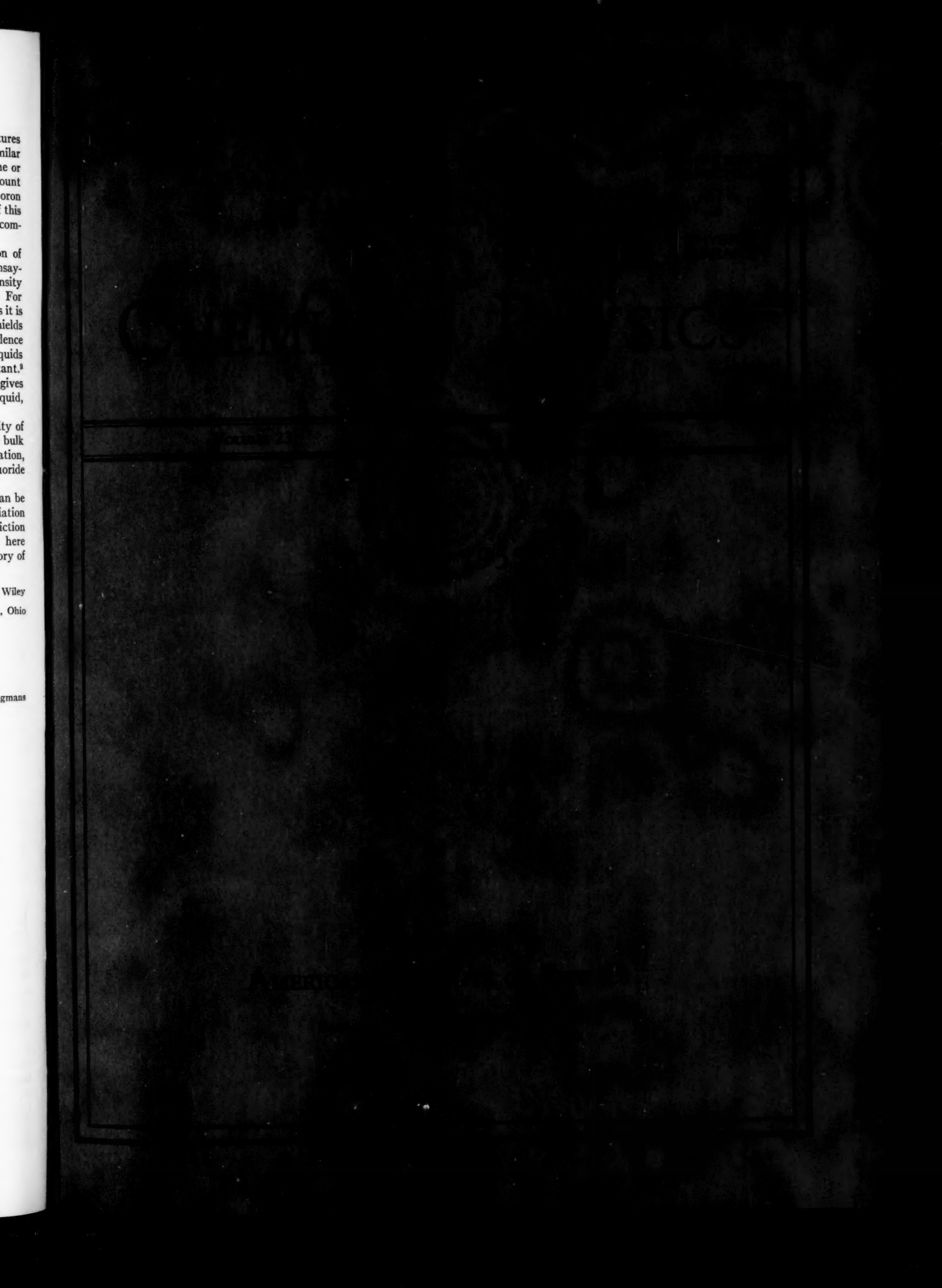

T. F. YOUNG

Physics and Chemical Abstracts (Chem.
(1951)).

typewritten on sheets separate from the
text. Each table must have a caption which will
the data in the table intelligible without reference
text. Avoid complicated column headings.

wherever possible figures should be planned for the
of a column (3 in.). A convenient reduction ratio is
2:1 or 3:1. Lettering should be large enough on the
that when reduced it shall not be less than about
(~1.5 mm). Line drawings should be in India ink on
paper or tracing cloth. Coordinate paper is not
but if used must be blue lined and the coordinate
which are to show must be inked over. Pictures of
etc., should be glossy prints and should have
black and white contrast. Identify each original
or photograph on the back with the author's name
the figure number. Figures should be numbered con-
Captions should be typed on a separate sheet
paper.

limited number of alterations in proof are unavoidable,
the cost of making extensive alterations after the
has been set in type will be charged to the author.
and all correspondence concerning papers in the
of publication should be addressed to the Publica-
Manager, American Institute of Physics, 57 East
Street, New York 22, New York.

Subscription Price

	In U.S. and Canada	Elsewhere
To members of the American Institute of Physics and Affiliated Societies	$12.00	$13.00
To all others	15.00	17.00

Back Numbers Price

Yearly rate when complete year is available: $18.00.
Single copies: $1.75 each.

Subscriptions, renewals, and orders for single copies should be addressed to the American Institute of Physics, 57 East 55 Street, New York 22, New York.

Changes of address should be sent to the American Institute of Physics.

[illegible] Lancaster, Pennsylvania

[illegible] Lancaster, Pa., under the Act of August 24, 1912.
[illegible] P. L. & R. authorized [illegible] February 2, 1923.

THE JOURNAL
OF
CHEMICAL PHYSICS

VOLUME 23, NUMBER 4 APRIL, 1955

Fluorescent Behavior of Solutions Containing More than One Solvent*

MILTON FURST AND HARTMUT KALLMANN
New York University, Physics Department, Washington Square, New York, New York
(Received May 20, 1954)

Fluorescent emission of organic solutions in combinations of solvents is investigated in order to determine the reasons for the suitability or unsuitability of solvents for high-energy induced fluorescence, particularly where these solvents do not influence the emission under ultraviolet irradiation. Basically two types of behavior under high-energy radiation are found in these combined solvent solutions. In type I a considerable drop in emitted intensity occurs only when the amount of the "poor" solvent greatly exceeds that of the "effective" solvent, whereas in type II small amounts of added "poor" solvent produce large decreases in emitted intensity. The fluorescence depends upon the concentration of solute, larger concentrations giving greater light outputs. The results obtained are explained by assuming that energy transfer occurs from the "poor" solvent to the "effective" one. At the same time a decrease in actual lifetime of excitation in the "effective" solvent occurs which is induced by the presence of the "poor" solvent molecules. This shows up as a quenching of the gamma-ray induced fluorescence in solutions even with solutes which are scarcely quenched at all under ultraviolet light excitation. For type I behavior this quenching is small while for type II it is considerable.

INTRODUCTION

COMPARISON of fluorescence induced by high energy and by ultraviolet-light excitation in solutions of various solutes in various solvents has shown striking differences between these modes of excitation. A number of solutions have similar relative efficiencies under both types of excitation; many others exhibit considerable variation. If the fluorescent emission of a given solute is tested in different solvents, nearly equal intensities are found under ultraviolet excitation whereas large differences are found under high-energy irradiation for these solvents. Thus some solvents ("poor") are unfavorable for producing high-energy fluorescence. It has further been observed that the addition of even small amounts of some "poor" solvents to a fluorescent solution results in a large decrease in high-energy induced fluorescence but only relatively small changes in ultraviolet-induced fluorescence.

The primary purposes of this investigation are (1) to attempt to determine why some substances (serving mainly as solvents) are favorable or unfavorable for high-energy induced fluorescence and (2) to explain the shapes of the various curves obtained for the fluorescent yield in solutions in combinations of solvents.

The basic experiments were studies of various solvent combinations, usually keeping the solute concentration (g/l of solution) unchanged. The solution was either placed in a "nonreflecting" beaker and excited by a one millicurie gamma-ray source, or was placed in a glass beaker and excited by light of a wavelength which is absorbed only by the solute (the light was directly incident upon the solution). The fluorescent output (integrated) was measured by means of an arrangement using a 1P28 photomultiplier.[1]

EXPERIMENTAL RESULTS

Pairs of solvents were used such that one solvent could usually be described as the "effective" solvent, and the other as the "poor" solvent. In an "effective" solvent rather strong fluorescence is produced under gamma-ray excitation when suitable solutes are dissolved in it, whereas in a "poor" solvent the same solutes produce only a small light output. Typical results are depicted in Figs. 1 to 4; in these graphs the fluorescence with 100 percent "effective" solvent is always shown on the left.

* This work was supported by contract with the Signal Corps Engineering Laboratories, Evans Signal Laboratory, Belmar, New Jersey.

[1] H. Kallmann and M. Furst, Phys. Rev. **79**, 870 (1950).

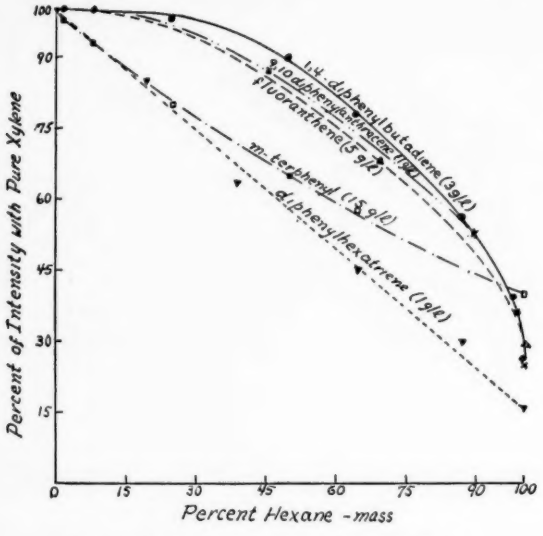

FIG. 1. Gamma-ray induced fluorescence in hexane-xylene mixtures.

There are essentially two different types of curves in these figures. Type I does not show a marked decrease in fluorescent output until large amounts of the "poor" solvent are added; only as 100 percent "poor" solvent is approached does the fluorescent output dip sharply.[1] Figure 1 presents examples of this type of behavior. Curves of Type II, on the other hand, show a sharp initial drop when only small amounts of the "poor" solvent have been added. This behavior is clearly shown, for example, when carbon tetrachloride is added to xylene solutions of fluoranthene (Fig. 4). Curves lying between these extremes are found in some of the experiments. The straight-line behavior of diphenylhexatriene in Fig. 1 is due in part to the decrease in fluorescence of diphenylhexatriene by hexane which is shown by measurements with ultraviolet light. The behavior of *m*-terphenyl in the same figure will be discussed later. The shape of the curve is also found to depend to some extent upon the concentration of the solute, thus further complicating the picture.

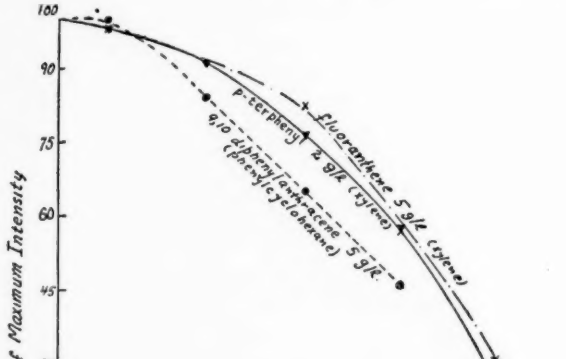
Percent of Maximum Intensity
Percent n-Butylphosphate -mass
p-terphenyl 2 g/l (xylene)
fluoranthene 5 g/l (xylene)
9,10 diphenylanthracene 5 g/l (phenylcyclohexane)

FIG. 2. Gamma-ray induced fluorescence in mixtures of *n*-Butylphosphate and xylene or phenylcyclohexane.

The curves of Figs. 1 to 4 depict results for gamma-ray excitation; under light excitation the shapes of the curves are often very different, as can be seen for example from Fig. 4. With many solvent combinations under ultraviolet excitation some solutes, (e.g., fluoranthene) have almost the same fluorescent yield with 100 percent "poor" solvent as is found with 100 percent effective solvent. These differences for the two types of excitation stem from the necessity for energy transfer from solvent to solute under gamma-ray excitation to produce strong fluorescence. Under light excitation the light-emitting solute molecule is directly excited, so that if a change because of variation of the solvent is found, it is to be attributed to a quenching of the excitation of the solute before the light-emission process occurs. A comparison between the results for light and gamma rays then makes it possible to differentiate between the effects due to solute quenching and those depending upon energy transfer. The results obtained with light excitation show that the light-emission efficiency, in many instances, is not impaired by the presence of the "poor" solvent. It can thus be definitely stated that in these experiments no new impurities which markedly affect the light output of the solute are introduced into a solution when the "poor" solvent is added.

TABLE I. Qualitative solvent ratings for gamma-ray induced fluorescence.

Effective	Moderate	Poor
Phenylcyclohexane	Cyclohexane	Acetone
Xylene	Hexane	*n*-Butylphosphate
Toluene	Paraffin oil	Carbontetrachloride
Benzene	1-Ethoxynaphthalene	Chloroform
Tetralin	Decalin	Ether
Phenyl ether	Tetrahydrofuran	Ethyl alcohol (95 percent)
Phenetole	Benzyl alcohol	Methyl alcohol
Cumene	Benzyl ether	
p-Cymene	Styrene	
p-Dioxane		
Iso-durene		

In Table I solvents are arranged according to their relative capabilities of energy transfer. We interpret this table by assuming that the solvents marked "effective" in the table have the longest actual lifetimes of excitation and those marked "poor" the shortest. Most of the better solvents contain double bonds. *p*-Dioxane is the only very good solvent we know which contains no double bonds, although there are many such with moderate transfer ability (e.g., cyclohexane and decalin). There are, of course, numerous solvents which do contain double bonds and have inferior transfer properties.

DISCUSSION

Consider first the behavior under gamma rays of a solution made with a "poor" solvent, that is, one in

which a low fluorescent output is obtained for all solutes, even for those which are efficient under ultraviolet excitation. The low output which occurs under high-energy irradiation in such solutions is then to be attributed to poor transfer of energy from the solvent to the solute. The assumption might be made that no transfer at all takes place from the "poor" solvent to the solute. This is, however, certainly not the case in many solutions made up with a single "poor" solvent rather than a combination of solvents; in these the light emission is found to increase considerably with increasing solute concentration (at concentrations sufficiently small to make direct excitation effects negligible). In addition, under the assumption of no transfer, the extended flat portions of some of the curves which are obtained using various solvent combinations cannot be explained. It is consequently assumed that energy transfer can take place to the solute from both types of solvent molecules of a combination, the probability of energy transfer being smaller for the "poor" solvent.

The probability of energy transfer, w, is approximately proportional to the concentration, c, of the molecules to which the energy is transferred, to the lifetime, τ, of the excited solvent molecule (this is determined mostly by the probabilities of internal and external quenching processes); and to a "collision" of cross section, σ, associated with the transfer of energy from the excited solvent molecule to the solute molecule. Thus approximately

$$w \sim \sigma \tau c. \tag{1}$$

This probability for energy transfer enters the expression for light emission under high-energy excitation in the following way: The equation

$$I = \frac{Pc}{(Q+c)(R+c)} \tag{2}$$

gives the intensity of fluorescent light output, I, as a function of solute concentration, c, and parameters P, Q, and R which are defined in reference (2). The parameter Q is proportional to the reciprocal of the energy transfer probability per unit concentration [i.e., to $(\sigma\tau)^{-1}$]. It has been found[2] that this parameter varies only slightly for a given efficient solvent (same τ) with many different efficient solutes, and furthermore, the concentration for efficient energy transfer is found to be of the same order of magnitude for most of these solutes. These findings imply that the cross section does not vary greatly for most efficient solutes. From the experimentally known decay times of the solute light flashes, one can also infer that the actual lifetime of the excited solvent molecules must be of the order of 10^{-9} second or smaller.

With reference to the above equations, the "poor" solvent is thought to be one in which the actual lifetime,

[2] M. Furst and H. Kallmann, Phys. Rev. 85, 816 (1952).

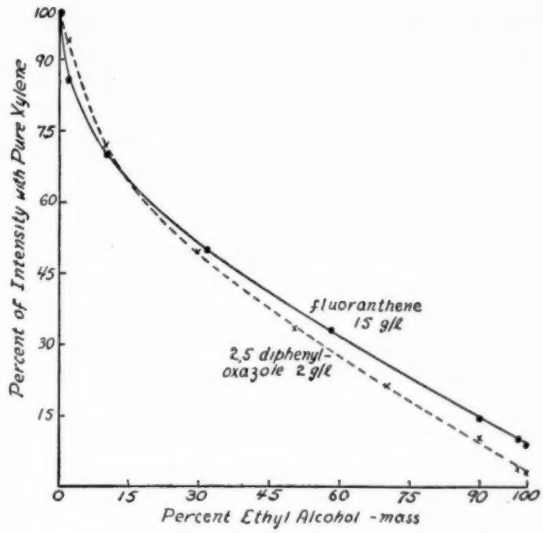

FIG. 3. Gamma-ray induced fluorescence in ethyl alcohol (95 percent)-xylene mixtures.

τ, of the excited solvent molecule is smaller than is the case for an "effective" solvent, which means a large Q in Eq. (2) for the "poor" solvent. One could also assume that σ the transfer cross section, is strongly reduced in a "poor" solvent, but then one would also have to assume that such a cross-section reduction occurs for all solutes. The expectation would then be a considerable variation in Q among the different solutes, but less variation than expected under such an assumption is found. Furthermore, it will be shown below that the shape of the curve can be understood more easily if the assumption is made that it is the lifetime of the excited molecule that is reduced. With a reduced τ at a given concentration of solute molecules, the number of "collisions" which are accompanied by energy transfer are insufficient to produce sizeable transfer during

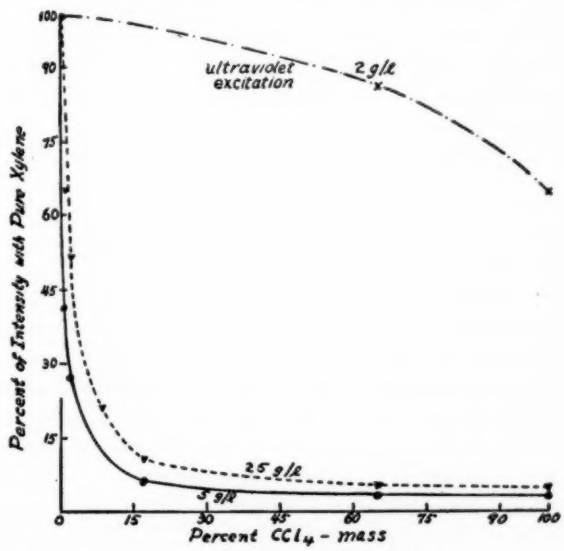

FIG. 4. Gamma-ray and light induced fluorescence in CCl_4-xylene mixtures, solute: fluoranthene.

the comparatively short actual lifetime of these excited solvent molecules. This idea is borne out by the fact that in "poor" solvents a considerable increase in fluorescence is obtained under gamma-ray excitation if greater concentrations of the solute are present than are needed in an "effective" solvent (see Fig. 4). These concentrations are in a range where an increase of light output is no longer obtained in an "effective" solvent but are still small enough for direct-excitation effects of the solute to be negligible. It is of interest to note that in solutions made with "poor" solvents the influence of self-quenching on the shape of the fluorescence *vs* concentration curve seems to be less evident since the usual decrease after reaching a maximum is almost completely eliminated. This comes about because of the poorer energy transfer which shows up in Eq. (2) as a relatively large value for the coefficient Q. Nevertheless the effect of self-quenching is still present and is even more important because of the higher solute concentrations necessary for obtaining maximum light outputs. The concentration $c_m=(QR)^{\frac{1}{2}}$, at which the maximum light output occurs according to Eq. (2), is shifted to higher concentrations in "poor" solvents because of their higher Q, and the maximum intensity $I_m=P/(Q^{\frac{1}{2}}+R^{\frac{1}{2}})^2$ is reduced for the same reason.[2]

If the fluorescence of a solute under ultraviolet light excitation and thus its internal quenching is known, and if its self-quenching coefficient [associated with factors P and R in formula (2)] is available, the fluorescence obtained under gamma-ray excitation can be adjusted for equal internal quenching and zero self-quenching of the solute, and then the effects due to energy transfer can be evaluated.

When small amounts of an "effective" solvent are added to a solution in a "poor" solvent or *vice versa*, one might expect a mixture curve to be followed since the high-energy radiation is absorbed in these organic solvents essentially in the ratio of the masses of the two solvents. Such a curve would be a straight line if the ultraviolet light induced fluorescence in the "poor" and "effective" solvents were of equal magnitude. With equal light fluorescence any chemical interaction influencing fluorescence would be ruled out or be equal. In most instances a straight line does not result as can be seen from the curves of Figs. 1 to 4.

The addition of relatively small amounts of "effective" solvent to a solution made in a "poor" solvent often produces a rapid increase in the gamma-ray induced fluorescence. This means that with small amounts of an effective solvent a considerable amount of energy absorbed in the "poor" solvent reaches the solute. In order to account for this, we assume that energy transfer occurs from excited molecules of the "poor" solvent to (unexcited) "effective" solvent molecules and then to the solute.

This assumption is made because: *a*. It is known that in these solutions with a given fraction of "effective" solvent present no more than about this fraction of incident energy is directly absorbed in the "effective" solvent, and *b*. a large portion of the available energy in the "effective" solvent goes to the solute at the concentrations used, whereas practically no energy transfer occurs from the "poor" solvent to the solute as shown by the experiments with only a single solvent present. Such transfer is possible if the lowest excitation energy of the "effective" solvent molecule is smaller than that of the "poor" solvent, and it takes place if a sufficient number of "effective" solvent molecules are present in the solution. (Ionization effects are not completely ruled out in these experiments with "poor" solvents.) Under such circumstances a considerable transfer may occur with only about 10 percent of "effective" solvent, despite the relatively short lifetime, τ, of the excited "poor" solvent molecule. In effective solvents energy transfer from the solvent occurs at solute concentrations of several grams per liter. Here the energy transfer from the "poor" solvent to the "effective" one occurs at concentrations of about 100 grams per liter. This indicates that the actual lifetime of the excited "poor" solvent is less than one tenth of that of the "effective" solvent. This is in agreement with the behavior that at a given solute concentration, the fluorescent yield under high-energy excitation is reduced by more than a factor of ten in a "poor" solvent. Once the energy resides in the "effective" solvent molecule, its actual lifetime is increased (now τ is the lifetime of the excited molecule of good solvent). Now the energy can easily be transferred again, this time from the "effective" solvent to the solute, with a corresponding increase in fluorescence.[3]

It should be here noted that in the process of energy transfer in solution only the lowest excited states need be considered since these states have the longest lifetimes. The higher excitation levels have comparatively short lifetimes on account of the many possibilities of degradation of energy to the lowest levels because of strong interaction with phonons. The lowest excited states of the "poor" solvent will consequently be reached very quickly, and effects connected with the higher states are unimportant. The energy will then be transferred to the lowest excited state of the "effective" solvent if this state has a smaller excitation energy than that of the "poor" solvent and if the "effective" solvent concentration is great enough. In such a case no return of the energy to the "poor" solvent is possible. It may be remarked that energy transfer has never been observed where the lowest excitation energy of the solvent is below that of the solute. The emission of the solute is always that of the lowest level.

Thus an energy transfer from the "poor" to the

[3] This mechanism very likely explains the successful use of mixtures for neutron and other particle detection, e.g., C. O. Muehlhause and G. E. Thomas, Jr., Phys. Rev. **85**, 926 (1952) and Nucleonics **11**, No. 1, 44 (1953); J. Kirkbridge, Nature **171**, 564 (1953); Cowan, Reines, Harrison, Anderson, and Hayes, Phys. Rev. **90**, 493 (1953).

"effective" solvent is assumed, similar to that which has been successful in explaining the high-energy induced fluorescence in dilute solutions in a single "effective" solvent.

If energy transfer from the "poor" solvent to the "effective" solvent and then to the solute were the only pertinent mechanism, the fluorescent intensity would increase more quickly than a mixture curve in practically all cases in which an "effective" solvent is added to a solution made in a "poor" one and the necessary energy condition is fulfilled. In numerous cases, however, this does not occur (e.g., curves of Fig. 3), indicating that other effects must be taken into account. This is particularly true for those curves which display a sharp drop in intensity when small amounts of "poor" solvent are added.

The behavior of solutions under light excitation helps clear up the situation. It is found that when some substances like xylene, durene, and *p*-terphenyl are used as solutes, their light-induced fluorescence (the solute molecules are directly excited) is tremendously decreased (quenched) upon the addition of even small amounts of "poor" solvents like carbon tetrachloride which exhibit a type II behavior. This quenching means that the actual lifetime of the excited state of these solutes is shortened by the addition of such a "poor" solvent. Solvents displaying a type I curve quench only to a slight extent if at all. These results provide experimental evidence that some "poor" solvents quench materials some of which are used as "effective" solvents, e.g., xylene. This supports the contention made above that the change in lifetime τ rather than that of cross section σ is of greater significance for the change of energy transfer.

Therefore, one must expect that a similar shortening of lifetime of excited molecules of the "effective" solvent is produced by the presence of even small amounts of a suitable "poor" solvent. Most of the curves can then be explained as follows: In a solution made with a combination of an "effective" and a "poor" solvent, all or practically all of the excitation energy initially induced in the "poor" solvent is transferred to the "effective" one (if the excited energy level of the "poor" solvent is above that of the "effective" solvent), so that most of the excitation energy eventually resides in the "effective" solvent. At the same time, however, the actual lifetime of the excited molecules of "effective" solvent (independently of whether their excitation is induced directly or by energy transfer from the "poor" solvent) can be decreased by the presence of the "poor" solvent, (markedly with type II solvents) and in such cases the energy transfer to the solute is diminished. Consequently the fluorescent-light output declines with increasing concentration of such "poor" solvents. If this quenching effect of "poor" solvents on excited molecules of "effective" solvents is very strong, a sharp decrease of fluorescence is observed with small amounts of added "poor" solvents. These considerations provide an explanation for the type II, sharply decreasing fluorescent-light output curves.

This idea of quenching of the excited solvent molecule is given further credence by the effects of increasing solute concentration upon these curves. It is found that at greater solute concentrations, the degree of the decrease in light output resulting from the addition of "poor" solvent is diminished. This shows that the excitation energy must not necessarily be lost; at larger solute concentrations the number of "collisions," with accompanying energy transfer, per unit time is increased so that more energy goes to the solute before the excited solvent molecule is quenched. In other cases the influence of the "poor" solvent on the "effective" solvent may be slight, and curves which lie above the mixture curve are obtained.

A pertinent example bearing out the above ideas is that in Fig. 4, where the fluorescence of fluoranthene in carbon tetrachloride-xylene combinations is shown. Under ultraviolet-light excitation the fluorescence of fluoranthene is only moderately decreased as one proceeds from pure xylene to pure carbon tetrachloride as solvent. Under gamma-ray excitation, however, the addition of only 5 percent carbon tetrachloride causes a reduction in fluorescence by more than a factor of 2. It is also readily observed in this figure that at large concentrations of fluoranthene less decrease in light emission occurs. The strong decrease in fluorescence under gamma-ray excitation is due to the reduction in the lifetime (quenching) of the excited xylene molecules produced by carbon tetrachloride molecules. At greater fluoranthene concentration this reduction in fluorescence is less in spite of the decreased lifetime of excitation of xylene molecules because a greater number of "collisions" with the solute molecules occur within this lifetime period.

Study of one solvent combination with different solutes shows that the shape of the light-output curve (whether type I or II) is generally unchanged; but this is not strictly true in all cases. For example, pyrene and *m*-terphenyl show anomalies in xylene-hexane and xylene-trimethylborate mixtures. These may be associated with the poorer energy transfer to these solutes when observed in xylene (this is deduced from the larger Q values obtained for these solutes).[2] Actually, hexane and trimethylborate produce only slight decreases in the actual lifetime of the excited solvent molecule (xylene) as is shown by the many type I curves obtained with these solvents. Because of the generally poor energy transfer to pyrene and *m*-terphenyl, however, the effect of this small decrease in τ is more easily noticeable in the range of concentrations here employed. Thus, in Eq. (2), if c is large compared to Q, relatively large changes in Q are necessary to produce sizeable changes in the light output; but if Q and c are of the same order, then a much smaller relative change in Q produces the same

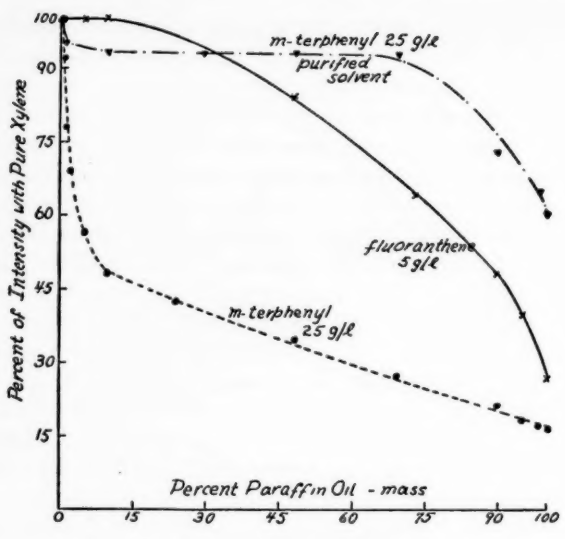

FIG. 5. Gamma-ray induced fluorescence in paraffin oil-xylene mixtures.

change in emission. In the solutions of pyrene and *m*-terphenyl the concentrations, c, at which considerable light emission occurs and the Q were of the same order of magnitude so that the effect of the comparatively small changes in Q produced by hexane and trimethyl borate were more easily observed.

A particularly unusual behavior was found in some experiments with xylene-paraffin oil combinations. With fluoranthene a type I curve was obtained, whereas a type II curve was exhibited with *m*-terphenyl (Fig. 5). Such a difference indicated the presence of impurities in the solvent since in no other cases were two different types of behavior found in the same solvent combination. Measurements with light excitation did indeed reveal the presence of an impurity affecting *m*-terphenyl but scarcely influencing fluoranthene (because of their different absorption spectra). As can be seen from Fig. 5, when a purer paraffin oil is used the result with *m*-terphenyl is also of type I if the effect of the high Q of *m*-terphenyl is taken into account. This experiment shows that such mixed solvent measurements can reveal the presence of impurities. In most of the experiments herein reported the role of impurities as causes of the large effects discussed in the earlier sections can be ruled out by theoretical considerations and previous studies of the importance of impurities.[4] Nevertheless many of the materials (both solvents and solutes) were additionally purified by continuous chromatography[5] or other means. These further purifications (including the removal of oxygen) produced only minor changes and did not alter the type I or type II behaviors. This shows that a "poor" solvent under high-energy induced fluorescence is not inferior because of the presence of impurities, but rather because of properties intrinsic to the solvent.

The experiment described above with mixed solvents using high energy show that two processes are mainly responsible for the observed effects: (1) the decrease in the lifetime of the excited molecule of "effective" solvent in the presence of a suitable "poor" one, and (2) the occurrence of energy transfer from "poor" to "effective" solvent. The process responsible for quenching of the "effective" solvent by the "poor" is as yet unknown. The following observation, however, may provide a clue. It is quite often found that molecules having greater excitation energies are more easily quenched by other molecules than those with smaller excitation energies.

If the "poor" solvent has a lowest (singlet) excitation level of smaller energy than the lowest level of the "effective" solvent, a decrease in light output by the addition of "poor" solvent could be attributed to an energy transfer from the "effective" to the "poor" solvent. In the cases of the addition of carbon tetrachloride or alcohol where the lowest excitation energies are above those of xylene, this certainly is not the reason for the decreased emission. In acetone, however, which has a lower excitation energy than xylene, the type II behavior found is very likely at least partially because of such an energy transfer.

According to these ideas, a solvent like 1-ethoxynapthalene which is less "effective" than xylene (Table I) with suitable solutes such as 9,10-diphenylanthracene, would be expected to show a type II behavior when mixed with xylene, since its excitation level is smaller than that of xylene. Experiments carried out with such xylene-1-ethoxynapthalene solvent combinations using the above solute have shown this type II behavior.

When energy transfer occurs from a molecule with shorter lifetime to one with a longer lifetime, the experiments described show that the fluorescent output is enhanced. It has been found that such a process can successfully be employed to make rather efficient solutions containing considerable amounts of substances which ordinarily exhibit inferior high-energy induced fluorescence properties.[6]

[4] H. Kallmann and M. Furst, Phys. Rev. **81**, 853 (1951).

[5] R. C. Sangster, Technical Report No. 55, Office of Naval Research, Contract with Massachusetts Institute of Technology (1952).

[6] M. Furst and H. Kallmann Phys. Rev. **97**, 583 (1955).

Surface Tension and Viscosity of Liquids

J. H. SIMONS AND W. H. WILSON
The University of Florida, Gainesville, Florida
(Received April 29, 1954)

Empirical relationships have been found between energy of vaporization, surface energy, energy of activation of viscosity, and the boiling temperature. This has been done by first considering the inert gases as the simplest type of liquid.

$$\Delta E_{vap}=\sigma_b A_b+\tfrac{1}{2}RT_b.$$
$$\Delta E_{vis}=1.212RT_b^{1.2}.$$

For the simplest type of polyatomic substance the normal fluorocarbons give

$$\Delta E_{vap}=\sigma_b A_b+\tfrac{1}{2}RT_b+1.212RT_b^{1.2},$$
$$\Delta E_{vis}=1.212RT_b^{1.2}.$$

The normal hydrocarbons give, as expected, liquids whose properties differ from those of the normal fluorocarbons.

$$\Delta E_{vap}=\sigma_b A_b+1.212RT_b^{1.2}.$$
$$\Delta E_{vis}=1.212RT_b^{1.2}-1000.$$

For normal heptane it is shown that $\Delta E_{vap}=\sigma A+1.212RT^{1.2}$ may be taken at temperatures other than T_b. Suggestions are given for theoretical reasons for these equations.

IT has long been apparent that advancements in the theory of the liquid state could be stimulated by expanding measurements of properties of liquids, both in amount and kind, and by finding new relationships between these measurements. The fluorocarbons have provided a new class of liquids, the physical properties of which are beginning to contribute to the available information upon which to correlate liquid properties. Considerable differences are obtained in the comparison of these properties with those of analogous hydrocarbons.[1] To correlate the properties of hydrocarbon-fluorocarbon mixtures, a type of internal entropy of the liquids was postulated for hydrocarbons and called interpenetration.[2] The solubility of organic substances in fluorocarbon solvents and the solubility of fluorocarbons in organic solvents shows the significant differences between these two classes of substances.[3] The solubilities of nitrogen and chlorine in both hydrocarbons and fluorocarbons also show the differences.[4] Other solubility studies, as for example the systems $WF_6-C_5F_{12}$ and $WF_6-C_5F_{10}$,[5] give additional information.

It is therefore beginning to appear that, just as water is a very untypical liquid, so hydrocarbons and other organic liquids are more complicated than nonhydrogen containing substances. A molecular interaction either of different kind (a hydrogen coupling) or of greater magnitude exists. This leads to the consideration of the inert gases and fluorocarbons as providing a better basis for comparison and for establishing ideas of normal or ideal liquids, the former for monatomic and the latter polyatomic substances.

In this paper, consideration is given to two other physically-determined properties of liquids, interfacial tension and flow: More particularly, the interfacial tension is that between the liquid and its vapor (surface tension), and the aspect of flow is the energy of activation of viscosity. Correlations are obtained with the energy of vaporization. First, the inert gases are considered as providing liquids of monatomic molecules the force fields of which are spherically symmetrical. Then the fluorocarbons are used as examples of liquids having molecules with moments of inertia thermodynamically significant and shape, i.e., force fields, not spherically symmetrical. Subsequently, hydrocarbons are shown to differ from fluorocarbons in both the nature of the force fields (interpenetration) and effects such as orientation on the surface.

SURFACE TENSION

The Inert Gases

The process of transferring a molecule of a monatomic substance from the body of the liquid to the surface can be looked upon as requiring two separate energy effects. The first of these is concerned with the environmental difference between the molecule in the body of the liquid and in the surface. In the body of the liquid a molecule has three degrees of freedom of translational kinetic energy. Its motion, however, is constrained by its near neighbors so that it undergoes what may be considered as nonuniform vibrations. This introduces three degrees of freedom of potential energy. At the

[1] J. H. Simons and R. K. Smith, J. Phys. Chem. **46**, 380 (1942); J. H. Simons and J. B. Hickman, J. Phys. Chem. **56**, 420 (1952).
[2] J. H. Simons and R. D. Dunlap, J. Chem. Phys. **18**, 335 (1950); J. H. Simons and J. W. Mausteller, J. Chem. Phys. **20**, 1516 (1952).
[3] Hildebrand, Fisher, and Benesi, J. Am. Chem. Soc. **72**, 4348 (1950); J. H. Simons and M. J. Linevsky, J. Am. Chem. Soc. **74**, 4750 (1952).
[4] J. Chr. Gjaldbaek and J. H. Hildebrand, J. Am. Chem. Soc. **71**, 3147 (1949); J. Chr. Gjaldbaek and J. H. Hildebrand, J. Am. Chem. Soc. **72**, 609 (1950).
[5] E. J. Barber and G. H. Cady, J. Am. Chem. Soc. **73**, 4247 (1951); G. H. Rohrback and G. H. Cady, J. Am. Chem. Soc. **73**, 4250 (1951).

TABLE I. Comparison of $\Delta E_{vap}-\frac{1}{2}RT_b$ and $\sigma_b T_b$ for the inert gases.

	T_b °K	$\frac{\Delta E_{vap}}{T}=\Delta S-R$ cal / mole, degree[a,b]	$\Delta E_{vap}\times10^{-10}$ ergs / mole at T_b	Density at T_b[a] g/cm³	$A_b\times10^{-9}$ cm²	σ_b dynes / cm	$\Delta E_{vap}-\frac{1}{2}RT_b\times10^{-10}$ ergs / mole at T_b	$\sigma_b A_b\times10^{-10}$ ergs / mole at T_b
Helium	4.2	3.7	0.065	0.126	4.098	0.12	0.048	0.049
Neon	27.2	13.3	1.514	1.204	2.675	5.50[c]	1.401	1.471
Argon	87.4	15.18	5.597	1.402	3.308	13.20[d]	5.232	5.030
Krypton	120.2	17.1	8.62	2.155	4.684		8.18	
Xenon	164	17.53	12.03	3.06	5.007		11.34	

[a] See reference 1.
[b] *International Critical Tables* Vol. IV, p. 445.
[c] Commun. Phys. Lab. Univ. Leiden, No. 182b.
[d] E. C. C. Baly and F. G. Donnan, J. Chem. Soc. (London) **81**, 907 (1920).

surface, however, there is one direction in which the translational motion is not constrained by repulsive forces of near neighbors so that a molecule on the surface can have one less degree of freedom of potential energy. The second effect is concerned with the increase in surface area caused by the molecule going into the surface. This is the surface tension, σ, multiplied by the increase in area. The total increase in surface for one mole of the monatomic substance going from bulk liquid to vapor is the total surface of the individual molecules minus the surface of the molal volume of liquid. The latter is negligible compared to the former. The former is not physically realizable or measurable, but a figure representing it can be obtained from the surface area of Avogadro's number of spheres, A, the density of which is the bulk density of the liquid at that temperature. In Table I, it can be seen that $\Delta E_{vap}-\frac{1}{2}RT_b$ is approximately equal to $A_b\sigma_b$ for the inert gases, helium, neon, and argon. The surface tension at the boiling point is not available for krypton and xenon.

$$\Delta E_{vap}=\tfrac{1}{2}RT_b+A_b\sigma_b. \qquad (1)$$

The Normal Fluorocarbons

The thermodynamically significant moment of inertia of polyatomic substances makes necessary a consideration of the differences of both rotations and oscillations in the body of the liquid, the surface, and in the vapor state. In the body of the liquid the molecular force fields are grossly uniform but minutely nonuniform, as the presence of near neighbors may prevent free rotation and cause rotational energy to be exhibited to some extent as oscillations with attendant potential terms. At the surface the gross force fields have a sharp gradient which causes changes in the rotations and oscillations. In the vapor, oscillations are nonexistent. Detailing these differences is not attempted here. In general, one would expect the over-all effect to be a function of temperature. Designating this rotational contribution as ΔE_{rot}, it has been found empirically to approximate $1.212RT_b^{1.2}$. For the normal fluorocarbons,

$$\Delta E_{vap}=\sigma_b A_b+1.212RT_b^{1.2}+\tfrac{1}{2}RT_b. \qquad (2)$$

In Table II can be seen the agreement of surface ten-

TABLE II. Comparison of surface tension calculated from Eq. (2) and observed for fluorocarbons.

	V_b/T_b cm³ per deg	$\frac{A_b}{T_b}\times10^{-8}$ cm² per deg	$\left(\frac{\Delta E_{vap}}{T_b}=\Delta S_{vap}-R\right)\times10^{-8}$ ergs per mole deg	$\frac{\Delta E_{rot}}{T}\times10^{-8}$ (calc) ergs per mole deg	σ_b (calc) dynes per cm	σ_b (obs) dynes per cm
methforane, CF_4	0.310	0.356	7.64	2.742	12.6	...
ethforane, C_2F_6	0.382	0.371	7.73	2.912	11.9	...
propforane, C_3F_8	0.551	0.445	7.91	3.024	10.05	...
n-butforane, C_4F_{10}	0.573	0.437	7.91	3.103	10.05	...
n-pentforane, C_5F_{12}	0.583	0.427	7.91	3.167	10.1	10.0[a]
n-hexforane, C_6F_{14}	0.633	0.435	8.06	3.233	10.1	...
n-heptforane, C_7F_{16}	0.665	0.435	7.91	3.284	9.7	10.0[b] 9.5[c]
n-octforane, C_8F_{18}	0.720	0.446	(7.91)	3.322	9.35	9.0[a]
n-nonforane, C_9F_{20}	0.766	0.458	(7.91)	3.356	9.0	9.3[d]
n-decforane, $C_{10}F_{22}$	0.828	0.475	(7.91)	3.394		

V_b = molal volume at T_b.
Observed at values of σ_b extrapolated from $\frac{\sigma}{\sigma_b}=3\left(\frac{T_c-T}{T_c}\right)^{1.23}$.
The ratio T_c/T_b is assumed constant for the fluorocarbon series.
[a] *Fluorine Chemistry*, J. H. Simons, Editor, (Academic Press, Inc., New York, 1950), Vol. I, p. 438.
[b] Fowler, Hamilton, Kaspor, Weber, Burford, and Anderson, Ind. Eng. Chem. **39**, 375 (1947).
[c] G. H. Rohrback, and G. H. Cady, J. Am. Chem. Soc. **71**, 1938 (1949).
[d] M. Stacey, Roy. Inst. Chem. G. Brit. Ireland, pp. 1–15, Preprint (1948).
The values in parentheses are estimated, based on the expected constancy of the entropy of vaporization for the higher members of the series. For fluorocarbons, ΔS_{vap} in cal/mole is taken from the tabulation in Simons and Smith (see reference 1) with additional information from the extrapolation of Burger and Cady's values [J. Am. Chem. Soc. **73**, 4243 (1951)] for pentforane and Brice and Coon's [J. Am. Chem. Soc. **75**, 2921 (1953)] for *n*-hexforane. All data were then converted to units proper for this work. In all cases $\Delta E_{rot}=1.212RT_b^{1.2}$ is the calculated value.

TABLE III. Comparison of surface tension calculated from Eq. (3) and observed for hydrocarbons.

	$\frac{V_b}{T_b}$	$\frac{A}{T_b}\times 10^{-8}$	$\left(\frac{\Delta E_{vap}}{T_b}=\Delta S_{vap}-R\right)\times 10^{-8}$ ergs per mole deg	$\frac{\Delta E_{rot}}{T_b}\times 10^{-8}$ (calc) ergs per mole deg	σ_b (calc) dynes per cm	σ_b (obs) dynes per cm
methane, CH_4	0.339[d]	0.412	6.49[e]	2.60	9.5	...
ethane, C_2H_6	0.298[d]	0.320	7.13[e]	2.88	13.3	...
propane, C_3H_8	0.328[d]	0.316	7.28[f]	3.01	13.5	...
n-butane, C_4H_{10}	0.354	0.315	7.36[g]	3.11	13.5	...
n-pentane, C_5H_{12}	0.382	0.318	7.64[h]	3.194	14.0	14.1[c]
n-hexane, C_6H_{14}	0.421	0.323	7.66[i]	3.260	13.62	13.6±0.3[a]
n-heptane, C_7H_{16}	0.451	0.334	(7.66)[i]	3.314	13.31	13.4[c]
n-octane, C_8H_{18}	0.470	0.336	7.90[i]	3.361	13.50	13.5[b]
n-nonane, C_9H_{20}	0.496	0.341	(7.66)	3.402	12.79	13.6[b]
n-decane, $C_{10}H_{22}$	0.524	0.347	(7.66)	3.439	12.48	12.45[b]

[a] *International Critical Tables* Vol. V, p. 137.
[b] Wibaut, Hoog, Langedijk, Overhoff, and Smittenberg, Rec. trav. chim. **58**, 329 (1939). These data are extrapolated to T_b from 0°C by

$$\frac{\sigma}{\sigma_b}=3\left(\frac{T_c-T}{T_c}\right)^{1.23}.$$

[c] G. W. Smith, J. Phys. Chem. **48**, 168–72 (1944) extrapolated from 20°C.
[d] Values of density at boiling point from G. Egloff, *Physical Constants of Hydrocarbons* (Reinhold Publishing Corporation, New York, 1939), Vol. I.
[e] Rossini, Wagman, Evans, Levine, and Jaffe, *Selected Values of Chemical Thermodynamic Properties, Bureau of Standards Circular 500*, (1952).
[f] J. D. Kemp and C. J. Egan, J. Am. Chem. Soc. **60**, 1521 (1938).
[g] J. G. Aston and G. H. Messerly, J. Am. Chem. Soc. **62**, 1917 (1940).
[h] G. H. Messerly, and R. M. Kennedy, J. Am. Chem. Soc. **62**, 2988 (1940).
[i] L. E. Steiner, *Introduction to Chemical Thermodynamics* (McGraw-Hill Book Company, Inc., New York, 1948), second edition. p. 212 from *American Petroleum Institute Research Project*, Natl. Bur. Standards; also see reference 1.

sions calculated from this equation and those that have been observed.

Hydrocarbons

In previous efforts to correlate the measured physical properties of liquids with empirical equations, a difference between fluorocarbons and hydrocarbons was found. In the above paragraph, fluorocarbons are pictured as liquids in which a molecule on the surface has one less degree of freedom of potential energy than one in the body of the liquid. For hydrocarbons, however, because of the phenomenon which has been called "interpenetration," a molecule on the surface is subject to constraints by its neighbors even in the direction normal to the surface. The result of this is such that most surface molecules have the same number of degrees of freedom of potential energy as molecules in the body of the liquid. The $\frac{1}{2}RT$ term, therefore, does not appear in the equation. As can be seen in Table III, a satisfactory fit with observed values is obtained for surface tension for hydrocarbons by the use of Eq. (3),

$$\Delta E_{vap}=\sigma_b A_b+1.212RT_b^{1.2}. \quad (3)$$

It would be convenient if the above equation were usable at temperatures other than that of boiling at atmospheric pressure. For normal hexane, as is shown in Table IV, the equation can be written

$$\Delta E_{vap}=\sigma A+1.212RT^{1.2}. \quad (4)$$

ENERGY OF ACTIVATION OF VISCOSITY

Simple Substances

A relationship between the energy of activation of viscosity ΔE_{vis} and the energy of vaporization has been discussed by Ewell and Eyring[6] and Eyring and Hirschfelder.[7] Hirschfelder, Stevenson, and Eyring[8] have pictured the process of flow in a liquid as involving the rotation of a pair of molecules about a common center of mass and movement into a hole in the liquid. The energy of activation of viscosity is, therefore, related to the energy of hole formation which is related to the energy of vaporization.

From the point of view of this paper, the above picture can be employed by considering the rotational energy of a molecule in going from a state of no flow to a state of flow. There will be a difference much the same as the difference between a molecule in the body of the liquid and in the surface. There is, however, one additional factor. The rotation of a molecule in flow is about its neighbor in this picture, so that even monatomic substances will have a moment of inertia for this type of motion. It is very interesting, therefore,

TABLE IV. Comparison of experimental and calculated ΔE_{vap} at various temperatures for normal hexane.

T°K	273.2	293.2	313.2	342
δg per cm³	0.6769	0.6596	0.6412	0.613
$A\times 10^{-10}$ (cm²)	1.034	1.053	1.072	1.101
σ ergs per cm²	20.52	18.43	16.3	13.6
$\sigma A\times 10^{-10}$ ergs per mole	21.22	19.41	17.47	14.97
σA cal per mole	5075	4624	4170	3586
ΔE_{rot} cal per mole (calc)	2034	2214	2396	2665
$\Delta E_{vap}=\sigma A+\Delta E_{rot}$ cal per mole (calc)	7109	6378	6566	6251
ΔH_{vap} cal per mole (exp)	7680	(7500)	(7300)	6950
ΔE_{vap} cal per mole (exp)	7136	6916	6678	6260
ΔE_{vap} (exp)−ΔE_{vap} (calc)	27	78	112	7

[6] R. H. Ewell and H. Eyring, J. Chem. Phys. **5**, 726 (1936).
[7] H. Eyring and J. Hirschfelder, J. Phys. Chem. **41**, 249 (1937).
[8] Hirschfelder, Stevenson, and Eyring, J. Chem. Phys. **5**, 896–907 (1937).

TABLE V. Energy of activation of viscosity for simple substances.

	T_b °K	$\Delta E_{vis}=1.212RT_b^{1.2}$ cal/mole	ΔE_{vis} (Exp)[a] cal/mole	Difference
Argon	87.5	520	520	0
N_2	72.4	448	449	1
CO	83.2	488	466	−22

[a] See reference 6.

TABLE VI. Energy of activation of viscosity for fluorocarbons.

	T_b °K	$\Delta E_{vis}=1.212RT_b$ cal/mole	ΔE_{vis} (Exp) cal/mole	Ref.	Difference
n-pentforane, C_5F_{12}	302.5	2289	2240	(a)	−49
n-hexforane, C_6F_{14}	329.5	2545	2600	(b)	+55
n-heptforane, C_7F_{16}	355.2	2787	2870	(b)	+83
n-octforane, C_8F_{18}	376.7	2990	3240	(b)	+250
cyclo $C_6F_{12}O$	328.2 (731 mm)	2909	2840	(b)	−69
n-dibutforyloxide, $(C_4F_9)_2O$	375.2	2976	2950	(b)	−26
n-propforyldiethforyl-nitride, $C_3F_7(C_2F_5)_2N$	365.2	2881	2940	(b)	+55
di-*n*-propforylethforyl-nitride $(C_3F_7)_2C_2F_5N$	383.2	3052	3040	(b)	−12
n-pentforane, C_5F_{12}	302.5	2289	2240	(a)	−49
isopentforane, C_5F_{12}	303.5	2305	2690	(a)	+385
cyclopentforane, C_5F_{10}	295.7	2236	2940	(a)	+704

[a] L. L. Burger and G. H. Cady, J. Am. Chem. Soc. **73**, 4243 (1951).
[b] T. J. Brice and R. I. Coon, J. Am. Chem. Soc. **75**, 2921 (1953).

that the term previously employed for rotational energy effects, $1.212RT_b^{1.2}$, should correlate empirically the energy of activation of viscosity at the boiling point for simple substances with argon as a representative of the inert gases. This is shown in Table V.

$$\Delta E_{vis}=1.212RT_b^{1.2}. \quad (5)$$

Fluorocarbons

Because viscosity depends on the shape of the molecules, it could hardly be expected that the viscosity of an entire class of substances, such as the fluorocarbons, could be correlated on the basis of a simple relationship in which shape is not represented. Straight chain fluorocarbons and their oxides and nitrides do form a class for which Eq. (5) is useful. This is shown in Table VI. To show the effect of shape, three pentforanes, *n*-C_5F_{12}, iso-C_5F_{12}, and cyclo-C_5F_{10}, are listed at the bottom of the table.

Normal Hydrocarbons

The normal hydrocarbons have experimental energies of activation that are less than $1.212RT_b^{1.2}$ by approximately 1000 calories per mole as is seen in Table VII. For normal hydrocarbons,

$$\Delta E_{vis}=1.212RT_b^{1.2}-1000. \quad (6)$$

At first sight, it would appear that hydrocarbons, with greater cohesive forces than fluorocarbons or inert gases, should have higher, rather than lower, energies of activation for viscosity. Closer examination of the process of flow shows that for a molecule to slip by its neighbor requires a compression of near neighbors. Substances with greater compressibilities would have, on this basis, lower energies of activation of viscosity. Bridgman[9] suggested from his studies at high pressure that organic molecules having hydrocarbon chains may have an actual interlocking effect between molecules. In his book, *Physics of High Pressure*, pp. 128 and 129, he shows the compressibility of a number of hydrocarbons and two nonhydrogen containing carbon compounds. Fluorocarbons were not available at that time. These data are seen in Table VIII. The nonhydrogen containing substances are less compressible than the hydrocarbons. This is in agreement with the concept of interpenetration that was advanced to explain hydrocarbon-fluorocarbon solubility effects.

TABLE VII. Energy of activation of viscosity for normal hydrocarbons.

	T_b °K	$1.212RT_b^{1.2}$	ΔE_{vis}[a]	cal/mole[b]	Difference ΔE_{vis}[a]	Difference $-1.2a12RT_b^{1.2}$[b]
methane	111.7	695				
ethane	184.9	1273				
propane	231.0	1663				
n-butane	272.8	2030				
n-pentane	309.4	2361	1580	1504	−781	−857
n-hexane	342.4	2665	1730	1690	−935	−975
n-heptane	371.7	2943	1910	1858	−1033	−1085
n-octane	399.0	3204	2140	2088	−1064	−1116
n-nonane	423.9	3445	2440	2394	−1005	−1051
n-decane	447.2	3674	2600	2565	−1074	−1109
n-undecane	469.0	3890	3060	2778	−830	−1112
n-dodecane	482	4020	...	3010	...	−1010
n-tetradecane	525.7	4461	3600	3203	−861	−1258
n-hexadecane	560.7	4819	4010	3652	−809	−1167
n-octadecane	590.2	5126	4150	3891	−976	−1235

[a] See reference 6.
[b] H. Kierstead and J. Turkevich, J. Chem. Phys. **12**, 24 (1944), Landolt-Bornstein, *Physical-Chemischo Tabellen Part 1*, pp. 130, 149–52; E. C. Bingham and H. Fornwalt, J. Rheol. **1**, 372 (1930).

TABLE VIII. Compressibility of hydrocarbons.

Substance	t°C	Pressure range atmos	Percent change in volume
CCl_4	50°	0–1000	8
CS_2	50°	0–1000	8
n-pentane	50°	0–1000	14
isopentane	50°	0–1000	14
n-hexane	50°	0–1000	11
n-octane	50°	0–1000	9
n-octane	95°	0–1000	13
CCl_4	95°	1000–3000	8.5
CS_2	80°	1000–3000	8.4
n-pentane	95°	1000–3000	11.2
isopentane	95°	1000–3000	11.2
n-heptane	95°	1000–3000	9.8
2,3 dimethylbutane	95°	1000–3000	10.2

[9] P. W. Bridgman, Proc. Natl. Acad. Sci. U. S. **11**, 603 (1925). Proc. Am. Acad. Arts Sci. **61**, 57–99 (1926). *Physics of High Pressure* (G. Bell and Sons, London, England, 1931), p. 352.

DISCUSSION

If the equations relating surface tension and energy of vaporization are valid at temperatures other than the boiling point at one atmosphere pressure, then,

$\Delta E_{vap}=\sigma A+\frac{1}{2}RT$ for inert gases,

$\Delta E_{vap}=\sigma A+\frac{1}{2}RT+1.212RT^{1.2}$ for normal fluorocarbons,

$\Delta E_{vap}=\sigma A+1.212RT^{1.2}$ for normal hydrocarbons.

It is to be expected that shape would contribute to the surface effects, particularly for hydrocarbons. Deviations from the simple equation may provide a parameter for shape and structure features.

The equations for the energy of activation of viscosity, $\Delta E_{vis}=1.212RT_b^{1.2}$, for inert gases and normal fluorocarbons, and $\Delta E_{vis}=1.212RT_b^{1.2}-1000$ for normal hydrocarbons contain a temperature related to the corresponding states of the different substances. These equations must show considerable deviation for shape and structure features, and a study of deviations from these simple laws may provide interesting parameters for these features. For the normal fluorocarbons a combination equation,

$$\Delta E_{vap}=\sigma_b A_b+\tfrac{1}{2}RT_b+\Delta E_{vis}, \tag{7}$$

valid at the normal boiling point, is interesting in that it relates properties of vaporization, surface tension, and viscosity in one equation. A similar equation for the normal hydrocarbons follows,

$$\Delta E_{vap}=\sigma_b A_b+\tfrac{1}{2}RT_b+\Delta E_{vis}-1000. \tag{8}$$

The authors wish to acknowledge the express appreciation for the sponsorship of part of this work by the Minnesota Mining and Manufacturing Company.

THE JOURNAL OF CHEMICAL PHYSICS VOLUME 23, NUMBER 4 APRIL, 1955

Molecular Clusters in Imperfect Gases

TERRELL L. HILL
Naval Medical Research Institute, Bethesda, Maryland
(Received November 30, 1953)

An exact, formal method for calculating the number of physical (as contrasted with Mayer's mathematical) clusters in an imperfect monatomic gas is developed. However, although the equations are exact, the definition of a physical cluster is somewhat arbitrary. This arbitrariness does not affect any of the purely thermodynamic properties of the gas. A particular pair-wise definition of physical clusters is discussed in some detail and compared with Mayer's pair-wise definition of mathematical clusters.

INTRODUCTION

CONSIDER a one-component, classical, monatomic gas with grand partition function[1]

$$\Xi=\sum_{N\geqslant 0}\mathfrak{z}^N Q_N, \tag{1}$$

where $\mathfrak{z}$ is the absolute activity

$$\mathfrak{z}=e^{\mu/kT}, \tag{2}$$

and

$$Q_N=Z_N/N!\Lambda^N, \tag{3}$$

$$Z_N=\int_V \exp(-U_N/kT)d\mathbf{r}_1 d\mathbf{r}_2\cdots d\mathbf{r}_N, \tag{4}$$

$$1/\Lambda=(2\pi mkT/h^2)^{\frac{1}{2}}, \tag{5}$$

$$d\mathbf{r}_i=dx_i dy_i dz_i.$$

The potential energy function U_N contains all the intermolecular forces of the system. Thus, if physical clusters between pairs, triplets, etc. of molecules are present in the gas because of strong attractive intermolecular forces, their existence and their influence on all thermodynamic properties are automatically taken care of without ever introducing them explicitly. For example, in Mayer's rigorous theory of gas condensation,[2] physical clusters are not discussed. On the other hand, it is illuminating as well as of practical interest (e.g., in the nonequilibrium problem of nucleation) to adopt an alternative but necessarily equivalent approach to imperfect gas theory in which physical clusters appear explicitly rather than only implicitly. This has been done in an approximate way by Frenkel[3] and Band.[4] Also, the subject has been revived recently by Reed,[5] Wooley,[6] and Kilpatrick.[7] The purpose of the

[1] See, for example, G. S. Rushbrooke, *Introduction to Statistical Mechanics* (Oxford University Press, London, 1949).

[2] J. E. Mayer and M. G. Mayer, *Statistical Mechanics* (John Wiley and Sons, Inc., New York, 1940). Mayer discusses "clusters" and "cluster integrals," but these have mathematical rather than physical significance (see following).

[3] J. Frankel, J. Chem. Phys. **7**, 200 (1939).

[4] W. Band, J. Chem. Phys. **7**, 324, 927 (1939). See also J. E. Mayer and S. F. Streeter, J. Chem. Phys. **7**, 1019 (1939).

[5] S. G. Reed, Jr., J. Chem. Phys. **20**, 208 (1952).

[6] H. W. Wooley, J. Chem. Phys. **21**, 236 (1953).

[7] J. E. Kilpatrick, J. Chem. Phys. **21**, 274, 1366 (1953).

present paper is to show how real (i.e., physical rather than mathematical) clusters can be treated in an exact way.

FORMAL RELATIONS

Whereas Eq. (1) forms the basis of an implicit treatment of cluster formation, from the alternative explicit point of view, we consider that the gas is made up of many different species, clusters of one, two, three, etc., molecules. Let ζ_s be the absolute activity of an s cluster and N_s the number of s clusters. Then we have also[1]

$$\Xi=\sum_{\mathbf{N}\geqslant 0}\left(\prod_s \zeta_s^{N_s}\right)Q_{\mathbf{N}}, \tag{6}$$

where $Q_{\mathbf{N}}$ is the partition function for a set of clusters $\mathbf{N}=N_1, N_2, \cdots$. However, the clusters are in equilibrium with each other so that

$$\begin{aligned}\mu_s&=s\mu_1\\ \zeta_s&=\zeta_1^{\,s}\end{aligned}\qquad s=1,2,\cdots. \tag{7}$$

(We must emphasize at this point that the zero of energy for interactions between the single molecules of clusters of all sizes is taken at infinite separation of the single molecules.) Equation (6) becomes, then,

$$\Xi=\sum_{\mathbf{N}\geqslant 0}\zeta_1^{\sum_s sN_s}Q_{\mathbf{N}}. \tag{8}$$

Now Eqs. (1) (clusters implicit) and (8) (clusters explicit) refer to the same system and so must be identical. We establish the detailed correspondence by first noting the limiting forms as ζ and ζ_1 approach zero

$$\begin{aligned}\Xi&=1+\zeta Q_1+\cdots\\ &=1+\zeta_1 Q_{1000\ldots}+\cdots.\end{aligned} \tag{9}$$

Q_1 and $Q_{1000\ldots}$ are the same quantity, the partition function of a single molecule in the volume V at T, hence $\zeta=\zeta_1$. Therefore the partition functions in Eqs. (1) and (8) must be related by

$$Q_N=Z_N/N!\Lambda^N=\sum_{\mathbf{N}}Q_{\mathbf{N}}, \tag{10}$$

where the sum is over all cluster sets $\mathbf{N}$ such that

$$\sum_{s=1}^{N} sN_s=N.$$

For example,

$$Q_1=Q_{1000\ldots}=V/\Lambda \tag{11a}$$

$$Q_2=Q_{2000\ldots}+Q_{0100\ldots} \tag{11b}$$

$$Q_3=Q_{3000\ldots}+Q_{1100\ldots}+Q_{00100\ldots} \tag{11c}$$

$$Q_4=Q_{4000\ldots}+Q_{2100\ldots}+Q_{0200\ldots}+Q_{10100\ldots}+Q_{00010\ldots}. \tag{11d}$$

The equilibrium number of s clusters is obtained by applying[1]

$$\bar{N}_s=\zeta_s\frac{\partial \ln\Xi}{\partial\zeta_s} \tag{12}$$

to Eq. (6); after the differentiation, we set $\zeta_s=\zeta^s$. This gives

$$\begin{aligned}\bar{N}_1&=\zeta Q_{100}+\zeta^2(2Q_{200}-Q_{100}^2)+\zeta^3(Q_{110}+3Q_{300}\\ &\qquad -Q_{100}Q_{010}-3Q_{100}Q_{200}+Q_{100}^3)+\cdots\\ \bar{N}_2&=\zeta^2 Q_{010}+\zeta^3(Q_{110}-Q_{100}Q_{010})+\cdots\\ &\vdots\\ \bar{N}_n&=\zeta^n Q_{00\ldots1}+\zeta^{n+1}(Q_{10\ldots1}-Q_{100}Q_{00\ldots1})+\cdots\\ &\vdots\end{aligned} \tag{13}$$

From the nature of Eqs. (6) and (12) (all $Q_{\mathbf{N}}$'s positive), the numbers $\bar{N}_1, \bar{N}_2, \cdots$ are necessarily all positive (unlike the numbers of Mayer's "mathematical clusters"—see following).

Equations (13) lead to the following "equilibrium quotients:"

$$\frac{\bar{N}_1^{\,n}}{\bar{N}_n}=\frac{Q_{100\ldots}^{\,n}}{Q_{00\ldots1}}\left\{1+\zeta\left[\frac{2nQ_{200\ldots}}{Q_{100\ldots}}-(n-1)Q_{100\ldots}-\frac{Q_{100\ldots1}}{Q_{00\ldots1}}\right]+\cdots\right\}\qquad n=2,3,\cdots. \tag{14}$$

The terms other than the leading terms in Eqs. (13) and (14) correct for the interactions between clusters; these interactions cannot properly be neglected in a discussion of *physical* clusters.

We can easily replace the variable ζ in Eqs. (13) by

$$\rho=\bar{N}/V=(\bar{N}_1+2\bar{N}_2+3\bar{N}_3+\cdots)/V. \tag{15}$$

For this purpose we define $Y_{\mathbf{N}}$ by

$$Q_{\mathbf{N}}=Y_{\mathbf{N}}/N!\Lambda^N. \tag{16}$$

Then, Eqs. (11) hold also between the Z_N's and $Y_{\mathbf{N}}$'s

$$Z_1=Y_{100\ldots}=V \tag{17a}$$

$$Z_2=Y_{2000\ldots}+Y_{0100\ldots},\quad \text{etc.} \tag{17b}$$

We now put Eqs. (13) into Eq. (15), giving ρ as a power series in ζ. On inverting this series, we have (as found by Mayer[2])

$$\zeta/\Lambda=\rho-2b_2\rho^2+(8b_2^2-3b_3)\rho^3+\cdots \tag{18}$$

$$2!Z_1b_2=Z_2-Z_1^2 \tag{19a}$$

$$3!Z_1b_3=Z_3-3Z_1Z_2+2Z_1^3,\quad \text{etc.} \tag{19b}$$

Finally, substitution of Eqs. (17)–(19) for ζ in Eqs. (13)

gives, to terms in ρ^3,

$$\rho_1=\bar{N}_1/V=\rho-\frac{Y_{010}}{Y_{100}}\rho^2+\left[2\frac{Y_{010}^2}{Y_{100}^2}-\frac{Y_{001}}{2Y_{100}}+\left(-\frac{1}{3}\frac{Y_{110}}{Y_{100}}-Y_{010}+2\frac{Y_{200}Y_{010}}{Y_{100}^2}\right)\right]\rho^3+\cdots \quad (20a)$$

$$\rho_2=-\frac{1}{2}\frac{Y_{010}}{Y_{100}}\rho^2+\left[-\frac{Y_{010}^2}{Y_{100}^2}+\left(-\frac{Y_{200}Y_{010}}{Y_{100}^2}+\frac{1}{2}Y_{010}+\frac{1}{6}\frac{Y_{110}}{Y_{100}}\right)\right]\rho^3+\cdots \quad (20b)$$

$$\rho_3=-\frac{1}{6}\frac{Y_{001}}{Y_{100}}\rho^3+\cdots. \quad (20c)$$

If, in the procedure just outlined [Eqs. (15)–(20)], only the first terms on the right-hand side of Eqs. (13) are used, the terms enclosed in parentheses are missing from Eqs. (20).

In conclusion, we want to stress that the equations of this section are formal but exact. With appropriate changes in definitions, these equations are valid for (1) polyatomic gases, (2) in quantum as well as in classical mechanics, and (3) for a solute in a solution (McMillan-Mayer solution theory).

DEFINITION OF A CLUSTER

It was not necessary above to define just what was meant by an s cluster, but we now turn to this point. The first conclusion one comes to is that for thermodynamic purposes the definition of a cluster is arbitrary. Equations (11) are the crux of the matter. In the absence of approximations, any definition will lead to the same thermodynamic predictions (e.g., virial coefficients) provided only that the definition specifies (1) how to divide the phase space of two molecules into two regions [Eq. (11b)], one region corresponding to $N_1=2$, $N_2=0$ and the other to $N_1=0$, $N_2=1$; (2) how to divide the phase space of three molecules into three regions, corresponding to $N_1=3$, $N_2=N_3=0$, or $N_1=N_2=1$, $N_3=0$, or $N_1=N_2=0$, $N_3=1$; etc. That is, the definition must give the recipe for assigning any particular element of volume in the phase space of N molecules to a subphase space corresponding to a particular cluster set $\mathbf{N}$. The equations of the preceding section will be applicable to any such definition. Of course the numbers $\bar{N}_1$, $\bar{N}_2$, etc. will in general be different for different definitions, but these are not measurable thermodynamic quantities.

A cluster is, however, a fairly definite physical concept (say, in nucleation theory) so that all physically reasonable definitions should lead to rather similar predictions of $\bar{N}_1$, $\bar{N}_2$, etc. In general, the stronger the forces leading to cluster formation, the greater the tendency of different reasonable definitions to converge on the same predictions.

In the special case of two monatomic molecules, there is a rather obvious single choice of a recipe for dividing Q_2 into two parts, Q_{20} and Q_{01}. Namely, when the two molecules are in an element of phase space such that the relative kinetic energy of the molecules exceeds the negative of the potential energy of interaction, then the two molecules are not "bound" to each other and the element belongs to Q_{20}. Otherwise, the molecules are "bound" and the element belongs to Q_{01}. Q_2, in this case,[2] is

$$Q_2=\frac{1}{2h^6}\int e^{-H/kT}\times dxdydzd\theta d\varphi drdp_xdp_ydp_zdp_\theta dp_\varphi dp_r, \quad (21)$$

$$H=\frac{1}{4m}(p_x^2+p_y^2+p_z^2)+\frac{1}{mr^2}\left(p_\theta^2+\frac{p_\varphi^2}{\sin^2\theta}\right)+\frac{p_r^2}{m}+u(r), \quad (22)$$

where x, y, and z refer to the center of mass, θ, φ, and r are the usual relative coordinates, and $u(r)$ is the intermolecular potential. The changes of variables

$$P_\theta=\frac{p_\theta}{(mr^2kT)^{\frac{1}{2}}}$$

$$P_\varphi=\frac{p_\varphi}{(mr^2kT\sin^2\theta)^{\frac{1}{2}}}$$

$$P_r=\frac{p_r}{(mkT)^{\frac{1}{2}}}$$

followed by integration over x, y, z, φ, θ, p_x, p_y, and p_z give

$$Q_2=\frac{V}{2\Lambda^2\pi^{\frac{1}{2}}}\int\exp[-u(r)/kT]4\pi r^2dr\times\int\exp[-(P_\theta^2+P_\varphi^2+P_r^2)]dP_\theta dP_\varphi dP_r \quad (23a)$$

$$=\frac{V}{2\Lambda^2}\int_V\exp[-u(r)/kT]4\pi r^2dr. \quad (23b)$$

According to Eq. (22), the condition for a bound pair is

$$P_\theta^2+P_\varphi^2+P_r^2\leqslant -u(r)/kT, \quad (24)$$

so Q_{01} is obtained by confining the integration over P_θ, P_φ, and P_r in Eq. (23a), for each r with negative $u(r)$, to the region satisfying Eq. (24). Contributions to Q_{20} come from values of r such that $u(r)>0$ or when $u(r)\leqslant 0$, but Eq. (24) is not satisfied.

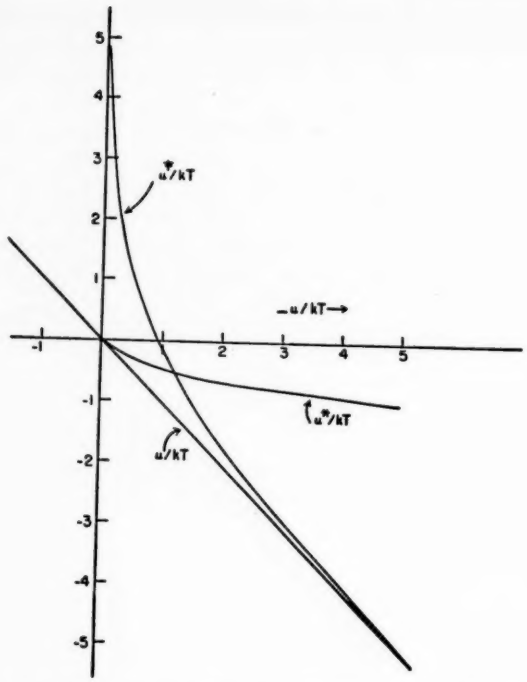

FIG. 1. Effective intermolecular potentials of bound (‡) and unbound (*) pairs.

Define $F(r)$ by

$$F(r)=\frac{1}{\pi^{\frac{3}{2}}}\int_{\text{Eq. (24)}}\exp[-(P_\theta^2+P_\varphi^2+P_r^2)]dP_\theta dP_\varphi dP_r$$

$$=\frac{4}{\pi^{\frac{1}{2}}}\int_0^{[-u(r)/kT]^{\frac{1}{2}}}e^{-R^2}R^2dR$$

$$=\frac{2}{\pi^{\frac{1}{2}}}\int_0^{-u(r)/kT}e^{-y}y^{\frac{1}{2}}dy=\frac{\Gamma[\frac{3}{2},(-u(r)/kT)]}{\Gamma(\frac{3}{2})}, \quad (25)$$

where $\Gamma(n,x)$ is the incomplete Γ function. Then we have, finally,

$$Q_{01}=\frac{V}{2\Lambda^2}\int_{u(r)\leqq 0}\exp[-u(r)/kT]4\pi r^2F(r)dr \quad (26a)$$

$$Q_{20}=\frac{V}{2\Lambda^2}\left\{\int_{u(r)>0}\exp[-u(r)/kT]4\pi r^2dr\right.$$

$$\left.+\int_{V,\,u(r)\leqq 0}\exp[-u(r)/kT]4\pi r^2\times[1-F(r)]dr\right\}. \quad (26b)$$

Q_{01} is the partition function of a pair of bound molecules, while Q_{20} is the partition function of a pair of molecules which are not bound. It is rather illuminating to rewrite Eqs. (26) as complete configuration integrals but using equivalent effective intermolecular potentials to distinguish the cases where the two molecules are bound or not bound. That is [compare Eq. (23b)],

$$Q_{01}=\frac{V}{2\Lambda^2}\int_V\exp[-u^\ddagger(r)/kT]4\pi r^2dr; \quad (27a)$$

$$Q_{20}=\frac{V}{2\Lambda^2}\int_V\exp[-u^*(r)/kT]4\pi r^2dr, \quad (27b)$$

where the effective potential between bound molecules is, from Eqs. (26a) and (27a),

$$\begin{aligned}u^\ddagger(r)&=+\infty \quad u(r)>0\\&=u(r)-kT\ln F(r) \quad u(r)\leqq 0\end{aligned} \quad (28a)$$

and the effective potential between unbound molecules is

$$\begin{aligned}u^*(r)&=u(r) \quad u(r)>0\\&=u(r)-kT\ln[1-F(r)] \quad u(r)\leqq 0.\end{aligned} \quad (28b)$$

The Lennard-Jones potential

$$u(r)=4\epsilon[(r_0/r)^{12}-(r_0/r)^6] \quad (29)$$

may be used to illustrate Eqs. (28). Figure 1 gives $u^\ddagger/kT$ and u^*/kT as functions of $-u/kT$, while Figs. 2 and 3 show u/kT, $u^\ddagger/kT$ and u^*/kT as functions of r for $\epsilon/kT=2$ and 5, using Eq. (29). As an aid in interpreting the figures, we note, from the properties of $\Gamma(n,x)$, that the asymptotic behavior of $u^\ddagger$ and u^* is

$$\left.\begin{aligned}&u^\ddagger/kT\to-\tfrac{3}{2}\ln(-u/kT)\to+\infty\\&u^*/kT\to u/kT\end{aligned}\right\}\text{ as } -u/kT\to 0+ \quad (30a)$$

$$\left.\begin{aligned}&u^\ddagger/kT\to u/kT\\&u^*/kT\to-\tfrac{1}{2}\ln(-u/kT)\end{aligned}\right\}\text{ as } -u/kT\to+\infty. \quad (30b)$$

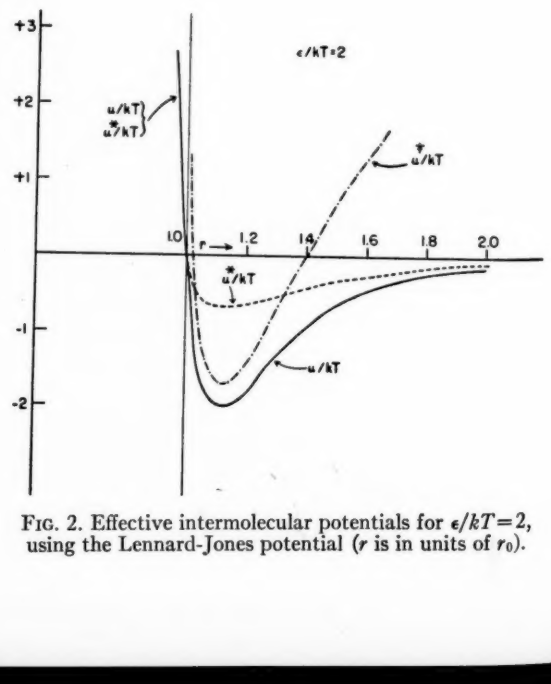

FIG. 2. Effective intermolecular potentials for $\epsilon/kT=2$, using the Lennard-Jones potential (r is in units of r_0).

When ϵ/kT is very large (strong binding), $u^{\ddagger}$ is indistinguishable from u in the region of the minimum in u and rises to infinity on both sides of the minimum, while u^* is indistinguishable from u for large r, has a relatively shallow minimum ($u^*/u^{\ddagger}\to 0$ as $-u/kT\to\infty$) where u has a minimum, and is equal to u (rises to $+\infty$) for small r. As a first approximation, in the absence of long range forces [where the long tail $u^*=u(r)$ for large r cannot be neglected], the interaction u^* between nonbinding molecules could be considered a hard sphere interaction; the explicit introduction of pairs substantially takes care of the strong attractive interaction. This justifies Band's[4] approximate hard sphere correction.

Of the various possible definitions of clusters of three and more monatomic molecules, one stands out as being especially simple and this is the only one we discuss. To introduce this definition, we consider first $N=2$:

$$Z_2=\int \exp(-u_{12}/kT)d\mathbf{r}_1d\mathbf{r}_2, \tag{31}$$

where $u_{12}=u(r_{12})$. Now we use Eqs. (28) to write

$$\exp(-u_{12}/kT)=\exp(-u_{12}^{\ddagger}/kT)+\exp(-u_{12}^*/kT) \tag{32}$$

and substitute Eq. (32) into Eq. (31). If this result is put in Eq. (10) for Z_2, we obtain the assignment of Q_{01} and Q_{20} already made in Eq. (27). Proceeding now to higher clusters, for $N=3$ we introduce Eq. (32) for each pair interaction, so that

$$\begin{aligned}\frac{Z_3}{3\,!\Lambda^3}&=\frac{1}{3\,!\Lambda^3}\int \exp[-(u_{12}+u_{13}+u_{23})/kT]d\mathbf{r}_1d\mathbf{r}_2d\mathbf{r}_3\\
&=\frac{1}{3\,!\Lambda^3}\int[\exp(-u_{12}^{\ddagger}/kT)+\exp(-u_{12}^*/kT)]\\
&\quad\times[\exp(-u_{13}^{\ddagger}/kT)+\exp(-u_{13}^*/kT)]\\
&\quad\times[\exp(-u_{23}^{\ddagger}/kT)+\exp(-u_{23}^*)/kT)]\\
&\qquad\qquad\times d\mathbf{r}_1d\mathbf{r}_2d\mathbf{r}_3 \qquad (33)\\
&=Q_{3000\ldots}+Q_{1100\ldots}+Q_{00100\ldots},\end{aligned}$$

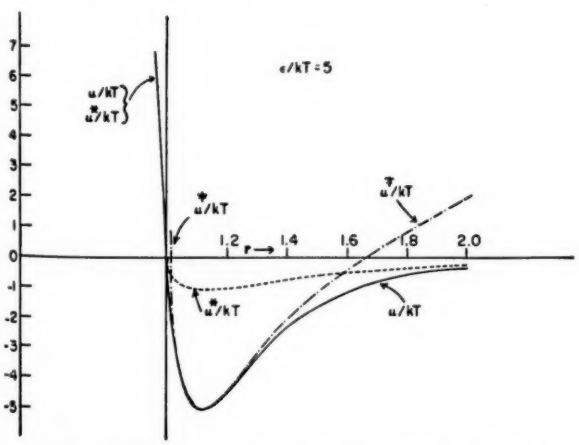

FIG. 3. Effective intermolecular potentials for $\epsilon/kT=5$, using the Lennard-Jones potential (r is in units of r_0).

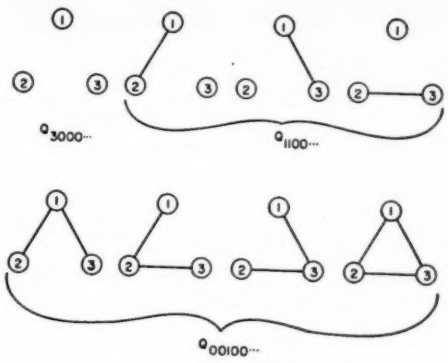

FIG. 4. Clusters of three molecules.

where

$$Q_{3000\ldots}=\frac{1}{3\,!\Lambda^3}\int \exp[-(u_{12}^*+u_{13}^*+u_{23}^*)/kT]\times d\mathbf{r}_1d\mathbf{r}_2d\mathbf{r}_3; \tag{34a}$$

$$Q_{1100\ldots}=\frac{3}{3\,!\Lambda^3}\int \exp[-(u_{12}^{\ddagger}+u_{13}^*+u_{23}^*)/kT]\times d\mathbf{r}_1d\mathbf{r}_2d\mathbf{r}_3; \tag{34b}$$

$$\begin{aligned}Q_{00100\ldots}=&\frac{3}{3\,!\Lambda^3}\int \exp[-(u_{12}^{\ddagger}+u_{13}^{\ddagger}+u_{23}^*)/kT]\\
&\times d\mathbf{r}_1d\mathbf{r}_2d\mathbf{r}_3+\frac{1}{3\,!\Lambda^3}\int \exp[-(u_{12}^{\ddagger}+u_{13}^{\ddagger}\\
&+u_{23}^{\ddagger})/kT]d\mathbf{r}_1d\mathbf{r}_2d\mathbf{r}_3. \qquad (34c)\end{aligned}$$

Equation (34) corresponds to the diagram shown in Fig. 4, where a line between two molecules represents a "bound" interaction (‡) and the absence of a line indicates a "nonbound" interaction (*). Thus, the three molecules form a 3 cluster, by the present definition, if they are all at least singly connected to each other by "bound" pair-wise interactions. For $N=4$, we obtain Fig. 5.

This scheme can obviously be extended to arbitrary N, and it is clearly analogous to Mayer's (pair-wise, mathematical) cluster expansion of Z_N. Whereas we put, for each pair,

$$\exp(-u_{ij}/kT)=\exp(-u_{ij}^{\ddagger}/kT)+\exp(-u_{ij}^*/kT), \tag{35a}$$

Mayer uses ↕ ↕

$$\exp(-u_{ij}/kT)=[\exp(-u_{ij}/kT)-1]+\ 1. \tag{35b}$$

Mayer's treatment is eventually simplified, however, because of the fact that unity in Eq. (35b) is independent of r_{ij}, whereas in our case $\exp(-u_{ij}^*/kT)$ in Eq. (35a) depends on r_{ij}. On the other hand, our clusters have some physical significance, whereas Mayer's are introduced for mathematical convenience only.

Mayer's procedure amounts formally to defining $u^{\ddagger}$ and u^* not by Eqs. (28) but by

$$u^{\ddagger}=-kT\ln[\exp(-u/kT)-1]; \tag{36a}$$

$$u^*=0. \tag{36b}$$

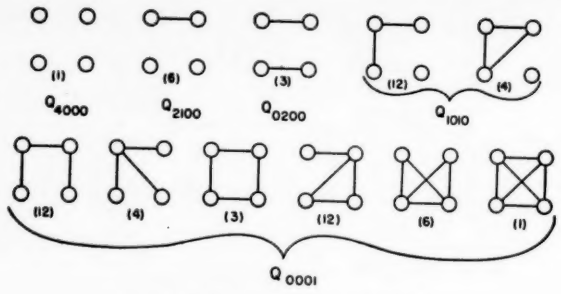

FIG. 5. Clusters of four molecules.

Since [ ] in Eqs. (35b) and (36a) can be negative, we have the possibility of complex values of $u^{\ddagger}$ and negative values of the Q_N's [Eqs. (11)] and $\bar{N}_i$'s [Eqs. (13)]. Also, in view of Eq. (36b), molecules in different (mathematical) clusters do not interact and the gas can be considered a perfect gas mixture of (mathematical) clusters—which is not the case with physical clusters or with any pair-wise definition of clusters except Mayer's [Eqs. (35b) and (36b)]. A consequence of this is that, with Mayer's clusters, all terms but the leading terms on the right-hand side of Eqs. (13) drop out.

As a simple example of an error arising from the treatment of an imperfect gas as a perfect gas mixture of physical clusters, consider the second virial coefficient B_2. From Mayer's work [or from Eqs. (1), (18), and $pV=kT\ln\Xi$], we know that

$$B_2=-b_2=(Y_{100}^2-Y_{200}-Y_{010})/2Y_{100}, \tag{37}$$

whereas if we use, incorrectly,

$$p/kT=\rho_1+\rho_2+\cdots, \tag{38}$$

we find from Eq. (20) that

$$\frac{p}{kT}=\rho-\frac{1}{2}\frac{Y_{010}}{Y_{100}}\rho^2+\cdots, \tag{39}$$

or

$$B_2=-Y_{010}/2Y_{100}. \tag{40}$$

Equation (40) is correct in general only if two unbound molecules do not interact ($Y_{200}=Y_{100}^2$), as in Eq. (36b) (Mayer).

The foregoing definition [Eqs. (28)] of a cluster in terms of pair-wise bound interactions is formally simple and is interesting because of the analogy to Mayer's theory. For molecules with very strong attractive interactions [e.g., when ϵ/kT in Eq. (29) is large], this definition is physically satisfactory for clusters of any size. However, if the interactions are weak, the present definition would exclude from a cluster a molecule which is not "bound" to any of the other molecules of the cluster taken singly, yet which would ordinarily be considered bound to the entire cluster because of the accumulation of attractive interactions with a number of molecules of the cluster.

It should be mentioned that, if one wishes to use an alternative pair-wise definition of physical clusters based simply on a "bound" interaction for $r<r'$ (where r' is some arbitrary but fixed intermolecular distance) and a "nonbound" interaction for $r>r'$, then the appropriate effective potentials are clearly

$$\begin{aligned} u^{\ddagger}&=u & r&<r' \\ &=+\infty & r&>r' \\ u^{*}&=+\infty & r&<r' \\ &=u & r&>r'. \end{aligned} \tag{41}$$

Equation (41) should be especially useful to avoid complications when considering clusters of polyatomic molecules.

The general approach of this paper is also applicable to cluster formation in polyatomic gases and to the equilibrium binding of one type of molecule on another. These aspects of the problem will be included in another paper concerned with the binding of ions and molecules on protein molecules in solution.[8] This method may also prove useful in treating clusters of ions in electrolyte-solution theory.

[8] T. L. Hill, J. Chem. Phys. (this issue).

Theory of Protein Solutions. I*†

TERRELL L. HILL
Naval Medical Research Institute, Bethesda, Maryland
(Received November 30, 1953)

A summary of a few results of the McMillan-Mayer solution theory is given in Sec. II, in order to have available necessary equations in a form required in later sections. It is pointed out in Sec. III that binding equilibria in a solution can in principle be discussed equally rigorously either implicitly or explicitly. The definition of "binding" in an explicit formulation is, strictly speaking, somewhat arbitrary but the arbitrariness disappears for practical purposes if the binding forces are very strong. However, the purely thermodynamic results are rigorously independent of the exact definition used. With the aid of Secs. II and III, it is possible to formulate in Sec. IV a general theory of protein solutions, including the effect of binding of ions or molecules on protein molecules. The discussion here is restricted to a single protein species and a single type of molecule capable of being bound, but the generalization to any number of protein or bound species is easy and will be published later. The topics discussed are osmotic pressure virial expansion, number of bound molecules per protein molecule expanded in powers of the protein concentration, distribution functions for sets of protein molecules (including the radial distribution function), potentials of average force on sets of protein molecules, superposition approximation in relation to the osmotic pressure and the Born-Green-Yvon integrodifferential equation for the distribution functions, and, finally, the relation to the recent Kirkwood—Shumaker theory. The theory applies equally well to polyelectrolyte, colloidal, and other solutions, but the "protein" language is used throughout for definiteness.

I. INTRODUCTION

IN 1945 McMillan and Mayer[1] published their very elegant general theory of solutions. The theory applies to any type of solution[2] and, in its quantum mechanical form, is formally exact if the forces between molecules of the solution are assumed known and if one accepts the general principles of quantum and statistical mechanics. The theory can be cast, in a very natural way, into the unsymmetrical form necessary if one wishes to distinguish "solutes" from "solvents" and to discuss properties such as the osmotic pressure (solute species impermeable to a membrane). This unsymmetrical approach is obviously the one of interest in protein solution theory.

An alternative but equivalent theory of solutions has been developed recently by Kirkwood and Buff.[3]

The McMillan-Mayer theory has already been applied to solutions of polymers and certain other large molecules by Zimm[4] and by Onsager.[5]

The properties of protein solutions are included in the general equations of McMillan and Mayer. In particular, interactions of protein molecules with small molecules or ions (including "binding") are taken care of *implicitly* by the inclusion of the appropriate forces. However, the binding of ions (especially hydrogen ions) and molecules on protein molecules is such an important property of these solutions that it is desirable to modify the theory in such a way that the binding referred to above appears *explicitly*. This modification is the main object of the present paper. With the explicit introduction of binding into the equations, it becomes possible, as we shall see, to discuss the formal interconnections between binding on proteins (e.g., titration curves), osmotic pressure virial coefficients, forces between protein molecules, protein aggregation, protein distribution functions, etc.

To simplify an already sufficiently complicated notation, we shall restrict ourselves here to solutions containing only one protein species and one species of ion or molecule whose binding to the protein is considered explicitly. The more general case will be discussed in a later paper of the series.

The aggregation of protein molecules into pairs, triplets, etc., is taken care of *implicitly* through protein-protein forces. Alternatively, as above for binding, aggregation can be treated *explicitly* (see Sec. III), but this also will be reserved for a later publication.

Actually, the present paper is not restricted to protein solutions. The discussion is equally applicable to any solution containing molecules of, say, type A each of which can bind or combine with one or more molecules of type B. The treatment includes, therefore, the binding of hydrogen ions to polyelectrolytes, polybasic acids, amino acids, etc. The Kirkwood-Westheimer[6] theory, including the extension to molecules with internal rotation,[7,8] is based on a particular model which is con-

* The opinions expressed herein are those of the author and not necessarily those of the Navy Department.

† This paper was summarized at a Gordon Research Conference on Proteins and Nucleic Acids, New Hampton, New Hampshire, August 25, 1953. A preliminary note has been published in J. Chem. Phys. **21**, 1395, 2242 (1953). The present paper is the more general account, mentioned in the preliminary paper, originally scheduled to be published in Ann. N. Y. Acad. Sci.

[1] W. G. McMillan and J. E. Mayer, J. Chem. Phys. **13**, 276 (1945).

[2] Electrolyte solutions are mentioned explicitly by, for example, T. L. Hill in *Ion Transport Across Membranes* (Academic Press, New York, 1954), edited by H. T. Clarke.

[3] J. G. Kirkwood and F. P. Buff, J. Chem. Phys. **19**, 774 (1951).

[4] B. H. Zimm, J. Chem. Phys. **14**, 164 (1946).

[5] L. Onsager, Ann. N. Y. Acad. Sci. **51**, 627 (1949).

[6] J. G. Kirkwood and F. H. Westheimer, J. Chem. Phys. **6**, 506, 513 (1938).

[7] T. L. Hill, J. Chem. Phys. **11**, 545, 552 (1943); **12**, 56, 147 (1944).

[8] H. M. Peek and T. L. Hill, J. Am. Chem. Soc. **73**, 5304 (1951).

sistent with the more general formal equations of the present paper.

In Sec. II we shall introduce (without derivations) the notation and fundamental equations of the McMillan-Mayer solution theory in a form necessary for our later purposes. Section III is a digression which is necessary in order to make clear the implications of taking into account binding equilibria for the phase integrals which arise. Clusters in a polyatomic gas are also discussed in this connection. Section IV is devoted to the formal theory of protein solutions, including the binding of ions or molecules.

II. McMILLAN-MAYER SOLUTION THEORY

We present here the fundamental equations needed in the following sections.[9] McMillan and Mayer treat all degrees of freedom classically or all quantally. For practical purposes in solution theory, we make the useful approximation here, at the outset, of assuming that vibrational degrees of freedom are separable. While this approximation is not at all essential to the argument, it would presumably almost always be made in applications in the field of solution physical chemistry.

We begin by considering a *closed* system containing a set of molecules[10] $\mathbf{N}=N_1, N_2, \cdots N_\nu$; that is, N_1 molecules of species 1, etc. Each molecule has the usual three translational and zero, two or three "external" rotational degrees of freedom. The remaining degrees of freedom are classed either as vibrational or internal rotational. One of these degrees of freedom which is separable, to a sufficient approximation, is called "vibrational" and is (or, rather, may be) treated quantally; one which is not separable is called "internal rotational" and is treated classically. (The translational and external rotational degrees of freedom are also treated classically.) The internal rotational degrees of freedom include, in particular, angular coordinates associated with rotation about bonds. Internal rotation is, of course, important in polymers and proteins, and also in much simpler molecules.[7,8] Because of internal rotation, molecules can take on different configurations and shapes. These may have different potential energies owing to interactions between groups, charges, etc., on the same molecule, and this is taken into account below.

In a strictly formal way, we could carry a *completely* quantal argument through the whole paper. This would be rigorous but useless (for our purposes).

The partition function in the canonical ensemble is written as

$$Q_{\mathbf{N}}=\frac{\prod_{s=1}^{\nu} q_{sv}{}^{N_s}}{\prod_{s=1}^{\nu}(N_s!h^{f_sN_s})}\int \exp(-H_{\mathbf{N}}/kT) \times d\{\mathbf{N}\}_x d\{\mathbf{P}\}_x d''\{\mathbf{N}\}_\theta d\{\mathbf{P}\}_\theta, \quad (1)$$

where q_{sv} is the (separable) vibrational partition function of a molecule of species s, f_s is the number of translational and rotational (internal and external) degrees of freedom of an s molecule, $H_{\mathbf{N}}$ is the classical Hamiltonian function for translation and rotation, $\{\mathbf{N}\}_x$ refers to all the translational coordinates of the set $\mathbf{N}$, and $\{\mathbf{P}\}_x$ represents the conjugate momenta, while $\{\mathbf{N}\}_\theta$ and $\{\mathbf{P}\}_\theta$ have similar meanings for the rotational degrees of freedom. The double prime on d in Eq. (1) is introduced to distinguish the magnitude of this element of volume from the magnitudes of $d'\{\mathbf{N}\}_\theta$ and $d\{\mathbf{N}\}_\theta$ encountered below.

In q_{sv} the zero of energy is chosen at the bottom of the vibrational potential well. $H_{\mathbf{N}}$ includes the potential energy $U_{\mathbf{N}}$; the zero of potential energy for *inter*molecular interactions is chosen at infinite separation of all molecules, but the zero for *intra*molecular interactions is left arbitrary for each species (until Sec. III).

We now integrate over the momenta in Eq. (1), and obtain

$$Q_{\mathbf{N}}=\frac{\prod_s q_{sv}{}^{N_s}}{\prod_s (N_s!\Lambda_{sx}{}^{N_s}\Lambda_{s\theta}{}^{N_s})}\int \exp(-U_{\mathbf{N}}/kT) \times d\{\mathbf{N}\}_x d'\{\mathbf{N}\}_\theta, \quad (2)$$

where

$$\frac{1}{\Lambda_{sx}}=\left(\frac{2\pi m_s kT}{h^2}\right)^{\frac{1}{2}}. \quad (3)$$

The integration over $\{\mathbf{P}\}_\theta$ gives a constant $1/\prod_s \Lambda_{s\theta}{}^{N_s}$ and also, in general, a function of rotational coordinates which, together with $d''\{\mathbf{N}\}_\theta$, is included in $d'\{\mathbf{N}\}_\theta$. For example, in the familiar case of a single rigid diatomic molecule of species s, we have[11]

$$\frac{1}{\Lambda_{s\theta}}=\frac{2\pi I_s kT}{h^2}; \quad d''(i_s)_\theta=d\theta_{i_s}d\varphi_{i_s}; \quad d'(i_s)_\theta=\sin\theta_{i_s}d\theta_{i_s}d\varphi_{i_s},$$

where (i_s) is used to denote the coordinates of molecule i of species s. The symbolic subscript θ is, of course, not to be confused with the angle θ_{i_s}.

When N_s/V is very small for all s, we have a perfect gas mixture. $U_{\mathbf{N}}$ is then the sum of separate contributions from each molecule; these contributions arise from *intra*molecular interactions. We have in this case, from Eq. (2),

$$Q_{\mathbf{N}}=\frac{(\prod_s q_{sv}{}^{N_s})(\prod_s V^{N_s}\lambda_{s\theta}{}^{N_s})}{\prod_s (N_s!\Lambda_{sx}{}^{N_s}\Lambda_{s\theta}{}^{N_s})}, \quad (4)$$

[9] A rather detailed review, with derivations, of the McMillan-Mayer solution theory can be obtained by writing the Naval Medical Research Institute, Bethesda, Maryland, for Lecture and Review Series Report No. 54–2 by T. L. Hill. Equations in this report will be referred to here by R.

[10] The notation is that of McMillan and Mayer, except that we use Kirkwood's notation for distribution functions.

[11] See G. S. Rushbrooke, *Introduction to Statistical Mechanics* (Oxford University Press, London, 1949), p. 87.

where

$$\lambda_{s\theta}=\int \exp[-U_{i_s}((i_s)_\theta)/kT]d'(i_s)_\theta. \quad (5)$$

$U_{i_s}\equiv U_{N_s=1}$ is a function of the (internal) rotational coordinates of molecule i_s. For the rigid rotator above, $U_{i_s}=$ constant and

$$\lambda_{s\theta}=\exp(-U_{i_s}/kT)\int \sin\theta_{i_s}d\theta_{i_s}d\varphi_{i_s}$$
$$=4\pi\exp(-U_{i_s}/kT).$$

It is convenient to rewrite Eq. (2) in the form

$$Q_{\mathbf{N}}=Z_{\mathbf{N}}/\prod_s (N_s!\Lambda_s^{N_s}), \quad (6)$$

where

$$\frac{1}{\Lambda_s}=\frac{q_{sv}\lambda_{s\theta}}{\Lambda_{sx}\Lambda_{s\theta}} \quad (7)$$

and

$$Z_{\mathbf{N}}=\frac{1}{\prod_s \lambda_{s\theta}^{N_s}}\int \exp(-U_{\mathbf{N}}/kT)d\{\mathbf{N}\}_x d'\{\mathbf{N}\}_\theta. \quad (8)$$

Or if we define $d(i_s)_\theta$ and $d\{\mathbf{N}\}_\theta$ by the equations

$$\frac{d'\{\mathbf{N}\}_\theta}{\prod_s \lambda_{s\theta}^{N_s}}=\prod_s \frac{d'(1_s)_\theta}{\lambda_{s\theta}}\frac{d'(2_s)_\theta}{\lambda_{s\theta}}\cdots\frac{d'(N_s)_\theta}{\lambda_{s\theta}}$$
$$=\prod_s d(1_s)_\theta d(2_s)_\theta\cdots d(N_s)_\theta$$
$$=d\{\mathbf{N}\}_\theta, \quad (9)$$

then

$$Z_{\mathbf{N}}=\int \exp(-U_{\mathbf{N}}/kT)d\{\mathbf{N}\}, \quad (10)$$

where

$$d\{\mathbf{N}\}\equiv d\{\mathbf{N}\}_x d\{\mathbf{N}\}_\theta. \quad (11)$$

Thus $Z_{\mathbf{N}}$, the configuration integral, is normalized in such a way that

$$Z_{\mathbf{N}}=\prod_s V^{N_s} \quad (12)$$

for a perfect gas mixture.

Distribution Functions in an Open System

In an *open* system, the grand partition function is

$$\Xi=e^{pV/kT}=\sum_{\mathbf{N}\geq 0}\exp[(N_1\mu_1+\cdots+N_\nu\mu_\nu)/kT]Q_{\mathbf{N}} \quad (13a)$$

$$=\sum_{\mathbf{N}\geq 0}\left(\prod_s \frac{z_s^{N_s}}{N_s!}\right)Z_{\mathbf{N}} \quad (13b)$$

$$=\sum_{\mathbf{N}\geq 0}\left(\prod_s \frac{z_s^{N_s}}{N_s!}\right)\int \times\exp(-U_{\mathbf{N}}/kT)d\{\mathbf{N}\}, \quad (13c)$$

where we have used Eq. (6) and

$$z_s=\frac{\exp(\mu_s/kT)}{\Lambda_s}. \quad (14)$$

We shall call z_s the activity of the species s. As the gas becomes infinitely dilute, $z_s\to\rho_s(=\bar{N}_s/V)$.

The probability of the open system containing exactly the numbers of molecules $\mathbf{N}$ is

$$P_{\mathbf{N}}=\left(\prod_s \frac{z_s^{N_s}}{N_s!}\right)Z_{\mathbf{N}}/\Xi. \quad (15)$$

Let $\rho_{\mathbf{n}}(\{\mathbf{n}\},\mathbf{z})d\{\mathbf{n}\}$ be the probability of observing any n_1 molecules of species 1, $\cdots$, and any n_ν molecules of species ν in $d\{\mathbf{n}\}$ at $\{\mathbf{n}\}$, where $\mathbf{z}$ represents the activity set $z_1,\cdots z_\nu$. Then one can show [Eq. (R-25)] that the "distribution function" $\rho_{\mathbf{n}}$ has the property that

$$\frac{\exp(pV/kT)\rho_{\mathbf{n}}(\{\mathbf{n}\},\mathbf{z})}{\prod_s z_s^{n_s}}=\sum_{\mathbf{m}\geq 0}\left(\prod_s \frac{z_s^{m_s}}{m_s!}\right)\int \times\exp(-U_{\mathbf{m}+\mathbf{n}}/kT)d\{\mathbf{m}\}. \quad (16)$$

It would be preferable to write the $\mathbf{n}$ of $\rho_{\mathbf{n}}$ as a superscript in parentheses, following Kirkwood, but this is not generally practical for the printer. We therefore follow the rule that in all distribution functions and potentials of average force, boldface letters representing the set of molecules are written as subscripts, but when the set can be represented by a lightface letter it is written as a superscript in parentheses.

We define $g_{\mathbf{n}}(\{\mathbf{n}\},\mathbf{z})$ and $W_{\mathbf{n}}(\{\mathbf{n}\},\mathbf{z})$ in terms of $\rho_{\mathbf{n}}(\{\mathbf{n}\},\mathbf{z})$ by

$$g_{\mathbf{n}}=\exp(-W_{\mathbf{n}}/kT)=\frac{\rho_{\mathbf{n}}}{\prod_s \rho_s^{n_s}}. \quad (17)$$

If each member of this equation is integrated over $\{\mathbf{n}\}_\theta$, we obtain

$$g_{\mathbf{n}x}(\{\mathbf{n}\}_x)=\exp[-W_{\mathbf{n}x}(\{\mathbf{n}\}_x)/kT]=\frac{\rho_{\mathbf{n}x}(\{\mathbf{n}\}_x)}{\prod_s \rho_s^{n_s}}, \quad (18)$$

where these functions are called "spatial" functions. That is,

$$g_{\mathbf{n}x}(\{\mathbf{n}\}_x)=\int g_{\mathbf{n}}(\{\mathbf{n}\})d\{\mathbf{n}\}_\theta, \quad (19)$$

etc. The special case $g_x^{(2)}$ is the well-known radial distribution function.

It is easy to prove [Eq. (R-42)] that $W_{\mathbf{n}}$ has the physical significance of a potential of the average force acting on the set $\mathbf{n}$. That is, let $q_{\mathbf{n}}$ represent an arbitrary coordinate associated with one of the molecules of the set $\mathbf{n}$. When there are $\mathbf{N}$ molecules in the system in the configuragion $\{\mathbf{N}\}$, including the set $\mathbf{n}$ in the configuration $\{\mathbf{n}\}$, the component of force along $q_{\mathbf{n}}$ is $-\partial U_{\mathbf{N}}/\partial q_{\mathbf{n}}$. $W_{\mathbf{n}}$ then satisfies

$$-\partial W_{\mathbf{n}}/\partial q_{\mathbf{n}}=\langle-\partial U_{\mathbf{N}}/\partial q_{\mathbf{n}}\rangle_{Av}, \quad (20)$$

where the force is averaged properly over all configurations of the $\mathbf{N}-\mathbf{n}$ molecules not in the set $\mathbf{n}$, for a given $\mathbf{N}$, and also over all $\mathbf{N}\geqslant\mathbf{n}$. Incidentally, $W_{\mathbf{n}}\rightarrow U_{\mathbf{n}}$ as the gas becomes infinitely dilute.

Osmotic Pressure

Equations (13c), (15), and (16) summarize the important properties (for our purposes) of a multicomponent gas in terms of integrals over $\exp(-U_{\mathbf{N}}/kT)$. McMillan and Mayer proved, without approximation, that completely analogous equations hold in an osmotic system.

Suppose we have a membrane permeable to "solvent" species (subscript τ) but not to "solute" species (subscript σ). On one side of the membrane we have a solution containing solvent species only. Let the value of each z_τ in this solution be denoted by z_τ^*, while each $z_\sigma=\rho_\sigma=0$. We summarize this activity set by $\mathbf{z}_\tau^*$, $\mathbf{0}_\sigma$. The solution on the other side of the membrane contains both solute and solvent species and is in equilibrium with the first solution with respect to each solvent species. The second activity set is $\mathbf{z}_\tau^*$, $\mathbf{z}_\sigma$, since each z_τ must have the same value, namely z_τ^*, in the two solutions. The pressure difference across the membrane is by definition just the osmotic pressure

$$\Pi=p(\mathbf{z}_\tau^*,\mathbf{z}_\sigma)-p(\mathbf{z}_\tau^*,\mathbf{0}_\sigma). \tag{21}$$

The analog of Eq. (13c) is [see Eq. (R-49)],

$$\exp(\Pi V/kT)=\sum_{\mathbf{m}_\sigma\geq\mathbf{0}}\left[\prod_\sigma\frac{(z_\sigma/\gamma_\sigma^{\,0})^{m_\sigma}}{m_\sigma!}\right]\times\int\exp[-W_{\mathbf{m}_\sigma}(\{\mathbf{m}_\sigma\},\mathbf{z}_\tau^*,\mathbf{0}_\sigma)/kT]\times d\{\mathbf{m}_\sigma\} \tag{22}$$

and of Eq. (15) [see Eq. (R-55)],

$$\mathfrak{P}_{\mathbf{m}_\sigma}=\left\{\left[\prod_\sigma\frac{(z_\sigma/\gamma_\sigma^{\,0})^{m_\sigma}}{m_\sigma!}\right]\times\int\exp[-W_{\mathbf{m}_\sigma}(\{\mathbf{m}_\sigma\},\mathbf{z}_\tau^*,\mathbf{0}_\sigma)/kT]\times d\{\mathbf{m}_\sigma\}\right\}\Big/\exp(\Pi V/kT), \tag{23}$$

and, finally, of Eq. (16) [see Eq. (R-52)],

$$\frac{\exp(\Pi V/kT)\rho_{\mathbf{n}_\sigma}(\{\mathbf{n}_\sigma\},\mathbf{z}_\tau^*,\mathbf{z}_\sigma)}{\prod_\sigma(z_\sigma/\gamma_\sigma^{\,0})^{n_\sigma}}=\sum_{\mathbf{m}_\sigma\geq\mathbf{0}}\left[\prod_\sigma\frac{(z_\sigma/\gamma_\sigma^{\,0})^{m_\sigma}}{m_\sigma!}\right]\times\int\exp[-W_{\mathbf{n}_\sigma+\mathbf{m}_\sigma}(\{\mathbf{n}_\sigma+\mathbf{m}_\sigma\},\mathbf{z}_\tau^*,\mathbf{0}_\sigma)/kT]\times d\{\mathbf{m}_\sigma\}, \tag{24}$$

where $\mathbf{m}_\sigma$ and $\mathbf{n}_\sigma$ refer to sets of solute molecules only. The "activity coefficient" γ_s is defined as z_s/ρ_s. In particular, $\gamma_\sigma^{\,0}$ denotes the activity coefficient of the solute species σ in the solution with activity set $\mathbf{z}_\tau^*$, $\mathbf{0}_\sigma$, that is, in a solution which is infinitely dilute with respect to all solute species but not with respect to solvent species. Similarly, $W_{\mathbf{m}_\sigma}$ in Eqs. (22)–(24) is the potential of average force associated with a fixed set of solute molecules $\mathbf{m}_\sigma$ in a solution which is infinitely dilute with respect to solute molecules; in other words, $W_{\mathbf{m}_\sigma}$ refers to a fixed set of solute molecules immersed in a medium which contains solvent species only (with activity set $\mathbf{z}_\tau^*$). Incidentally, although each solvent species has the same activity in the two solutions, in general the solvent will have a different composition on the two sides of the membrane.

Equations (22)–(24) are remarkable results. For example, Eq. (22) states that the osmotic pressure depends on $z_\sigma/\gamma_\sigma^{\,0}$ for solute species and on the potential of average force on solute molecules in an infinitely dilute solution in a way which is formally identical with the dependence of the pressure of a gas [Eq. (13c)] on z_s for all species and on the potential energy (which is the potential of average force when *all* species are infinitely dilute). Solvent species do not enter explicitly into Eqs. (22)–(24). However, the solvent must be important and in fact plays its role implicitly through $\gamma_\sigma^{\,0}$ and $W_{\mathbf{m}_\sigma}(\mathbf{z}_\tau^*,\mathbf{0}_\sigma)$.

Aside from the elegance of these results, for practical purposes these analogies make it possible to take over without modification the formal procedures familiar in the theory of the gaseous state (virial expansions, integral equations for distribution functions, etc.) and apply them to solutes in solution. To make real progress, however, the potential of average force and the activity coefficients for solute molecules at infinite dilution must be specified. This can usually be done only in an approximate way.

III. DEFINITION OF "BINDING"

If Eq. (13a) is applied to a protein solution, the forces between all the molecules of the system are contained, of course, in $U_{\mathbf{N}}$. In particular, if certain small molecules are "bound" to the protein as a result of strong attractive forces, this binding does not appear explicitly in the theory but it is nevertheless taken into account. However, it would be of considerable assistance in the understanding of the behavior of protein solutions on a molecular level to have available an alternative but equivalent theory which introduces binding explicitly. Such a theory is discussed in Sec. IV, following the necessary preliminary considerations of the present section.

Remarks analogous to those above apply in general to any system of molecules in which it is convenient to recognize explicitly new molecular species formed by combinations of molecules belonging to other species. The simplest example is molecular cluster formation in a

one-component monatomic gas. We have treated this case elsewhere,[12] and we shall use this treatment as a point of departure here, without repeating definitions, etc. It was found[12] that clusters can be introduced explicitly, without any approximations, but that the definition of a cluster is in general somewhat arbitrary (except perhaps in the case of a cluster of two monatomic molecules). This arbitrariness does not affect thermodynamic properties, however.

In this section we consider first cluster formation in a polyatomic gas and then turn to the definition of binding.

Polyatomic Gas

The formal equations (M-6) to (M-20) apply here as well as to a monatomic gas except for the definition of Λ.

The definition of a cluster of even two identical polyatomic molecules is rather arbitrary. Perhaps the most obvious possibility to consider is the following. For the two molecules in any element of phase space,[13] the total energy can be written

$$H=\mathrm{KE}_{x,\,\mathrm{c.m.}}+\mathrm{KE}_{x,\,\mathrm{rel}}+\mathrm{KE}_\theta +u_{12}(r_{12},(1)_\theta,(2)_\theta)+U_1((1)_\theta)+U_2((2)_\theta), \quad (25)$$

where u_{12} is the intermolecular potential, c.m. = center of mass, rel = relative, and otherwise the notation has been used before or is obvious. Let $U_1^0=U_2^0$ be the minimum value of the intramolecular potentials U_1 and U_2. The two molecules are considered "not bound" if

$$\mathrm{KE}_{x,\,\mathrm{rel}}+\mathrm{KE}_\theta+u_{12}+U_1+U_2\geqslant U_1^0+U_2^0. \quad (26)$$

Otherwise they are "bound." The point of view here is that if the detailed trajectory of two molecules is followed for a long enough time, and if the "not bound" criterion above is satisfied, then eventually sufficient rotational kinetic energy and excess intramolecular potential energy will be transferred to relative translational kinetic energy so that the two molecules can escape from each other. The difficulty is that the time required for escape may be long relative to the time of a hypothetical experimental observation, especially if practically all of the rotational kinetic energy and excess intramolecular potential energy is required for escape, and if there are a large number of rotational degrees of freedom. If the escape time is this long, it is more reasonable to consider the pair "bound" than "not bound."

An arbitrary but probably more realistic criterion, on the average, is, instead of Eq. (26),

$$\mathrm{KE}_{x,\,\mathrm{rel}}+u_{12}\geqslant 0, \quad (27)$$

in which it is assumed[14] that there is no transfer of energy (of the type discussed in the foregoing), positive or negative. If we adopt Eq. (27), the argument of Eqs. (M-21)–(M-35) goes through, for polyatomic molecules, substantially without change. Integration over $\{P\}_\theta$ in Eq. (1) with $N=2$ leads to

$$Q_2=\frac{q_v^2\lambda_\theta^2}{2h^6\Lambda_\theta^2}\int \exp(-H'/kT)d(1)_\theta d(2)_\theta \times dxdydzd\theta d\varphi dr_{12}dp_xdp_ydp_zdp_\theta dp_\varphi dp_{r_{12}} \quad (28a)$$

where

$$H'=\frac{1}{4m}(p_x^2+p_y^2+p_z^2)+\frac{1}{mr_{12}^2}\left(p_\theta^2+\frac{p_\varphi^2}{\sin^2\theta}\right)+\frac{p_{r_{12}}^2}{m}+u_{12}+U_1+U_2. \quad (28b)$$

Following Eqs. (M-21)–(M-26), we find

$$Q_{01}=\frac{V}{2\Lambda^2}\int_{u_{12}\leq 0}\exp[-(u_{12}+U_1+U_2)/kT] \times 4\pi r_{12}^2F(r_{12},(1)_\theta,(2)_\theta)dr_{12}d(1)_\theta d(2)_\theta \quad (29a)$$

$$Q_{20}=\frac{V}{2\Lambda^2}\left\{\int_{u_{12}>0}\exp[-(u_{12}+U_1+U_2)/kT] \times 4\pi r_{12}^2dr_{12}d(1)_\theta d(2)_\theta +\int_{V,\,u_{12}\leq 0}\exp[-(u_{12}+U_1+U_2)/kT] \times 4\pi r_{12}^2[1-F(r_{12},(1)_\theta,(2)_\theta)]dr_{12}d(1)_\theta d(2)_\theta, \quad (29b)$$

where F is defined as in Eq. (M-25) except that u_{12} is a function of r_{12}, $(1)_\theta$ and $(2)_\theta$. Q_{01} and Q_{20} can also be written with u_{12} replaced by $u_{12}^\ddagger$ and u_{12}^*, respectively, as in Eqs. (M-27) and (M-28). The extension to larger clusters is also obvious. For example,

$$\frac{Z_3}{3!\Lambda^3}=\frac{1}{3!\Lambda^3}\int[\exp(-u_{12}^\ddagger/kT)+\exp(-u_{12}^*/kT)] \times[\exp(-u_{13}^\ddagger/kT)+\exp(-u_{13}^*/kT)] \times[\exp(-u_{23}^\ddagger/kT)+\exp(-u_{23}^*/kT)] \times\exp[-(U_1+U_2+U_3)/kT]d(1)d(2)d(3) =Q_{300}+Q_{110}+Q_{001}, \quad (30)$$

where

$$Q_{300}=\frac{1}{3!\Lambda^3}\int\exp[-(u_{12}^*+u_{13}^*+u_{23}^* +U_1+U_2+U_3)/kT]d(1)d(2)d(3), \text{ etc.} \quad (31)$$

[12] T. L. Hill, J. Chem. Phys. **22**, 617 (1955). Equations in this paper will be referred to by M.

[13] We refer to the translational-rotational phase space of Sec. II for consistency.

[14] This procedure has been applied to the adsorption of a diatomic molecule on a surface by T. L. Hill, J. Chem. Phys. **16**, 181 (1948).

Binding of One Species to Another in a Solution

Let $x=\exp(\mu_a/kT)$ and N_a be the absolute activity and number of molecules of a species a which interacts sufficiently strongly with another species P ($\zeta=e^{\mu/kT}$ and N) so that it is worthwhile to introduce a formulation in which this interaction is treated explicitly as binding of a on P. (This x is of course not be be confused with our symbolic subscript x.) Also present in the solution are other species ($y_q=\exp(\mu_q/kT)$ and L_q, for the qth of these). Let $Q_{N_aN\mathbf{L}}$ be the partition function. Thus the grand partition function is

$$\Xi=\sum_{N_a,N,\mathbf{L}}\left(\prod_q y_q^{L_q}\right)x^{N_a}\zeta^N Q_{N_aN\mathbf{L}}. \tag{32}$$

This equation treats any binding of a on P implicity. To consider the binding explicitly, let $\zeta_s=\exp(\mu_s/kT)$ and N_s refer to molecules of P, P_s, with s bound molecules of a. Let $\mathbf{N}=N_0, N_1, N_2,\cdots$. Let Ω_a be the number of *free* molecules of a in the solution, and let the partition function for Ω_a, $\mathbf{N}$, $\mathbf{L}$ be $Q_{\Omega_a\mathbf{NL}}$. Then the grand partition function is

$$\Xi=\sum_{\Omega_a,\mathbf{N},\mathbf{L}}\left(\prod_q y_q^{L_q}\right)x^{N_a}\left(\prod_{s\geq 0}\zeta_s^{N_s}\right)Q_{\Omega_a\mathbf{NL}}. \tag{33}$$

Now of course P_s is in equilibrium with a and P_0 so that

$$\mu_s=s\mu_a+\mu_0 \qquad s=0,1,2,\cdots. \tag{34}$$
$$\zeta_s=x^s\zeta_0$$

The zeros of energy of the various species P_s must be chosen to be consistent with zero interaction energy between P_0 and a at infinite separation. Equations (33) and (34) give

$$\Xi=\sum_{\Omega_a,\mathbf{N},\mathbf{L}}\left(\prod_q y_q^{L_q}\right)x^{\Omega_a+\Sigma_s sN_s}\zeta_0^{\Sigma_s N_s}Q_{\Omega_a\mathbf{NL}}. \tag{35}$$

Equations (32) and (35) must be identical. On letting $x\to 0$, we see that $\zeta_0=\zeta$. Then the partition functions are seen to be related by

$$Q_{N_aN\mathbf{L}}=\sum_{\Omega_a,\mathbf{N}}Q_{\Omega_a\mathbf{NL}}, \tag{36}$$

where the sum is over all Ω_a and $\mathbf{N}$ such that

$$N_a=\Omega_a+\sum_{s=0}^{N_a}sN_s \quad\text{and}\quad N=\sum_{s=0}^{N_a}N_s.$$

All purely thermodynamic predictions based on Eqs. (33)–(35) will be the same regardless of the definition of "binding," provided only that the definition satisfies Eq. (36). However, average values of nonthermodynamic quantities such as

$$\langle\textstyle\sum_s sN_s\rangle_{Av}=\dfrac{\sum_{\Omega_a\,\mathbf{N},\mathbf{L}}\left(\prod_q y_q^{L_q}\right)[\sum_s sN_s]x^{\Omega_a+\Sigma_s sN_s}\zeta^{\Sigma sN_s}Q_{\Omega_a,\mathbf{N},\mathbf{L}}}{\Xi} \tag{37}$$

and $\langle\Omega_a\rangle_{Av}$ (replace $[\sum sN_s]$ by Ω_a in Eq. (37)) will depend on the definition. But if the binding is strong, all physically reasonable definitions will give essentially the same results. If ambiguity exists because of weak binding, the explicit formulation should be given up in favor of the implicit treatment of interactions [Eq. (32)].

If we write $\bar{N}_a=\langle\Omega_a\rangle_{Av}+\langle\sum sN_s\rangle_{Av}$ and let $\bar{N}_a{}^0$ be the value of $\bar{N}_a$ when $\zeta\to 0$ holding x and $\mathbf{y}$ constant, then in the equation

$$\langle\textstyle\sum sN_s\rangle_{Av}=(\bar{N}_a-\bar{N}_a{}^0)-(\langle\Omega_a\rangle_{Av}-\bar{N}_a{}^0) \tag{38}$$

the quantity $\bar{N}_a-\bar{N}_a{}^0$ is thermodynamically defined and independent of our definition of binding (but not so for the other two terms in the equation separately). In the equilibrium dialysis method of measuring binding on proteins, it is, in effect, customary, at low protein concentrations, to assume that $\langle\Omega_a\rangle_{Av}-\bar{N}_a{}^0$ is negligible so that $\bar{N}_a-\bar{N}_a{}^0$ represents the amount of binding $\langle\sum sN_s\rangle_{Av}$.

Although the quantity $\bar{N}_a-\bar{N}_a{}^0$ is convenient because it is always operationally defined and may be acceptable for $\langle\sum sN_s\rangle_{Av}$ in special cases in practice, it would not be satisfactory for interpretive purposes as a *general* definition of the amount of binding. The quantity $\langle\sum sN_s\rangle_{Av}$, on the other hand, although of no thermodynamic-operational significance in general, is of considerable interest (if defined in a physically reasonable way) in trying to understand the properties of protein solutions on a molecular scale. This is the quantity which will be discussed in detail in Sec. IV.

Pair-Wise Definition of Binding

As an example of a specific choice of a definition of binding, let us adopt the method of Eqs. (27)–(31). If the two polyatomic molecules of Eq. (29) are different, the only significant change is to replace $1/2\Lambda^2$ by $1/\Lambda_1\Lambda_2$; $u_{12}{}^{\ddagger}$ and $u_{12}{}^{*}$ can still be defined as before.

As a simple illustration of Eq. (36), which exhibits the essential points, take $N_a=2$, $N=2$ and leave $\mathbf{L}$

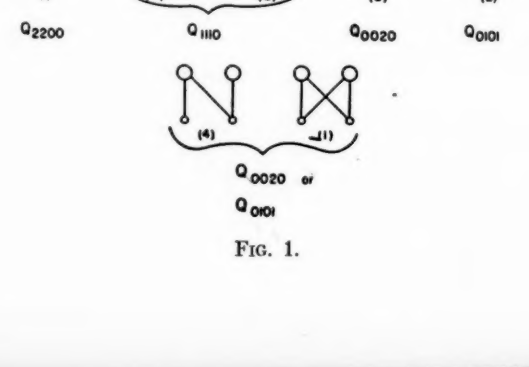

FIG. 1.

arbitrary. Then (using the order $Q_{\mathfrak{a}_a N_0 N_1 N_2 \mathbf{L}}$ on the right-hand side)

$$Q_{22\mathbf{L}}=Q_{2200\mathbf{L}}+Q_{1110\mathbf{L}}+Q_{0020\mathbf{L}}+Q_{0101\mathbf{L}}. \quad (39)$$

Let us label the two a molecules 1 and 2 and the two P molecules A and B. The potential energy can be written

$$U_{22\mathbf{L}}=u_{1A}+u_{1B}+u_{2A}+u_{2B}+u_{AB}+u_{12}+u_{\mathbf{L}} +U_1+U_2+U_A+U_B+U_{\mathbf{L}}, \quad (40)$$

where $u_{\mathbf{L}}$ represents all pair interactions involving one or two molecules of the set $\mathbf{L}$, and $U_{\mathbf{L}}$ represents the total intramolecular potential energy of the set $\mathbf{L}$. Then

$$Q_{22\mathbf{L}}=\left[\int \exp(-U_{22\mathbf{L}}/kT)d\{22\mathbf{L}\}\right]\Big/(2\Lambda_a{}^2) \times(2\Lambda_P{}^2)(\textstyle\prod_q L_q!\Lambda_q{}^{Lq}). \quad (41)$$

In Eq. (41) we introduce Eq. (M-32) for u_{1A}, u_{1B}, u_{2A}, and u_{2B}, since these interactions are to be treated as explicit binding. Then we find, for example,

$$Q_{2200\mathbf{L}}=\frac{\int \exp[-(u_{1A}{}^*+u_{1B}{}^*+u_{2A}{}^*+u_{2B}{}^*+u_{AB}+\cdots+U_{\mathbf{L}})/kT]d\{22\mathbf{L}\}}{(2\Lambda_a{}^2)(2\Lambda_P{}^2)(\prod_q L_q!\Lambda_q{}^{Lq})} \quad (42)$$

[see Fig. 1 for diagram form (omitting the set $\mathbf{L}$)]. For any element of volume in configuration space in the integrals corresponding to the three diagrams of Fig. 1 in which an a molecule is bonded to more than one P molecule, the a molecule is considered bonded to that P molecule for which the corresponding $u^\ddagger$ has the lower value. (The lowest value of $u^\ddagger$ is chosen when $N>2$.) This provides a unique assignment in every case, but actually integrals of this type will always be negligible in magnitude anyhow, relative to other contributions to the same $Q_{\mathfrak{a}_a \mathbf{NL}}$, because appreciable contributions to the integral come only from that part of the configuration space of the two P molecules in which the P molecules are within molecular dimensions of each other (see $u^\ddagger$ in Figs. M-2 and M-3), instead of from the entire configuration space of the two P molecules.

In small molecule (or ion)—protein binding, a pair-wise definition is particularly appropriate because the dominant force leading to binding is between the small molecule and a single protein molecule.

Conclusion

The general conclusion we come to is the following. Binding can be introduced explicitly and, in principle, without approximation. The definition of a bound molecule introduces nonthermodynamic (i.e., molecular) concepts and is not unique, but in actual practice the arbitrariness is not important if the binding is strong and if a physically reasonable definition is used. A pair-wise definition is particularly convenient, though by no means essential. In the $a-P$ intermolecular potential curve, the region of strong attractive interaction plays its part in the treatment of binding as essentially the interaction between a bound a and the P to which it is attached; the repulsive part of the $a-P$ interaction and any weak attractive tail appear as the interaction between a *free* a and a P molecule.

IV. THEORY OF PROTEIN SOLUTIONS

We discuss some of the properties of protein solutions here, introducing binding explicitly. We have seen in Sec. III how this can be done, in principle, without approximation. Of course in practice one can never carry out the complicated phase integrals which arise in solution theory, but an exact formal analysis is valuable, nevertheless, in that it provides the only completely reliable starting point in the development of approximate models.

With the understanding reached in Sec. III (see especially the last paragraph) concerning the significance of partition functions and intermolecular interactions when binding is treated explicitly, we adopt here the methods of Eqs. (13a) to (24) to go over to the osmotic equations of McMillan and Mayer. The protein species P_s are regarded as solutes and all other species as solvents. The solvent species play only an implicit role, as we have seen in Sec. II, with the exception of the species a being bound, which appears both implicitly and explicitly in the fundamental equations (see below).

We introduce two modifications in the approach of Sec. III before proceeding further. (1) In Sec. II we adopted the scheme of dividing the coordinates of a given molecule into translational (classical treatment), external rotational (classical), internal rotational (nonseparable, classical), and vibrational (separable, quantal). The $a-P$ and $a-a$ interactions between the s molecules of a and P in P_s are thus treated classically in Sec. III. It will simplify our notation considerably and in general improve the theory (in the sense that some additional degrees of freedom are treated quantally instead of classically) if, instead of regarding the coordinates of P_s as a composite of a coordinates and P coordinates (as in Sec. III), we make a new assignment of translational, rotational and vibrational coordinates for the molecule P_s as a whole, following the scheme of Sec. II. That is, the $a-P$ and $a-a$ interactions are included in the total potential energy surface of P_s along with the various atom-atom interactions of the mole-

cule P. This modification is not essential; in fact, in most simple approximate models it will be more convenient to omit it. (2) In the binding of one molecule to another larger one, the case of most interest is "localized" binding. That is, there are specific sites (say B in number, and in general not equivalent) at which a molecules are attached relatively strongly to P; the bound a molecules are not free to move over the "surface" of P because of deep potential wells at the sites. The total potential energy surface for P_s mentioned above will, in other words, have minima corresponding to the $B!/s!(B-s)!$ different distributions of the s bound molecules among the B sites. We designate an arbitrary one of these distributions by the symbol $\omega(s)$. The only significant contributions to the partition function of P_s will arise from the neighborhoods of these minima. It is therefore possible, without approximation (or the binding should not be called "localized"), to regard each distribution $\omega(s)$ as a different solute species $P_{\omega(s)}$ with a partition function arising from the neighborhood of the appropriate minimum in the P_s potential surface. It is not at all necessary to break up P_s into subspecies $P_{\omega(s)}$ in this way, but it is convenient and natural to do so with localized binding. If the binding is not "localized," this procedure is of course not permissible.

Osmotic Pressure and Amount of Binding

With the foregoing modification, Eq. (33) become

$$\Xi=\sum_{\Omega_a,\mathbf{N},\mathbf{L}}\Big(\prod_q y_q^{L_q}\Big)x^{\Omega_a}\Big(\prod_{s,\omega(s)}\mathfrak{z}_{\omega(s)}^{N_{\omega(s)}}\Big)Q_{\Omega_a\mathbf{NL}}, \quad (43)$$

where $\mathbf{N}$ represents a set of $N_{\omega(s)}$ (when $\omega(s)$ is used as a subscript it implies s, $\omega(s)$). This is the grand partition function for the inside solution in the osmotic equilibrium. That is, "inside" we have solutes ($P_{\omega(s)}$) and solvents at absolute activities $\mathfrak{z}$, $\mathbf{y}$, and x separated by a membrane (not permeable to the $P_{\omega(s)}$) from the "outside" where the absolute activities are $\mathfrak{z}=\mathbf{0}$, $\mathbf{y}$, and x. From Eqs. (14) and (22), the osmotic pressure Π is then given by

$$\exp(\Pi V/kT)=\sum_{\mathbf{m}\geq\mathbf{0}}\Big[\prod_{s,\omega(s)}\frac{(\mathfrak{z}_{\omega(s)}/\Lambda_{\omega(s)}\gamma_{\omega(s)}{}^0)^{m_{\omega(s)}}}{m_{\omega(s)}!}\Big]\times\int\exp[-W_{\mathbf{m}}(\{\mathbf{m}\},x,\mathbf{y},\mathbf{0}_{\omega(s)})/kT]\times d\{\mathbf{m}\}, \quad (44)$$

where $\mathbf{m}$ represents a set of $m_{\omega(s)}$. Of course, $\gamma_{\omega(s)}{}^0$ is a function of x and $\mathbf{y}$ (and T). By virtue of the equilibria existing [Eq. (34)], we have

$$\mathfrak{z}_{\omega(s)}=x^s\mathfrak{z} \quad (45)$$

for all $\omega(s)$ belonging to s, where $\mathfrak{z}$ is the absolute activity of a protein molecule with $s=0$ [see Eqs. (32) and (35)].

Then

$$\exp(\Pi V/kT)=\sum_{\mathbf{m}\geq\mathbf{0}}\Big[\prod_{s,\omega(s)}\frac{(\mathfrak{z}x^s/\Lambda_{\omega(s)}\gamma_{\omega(s)}{}^0)^{m_{\omega(s)}}}{m_{\omega(s)}!}\Big]\times\int\exp(-W_{\mathbf{m}}(0)/kT)d\{\mathbf{m}\}, \quad (46)$$

where we have used $W_{\mathbf{m}}(0)$ as shorthand for $W_{\mathbf{m}}(\{\mathbf{m}\},x,\mathbf{y},\mathfrak{z}=0)$.

With the aid of Eq. (23), we can write down immediately expressions for the mean number of protein molecules $\bar{M}_P$ and the mean number of a molecules $\bar{M}_a$ bound to protein in the inside solution:

$$\bar{M}_P=\Big\langle\sum_{s,\omega(s)}m_{\omega(s)}\Big\rangle_{\mathrm{AV}}=\frac{1}{\exp(\Pi V/kT)}\sum_{\mathbf{m}\geq\mathbf{0}}\Big(\sum_{s,\omega(s)}m_{\omega(s)}\Big)\times\Big[\prod_{s,\omega(s)}\frac{(\mathfrak{z}x^s/\Lambda_{\omega(s)}\gamma_{\omega(s)}{}^0)^{m_{\omega(s)}}}{m_{\omega(s)}!}\Big]\times\int\exp(-W_{\mathbf{m}}(0)/kT)d\{\mathbf{m}\} \quad (47)$$

$$\bar{M}_a=\Big\langle\sum_{s,\omega(s)}sm_{\omega(s)}\Big\rangle_{\mathrm{AV}}=\frac{1}{\exp(\Pi V/kT)}\sum_{\mathbf{m}\geq\mathbf{0}}\Big(\sum_{s,\omega(s)}sm_{\omega(s)}\Big)\times\Big[\prod_{s,\omega(s)}\frac{(\mathfrak{z}x^s/\Lambda_{\omega(s)}\gamma_{\omega(s)}{}^0)^{m_{\omega(s)}}}{m_{\omega(s)}!}\Big]\times\int\exp(-W_{\mathbf{m}}(0)/kT)d\{\mathbf{m}\}. \quad (48)$$

We note that

$$\bar{M}_P=\mathfrak{z}\Big[\frac{\partial\ln\exp(\Pi V/kT)}{\partial\mathfrak{z}}\Big]_{x,\mathbf{y},T,V} \quad (49)$$

and, formally,

$$\bar{M}_a=x\Big[\frac{\partial\ln\exp(\Pi V/kT)}{\partial x}\Big]_{\mathfrak{z},T,V,\gamma,W}, \quad (50)$$

where the subscripts γ and W signify that $\gamma_{\omega(s)}{}^0$ and $W_{\mathbf{m}}(0)$ are held constant in the differentiation with respect to x.

In Eq. (46), let us replace $W_{\mathbf{m}}(0)$ by $\mathfrak{W}_{\mathbf{m}}(0)$, using

$$\mathfrak{W}_{\mathbf{m}}(0)=W_{\mathbf{m}}(0)-\sum_{s,\omega(s)}[W^{(1)}((1_{\omega(s)}),0)+\cdots+W^{(1)}((m_{\omega(s)}),0)] \quad (51)$$

as the definition of $\mathfrak{W}_{\mathbf{m}}(0)$. Since each $W^{(1)}(0)$ depends only on rotational coordinates in a fluid, $\exp(-W^{(1)}(0)/kT)$ can be placed in front of the translational coordinate integral sign if we restrict ourselves to an infinitely dilute solution (solvent) which is a fluid (the analysis can be carried through without this restriction, but there would be little point in doing

this). Thus we can write

$$\exp(\Pi V/kT)=\sum_{\mathbf{m}\geq 0}\int d'\{\mathbf{m}\}_\theta \prod_{s,\omega(s)} \times\left\{\frac{(\mathfrak{z}x^s)^{m_{\omega(s)}}}{m_{\omega(s)}!}\prod_{(m_{\omega(s)})} H_{\omega(s)}\right\} \times\int \exp[-\mathfrak{W}_{\mathbf{m}}(0)/kT]d\{\mathbf{m}\}_x, \quad (52)$$

where

$$\prod_{(m_{\omega(s)})} H_{\omega(s)}=H_{\omega(s)}((1_{\omega(s)})_\theta)H_{\omega(s)}((2_{\omega(s)})_\theta)\cdots \times H_{\omega(s)}((m_{\omega(s)})_\theta) \quad (53a)$$

$$H_{\omega(s)}((i_{\omega(s)})_\theta)=\frac{\exp\{-W^{(1)}[(i_{\omega(s)})_\theta,x,\mathbf{y},\mathfrak{z}=0]/kT\}}{\Lambda_{\omega(s)}\lambda_{\omega(s)\theta}\gamma_{\omega(s)}{}^0(x,\mathbf{y})}. \quad (53b)$$

From Eqs. (7) and (R-61) we see that, roughly speaking, $H_{\omega(s)}$ is a partition function for a single molecule of species $s,\omega(s)$ in a particular rotational configuration and includes interactions between a molecules bound to the same protein molecule. Actually, $H_{\omega(s)}$ will depend only on the internal rotational configuration, and not the external [see Eq. (R-61)]. $\mathfrak{W}_{\mathbf{m}}(0)$ has the property [Eqs. (51) and (R-73)] that it approaches zero when the molecules of the set $\mathbf{m}$ are widely separated; also $\mathfrak{W}^{(1)}=0$ by definition. Equation (52) is the generalization and rigorous justification of Eq. (3) of the preliminary note.[2]

We now introduce the notation

$$\sum_{(s)}=\sum_{s,\omega(s)}\int d'(1_{\omega(s)})_\theta. \quad (54)$$

That is, $\sum_{(s)}$ is a sum over all values of s, over all distributions $\omega(s)$ for each s, and over all rotational configurations for each $s,\omega(s)$. Using this notation, let us write Eq. (52) in the form of a power series in $\mathfrak{z}$:

$$\exp(\Pi V/kT)=1+\mathfrak{z}C_1+\frac{\mathfrak{z}^2}{2!}C_2+\frac{\mathfrak{z}^3}{3!}C_3+\cdots, \quad (55)$$

where

$$C_1=c_1V,\quad c_1=\sum_{(s)}x^sH_{\omega(s)} \quad (56a)$$

$$C_2=\sum_{(s)}\sum_{(s')}(x^sH_{\omega(s)})(x^{s'}H_{\omega(s)'}) \times\int\exp[-\mathfrak{W}^{(2)}((1_{\omega(s)}),(1_{\omega(s)'}),0)/kT] \times d(1_{\omega(s)})_x d(1_{\omega(s)'})_x \quad (56b)$$

$$C_3=\sum_{(s)}\sum_{(s')}\sum_{(s'')}(x^sH_{\omega(s)})(x^{s'}H_{\omega(s)'})(x^{s''}H_{\omega(s)''}) \times\int\exp[-\mathfrak{W}^{(3)}((1_{\omega(s)}),(1_{\omega(s)'}),(1_{\omega(s)''}),0)/kT] \times d(1_{\omega(s)})_x d(1_{\omega(s)'})_x d(1_{\omega(s)''})_x \quad (56c)$$

etc., where the subscript $\omega(s)'$ should be understood as $s',\omega'(s')$ etc., and terms with $(s)=(s')$, etc., are included in the sums. If Eq. (55) is rewritten as

$$\exp(\Pi V/kT)=1+(\mathfrak{z}c_1)[V]+\frac{(\mathfrak{z}c_1)^2}{2!}\left[\frac{C_2}{c_1{}^2}\right]+\frac{(\mathfrak{z}c_1)^3}{3!}\left[\frac{C_3}{c_1{}^3}\right]+\cdots, \quad (57)$$

and we take the logarithm of both sides of this equation, we obtain

$$\Pi/kT=\sum_{j\geq 1}\mathfrak{b}_j(\mathfrak{z}c_1)^j, \quad (58)$$

where

$$1!V\mathfrak{b}_1=V \quad (59a)$$

$$2!V\mathfrak{b}_2=C_2/c_1{}^2-V^2 \quad (59b)$$

$$3!V\mathfrak{b}_3=\frac{C_3}{c_1{}^3}-3V\frac{C_2}{c_1{}^2}+2V^3, \quad (59c)$$

etc., Eqs. (49) and (58) then lead to

$$\rho=\frac{\bar{M}_P}{V}=\sum_{j\geq 1}j\mathfrak{b}_j(\mathfrak{z}c_1)^j \quad (60)$$

and to the inverse relation

$$\mathfrak{z}c_1=\rho-2\mathfrak{b}_2\rho^2+(8\mathfrak{b}_2{}^2-3\mathfrak{b}_3)\rho^3+\cdots. \quad (61)$$

Substitution of Eq. (61) in Eq. (58) gives the virial expansion of the osmotic pressure

$$\Pi/kT=\rho+\mathfrak{B}_2\rho^2+\mathfrak{B}_3\rho^3+\cdots, \quad (62)$$

where

$$\mathfrak{B}_2=-\mathfrak{b}_2 \quad (63a)$$

$$\mathfrak{B}_3=-2(\mathfrak{b}_3-2\mathfrak{b}_2{}^2), \quad (63b)$$

etc. From Eqs. (56a), (56b), (59b), and (63a), the explicit expression for the second virial coefficient is

$$\mathfrak{B}_2=-\frac{1}{2}\frac{\sum_{(s)}\sum_{(s')}[s,s'](x^sH_{\omega(s)})(x^{s'}H_{\omega(s)'})}{(\sum_{(s)}x^sH_{\omega(s)})^2}, \quad (64)$$

where

$$[s,s']=\int_0^\infty\{\exp[-\mathfrak{W}^{(2)}(r,(1_{\omega(s)})_\theta,(1_{\omega(s)'})_\theta,0)/kT] -1\}4\pi r^2dr. \quad (65)$$

Equation (65) contains the conventional type of integral for the second virial coefficient [see Eq. (R-83a)], and Eq. (64) shows the proper type of averaging of this integral to use, for given x, with respect to the number of molecules bound, the distribution of bound molecules among sites and the rotational configurations of the protein molecules. When x is small (x is proportional to the activity of a in solution), $\mathfrak{B}_2$ in Eq. (64) can be expanded[2] in powers of x. If $\mathfrak{W}^{(2)}(0)$ happens to be the

same for all (s), (s'), Eq. (64) reduces to

$$\mathfrak{B}_2=-\tfrac{1}{2}\int_0^\infty\{\exp[-\mathfrak{W}^{(2)}(0)/kT]-1\}4\pi r^2dr. \quad (66)$$

The amount of binding of a per protein molecule is, from Eqs. (49), (50), and (55),

$$\frac{\bar{M}_a}{\bar{M}_P}=\frac{x[\partial\exp(\Pi V/kT)/\partial x]_{\mathfrak{z},T,V,\gamma,W}}{\mathfrak{z}[\partial\exp(\Pi V/kT)/\partial\mathfrak{z}]_{x,y,T,V}}$$
$$=\frac{\mathfrak{z}E_1+\frac{\mathfrak{z}^2E_2}{1!}+\frac{\mathfrak{z}^3E_3}{2!}+\cdots}{\mathfrak{z}C_1+\frac{\mathfrak{z}^2C_2}{1!}+\frac{\mathfrak{z}^3C_3}{2!}+\cdots}, \quad (67)$$

where

$$E_1=e_1V,\quad e_1=\sum_{(s)}sx^sH_{\omega(s)} \quad (68a)$$

$$E_2=\sum_{(s)}\sum_{(s')}(s+s')(x^sH_{\omega(s)})(x^{s'}H_{\omega(s)'})$$
$$\times\int\exp[-\mathfrak{W}^{(2)}((1_{\omega(s)}),(1_{\omega(s)'}),0)/kT]$$
$$\times d(1_{\omega(s)})_x d(1_{\omega(s)'})_x \quad (68b)$$

$$E_3=\sum_{(s)}\sum_{(s')}\sum_{(s'')}$$
$$\times(s+s'+s'')(x^sH_{\omega(s)})(x^{s'}H_{\omega(s)'})(x^{s''}H_{\omega(s)''})$$
$$\times\int\exp[-\mathfrak{W}^{(3)}((1_{\omega(s)}),(1_{\omega(s)'}),(1_{\omega(s)''}),0)/kT]$$
$$\times d(1_{\omega(s)})_x d(1_{\omega(s)'})_x d(1_{\omega(s)''})_x, \quad (68c)$$

etc. Equation (67) can also be written as

$$\frac{\bar{M}_a}{\bar{M}_P}=\frac{e_1}{c_1}\left[1+\mathfrak{z}\left(\frac{E_2}{2E_1}-\frac{C_2}{C_1}\right)\right.$$
$$\left.+\mathfrak{z}^2\left(\frac{E_3}{6E_1}-\frac{E_2C_2}{2E_1C_1}-\frac{C_3}{2C_1}+\frac{C_2^2}{C_1^2}\right)+\cdots\right], \quad (69)$$

or using Eq. (61),

$$\frac{\bar{M}_a}{\bar{M}_P}=\frac{e_1}{c_1}\left[1+\frac{\rho}{c_1}\left(\frac{E_2}{2E_1}-\frac{C_2}{C_1}\right)\right.$$
$$+\left(\frac{\rho}{c_1}\right)^2\left(\frac{E_3}{6E_1}-\frac{E_2C_2}{E_1C_1}-\frac{C_3}{2C_1}+\frac{2C_2^2}{C_1^2}\right.$$
$$\left.\left.+\frac{E_2C_1}{2E_1}-C_2\right)+\cdots\right]. \quad (70)$$

In the limit $\rho\to0$, the amount of binding,

$$\frac{\bar{M}_a}{\bar{M}_P}=\frac{e_1}{c_1}=\frac{\sum_{(s)}sx^sH_{\omega(s)}}{\sum_{(s)}x^sH_{\omega(s)}}\quad(\rho=0), \quad (71)$$

is in a form which is familiar from the usual discussion of protein binding neglecting protein-protein interactions.[15–18] However, the present theory provides the precise statistical mechanical significance of $H_{\omega(s)}$ in Eq. (71).

At finite protein concentrations, correction terms owing to the influence of protein-protein interactions must be considered in Eq. (70). The question of interest is: under what conditions is $(\rho/c_1)[(E_2/2E_1)-(C_2/C_1)]$ not negligible compared to unity? We intend to make calculations on this point using approximate models. For the present, it can be stated that while no experimental data appear to be available to answer this question directly, there is some indirect evidence that indicates that under ordinary conditions in light scattering and osmotic pressure work the correction term is probably of the order of about 0.02 (2 percent of the leading term). This tentative conclusion has been reached as follows. From Eqs. (59b) and (63a) we observe that

$$\frac{-\rho(\partial\mathfrak{B}_2/\partial\ln x)_{T,\gamma,W}}{e_1/c_1}=\frac{\rho}{c_1}\left(\frac{E_2}{2E_1}-\frac{C_2}{C_1}\right). \quad (72)$$

Now the change of the second virial coefficient with concentration of the ion being bound (e.g., H^+) is available experimentally in several cases, but not under conditions which correspond exactly to the unusual derivative in Eq. (72). If we ignore this difference for order of magnitude purposes, four different sets of data[19–21] (H^+ on insulin, H^+ on insulin, CNS^- on insulin and H^+ on serum albumin) were found to give of the order of 0.02 in Eq. (72). It seems reasonable, for the present at least, to expect that, except in unusual cases, the influence of protein-protein interactions on binding will be small, though of course the converse effect of binding on protein-protein interactions is certainly not small in many systems.

---

[15] I. M. Klotz in *Modern Trends in Physiology and Biochemistry* (Academic Press, New York, 1952), edited by E. S. G. Barron.

[16] G. Scatchard, Ann. N. Y. Acad. Sci. **51**, 660 (1949).

[17] E. J. Cohn and J. T. Edsall, *Proteins, Amino Acids and Peptides* (Reinhold Publishing Corporation, New York, 1943), Chapter 20.

[18] T. L. Hill, J. Phys. Chem. **57**, 324 (1953).

[19] Reference 17, p. 387.

[20] P. Doty and J. T. Edsall, Advances in Protein Chem. **6**, 35 (1951).

[21] R. F. Steiner, Arch. Biochem. and Biophys. **39**, 333 (1952).

Distribution Functions and Potentials of Average Force

In Eq. (24) we replace $\mathbf{m}+\mathbf{n}$ by $\mathbf{m}$ and obtain for the distribution function of a set of protein molecules

$$\rho_{\mathbf{n}}(\{\mathbf{n}\},x,\mathbf{y},\mathfrak{z})$$

$$=\frac{1}{\exp(\Pi V/kT)}\sum_{\mathbf{m}\geq\mathbf{n}}\left[\prod_{s,\omega(s)}\frac{(\mathfrak{z}x^s/\Lambda_{\omega(s)}\gamma_{\omega(s)}{}^0)^{m_{\omega(s)}}}{(m_{\omega(s)}-n_{\omega(s)})\,!}\right]\times\int\exp(-W_{\mathbf{m}}(0)/kT)d\{\mathbf{m}-\mathbf{n}\} \quad (73)$$

$$=\frac{1}{\exp(\Pi V/kT)}\sum_{\mathbf{m}\geq\mathbf{n}}\int d'\{\mathbf{m}-\mathbf{n}\}_\theta\prod_{s,\omega(s)}\times\left\{\frac{(\mathfrak{z}x^s)^{m_{\omega(s)}}\lambda_{\omega(s)\theta}{}^{n_{\omega(s)}}}{(m_{\omega(s)}-n_{\omega(s)})\,!}\prod_{(m_{\omega(s)})}H_{\omega(s)}\right\}\times\int\exp(-\mathfrak{W}_{\mathbf{m}}(0)/kT)d\{\mathbf{m}-\mathbf{n}\}_x, \quad (74)$$

where $\mathbf{m}$ and $\mathbf{n}$ both refer to solute sets. Also, the spatial distribution function for the set $\mathbf{n}$ is

$$\rho_{\mathbf{n}x}(\{\mathbf{n}\}_x,x,\mathbf{y},\mathfrak{z})$$

$$=\int\rho_{\mathbf{n}}d\{\mathbf{n}\}_\theta$$

$$=\frac{1}{\exp(\Pi V/kT)}\sum_{\mathbf{m}\geq\mathbf{n}}\int d'\{\mathbf{m}\}_\theta\prod_{s,\omega(s)}\times\left\{\frac{(\mathfrak{z}x^s)^{m_{\omega(s)}}}{(m_{\omega(s)}-n_{\omega(s)})\,!}\prod_{(m_{\omega(s)})}H_{\omega(s)}\right\}\times\int\exp(-\mathfrak{W}_{\mathbf{m}}(0)/kT)d\{\mathbf{m}-\mathbf{n}\}_x. \quad (75)$$

In the limit ρ or $\mathfrak{z}\to 0$, we set $\exp(\Pi V/kT)=1$, $\mathfrak{z}=\rho/c_1$ and retain only the term $\mathbf{m}=\mathbf{n}$:

$$\rho_{\mathbf{n}}(0)=(\rho/c_1)^n\prod_{s,\omega(s)}\{(x^s\lambda_{\omega(s)\theta})^{n_{\omega(s)}}\prod_{(n_{\omega(s)})}H_{\omega(s)}\}\times\exp[-\mathfrak{W}_{\mathbf{n}}(0)/kT] \quad (76)$$

$$\rho_{\mathbf{n}x}(0)=\left(\frac{\rho}{c_1}\right)^n\int d'\{\mathbf{n}\}_\theta\prod_{s,\omega(s)}\{x^{sn_{\omega(s)}}\prod_{(n_{\omega(s)})}H_{\omega(s)}\}\times\exp[-\mathfrak{W}_{\mathbf{n}}(0)/kT], \quad (77)$$

where

$$n=\sum_{s,\omega(s)}n_{\omega(s)}.$$

The quantity $\rho_{\mathbf{n}}d\{\mathbf{n}\}$ is the probability of observing the set $\mathbf{n}$ in $d\{\mathbf{n}\}$ at $\{\mathbf{n}\}$. Of greater interest is a probability such as this for a set of n protein molecules irrespective of species $s,\omega(s)$. Especially important is the probability of finding any n protein molecules in the spatial volume element $d\{n\}_x$ (i.e., irrespective of species $s,\omega(s)$ and also of rotational configurations). We denote this probability by $\rho_x{}^{(n)}d\{n\}_x$. It is clearly just the sum of the separate (spatial) probabilities for the various possible sets $\mathbf{n}$ obtained by letting each of the positions $(1)_x$, $(2)_x$, $\cdots(n)_x$ be occupied by every different species $s,\omega(s)$. That is,

$$\rho_x{}^{(n)}(\{n\}_x)d\{n\}_x=\sum_{2^{nB}}\rho_{\mathbf{n}x}(\{\mathbf{n}\}_x)d\{n\}_x, \quad (78)$$

or

$$\rho_x{}^{(n)}(\{n\}_x)=\sum_{2^{nB}}\rho_{\mathbf{n}x}(\{\mathbf{n}\}_x), \quad (79)$$

where $\rho_{\mathbf{n}x}$ is given by Eq. (75) and the sum is over the

$$2^{nB}=\left[\sum_{s=0}^{B}\frac{B\,!}{s\,!(B-s)\,!}\right]^n$$

different assignments of 2^B species $s,\omega(s)$ to n positions in space. Of these assignments, $n\,!/\prod_{s,\omega(s)}n_{\omega(s)}\,!$ will correspond to the same $\mathbf{n}$, but $\rho_{\mathbf{n}x}$ will in general be different because of its dependence on $\{\mathbf{n}\}_x$ (not just $\mathbf{n}$), for $n>2$.

Distribution functions for other coordinates than just $\{\mathbf{n}\}_x$ can be obtained by summing as in Eq. (78). But one is restricted to a set of coordinates belonging to every species $s,\omega(s)$. So in general one cannot use the complete distribution function $\rho_{\mathbf{n}}(\{\mathbf{n}\})$ for this purpose, since different species may have different choices for or numbers of rotational coordinates.

Returning to Eq. (79), we define $g_x{}^{(n)}$ and $W_x{}^{(n)}$ for the set of protein molecules by

$$g_x{}^{(n)}=\exp(-W_x{}^{(n)}/kT)=\rho_x{}^{(n)}/\rho^n. \quad (80)$$

The quantity $g_x{}^{(2)}$ is the radial distribution function. We should now verify that $\rho_x{}^{(n)}$, $g_x{}^{(n)}$, and $W_x{}^{(n)}$ have the expected properties of one-component functions (i.e., these functions refer to the single protein species in the solution, irrespective of the subspecies classification $s,\omega(s)$). (1) We recall from Eq. (78) that $\rho_x{}^{(n)}$ has the usual probability definition. (2) At infinite separation of the n molecules [Eq. (R-31)],

$$\rho_x{}^{(n)}\to\sum_{2^{nB}}\left(\prod_{s,\omega(s)}\rho_{\omega(s)}{}^{n_{\omega(s)}}\right)=\left(\sum_{s,\omega(s)}\rho_{\omega(s)}\right)^n=\rho^n, \quad (81a)$$

and

$$g_x{}^{(n)}\to 1 \quad (81b)$$

$$W_x{}^{(n)}\to 0. \quad (81c)$$

(3) As regards normalization [Eq. (R-21)],

$$\int\rho_x{}^{(n)}d\{n\}_x=\sum_{2^{nB}}\left\langle\prod_{s,\omega(s)}\frac{m_{\omega(s)}\,!}{(m_{\omega(s)}-n_{\omega(s)})\,!}\right\rangle_{\text{Av}}=\left\langle\sum_{2^{nB}}\left[\prod_{s,\omega(s)}\frac{m_{\omega(s)}\,!}{(m_{\omega(s)}-n_{\omega(s)})\,!}\right]\right\rangle_{\text{Av}}. \quad (82)$$

It is not difficult to see that the sum in Eq. (82) ex-

hausts all the ways of selecting $n=\sum_{s,\omega(s)} n_{\omega(s)}$ molecules from $M_P=\sum_{s,\omega(s)} m_{\omega(s)}$. That is,

$$\int \rho_x^{(n)} d\{n\}_x = \left\langle \frac{M_P!}{(M_P-n)!} \right\rangle_{Av}. \tag{83}$$

(4) It can be shown that [see Eq. (R-67)] $-\nabla_\alpha W_{\mathbf{n}x}$ is the average force on a molecule α of the set $\mathbf{n}$, including proper averaging over rotational configurations. Let us now average this force further over different sets $\mathbf{n}$. The probability that the element of volume $d\{n\}_x$ is occupied by the set $\mathbf{n}$ in the configuration $\{\mathbf{n}\}_x$ is, from Eq. (78),

$$\frac{\rho_{\mathbf{n}x}(\{\mathbf{n}\}_x)d\{n\}_x}{\rho_x^{(n)}(\{n\}_x)d\{n\}_x}. \tag{84}$$

Hence the desired average force is

$$\frac{\sum_{2^{nB}} \rho_{\mathbf{n}x}(-\nabla_\alpha W_{\mathbf{n}x})}{\rho_x^{(n)}}. \tag{85}$$

Now it is easy to show that $W_x^{(n)}$ is the potential of this average force. On taking the gradient ∇_α of

$$\exp(-W_x^{(n)}/kT) = \frac{\sum_{2^{nB}} [(\prod_{s,\omega(s)} \rho_{\omega(s)}^{n\omega(s)}) \exp(-W_{\mathbf{n}x}/kT)]}{\rho^n}, \tag{86}$$

where the square bracket is $\rho_{\mathbf{n}x}$, we find immediately that $-\nabla_\alpha W_x^{(n)}$ is equal to the expression (85). Thus $W_x^{(n)}$ is the potential of the average force on protein molecules of the set n, including averaging over all rotational configurations and species $s,\omega(s)$.

Equations (75), (79), and (80) provide us with general expressions for $\rho_x^{(n)}$, $g_x^{(n)}$, and $W_x^{(n)}$ as functions of $\{\mathbf{n}\}_x$, x, $\mathbf{y}$, and $\mathfrak{z}$. Expansions of these functions in powers of $\mathfrak{z}$ or ρ [using Eq. (61)] can be written out, but we omit them here. The leading terms in these series correspond to ρ or $\mathfrak{z}=0$ and we now consider this special case. From Eqs. (77), (79), and (80):

$$g_x^{(n)}(0)=\frac{\rho_x^{(n)}(0)}{\rho^n}=\exp[-W_x^{(n)}(0)/kT]$$

$$=\frac{\sum_{(s)}\sum_{(s')}\sum_{(s'')}\cdots\sum_{(s^{(n)})}(x^s H_{\omega(s)})(x^{s'}H_{\omega(s)'})\cdots(x^{s^{(n)}}H_{\omega(s)^{(n)}})\exp[-\mathfrak{W}^{(n)}((1_{\omega(s)}),\cdots,(1_{\omega(s)^{(n)}}),0)/kT]}{(\sum_{(s)} x^s H_{\omega(s)})^n}. \tag{87}$$

Equation (87) is closely related to Eq. (56),

$$\int g_x^{(n)}(0)d\{n\}_x=\int \exp[-W_x^{(n)}(0)/kT]d\{n\}_x$$

$$=C_n/c_1{}^n, \tag{88}$$

which result may be compared with Eqs. (R-74), (R-75), and (57). In particular, from Eqs. (59b) and (88), the second virial coefficient can be written in the alternative form

$$\mathfrak{B}_2=-\mathfrak{b}_2=-\frac{1}{2V}\left(\frac{C_2}{c_1{}^2}-V^2\right)$$

$$=-\frac{1}{2}\int_0^\infty \{g_x^{(2)}(0)-1\}4\pi r^2 dr, \tag{89}$$

where $g_x^{(2)}(0)$ is given by Eq. (87). This is a standard form for the second virial coefficient [see Eq. (R-83a)], and we see, as expected, that binding on a protein does not alter it.

Equation (87) also shows how to calculate the potential of average force $W_x^{(n)}(0)$ on a set of isolated ($\rho=0$) protein molecules in solution, taking into account binding.

Superposition Approximation

We introduce here the superposition approximation in the potential of average force for sets of protein molecules at infinite dilution. In the present case this means [see Eqs. (R-73a), (R-86) and (53b)]

$$\mathfrak{W}_{\mathbf{m}}(0)=\sum_{\text{pairs in }\mathbf{m}} w_{\omega(s)\omega(s)'}(0), \tag{90}$$

where

$$w_{\omega(s)\omega(s)'}(0)=\mathfrak{W}^{(2)}((1_{\omega(s)}),(1_{\omega(s)'}),x,\mathbf{y},\mathfrak{z}=0). \tag{91}$$

This approximation makes it possible to write a "condensed" equation of state [see Eqs. (R-90) and (R-94) for the monatomic case]

$$\frac{\Pi}{kT}=\rho-\frac{1}{6VkT}\sum_{s,\omega(s)}\sum_{s',\omega(s)'}\int r\frac{\partial w_{\omega(s)\omega(s)'}(0)}{\partial r}$$

$$\times\rho_{\omega(s)\omega(s)'}{}^{(2)}(\mathfrak{z})d(1_{\omega(s)})d(1_{\omega(s)'}), \tag{92}$$

where r is the intermolecular distance (regarding $w_{\omega(s)\omega(s)'}(0)$ as a function of r, $(1_{\omega(s)})_\theta$ and $(1_{\omega(s)'})_\theta$) and $\rho_{\omega(s)\omega(s)'}{}^{(2)}$ is the distribution function of Eq. (74) for a set of two protein molecules, one of species $s,\omega(s)$ and the other of species $s',\omega(s)'$. An equivalent form [see Eq. (R-91)], when the protein solution at $\mathfrak{z}$ (as well as at $\mathfrak{z}=0$) is a fluid, is

$$\frac{\Pi}{kT}=\rho-\frac{\rho^2}{6kT}\int_0^\infty r\left\langle\frac{\partial w}{\partial r}\right\rangle_{Av}(\mathfrak{z})g_x^{(2)}(\mathfrak{z})4\pi r^2 dr, \tag{93}$$

where

$$\left\langle \frac{\partial w}{\partial r} \right\rangle_{Av}(\mathfrak{z}) = \frac{\sum_{s,\omega(s)} \sum_{s',\omega(s)'} \int \frac{\partial w_{\omega(s)\omega(s)'}(0)}{\partial r} \rho_{\omega(s)\omega(s)'}{}^{(2)}(\mathfrak{z}) d(1_{\omega(s)})_\theta d(1_{\omega(s)'})_\theta}{\sum_{s,\omega(s)} \sum_{s',\omega(s)'} \int \rho_{\omega(s)\omega(s)'}{}^{(2)}(\mathfrak{z}) d(1_{\omega(s)})_\theta d(1_{\omega(s)'})_\theta}, \tag{94}$$

and $g_x{}^{(2)}(\mathfrak{z})$ is the pair (radial) distribution function of Eq. (80). Since an alternative form of (85) is

$$\frac{\sum_{2^{nB}} \int \rho_{\mathbf{n}}(-\nabla_\alpha W_{\mathbf{n}}) d\{\mathbf{n}\}_\theta}{\rho_x{}^{(n)}}, \tag{95}$$

$-\langle \partial w/\partial r \rangle_{Av}$ is an average force similar to (85), *except* for the mixed character of Eq. (94) with respect to $\mathfrak{z}$ ($\mathfrak{z}=0$ and $\mathfrak{z}=\mathfrak{z}$). Equation (92) agrees with Eq. (62) only as far as the second virial coefficient, since the superposition approximation was not made in Eq. (62). That is, the leading term, $\rho_{\omega(s)\omega(s)'}{}^{(2)}(0)$, in the expansion of $\rho_{\omega(s)\omega(s)'}{}^{(2)}(\mathfrak{z})$ in Eq. (92) in powers of ρ or $\mathfrak{z}$ leads to the second virial coefficient.

Born-Green-Yvon Integrodifferential Equation

In this subsection we employ the superposition approximation introduced above to derive an integrodifferential equation which is the analog of the well-known Born-Green-Yvon equation for a one component monatomic system. Let molecule 1 be a member of the set $\mathbf{n}$ in Eq. (75). We take the gradient $\nabla_1 \rho_{\mathbf{n}x}$ of both sides of this equation[22] and use the notation

$$\mathfrak{W}_{\mathbf{m}}(0) = \sum_{\text{pairs } i,j \text{ in } \mathbf{m}} w(i,j) \tag{96}$$

$$\nabla_1 \mathfrak{W}_{\mathbf{m}}(0) = \sum_{i \text{ in } \mathbf{n},\, i \neq 1} \nabla_1 w(1,i) + \sum_{i \text{ in } \mathbf{m}-\mathbf{n}} \nabla_1 w(1,i) \tag{97}$$

instead of that of Eqs. (90) and (91). It is understood that $w(i,j)$ refers to x, $\mathbf{y}$, $\mathfrak{z}=0$. After taking the gradient as indicated, the right-hand side of Eq. (75) breaks up into two parts corresponding to the two sums in Eq. (97). The first part (i in $\mathbf{n}$) can be written

$$\begin{aligned} &-\frac{1}{kT}\frac{1}{\exp(\Pi V/kT)} \int d\{\mathbf{n}\}_\theta \\ &\quad \times [\sum_i \nabla_1 w(1,i)] \sum_{\mathbf{m} \geq \mathbf{n}} \int d'\{\mathbf{m}-\mathbf{n}\}_\theta \prod_{s,\omega(s)} \\ &\quad \times \left\{ \frac{(\mathfrak{z} x^s)^{m_{\omega(s)}}}{(m_{\omega(s)} - n_{\omega(s)})!} \lambda_{\omega(s)\theta}{}^{n_{\omega(s)}} \prod_{(m_{\omega(s)})} H_{\omega(s)} \right\} \\ &\quad \times \int \exp[-\mathfrak{W}_{\mathbf{m}}(0)/kT] d\{\mathbf{m}-\mathbf{n}\}_x \\ &= -\frac{1}{kT} \int [\sum_i \nabla_1 w(1,i)] \rho_{\mathbf{n}}(\mathfrak{z}) d\{\mathbf{n}\}_\theta. \end{aligned} \tag{98}$$

[22] Only $\mathfrak{W}_{\mathbf{m}}$ is a function of $(1)_x$ as the infinitely dilute solution is assumed a fluid. See Eq. (53b).

There are $m_{\omega(s)^0} - n_{\omega(s)^0}$ identical contributions to the second part (i in $\mathbf{m}-\mathbf{n}$) as i runs through $n_{\omega(s)^0}+1$, $n_{\omega(s)^0}+2$, $\cdots m_{\omega(s)^0}$ for each species $s^0,\omega(s)^0$. Thus the second part is

$$\begin{aligned} &-\frac{1}{kT}\frac{1}{\exp(\Pi V/kT)} \sum_{s^0,\omega(s)^0} \int d\{\mathbf{n}+1_{\omega(s)^0}\}_\theta \\ &\quad \times \int \nabla_1 w(1, n_{\omega(s)^0}+1) d(n_{\omega(s)^0}+1)_x \\ &\quad \times \Big[\sum_{\mathbf{m} \geq \mathbf{n}} \int d'\{\mathbf{m}-\mathbf{n}-1_{\omega(s)^0}\}_\theta \\ &\quad \times \prod_{s,\omega(s)} \left\{ \frac{(\mathfrak{z} x^s)^{m_{\omega(s)}}}{(m_{\omega(s)} - n_{\omega(s)})!} \lambda_{\omega(s)\theta}{}^{n_{\omega(s)}} \prod_{(m_{\omega(s)})} H_{\omega(s)} \right\} \\ &\quad \times \lambda_{\omega(s)^0\theta} (m_{\omega(s)^0} - n_{\omega(s)^0}) \int \exp(-\mathfrak{W}_{\mathbf{m}}/kT) \\ &\qquad \times d\{\mathbf{m}-\mathbf{n}-1_{\omega(s)^0}\}_x \Big] \\ &= -\frac{1}{kT} \sum_{s^0,\omega(s)^0} \int \nabla_1 w(1, n_{\omega(s)^0}+1) \rho_{\mathbf{n}+1\omega(s)^0}(\mathfrak{z}) \\ &\qquad \times d(n_{\omega(s)^0}+1)_x d\{\mathbf{n}+1_{\omega(s)^0}\}_\theta. \end{aligned} \tag{99}$$

The sum of (98) and (99) is $\nabla_1 \rho_{\mathbf{n}x}$. To obtain $\nabla_1 \rho_x{}^{(n)}$, we sum $\nabla_1 \rho_{\mathbf{n}x}$ over the 2^{nB} different assignments of species to the n positions $(1)_x$, $(2)_x$, $\cdots (n)_x$ of the set, with the understanding that, in each set $\mathbf{n}$, "molecule 1" is the molecule, of whatever species $s,\omega(s)$, located at the same position $(1)_x$. Then

$$\begin{aligned} -kT\nabla_1 \rho_x{}^{(n)} &= \sum_{2^{nB}} \int [\sum_{i=2}^{n} \nabla_1 w(1,i)] \rho_{\mathbf{n}}(\mathfrak{z}) d\{\mathbf{n}\}_\theta \\ &\quad + \sum_{2^{nB}} \sum_{s^0,\omega(s)^0} \int \nabla_1 w(1, n_{\omega(s)^0}+1) \\ &\quad \times \rho_{\mathbf{n}+1\omega(s)^0}(\mathfrak{z}) d(n_{\omega(s)^0}+1)_x \\ &\quad \times d\{\mathbf{n}+1_{\omega(s)^0}\}_\theta. \end{aligned} \tag{100}$$

Equation (100) can also be written as

$$\begin{aligned} -kT\nabla_1 \rho_x{}^{(n)} &= \rho_x{}^{(n)} \sum_{i=2}^{n} \langle \nabla_1 w(1,i) \rangle_{Av} \\ &\quad + \int \langle \nabla_1 w(1, n+1) \rangle_{Av} \rho_x{}^{(n+1)}(\mathfrak{z}) d(n+1)_x, \end{aligned} \tag{101}$$

where

$$\langle \nabla_1 w(1,i)\rangle_{Av} = \frac{\sum_{2^n B} \int \nabla_1 w(1,i)\rho_n(\mathfrak{z}) d\{\mathbf{n}\}_\theta}{\rho_x{}^{(n)}(\mathfrak{z})}, \quad (102)$$

and

$$\langle \nabla_1 w(1,n+1)\rangle_{Av} = \frac{\sum_{2^{(n+1)}B} \int \nabla_1 w(1,n+1)\rho_{n+1}(\mathfrak{z}) d\{\mathbf{n+1}\}_\theta}{\rho_x{}^{(n+1)}(\mathfrak{z})}. \quad (103)$$

Equation (101) has the same formal appearance as the simple Born-Green-Yvon equation, but average forces replace forces. Since $w(1,i)$ refers to $\mathfrak{z}=0$, we see that the averages here are of the same mixed type already encountered in Eqs. (93) and (94). To make appreciable further progress, a superposition approximation at $\mathfrak{z}$ (as well as at $\mathfrak{z}=0$) must be introduced (as in the case of a monatomic fluid).

In deriving Eq. (101), we have used the fact that the solvent is a fluid [see Eqs. (53b) and footnote 22 $-W^{(1)}(0)$ is taken independent of $(1)_x$]. However, Eq. (101) does not exclude the possibility that the protein molecules themselves may have long range order when $\mathfrak{z}$ is sufficiently large—as for example in gel formation or when the protein precipitates. The case $n=1$ is then particularly important.[23,24]

Relation to the Kirkwood-Shumaker Theory

The equations of this section are quite general and should be useful as a reliable point of departure in making detailed approximate calculations for special cases. However, we wish to point out here that one such calculation has already been carried out. Kirkwood and Shumaker[25] have made an explicit approximate evaluation of the potential of average force between two isolated ($\rho=0$) protein molecules at a distance r apart, for a particular model, including averaging with respect to external rotational orientation and the number s and distribution $\omega(s)$ of bound hydrogen ions. The precise nature of their averaging is exhibited in their Eq. (8). From this equation it is clear that the averaging is in fact the same as in our Eq. (87) with $n=2$ (as modified to suit their special model). The Kirkwood-Shumaker V and W [see their Eq. (2)] are in our notation $\mathfrak{W}^{(2)}((1_{\omega(s)}),(1_{\omega(s)'}),0)$ and $W_x{}^{(2)}(0)$, respectively. They use the method, in the calculation of $g_x{}^{(2)}(0)$ and $W_x{}^{(2)}(0)$, of expanding the exponential in the summation of Eq. (87) to the term[26] in $(1/kT)^2$.

The "fluctuation" origin of an average attractive force[25] between two isolated protein molecules at the isoionic point refers to the fact that every combination of rotational orientations $(1_{\omega(s)})_\theta$, $(1_{\omega(s)'})_\theta$, numbers of bound molecules s,s', and distributions of bound molecules $\omega(s)$, $\omega(s)'$ is represented by a term in the numerator of the right-hand side of Eq. (87), and that those terms with negative $\mathfrak{W}^{(2)}(0)$ will tend to predominate in the sum, making the weighted average value $W_x{}^{(2)}(0)$ negative (attraction). Negative values of $\mathfrak{W}^{(2)}(0)$ arise, for example, when s and s' are such that the two proteins have opposite charges, or when $\omega(s)$ and $\omega(s)'$ are such that both charge distributions are unsymmetrical with the positively charged side of one protein molecule adjacent to the negatively charged side of the other. Away from the isoionic point, the net charge on the protein molecules predominates in determining the force: there will be a repulsion between identical protein molecules, reduced slightly in magnitude by the statistical favoring [Eq. (87)] of orientations and distributions with charges arranged so as to reduce the repulsion.

ACKNOWLEDGMENTS

The author is indebted to Professor J. T. Edsall, Professor I. M. Klotz, and Professor G. Scatchard for helpful comments and criticisms, and to Dr. H. Gutfreund for many stimulating discussions. Most of this work was done while the author was a Fellow of the John Simon Guggenheim Memorial Foundation in the Department of Chemistry, Yale University.

[23] J. G. Kirkwood in *Phase Transformations in Solids* (John Wiley and Sons, Inc., New York, 1951), edited by Smoluchowski, Mayer, and Weyl.

[24] J. G. Kirkwood and J. Mazur, Compt. rend. réunion ann., Union intern. phys. (Paris) 1952, p. 143.

[25] J. G. Kirkwood and J. B. Shumaker, Proc. Natl. Acad. Sci. **38**, 863 (1952).

[26] There appears to be a typographical error in their Eq. (2): $\langle V^2\rangle_{Av}$ should be replaced by $\langle V^2\rangle_{Av}-\langle V\rangle_{Av}{}^2$, with corresponding changes in Eqs. (3) and (5) [replace f_{ikls} by $f_{ikls}-1$ in $W^{00}(R)$].

Influence of Vibration-Rotation Interaction on Line Intensities in Vibration-Rotation Bands of Diatomic Molecules*,†

ROBERT HERMAN AND RICHARD F. WALLIS
Applied Physics Laboratory, The Johns Hopkins University, Silver Spring, Maryland

(Received June 24, 1954)

The influence of vibration-rotation interaction on line intensities in vibration-rotation bands of diatomic molecules had been recognized and treated approximately many years ago. In the present paper matrix elements have been calculated for the P and R branches of the 0–1, 0–2 and 1–2 transitions taking into account the interaction of rotation and vibration as well as the mechanical and electrical anharmonicity. For the 0–1 and 1–2 transitions the intensities of corresponding absorption lines in the P and R branches are proportional, in first order approximation, to $[1+4\gamma\theta J]J$ and $[1-4\gamma\theta(J+1)](J+1)$, respectively, where J is the rotational quantum number of the initial state, $\gamma=2Be/\omega_e$, $\theta=M_0/M_1r_e$ and M_0 and M_1 are the first two coefficients in the electric dipole moment expansion about the equilibrium internuclear distance r_e. Corrections to the above expressions that are proportional to γ^2 have also been obtained. Formulas are given for the total integrated band intensity and for the line intensities summed over each branch taken individually. In the case of certain molecules, such as HCl for which $\theta\cong1$, it is possible to determine the magnitude of sign of θ by applying the above analyses to experimental data. For molecules such as CO, where $\theta\ll1$, the effect is negligible for the fundamental transition. A semiclassical interpretation of the influence of vibration-rotation interaction on line intensity has also been given.

I. INTRODUCTION

DURING recent years there has been a renewed interest in studying the intensities of individual vibration-rotation lines of diatomic molecules as well as the integrated intensity of all the lines in a given vibrational transition. The experimental measurement of line intensities in the vibration-rotation band spectra of gaseous diatomic molecules provides a method for the determination of a so-called rotational temperature as well as information concerning the population of the individual rotational energy states. From measurements of integrated intensities of the fundamental and overtone bands one may obtain a vibrational temperature as well as information concerning the coefficients in the expansion of the electric dipole moment about the equilibrium internuclear distance. In addition, a knowledge of line intensity is required in determinations of individual line widths. Finally, the presently available experimental techniques make it worthwhile to examine again the degree to which theory can predict individual line intensities in vibration-rotation bands, and particularly to investigate the importance of the vibration-rotation interaction.

The present paper is concerned with the problem of calculating the intensity of the line associated with the transition $v,J\rightarrow v',J'$. According to the quantum theory of radiation the line intensity is given by

$$I_{v,J}{}^{v',J'}\propto\sum_{M,M'}\sum_{\tau}|(v,J,M|M_\tau(r,\theta,\phi)|v',J',M')|^2 \quad (1)$$

where v, J, and M are the vibrational, rotational, and magnetic quantum numbers, respectively. In Eq. (1) the quantity

$$(v,J,M|M_\tau(r,\theta,\phi)|v',J',M')$$

is the matrix element of the τth Cartesian component of the electric dipole moment $\mathbf{M}(r,\theta,\phi)$ for the transition $v,J,M\rightarrow v',J',M'$. It should be noted that we consider molecules whose electronic angular momentum and spin are zero. The value of the matrix element depends on the particular model chosen to represent the diatomic molecule. Since for the diatomic molecule Schrödinger's equation is separable, one has

$$\sum_{M,M'}\sum_{\tau}|(v,J,M|M_\tau(r,\theta,\phi)|v',J',M')|^2$$
$$=|(v,J|M(r)|v',J')|^2\sum_{M,M'}\sum_{\tau}$$
$$\times|(J,M|f_\tau(\theta,\phi)|J',M')|^2 \quad (2)$$
$$=|\mathfrak{M}_{v,J}{}^{v',J'}|^2\{J\delta_{J-1,J'}+(J+1)\delta_{J+1,J'}\} \quad (2a)$$

where

$$M_\tau(r,\theta,\phi)=f_\tau(\theta,\phi)M(r), \quad (2b)$$
$$\tau=x,\ y,\ \text{or}\ z, \quad (2c)$$
$$f_x(\theta,\phi)=\sin\theta\cos\phi, \quad (2d)$$
$$f_y(\theta,\phi)=\sin\theta\sin\phi, \quad (2e)$$
$$f_z(\theta,\phi)=\cos\theta, \quad (2f)$$
$$M(r)=\sum_i M_i(r-r_e)^i, \quad (2g)$$
$$\mathfrak{M}_{v,J}{}^{v',J'}=(v,J|M(r)|v',J'), \quad (2h)$$

where $\delta_{i,j}$ is the Kronecker delta, and r_e is taken as the equilibrium internuclear separation. The multiple sum in Eq. (2) represents the contribution to the intensity of the molecule considered as a rigid rotator and has the values J and $J+1$ for the P- and R-branches, respectively. The entire problem rests in the evaluation of the

* A preliminary account of a portion of this work was reported at the New York Meeting of the American Physical Society, January, 1954.

† The work reported herein was supported by the Bureau of Ordnance, Department of the Navy, under Contract NOrd-7386.

vibrational matrix element taking into account the interaction of the vibrational motion with the rotation.

This problem was studied many years ago on the basis of the old quantum theory and Bohr correspondence principle. The dominant term in the intensity of a vibration-rotation line was obtained by Fowler[1] who neglected the additional terms arising from the vibration-rotation interaction. The first correction was computed by Kemble[2] who recognized that the interaction arose from the Coriolis force. These results suffered from ambiguity because the old quantum theory did not provide a unique or correct prescription for the calculation of intensities. With the advent of the quantum mechanics, Oppenheimer[3] applied the Heisenberg matrix method to the special model of a harmonic oscillator including vibration-rotation interaction. It should be noted that this model was studied for the case of point charges and the fundamental 0–1 transition only. The correction factor to the intensity obtained by Oppenheimer for the 0–1 transition is given by

$$F_R=1-4\gamma(J+1)[1-\tfrac{5}{8}\gamma(J+1)-\tfrac{3}{8}\gamma], \quad (3a)$$

and

$$F_P=1+4\gamma J[1+\tfrac{5}{8}\gamma J-\tfrac{3}{8}\gamma] \quad (3b)$$

for the R- and P-branches, respectively, where

$$\gamma=\frac{2B_e}{\omega_e}=\frac{\omega_r}{\omega_e} \quad (3c)$$

and ω_r is the fundamental rotational frequency. According to Eq. (3) the correction obtained by Oppenheimer would be considerable for molecules like HCl and CO for the lines of high J-value observed experimentally. The application of Oppenheimer's result to HCl was made quite early by Dennison[4] and recently to HCl and CO by Penner.[5]

General formulas for the first-order correction to the intensity also have been derived by Dunham[6] using wave mechanics. Dunham considered the Morse potential energy function and used the Morse wave functions as zero-order functions for a perturbation calculation in which the rotation-vibration interaction term was treated as the perturbation. In evaluating the matrix elements of the interaction term, the latter was expanded in power series and only the dominant term of the matrix element retained. Dunham made specific application of his results only to the 0–2 transition in HCl.

During the course of our studies of the intensity of infrared vibration-rotation bands we attempted to understand more fully the physical significance of the above correction found by Oppenheimer. We realized that his results given in Eq. (3) applied as stated above to a rather special case. It was deemed important to re-examine the question in somewhat greater generality to determine how good Oppenheimer's model is for molecules like HCl and CO to which it had already been applied. In addition, new experimental results on CO seemed to indicate that the formulas in Eq. (3) were not accurate.[7] It is the purpose of this paper to give the correction to the intensity which arises from the vibration-rotation interaction for the case of a diatomic molecule possessing mechanical anharmonicity and electronic charge distributed about the nuclei. The analysis has been carried out for the fundamental, 1–2 and 0–2 vibrational transitions.

II. THEORY

A. General Formulation

In order to calculate theoretically the intensity of the line associated with the transition $v,J\rightarrow v',J'$ it is necessary to evaluate the matrix element $(vJ|M(r)|v'J')$ which involves the radial wave functions of the diatomic molecule. The radial wave equation obtained by separation of Schrödinger's equation is

$$\frac{1}{r^2}\frac{d}{dr}\left(r^2\frac{dR}{dr}\right)+\left\{-\frac{J(J+1)}{r^2}+\frac{2\mu}{\hbar^2}[E-U(r)]\right\}R=0, \quad (4)$$

where μ is the reduced mass. The term $-J(J+1)/r^2$ represents the rotational energy and introduces the interaction between the vibrational and rotational motions. Equation (4) has been solved exactly by Fues[8] for the special potential function

$$U(r)=-A\left(\frac{1}{\rho}-\frac{1}{2\rho^2}\right), \quad (5)$$

where

$$\rho=r/r_e, \quad (5a)$$

$$A=\frac{\hbar^2}{\gamma^2\mu r_e^2} \quad (5b)$$

and γ is as defined in Eq. (3c). The matrix elements can be evaluated in closed form and will be discussed later. The Fues potential lacks flexibility in that it specifies a fixed value for the mechanical anharmonicity. Solutions for more general potential functions have been obtained by expanding the vibration-rotation interaction term $-J(J+1)/r^2$. This has been done by Pekeris[9] for the case of the Morse potential function. The resulting wave functions are given in terms of the confluent hypergeometric functions and as yet the evaluation of the matrix elements does not appear to have been carried out. Relatively simple wave functions are obtained in the case of the harmonic oscillator using terms

[1] R. H. Fowler, Phil. Mag. **49**, 1272 (1925).
[2] E. C. Kemble, Phys. Rev. **25**, 1 (1925).
[3] J. R. Oppenheimer, Proc. Cambridge Phil. Soc. **23**, 327 (1926).
[4] D. M. Dennison, Phys. Rev. **31**, 503 (1928).
[5] S. S. Penner, J. Chem. Phys. **19**, 272 (1951).
[6] J. L. Dunham, Phys. Rev. **34**, 438 (1929).
[7] Herman, Silverman, and Wallis, Phys. Rev. **94**, 752 (1954).
[8] E. Fues, Ann. Physik **80**, 367 (1926); **81**, 281 (1926).
[9] C. L. Pekeris, Phys. Rev. **45**, 98 (1934).

through the quadratic terms in the expansion of the interaction in powers of $(r-r_e)$. These wave functions have been utilized by us in the following treatment of the matrix elements of the electric moment for an anharmonic oscillator.

The potential energy $U(r)$ and the term $J(J+1)/r^2$ which appear in Eq. (4) may be expanded in power series about the equilibrium internuclear distance r_e as follows:

$$U(r)=\tfrac{1}{2}ku^2+k'u^3+\cdots, \tag{6a}$$

and

$$\frac{J(J+1)}{r^2}=\frac{J(J+1)}{r_e^2}[1-2\xi+3\xi^2-4\xi^3+\cdots], \tag{6b}$$

where

$$u=r-r_e, \tag{6c}$$

and

$$\xi=u/r_e. \tag{6d}$$

The constants k and k' may be expressed in terms of the coefficients in the Dunham expansion for $U(r)$ by the equations

$$k=\frac{2hca_0}{r_e^2}$$

$$k'=\frac{hca_0a_1}{r_e^3}.$$

The coefficients a_0 and a_1 are defined by the expansion

$$U(r)=hca_0\xi^2(1+a_1\xi+\cdots)$$

and are related to the spectroscopic constants by the equations

$$a_0=\frac{\omega_e^2}{4B_e}$$

$$-a_1=1+\frac{\alpha_e\omega_e}{6B_e^2}.$$

If only terms through the quadratic terms are retained in the expansions (6a) and (6b), Eq. (4) may be solved yielding the following wave functions[10]:

$$S^0_{v,J}(\eta_J)=rR^0_{v,J}(r)$$

$$=\left[\left(\frac{\alpha_J}{\pi}\right)^{\frac{1}{2}}\frac{1}{2^v v!}\right]^{\frac{1}{2}}\exp(-\tfrac{1}{2}\eta_J^2)H_v(\eta_J) \tag{7}$$

where

$$\eta_J=\alpha_J^{\frac{1}{2}}\zeta_J, \tag{7a}$$

$$\zeta_J=u-a_J, \tag{7b}$$

$$a_J=\frac{J(J+1)\gamma^2r_e}{1+3J(J+1)\gamma^2} \tag{7c}$$

$$\alpha_J=\frac{2\pi\mu c\omega_e'}{h}, \tag{7d}$$

$$\omega_e'=\omega_e\{1+3J(J+1)\gamma^2\}^{\frac{1}{2}}, \tag{7e}$$

$$\omega_e=\frac{1}{2\pi c}\left(\frac{k}{\mu}\right)^{\frac{1}{2}} \tag{7f}$$

and H_v is the vth Hermite polynomial. The energy levels $E^0_{v,J}$ are given by

$$E^0_{v,J}=J(J+1)\sigma\left\{1-\frac{a_J}{r_e}\right\}+(v+\tfrac{1}{2})hc\omega_e' \tag{8}$$

where

$$\sigma\equiv hcB_e=\tfrac{1}{2}kr_e^2\gamma^2 \tag{8a}$$

and

$$B_e=h/(8\pi^2c\mu r_e^2). \tag{8b}$$

The quantity r_e+a_J may be interpreted as the equilibrium internuclear distance in the rotating molecule. The quantity $k[1+3J(J+1)\gamma^2]$ which occurs in Eq. (7d) may be considered to be an effective force constant.

First-order perturbed solutions to Eq. (4) may be obtained by treating the cubic terms in the expansions of $U(r)$ and $J(J+1)/r^2$ as the perturbation H'. The latter may be written as

$$H'=hc\omega_eb_J\alpha^{\frac{1}{2}}u^3 \tag{9}$$

where

$$b_J=b\left[1-\frac{2\gamma^{5/2}}{b}J(J+1)\right], \tag{9a}$$

$$b=k'/(hc\omega_e\alpha^{\frac{1}{2}}), \tag{9b}$$

and

$$\alpha=1/(\gamma r_e^2). \tag{9c}$$

The constant b is related to the spectroscopic constants by

$$b=-\frac{1}{2}\gamma^{\frac{1}{2}}\left[1+\frac{\alpha_e}{3\gamma B_e}\right].$$

The quantity b_J is a dimensionless measure of the effective mechanical anharmonicity of the molecule. The first term, b, arises from the anharmonicity of $U(r)$; the second term arises from the interaction of rotation and vibration.

The first-order perturbed wave functions $R_{v,J}$ may be expressed in the form[11]

$$R_{v,J}=\frac{S_{v,J}}{r}, \tag{10}$$

where

$$S_{v,J}=S^0_{v,J}+\sum_{m=0}^{\infty}{}'C_{v,m,J}S^0_{m,J}, \tag{10a}$$

and

$$C_{v,m,J}=\frac{\int_{-\infty}^{\infty}S^0_{m,J}H'S^0_{v,J}\,dr}{E^0_{v,J}-E^0_{m,J}}. \tag{10b}$$

[10] See L. Pauling and E. B. Wilson, Jr., *Introduction to Quantum Mechanics* (McGraw-Hill Book Company, Inc., New York, 1935), pp. 267–271.

[11] R. C. Herman and K. E. Shuler, J. Chem. Phys. **22**, 481 (1954).

If the expression for H' given by Eq. (9) is substituted into Eq. (10b), the coefficients $C_{v,m,J}$ may be written in the form

$$C_{v,m,J}=[b_J'/(v-m)]\int_{-\infty}^{\infty}\psi_m{}^0(q)q^3\psi_v{}^0(q)dq +[3b_JJ(J+1)\gamma^{\frac{1}{2}}/(v-m)] \times\int_{-\infty}^{\infty}\psi_m{}^0(q)q^2\psi_v{}^0(q)dq, \quad (11)$$

$$q=\eta_J, \quad (11a)$$

$$\psi_v{}^0(q)=\alpha_J{}^{-\frac{1}{2}}S^0{}_{v,J}(q), \quad (11b)$$

$$b_J'=b\left[1-\left(2\frac{\gamma^{\frac{1}{2}}}{b}+\frac{15}{4}\right)J(J+1)\gamma^2\right] \quad (11c)$$

and terms of order greater than γ^2 have been neglected. The quantity b has been considered to be of order $\gamma^{\frac{1}{2}}$. The justification for this assumption will be given later under the discussion of the Fues potential [see paragraph following Eq. (23)].

The quantity b_J' differs from b_J by a term which may be interpreted to arise from the dependence of the effective force constant on J. The second term in Eq. (11) may be interpreted to arise from the dependence of the equilibrium internuclear distance on J.

The integrals in Eq. (11) may be evaluated by standard methods.[12] Explicit expressions for the first order perturbed functions $S_{v,J}$ for $v=0$, 1, and 2 are

$$S_{0,J}=S^0{}_{0,J}-\frac{3}{2\sqrt{2}}b_J'S^0{}_{1,J}-\frac{3}{2\sqrt{2}}b_JJ(J+1)\gamma^{\frac{1}{2}}S^0{}_{2,J} -\frac{1}{2\sqrt{3}}b_J'S^0{}_{3,J}, \quad (12)$$

$$S_{1,J}=S^0{}_{1,J}+\frac{3}{2\sqrt{2}}b_J'S^0{}_{0,J}-3b_J'S^0{}_{2,J} -\frac{3\sqrt{3}}{2\sqrt{2}}b_JJ(J+1)\gamma^{\frac{1}{2}}S^0{}_{3,J}-\frac{1}{\sqrt{3}}b_J'S^0{}_{4,J}, \quad (12a)$$

and

$$S_{2,J}=S^0{}_{2,J}+\frac{3}{2\sqrt{2}}b_JJ(J+1)\gamma^{\frac{1}{2}}S^0{}_{0,J}+3b_J'S^0{}_{1,J} -\frac{9\sqrt{3}}{2\sqrt{2}}b_J'S^0{}_{3,J}-\frac{3\sqrt{3}}{2}b_JJ(J+1)\gamma^{\frac{1}{2}}S^0{}_{4,J} -\frac{\sqrt{5}}{\sqrt{6}}b_J'S^0{}_{5,J}. \quad (12b)$$

[12] The integrals required in the perturbation calculation can be obtained from formulas given by E. Fues in reference 8 or from the recursion formulas for the harmonic oscillator wave functions given by E. Hutchisson, Phys. Rev. **37**, 45 (1931).

The calculation of the line intensity for the transition $v,J\rightarrow v',J'$ requires the evaluation of the matrix element

$$\mathfrak{M}_{v,J}{}^{v',J'}=(v,J\,|\,M(r)\,|\,v',J') \quad (13)$$

$$=\int_0^{\infty}R_{v,J}(r)M(r)R_{v',J'}(r)r^2dr \quad (13a)$$

$$\simeq\int_{-\infty}^{\infty}S_{v,J}(\eta_J)M(r)S_{v',J'}(\eta_{J'})dr. \quad (13b)$$

The extension of the range of integration in Eq. (13b) involves the customary assumption that the functions $S_{v,J}$ are sufficiently small for r negative.[10,13] If the expansion for $M(r)$ given by Eq. (2g) is substituted into Eq. (13b) the following general expression for the matrix element $\mathfrak{M}$ is obtained.

$$\begin{aligned}\mathfrak{M}_{v,J}{}^{v',J'}=&\alpha_J{}^{-\frac{1}{2}}[\sum_{i=0}^{\infty}M_ia_J{}^i]\\ &\times\int_{-\infty}^{\infty}S_{v,J}(\eta_J)S_{v',J'}(\eta_{J'})d\eta_J\\ &+\alpha_J{}^{-1}[\sum_{i=1}^{\infty}M_ia_J{}^{i-1}i]\\ &\times\int_{-\infty}^{\infty}S_{v,J}(\eta_J)\eta_JS_{v',J'}(\eta_{J'})d\eta_J\\ &+\alpha_J{}^{-\frac{3}{2}}[\sum_{i=2}^{\infty}M_ia_J{}^{i-2}i(i-1)/2]\\ &\times\int_{-\infty}^{\infty}S_{v,J}(\eta_J)\eta^2S_{v',J'}(\eta_{J'})d\eta_J\\ &+\cdots\end{aligned} \quad (14)$$

Since a_J is of the order of γ^2, the terms in the square brackets drop off as powers of γ^2.

The matrix elements for the 0–1, 0–2, and 1–2 vibrational transitions have been calculated explicitly using the first-order perturbed functions given by Eqs. (12), (12a), and (12b). The required integrals have the form

$$\int_{-\infty}^{\infty}\exp(-\tfrac{1}{2}z^2)\exp[-\tfrac{1}{2}(\beta z+\delta)^2] \times H_v(z)H_{v'}(\beta z+\delta)z^pdz \quad (15)$$

where

$$\beta=(\alpha_{J'}/\alpha_J)^{\frac{1}{2}} \quad (15a)$$

and

$$\delta=(\alpha_{J'})^{\frac{1}{2}}(a_J-a_{J'}). \quad (15b)$$

The integrals were evaluated with the aid of the generating function[14] $\mathcal{S}(z,s)$ for the Hermite polynomials.

$$\mathcal{S}(z,s)=\sum_n\frac{H_n(z)}{n!}s^n \quad (15c)$$

$$=\exp[z^2-(s-z)^2]. \quad (15d)$$

[13] D. ter Haar, Phys. Rev. **70**, 222 (1946).

[14] See reference 10, p. 80.

Consider the integral

$$\int_{-\infty}^{\infty} \mathcal{S}(z,s)\mathcal{S}(\beta z+\delta,t)\exp[-\tfrac{1}{2}z^2-\tfrac{1}{2}(\beta z+\delta)^2]z^p dz$$
$$=\sum_n\sum_m \frac{s^n t^m}{n!m!}\int_{-\infty}^{\infty} H_n(z)H_m(\beta z+\delta)$$
$$\times\exp[-\tfrac{1}{2}z^2-\tfrac{1}{2}(\beta z+\delta)^2]z^p dz. \quad (15e)$$

If the generating functions on the left-hand side of Eq. (15e) are replaced by their values specified by Eq. (15d), then the left-hand side may be integrated. The result may be expanded in power series in s and t. The integrals defined by Eq. (15) may then be obtained by equating the coefficients of $s^v t^{v'}$ on each side of Eq. (15e).

The matrix elements are given as power series in the parameter γ through terms in γ^2. The first two terms in the expansion of $M(r)$ given by Eq. (2g) have been included in the formulas.

The results for the 0–1 and 1–2 transitions are

$$\mathfrak{M}_{0-1}(m)\cong\frac{M_1}{(2\alpha)^{\frac{1}{2}}}\left\{1-2\theta\gamma m\left[1+\frac{15}{2}b\gamma^{\frac{1}{2}}+3\gamma-\frac{5}{2}\frac{b\gamma^{\frac{1}{2}}}{\theta}\right.\right.$$
$$\left.\left.+\frac{3}{4}\frac{b\gamma^{\frac{1}{2}}}{\theta}(m-1)+\frac{3}{8}\frac{\gamma}{\theta}(m-1)\right]\right\}, \quad (16)$$

$$\mathfrak{M}_{1-2}(m)\cong\frac{M_1}{(\alpha)^{\frac{1}{2}}}\left\{1-2\theta\gamma m\left[1+15b\gamma^{\frac{1}{2}}+6\gamma-\frac{23}{4}\frac{b\gamma^{\frac{1}{2}}}{\theta}\right.\right.$$
$$\left.\left.+\frac{3}{4}\frac{b\gamma^{\frac{1}{2}}}{\theta}(m-1)+\frac{3}{8}\frac{\gamma}{\theta}(m-2)\right]\right\}, \quad (16a)$$

where

$$\theta=\frac{M_0}{M_1 r_e} \quad (16b)$$

$$m=\begin{cases} J+1, & R\text{-branch} \\ -J, & P\text{-branch} \end{cases}, \quad (16c)$$

and J is the rotational quantum number for the initial state. As will be discussed in more detail, later the quantity θ appearing in Eq. (16) introduces a dependence on the dipole moment and its variation with internuclear separation which does not appear in Oppenheimer's results.

Equations (16) and (16a) express the matrix element as the matrix element for a pure harmonic oscillator without rotation multiplied by a correction factor arising from the interaction of rotation and vibration. It is perhaps worthwhile to point out a formal interpretation of the various terms in the correction factors. The linear term in γ arises from the difference in equilibrium internuclear distances in the initial and final rotational states. The first term quadratic in γ (taking, as before, $b\sim\gamma^{\frac{1}{2}}$) is a contribution from the mechanical anharmonicity of $U(r)$ and the J dependence of the effective force constant. The next term arises from the contribution of the rotation-vibration interaction to the mechanical anharmonicity. The third and fourth quadratic terms in γ arise from the mechanical anharmonicity of $U(r)$ and the J dependence of the equilibrium internuclear distance. The last term is a contribution from the J dependence of the effective force constant.

The result for the matrix element of the 0–2 transition is

$$\mathfrak{M}_{0-2}(m)\cong\frac{M_1 b}{(2\alpha)^{\frac{1}{2}}}\left\{1-2\frac{\gamma^{\frac{1}{2}}}{b}m\left[\left(1-\frac{3\theta}{4}+\frac{\theta}{2}\frac{b}{\gamma^{\frac{1}{2}}}\right)-\theta\gamma m\right.\right.$$
$$+\frac{1}{2}\left(2\frac{\gamma^{\frac{1}{2}}}{b}+\frac{15}{4}\right)\gamma^{\frac{1}{2}}b(m+5)$$
$$\left.\left.+\frac{3}{16}\gamma^{\frac{1}{2}}b(2m-3)\right]\right\}. \quad (17)$$

The matrix element given by Eq. (17) is the product of the matrix element of a nonrotating anharmonic oscillator and a correction factor. The terms in the latter may be interpreted formally as was done for the 0–1 and 1–2 transitions but this is omitted here. It may be mentioned, however, that $\mathfrak{M}_{0-2}(m)$ does not vanish even if the mechanical anharmonicity constant b vanishes. The interaction of rotation and vibration therefore leads to a violation of the selection rule $\Delta v=\pm 1$ for a pure harmonic oscillator.

The intensity of the absorption line corresponding to the transition $v,J\to v',J'$ is given by

$$I_{v,J}{}^{v',J'}=\frac{8\pi^3 N_{v,J}}{3hc(2J+1)}\omega_{v,J}{}^{v',J'}\sum_{M',M}\sum_{\tau}$$
$$\times|(v,J,M|M_\tau(r,\theta,\phi)|v',J',M')|^2, \quad (18)$$

where $N_{v,J}$ is the number of molecules in the initial state and $\omega_{v,J}{}^{v',J'}$ is the frequency for the transition in wave numbers. If the multiple sum in Eq. (18) is replaced by its value given by Eq. (2a), one obtains

$$I_v{}^{v'}(m)=\frac{8\pi^3 N_{v,J}}{3hc(2J+1)}\omega_v{}^{v'}(m)|m||\mathfrak{M}_v{}^{v'}(m)|^2, \quad (19)$$

where m takes on the values previously given in Eq. (16c). The square of the vibrational matrix element may be written in the form

$$|\mathfrak{M}_v{}^{v'}(m)|^2=|R_v{}^{v'}|^2 F_v{}^{v'}(m), \quad (20)$$

where $R_v{}^{v'}$ is the matrix element of the electric dipole moment for a nonrotating anharmonic oscillator and $F_v{}^{v'}(m)$ is a correction factor taking into account the interaction of rotation and vibration.

Explicit expressions for $F_v{}^{v'}(m)$ for the 0–1, 1–2, and 0–2 transitions may be obtained from Eqs. (16), (16a),

and (17). They are

$$F_{0-1}(m)\cong 1-4\theta\gamma m \times\left[1+3\gamma\left(1+\frac{5}{2}\frac{b}{\gamma^{\frac{1}{2}}}-\frac{13}{12}\frac{b}{\gamma^{\frac{1}{2}}\theta}-\frac{1}{8\theta}\right)-m\left(\theta\gamma-\frac{3}{8}\frac{\gamma}{\theta}-\frac{3}{4}\frac{b\gamma^{\frac{1}{2}}}{\theta}\right)\right] \quad (21)$$

$$F_{1-2}(m)\cong 1-4\theta\gamma m \times\left[1+6\gamma\left(1+\frac{5}{2}\frac{b}{\gamma^{\frac{1}{2}}}-\frac{13}{12}\frac{b}{\gamma^{\frac{1}{2}}\theta}-\frac{1}{8\theta}\right)-m\left(\theta\gamma-\frac{3}{8}\frac{\gamma}{\theta}-\frac{3}{4}\frac{b\gamma^{\frac{1}{2}}}{\theta}\right)\right] \quad (21a)$$

and

$$F_{0-2}(m)\cong 1-4\frac{\gamma^{\frac{1}{2}}}{b}m\left[\left(1-\frac{3\theta}{4}+\frac{\theta}{2}\frac{b}{\gamma^{\frac{1}{2}}}\right)-\theta\gamma m+\frac{1}{2}\left(2\frac{\gamma^{\frac{1}{2}}}{b}+\frac{15}{4}\right)\gamma^{\frac{1}{2}}b(m+5)+\frac{3}{16}\gamma^{\frac{1}{2}}b(2m-3)-\frac{\gamma^{\frac{1}{2}}}{b}\left(1-\frac{3\theta}{4}+\frac{\theta}{2}\frac{b}{\gamma^{\frac{1}{2}}}\right)^2 m\right]. \quad (21b)$$

The derivation of Eqs. (21), (21a), and (21b) involved a number of approximations. Only the cubic term in the expansion of $U(r)$ was retained in the calculation of the perturbed wave function coefficients $C_{v,m,J}$. This approximation is reasonable for the low-vibrational states considered here. For transitions involving higher states having relatively large vibration amplitudes, additional terms in the expansion would be required.

The first two terms of the electric dipole moment expansion were employed in the derivations. The contributions arising from the matrix elements of the third term $M_2(r-r_e)^2$ were examined and were found to add no new qualitative features to the behavior of the F-factors.

On numerous occasions power series expansions in a variable of the order of $J(J+1)\gamma^2$ were made. Such expansions are valid only if $J(J+1)\gamma^2\ll 1$. Since $\gamma^2\sim 10^{-4}$ for many molecules, this condition becomes $J\ll 100$.

In the calculation of the first-order perturbed wave functions the rotation-vibration interaction term was expanded in power series according to Eq. (6b) and terms higher than cubic neglected. The effect of this approximation may be investigated if one employs the Fues potential function given by Eq. (5). For this potential the exact solutions to the radial equation [Eq. (4)] are[8]

$$R(\rho)=\rho^{\alpha-1}e^{-\beta\rho}L^s_{t+s}(2\beta\rho) \quad (22)$$

where $L^s_{t+s}(2\beta\rho)$ is the associated Laguerre polynomial of order s and degree t and

$$\beta=[\gamma^2(t+\alpha)]^{-1}, \quad (22a)$$

$$s=2\alpha-1, \quad (22b)$$

and

$$\alpha=\tfrac{1}{2}+\gamma^{-1}[1+\tfrac{1}{4}\gamma^2+J(J+1)\gamma^2]^{\frac{1}{2}}. \quad (22c)$$

The quantity t is an integer and plays the role of the vibrational quantum number.

The matrix elements for the 0–1, 1–2, and 0–2 transitions were evaluated using the wave functions given by Eq. (22) and the first two terms of the electric dipole moment expansion. The results for the F-factors in the case of the Fues potential are as follows:

$$F_{0-1}(m)\cong 1-4\gamma\theta m\left[1+\gamma\left(\frac{23-12\theta}{8\theta}\right)-m\gamma\left(\theta+\frac{3}{8\theta}\right)\right], \quad (23)$$

$$F_{0-2}(m)\cong 1+4\gamma m \quad (23a)$$

and

$$F_{1-2}(m)\cong 1. \quad (23b)$$

Terms through order γ^2 have been retained in Eq. (23). Only terms through order γ in Eqs. (23a) and (23b) have been retained because of the labor involved in obtaining the higher order corrections in this case.

A comparison of these expressions with those obtained using perturbed harmonic oscillator functions can be made if one expands the Fues potential function about the equilibrium internuclear distance. If one equates the cubic term in the latter expansion to $bhc\omega_e\alpha^{\frac{1}{2}}(r-r_e)^3$, one finds that $b=-\gamma^{\frac{1}{2}}$. Substitution of this value of b into Eq. (21), which gives the F-factor derived for the perturbed harmonic oscillator, leads to the expression

$$F_{0-1}(m)\cong 1-4\theta\gamma m\left[1+\gamma\left(\frac{23-36\theta}{8\theta}\right)-m\gamma\left(\theta+\frac{3}{8\theta}\right)\right] \quad (24)$$

which differs from Eq. (23) only in one of the terms quadratic in γ. For the 0–2 transition it may be seen that with the substitution $b=-\gamma^{\frac{1}{2}}$, Eq. (21b) for the perturbed harmonic oscillator differs from Eq. (23a) for the Fues potential in the dependence of the first-order term in γ on θ. For these two transitions the F factor is rather insensitive to the omission of the higher terms in the rotation-vibration interaction term expansion or to the exact form of the potential function $U(r)$.

Equation (23b) for the 1–2 transition, on the other hand, shows no J dependence to order γ in contrast to Eq. (21a). Formally, this result is a consequence of the orthogonality of the radial functions to the order of γ considered, but the physical significance of the result is not clear.

The quantity θ which occurs in the F factors involves M_0, the electric dipole moment at the equilibrium internuclear distance, and M_1, the so-called "effective charge." The value of M_0 may be obtained from dielectric constant measurements. The value of M_1 may be determined from the total integrated intensity of a transition such as the 0–1 transition.

Expressions for the total integrated intensity of a vibration-rotation band can be obtained in general by summing Eq. (19) over all non-negative integral values of J and over the P and R branches. The number of molecules $N_{v,J}$ in the Jth rotational state of the vth vibrational state is given by

$$N_{v,J}=N_v Z_v^{-1}(2J+1)\exp[-E_v(J)/kT] \quad (25)$$

where N_v is the total number of molecules in the vth vibrational state, Z_v is the rotational partition function for the vth state given by

$$Z_v=\sum_{J=0}^{\infty}(2J+1)\exp[-E_v(J)/kT], \quad (25a)$$

and $E_v(J)$ is the energy of the state having quantum numbers v,J referred to the state $v=v$, $J=0$. The energy $E_v(J)$ has been approximated by the expression

$$E_v(J)=hcB_vJ(J+1) \quad (25b)$$

where

$$B_v=B_e-\alpha_e(v+\tfrac{1}{2}) \quad (25c)$$

and α_e is a constant. The frequency $\omega_v{}^{v'}(m)$ has been approximated by

$$\omega_v{}^{v'}(m)=\omega_v{}^{v'}+2\bar{B}m+B_-m^2 \quad (25d)$$

where

$$B_-=B_{v'}-B_v, \quad (25e)$$

$$2\bar{B}=B_{v'}+B_v, \quad (25f)$$

$$\omega_v{}^{v'}=\omega_e(v-v')[1-x_e(v'+v+1)], \quad (25g)$$

and x_e is a constant which takes into account the mechanical anharmonicity. The F factor for the various transitions may be expressed by the following general formula

$$F(m)=1-c_1m+c_2m^2 \quad (26)$$

where, for example, expressions for c_1 and c_2 for the various transitions discussed may be obtained by rearrangement of Eqs. (21), (21a), and (21b) or Eqs. (23), (23a), and (23b).

In addition to the partition function the sums which occur in summing Eq. (19) may be expressed in the form

$$Y(v,p)=\sum_{j=0}^{\infty}[J(J+1)]^p(2J+1)\exp[-\sigma_vJ(J+1)] \quad (27)$$

where

$$p=1,2 \quad (27a)$$

and

$$\sigma_v=\frac{hcB_v}{kT}. \quad (27b)$$

The sums were evaluated approximately using the Euler-Maclaurin summation formula. The results are

$$Z_v=\left(1+\frac{1}{3}\sigma_v+\frac{1}{15}\sigma_v^2\right)\Big/\sigma_v, \quad (28)$$

$$Y(v,1)=\left(1-\frac{1}{15}\sigma_v^2-\frac{1}{30}\sigma_v^3\right)\Big/\sigma_v^2, \quad (28a)$$

and

$$Y(v,2)=\left(2+\frac{1}{30}\sigma_v^3-\frac{1}{120}\sigma_v^4\right)\Big/\sigma_v^3. \quad (28b)$$

The expression for the total integrated intensity $I_v{}^{v'}$ may be written in the form

$$I_v{}^{v'}=\frac{8\pi^3N_v}{3hc}|R_v{}^{v'}|^2\bar{\omega}_v{}^{v'} \quad (29)$$

where

$$\bar{\omega}_v{}^{v'}=\omega_v{}^{v'}(1+\epsilon_1)+2\bar{B}(1+\epsilon_2)+B_-(\kappa_1+\epsilon_3), \quad (29a)$$

$$\epsilon_1=-\tau-c_1(1+\tau)+c_2(\kappa_1-\kappa_1'\tau), \quad (29b)$$

$$\epsilon_2=\tau-c_1(\kappa_1-\kappa_1'\tau)+c_2[(2\kappa_1-1)+(2\kappa_1'-1)\tau], \quad (29c)$$

$$\epsilon_3=-\kappa_1'\tau-c_1[(2\kappa_1-1)+(2\kappa_1'-1)\tau]+c_2[(3\kappa_1+\kappa_2-2)-(3\kappa_1'+\kappa_2'-2)\tau], \quad (29d)$$

$$\kappa_1=1+Y(v,1)/Z_v, \quad (29e)$$

$$\kappa_1'=1+Y(v',1)/Z_{v'}, \quad (29f)$$

$$\kappa_2=Y(v,2)/Z_v, \quad (29g)$$

$$\kappa_2'=Y(v',2)/Z_{v'}, \quad (29h)$$

and

$$\tau=(Z_{v'}/Z_v)\exp(-hc\omega_v{}^{v'}/kT). \quad (29i)$$

Crawford and Dinsmore[15] have derived an expression for the total integrated intensity which is similar to Eq. (29) but which does not contain the small corrections arising from the vibration-rotation interaction contained in the F-factor. The quantity τ is introduced to allow for the contribution of induced emission to the apparent intensity of absorption.

[15] B. L. Crawford, Jr., and H. L. Dinsmore, J. Chem. Phys. **18**, 983 (1950); **18**, 1682 (1950).

The coefficient M_1 may be determined by successive approximations from Eq. (29) applied to, say, the 0–1 transition. If one sets c_1 and c_2 equal to zero and replaces $R_v^{v'}$ by $M_1/2\alpha$, one may calculate a first approximation to M_1 using Eq. (29), measured values of I_0[1] and N_v, and known values of the necessary molecular constants. This value of M_1 can then be used to calculate c_1, c_2, and $\bar{\omega}_v^{v'}$ after which a second approximation to M_1 can be obtained.

Qualitatively, the effect of the interaction of rotation and vibration is to enhance or depress the intensity of a line in the R branch relative to the corresponding line in the P branch. The value of the ratio of the intensities of two such lines depends on the sign and magnitude of the molecular constant θ. The latter may in principle be determined from this intensity ratio or from the ratio of the integrated intensities of the R and P branches taken separately. Theoretical expressions for the R and P branch integrated intensities, $I_v^{v'}(R)$ and $I_v^{v'}(P)$, have been derived from Eq. (18) with the aid of the Euler-Maclaurin summation formula. The result for the P branch is

$$I_v^{v'}(P)=\frac{8\pi^3 N_v}{3hcZ_v}|R_v^{v'}|^2(\Phi_{1,P}-\Phi_{2,P}), \tag{30}$$

where

$$\Phi_{1,P}=\{\omega_v^{v'}[K_{1,P}+c_1K_{2,P}+c_2K_{3,P}]+2\bar{B}[-K_{2,P}-c_1K_{3,P}-c_2K_{4,P}]+B_-[K_{3,P}+c_1K_{4,P}+c_2K_{5,P}]\}, \tag{30a}$$

$$\Phi_{2,P}=\exp(-hc\omega_v^{v'}/kT)\times\{\omega_v^{v'}[K'_{1,P}-c_1K'_{2,P}+c_2K'_{3,P}]+2\bar{B}[K'_{2,P}-c_1K'_{3,P}+c_2K'_{4,P}]+B_-[K'_{3,P}-c_1K'_{4,P}+c_2K'_{5,P}]\}, \tag{30b}$$

$$K_{1,P}=\frac{1}{2\sigma_v}-\frac{1}{2}K_0-\frac{1}{12}-\frac{1}{240}(2-\sigma_v)\sigma_v, \tag{30c}$$

$$K_{2,P}=-\frac{1}{4\sigma_v}+\left(\frac{1}{2\sigma_v}+\frac{1}{4}\right)K_0-\frac{1}{120}\sigma_v, \tag{30d}$$

$$K_{3,P}=\frac{1}{2\sigma_v^2}+\frac{1}{8\sigma_v}-\frac{1}{4}\left(\frac{3}{\sigma_v}+\frac{1}{2}\right)K_0+\frac{1}{120}, \tag{30e}$$

$$K_{4,P}=-\frac{5}{8\sigma_v^2}-\frac{1}{16\sigma_v}+\frac{1}{4}\left(\frac{3}{\sigma_v^2}+\frac{3}{\sigma_v}+\frac{1}{4}\right)K_0, \tag{30f}$$

$$K_{5,P}=\frac{1}{\sigma_v^3}+\frac{9}{16\sigma_v^2}+\frac{1}{32\sigma_v}-\frac{1}{8}\left(\frac{15}{\sigma_v^2}+\frac{5}{\sigma_v}+\frac{1}{4}\right)K_0, \tag{30g}$$

$$K_0=[\pi/(4\sigma_v)]^{\frac{1}{2}}\exp(\sigma_v/4)\operatorname{erfc}(\sigma_v^{\frac{1}{2}}/2), \tag{30h}$$

and

$$\operatorname{erfc}(a)=(2/\sqrt{\pi})\int_a^\infty \exp(-t^2)dt. \tag{30i}$$

The quantities $K'_{i,P}$, $i=1, 2, \cdots 5$ are obtained from the quantities $K_{i,P}$ by replacing σ_v by $\sigma_{v'}$.

The result for R branch is

$$I_v^{v'}(R)=\frac{8\pi^3 N_v}{3hcZ_v}|R_v^{v'}|^2(\Phi_{1,R}-\Phi_{2,R}) \tag{31}$$

where

$$\Phi_{1,R}=\omega_v^{v'}[K_{1,R}-c_1K_{2,R}+c_2K_{3,R}]+2\bar{B}[K_{2,R}-c_1K_{3,R}+c_2K_{4,R}]+B_-[K_{3,R}-c_1K_{4,R}+c_2K_{5,R}], \tag{31a}$$

$$\Phi_{2,R}=\exp(-hc\omega_v^{v'}/kT)\times\{\omega_v^{v'}[K'_{1,R}+c_1K'_{2,R}+c_2K'_{3,R}]-2\bar{B}[K'_{2,R}+c_1K'_{3,R}+c_2K'_{4,R}]+B_-[K'_{3,R}+c_1K'_{4,R}+c_2K'_{5,R})\}, \tag{31b}$$

$$K_{m,R}=\sum_{n=0}^{m}\binom{m}{n}K_{n,P}, \tag{31c}$$

and

$$K_{0,P}=K_0+\frac{1}{2}+\frac{1}{12}\sigma_v. \tag{31d}$$

As with the P branch the $K'_{i,R}$ are obtained from the $K_{i,R}$ by replacing σ_v by $\sigma_{v'}$. The quantities $\Phi_{2,P}$ and $\Phi_{2,R}$ represent contributions of induced emission to the apparent absorption intensities.

If one takes the ratio of Eqs. (30) and (31) one obtains

$$\frac{I_v^{v'}(P)}{I_v^{v'}(R)}=\frac{\Phi_{1,P}-\Phi_{2,P}}{\Phi_{1,R}-\Phi_{2,R}}. \tag{32}$$

If experimental values are substituted for $I_v^{v'}(P)$ and $I_v^{v'}(R)$ in Eq. (32) one has an equation quadratic in θ which may be solved to yield the value of θ.

III. DISCUSSION

The results contained in this paper constitute a generalization of those obtained by Oppenheimer[3] who considered a special model of a molecule having $\theta=+1$ where θ is the ratio of the permanent dipole moment to the product of the effective charge and equilibrium internuclear distance, i.e., $M_0/(M_1 r_e)$. Our formula for the intensity of a line in the 0–1 transition reduces to that of Oppenheimer if $\theta=+1$ and if anharmonicity is neglected. The case $\theta=+1$ is valid for a molecule consisting of point charges or may occur fortuitiously in a more realistic model. From the experimental work of Rollefson and Rollefson[16] and Havens[17] and our own to appear in a subsequent publication it would appear

[16] R. Rollefson and A. H. Rollefson, Phys. Rev. **48**, 779 (1935).
[17] R. J. Havens, "The variation of the electric moment of carbon monoxide and of nitric oxide with internuclear distance," Doctoral Dissertation, University of Wisconsin, 1938.

that for carbon monoxide $|\theta| \ll 1$ whereas for hydrogen chloride $\theta \sim +1$.

Our result for the F-factor for the 0–2 transition as given by Eq. (21b) is qualitatively similar to that of Dunham[6] but differs in the dependence of the first order term on θ. The difference in the two results appears to arise from the use of different potential functions and different approximations. Dunham does not give the second-order term.

For molecules having $|\theta| \ll 1$ the F-factors for the 0–1 and 1–2 transitions as given by Eqs. (21) and (21a) are very close to unity for moderate J values. The effect of the interaction of rotation and vibration is therefore quite small and the use of Oppenheimer's result leads to erroneous results.

For the 0–2 transition the effect may be appreciable even though $|\theta| \ll 1$. The magnitude of the effect depends primarily on the values of γ and b rather than on that of θ. It may be noted in this connection that the sign of b is ordinarily negative whereas that of γ is positive. Calculations by the present authors to be reported indicate that for CO the F factor leads to an enhancement of the R branch and a depression of the P branch by about five percent at $J=10$. Goldberg and Müller[18] have concluded from a study of the 2–0, 3–1, 4–2, and 5–3 transitions in the solar spectrum of CO that the F factor is much closer to unity for these transitions than is the F factor calculated from Oppenheimer's formula. Further theoretical and experimental work seems required to determine whether the results of Goldberg and Müller are consistent with those of the present authors.

For molecules having $|\theta| \sim 1$ the effect of the interaction in the 0–1 and 1–2 transitions depends drastically on the sign of θ. If θ is positive the R branch is depressed and the P branch is enhanced for moderate J values. The reverse is true if θ is negative. In a subsequent paper it is shown that the experimental individual line intensities for HCl are sufficiently precise so that the sign of θ can be unambiguously determined to be positive. For the 0–2 transition in this case the sign of θ is quite important in contrast to the case of $|\theta| \ll 1$. Calculations for HCl indicate that if $\theta \sim +1$, the R branch is depressed by about fifteen percent and the P branch is enhanced by about five percent at $J=10$. For $\theta \sim -1$, on the other hand the R branch is enhanced by about seventy percent while the P branch is depressed by about fifty percent at $J=10$.

It may elucidate the above discussion if one gives a semi-classical description of the influence of the vibration-rotation interaction on the intensity of a vibration-rotation line. Because of the conservation of angular momentum the angular velocity of a vibrating-rotating diatomic molecule decreases and increases about the mean value Ω as the atoms are farther or less apart than the mean value r_e. In another manner of speaking the atoms execute small vibrations in a direction perpendicular to their line of centers. If one assumes simple harmonic motions, then the component of the acceleration (neglecting the centripetal acceleration) of one of the nuclei along the line of centers can be written as

$$a_x = a_0 \cos\omega_v t$$

while the component perpendicular to the line of centers can be obtained from the Coriolis acceleration and is

$$a_y = -\frac{2\Omega}{\omega_v} a_0 \sin\omega_v t$$

where the angular velocity of the molecule Ω is given by $\Omega = J\omega_r$. It should be noted that with respect to the coordinate system rotating with the mean angular velocity Ω the nuclei move in retrograde ellipses.

In classical theory the rate of radiation of energy from an accelerating point charge is proportional to the square of the product of the magnitudes of the charge and acceleration. The effective charge displaced perpendicular to the line of centers in the rotation is M_0/r_e while that displaced along the line of centers in the vibration is M_1. In the foregoing frame of reference just noted these quantities can be resolved into two circularly polarized components, namely,

$$A_1 = (a_0 M_1/2)(1 - 2\gamma'\theta J)$$

and

$$A_2 = (a_0 M_1/2)(1 + 2\gamma'\theta J)$$

where $\gamma' = \omega_r/\omega_v$. The quantities A_1 and A_2 refer to the advanced and retrograde motions of the nuclei with respect to the direction of the angular velocity of the molecule as a whole.

The ratio of the intensities of the radiation emitted in these two types of motion according to classical theory is given by

$$\left|\frac{A_1}{A_2}\right|^2 = \frac{1 - 4\gamma'\theta J}{1 + 4\gamma'\theta J}. \tag{33}$$

This is the essential result obtained in the body of this paper if one notes that the circularly polarized radiation is emitted with its angular momentum vector parallel to the angular momentum vector of the circulating charge. In the advanced and retrograde motions the the emitted quanta are radiated with angular momenta such as to decrease and increase the total angular momentum of the molecule; hence, the numerator and denominator in Eq. (33) refer to the R and P branches, respectively.

The result given by Eq. (33) is identical to first order in γ to that specified by Eqs. (21) and (21a) for the 0–1 and 1–2 transitions if one sets $\gamma' = \gamma = \omega_r/\omega_e$. To compare Eq. (33) with the results for the 0–2 transition given by Eq. (21b) it is convenient to let b become very large so that the terms depending on the anharmonicity

[18] L. Goldberg and E. A. Müller, Astrophys. J. 118, 397 (1953).

are isolated and terms depending only on the rotation-vibration interaction are neglected. Then if one sets $\omega_v = 2\omega_e$ so that $\gamma' = \gamma/2$, the results specified by Eq. (21b) agree with those of Eq. (33).

In conclusion one might re-emphasize the importance of taking into account properly the rather large influence of the vibration-rotation interaction on line intensities for many molecules especially in determining "temperature" from line intensity distributions. Experimental values of vibration-rotation line intensities of HCl and of CO to be reported in a subsequent paper confirm the importance of the vibration-rotation interaction as well as the strong dependence of the F-factor on θ. The data show unequivocally that the sign of θ for HCl is positive rather than negative. Work is in progress on extending the results of this paper to molecules in states other than Σ-states such as OH and NO as well as in examining the feasibility of extending the treatment to molecules described by a Morse potential function. Finally, it should be noted that the influence of vibration-rotation interaction on line intensities might be important in forbidden electronic transitions.

IV. ACKNOWLEDGMENTS

The authors wish to express their appreciation to Dr. K. E. Shuler who provided much of the stimulation to carry out the present research. We also thank Dr. W. S. Benedict and Dr. S. Silverman for their interest and many profitable discussions. We are especially indebted to Dr. J. W. Follin, Jr. for his invaluable assistance in developing the semiclassical interpretation of the influence of vibration-rotation interaction on line intensity. Finally, we thank Miss Shirley Thomas for her aid in the preparation of this manuscript.

THE JOURNAL OF CHEMICAL PHYSICS VOLUME 23, NUMBER 4 APRIL, 1955

Vapor Absorption Spectra of Light and Heavy Naphthalenes at 2900–2500 A*

H. SPONER AND C. D. COOPER†
Department of Physics, Duke University, Durham, North Carolina
(Received August 23, 1954)

The 2900–2500 A region of absorption in both light and heavy naphthalene is interpreted as an allowed $A_{1g}-B_{2u}$ transition, and the bands at 35 910 and 36 040 cm^{-1} are assigned as the respective 0,0 bands. Upper-state frequencies of 485, 710, 995, 1390, 1520, and 1600 cm^{-1} and the ground-state frequencies of 495, 755, 1024, and 1380 cm^{-1} in the ordinary naphthalene spectrum are correlated with previously reported Raman frequencies. A corresponding interpretation is given for the vibrational frequencies occurring in the spectrum of deuterated naphthalene. The general appearance of the spectrum is compared with recent absorption curves in solid solution by Passerini and Ross, and with crystal data obtained with polarized light. Possible occurrence of vibrationally induced "forbidden" bands is discussed.

INTRODUCTION

THE near-ultraviolet absorption spectra of naphthalene have been studied by many investigators. As early as 1881 the solution spectrum[1] was reported. Since then more reliable data have been published, for example, by Morton and de Gouveia,[2] Mayneord and Roe,[3] and the American Petroleum Institute.[4] The vapor spectrum was first reported by Purvis[5] in 1912. More detailed spectrograms and detailed tables were published by Henri and de Laszlo[6,7] in 1924. The absorption spectrum of the solid was studied by Seshan,[8] Sirkar,[9] and Prikhotjko.[10,11] Both the infrared[12–14] and Raman spectra[15,16] of naphthalene are known.

For deuterated naphthalene, the spectroscopic data available are rather meager because many of them are in abstract or review form or unpublished‡ (infrared,[17,18] Raman,[19,20] electronic spectra[21,22]).

* Research assisted by the Office of Naval Research under contract with Duke University.

† Present address: Physics Department, University of Georgia, Athens, Georgia.

[1] W. N. Hartley, J. Chem. Soc. **39**, 153 (1881).

[2] R. H. Morton and A. J. A. de Gouveia, J. Chem. Soc. **137**, 911 (1934).

[3] W. V. Mayneord and E. M. F. Roe, Proc. Roy. Soc. (London) **A152**, 299 (1935).

[4] A. P. I. Research Project 44 at N. B. S., Catalog of Ultraviolet Spectrograms. Ser. No. 87, California Research Corporation.

[5] J. E. Purvis, J. Chem. Soc. **101**, 1315 (1912).

[6] V. Henri and H. de Laszlo, Proc. Roy. Soc. (London) **A105**, 662 (1924).

[7] H. de Laszlo, Z. phys. Chem. **118**, 369 (1925).

[8] P. K. Seshan, Proc. Indian Acad. Sci. **3**, 148 (1936).

[9] S. C. Sirkar, Indian J. Phys. **10**, 109 (1936).

[10] A. Prikhotjko, J. Phys. (USSR) **8**, 257 (1944).

[11] A. Prikhotjko, Izvest. Akad. Nauk USSR, Ser. Fiz. **12**, 499 (1948).

[12] P. Lambert and J. Lecomte, Ann. phys. **18**, 329 (1932).

[13] Barnes, Gore, Liddell, and Williams, *Infrared Spectroscopy* (Reinhold Publishing Corporation, New York, 1944), p. 56.

[14] G. C. Pimentel and A. L. McClellan, J. Chem. Phys. **20**, 270 (1952).

[15] K. W. F. Kohlrausch, *Ramanspektren, Akademische Verlagsgesellschaft*, (Becker and Erler, Leipzig, 1943), pp. 385–390.

[16] H. Luther and B. Hampel, Z. physik. Chem. **202**, 390 (1954).

‡ *Note added in proof.*—These papers have been published in the meantime: reference 18, Person, Pimentel, and Schnepp, J. Chem. Phys. **23**, 230 (1955); A. L. McClellan and G. C. Pimentel, J. Chem. Phys. **23**, 245 (1955); reference 20, E. R. Lippincott and E. J. O'Reilly, Jr., J. Chem. Phys. **23**, 238 (1955); reference 32, Donald S. McClure, J. Chem. Phys. **22**, 1668 (1954).

[17] L. Corrsin, Phys. Rev. **79**, 235A (1950).

[18] Person, Pimentel, and Schnepp, J. Chem. Phys. (to be published).

[19] H. Luther, Abh. Braunschweig. Wiss. Ges. **1**, 33 (1949); Goubeau, Luther, Feldmann, and Brandes, Ber. deut. chem. ges. **86**, 214 (1953).

EXPERIMENTAL PROCEDURE

The naphthalene used in this research was purified by Dr. L. Corrsin. He obtained Eastman Kodak's highest purity naphthalene and refluxed it over sodium to remove a suspected thionaphthene impurity. Further purification was carried out by repeated recrystallization. Dr. Corrsin also prepared the deuterated naphthalene by exchange with D_2SO_4. The sample used contained about 99 atom percent deuterium.

The optical arrangement used in this research and the method of controlling the number of molecules in the light path are the same as that used for previous studies from this laboratory. A quartz absorption cell 75 cm in length was used. A 2300-volt ac hydrogen lamp served as a light source and an iron arc was utilized to produce a comparison spectrum. The spectrograph consisted of a 3-meter reflection grating in a modified Eagle mounting. The grating was used in the first order giving a practically linear dispersion of 5.535 A/mm Eastman Kodak II-0 and II-0 U.V. spectroscopic plates were used and they were developed for five minutes in D-19 developer. The vapor pressures for the different temperatures were obtained from the measurements of Schlumberger[23] and Speranski.[24]

EXPERIMENTAL RESULTS

The light and heavy naphthalene spectra were studied in dependence on their temperature and vapor pressure for temperatures between −15° and 130°C. For both compounds a few broad absorption bands are observed around 2250 to 2050 A for a substance temperature of 0°C (0.006 mm Hg). At the higher temperature of 20°C (0.054 mm Hg) there is complete absorption in the above region and many diffuse bands are found between 2900 and 2500 A. For a temperature of 65°C (2.65 mm Hg) many sharp bands are observed between 3100 and 2900 A.

Primarily, this paper deals with the absorption system of medium intensity between 2900 and 2500 A, but the absence in our spectra of the strong bands reported by Henri and de Laszlo between 2935 and 2948 A should be noted. A study of the thionaphthene spectrum in our laboratory[22,25] showed that these bands as well as some weaker ones in the 2900 A region were due to a thionaphthene impurity in Henri and de Laszlo's sample.

The strongest bands in the 2900–2500 A region of the naphthalene spectrum are located at 35 910, 37 300, and 38 720 cm^{-1}. These bands are diffuse and are just detectable on a spectroscopic plate for a substance temperature of 0°C (0.006 mm Hg). With increasing temperature and pressure, close lying diffuse bands appear on the red side of each band. Figure 1 shows the fully-developed band system at 20°C (0.05 mm Hg) and here it can be seen that most of the bands fit into three reoccurring groups which have the three strong bands mentioned above as their band of longest wavelength. The bands are degraded toward the red and the ultraviolet edge of each band was measured. All of the measured bands are given in Table I. The 2900–2500 A absorption region in the deuterated naphthalene spectrum resembles very closely the corresponding absorption in naphthalene. The most noticeable difference is the shift of the 35 910 cm^{-1} naphthalene band to 36 040 cm^{-1} in the spectrum of the deuterated sample. A print of this spectrum is shown in Fig. 1 and the measured bands are recorded in Table II. In both Tables I and II, column one contains the wavelengths. Column two gives the separation from the chosen 0,0 band, and column three gives intensity data for different temperatures and pressures. Assignments are given in the last column. Most of the wavelength measurements were recorded to the nearest Angstrom because of the diffuseness of the bands involved. The wave numbers are accurate to within 10 or 15 wave numbers, except for those

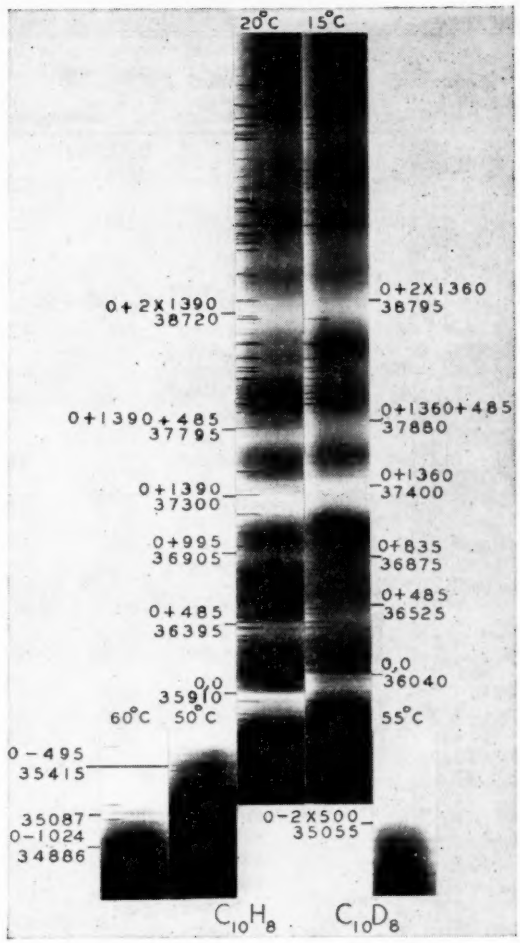

Fig. 1. Absorption spectra of light and heavy naphthalene at 2900–2500 A.

[20] E. R. Lippincott and E. J. O'Reilly, Jr., J. Chem. Phys. (to be published).
[21] C. D. Cooper and H. Sponer, Phys. Rev. **87**, 213A (1952).
[22] H. Sponer and Gertrud P. Nordheim, Discussions Faraday Soc. **9**, 19 (1950).
[23] E. Schlumberger, J. Gasbel **55**, 1257 (1912).
[24] A. Speranski, Z. phys. Chem. **46**, 74 (1903).
[25] R. C. Heckman, Phys. Rev. **91**, 242A (1953).

TABLE I. Absorption bands of naphthalene vapor in the 2900 to 2500 A region.

Wave number cm^{-1}	Separation from 0,0 band	Intensity $t=60°C$ $p=1.83$ mm Hg	Intensity $t=70°C$ $p=3.95$ mm Hg	Assignments
34 537	−1373	vw-d-B	mw	0−1380?
555	−1355		mw-d	
558	−1352	ew	m-d	
569	−1341	ew	m-d	
580	−1330	vw	m-d	
592	−1318	mw	m-sd	
614	−1296	w	m-d	
624	−1286	w	m-sd	0−1380+90?
831	−1079	ew-d		
			$t=50°C$ $p=0.82$ mm Hg	
844	−1066	vw-d	ew	
856	−1054	vw-d	vw	
877	−1033	w-sd	vw	
886	−1024	mw-sh		0−1024?
965	−945	ew-ed-B		0−943?
35 004	−906		ew	
012	−898	ew-d	ew	
021	−889	vw-d	ew	
032	−878	vw-sd	ew	0−878?
047	−863	m-d	w	
058	−852	ms-d	ms	
068	−842	s-sd	ms	
077	−833	s-sd	ms	
087	−823	s-sd	ms	
		$t=20°C$ $p=0.05$ mm Hg		
155	−755		ew-ed-B	0−755
325	−585		vw-ed-B	
415	−495		m-ed-B	0−495(512R)
475	−435		vs-vd	
534	−376		s-sd	0−2×191?
544	−366		s-sd	0−2×176?
715	−195	vw-ed		0−195
730	−180	vw-ed		0−130−50
770	−140	vw-vd		0−140
780	−130	mw-vd		0−130; 0−2×65
820	−90	w-vd		0−90; 0−2×50
845	−65	w-vd		0−65; 0−195+130
860	−50	vw-vd		0−50
910	0	s-vd		0,0
920	10	s-d		0+10
935	25	ew-vd		
36 000	90	w-vd		0+90
025	115	ew-d		
040	130	ew-d		0+130
285	375	vw-d		0+485−2×50
315	405	vw-d		0+485−80

Wave number cm^{-1}	Separation from 0,0 band	Intensity $t=20°C$ $p=0.05$ mm Hg	Assignments
340	430	mw-vd	0+485−50
395	485	mw-vd	0+485
500	590	ew-ed	
525	615	ew-d	0+485+130
550	640	ew-d	0+710−65
620	710	ew-vd	0+710
780	870	ew-ed	0+995−130
850	940	ew-ed	0+995−50
905	995	w-ed	0+995
960	1050	ew-ed	
37 080	1170	ew-ed	
135	1225	ew-ed	
165	1255	vw-ed	0+1390−130
220	1310	m-ed	0+1390−80
245	1335	ms-ed	0+1390−65
260	1350	s-ed	0+1390−50
300	1390	vs-vd	0+1390
315	1405	m-vd	0+1390+15
360	1450	w-ed	0+1520−65
430	1520	m-ed	0+1390+130; 0+1520
455	1545	ew-ed	0+1600−50
470	1560	ew-ed	
510	1600	vw-ed	0+1600
585	1675	ew-vd	
710	1800	w-ed	0+485+1390−80
755	1845	ms-ed	0+485+1390−50
795	1885	ms-ed	0+485+1390
810	1900	m-ed	0+485+1390+15
870	1960	ew-ed	
925	2015	vw-ed	0+485+1390+130
38 025	2115	ew-ed	0+710+1390
155	2245	ew-ed	0+995+1390−140
185	2275	ew-ed	0+995+1390 −2×50
245	2335	w-ed	0+995+1390−50
290	2380	mw-ed	0+995+1390
360	2450	ew-ed	
630	2720	m-ed	0+2×1390−80
675	2765	ms-ed	0+2×1390−50
720	2810	ms-ed	0+2×1390
765	2855	mw-ed	0+1520+1390−50
810	2900	mw-ed	0+1520+1390
39 125	3215	w-vd	0+2×1600
175	3265	vw-ed	
205	3295	vw-ed	0+485+2×1390
265	3355	ew-ed	
325	3415	ew-ed	
40 150[a]	4240	ew-ed-B	0+3×1390; 0+1520+1390

[a] Center of absorption about 200 cm^{-1} in width.

bands that are extremely diffuse. For these extremely diffuse bands the measurement may be in error by 30 cm^{-1} or more. Under the intensity column, estimates of the band intensity are given. They were obtained from microphotometer tracings (Jarrell-Ash microphotometer) and have been supplemented by visual estimates where necessary. The scale used is as follows: vs—very strong, s—strong, ms—medium strong, m—medium, mw—medium weak, w—weak, vw—very weak, and ew—extremely weak. Other notations used in the intensity column to indicate the diffuseness of the band head and to designate the broad bands are: sh—sharp, sd—slightly diffuse, d—diffuse vd—very diffuse, ed—extremely diffuse, β-broad.

DISCUSSION

The spectrum studied here represents the second absorption region of the naphthalene molecules for which an allowed transition is expected with polarization along the short axis.[26] Since both light and heavy naphthalene have D_{2h} symmetry, the transition is of type $A_{1g}-B_{2u}$.

The strong bands at 35 910 cm^{-1} in light naphthalene and 36 040 cm^{-1} in heavy naphthalene suggests themselves as the respective 0,0 bands. The observed 130 cm^{-1} shift of the 0,0 band, caused by the substitution of

[26] For latest discussion see W. Moffitt, J. Chem. Phys. 22, 320 (1954).

TABLE II. Absorption bands of deuterated naphthalene vapor in the 2900 to 2500 A region.

Wave number cm^{-1}	Separation from 0,0 band	Intensity $t=65°C$ $p=2.65$ mm Hg	Intensity $t=55°C$ $p=1.26$ mm Hg	Assignments
34 562	−1480	ew-ed	ew	
572	−1470	ew-d	ew	
591	−1450	ew-sd		
602	−1440	ew-sd		
612	−1430	ew-d		
631	−1410	ew-d		
		$t=45°C$ $p=0.52$ mm Hg		
820	−1220	ew	ew-ed-B	
895	−1145	ew	ew-ed-B	
995	−1085	ew	vw-vd-B	
35 000	−1035		ew-ed	0−2×500−45?
055	−985	ew	ew-ed-B	0−2×500?
225	−815	ew	ew-ed-B	
250	−790	ew-ed		
315	−725	ew-ed		
365	−675	ew-ed		0−500−185
400	−640	ew-ed		0−500−145
			$t=35°C$ $p=0.21$ mm Hg	
490	−550	mw-ed-B	vw	0−500−45
540	−500	s-ed-B	mw	0−500(491R)
600	−440		vw-ed-B	0−500+50
		$t=15°C$ $p=0.04$ mm Hg		
855	−185	vw-vd		0−185
895	−145	vw-vd		0−145
910	−130	vw-vd		0−130; 0−2×65
950	−90	s-vd		0−90
975	−65	s-vd		0−65; 0−185+115
36 000	−40	w-vd		0−45
040	0	ms-vd		0,0
050	10	vw-vd		0+10
090	50	mw-vd		0+50
155	115	ew-vd		0+115
195	155	ew-ed		0+155
340	300	w-ed		0+485−185
365	325	w-vd		0+485−160
380	340	mw-vd		0+485−145
430	390	vw-vd		0+485−90
460	420	w-vd		0+485−65
475	435	vw-vd		0+485−45

Wave number cm^{-1}	Separation from 0,0 band	Intensity $t=15°C$ $p=0.04$ mm Hg	Assignments
525	485	w-vd	0+485
565	525	vw-vd	0+485+50
675	635	ew-ed	0+635; 0+485+155
725	685	ew-vd	0+835−145; 0+635+50
820	780	vw-ed	0+835−65?
875	835	w-ed	0+835
930	890	vw-ed	0+835+50; 0+890
37 025	985	ew-ed	0+835+155; 0+2×485?
260	1220	mw-ed-vB	0+1360−145
300	1260	m-ed	485+835−65?; 0+2×635?
315	1275	m-ed	0+1360−90
360	1320	ms-vd	0+1360−45; 0+485+835
400	1360	vs-vd	0+1360; 0+485 +835+50
455	1415	s-vd	0+1360+50
500	1460	ms-vd	0+1500−45; 0+1360+115
540	1500	m-vd	0+1500
595	1555	mw-vd	0+1500+50
740	1700	mw-vd	0+485+1360 −2×65
810	1770	m-vd	0+485+1360−65
880	1840	ms-vd	0+485+1360
925	1885	m-vd	0+485+1360+50
38 025	1985	ew-vd	0+485+1500; 0+485+1360 +155
070	2030	ew-vd	0+485+1500+50
230	2190	w-vd	0+835+1360
315	2275	w-vd	0+835+1500−45
360	2320	w-vd	0+835+1500
405	2365	vw-vd	0+835+1500+50
735	2695	m-vd	0+2×1360−65
795	2755	ms-vd	0+2×1360
840	2800	m-vd	0+2×1360+50
900	2860	ew-vd	0+1360+1500
945	2905	ew-vd	0+2×1500−50?
990	2950	w-vd	0+2×1500?
39 080	3040	ew-vd	
200	3160	w-ed-B	0+485+2×1360
40 180[a]	4140	vw-ed-B	0+3×1360

[a] Center of broad band.

heavy hydrogen, is due to a change in the zero-point vibrational energies. From the appearance of the spectra it is seen that all strong bands can be explained as resulting from two vibrations with upper state values of 1390 and 485 cm^{-1} in light naphthalene, and 1360 and 485 cm^{-1} in heavy naphthalene. The 1390 and 1360 vibrations occur in progressions and in combination with the 485 vibration. (See Tables I and II). There is no doubt that the 1390 has to be associated with the very strong, polarized Raman line of frequency 1380 cm^{-1} in ordinary naphthalene[15] which had been assigned to a totally symmetric carbon ring vibration. The same value, namely 1380 cm^{-1}, has been found by Lippincott[27] and O'Reilly as a strong line in the Raman spectrum[20] of deuterated naphthalene. Whether this vibrational frequency does increase in the excited state of light naphthalene and decrease in heavy naphthalene cannot be determined with certainty due to the diffuseness and broadness of the absorption bands. In fact, the ground-state frequency of the 1360 vibration could not be ascertained in the spectrum of the heavy molecule. However, the finding of a ground state value of only 1373 for light naphthalene is in agreement with new results in the Raman spectrum,[20] and is there explained[28] as resulting from an accidental degeneracy (Fermi degeneracy) with another vibrational mode.

The 485-cm^{-1} frequency occurs singly excited. It is probably represented in the ground state by the bands at 35 415 (light) and at 35 155 cm^{-1} (heavy) giving fre-

[27] We are grateful to Dr. Lippincott for furnishing us the data on heavy naphthalene prior to their publication.

[28] Information obtained in private discussions with Dr. O'Reilly, Dr. Lippincott, and Dr. Pimentel (see note added in proof on p. 646).

quencies of 495 and 500 cm^{-1}, respectively. It seems logical to associate these frequencies with the strong Raman lines at 512 cm^{-1} (light) and 491 cm^{-1} (heavy). (The reversal in values is probably not genuine in view of the diffuseness and broadness of the bands.) The 512 line has been reported[15] as polarized and hence was assigned to a totally symmetric vibration. The only band that might result from a two-fold excitation of the 485 occurs at 37 025 in the heavy molecule, but no counterpart was found in the spectrum of the light compound. Therefore, the last assignment is considered doubtful. We will come back to the question of the selective excitation of this vibration further below.

Another vibrational frequency is represented by the bands at 36 905 (Table I) and at 36 875 (Table II) giving 995 cm^{-1} in the upper electronic state of light naphthalene and 835 cm^{-1} in heavy naphthalene, respectively. If the bands are associated with the vibration which produces the strong polarized Raman lines at 1022 cm^{-1} [15] and at 862 cm^{-1},[20] the latter frequencies might take part in bands on the red side of the 0,0 band. However, no such band was found in the spectrum of heavy naphthalene, and in light naphthalene, the assignment of band 34 886 to an excitation of the 1022 in the ground state is uncertain because this band may belong to the weaker long wavelength transition. Nevertheless, the mentioned correlation of the 995 and 835 with the Raman values is considered correct. The 1022 cm^{-1} frequency was interpreted by Kohlrausch[15] as a totally-symmetric CH-deformation vibration in the plane.

There is a very weak band at 36 620 cm^{-1} in light naphthalene which may be assigned to a 0–710 transition (Table I). The 710 occurs in combination with the 1380 separation. If it is taken as the upper-state value of the vibration represented in the strong, polarized Raman line of 762 cm^{-1}, it represents a totally-symmetric carbon-ring vibration assuming the interpretation of the Raman line to be correct. The vibration may be present in the ground state in the very weak band at 35 155 cm^{-1}. Bands indicating the corresponding vibration in heavy naphthalene are not obvious, but the extremely weak band at 36 675 may contain the corresponding upper-state vibration of 635 in heavy naphthalene.

There are several bands in both naphthalenes which contain vibrational contributions in the range 1500–1600 cm^{-1}. The interpretation of these bands does not give a complete correspondence for the two molecules but rather leads to some peculiarities which indicate that the interpretation may not be conclusive. For example, there is a medium-intense band at 37 430 in the light naphthalene spectrum giving a vibrational frequency of 1520 which occurs also combined with the 1390 frequency. There are the bands at 37 510 and 39 125 cm^{-1}, also in light naphthalene, which might be members of a 1600 progression, and there are in the spectrum of deuterated naphthalene members of a possible 1500 progression located at 37 540 and 38 990 cm^{-1}. The 1600, if a fundamental, could only be linked with the Raman line at 1625 which Kohlrausch had considered to be totally symmetric, and the 1520 could be linked with the medium strong 1576 Raman line assigned to class β_{1g} by Kohlrausch.[15] It is suggestive to consider the 1500 frequency in the heavy naphthalene spectrum as counterpart of the 1520 in light naphthalene, thus relating it to the Raman line 1548 of deuterated naphthalene.[20] We understand, however, that the tentative assignment of Kohlrausch probably should be reversed.[28] In our case, it means that the bands connected with the 1600 vibration—if it is a fundamental—are longitudinally polarized.

Assignments of most of the companion bands accompanying the main bands are uncertain since their diffuseness allows more than one equally good assignment. The band at 35 715 cm^{-1} in the spectrum of ordinary naphthalene is separated from the 0,0 band by 195 wave numbers and this value coincides with the 191-cm^{-1} Raman frequency. A corresponding band was found in the heavy compound 185 cm^{-1} to the red from the 0,0 band and it coincides well enough with a Raman frequency[20] of 180 cm^{-1}. It should be noted that extremely weak bands were observed 130 cm^{-1} and 115 cm^{-1} to the violet from the 0,0 band in light and heavy naphthalene, respectively, and if taken as upper-state values of the 195 and 185 frequencies, the 65–70 differences in the two spectra could be interpreted as 1,1 and 2,2 transitions of these vibrations. From all this we should like to suggest, although quite tentatively, the 195 and 185 as β_{3g} vibrations. Vibrational analysis from infrared and Raman data favors β_{2g} or β_{3g} type for this vibration[28] but no electric moment is associated with excitation of a β_{2g}-type vibration in an $A_g - B_{2u}$ transition. We would not discuss the assignment of the 195–185 pair to fundamentals had we not observed so many apparently fitting correlations. The assignment is somewhat uncertain since the respective bands would have to be polarized perpendicular to the molecular plane, and such bands have not been identified with certainty in the observed $\pi - \pi$ transitions of aromatic molecules. Of course, the 195 could represent 3×65 ($v - v$ transition) of another vibration, and the 185 could be 3×65 or 2×90, correspondingly. It is indeed possible to find plausible interpretations of many of the smaller separations on the long wavelength side and of some of the short wavelength side of the 0,0 band by assuming plausible frequency decreases of the low vibrations of types β_{1u}, β_{2u}, β_{2g}, β_{3g}, in the upper state, and by using $v - v$ transitions of the same vibration and of different type vibrations so as to give a vibronic transition moment. At present, it is considered premature to report these attempts. This discussion shows the well-known difficulties encountered in the assignment of bands occurring on the red side of the strong bands. They are typical for vapor spectra of aromatic compounds.

Many bands in the region of overlap of the two electronic transitions are not discussed here (some lying beyond the range of Table I and II) because it is believed that they belong to the first weaker transition.

The vibrational frequencies determined from the 2900–2500 A absorption region of both light and heavy naphthalene are collected in Table III.

The analysis presented is neither complete nor entirely satisfactory, but is believed to account for the main features of the spectrum. The outstanding bands involve two vibrations only, the 500 and the 1390 (1360 resp.). In fact, Prikhotjko[11] reported only on these. Their prominence is particularly clear from microphotometer tracings of the plates. We found a comparison very interesting of our plates and tracings with a very good reproduction of the second electronic transition in naphthalene published recently by Passerini and Ross.[29] It shows spectral curves taken in ethanol solution at 50°C, 20°C, and −80°C, and in 4:1 ethanol-methanol mixture at −183°C. The comparison reveals a close resemblance of the spectrum at −183°C with the vapor spectrum. The first peak occurs in solid solution at 34 700, thus establishing a shift of about 1200 cm^{-1} to the red with respect to the vapor. The strong peaks are about 1400 cm^{-1} apart and there are weaker maxima about 500 cm^{-1} toward the short wavelength side of each of the strong peaks. The 995 frequency in the vapor is, in the solid solution curve, recognizable as a step-out.[30]

When analyzing the spectrum it was expected to find "forbidden" bands of noticeable intensity, i.e., bands with longitudinal polarization. The proximity of the strong third electronic transition assumed to be polarized in the long axis could induce appearance of such bands through coupling with a β_{1g} vibration. Theoretically, a strong interaction of this type has been expected for the second transition of naphthalene.[26] Corresponding forbidden bands have been found in the near-ultraviolet absorption spectra (first electronic transitions) of benzene derivatives, and it was observed that their appearance is slightly different from that of the regular bands of the system.[31] Unfortunately, the diffuseness of the second absorption system in naphthalene invalidates this criterion. However, excitation of a β_{1g} vibration (433 cm^{-1} upper-state value) is now being held responsible[32] for the strong portion of the first electronic transition ($A_{1g}-B_{3u}$). Consequently, this portion is short-axis polarized (connecting the 0−1 band of Nordheim and Sponer with a β_{1g} rather than with a β_{1u} vibration). As previously mentioned, a 485-cm^{-1} vibration appears strongly in the second transition of both naphthalenes. It may be added at this point that a separation of 485 is also found in the overlap region of the two systems. Although the 485 occurs apparently singly excited in the second system, it was pointed out above that a correlation with the polarized Raman lines of 512 and 491 cm^{-1} is suggestive. However, from the vapor spectrum alone it cannot be ruled out entirely that a β_{1g} vibration may be involved in the bands under discussion. The 485 could represent a β_{1g} vibration, or the band 0+485−55 (Table I) might involve a separate vibration of 430 cm^{-1}. In the first case, a noticeable portion of the spectrum would have to be long axis polarized. Comparison with the crystal spectrum[10] (taken with polarized and unpolarized light) is difficult, as has been mentioned previously.[22] Considering the geometrical arrangement of the molecules in the crystal,[33] it seems that mainly short-axis polarization was observed whether the electric vector of the incident light was parallel to the *a* or to the *b* axis of the crystal. The latter case gave the more intense spectra, which was confirmed in later work by Craig and Lyons.[34] However, new results by McClure[32,35] in mixed crystals of naphthalene and durene show conclusively that the second transition is predominantly short-axis polarized. Taking the short-axis polarization as established, the structure and appearance of the vapor spectrum indicates that the longitudinal component of the system is very weak if the plausible assumption is made that the 485-cm^{-1} separation represents a totally symmetric vibration.

TABLE III. Vibrational frequencies obtained from the 2900–2500 A spectral region of light and heavy naphthalene.

Light naphthalene		Heavy naphthalene		
Lower state cm^{-1}	Upper state cm^{-1}	Lower state cm^{-1}	Upper state cm^{-1}	Symmetry
195	130	185	115	β_{3g}?
495	485	500	485	α_{1g}
755	710		635	α_{1g}
1024	995		835	α_{1g}
	1390		1360	α_{1g}
	1600			
	1520		1500	

We are indebted to Dr. E. R. Lippincott, Dr. D. S. McClure, Dr. E. J. O'Reilly, Jr., and Dr. G. C. Pimentel for stimulating discussions.

[29] R. Passerini and I. G. Ross, J. Sci. Instr. **30**, 274 (1953).

[30] After completion of this paper, a second article by Passerini and Ross appeared in the June issue of J. Chem. Phys. [**22**, 1012 (1954)] dealing with naphthalene. It substantiates our comparison with the only difference that these authors consider the second transition as long-axis polarized whereas we assume it to be short-axis polarized.

[31] For example, S. H. Wollman, J. Chem. Phys. **14**, 123 (1946).

[32] Donald S. McClure, private communication (see note added in proof on p. 646).

[33] Abrahams, Robertson, and White, Acta Cryst. **2**, 238 (1949).

[34] D. P. Craig and L. E. Lyons, J. Chem. Phys. **20**, 1499 (1952).

[35] Donald S. McClure, J. Chem. Phys. **22**, 1256 (1954).

Experimental Study of the Mechanism of Thermoluminescence in Irradiated Sodium Chloride

J. J. HILL* AND P. SCHWED
Lewis Flight Propulsion Laboratory, National Advisory Committee for Aeronautics, Cleveland, Ohio
(Received April 8, 1954)

The general configuration of the emission spectrum of synthetic NaCl crystals which had been irradiated with $7\times10^5 r$ of x-rays at room temperature and were then permitted to luminesce at 500°K was determined, and bands were located with maxima at 362, 418, 432, and 525 millimicrons. The glow curves for NaCl crystals irradiated with x-rays or ultraviolet light were investigated, and eight bursts of light (glow peaks) were found with peaks at temperatures between 334 and 625°K. The relative contribution of the different bursts to the total glow curve was determined as a function of the amount of x-ray irradiation. The activation energies for five of the bursts were measured and in each case turned out to be about 1.25 ev. It is suggested that these results indicate that the thermoluminescence takes place by means of a two-stage process of the following sort. The first stage, which is the same for all the bursts and is thermally activated with the measured activation energy, takes place when trapped electrons are raised from *F*-centers into the conduction band. In the second stage, electrons in the conduction band fall into different empty energy levels, there being one type of level for each burst. The large observed differences between the peak temperatures of the different bursts is then due to large variations in the probabilities of this second process for different levels.

INTRODUCTION

CRYSTALS which have been colored by irradiation[1] at room temperature display a tendency to luminesce if afterwards brought to a sufficiently high temperature.[2] The occurrence of this thermoluminescence indicates that, as a consequence of the irradiation, electrons are brought into metastable states of relatively high energy (ordinarily called traps) from which they pass to a higher level as the result of a thermally activated process and, thence, to a final stable state *via* an optical transition in the course of which all, or part, of their excess energy is given up in the form of light.

The following more explicit scheme is due to Johnson[3] who applied it to ZnS:Cu. Figure 1 shows the electronic energy levels of a crystal which exhibits the phenomenon of thermoluminescence. As usual in an insulator the situation before irradiation is that one energy band is completely filled, while the next higher one is completely empty. Besides the bands, there exist two sorts of localized levels: first, those associated with several types of traps, which are normally not occupied by electrons, and second, those associated with several types of imperfections (such as impurity atoms) to each of which an electron is ordinarily attached and which retain their electrons as long as the lower band is completely filled. In the figure the energy levels corresponding to trapped electrons are designated as trap levels T_1, T_2, etc. while the energy levels corresponding to electrons attached to the other type of imperfection are designated as luminescence levels L_1, L_2, etc. The individual diagrams indicate the sequence occurring when a *single* electron is excited from the filled band and trapped. As usual the electron is represented by a filled circle, and a hole in a band by an open circle. Figure 1(a) refers to the normal state of the crystal in which all the luminescence levels are filled and the trap levels are empty. Figure 1(b) refers to the state immediately after irradiation during which one of the electrons was lifted from the lower band into the trap level T_2 leaving a hole in the lower band. Figure 1(c) represents the situation after the next step during which the electron from the luminescence level L_3 falls into the hole in the lower band. Under the influence of thermal excitation the trapped electron is raised to the conduction band as shown in Fig. 1(d) from which it returns to the level L_3 by the emission of light. Since, in addition to the luminescence and trap levels, there might be localized lower states associated with a given trap level (some of which may be connected to a level T by radiationless transitions), the kinetics of the process of thermoluminescence may be quite complex.[4]

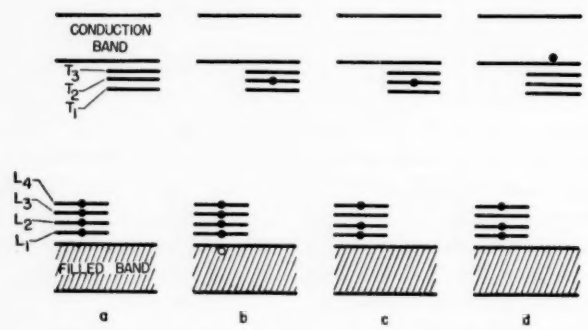

FIG. 1. Energy diagram for an electron participating in thermoluminescence.

* Now at Rockhurst College, Kansas City, Missouri.
[1] F. Seitz, Revs. Modern Phys. **18**, 384 (1946).
[2] For a general review see, e.g., Karl Przibram, *Verbaerfung und Lumineszenz* (Springer, Vienna, 1953).
[3] R. P. Johnson, J. Opt. Soc. Am. **29**, 387 (1939).
[4] F. E. Williams, *Preparation and Characteristics of Solid Luminescent Materials*, Cornell Symposium of The American Physical Society (John Wiley and Sons, Inc., New York, 1948), Chap. 20, p. 337.

From an experimental viewpoint, it is usual to study thermoluminescence by means of a procedure, due to Urbach,[5] which consists of raising the temperature of the crystal at a constant rate and measuring the intensity of the emitted light as a function of time, the resulting plot of intensity against time being known as a glow curve.

In case there is only one type of trap T and one type of luminescence level L (see Fig. 1), the glow curve has the form shown in Fig. 2(d) and can generally be fairly well represented by means of a theoretical expression which is a solution of the equation:

$$I=-\alpha(T)\frac{dn}{dt}=\alpha(T)n^{p}\nu\exp(-E/kT) \qquad (1)$$

for the case where the absolute temperature T increases linearly with time at a constant rate. Here n is the number of trapped electrons; I is the intensity of the emitted light; p is the effective order of the process—usually one but sometimes two; α represents the amount of radiation emitted per trapped electron released which may be temperature dependent if a competing radiationless process exists; ν is the frequency factor; T is the absolute temperature; and k is Boltzmann's constant. In the following, a pulse shaped curve like that shown in Fig. 2(d) will be called a luminescence "burst."

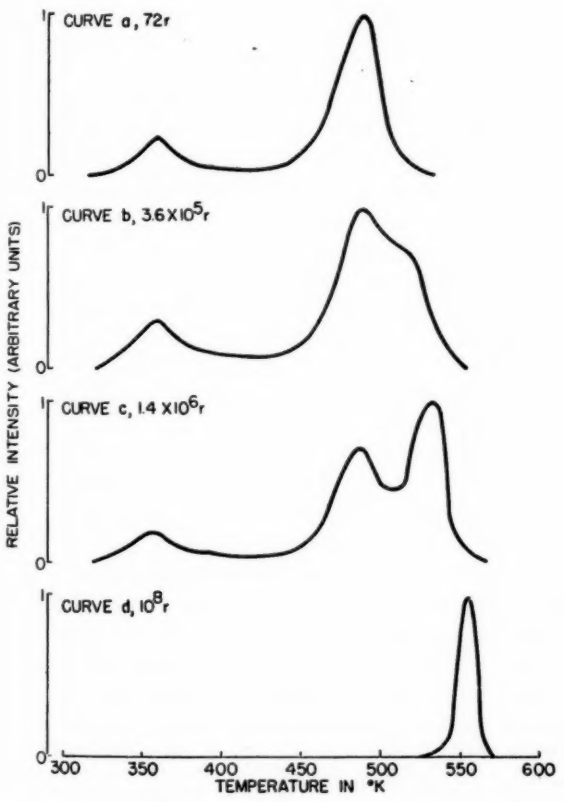

FIG. 2. Glow curves of NaCl crystals exposed to varying amounts of irradiation with x-rays. The units of light intensity are adjusted so that the maximum intensity is unity for each curve.

[5] F. Urbach, Wien. Ber. (IIA) **139**, 363 (1930).

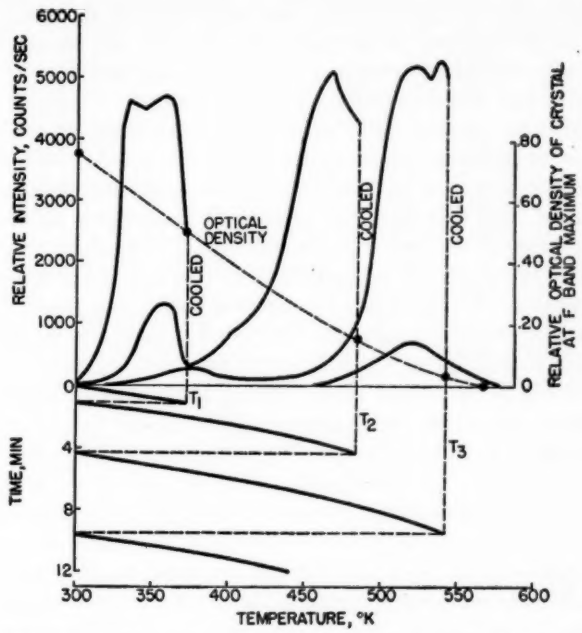

FIG. 3. Glow curve for an NaCl crystal irradiated with $3\times10^{5}r$ of x-rays as obtained by the method of "saw-tooth annealing." The lower part of the figure shows the variation of the temperature of the crystal during the annealing. The upper part shows the measured light intensities as a function of temperature. Also shown are the values of the optical density (in relative units) each time the crystal was cooled to room temperature.

In case there are several types of traps T and luminescence levels L, the resulting curve is, of course, more complex, especially if the individual bursts should overlap; [see, for instance, Fig. 2(b)]. To analyze a curve of this sort, it is usually necessary to specialize[6,7] Eq. (1) somewhat by taking α constant and assuming a value for p. If the overlapping is large, it is possible to determine only the locations of the peaks of the individual bursts. For a simple first-order process, this is approximately related[8] to quantities entering Eq. (1) by Eq. (2)

$$E=kT_G\ln\frac{12\nu}{r}, \qquad (2)$$

where T_G is the temperature of the crystal at the time the intensity passes through its maximum and r is the time rate at which the temperature of the crystal increases, ν being measured in sec^{-1} and r in °K sec^{-1}. Several procedures have been introduced for determining E and ν individually in such cases.[6,9] In the present investigation use was made of that of Ghormley and Levy[9] which can be described with the aid of the

[6] J. T. Randall and M. H. F. Wilkins, Proc. Roy. Soc. (London) **A184**, 366 (1945).

[7] F. E. Williams and H. Eyring, J. Chem. Phys. **15**, 289 (1947).

[8] P. Schwed, NACA Report RM E51G24.

[9] J. A. Ghormley and H. A. Levy, J. Phys. Chem. **56**, 548 (1952).

lower part of Fig. 3. First, the early part of the glow curve is obtained in the usual fashion, but the heating of the crystal is interrupted at a temperature T_1 just above the temperature at which the burst of interest begins to appear and the crystal is allowed to cool rapidly to room temperature. A second glow curve for the same crystal is then obtained in a similar fashion except that this time the heating is interrupted when the crystal reaches the temperature T_2 at which the burst of interest is completed. For this curve the contribution corresponding to bursts below the one of interest is greatly attentuated so that the ascending part of the latter is quite well resolved. It is then possible to determine directly from a curve of this sort both ν and E for the process responsible for the burst in question. As indicated on Fig. 3 the procedure can be repeated; and we shall refer to the general method as saw-tooth annealing because of the shape of the resulting temperature-time curve.

Although the thermoluminescence of x-ray irradiated NaCl has been studied extensively,[5,9–13] there remain a number of matters which are not as yet fully understood. The most direct experimental question, of course, has to do with the values of ν, E, and p to be associated with each process contributing a luminescence burst to the curve. Also of interest are the reason for the dependence of the shape of the glow curve (relative strength of the individual bursts) upon the amount of irradiation to which the crystal has been subjected, which was first investigated by Urbach and Schwartz[11] and more recently by Hecklesberg,[14] and the relation between the thermoluminescence and the bleaching of color centers.

The present paper is devoted to an account of a series of experiments carried out for the purpose of studying these matters. Glow curves were obtained for crystals subjected to varying amounts of irradiation by x-rays and by ultraviolet light. These curves were analyzed in order to determine the relative contributions of the individual bursts as well as the associated values of E and ν. For two cases in which the glow curve was especially complex, the method of saw-tooth annealing was used. The results obtained served as the basis for applying Johnson's scheme to the thermoluminescence of colored NaCl.

EXPERIMENTAL PROCEDURE

The method used to determine the emission spectra and the glow curves was essentially the same as that described in a previous article.[15] Briefly, to obtain a glow curve, the crystal was placed in an electric furnace, and the crystal temperature, which was recorded as a function of time, raised at the rate of 0.6°K per second from 280°K to 625°K. The light emitted by the crystal was permitted to fall upon a type 5819 photomultiplier, the output of which was recorded on a moving chart. The light intensity measured was that of the whole thermoluminescence spectrum as weighted by the spectral sensitivity of the photomultiplier. Because the amount of light emitted by the crystals was, in general, quite small, we made no attempt to obtain simultaneously the spectral and temperature dependence of the luminescence or even to determine whether there is any change in the spectral distribution of the emitted light as the temperature of the crystal is raised. If this latter should be the case, then the detailed form of the glow curve, measured in this fashion, necessarily depends on the spectral characteristics of the phototube. In order to obtain the general configuration of the optical emission spectrum at a fixed temperature, a similar arrangement was used, except that a Beckman monochromator, which served to analyze the light, was placed between the crystal and the photomultiplier. As was the case in the earlier work,[15] the monochromator was adapted to scan the spectrum automatically; in the course of each determination, the spectrum was traversed in both directions and an appropriate average taken so as to compensate for the error in the position of the band maximum due to the time lag in the counting rate meter and in the recorder.

The samples used were synthetic single crystals of NaCl obtained from the Harshaw Chemical Company. Before being irradiated, the crystals were freshly cleaved to appropriate dimensions. Crystals 6×6×10 mm were used for spectrum determinations in order to obtain sufficient light intensities while crystals 2×2×6 mm sufficed for the other work. The freshly cleaved crystals were wrapped in aluminum foil to shield them from light and irradiated for appropriate intervals at room temperature with a beryllium window x-ray tube operated at 45 kv and 30 ma at varying distances from the window. At the conclusion of the irradiation they were left at room temperature for 40 minutes and then stored at dry ice temperature still wrapped in aluminum foil. Consequently, any F' centers formed during the irradiation should have bleached out as a consequence of the annealing at room temperature.[16,17] When the crystal was placed in the furnace, the part of the foil in contact with the face of the crystal placed opposite the detector was removed while the remainder of the foil was left in place to serve as a reflector. The care taken to prevent exposure of the crystal to visible light insured the presence of only the F and M absorption bands in the visible region.[18]

[10] F. Urbach, Wien. Ber. (IIA) **139**, 353 (1930).
[11] F. Urbach and G. Schwartz, Wien. Ber. (IIA) **139**, 483 (1930).
[12] M. L. Katz, Zh. Eksper. Teor. Fiz. **20**, 166 (1950).
[13] M. Lautout, Compt. rend. **232**, 2025 (1951).
[14] L. F. Hecklesberg, "Thermoluminescence and related properties of the alkali halides" in *The Thermoluminescence of Crystals*, AECU 1583.
[15] J. J. Hill and J. Aron, J. Chem. Phys. **21**, 223 (1953).
[16] H. Pick, Ann. Physik **31**, 365 (1938); **37**, 421 (1940).
[17] R. T. Platt and J. J. Markham, Phys. Rev. **92**, 40 (1953).
[18] The complex R bands, in general, do not appear as long as the crystal is not exposed to visible light during or after irradiation. Heating lowers the intensities of the F and M bands but introduces no additional bands (reference 1).

Measurements of the amount of x-ray irradiation were made by monitoring the beam with an ionization chamber used in conjunction with a quartz fiber electrometer. The chamber was placed a distance of 10 feet from the target; and it was assumed that the inverse square law applied.

RESULTS

The Emission Spectrum

Three main bands with maxima at 362, 418, and 432 millimicrons and a weaker band with a maximum at 525 millimicrons were detected in the emission spectrum of an NaCl crystal which had been irradiated with $7\times10^5 r$ of x-rays and was permitted to luminesce at 500°K. It proved impossible, however, to determine any further details of the emission spectrum because the weakness of the luminescence and its rapid decay necessitated the use of a large slit width and fast scanning. In obtaining the positions quoted for the maxima, the data were corrected for the nonlinear dispersion of the monochromator and for the way the photomultiplier sensitivity varies with wavelength.

Variation of the Relative Intensities of Bursts of Luminescence with Amount and Type of Irradiation

(a) *Irradiation with X-Rays*

Our first experiments represent an extension of Hecklesberg's work[14] on the relation between the amount of x-ray exposure and the shape of the glow curve displayed by NaCl crystals. As a preliminary to this study the glow curves of a large number of NaCl crystals irradiated in different ways were obtained; and the temperatures corresponding to the maxima of the eight different bursts which were found in the curves are included in Table I. Some of these bursts were always quite low in intensity and such bursts did not appear consistently even in the glow curves of crystals which had been irradiated in the same fashion. No further study was made of these.

A number of crystals, selected from a single batch in order to avoid effects due to variations among batches, were exposed to amounts of radiation varying from $8r$ to $10^8 r$ and the glow curves recorded. Some of these curves are shown in Fig. 2, the results being plotted on such a scale that the highest value attained by the ordinate in each curve is unity. It can be seen that, as originally observed by Urbach and Schwartz,[11] the relative intensity of the burst appearing at the highest temperature always increases with increasing amount of irradiation (within the range employed here) while that of the lower temperature peaks reaches a maximum and then begins to decrease. It may be remarked that the absolute intensity of a given burst varies with the amount of irradiation in much the same fashion as does its relative intensity. In particular, for crystals which were saturated with color centers (containing about 10^{19} per cm^3) only the highest temperature burst appeared (Fig. 2(d)). Figure 4 shows the peak intensities of the major bursts as a function of the total amount of irradiation in units adjusted so that the total light sum for each glow curve is normalized to unity.

TABLE I. Activation energies E and frequency factors ν for luminescence bursts with maxima occurring at temperatures T_G in irradiated NaCl. [The values E_{Av} are obtained from Table II. The values of ν given are calculated on the assumption that the true value of E is the same for all bursts and is equal to 1.26 ev (see text).]

T_G, °K	E_{Av} ev	ν, sec^{-1}
334	1.35	7×10^{17}
354	1.25	6×10^{16}
379	···	4×10^{15}
405	···	3×10^{14}
433	···	3×10^{13}
474	1.25	2×10^{12}
518	1.27	1×10^{11}
562	1.28	1×10^{10}

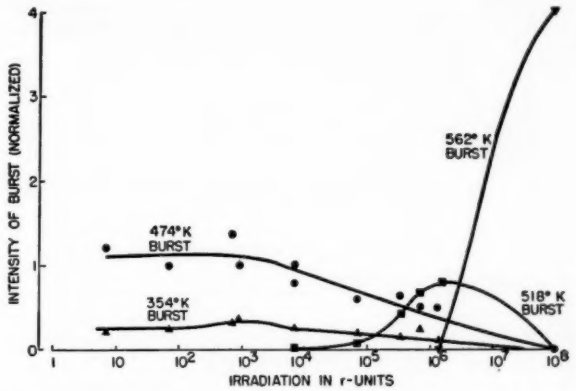

FIG. 4. Relation between the light intensity at the peak of an individual burst and the amount of irradiation. The units of light intensity employed were normalized so as to make the measured luminescence light sum equal to unity.

(b) *Irradiation with Ultraviolet Light*

We also investigated in a similar fashion the glow curves of NaCl crystals irradiated with ultraviolet light.[13] The first irradiations were done at 300°K with the crystals placed 10 cm from the quartz envelope of a Hanovia low-pressure mercury arc lamp. None of these crystals showed any coloration even for fairly long exposures (20 hours), a result which might be expected in view of the results of earlier studies of synthetic crystals.[19] Furthermore, the total amount of light emitted during the luminescence was always quite small. The glow curves for three of these crystals are shown in Fig. 5 (curves *a*, *b*, and *c*). The locations of the maxima of the bursts coincide with those found for x-ray irradiated crystals; and the highest temperature bursts are missing, as would be expected in view of the small light sum. Of the bursts appearing, the

[19] H. J. Schroeder, Z. Physik **76**, 608 (1932).

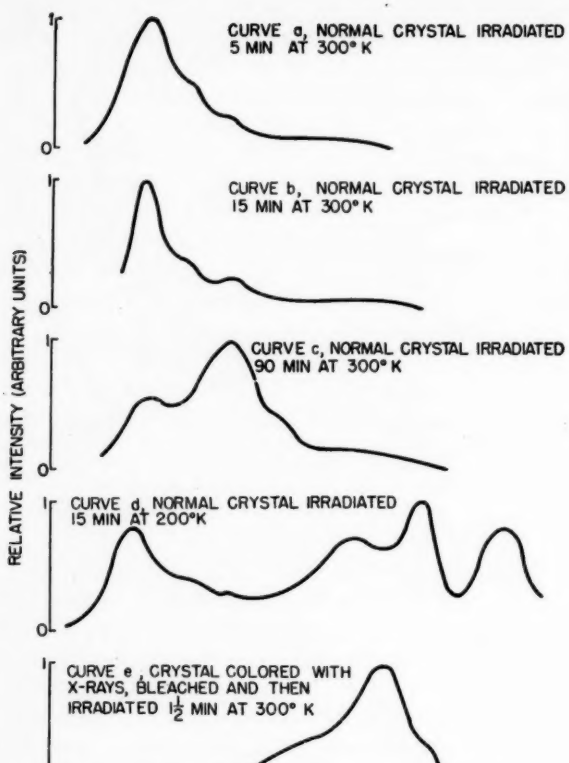
CURVE a, NORMAL CRYSTAL IRRADIATED 5 MIN AT 300° K
CURVE b, NORMAL CRYSTAL IRRADIATED 15 MIN AT 300° K
CURVE c, NORMAL CRYSTAL IRRADIATED 90 MIN AT 300° K
CURVE d, NORMAL CRYSTAL IRRADIATED 15 MIN AT 200°K
CURVE e, CRYSTAL COLORED WITH X-RAYS, BLEACHED AND THEN IRRADIATED ½ MIN AT 300° K
RELATIVE INTENSITY (ARBITRARY UNITS)
0
300
350
400
450
500
550
600
TEMPERATURE IN °K

FIG. 5. Glow curves of NaCl crystals irradiated with ultra-violet light. The units of light intensity are adjusted so that the maximum intensity is unity for each curve.

higher temperature ones become relatively more prominent for longer exposures.

In order to obtain crystals which luminesced more strongly, some ultraviolet irradiations were undertaken at 200°K since according to Casler, Pringsheim, and Yuster,[20] the rate of production of color centers in NaCl by x-rays is a maximum at this temperature. We found that the light sum of the luminescence of crystals irradiated with ultraviolet light at this temperature was about ten times greater than that for crystals irradiated at room temperature under the same circumstances and thus corresponds to an F center concentration just at the threshold of detectability. Once again, no coloration could be detected; but, as can be seen from curve d of Fig. 5, the highest-temperature luminescence bursts appear.

According to Lautout,[13] an NaCl crystal, which is first colored by x-rays and then bleached before being exposed to ultraviolet light, shows a greater luminescence light sum than an ordinary crystal exposed to the same amount of ultraviolet irradiation. In investigating this effect, we first colored a crystal fairly heavily by irradiation with x-rays and next heated it until the coloration just disappeared. After a one minute exposure to ultraviolet light at room temperature, the crystal became colored, an effect reported by Smekal.[21] The luminescence light sum of such a crystal was about the same as that of a normal crystal colored directly with x-rays to the same extent; and as can be seen from curve e of Fig. 5 the bursts at higher temperatures became more pronounced in this case.

Analysis of Glow Curves

The individual bursts contributing to the glow curves of a number of crystals irradiated with x-rays or ultraviolet light for various lengths of time were subjected to detailed analysis in order to determine E and ν separately on the assumption that α is constant and p equals one in Eq. (1). Then the intensity of the emitted light following from Eq. (1) can be written[22] as

$$I = c\nu \exp(-E/kT) \exp\left(-\int_{t_0}^{t} \frac{\nu}{r} \exp(-E/kT)dt\right), \quad (3)$$

where $T_0 (\ll T_G)$ and T are the temperatures at the times t_0 and t, respectively, and c defined as

$$c = \int_{t_0}^{\infty} I dt$$

equals the total intensity of light emitted subsequent to time t_0. It follows from the equation that for t near t_0 (when the integral entering the right side is small) the quantity I varies nearly exponentially with $-E/kT$. Consequently, it is possible to determine E from the slope of the linear portion of the curve of $\ln I$ against $1/T$. The quantity ν can be obtained with the aid of Eq. (2). (It may be noted that this procedure for finding E is equally valid in case the process is not first order.)

The glow curves for a number of different crystals were studied in this fashion. In the case of two crystals which had been irradiated with $1.5\times10^5 r$ and $3\times10^5 r$ of x-rays, respectively, the method of saw-tooth annealing was applied, the resultant glow curve for the latter case being shown in the upper part of Fig. 3. The optical density of this crystal was also determined each time it was brought to room temperature; and the results of these measurements are also shown on the figure.[23] It may be seen that over most of the glow curve the decrease in optical density is roughly proportional to the total light emitted during the luminescence between measurements. Including the results of these saw-tooth annealing experiments, it finally proved possible to determine E for five of the eight bursts in

[20] Casler, Pringsheim, and Yuster, J. Chem. Phys. **18**, 887 (1950).

[21] See reference 2, p. 43.

[22] G. F. J. Garlick and A. F. Gibson, Proc. Phys. Soc. (London) **60**, 574 (1948).

[23] The dotted line shown connecting the points representing the measured optical density after the completion of each burst is, of course, not supposed to represent the actual variation of this quantity during the annealing but only to indicate the general trend.

question. In Fig. 6 are shown typical plots of $\ln I$ against $1/T$. It can be seen that these are, indeed, very nearly straight over most of the early part of the bursts as is to be expected from the theory. In Table II are given the results of nineteen such individual determinations of E for the five bursts which could be studied in this way for crystals irradiated as specified. The resulting values of E appear to be very nearly the same for all the bursts and to be independent of the method of irradiation. It therefore seems reasonable to assume that E is the same for the five bursts for which it was determined and also for the three others; and we have taken for this common value of E the average of all the observations listed (i.e., 1.26±0.05 ev). The value of ν for each burst has been computed by the use of Eq. (2) using this particular value of E; and the results are given in Table I. The ratio of the values of ν for successive bursts is of the order of ten.

Conclusions as to the Mechanism of Thermoluminescence in Irradiated NaCl

The central results of the present investigation are that (1) the activation energies for luminescence bursts occurring at a given temperature in NaCl crystals irradiated for different periods with x-rays and with ultraviolet light and, more surprisingly, the activation energies for bursts occurring at different temperatures in such crystals are identical; and that (2) the frequency factors associated with different bursts differ by factors as large as 10^8. If one assumes that the observed values of ν and E specify a simple rate process governing the escape of electrons from different types of traps, it becomes quite difficult to understand how individual traps can differ so greatly with respect to the properties which determine ν and not with regard to those entering E and (even disregarding the latter fact) to explain the fact that the range of values of ν

TABLE II. Experimentally determined activation energies E for luminescence bursts of NaCl crystals irradiated under various conditions.

T_0, °K	State of crystal	Type of irradiation	E, ev	E_{Av}, ev
334	normal	x-ray 1.5×10^5r	1.35	1.35
354	normal	x-ray 7×10^4r	1.28	
	normal	x-ray 7×10^4r	1.25	
	normal	x-ray 1.5×10^5r	1.10	
	normal	x-ray 1.5×10^5r	1.37	
	normal	x-ray 5×10^5r	1.27	
	normal	x-ray 7×10^5r	1.20	
	normal	x-ray 7×10^5r	1.26	
	normal	U. V.	1.38	
	normal	U. V.	1.29	
	x-rayed and bleached	U. V.	1.13	1.25±0.09
474	normal	x-ray 7×10^3r	1.23	
	normal	x-ray 3.5×10^5r	1.29	
	normal	x-ray 1.4×10^6r	1.23	1.25±0.03
518	normal	x-ray 10^3r	1.27	
	normal	x-ray 5×10^3r	1.26	1.27±0.01
	normal	x-ray 1.5×10^5r	1.29	
548	normal	U. V.	1.29	
	x-rayed and bleached	U. V.	1.26	1.27

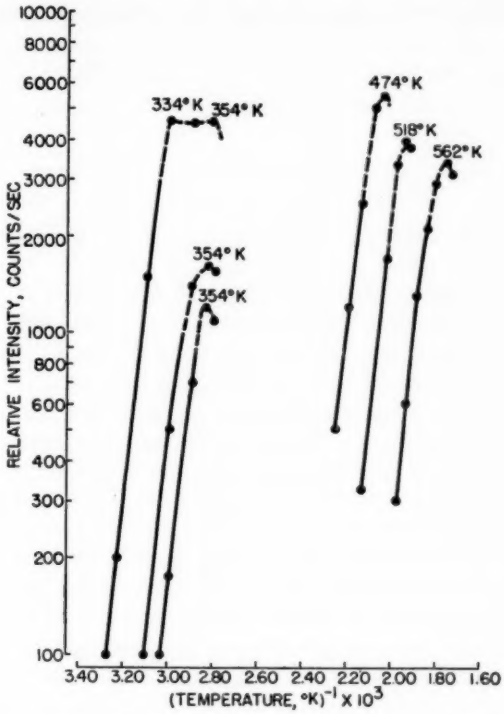

FIG. 6. Plot of the logarithm of light intensity against the reciprocal of the absolute temperature for various bursts.

(from 10^{10}/sec to 10^{18}/sec) far exceeds that usually assumed for such processes in solids (10^8/sec to 10^{13}/sec). It seems reasonable, therefore, to assume that the emission of each quantum of light during the thermoluminescence is the result of a process composed of two quite independent steps of which only one requires a thermal activation. A fairly explicit physical picture which accounts for most of the observations can be presented in terms of a modification of the scheme proposed by Johnson[3] (see Fig. 1) as follows. We assume that there exists only one type of trap T and that in spite of the occurrence of the luminescence the electrons are always distributed between them and the conduction band approximately according to the equilibrium law:

$$n_c = n_t e^{-E/kT}, \tag{4}$$

where E is a constant and n_c and n_t are the number of electrons in the conduction band and in traps at a given moment. Further, we assume that there are at least eight different types of luminescence levels,[24] $L_1, L_2, \cdots, L_8$ to which electrons are bound in the normal state of the crystal; that certain of these become empty when their electrons replace those removed from the lower filled band by the irradiation; and that the probability per unit time that a single electron in the conduction band enter an empty level L_i when a single electron is missing

[24] Certain of these levels may be connected with the presence of impurities as might be inferred from the relationship between the spectrum of the thermoluminescence and the impurity content in CaF_2 found by Prizbram and his collaborators (Haberland, Karlik, and Prizbram, Wien. Ber. **144**, 77 (1935)).

from this level is a temperature independent quantity p_i. Thus, the rate $(-dN_i/dt)$ at which electrons from the conduction band combine with empty levels of the type L_i in the course of the luminescence is equal to

$$-\frac{dN_i}{dt}=p_iN_in_te^{-E/kT}, \tag{5}$$

where N_i represents the number of empty levels of the type L_i.

If we consider an isolated burst, the intensity of the emitted light is proportional to $-dNi/dt$ so that Eq. (5) has the same significance and form as Eq. (1) except that ν is replaced by p_in_t. Although the latter product varies to some extent during the luminescence, Eq. (5) nevertheless defines a burst of the same general shape as does Eq. (1). Furthermore, if the activation energy associated with a burst defined by Eq. (5) is measured by the method employed in the present experiments, the value obtained will be equal to E as follows from the remarks subsequent to Eq. (3). Thus, Eq. (5) represents a set of bursts with a common E but different ν's. It follows also that ν does not really remain a constant over the course of a single burst and that there is a slight variation in the value of ν and, hence, of T_G for a given burst between crystals subjected to different amounts of irradiation (since ν is proportional to n_t). The accuracy of our measurements was, however, not sufficient to permit an investigation of these effects. It also seems possible that, in general, the spectrum of the light emitted during the luminescence should be different for different bursts.

For the reason that the coloration of the NaCl crystals diminishes steadily during the course of the thermoluminescence and disappears at the temperature at which the luminescence is completed, it appears reasonable to identify the traps T with the F-centers. In this case the measured energy E required for the transition of the trapped electrons from the trap level T into the conduction band should be identical with the effective activation energy E_C for the thermal dissociation of the F-centers. Smakula[25] has measured this quantity for NaCl crystals which had a stoichiometric excess of sodium and, consequently, contained permanent color centers. He obtained a value of 0.94 ± 0.19 ev which is to be compared with our value of 1.26 ± 0.05 ev for E. The discrepancy is somewhat larger than should be expected on the basis of the quoted experimental errors. However, in a theoretical analysis[26] of the factors determining E_c, Mott and Gurney have shown that the quantity measured by Smakula depends not only upon the energy required to remove an electron from an F-center into the conduction band, but also upon the interaction between the vacancy thus produced and the other vacancies in the crystal. This interaction may depend upon whether the color centers are permanent (as in Smakula's measurements) or temporary (as in our measurements) so that the occurrence of a small difference between the E's measured in these two ways does not appear unreasonable.

The observed change of the shape of the glow curves with the amount of irradiation indicates that if the irradiation is interrupted after a relatively short time, there will be more electrons missing from the low-temperature luminescence levels than from the high-temperature levels. If the irradiation, however, is interrupted after a sufficiently long time, the situation is reversed. This implies that the probability that an electron missing from the filled band be replaced by one of the electrons from the luminescence levels is higher for the low-temperature levels than for the high-temperature levels, so that in the early stages of the irradiation more of the low-temperature levels than the high-temperature ones are emptied. During the course of the irradiation electrons are excited from the filled band by the x-rays and the ones which do not return directly into the band or become trapped replace electrons missing from the luminescence levels. In this latter process the low-temperature levels must be preferred to such an extent that virtually all of them become filled and thus, in effect, most of the trapped electrons are supplied from the high-temperature luminescence levels. This means that the number of imperfections responsible for the high-temperature levels is at least as large as the number of trapped electrons.

If thermoluminescence is the only mechanism by which F-centers decay, it follows that the average stability of an F center in NaCl should increase with the amount of irradiation to which the crystal was subjected, since the more deeply colored the crystal, the higher is the temperature at which thermoluminescence occurs (see Fig. 4). This is in qualitative agreement with the results of a study of the influence of the amount of irradiation upon the stability of the F centers conducted by Casler, Pringsheim, and Yuster.[20]

Thanks are due Gerhart Groetzinger for many helpful discussions and for valuable counsel throughout the course of this work.

[25] A. Smakula, Nachr. Goett. Wiss. **NF 1**, 55 (1934).

[26] N. F. Mott and R. W. Gurney, *Electronic Processes in Ionic Crystals* (Oxford University Press, London, 1948), second edition, pp. 140–143.

Self-Diffusion of Carbon Tetrachloride, Isobars and Isochores

H. WATTS, B. J. ALDER, AND J. H. HILDEBRAND
Department of Chemistry and Chemical Engineering, University of California, Berkeley, California
(Received August 20, 1954)

The self-diffusion coefficient of CCl_4 has been measured over a range of temperature between 25° and 50°C and at 1 and 200 atmospheres. The results can be expressed by the equations: for 1 atmos, $D=325\exp(-3300/RT)$, for 200 atmos, $D=264\exp(-3300/RT)$. The activation energy for constant volume is 1070 Cal. These activation energies are identical with those previously found for the diffusion of I_2 in CCl_4. The temperature coefficient of diffusion at constant volume parallels in both cases the increase of kinetic energy. $D\eta/T$ is constant within 7 percent in the range studied, where η denotes viscosity. These results are discussed in relation to various theories for the mechanism of diffusion.

THE work herein described is a sequel to the recent investigation by Haycock, Alder, and Hildebrand,[1] of the isobaric and isochoric diffusion rates of iodine in carbon tetrachloride.

APPARATUS AND PROCEDURE

Diffusion was measured by the capillary cell method described by Anderson and Saddington[2] and by Wang,[3] and adapted for high pressures as described in the earlier paper.[1]

The diffusion cells were accurately calibrated capillaries, approximately 4 cm in length and 0.02 cc in volume. They were filled with CCl_4 containing Cl^{36} sufficient to give 1100 counts per minute in the counting system used. The cells were immersed in a liter reservoir of pure, inactive CCl_4, in a thermostat constant to 0.01°, and diffusion was allowed to proceed for about 3 days, after which the residual activity in the tubes was determined as described below.

The radioactive CCl_4 was prepared from active KCl supplied by the Union Carbide and Carbon Company, Oakridge, Tennessee. The half-life of Cl^{36} is 4×10^5 years, and it emits 0.716 Mev electrons. All other radioactive impurities present have short half-lives, therefore the material was kept three months before using to allow these to decay. The chlorine of the KCl was first precipitated as AgCl, then transposed to $Al_2Cl_5Cl^{36}$ by reaction with Al-turnings *in vacuo*. This in turn was equilibrated with vapor of CCl_4, by the method of Wallace and Willard,[4] to produce CCl_3Cl^{36}. It was found that by continually resubliming the aluminum chloride a specimen of CCl_4 was produced with an activity higher than that previously obtained from a three day contact at room temperature. Possible traces of $ClCl^{36}$ or HCl^{36} were removed by treatment with 50 percent KOH, and two distillations *in vacuo* from freshly resublimed P_2O_5.

The CCl_4 used for the exchange had been purified by shaking repeatedly with distilled mercury until no black sediment formed, filtered, washed with 10 percent KOH, dried over Drierite, and fractionated in a 30-plate column at a reflux ratio of 30:1. Its boiling point was 76.8°C at 761.3 mm.

The activity of the CCl_4 was counted by the apparatus shown in Fig. 1. A Victoreen tube, No. 1B85, designated by *A* in the diagram, was sealed into a glass envelope, *B*, 10 cm long and 4.5 cm in diameter, by means of red sealing wax, *C*. This section was surrounded by 3 inches of lead shielding to reduce background. A manometer, *D*, indicated the pressure in the counting system. The procedure of transferring the specimen from the diffusion cell to the counting chamber was as follows: the cell, after removal from the bath on conclusion of an experiment, was rapidly dried on the outside, placed in a tube, *E*, and capped by a standard taper carrying a stopcock, *F*. This assembly was then connected to the counting system through another taper and stopcock *G*. The carbon tetrachloride was frozen in the cell by means of a liquid N_2 bath and the whole system evacuated to 10^{-5} mm Hg. Stopcock *H* was then closed. The CCl_4 was condensed into *J*, and *G* was closed. The CCl_4 was vaporized and recondensed into *J* several times to insure homogeneity. From *J* it was vaporized into the counting chamber, giving rise to a pressure of about 4.5 cm of Hg.

The activity was then counted using the Victoreen tube in conjunction with a scaler developed by the

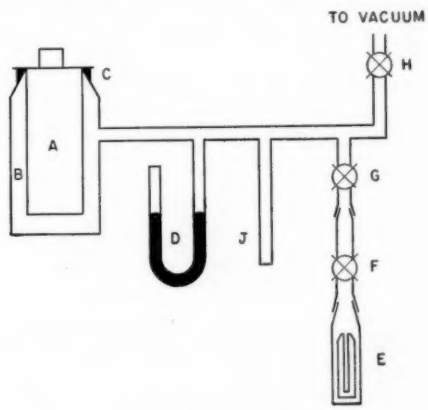

FIG. 1. Apparatus.

[1] Haycock, Alder, and Hildebrand, J. Chem. Phys. **21**, 1601 (1953).
[2] J. S. Anderson and K. Saddington, J. Chem. Soc. 5381 (1949).
[3] J. H. Wang, J. Am. Chem. Soc. **72**, 510 (1951).
[4] C. H. Wallace and J. E. Willard, J. Am. Chem. Soc. **72**, 5275 (1950).

Berkeley Radiation Laboratory. The counts were found to be proportional to the pressure of CCl_4 in the counting section. The addition of a small amount of inert CCl_4 to active CCl_4 already in this section did not alter the count. Three-hour counts were taken on each specimen in order to reduce statistical counting errors.[5] After counting, the CCl_4 was condensed into a storage vessel, not shown on the diagram, and the counting section was flushed with inert CCl_4 vapor and pumped for 15 minutes, after which time the background count returned to normal, 33 ± 3 counts per minute, small compared with the specimen count. The background was checked before and after each run.

EXPERIMENTAL RESULTS

The diffusion coefficients, D, were calculated using the relationship[6]

$$\frac{C_{av}}{C_0}=\frac{8}{\pi^2}\sum_{n=0}^{\infty}\frac{1}{(2n+1)^2}\exp\left[\frac{-(2n+1)^2\pi^2Dt}{4L^2}\right],$$

where L is the length of the cells and t is the time during which diffusion took place. C_{av} is the average concentration of active CCl_4 in the cell after diffusion, C_0 is the initial concentration. C_0 was found by filling the cells with active CCl_4 and running a count on it by the procedure described above. Three cells were used in each experiment and two experiments were performed at each temperature, hence, each reported diffusion coefficient is a mean of 6 value.

Values of the diffusion coefficient were obtained at 1 and 200 atmos over a temperature range of 25° to 50°C as indicated in Table I and Fig. 2. The heavy solid lines represent the self-diffusion data for CCl_4. The light solid lines represent the former results on the diffusion of I_2 in CCl_4. The results for I_2 indicated a linear relation, except, possibly, at the lowest temperature and highest pressure; and since there is no reason to expect the self-diffusion to behave otherwise, we have drawn the main portion of the lines straight, assuming the small deviations from linearity to result from errors of measurement.

The short vertical lines on each experimental point correspond to the root mean square experimental deviations. They are approximately 4 percent. The errors connected with this diffusion technique were discussed in the earlier paper.[1] An additional error in this case comes from evaporation occurring during transfer to the counting apparatus. This was reduced as much as possible by rapid, careful operation.

TABLE I. Values of the diffusion coefficient.

1 atmos			200 atmos	
T°C	D (cm²/day)	$\frac{D\eta^a}{T}\times10^5$	T°C	D (cm²/day)
25.0	1.22	3.71	25.0	0.93
35.0	1.51	3.87	37.5	1.29
45.0	1.72	3.80	50.0	1.56

[a] D is in cm²/day; η is in poises, from J. Timmermans, *Physico-Chemical Constants of Pure Organic Compounds* (Elsevier Publishing Company, Inc., New York, Amsterdam, London, Brussels, 1950).

[5] G. B. Cook and J. F. Duncan, J. Chem. Soc. S369, (1949).
[6] H. S. Carslaw and J. C. Jaeger, *Conductivity of Heat in Solids* (Oxford University Press, London, 1947), p. 79.

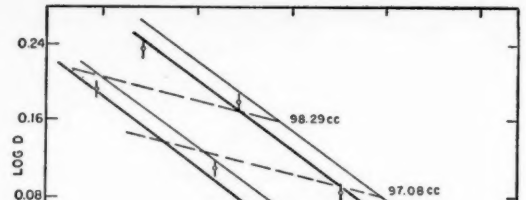

FIG. 2. Self-diffusion of CCl_4, heavy lines, compared with diffusion of I_2 in CCl_4, light lines. Dashed lines are isochores.

The slopes of the isobaric lines are identical for the two systems at both 1 and 200 atmos, therefore they have the same activation energy, 3300 Cal/mole. The broken lines are isochores, calculated from the data of Hildebrand and Carter,[7] recently confirmed for higher pressures by Alder, Haycock, Hildebrand, and Watts.[8] The activation energy for constant volume is, as before, 1070 Cal/mole.

The linear portion of the isobars for self-diffusion of CCl_4 can be represented by the expressions,

$$\text{1 atmos,}\quad D=325\exp(-1662/T),$$
$$\text{200 atmos,}\quad D=264\exp(-1662/T),$$

where D is in cm²/day.

DISCUSSION

The questions naturally presenting themselves concern (1) the temperature coefficient of diffusion, (2) the relative magnitudes of the diffusion of CCl_4 and I_2 in CCl_4, and (3) the absolute magnitude of the diffusion coefficients.

The present work confirms the conclusion drawn from the diffusion of I_2 that the rate of change of the diffusion coefficient with temperature at constant volume roughly parallels the rate of change of kinetic energy with temperature, and that the probability of forming a sufficiently large gap in the "cage" is not substantially altered at constant volume. It may also be inferred that the height of the barrier to be overcome in CCl_4 is practically the same for both I_2 and CCl_4.

Regarding the second question, since the activation energies are the same, the relative magnitude of the

[7] J. H. Hildebrand and J. M. Carter, J. Am. Chem. Soc. **54**, 3592 (1932).
[8] Alder, Haycock, Hildebrand, and Watts, J. Chem. Phys. **22**, 1060 (1954).

diffusion of I_2 and CCl_4 may be referred to the relative frequency with which the barrier is overcome. We may assume that this, in turn, depends in large part both upon their relative velocities, given by the square root of the inverse ratio of their masses, 1.28, and upon the inverse ratio of their cross sections, taken as the $\frac{2}{3}$ power of their liquid molar volumes, 59/97, which is 0.72. According to this concept, the ratio of their diffusion coefficients would be $1.28\times0.72=0.92$. The experimental values give 0.96, a quite satisfactory agreement.

In order to formulate tractable theories for the absolute magnitude of diffusion rates, all those who have attacked the problem have of necessity simplified it by assuming that the molecules are spherically symmetrical.

Eyring[9] has proposed the following now well-known expression,

$$D=e\lambda^2kT/h\,\exp\Delta S/R\,\exp-E/RT,$$

where λ is of the order of an intermolecular distance, ΔS is the entropy and E the energy of activation. If we assume that the entropy of activation is negligibly small, and use the experimental activation energy for constant pressure, our value for the self-diffusion of CCl_4 gives $\lambda=1.5$ A, whereas the C-C distance from x-ray scattering[10] is 6.4 A. If the activation energy at constant volume is used, the calculated value of λ is even smaller. This equation would also predict a smaller diffusion coefficient for I_2 than for CCl_4, whereas the reverse is true.

Eyring's theory gives the relation, $D\eta/kT=1/\lambda$, where η is the viscosity. Our data give $\lambda=31.5$ A, far too large for an intermolecular distance.

Einstein[11] defined the mobility of an individual particle as $\alpha=D/kT$. The friction constant, ζ, of Kirkwood's[12] theory is the reciprocal of α, and occurs in the Langevin[13] equation to describe the frictional forces experienced by a molecule undergoing Brownian motion. Since ζ can be considered as essentially a microscopic viscosity, and proportional to η, then the relation, $D\eta/kT=$const is again obtained. Our data confirm this over a wide range.[1] The maximum variation found was 7 percent. The near constancy of this quantity is useful.

Using the methods for calculating ζ developed by Kirkwood, a value of approximately 7×10^{-10} g/sec results for CCl_4. This gives a value of D twice as large as that from experiment.

The "Einstein-Stokes" equation, $D\eta/kT=1/3\pi\lambda$, was derived by assuming that the frictional forces are those given by the Stokes expression for a relatively large particle falling through a continuous medium. According to this equation, $\lambda=3.4$ A, smaller than the intermolecular distance, 6.4 A. It is to be noted that the use of the Stokes expression, in the case of a particle of molecular dimensions, does not take into account the difference between a large, freely falling sphere and a molecule participating in the molecular motion of the medium.

The original purpose of these two investigations was to test the concept that the essential condition for the escape of a molecule from its "cage" is not the occurrence of a "hole" of molecular size such as can exist in a crystal, but rather its possession of kinetic energy sufficient to penetrate an energy barrier consisting of the creation of a partial gap between surrounding molecules. The senior author[14] has argued against the quasi-crystalline model of liquid structure. For this reason we studied the effect of increasing temperature while keeping volume, and consequently intermolecular space, constant. But one must admit that these two concepts are not necessarily as different as they seem to be when stated in those words. If the holes are conceived, not as vacant crystal lattice sites, but as regions of weakness in the "cage" into which a molecule can move when impelled by the unsymmetrical bombardment of its neighbors, then the two concepts are not so very different. The chief difference would appear to be that diffusion could take place in much smaller steps, which accords with the fact that the values of λ calculated from our data are considerably smaller than the intermolecular distances. To debate whether a kinetic energy vector of the diffusing molecule or the spontaneous formation of an adjacent hole is to be regarded as the cause of the displacement is to forget that cause and effect in such an interaction are not truly separable.

We wish to mention in this connection the recent diffusion measurements of Drickamer[15] and co-workers over a wider range of pressure than our own, sure to prove significant in the further development of diffusion theory, also those of Stokes[16] on the diffusion of iodine in various liquids, whose value for I_2 in CCl_4 agrees well with our own.

We wish to acknowledge the assistance of Dr. E. W. Haycock in the initial stages of this investigation, also, the generous support of the investigation by the Atomic Energy Commission.

[9] Glasstone, Laidler, and Eyring, *The Theory of Rate Processes* (McGraw-Hill Book Company, Inc., New York, 1941), p. 524.
[10] F. F. Bray and N. S. Gingrich, J. Chem. Phys. **11**, 351 (1943).
[11] A. Einstein, Ann. Physik **19**(4), 289 (1906).
[12] Zwanzig, Kirkwood, Oppenheim, and Alder, J. Chem. Phys. **22**, 783 (1954).
[13] J. G. Kirkwood, J. Chem. Phys. **14**, 180 (1946).
[14] J. H. Hildebrand, Discussions Faraday Soc., No. 15, p. 9 (1953).
[15] W. M. Rutherford and H. G. Drickamer, J. Chem. Phys. **22**, 1157 (1954); Saxon, Dougherty, and Drickamer, *ibid*, p. 1166.
[16] R. H. Stokes, Trans. Faraday Soc. **49**, 886 (1953).

Infrared Spectrum and the Structure of the Low-Temperature Phases of Crystalline HCl, HBr, and HI*

D. F. Hornig and W. E. Osberg†
Metcalf Research Laboratory, Brown University, Providence, Rhode Island
(Received July 9, 1954)

The infrared spectra of crystalline HCl, HBr, and HI have been studied at −205°C. The fundamental vibrations were observed in HCl at 2704 and 2746 cm^{-1}, in HBr at 2404 and 2438 cm^{-1}, and in HI at 2120 cm^{-1}. In addition, low-frequency bands associated with torsional lattice vibrations were observed directly and in combination with the fundamental vibrations of the molecules. It is concluded that in the low-temperature crystalline phases both HCl and HBr form zigzag hydrogen-bonded chains, the angle between adjacent molecules being about 107° in HCl and 97° in HBr. The crystalline potential function is investigated for all three molecules.

INTRODUCTION

Up to the present time the structures of the hydrogen halide crystals have not been fully determined. The positions of the halogen atoms in the lowest temperature phases have been measured by x-ray methods, and the determination is probably fairly reliable in the case of hydrogen chloride, but the arrangement of the hydrogen atoms, upon which many of the physical properties of these crystals depend, is unknown. Until the structures of the lowest temperature phases are available, there is little hope of understanding the principles on which these simple crystals are constructed or the nature of the solid state phase transitions which occur in HCl, HBr, and HI.

These transitions are probably connected with the reorientation and disordering of the molecules, but although they have been studied by thermodynamic, optical, spectroscopic, x-ray, and dielectric techniques, the nature of the structural changes is not understood. Much of the information (prior to 1938) concerning these transitions is summarized in a review by Eucken.[1] However, it is clear from the previous infrared studies[2,3] and the more recent nuclear magnetic resonance experiments[4] that there is no free or nearly free molecular rotation in any of the phases.

Most recent theoretical discussions of the structures and the phase transitions are based on models consisting of dipole arrays. Since the intermolecular distance is not much greater than the interatomic distance in a single molecule, there is a real question as to whether such models are applicable. In any case, Luttinger and Tisza[5] have predicted on the basis of such a model that the lowest ordered phase consists of antiparallel strings of dipoles, and this can be checked from the infrared spectrum.

Since these molecules have but a single internal mode of vibration there should be little ambiguity in the interpretation of the infrared spectrum in terms of the present theory of molecular vibrations in crystals.[6] A completely unambiguous determination of the crystal structure is out of the question but certain features of the structure can be obtained. For example, it should be possible to decide whether or not the structure is ordered; and if it is ordered to gain some knowledge of the number and arrangement of the molecules in a unit cell from the *number* of absorption peaks associated with the single mode of vibration. The orientation of the molecules should be revealed by the relative intensities of these coupling components. In addition a quantitative measure of the intermolecular forces should be available from (a) the change in the mean internal frequency in passing from gas to crystal (b) the magnitude of the separation between coupling components (c) the magnitude of the torsional oscillation frequency in the crystal (which has not been observed heretofore).

The infrared spectra of crystalline HCl, HBr, and HI have all been studied before[2,3,7] although HBr and HI were not obtained in the lowest temperature phases, which exist below 89°K and 70°K respectively. The spectrum of HCl has been studied between 1.5μ and 4.15μ and the existence of two distinct peaks at about 2705 cm^{-1} and 2746 cm^{-1} noted in the low-temperature phase (i.e., below 98.4°K).[2,3] Since the completion of the work reported here a study of the infrared spectrum of a dilute solution of HCl in crystalline DCl has led to the conclusion that the angle between adjacent hydrogen-bonded HCl molecules is either 102° or 78°,[8] contrary to the theoretical expectations. The Raman spectrum of HCl has also been studied[2,9] and

* Based on a thesis submitted by W. E. Osberg in partial fulfillment of the requirements for the Ph.D., Brown University, 1951. The work reported here was supported by the Office of Naval Research.

† Present Address: Hercules Powder Company, Wilmington, Delaware.

[1] A. Eucken, Z. Elektrochem. **45**, 126 (1939).
[2] G. Hettner, Z. Physik **78**, 141 (1932); *ibid.* **89**, 234 (1934); Ann. Physik **32**, 141 (1938).
[3] Lee, Sutherland, and Wu, Nature **142**, 669 (1938); Proc. Roy. Soc. (London) **A176**, 493 (1940).
[4] N. L. Alpert, Phys. Rev. **75**, 398 (1949).
[5] J. M. Luttinger and L. Tisza, Phys. Rev. **70**, 954 (1946).
[6] D. F. Hornig, J. Chem. Phys. **16**, 1063 (1948); H. Winston and R. S. Halford, *ibid.* **17**, 607 (1949).
[7] J. Zunino, Z. Physik **100**, 335 (1936).
[8] G. L. Hiebert and D. F. Hornig, J. Chem. Phys. **20**, 918 (1952).
[9] D. Callihan and E. O. Salant, J. Chem. Phys. **2**, 317 (1934).

two peaks observed in the low-temperature phase,[2] only one of them coinciding in frequency with an infrared absorption maximum to within the combined experimental errors.

However, these observations have not been interpreted satisfactorily.

EXPERIMENTAL TECHNIQUES

Two different samples of hydrogen chloride were used in this work, commercial hydrogen chloride whose purity was stated to be 99.5 percent, the impurities consisting of 0.2 percent acetylene and 0.3 percent chlorinated hydrocarbon, and a sample prepared from reagent grade sodium chloride plus sulfuric acid. The first sample was used without further purification; the second was dried over anhydrous aluminum chloride and collected at liquid nitrogen temperature. The spectra obtained from the two samples were identical.

Commercial hydrogen bromide[10] was used without further purification. The purity of the material was reported as 99.5 percent, the gas containing no bromine or moisture; the principal impurity was nitrogen.

Hydrogen iodide was prepared by adding sodium iodide to phosphoric acid at dry ice temperature, sealing and evacuating the system, and then allowing the mixture to warm until reaction took place. The gas passed through a trap at $-35°C$ to remove water or iodine and collected as a solid in a trap at liquid nitrogen temperature. The entire system was wrapped in aluminum foil to prevent the photodecomposition which occurred when this precaution was not taken.

The samples were studied in a low-temperature cell similar to that described previously,[10a] except that provision was made for cooling the liquid nitrogen to its triple point by reducing the pressure in the reservoir.[11] To do so a chimney with a sidearm was added to the liquid nitrogen reservoir. When pumping through the sidearm an adequate vacuum seal was obtained if a plastic plate was simply rested on the top of the chimney. To replenish the liquid nitrogen, the plastic plate was removed without disconnecting the pump, liquid nitrogen added, and the plate replaced. No detectable fluctuation in the temperature of the copper block in which the sample was mounted was observed during this process.

The only other changes were the addition of a second sidearm to the outer jacket, through which the sample was sublimed onto the mounting plate, and the inclusion of a threaded retaining ring and spring to hold the sample plate in firm thermal contact with the copper block.

The temperature of the block was measured by a thermocouple and for most of the experiments reported here this was the only temperature measured. On a number of occasions the temperature difference between the block and the salt window on which the samples were deposited was measured by inserting a thermocouple into a small hole drilled in the window; it never exceeded 3°C when the block was at the temperature of liquid nitrogen.

The films were prepared by condensing the gas in a trap, cooling the cell to approximately 63°K, and then partially removing the liquid nitrogen coolant from around the trap to sublime material into the cell at a vapor pressure of about 5 mm Hg. Of course a large part of the material actually condensed on the copper block rather than the salt window, but this was of no consequence. After the film was deposited, the jacket was re-evacuated with a diffusion pump to minimize the heat loss to the outer walls. The films prepared by this technique were quite transparent to the eye and showed little or no scattering of infrared radiation. They evaporated rapidly from the window at $-195°C$ but could be retained for long periods at $-210°C$.

The spectra of the films were studied from 300 cm^{-1} to 4000 cm^{-1} with a double beam spectrophotometer,[12] the low-temperature cell being in one path and an evacuated cell of the same length with similar windows in the other. CaF_2, KBr, and KRS-5 prisms were used. The spectrometer housing was flushed with dry nitrogen to remove CO_2 and H_2O, but in the spectra of some of the HBr films is evidence that the flushing may not have been equally efficient in both beams. Stray radiation in the KBr region was eliminated by a scattering filter and that in the KRS-5 region minimized by replacing the mirror before the entrance slit with a stainless steel mirror, roughened by grinding with Aluminox No. 120. Nevertheless, when the prism was set to 310 cm^{-1}, 31 percent of the total radiation was transmitted by an NaCl plate and was therefore stray. It should be noted that the low-frequency limit of the spectral region investigated was determined by the transmission of the KBr window on the thermocouple.

The spectrometer calibration was checked against atmospheric water and CO_2 bands. The frequencies reported are believed to be accurate to ± 3 cm^{-1} at 2700 cm^{-1}, 1.5 cm^{-1} at 2100 cm^{-1}, and better than 1 cm^{-1} in the low-frequency region.

EXPERIMENTAL RESULTS

a. Hydrogen Chloride

Typical spectra obtained at a temperature of 73°K, well below the temperature of the phase transition at 98.8°K, with the film on a KBr backing, are shown in Fig. 1. A film of HCl deposited on NaCl to check the effect of the substrate yielded a similar spectrum, although the intensity of the two peaks was more nearly equal.

The spectra of thin films (e.g., Fig. 1) in good

[10] The Matheson Company, Inc.

[10a] E. L. Wagner and D. F. Hornig, J. Chem. Phys. **18**, 296 (1950).

[11] J.B. Lohman, Ph.D. thesis, Brown University, 1951.

[12] Hornig, Hyde, and Adcock, J. Opt. Soc. Am. **40**, 497 (1950).

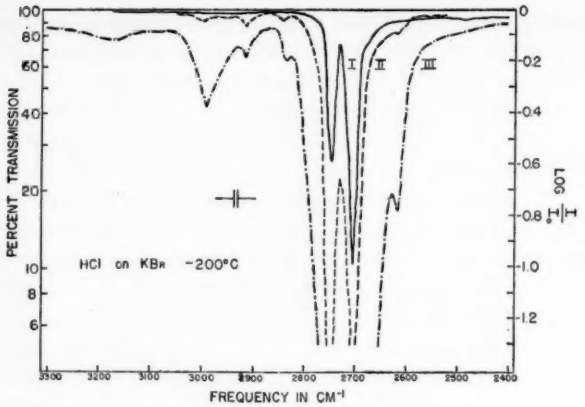

FIG. 1. Infrared spectrum of HCl in the low-temperature crystalline phase.

agreement with the high resolution study of Lee, Wu, and Sutherland who found maxima at 2701 cm^{-1} and 2744 cm^{-1}, consist of two sharp lines at 2704±3 cm^{-1} and 2746±3 cm^{-1}, whose widths at half peak intensity are approximately 30 cm^{-1}. The spectra of thick films show a number of previously unreported regions of absorption, a sharp line at 2616±3 cm^{-1}, a somewhat weaker band at 2991 cm^{-1} whose width is roughly 50 cm^{-1}, and a very weak band at 3171 cm^{-1}. Two other peaks, at 2837 cm^{-1} and 2916 cm^{-1}, are believed to originate in Apiezon-*M* stopcock grease which was carried into the cell from the vacuum system with the HCl. They occur in the spectrum of Apiezon-*M* and were not found in other HCl spectra taken when a fluorocarbon grease (DuPont FXC-441) was used as a stopcock lubricant.

A very thick film (Fig. 2) also showed absorption maxima at 315 cm^{-1}, 496 cm^{-1} and roughly 650 cm^{-1}. The true maximum of the lowest frequency peak may be at a still lower frequency since it occurs just at the limit of our measurements, where stray radiation is a very serious problem. The width of the 496 cm^{-1} line is about 55 cm^{-1} and of the 650 cm^{-1} line about 75 cm^{-1}.

The two strong sharp lines are certainly coupling components of the fundamental stretching vibration. The origin of the sharp weak line at 2616 cm^{-1} is doubtful. Although it may be a third component of the stretching vibration, there are strong reasons to believe this is not the case. It might be a difference vibration involving a lattice frequency of about 100 cm^{-1} but the corresponding sum is absent. If it is caused by an impurity it is not easy to find any reasonable possibilities. The intensity of the peak is about the same in the spectrum of HCl from different sources. The most likely impurity is the OH_3^+ ion resulting from traces of H_2O, perhaps adsorbed on the KBr or NaCl. A broad absorption maximum has been observed recently at 2600 cm^{-1} in the compound OH_3Cl;[13] however, subsequent studies of dilute solutions of H_2O in crystalline HCl[14] did not disclose a corresponding sharp line, nor is a corresponding peak found in our spectra of HBr, although the maximum at 2600 cm^{-1} was also found in OH_3Br.

Nevertheless, it is our opinion that the weak line at 2616 cm^{-1} is not to be ascribed to a fundamental vibration for the following reasons, some of which are elaborated later:

(a) No corresponding line has been found in recent studies of thick films of DCl.[15]

(b) Sutherland found a Raman line at 2709±5 cm^{-1} and an infrared line at 2701±1 cm^{-1}. Unless they actually coincide, no assignment is available for the line in question.

(c) The existence of a component at 2616 cm^{-1} would imply strong coupling between each HCl molecule and one neighbor in addition to the one to which it is hydrogen bonded. If this were the case, two different sets of "wings" should have been obtained in the spectra of dilute solutions of HCl in DCl. The second set, which would be separated by about 24 cm^{-1} from the main peak, was not observed.

(d) The existence of a coupling component at a frequency as low as 2616 cm^{-1} would imply a spread of over 100 cm^{-1} in the broad band in the disordered phase above 98.8°K, since all of the vibrational frequencies may then appear in the spectrum. In fact, the spread of the band is about 50 cm^{-1}, roughly equal to the separation of the two Raman peaks and the two infrared maxima,[2] as would be expected if these were at the ends of the frequency distribution.

In the subsequent discussion it will be assumed that the peak at 2616 cm^{-1} cannot be ascribed to a fundamental vibration. However, the changes in the reasoning which are necessary if it is will be pointed out explicitly.

The frequencies 496 cm^{-1} and 650 cm^{-1} cannot be the fundamental lattice torsions since they could be expected to be very intense, even more so than in NH_3 where the torson is the strongest band in the spectrum.[16]

These bands were observed only in thick films and are probably overtones or combinations of still lower frequency lattice modes. The broad peaks at 2991 cm^{-1}

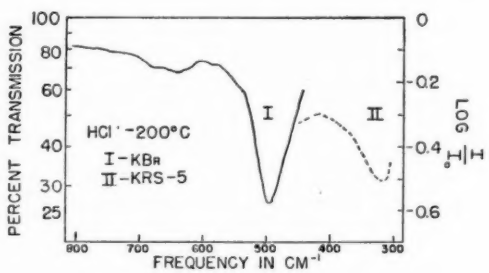

FIG. 2. Lattice spectrum of HCl in the low-temperature phase.

[13] C. C. Ferriso and D. F. Hornig, J. Am. Chem. Soc. **75**, 4113 (1953).

[14] C. C. Ferriso (unpublished).

[15] G. L. Hiebert (unpublished).

[16] F. P. Reding and D. F. Hornig, J. Chem. Phys. **19**, 594 (1951).

and 3171 cm^{-1} are probably combinations of the stretching vibration with lattice frequencies (probably largely torsional) near 266 cm^{-1} and 446 cm^{-1} respectively. The latter may be some of the same levels which give rise to the 496 cm^{-1} band.

b. Hydrogen Bromide

Hydrogen bromide was studied on KBr, NaCl, and CaF_2 backing plates. Typical transmission curves obtained for the lowest temperature phase on KBr are reproduced in Figs. 3 and 4. The temperature of the films (73°K) was well below the transition temperature (89°K). The spectra of thin films closely resemble the corresponding spectra of hydrogen chloride, showing two sharp lines at 2404±3 cm^{-1} and 2438±4 cm^{-1}, in contrast to the single broad band centered at 2420 cm^{-1} reported by Zunino for the crystal at 88°K. It is apparent that Zunino's crystal was not in the lowest temperature phase. The two bands are quite narrow, their widths at half peak intensity being 25 cm^{-1} and 20 cm^{-1} respectively.

The spectra of very thick films show another sharp line (approximately 20 cm^{-1} wide) at 2727 cm^{-1}, which may be analogous to the high-frequency band in hydrogen chloride. However, it seems most likely that this line arises from traces of HCl in the HBr. It has been pointed out previously[17,8] that such a dilute solid solution should show only one sharp line, and the observed line corresponds very closely to the mean of the HCl components, 2729 cm^{-1}. The very weak absorption maxima at about 2660 cm^{-1}, and possibly 2850 cm^{-1}, may actually correspond to the high-frequency peaks in HCl. A weak line whose width is about 100 cm^{-1} has its center at 400 cm^{-1} (Fig. 4) and another very weak absorption is barely evident at 575 cm^{-1}. The structure on the 400 cm^{-1} band is probably caused by water vapor, which has very intense rotational lines in this region.

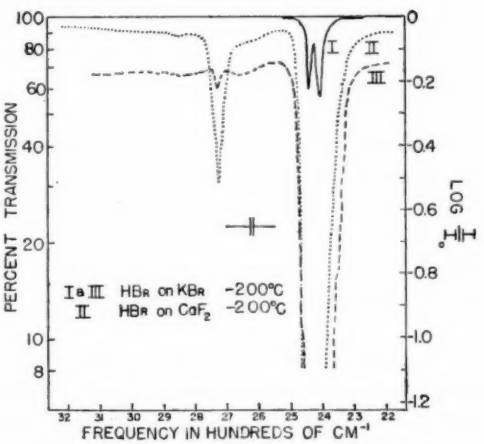

FIG. 3. Infrared spectrum of HBr in the low-temperature phase.

[17] H. J. Hrostowski and G. C. Pimentel, J. Chem. Phys. **19**, 661 (1951).

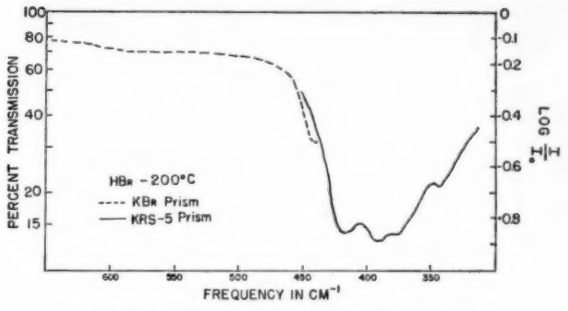

FIG. 4. Lattice spectrum of HBr in the low-temperature crystalline phase.

It was not possible to find a low-frequency component of the strong absorption doublet similar to that found in hydrogen chloride. Several of the films showed an absorption region at 2349 cm^{-1}, a frequency identical with that of carbon dioxide, but it was not reproducible.

c. Hydrogen Iodide

Since hydrogen iodide undergoes a λ-type transition to its low-temperature phase at 70°K, nearly the lowest temperature we could reach, an unambiguous spectrum of this phase was not obtained. Instead, a spectrum of a film was taken on KBr at 83°K, (above the transition temperature); the pressure above the liquid nitrogen was then reduced, and the spectrum was followed as the film cooled to about 66°K. The results are shown in Fig. 5. The thin films reached equilibrium after approximately forty minutes while the spectrum of a medium thick film changed slowly through a period of an hour. The spectrum of a very thick film (not reproduced) gave no indication of passing through the transition point although the nitrogen reservoir was maintained at the nitrogen triple point (63°K) for a period of ninety minutes.

The frequency of maximum absorption, 2120 cm^{-1}, was independent of the temperature throughout the small range studied. However, the transition showed itself by the growth of a single sharp spike (width at half-height, approx. 10 cm^{-1}) above the broader peak (width, approx. 30 cm^{-1}) characterizing HI above 70°K. It is not clear whether the thin film underwent complete transition or not. The base in *B* and *C* of Fig. 5 may be regarded as a remnant of the higher temperature spectrum. However there are indications that additional sharp components exist about 10 cm^{-1} on either side of the central peak, one of which may be just resolved in *C*.

There also appears to be a weak band at about 2075 cm^{-1} in Fig. 5, and a still weaker band at about 2180 cm^{-1} in the spectrum of a very thick film at 83°K. These appear to be a sum and difference band involving a lattice frequency of about 50 cm^{-1}.

CRYSTAL STRUCTURE OF THE HYDROGEN HALIDES

According to the available x-ray information, HCl and HBr are both face-centered orthorhombic crystals

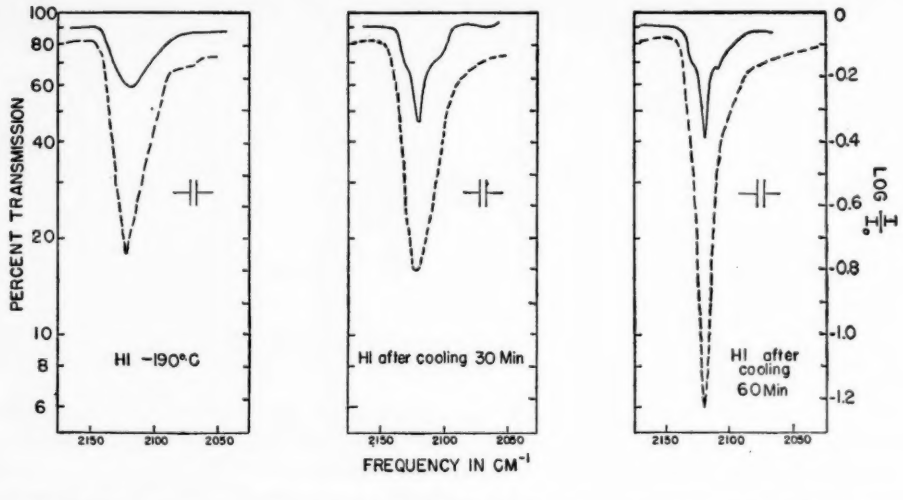

FIG. 5. Spectrum of HI on cooling through phase transition at 70°K.

in their low-temperature phases, the lattice dimensions being 5.03, 5.35, and 5.46 A in HCl, and 5.56, 5.64, and 6.06 A in HBr.[18] The latter are open to some question because the same investigator found an almost identical orthorhombic structure above 117°K whereas optical studies[19] indicate an isotropic structure above this temperature and anisotropic structures below. HI is reported to have a face-centered tetragonal structure with an axial ratio of 1.08:1[20] at all temperatures. However, here too the optical investigation found anisotropy only below 70°K.

If the HCl and HBr structures are face-centered orthorhombic as reported, the x-ray unit cells contain four halogen atoms. The true primitive cell may contain one, two, four or more molecules. On the basis of the present results and the published Raman spectrum, the following conclusions are possible.

(1) The presence of at least two infrared active components in both HCl and HBr demonstrates that there are at least two molecules per primitive unit cell. The orthorhombic symmetry requires that if there are only two molecules per primitive unit cell, they must lie in a plane or in parallel planes. If there are more than two molecules they still lie in parallel planes unless there is a third infrared active component which would indicate a dipole moment perpendicular to the planes (assuming that the direction of dipole moment change is not far from the molecular axis during a stretching vibration). The line at 2616 cm^{-1} is so weak that even if it is a third component the structure is substantially planar.

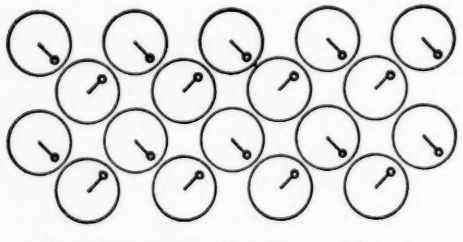

FIG. 6. Two molecule unit cell with both molecules in a single plane.

(2) Unless both of the Raman lines which have been reported in HCl at 2709±5 cm^{-1} and 2759±5 cm^{-1} coincide with the infrared peaks at 2704 and 2746 cm^{-1}, there must be at least four molecules per unit cell in HCl. It seems probable, therefore, that the primitive unit cell contains four molecules, but it is possible that it contains only two.

(3) If there are but *two* molecules in a primitive unit cell there are only two basic structural possibilities.

(a) Both of the molecules lie in a single plane and the crystal is built of planes such as that illustrated in Fig. 6 containing parallel zigzag chains. In this structure, described by space group C_{2v}^{12}, each sheet can be obtained from the others by simple translation.

(b) All of the molecules in a given plane are parallel but the two molecules lie in alternate planes. This possibility is illustrated in Fig. 7 and would consist alternately of planes *a* and *b*.

This second possibility is ruled out by the studies of dilute solutions of HCl in DCl crystals[8] which show that there is an angle of 102° between interacting pairs of molecules and that there is only one kind of pair showing appreciable interaction. It is unreasonable to anticipate that the interacting pair is not the hydrogen-bonded pair.

(4) If there are *four* molecules per primitive unit cell the number of reasonable possibilities is still limited.

(a) If the four molecules lie in a single plane and it is assumed first that one hydrogen atom is bonded to each chlorine and second that the angle between all hydrogen-bonded pairs is identical, the crystal must consist of the planes shown in Fig. 8. Successive planes would be derived from each other by simple lattice translation from the starred molecule to the approxi-

[18] G. Natta, Gazz. chim. Ital. **63**, 425 (1933).
[19] A. Kruis and R. Kaischew, Z. physik. Chem. **B41**, 427 (1938).
[20] B. Ruheman and F. Simon, Z. physik. Chem. **B15**, 389 (1931–1932).

mately face-centered position in the xz or yz plane. Neither of the resultant lattices are orthorhombic so they must be considered improbable, but not impossible, since the powder x-ray study could not have detected small deviations from orthorhombic symmetry.

(b) If two molecules lie in each of two parallel planes, the structure must be built from planes like that in Fig. 6 with the directions of the chains in adjacent planes reversed. There are two possibilities of this sort, depending on whether the reversed plane is displaced by a half unit cell along or perpendicular to the chains. Unless the face-centering is quite exact, and this cannot be determined from powder x-ray studies, displacement along the chain leads to packing difficulties. Displacement perpendicular to the chains results in a lattice of symmetry D_{2h}^{16} and a structure which is identical with one of the possibilities found for HF by Atoji and Lipscomb.[21]

(c) If one molecule lies in each of four planes, the structure is similar to that shown in Fig. 7, planes c and d being obtained by reversing the direction of the chains in a and b. This structure is ruled out by the same arguments as is that of paragraph 3(b).

In summary, the basic structural unit in the HCl and HBr crystals is a zigzag hydrogen-bonded chain. In HCl, at least, the crystal appears to be built from antiparallel pairs of such chains but the relative position of the chains is uncertain. The most probable structures seem to be the two described in paragraph 4b.

It is interesting to compare this result with that obtained for HF in a single crystal x-ray study by Atoji and Lipscomb.[21] They found zigzag hydrogen-bonded chains with an angle between adjacent molecules of 120°. A Fourier analysis based on the space group C_{2v}^{12} (i.e., the structure of Fig. 6) showed a statistical distribution of H atoms on both sides of each F atom, i.e., a structure with symmetry D_{2h}.[17] However, in a footnote they stated that the structure of symmetry D_{2h}^{16} which is not genuinely face-centered is almost as satisfactorily as the random structure.

Not much can be said about the structure of HI. A single sharp component of the stretching vibration

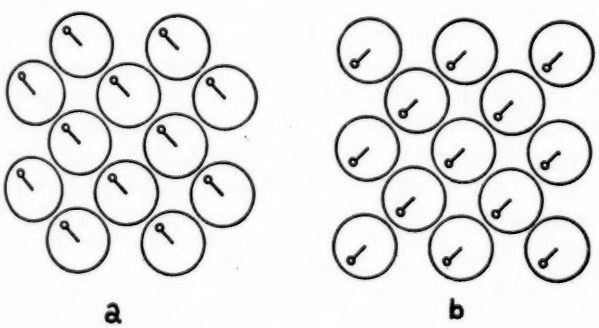

FIG. 7. Crystal planes of two molecule unit cell with molecules in successive planes.

[21] M. Atoji and W. Lipscomb, Acta Cryst. **7**, 173 (1954).

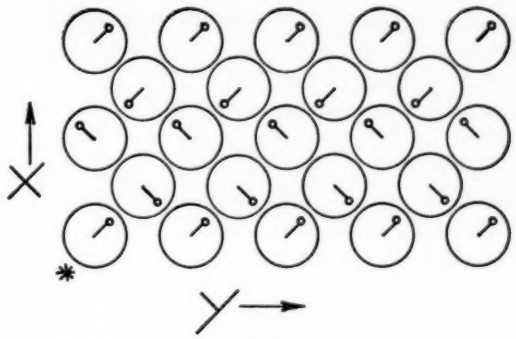

FIG. 8. Four molecule unit cell with four molecules in a single plane.

would be consistent with the tetragonal x-ray structure. In this case there are two basic structural possibilities: (a) the molecules are arranged in parallel or antiparallel chains along the tetragonal axis or (b) sets of four are arrayed perpendicular to the tetragonal axis. However, as pointed out before, it is exactly this question, whether there is but a single component, which remains uncertain in the spectrum. The structure is almost certainly different from HCl and HBr, for the observed peak is probably too sharp to be interpreted as an unresolved pair of peaks; only by this interpretation could a similar structure be supported. A final conclusion in this case must await further study.

THE ANGLE BETWEEN MOLECULES IN HCl AND HBr

In an orthorhombic crystal the dipole moment generated by each normal vibration must be along the x, y, or z axis, and the intensities of the components proportional to the quantities $(\mu_x)_{01}^2$, $(\mu_y)_{01}^2$, and $(\mu_z)_{01}^2$, where μ is the dipole moment matrix of the crystal. If it is assumed that moments are developed along the bond directions when the molecules are stretched, and that the moment of the crystal is the sum of the moments of the molecules, the intensity of each component is proportional to the square of the direction cosines of the molecular axes. It therefore follows immediately that the intensity ratio of the two components in the planar case is given by the expression

$$I_z/I_y = \tan^2\alpha/2, \qquad (1)$$

where α is the angle between bonds.

An estimate of the relative integrated intensities was made by comparing the products of the peak intensities and the line widths at half of the maximum absorption coefficients. The ratios obtained for four HCl films whose peak absorption occurred in a suitable range were 2.25 (Fig. 1), 1.83, and 1.69 on KBr backing and 1.62 on NaCl backing. The corresponding values of α (or $\pi-\alpha$) were 113°, 107°, 105°, and 104°. The reason for the variation is not known although it may be that the films were partially oriented. In this

connection it should be noted that the ratio of peak intensities was only 1.17 on the single film deposited on NaCl whereas values 1.30, 1.32, and 1.69 were obtained for those deposited on KBr.

Similar variations were found by the previous investigators,[2,3] but in all cases the line at 2704 cm^{-1} was more intense, although films were deposited on both salt plates and metal mirrors.

If in fact the films were partially oriented, the accuracy of these angles is open to question, but orientation cannot have been too serious since highly scattering films gave similar ratios. Even if there is no orientation effect, the angles may be in error because of a failure of the initial assumptions. It should be noted that this same objection applies to the angles measured on molecular pairs.[8]

When the same estimate was made for HBr, ratios of 1.28, 1.26, and 1.23 were obtained from three films, all of them on KBr. The corresponding mean angle is either 97° or 83°. Although the same objections apply here as in the case of HCl, it does seem very likely that the intermolecular angle actually is much nearer to 90° than in HCl.

FORCE CONSTANTS IN THE HCl AND HBr CRYSTALS

If it is assumed that the coupling between internal and external motions of the molecules is negligible, and it is shown in appendix A that this is true to a good approximation, the potential energy change when the molecules in a crystal are distorted is

$$2V=\sum_i\sum_j\sum_k\sum_l f_{ij}{}^{kl}r_i{}^k r_j{}^l, \tag{2}$$

where $r_i{}^k$ and $r_j{}^l$ are the ith and jth internal displacement coordinates of the kth and lth unit cells.

If the momentum conjugate to an r is designated p, the kinetic energy is

$$2T=\sum_i\sum_j\sum_k\sum_l g_{ij}{}^{kl}p_i{}^k p_j{}^l. \tag{3}$$

It is worth noting here that the kinetic energy contains cross terms only between coordinates which are common to the same molecule.

In the case of motions which may give rise to spectral activity, either infrared or Raman, corresponding coordinates of all unit cells are equal. That is,

$$r_i{}^1=r_i{}^2=\cdots r_i{}^k=r_i, \tag{4}$$

$$p_i{}^1=p_i{}^2=\cdots p_i{}^k=p_i, \tag{5}$$

so that Eqs. (2) and (3) become

$$2V=N\sum_i\sum_j f_{ij}r_i r_j, \tag{6}$$

$$2T=N\sum_i\sum_j g_{ij}p_i p_j, \tag{7}$$

where

$$f_{ij}=\sum_{k=1}^{N} f_{ij}{}^{kl}, \tag{8}$$

$$g_{ij}=\sum_{k=1}^{N} g_{ij}{}^{kl}. \tag{9}$$

The factor N, the total number of unit cells in the crystal, factors from the equations of motion so that the secular determinant is simply

$$|gf-\lambda I|=0. \tag{10}$$

Its dimensions equal the number of internal coordinates in a single unit cell. In the problem at hand these are just the four H-Cl stretching coordinates.

If the HCl and HBr crystals are orthorhombic, each must belong to one of the D_{2h}, D_2, or C_{2v} space groups. No matter which one, an appropriate set of symmetry coordinates for a unit cell containing four molecules is

$$\begin{aligned} S_1&=\tfrac{1}{2}(r_1+r_2+r_3+r_4)\\ S_2&=\tfrac{1}{2}(r_1+r_2-r_3-r_4)\\ S_3&=\tfrac{1}{2}(r_1-r_2-r_3+r_4)\\ S_4&=\tfrac{1}{2}(r_1-r_2+r_3-r_4). \end{aligned} \tag{11}$$

The symmetry classification of the coordinates depends on the particular structure. These coordinates factor the secular determinant and yield

$$\lambda_i=G_{ii}F_{ii}, \quad i=1\cdots 4. \tag{12}$$

In Eq. (12)

$$G_{ii}=\mu_H+\mu_{Cl}, \tag{13}$$

if μ_H and μ_{Cl} are the reciprocals of the mass of H and Cl, respectively. It is clear from Eq. (12) that for an orthorhombic crystal with four molecules per unit cell there are but four independent force constants. In terms of the symmetry force constants determined from Eq. (12) they are

$$\begin{aligned} f_{11}=f_{22}=f_{33}=f_{44}&=\tfrac{1}{4}(F_{11}+F_{12}+F_{13}+F_{14}),\\ f_{12}=f_{34}&=\tfrac{1}{4}(F_{11}+F_{22}-F_{33}-F_{44}),\\ f_{13}=f_{24}&=\tfrac{1}{4}(F_{11}-F_{22}-F_{33}+F_{44}),\\ f_{14}=f_{23}&=\tfrac{1}{4}(F_{11}-F_{22}+F_{33}-F_{44}). \end{aligned} \tag{14}$$

Assuming that HCl and HBr are actually built of antiparallel zigzag chains, we shall designate the hydrogen-bonded pair in the first chain by r_1 and r_2, the antiparallel pair by r_3 and r_4. Then λ_2 and λ_3 are infrared active, with λ_2 polarized along the chain axis and λ_3 perpendicular to it. Although all four may be Raman active, we will assume that the observed Raman lines in HCl are λ_1 and λ_4. The most reasonable assignments of the observed frequencies in HCl are then as follows:

	A	B
ν_1	2709	2759
ν_2	2704	2746
ν_3	2746	2704
ν_4	2759	2709

Other permutations are possible but these two assignments are the only ones consistent with the assumption that no other interactions are nearly as strong as those between hydrogen-bonded pairs. This assumption is justified by the previous finding that only one variety of significantly interacting molecular pairs occurs in dilute solutions of HCl in DCl. We thus obtain the force constants

$$f_{11}=4.31\times10^5 \text{ dynes/cm}, \quad (\text{gas}=4.806\times10^5 \text{ dynes/cm})$$

$$f_{12}=f_{34}=\mp0.072\times10^5,$$

$$f_{13}=f_{24}=\ \ 0.012\times10^5,$$

$$f_{14}=f_{23}=\pm0.006\times10^5.$$

It is of some interest to compare the principal force constant, f_{11}, and the force constant connecting hydrogen-bonded molecules, f_{12}, with those obtained from the data of Hiebert and Hornig on molecular pairs. In the case of a pair of HCl molecules which are coupled to each other,

$$4\pi^2\nu_1^2=(f_{11}+f_{12}')(\mu_H+\mu_{Cl}),$$

$$4\pi^2\nu_2^2=(f_{11}-f_{12}')(\mu_H+\mu_{Cl}).$$

It is to be anticipated that $f_{12}'=f_{12}/2$ since according to Eq. (9) f_{12} is the sum of the interactions between a single molecule (1) and *all* molecules (2). If only the two nearest neighbor molecules in the chain contributed, the factor would be exactly $\frac{1}{2}$. Using 2715 cm^{-1} and 2737 cm^{-1} for the frequencies, one obtains

$$f_{11}=4.29\times10^5 \text{ dynes/cm},$$

$$f_{12}'=\pm0.035\times10^5 \text{ dynes/cm},$$

both in good agreement with those derived from the present work.

The only alternative interpretation of the spectrum, that the Raman line at 2709 cm^{-1} actually coincides with the infrared line at 2704 cm^{-1}, and that the fourth component is the infrared line at 2616 cm^{-1}, leads to a somewhat different result, namely, that $f_{11}=4.20\times10^5$ dynes/cm and the three cross-terms equal ±0.14, ±0.078 and $\pm0.058\times10^5$ dynes/cm. The principal force constant is in substantial agreement but the existence of three sizeable coupling constants leads to the prediction that three different kinds of interacting pairs would be observed in the dilute solution experiment. These three pairs would have vibration frequencies separated by 12 cm^{-1}, 14 cm^{-1}, and 24 cm^{-1} from the central peak. The first two coincide well with the 12 cm^{-1} separation observed, but the absence of the last peak rules this interpretation out.

Since the Raman spectrum of low-temperature HBr is unavailable, a complete treatment is impossible. However, if it is assumed that coupling between chains is negligible, and it is almost certainly less important than in HCl, the result is

$$f_{11}=3.45\times10^5, \quad (\text{gas}=3.85\times10^5 \text{ dynes/cm}).$$
$$f_{12}=0.048\times10^5$$

In HI it is only possible to obtain a rough value of the principal force constant for comparison with the gas value. It is

$$f_{11}=2.66\times10^5 \quad (\text{gas}=2.95\times10^5 \text{ dynes/cm}).$$

There is evidence of considerable intermolecular interaction, whether or not it be called hydrogen bonding, in all three molecules. Even in HI the fundamental frequency decreases 100 cm^{-1} and the principal force constant by 9.5 percent from the gas value.

Aside from the stretching modes the molecules may also oscillate about axes through their centers of gravity. Since each molecule of the unit cell has two of these motions, eight different modes of this type may be expected; three of them may be infrared active. They have not all been observed. Their magnitude may be estimated as approximately 266 cm^{-1} in HCl from the combination band at 2991 cm^{-1}. If coupling is neglected

$$4\pi^2\nu_T^2=k_T r_0^2/I,$$

where r_0 is the equilibrium internuclear distance, I the moment of inertia, and k_T the force constant for perpendicular displacements of the protons. Using 266 cm^{-1}, we find roughly that

$$k_T=0.041\times10^5 \text{ dynes/cm}.$$

It is interesting that this is of the same order of magnitude as the intermolecular interaction constants found previously. If the corresponding torsional frequency in HBr is 240 cm^{-1}, obtained from the band at 2660 cm^{-1}, the force constant is

$$k_T=0.033\times10^5 \text{ dynes/cm}.$$

CONCLUSION

In both HCl and HBr the low-temperature phases are composed of antiparallel zigzag chains of hydrogen-bonded molecules with angles not too different from 90° between adjacent molecules. This structure is qualitatively similar to that found in gaseous and crystalline HF and indicates that the structure is based, not on a dipole array, but on hydrogen bonds to the nonbonding orbitals of the adjacent molecule. This has the effect of preserving external valence angles.

APPENDIX A

In the calculation of the force constants in the HCl and HBr crystals, it was assumed that to a good approximation there was no interaction between internal and external motions of the molecules in a crystal. This can be shown as follows. According to

second order perturbation theory the ith eigenvalue of a set of coupled harmonic oscillators is displaced by an amount

$$\Delta\lambda_i=\sum_{j\neq i}(GF)_{ji}(GF)_{ij}/(\lambda_i^0-\lambda_j^0) \qquad \text{(A1)}$$

by the introduction of the coupling GF. In Eq. (A1) $\lambda_i^0=4\pi^2\nu_i^2c^2$, if ν_i is the frequency (cm^{-1}) in the absence of the coupling. In the present case the eigenvalues corresponding to lattice frequencies may be neglected in comparison to those representing the internal vibrations and the matrix G contains no cross terms connecting internal and lattice coordinates. The shift in frequency of an internal vibration then becomes

$$32\pi^4c^4\nu_i^3\Delta\nu_i=\sum_{j\neq i}G_{ii}G_{jj}F_{ij}^2. \qquad \text{(A2)}$$

If it is assumed that the order of magnitude of the coupling elements F_{ij} is that of those coupling internal vibrations, or the diagonal elements for the torsional lattice vibrations, then the frequency shift arising from coupling between internal and lattice modes would be less than 0.2 cm^{-1}. Even if this estimate were in considerable error it would still be justifiable to neglect the interaction with lattice modes when obtaining the frequencies of internal vibrations.

THE JOURNAL OF CHEMICAL PHYSICS VOLUME 23, NUMBER 4 APRIL, 1955

Note on an Analytical Proof of Wulff's Theorem in Three Dimensions*

G. C. Benson and D. Patterson†
Division of Pure Chemistry, National Research Council, Ottawa, Canada
(Received August 19, 1954)

A proof of Wulff's theorem for the equilibrium shape of a two-dimensional crystal has been given by Burton, Cabrera, and Frank. This has been extended to three dimensions in the present note and an expression has been derived for the principal radii of curvature of the crystal.

INTRODUCTION

THE equilibrium shape of a crystal is determined by minimizing the surface free energy keeping the volume constant. Wulff's theorem states that the result is a figure in which it is possible to locate a point whose distances from the various faces of the crystal are proportional to their surface free energies per unit area. A number of types of proof of varying degrees of generality have been given for this statement, and critical reviews of the subject have been rewritten by von Laue[1] and Herring.[2] The most satisfactory proof has been given by Dinghas.[3] Using a Brunn-Minkowski inequality, he proved that the Wulff construction gives an absolute minimum for the free energy of a convex crystal. Herring[2] has indicated that this proof is also valid for any shape of crystal. Until recently, however, an analytical proof has been lacking. This has been supplied in the two-dimensional case by Burton, Cabrera, and Frank[4] and also by Nielsen and Garfinkel.[5] The present note describes an attempt to extend the former proof to three dimensions.

FORMULATION AND SOLUTION OF THE VARIATIONAL PROBLEM

The specific surface free energy at a point on the surface of a given crystalline material is assumed to be a function only of the orientation $\mathbf{n}$ of the unit outward normal vector at that point and will be denoted by $f(\mathbf{n})$. Hence the total surface free energy F associated with a closed form is

$$F=\int f(\mathbf{n})d\sigma, \qquad (1)$$

where the integral extends over the entire surface. The volume of the crystal can be expressed as

$$V=\int d\tau=\tfrac{1}{3}\int \mathrm{div}\mathbf{r}\,d\tau, \qquad (2)$$

where $\mathbf{r}$ is the radius vector from some arbitrary fixed origin to a point of the crystal, and the integration is taken throughout the volume of the crystal.

The integral in Eq. (2) can be converted by Gauss' theorem to a surface integral

$$V=\tfrac{1}{3}\int \mathbf{r}\cdot\mathbf{n}\,d\sigma=\tfrac{1}{3}\int p\,d\sigma. \qquad (3)$$

The pedal p is defined as

$$p=\mathbf{r}\cdot\mathbf{n}=xn_x+yn_y+zn_z, \qquad (4)$$

* Issued as N. R. C. No. 3574.
† National Research Laboratories Postdoctorate Research Fellow.
[1] M. von Laue, Z. Krist. **105**, 124 (1943).
[2] C. Herring, *Structure and Properties of Solid Surfaces* (University of Chicago Press, Chicago, Illinois, 1953), p. 5.
[3] A. Dinghas, Z. Krist. **105**, 304 (1944).
[4] Burton, Cabrera, and Frank, Trans. Roy. Soc. (London) **A243**, 299 (1951).
[5] J. P. Nielsen and B. Garfinkel, Phys. Rev. **86**, 624(A) (1952).

and represents the perpendicular distance from the origin to the tangent plane at the surface point **r**. This is illustrated in Fig. 1.

The components of **n** relative to a set of orthogonal Cartesian axes can be written

$$n_x=\sin\theta\cos\phi,\quad n_y=\sin\theta\sin\phi,\quad n_z=\cos\theta, \tag{5}$$

where θ and ϕ are the polar angles of **n** and fall in the ranges $0\leq\theta<\pi$ and $0\leq\phi<2\pi$.

Using θ and ϕ as independent variables the partial derivatives of p are

$$p_\theta=\frac{\partial\mathbf{n}}{\partial\theta}\cdot\mathbf{r}+\mathbf{n}\cdot\frac{\partial\mathbf{r}}{\partial\theta}=\frac{\partial\mathbf{n}}{\partial\theta}\cdot\mathbf{r}, \tag{6}$$

and

$$p_\phi=\frac{\partial\mathbf{n}}{\partial\phi}\cdot\mathbf{r}+\mathbf{n}\cdot\frac{\partial\mathbf{r}}{\partial\phi}=\frac{\partial\mathbf{n}}{\partial\phi}\cdot\mathbf{r}. \tag{7}$$

In Eqs. (6) and (7), $\partial\mathbf{r}/\partial\theta$ and $\partial\mathbf{r}/\partial\phi$ are vectors in the tangent plane and hence their scalar products with **n** vanish. Equations (4), (6), and (7), after substituting the components of **n** from Eq. (5), can be solved for the x, y, z coordinates of a surface point in terms of θ, ϕ, p and the first derivatives of p. Thus

$$\begin{aligned}x&=p\sin\theta\cos\phi+p_\theta\cos\theta\cos\phi-p_\phi\sin\phi/\sin\theta\\ y&=p\sin\theta\sin\phi+p_\theta\cos\theta\sin\phi+p_\phi\cos\phi/\sin\theta\\ z&=p\cos\theta-p_\theta\sin\theta.\end{aligned} \tag{8}$$

The element of area $d\sigma$ can be expressed[6] by

$$d\sigma=Qd\theta d\phi, \tag{9}$$

where

$$Q=\left[\left(\frac{\partial(y,z)}{\partial(\theta,\phi)}\right)^2+\left(\frac{\partial(z,x)}{\partial(\theta,\phi)}\right)^2+\left(\frac{\partial(x,y)}{\partial(\theta,\phi)}\right)^2\right]^{\frac{1}{2}} \tag{10}$$

$$=KM-L^2/\sin^3\theta. \tag{11}$$

Here,

$$\begin{aligned}K&=p+p_{\theta\theta}\\ L&=p_{\theta\phi}\sin\theta-p_\phi\cos\theta\\ M&=p\sin\theta+p_\theta\cos\theta+p_{\phi\phi}/\sin\theta.\end{aligned} \tag{12}$$

The variational problem now is to determine a function $p(\theta,\phi)$ which makes

$$F=\int f(\mathbf{n})Qd\theta d\phi \tag{13}$$

a minimum subject to the condition that

$$V=\tfrac{1}{3}\int pQd\theta d\phi \tag{14}$$

is held constant. After introducing $2/\lambda$ as a convenient

[6] H. Jeffreys and B. S. Jeffreys, *Methods of Mathematical Physics* (Cambridge University Press, Cambridge, England, 1950), second edition, p. 192.

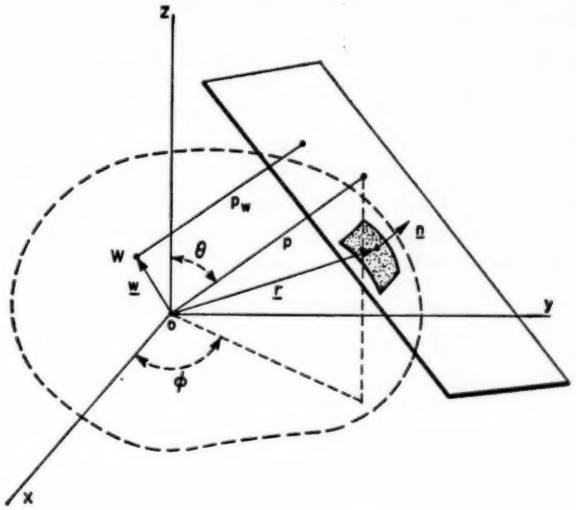

FIG. 1. The coordinate system.

form of the Lagrange multiplier, the problem reduces to making

$$I=F-2V/\lambda=\int G(\theta,\phi,p,p_\theta,p_\phi,p_{\theta\theta},p_{\theta\phi},p_{\phi\phi})d\theta d\phi \tag{15}$$

an extremum, where

$$G(\theta,\phi,p,p_\theta,p_\phi,p_{\theta\theta},p_{\theta\phi},p_{\phi\phi})=[f(\mathbf{n})-2(3\lambda)^{-1}p]Q. \tag{16}$$

Euler's condition for a stationary value in this case can be written

$$\begin{aligned}\frac{\partial G}{\partial p}-\frac{\partial}{\partial\theta}\frac{\partial G}{\partial p_\theta}-\frac{\partial}{\partial\phi}\frac{\partial G}{\partial p_\phi}+\frac{\partial^2}{\partial\theta^2}\frac{\partial G}{\partial p_{\theta\theta}}\\ +\frac{\partial^2}{\partial\theta\partial\phi}\frac{\partial G}{\partial p_{\theta\phi}}+\frac{\partial^2}{\partial\phi^2}\frac{\partial G}{\partial p_{\phi\phi}}=0.\end{aligned} \tag{17}$$

After substitution for G, Eq. (17) becomes

$$\begin{aligned}&(p-\lambda f)[M+K\sin\theta]+(p_\theta-\lambda f_\theta)[K\cos\theta]\\ &\quad+(p_\phi-\lambda f_\phi)[2L\cos\theta/\sin^3\theta]+(p_{\theta\theta}-\lambda f_{\theta\theta})[M]\\ &\quad+(p_{\theta\phi}-\lambda f_{\theta\phi})[-2L/\sin^2\theta]\\ &\qquad+(p_{\phi\phi}-\lambda f_{\phi\phi})[K/\sin\theta]=0.\end{aligned} \tag{18}$$

After regrouping the terms, Eq. (18) leads to

$$Rp_{\theta\theta}+Sp_{\theta\phi}+Tp_{\phi\phi}+U(p_{\theta\theta}p_{\phi\phi}-p_{\theta\phi}^2)=V, \tag{19}$$

where R, S, T, U, and V are functions of θ, ϕ, p, p_θ, and p_ϕ. This form is known as Ampère's extension of Monge's equation and its solution is outlined in standard texts on differential equations. In the present case, however, V is an awkward function of f and its derivatives and application of this method does not appear feasible.

As an alternative method of finding a solution the following procedure was adopted. Equation (18) is symmetrical in $(p-\lambda f)$ and p; thus, setting

$$p-\lambda f(\mathbf{n})=Z(\theta,\phi), \tag{20}$$

it can be rewritten as

$$p[\bar{M}+\bar{K}\sin\theta]+p_\theta[\bar{K}\cos\theta]+p_\phi[2\bar{L}\cos\theta/\sin^3\theta]+p_{\theta\theta}[\bar{M}]+p_{\theta\phi}[-2\bar{L}/\sin^2\theta]+p_{\phi\phi}[\bar{K}/\sin\theta]=0. \quad (21)$$

Here $\bar{K}$, $\bar{L}$, and $\bar{M}$ are defined by Eqs. (12) with p and its derivatives replaced by Z and its corresponding derivatives. Each of the terms in square brackets will vanish if it is possible to find a $Z(\theta,\phi)$ which satisfies the three simultaneous equations

$$\begin{aligned}\bar{K}&=Z+Z_{\theta\theta}=0\\ \bar{L}&=Z_{\theta\phi}\sin\theta-Z_\phi\cos\theta=0\\ \bar{M}&=Z\sin\theta+Z_\theta\cos\theta+Z_{\phi\phi}/\sin\theta=0.\end{aligned} \quad (22)$$

The general solution of these equations is

$$Z=A\sin(\phi-\alpha)\sin\theta+B\cos\theta, \quad (23)$$

where A, B, and α are constants. Thus

$$p=\lambda f(\mathbf{n})+A\sin(\phi-\alpha)\sin\theta+B\cos\theta \quad (24)$$

is a solution of the variational problem.

DISCUSSION

It has not been possible to prove that Eq. (24) is the most general form of solution. However it does appear to be a reasonable extension of the general solution in two dimensions given by Burton, Cabrera, and Frank. From the symmetry noted in connection with Eqs. (18) and (21), it follows that

$$p=A'\sin(\phi-\alpha')\sin\theta+B'\cos\theta \quad (25)$$

is also a solution. This is independent of $f(\mathbf{n})$ and is of no physical significance.

If the origin is shifted by a vector $\mathbf{w}$ to a new point W, p_w, the corresponding value of p measured from W, is given by

$$p_w=p-\mathbf{w}\cdot\mathbf{n}=\lambda f(\mathbf{n})-[A\sin\alpha+w_x]\sin\theta\cos\phi+[A\cos\alpha-w_y]\sin\theta\sin\phi+[B-w_z]\cos\theta. \quad (26)$$

It is possible to choose the point W such that the square-bracketed terms of Eq. (26) all vanish. Then, using W the Wulff point as origin,

$$p_w=\lambda f(\mathbf{n}). \quad (27)$$

This equation leads to the statement of Wulff's theorem given in the introduction.

If F_m is the total surface free energy corresponding to the equilibrium shape, then Eqs. (1), (3), and (27) give a physical interpretation for the Lagrange parameter. Thus

$$2/\lambda=2F_m/(3V). \quad (28)$$

The principal radii of curvature ρ_1 and ρ_2 may be obtained for the equilibrium shape determined by Eq. (27). ρ_1 and ρ_2 are found as the roots of the equation

$$\rho^2+\rho(K+M/\sin\theta)+(KM-L^2/\sin^3\theta)/\sin\theta=0, \quad (29)$$

where K, L, and M are as defined previously.

It has been implicitly assumed in the above proof that the equilibrium shape possesses no sharp edges or corners, i.e., that p is a continuous function of θ and ϕ. For the two-dimensional case the possibility of discontinuities has been discussed by Burton, Cabrera, and Frank, who conclude that the proof is still valid. Presumably a similar statement is true for edges and corners in three dimensions, although it seems difficult to give a rigorous proof in either case.

Finally, it may be noted that the Euler condition stated in Eq. (17) is for a relative extremum. Hence the foregoing treatment has not established that the Wulff's construction leads to an absolute minimum of the surface energy. The same criticism is applicable to the corresponding proof in two dimensions. In the case of a constant value of f it can be shown that Eq. (27) leads to the expected result that a sphere has the minimum surface area for a fixed volume. Here, if $p=\lambda f$ and f is constant, Eq. (12) gives

$$K=\lambda f,\quad M=\lambda f\sin\theta,\quad L=0,$$

whence, $\rho_1=\rho_2=-\lambda f$. The negative sign of ρ_1 and ρ_2 indicates that the surface is convex in the direction of the outward normal, and it is apparent that the equilibrium shape is a sphere. However, to prove in general that Eq. (27) corresponds to a minimum it would be necessary to examine the behavior of the higher derivatives in accordance with Legendre's theory. This does not appear worthwhile since the minimal character of the extremum is assured by the physical nature of the problem.

ACKNOWLEDGMENT

The authors wish to thank Dr. P. Mandl of the National Research Council Aerodynamics Laboratory for an interesting discussion of the Monge-Ampère differential equation.

An LCAO MO Study of the Structure of Chlorophyll Prototypes*

SHELDON L. MATLOW
Chemistry Department, Brookhaven National Laboratory, Upton, Long Island, New York

(Received April 29, 1954)

By means of Wheland's method of treating systems with hetero-atoms three possible isomers of porphyrin and five of dihydroporphyrin are studied from the viewpoint of the energies of the ground states and the transition energies to the lowest lying excited states. In the case of porphyrin it is found that, within the limits of accuracy of the method used, two of the structures, PA (porphyrin-adjacently bonded hydrogens) and PO (porphyrin-oppositely bonded hydrogens), have identical ground state energies. In the case of dihydroporphyrin the DHP-AI (DHP-A—dihydroporphyrin-adjacently bonded hydrogens) isomer is most stable and the DHP-AII and DHP-OII (DHP-O—dihydroporphyrin-oppositely bonded hydrogens) isomers are more energetic by 1.06 and 1.20 kcal/mole, respectively. With respect to the transition energies and the resulting spectra it is possible that the peaks in the spectrum of porphyrin are not due mainly to vibrational fine structure of a single electronic transition, as is proposed by Rabinowitch, but rather are the combination of the electronic spectra of the PA and PO isomers. The dihydroporphyrin spectral analysis, however, indicates that several of the peaks are probably vibrational fine structure of a single electronic transition. The calculated bond orders are given for the various structures discussed.

INTRODUCTION

THE structure of porphyrin ($C_{20}H_{14}N_4$) is of great interest not only in its own right, but also because the porphyrin skeleton is basic to such naturally occurring compounds as chlorophyll and hemin. The positions of the nitrogens and carbons are quite well known. Very little is known, however, about the positions and the nature of the binding, of the hydrogens bound to the nitrogens. Erdman and Corwin give some spectroscopic evidence indicating that the hydrogens are not symmetrically bound to the nitrogens.[1] Their argument is based upon the fact that etioporphyrin II (1,4,5,8-tetramethyl-2,3,6,7-tetraethyl porphyrin) and *N*-methyl etioporphyrin II have similar spectra. These spectra, however, differ considerably from the spectra of the disodium salt, the dihydrochloride, and the metallic complexes of etioporphyrin II, compounds which have similar spectra.

Several theoretical studies have been made of the structure of porphyrin. Kuhn,[2] Simpson,[3] and Nakajima and Kon[4] have made free electron model (FEM) calculations while Longuet-Higgins, Rector, and Platt[5] have used the LCAO MO (Linear Combination of Atomic Orbitals-Molecular Orbital) approximation (Simpson[3] also made some LCAO MO calculations). Although Kuhn states that he has made an FEM study and that the study will be published,[2] this author has not been able to find the publication; therefore, no comment can be made as to Kuhn's methods or results. Simpson[3] used a simple FEM method approximating the molecule by an eighteen atom, single ring system, neglecting branching and the difference between nitrogen and carbon atoms. His approximation also neglects any possibility of the nitrogens differing somewhat because of the attached hydrogens. Nakajima and Kon[4] take into consideration the actual branching in the molecule. They explicitly distinguish the nitrogens from the carbons by using a deeper potential well for the sub-boxes representing the nitrogens. However, they do not distinguish between nitrogens bonded to hydrogen and nitrogens not bonded to hydrogen. Longuet-Higgins, Rector, and Platt[5] use the standard LCAO MO method including overlap. They distinguish between nitrogen and carbon by a perturbation correction on a calculation which assumes that all the atomic orbitals are carbon $2p\pi$ orbitals. As is the case with the authors using the FEM method, they assume all the nitrogens to be identical.

The work of Erdman and Corwin,[1] indicating that the nitrogens are not identical, makes it desirable that a theoretical study be made of porphyrin explicitly taking into consideration the possibility that the nitrogens are not identical. It is the purpose of this paper to report on such a study. The method used here is Wheland's[6] modification of the LCAO MO approximation for hetero-atom systems. The structure of porphyrin, as well as that of its reduction product, dihydroporphyrin, will be considered from two viewpoints. First, the possible isomeric structures will be compared with regard to the energies of the respective ground states. Second, the spectra calculated for the transitions from the ground states to the lowest lying excited states will be compared with the available experimental data. In the calculation of the spectra, no consideration will be given to the effect of configuration interaction nor to singlet-triplet energy separations.

In the Wheland method for treating hetero-atom systems,[6] the hetero-atoms are introduced by means of

* Research carried out under the auspices of the U. S. Atomic Energy Commission.

[1] J. G. Erdman and A. H. Corwin, J. Am. Chem. Soc. **68**, 1885 (1946).

[2] H. Kuhn, J. Chem. Phys. **17**, 1198 (1949).

[3] W. T. Simpson, J. Chem. Phys. **17**, 1218 (1949).

[4] T. Nakajima and H. Kon, J. Chem. Phys. **20**, 750 (1952).

[5] Longuet-Higgins, Rector, and Platt, J. Chem. Phys. **18**, 1174 (1950).

[6] G. W. Wheland, J. Am. Chem. Soc. **64**, 900 (1942). For a detailed analysis of the method, see S. L. Matlow, Doctoral thesis, Department of Chemistry, University of Chicago, 1953.

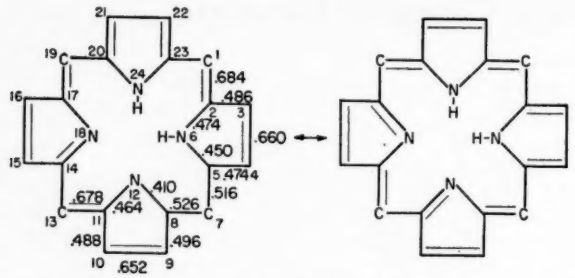

FIG. 1. PA (porphyrin-adjacently bonded hydrogens). (Note: the three digit numbers are the bond orders.)

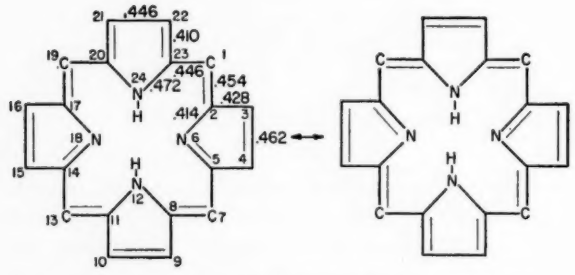

FIG. 2. PO (porphyrin-oppositely bonded hydrogens).

the electronegativity parameter, δ_k. The usual rule for evaluating the δ_k's, which is necessary to predict the correct dipole moments, is to assign the greater electronegativity to the atom, which in the classical structure for the compound, shares its "unshared" electrons to the least extent with adjacent atoms. In this treatment, however, the atom in the classical structure, which can most easily accept a pair of electrons from other atoms of the molecule is considered the most electronegative. This modification of the usual rule is necessary in order to bring the results on dihydroporphyrin into agreement with the predictions of the theory of resonance. The value of δ_{nitrogen} used here is 0.8 for singly bonded nitrogens and 1.0 for doubly bonded nitrogens (doubly bonded, that is, in a classical structure). In other words, a nitrogen which is bonded to a hydrogen is given a δ value of 0.8, and a nitrogen which is not bonded to a hydrogen is given a δ value of 1.0. In the cases in which the central hydrogens are assumed to be symmetrically bonded to all four nitrogens, δ_{nitrogen} is given the intermediate value of 0.9.

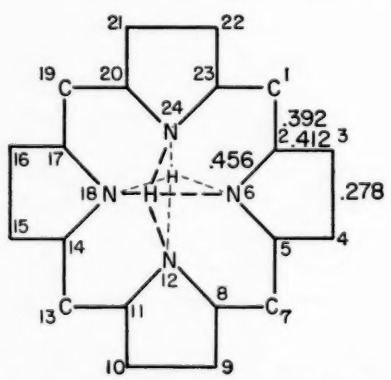

FIG. 3. PS (porphyrin-symmetrically bonded hydrogens).

GROUND-STATE ENERGIES

Porphyrin

Assuming that the central hydrogens are bonded to the nitrogens by means of classical valence forces, one can draw two isomeric structures for porphyrin, PA (porphyrin-adjacently bonded hydrogens) (Fig. 1) and PO (porphyrin-oppositely bonded hydrogens) (Fig. 2). If one includes nonclassical valence forces such as π-complex binding, a third isomeric structure can be drawn, PS (porphyrin-symmetrically bonded hydrogens) (Fig. 3). In Table I are listed the first fifteen π-electronic energy levels for PA, PO, and PS. The total energy is calculated by placing two electrons in each level.† On this basis the energies of the structures are

$$E_{\text{PA}}=26\alpha+26.7672\beta \quad (1)$$

$$E_{\text{PO}}=26\alpha+26.7666\beta \quad (2)$$

$$E_{\text{PS}}=26\alpha+26.7589\beta. \quad (3)$$

TABLE I. π-electronic energy levels for isomeric structures of porphyrin.

Level	Structure PA	PO	PS
I	$\alpha+1.5820\beta$	$\alpha+1.5765\beta$	$\alpha+1.5673\beta$
II	$\alpha+1.5372\beta$	$\alpha+1.5536\beta$	$\alpha+1.5228\beta$
III	$\alpha+1.5123\beta$	$\alpha+1.4966\beta$	$\alpha+1.5228\beta$
IV	$\alpha+1.4399\beta$	$\alpha+1.4449\beta$	$\alpha+1.4491\beta$
V	$\alpha+1.1520\beta$	$\alpha+1.1520\beta$	$\alpha+1.1520\beta$
VI	$\alpha+0.9484\beta$	$\alpha+0.9600\beta$	$\alpha+0.9429\beta$
VII	$\alpha+0.9467\beta$	$\alpha+0.9324\beta$	$\alpha+0.9429\beta$
VIII	$\alpha+0.8688\beta$	$\alpha+0.8753\beta$	$\alpha+0.8396\beta$
IX	$\alpha+0.8652\beta$	$\alpha+0.8611\beta$	$\alpha+0.8369\beta$
X	$\alpha+0.8000\beta$	$\alpha+0.8000\beta$	$\alpha+0.8350\beta$
XI	$\alpha+0.8000\beta$	$\alpha+0.8000\beta$	$\alpha+0.8350\beta$
XII	$\alpha+0.5353\beta$	$\alpha+0.5353\beta$	$\alpha+0.5353\beta$
XIII	$\alpha+0.3958\beta$	$\alpha+0.3965\beta$	$\alpha+0.3978\beta$
XIV	$\alpha-0.1918\beta$	$\alpha-0.1804\beta$	$\alpha-0.1913\beta$
XV	$\alpha-0.1923\beta$	$\alpha-0.2034\beta$	$\alpha-0.1913\beta$

Thus, within the limitations of the method used, the three isomeric structures have the same energy, except for the uncertain σ-bond energy correction term for PS, which makes PS much more unstable than the other two structures. It is to be expected, therefore, that porphyrin at room temperature is a mixture of

† This procedure assumes that the σ-electronic energies are identical for the three structures. This assumption is essentially correct if the comparison is between PA and PO. PS, however, has two less σ-bonds than PA and PO, namely the two hydrogen-nitrogen bonds. The hydrogen-nitrogen bond energy is 83.7 kcal/mole (L. Pauling, *The Nature of the Chemical Bond* (Cornell University Press, Ithaca, 1948), second edition, p. 53). Thus the σ-bond energy of PS (as well as that of DHP-S discussed below) is 167.4 kcal/mole greater than that of the other isomers. However, this difference is partially compensated by having the hydrogens "in the midst of an electronic sea." This author knows of no way of accurately estimating this energy effect. It is, in all probability, less than 80 kcal/mole for the entire molecule. Therefore, a correction term of about 80 kcal/mole should be added to the energy calculated for PS (similarly for DHP-S).

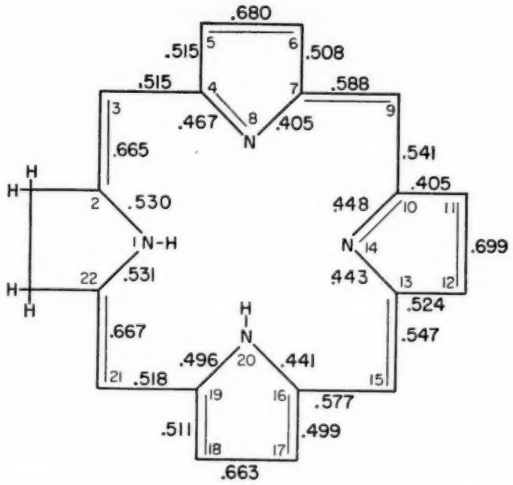

FIG. 4. DHP-AI (dihydroporphyrin-adjacently bonded hydrogens) (three digit numbers are bond orders).

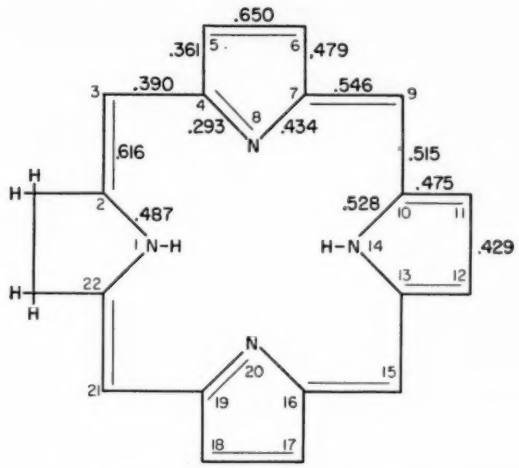

FIG. 6. DHP-OI (dihydroporphyrin-oppositely bonded hydrogens).

equal amounts of PA and PO. This author knows of no experimental data available at the present to test this prediction. Dorough and Shen,[7] however, do report some spectral evidence indicating that α, β, γ, δ-tetraphenyl porphyrine is a mixture of two isomers.

Dihydroporphyrin

As is the case with porphyrin the central hydrogens of dihydroporphyrin can be bonded in three ways, (1) to adjacent nitrogens, DHP-A (dihydroporphyrin-adjacently bonded hydrogens), (2) to opposite nitrogens, DHP-O (dihydroporphyrin-oppositely bonded hydrogens), and (3) symmetrically to all four nitrogens, DHP-S (dihydroporphyrin-symmetrically bonded hydrogens). However, unlike porphyrin, the four pyrrole rings in dihydroporphyrin are not identical. One of the rings is partially reduced. This idiosyncrasy of the dihydroporphyrin ring system results in there being two DHP-A and two DHP-O isomers. These isomers shall be distinguished according to the following rule. If one of the hydrogens is bonded to the nitrogen of the reduced ring, the isomer designation will be followed by the roman numeral I. If neither hydrogen is bonded to the nitrogen of the reduced ring, the isomer designation will be followed by the roman numeral II. Thus, the four classically bonded isomers are DHP-AI, DHP-AII, DHP-OI, and DHP-OII (Figs. 4–7). Only one π-bonded isomer will be considered here, DHP-S (Fig. 8). That is, with regard to the symmetrical isomer, no consideration will be made of possible further isomerization resulting from the nonequivalence of the four rings. In Table II are listed the first fourteen π-electronic energy levels for the dihydroporphyrin isomers under discussion. Proceeding as in the porphyrin case, we have

$$E(\text{DHP-AI}) = 24\alpha + 24.5844\beta \qquad (4)$$

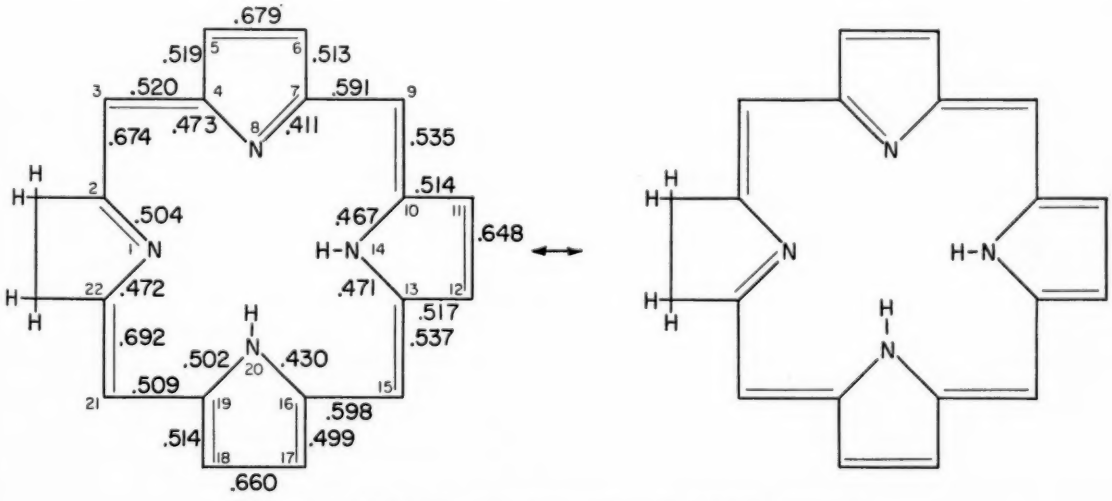

FIG. 5. DHP-AII (dihydroporphyrin-adjacently bonded hydrogens).

[7] G. D. Dorough and K. T. Shen, J. Am. Chem. Soc. **72**, 3939 (1950).

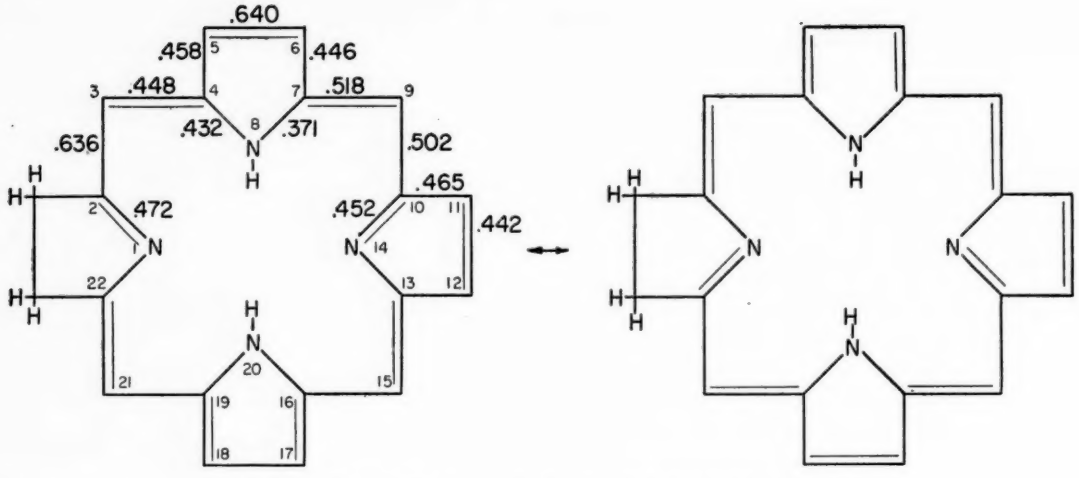

FIG. 7. DHP-OII (dihydroporphyrin-oppositely bonded hydrogens).

$$E(\text{DHP-AII}) = 24\alpha + 24.5580\beta \quad (5)$$

$$E(\text{DHP-OI}) = 24\alpha + 24.0300\beta \quad (6)$$

$$E(\text{DHP-OII}) = 24\alpha + 24.5544\beta \quad (7)$$

$$E(\text{DHP-S}) = 24\alpha + 24.5622\beta. \quad (8)$$

If the energy of DHP-AI is taken as the standard, the energies of the other isomers are greater by the following amounts:

$$\Delta E(\text{DHP-AII}) = -0.0264\beta = 1.06 \text{ kcal/mole} \quad (9)$$

$$\Delta E(\text{DHP-OI}) = -0.5544\beta = 22.18 \text{ kcal/mole} \quad (10)$$

$$\Delta E(\text{DHP-OII}) = -0.0300\beta = 1.20 \text{ kcal/mole} \quad (11)$$

$$\Delta E(\text{DHP-S}) = -0.0222\beta = 0.89 \text{ kcal/mole}. \quad (12)$$

The value used for β is -40 kcal/mole.[8] As was pointed out above ΔE(DHP-S) should be corrected by a factor of about 80 kcal/mole. Thus

$$\Delta E'(\text{DHP-S}) = 0.89 + 80 = 80.89 \text{ kcal/mole}. \quad (12')$$

On the basis of these calculations, it appears that at room temperature dihydroporphyrin is a mixture of three isomers DHP-AI, DHP-AII, and DHP-OII. Furthermore, two of the isomers, DHP-AII and DHP-OII, are about one kcal more energetic than DHP-AI. (It was pointed out above that the calculations in this series were made using an electronegativity rule different from the one necessary to predict dipole moments correctly. If the latter rule were used for these calculations, the I and II designations would reverse for the energy values of Table II. This would result in DHP-OII being the least stable of the classical valence isomers. According to the theory of resonance this does not seem reasonable since DHP-OII has two Kekule structures contributing to the hybrid while DHP-OI has only one.)

FIG. 8. DHP-S (dihydroporphyrin-symmetrically bonded hydrogens).

[8] G. W. Wheland, J. Am. Chem. Soc. **63**, 2025 (1941).

TRANSITION ENERGETICS

Porphyrin

The available data on the spectrum of porphyrin are listed in Table III. The data of Stern *et al.*[9–11] appear to be the most consistent and reproducible of the entire group. Rabinowitch[12] apparently concurs with this opinion since he considers only their work in his discussion of the spectrum of porphyrin. In Table IV are listed the values obtained by averaging the three spectra of Stern *et al.*[9–11] Rabinowitch[12] does not consider the 634 or the 602 mμ peaks at all. He includes a

[9] A. Stern and H. Wenderlein, Z. physik. Chem. **175A**, 405 (1936).

[10] Stern, Wenderlein, and Molvig, Z. physik. Chem. **177A**, 40 (1936).

[11] F. Pruckner and A. Stern, Z. physik. Chem. **177A**, 387 (1936).

[12] E. I. Rabinowitch, *Photosynthesis and Related Processes* (Interscience Publishers, Inc., New York, 1951), Vol. II, Part 1, pp. 619–22.

TABLE II. π-electronic energy levels of dihydroporphyrin isomers.

Level	DHP-AI[a]	DHP-AII	DHP-OI	DHP-OII	DHP-S
I	$\alpha+1.5794\beta$[b]	$\alpha+1.5659\beta$	$\alpha+1.5698\beta$	$\alpha+1.5685\beta$	$\alpha+1.5580\beta$
II	$\alpha+1.5342\beta$	$\alpha+1.5154\beta$	$\alpha+1.4733\beta$	$\alpha+1.4986\beta$	$\alpha+1.5218\beta$
III	$\alpha+1.4853\beta$	$\alpha+1.4797\beta$	$\alpha+1.4698\beta$	$\alpha+1.4954\beta$	$\alpha+1.4870\beta$
IV	$\alpha+1.3472\beta$	$\alpha+1.4169\beta$	$\alpha+1.3502\beta$	$\alpha+1.4154\beta$	$\alpha+1.3857\beta$
V	$\alpha+1.1335\beta$	$\alpha+1.1335\beta$	$\alpha+1.1331\beta$	$\alpha+1.1333\beta$	$\alpha+1.1335\beta$
VI	$\alpha+0.9425\beta$	$\alpha+0.9462\beta$	$\alpha+0.9272\beta$	$\alpha+0.9595\beta$	$\alpha+0.9422\beta$
VII	$\alpha+0.9015\beta$	$\alpha+0.9015\beta$	$\alpha+0.8753\beta$	$\alpha+0.8720\beta$	$\alpha+0.8863\beta$
VIII	$\alpha+0.8667\beta$	$\alpha+0.8529\beta$	$\alpha+0.8645\beta$	$\alpha+0.8686\beta$	$\alpha+0.8388\beta$
IX	$\alpha+0.8527\beta$	$\alpha+0.8000\beta$	$\alpha+0.8000\beta$	$\alpha+0.8000\beta$	$\alpha+0.8363\beta$
X	$\alpha+0.8000\beta$	$\alpha+0.8000\beta$	$\alpha+0.7070\beta$	$\alpha+0.8000\beta$	$\alpha+0.8315\beta$
XI	$\alpha+0.4306\beta$	$\alpha+0.4382\beta$	$\alpha+0.4253\beta$	$\alpha+0.4369\beta$	$\alpha+0.4302\beta$
XII	$\alpha+0.4186\beta$	$\alpha+0.4288\beta$	$\alpha+0.4195\beta$	$\alpha+0.4290\beta$	$\alpha+0.4298\beta$
XIII	$\alpha-0.1393\beta$	$\alpha-0.1302\beta$	$\alpha-0.1510\beta$	$\alpha-0.1181\beta$	$\alpha-0.1338\beta$
XIV	$\alpha-0.3700\beta$	$\alpha-0.3700\beta$	$\alpha-0.4224\beta$	$\alpha-0.3797\beta$	$\alpha-0.3697\beta$

[a] The isomer designations are defined as follows: DHP, dihydroporphyrin; A, adjacently bonded hydrogens; O, oppositely bonded hydrogens; S, symmetrically bonded hydrogens; I, one of the hydrogens is bonded to the nitrogen of the reduced ring; II, neither hydrogen is bonded to the nitrogen of the reduced ring.
[b] α and β are, respectively, the Coulombic and modified exchange integrals.

TABLE IV. Averaged spectrum of porphyrin.[a]

mμ	Wave numbers	Molar extinction coefficient $\times10^{-4}$
634±0[b]	15 800±000[c]	0.020±0.003
614±1	16 300±265	0.082±0.006
602	16 700	0.051
561±0.5	17 800±159	0.484±0.016
518±0.5	19 300±186	0.269±0.014
489±1	20 400±418	1.485±0.028
392	25 500	35.8

[a] Taken from the data of Stern *et al.* given in Table III.
[b] The limit value given for the mμ data are the average deviations of the three spectra of Stern *et al.* The limit value given for the wave number values are calculated by assuming the percentage average deviation as is listed for the mμ values. The limit values for the extinction coefficients are the average deviation values.
[c] The final two zeros of the wave-number values are not significant and are inserted only to facilitate the writing of the values.

peak at 430 mμ which in an earlier publication[13] he attributes to Stern, Wenderlein, and Molvig.[10] This author has been unable to find any reference in the papers of Stern *et al.* to such a peak. Rabinowitch[12] also does not include in his table the 392 mμ peak reported by Pruckner and Stern.[11] Rabinowitch[12,13] attributes the 613, 560.5, 517.5, and 487 mμ peaks to vibrational bands of a single electronic transition and the 430 mμ (?) peak to a second electronic transition. An alternate explanation which bears investigation is that the 634, 602, 561, and 489 mμ peaks are due to the first four transitions of PO; that the 614 and 518 mμ peaks are doublets due to the first two pairs of transitions of PA; and that the Soret band at 392 mμ is due to the overlap of the fourth through the eighth transitions of PA and the sixth and eighth transitions of PO.

If the possible variation in the experimental spectrum resulting from the difference in energy between singlet and triplet transitions is neglected, the values of Nakajima and Kon[4] (among the previous authors) best fit the experimental data. It is to be remembered, however, that the calculations of Nakajima and Kon assume that all four nitrogens are equivalent, an assumption which is made questionable by the experimental work of Erdman and Corwin.[1] The calculations of the present author (Table V) were made in two ways. The π-electronic levels X to XV for the three isomeric structures are listed in Table I. By means of the assumption that the spectroscopic transitions are one electron transitions (the usual MO assumption), the transitions listed in Table VI are calculated. The PA calculations indicate that for that isomer the spectrum should consist of three peaks, the first two of which are doublets and the third of which is a quadruplet. A similar interpretation can be given to the spectrum calculated for the transitions of PO. In this case, however, the separations in the doublets are considerably greater. The PS

TABLE III. Spectrum of porphyrin in various solvents.

Pyridine-Ether						Pyridine		Benzene		Dioxane	
683[a,b]	1.50										
671	1.57										
630	0.67			632.3[c,d]	1	634[f,g]	0.019	634[f,g]	0.016	634[f,g]	0.024
612	0.85	616.8[e,d]	4	617.8	5	613	0.075	615	0.080	613[h,g]	0.091
		606.5	3	605.4	1					602	0.051
585	0.78	590.9	2	590.6	2						
		572.1	6	571.6	6						
565	2.73										
		564.4	7	561.9	7	561	0.471	562	0.474	560.5	0.508
559	3.20										
				552.7	3						
515	2.55	518.2	5	522.4	4	518	0.262	519	0.255	517.5	0.290
485	9.83	486.7	8	489.9	8	490	1.449	489	1.480	487	1.527
		460	1								
390	168									392[i,g]	35.8

[a] V. M. Albers and H. V. Knorr, J. Chem. Phys. **4**, 22 (1936).
[b] The first column lists the absorption peaks in mμ. The second column lists the molar extinction coefficients $\times10^{-3}$.
[c] H. Fischer and W. Gleim, Ann. **521**, 157 (1936).
[d] The first column lists the absorption peaks in mμ. The second column lists the sequence of intensities in ascending order.
[e] P. Rothemund, J. Am. Chem. Soc. **58**, 625 (1936).
[f] Stern, Wenderlein, and Molvig, Z. physik. Chem. **177A**, 40 (1936).
[g] The first column lists the absorption peaks in mμ. The second column lists the molar extinction coefficients $\times10^{-4}$.
[h] A. Stern and H. Wenderlein, Z. physik. Chem. **175A**, 405 (1936).
[i] F. Pruckner and A. Stern, Z. physik. Chem. **177A**, 387 (1936).

[13] E. I. Rabinowitch, Revs. Modern Phys. **16**, 226 (1944).

TABLE V. Calculated spectrum of porphyrin.

Experimental values[a]	Simpson[b]	Theoretical values Nakajima and Kon[c,e]	Longuet-Higgins, Rector, and Platt[d,e]	Composite[f]	Present author PO[g,h]	PA
15 800		15 600 (9300)	14 500 (9000)	15 800	15 800	
16 300	16 260					16 124
16 700			16 500 (21 300)		16 431	
17 800					19 632	
19 300				19 549		19 950
20 400		20 200 (20 200)			20 263	
25 500		25 600 (26 800)	23 000 (21 300)	26 668	26 893	
						27 212
					27 524	

[a] See Table IV, values given in cm^{-1}.
[b] W. T. Simpson, J. Chem. Phys. **17**, 1218 (1949).
[c] T. Nakajima and H. Kon, J. Chem. Phys. **20**, 750 (1952).
[d] Longuet-Higgins, Rector, and Platt, J. Chem. Phys. **18**, 1174 (1950).
[e] The values given in parentheses are those calculated by approximating the nitrogens as carbons.
[f] The composite calculation was made by averaging the PA and PO values, taking the first averaged value, -0.5877β, as corresponding to 15 800 cm^{-1} and calculating β thereby.
[g] PO and PA designate porphyrin-oppositely bonded hydrogens and porphyrin-adjacently bonded hydrogens, respectively.
[h] The PO and PA columns were calculated by taking -0.5760β of PO as corresponding to 15 800 cm^{-1} and calculating β thereby.

isomer calculation predicts two doublet peaks and a quadruplet peak which is a group theoretically forbidden transition. If the doublets and quadruplets of PA and PO are averaged and the first averaged peak is assigned the value 15 800 cm^{-1} (to set the value of β) the "composite" spectrum is obtained. It is to be noted that the composite spectrum is quite similar to the spectrum predicted by Nakajima and Kon.[4] (The PS spectrum is neglected in this calculation since this isomer is probably much higher in energy than PA and PO, and, if present at all, is present in a considerably smaller amount than the other two isomers. Even if the two doublets of PS were to be included, the composite spectrum would not change very much since the PS doublets have about the same values as the average of the PA and PO doublets.)

If the separation in the PO doublets is assumed to be real and significant, a second calculation is possible. In this case the -0.5760β peak of PO is assigned the value 15 800 cm^{-1}, and the other peaks are evaluated accordingly. These are the values listed in the last two columns of Table V. The terms resulting from PS are again neglected. The poorest values obtained by this method appear to be the 19 632 cm^{-1} peak and the 26 893–27 524 cm^{-1} Soret band, the deviation from the experimental values being 1832 cm^{-1} and 1708 cm^{-1}, respectively. Considering the crudeness of the approximations used, one could not have expected as good an over-all fit between the experimental and theoretical spectra as was obtained. While this is by no means conclusive proof as to the nature of the peaks in the porphyrin spectrum, it does indicate that this interpretation should be investigated more thoroughly. It should be noted that the theoretical Soret band results from the overlap of six and possibly seven transitions. This might explain why the molar extinction coefficient of the Soret band is so much greater than those of the other peaks (see Table IV).

It is not at all unlikely that an even better fit could be obtained between the experimental and theoretical spectra by a "more judicious" choice of electronegativity parameters. If the present interpretation is correct, one should be able to resolve the 16 300, 19 300, and the 25 500 cm^{-1} peaks while the other should not be resolvable, except for vibrational-rotational fine structure.

There are three possible configurations for the PA isomer depending on whether the central hydrogens are both on one side of the ring system, co-planar with the ring system, or on opposite sides of the ring system.

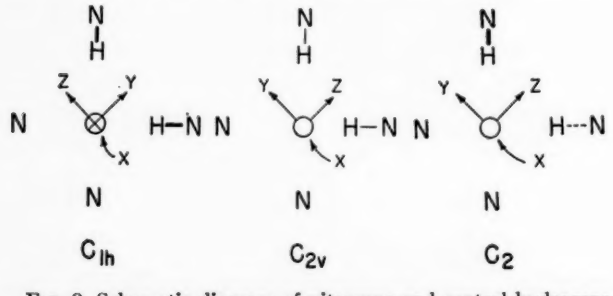

FIG. 9. Schematic diagram of nitrogens and central hydrogens of the PA (porphyrin-adjacently bonded hydrogens) configurations. —— bond coming out of the paper; —— bond in the plane of the paper; – – – bond going into the paper. The arrows designate the directions of the dipole axes. ⊗ axis points toward the reader; ○ axis points away from the reader.

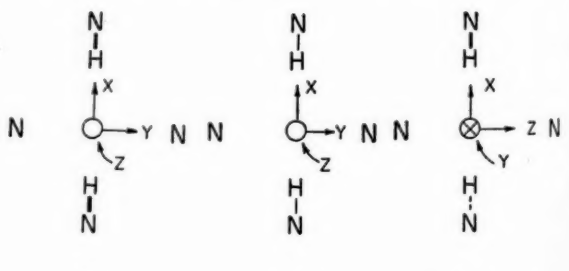

FIG. 10. Schematic diagram of nitrogens and central hydrogens of the PO (porphyrin-oppositely bonded hydrogens) configurations, showing the directions of the dipole axes.

TABLE VI. Calculated π-electronic transitions.

Transition	ΔE[a]	Structure PA C_{1h}[b]	PA C_{2v}	PA C_2	ΔE	PO C_{2v}	PO D_{2h}	PO C_{2h}	ΔE	PS D_{4h}
XIII–XIV	0.5876	A'–A''[c] A (z)[d]	B_1–B_2 A (y)	B–A A (x,y)	0.5760	A_1–B_2 A (y)	B_{1u}–B_{2g} A (y)	B_u–B_g A (z)	0.5891	A_{2u}–E_g A (x,y)
XIII–XV	0.5881	A'–A' A (x,y)	B_1–B_1 A (z)	B–B A (z)	0.5990	A_1–B_1 A (x)	B_{1u}–B_{2g} A (x)	B_u–A_g A (x,y)	0.5891	
XII–XIV	0.7271	A''–A'' A (x,y)	A_2–A_2 A (z)	A–A A (z)	0.7157	A_2–B_2 A (x)	A_{1u}–B_{2g} A (x)	A_u–B_g A (x,y)	0.7266	A_{1u}–E_g A (x,y)
XII–XV	0.7275	A''–A' A (z)	A_2–B_1 A (y)	A–B A (x,y)	0.7387	A_2–B_1 A (y)	A_{1u}–B_{2g} A (y)	A_u–A_g A (z)	0.7266	
XI–XIV	0.9918	A''–A'' A (x,y)	A_2–A_2 A (z)	A–A A (z)	0.9804	B_1–B_2 F	B_{2g}–B_{3g} F	A_g–B_g F	1.0263	E_g–E_g F
X–XIV	0.9918	A'–A'' A (z)	B_1–A_2 A (y)	B–A A (x,y)	0.9804	A_1–B_2 A (y)	B_{1u}–B_{3g} A (y)	B_u–B_g A (z)	1.0263	
XI–XV	0.9923	A''–A' A (z)	A_2–B_1 A (y)	A–B A (x,y)	1.0034	B_1–B_1 A (z)	B_{2g}–B_{2g} F	A_g–A_g F	1.0263	
X–XV	0.9923	A'–A' A (x,y)	B_1–B_1 A (z)	B–B A (z)	1.0034	A_1–B_1 A (x)	B_{1u}–B_{2g} A (x)	B_u–A_g A (x,y)	1.0263	

[a] ΔE is given in units of $-\beta$. See Table I for the individual energy levels.
[b] The group theoretic designation refers to the symmetry of the molecule with regard to the position and orientation of the nitrogen-hydrogen bonds.
[c] The group theoretic designation refers to the symmetry of the wave function of the electron being excited in the transition, before and after the transition.
[d] The symbols A and F designate that the transition is allowed or forbidden, respectively. The x, y, or z designation refers to the direction of the dipole of the dipole transition under consideration. For the relation between the dipole directions and the configuration, see Figs. 9, 10, and 11.

These configurations have C_{1h}, C_{2v}, and C_2 symmetry, respectively. In Fig. 9 the three configurations and the electric dipole directions are shown. From steric considerations the most likely configuration is C_2. According to the group theoretic data listed in Table VI, a spectral study with polarized light will give no additional information, except for a possible slight shift of the 16 700 and 19 300 cm^{-1} peaks (assuming that the interpretation given above for the spectrum of porphyrin is correct).

The corresponding configurations for PO are C_{2v}, D_{2h}, and C_{2h} (see Fig. 10). Again because of steric considerations, the most likely configuration is that with the hydrogens on opposite sides of the ring system, which configuration in this case is C_{2h}. In this case some information could be obtained by a spectral study with polarized light. The spectrum obtained when the dipole is perpendicular to the plane of the molecule should be the same as that obtained when the dipole lies along one of the two lines joining two opposite nitrogens, and should not have the 15 800 or the 20 400 cm^{-1} peaks. With the dipole along the other line joining two opposite nitrogens, the spectrum should be different, and the 16 700 and 17 800 cm^{-1} peaks should be missing.‡

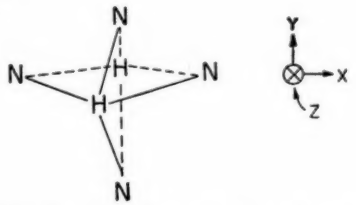

FIG. 11. Schematic diagram of nitrogens and central hydrogens of the PS (porphyrin-symmetrically bonded hydrogens) configuration D_{4h}, showing the directions of the dipole axes.

‡ The discussion of the possible anisotropy of the prophyrin spectrum has, to this point, been made in terms of the spectrum in solution although any anisotropy investigation would have to be made on a single crystal. The spectrum of the solid is, however, somewhat different than that of porphyrin in solution, the peaks occurring at 650, 625, 568, 537, and 495 mμ (Stern, Wenderlein, and Molvig, Z. physik. Chem. **177A**, 40 (1936)). Except for a shifting of maxima the only peak missing is the 602 mμ one. The Soret band at 392 mμ is also not present but that might be due to the investigators not having taken the spectrum out that far.

There is only one possible configuration for PS and that is D_{4h} (Fig. 11). If the molecule had this configuration there would be only two peaks, the E_g–E_g transitions being forbidden. The two peaks which are allowed would not appear if the dipole is along the z-direction, which is perpendicular to the plane of the ring system.

Dihydroporphyrin

In Table VII are listed the transition energies for the first six π-electronic transitions for the five isomers of dihydroporphyrin. The values are given in terms of $-\beta$. In Table VIII are listed these same transitions for the three isomers of lowest energy and the values of the transition energies in cm^{-1}. The values in cm^{-1} were obtained by setting $-\beta$ equal to 27 430 cm^{-1}. This value is taken from the porphyrin calculations above in which the -0.5760β transition was set equal to 15 800 cm^{-1}. Unlike the porphyrin case the spread of spectral values is not very great from isomer to isomer. Unfortunately this author does not know of any experimental data on the spectrum of dihydroporphyrin itself. The best data available to the author is the spectrum of dihydrochlorin-e_4-dimethyl ester (1,3,5,8,γ-pentamethyl-2,4-diethyl-6-methyl formate-7-methyl propionate-chlorin)[14]

TABLE VII. Calculated transition energies of dihydroporphyrin isomers.

Transition	DHP-AI	DHP-AII	DHP-OI	DHP-OII	DHP-S
XII–XIII	0.5579[a]	0.5590	0.5705	0.5471	0.5636
XI–XIII	0.5699	0.5684	0.5763	0.5550	0.5640
XII–XIV	0.7886	0.7988	0.8419	0.8087	0.7995
XI–XIV	0.8006	0.8082	0.8477	0.8166	0.7999
X–XIII	0.9393	0.9302	0.8580	0.9181	0.9653
IX–XIII	0.9920	0.9302	0.9510	0.9181	0.9701

[a] Values are in units of $-\beta$.

[14] A. Stern and H. Wenderlein, Z. physik. Chem. **174A**, 321 (1935).

TABLE VIII. Calculated spectrum of dihydroporphyrin.

DHP-AI	DHP-AII	DHP-OII	Wave numbers	Ave. value
		0.5471[a]	15 007[b]	
		0.5550	15 224	
0.5579			15 303	15 348
	0.5590		15 333	
	0.5684		15 591	
0.5699			15 632	
0.7886			21 631	
	0.7988		21 911	
0.8006			21 960	22 042
	0.8082		22 169	
		0.8087	22 183	
		0.8166	22 399	
		0.9181[c]	25 183	
	0.9302[c]		25 515	25 488
0.9393			25 765	
0.9920			27 210	27 210

[a] Values are in units of $-\beta$.
[b] Values are obtained in taking $-\beta$ equal to 27 430 cm^{-1}.
[c] Doublet.

TABLE IX. Spectrum of dihydrochlorin-e_4-dimethyl ester.[a]

λ mμ	cm^{-1}	$\epsilon \times 10^{-4}$
647.5	15 440	5.760
596	16 800	0.557
548	18 200	0.212
522	19 200	0.382
496	20 200	1.367

[a] Taken from A. Stern and H. Wenderlein, Z. physik. Chem. **174A**, 321 (1935).

(see Fig. 12 for the positions of the substituents). The most serious perturbing substituent is the 6-methyl formate group. The other substituents are alkyl groups and would affect the spectrum only by second-order effects (hyperconjugation). The propionic acid group is joined to the ring system by the terminal carbon atom. Therefore, the carboxyl group does not affect the spectrum except by still higher order effects. In Table IX are listed the spectral data for dihydrochlorin-e_4-dimethyl ester. The 15 440 cm^{-1} peak is well matched by the predicted peak at 15 348 cm^{-1}. The 20 200 cm^{-1} peak is somewhat more poorly matched by the predicted 22 042 cm^{-1} peak. This difference of 1842 cm^{-1} could possibly be due to the perturbing affect of the

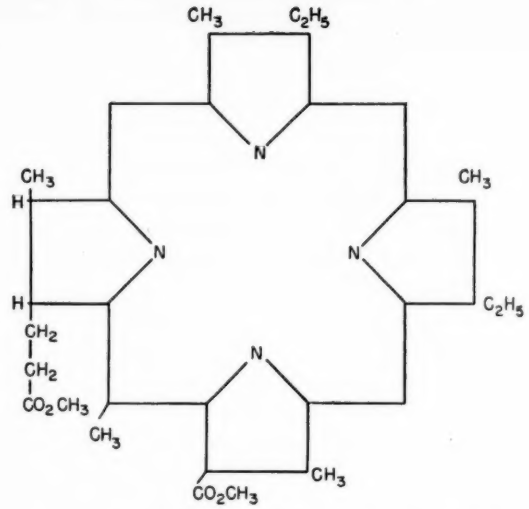

FIG. 12. Dihydrochlorin-e_4-dimethylester (not showing the positions of the central hydrogens).

formate group. However, it is unlikely that such an explanation can hold for the failure to predict the 16 800, 18 200, and 19 200 cm^{-1} peaks. Unlike the porphyrin case, in which the various peaks could be explained by the difference in the spectra of the isomers, the most reasonable explanation is one similar to that offered by Rabinowitch[12] for the porphyrin case, namely that the first four peaks are vibrational fine structure of a single electronic transition and that the fifth peak is a separate electronic transition.

BOND ORDERS

The three digit numbers given in the diagrams of the isomeric forms of porphyrin and dihydroporphyrin are the bond orders of the π electrons. One should not attempt to attribute any significance to variations from structure to structure in the values for a given bond. What are significant, however, are the variations of bond orders for the bonds of a given structure.

The author is indebted to Dr. Wallace Givens and Mr. J. H. Alexander and Mr. W. Miranker of the U. S. Atomic Energy Commission Computing Facility at New York University for their aid in making these calculations, and to Dr. Edward V. Sayre of the Brookhaven National Laboratory for his aid in making the group theoretic analyses.

Equation of State and the Thermal Dependence of the Elastic Coefficients of Crystalline Argon

JOHN H. HENKEL
Field Research Laboratories, Magnolia Petroleum Company, Dallas, Texas
(Received July 19, 1954)

An interaction potential of the form $A/R^{10}-B/R^6$ for two argon atoms is assumed. The values of A and B are evaluated using the heat of sublimation and the lattice constant at temperature $T=0°K$ and pressure $p=0$. By assuming that each atom moves in a potential field because of all the other atoms at rest in their mean positions, a theory is developed for anharmonic vibrations using the perturbation theory for a harmonic oscillator. The partition function for each argon atom is obtained and the equation of state is calculated. The specific-heat equation obtained represents a correction of the Einstein form. The specific heats at constant pressure are calculated as a function of temperature and deviate from the experimental ones by only 3 percent at low temperatures (15°K–30°K) and only 1 percent at higher temperatures. The isothermal elastic coefficients C_{11}, C_{12}, and C_{44} are calculated by Born's method without neglecting the part played by the thermal energy. The Cauchy relation is found to be invalid, C_{44} being about twice C_{12} at the higher temperatures.

I. INTRODUCTION

BETWEEN 1934 and 1940 there appeared several articles (by Herzfeld and Goeppert Mayer,[1] Kane,[2] Brillouin,[3] and Born[4]) associating the melting point of a solid with the vanishing of an elastic constant. In the development of the equations of state needed in their discussions, the above authors restricted their developments to harmonic vibrations. Since the specific heats obtained by Kane deviate from the experimental ones at the higher temperatures, it is felt that there is need for a theory treating anharmonic vibrations. The present paper endeavors to supply this need by extending Born's developments to anharmonic vibrations and to the calculation of specific heats and the isothermal elastic coefficients for crystalline solid argon.

Born defines a unit cell of a cubic lattice in terms of three vectors a_1, a_2, and a_3, and introduces the strain components

$$e_1=\frac{a_1\cdot a_1-a^2}{2a^2},\quad e_4=\frac{a_2\cdot a_3}{a^2},$$
$$e_2=\frac{a_2\cdot a_2-a^2}{2a^2},\quad e_5=\frac{a_1\cdot a_3}{a^2},\qquad(1)$$
$$e_3=\frac{a_3\cdot a_3-a^2}{2a^2},\quad e_6=\frac{a_1\cdot a_2}{a^2},$$

where a is the side of the undeformed cubic element. He then develops in terms of the Helmholtz free energy per particle $f(T,a,e_1,e_2,\cdots e_6)$ the following quantities:

$$p=-\frac{1}{3\beta a^2}\frac{\partial f}{\partial a},\qquad(2)$$

$$C_{11}=\frac{1}{\beta a^3}\frac{\partial^2 f}{\partial e_1{}^2},\qquad(3)$$

$$C_{12}=\frac{1}{\beta a^3}\frac{\partial^2 f}{\partial e_1\partial e_2},\qquad(4)$$

$$C_{44}=\frac{1}{\beta a^3}\frac{\partial^2 f}{\partial e_4{}^2},\qquad(5)$$

$$3K=C_{11}+2C_{12}=-\frac{\partial(ap)}{\partial a},\qquad(6)$$

where all derivatives are evaluated at $e_1=e_2=e_3=e_4=e_5=e_6=0$, and where βa^3 is the volume of one particle, p the pressure, C_{11}, C_{12}, and C_{44} are the isothermal elastic coefficients, and K is the bulk modulus.

II. ENERGY EIGENVALUES

It is assumed that each argon atom in its face-centered cubic lattice moves in a potential field because of all the others at rest in their mean positions, that boundary effects are negligible, that the forces between the atoms are central, and that the interaction potential

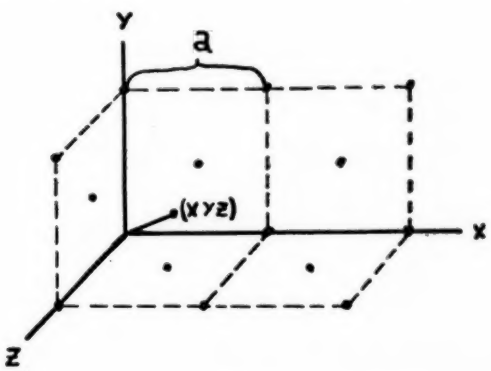

FIG. 1.

[1] K. F. Herzfeld and M. G. Mayer, Phys. Rev. **46**, 995 (1934).
[2] G. Kane, J. Chem. Phys. **7**, 603 (1939).
[3] M. L. Brillouin, Phys. Rev. **54**, 916 (1938); Mém. Sci. Math. **99**.
[4] M. Born, J. Chem. Phys. **7**, 591 (1939).

between two argon atoms has the elementary form

$$\phi(r)=A/r^{10}-B/r^6. \tag{7}$$

For the present we will use the form A/r^N where N is

$$P=-P_0/2+\sum_{ijk,-\infty}^{+\infty}{}'\frac{A}{[(ia-x)^2+(ja-y)^2+(ka-z)^2]^{N/2}}+\sum_{ijk,-\infty}^{+\infty}\left[\frac{A}{\left[(ia-x)^2+\left(ja+\frac{a}{2}-y\right)^2+\left(ka+\frac{a}{2}-z\right)^2\right]^{N/2}}\right.$$

$$\left.+\frac{A}{\left[\left(ia+\frac{a}{2}-x\right)^2+(ja-x)^2+\left(ka+\frac{a}{2}-z\right)^2\right]^{N/2}}+\frac{A}{\left[\left(ia+\frac{a}{2}-x\right)^2+\left(ja+\frac{a}{2}-y\right)^2+(ka-z)^2\right]^{N/2}}\right], \tag{8}$$

where i, j, and k are integers, where the prime denotes omission of the term $i=j=k=0$, and where P_0 is the value of the summations evaluated at $x=y=z=0$. Here, $a=\sqrt{2}d$, and d is the distance between nearest neighbors. $P_0/2$ is subtracted so that atoms will not be counted twice in forming the total energy of the crystal. Expanding P in a series and keeping terms to the fourth degree, we obtain because of symmetry

$$P=P_0/2+P_2(x^2+y^2+z^2)+P_{x^4}(x^4+y^4+z^4)+P_{x^2y^2}(x^2y^2+y^2z^2+z^2x^2). \tag{9}$$

The author shows in another place[5] that by the use of certain approximations $P_{x^2y^2}(x^2y^2+y^2z^2+z^2x^2)$ may be replaced by $\frac{1}{3}P_{x^2y^2}(x^4+y^4+z^4)$. It should be noted that these two expressions have the same symmetry and the same average value over a sphere. Employing this replacement Eq. (9) becomes

$$P=P_0/2+P_2(x^2+y^2+z^2)+P_4(x^4+y^4+z^4), \tag{10}$$

where

$$P_4=P_{x^4}+P_{x^2y^2}/3. \tag{11}$$

Letting

$$D_L=\sum_{ijk,-\infty}^{+\infty}{}'\frac{1}{[i^2+j^2+k^2]^L}+3\sum_{ijk,-\infty}^{+\infty}\frac{1}{[i^2+(j+\frac{1}{2})^2+(k+\frac{1}{2})^2]^L}, \tag{12}$$

then

$$P_0=\frac{A}{a^N}D_{N/2}, \tag{13}$$

$$P_2=\frac{(N-1)NA}{6a^{N+2}}D_{N/2+1}, \tag{14}$$

$$P_4=\frac{(N-1)N(N+1)(N+2)}{72a^{N+4}}D_{N/2+2}. \tag{15}$$

If the energy levels ϵ_j are treated as discrete, the partition function per atom becomes

$$Q(a,T)=\sum g_j e^{-\epsilon_j/kT}, \tag{16}$$

where the g_j's are weighting factors. The energy levels are given by the time-independent Schrödinger equation

$$\left[-\frac{\hbar^2}{2M}\nabla^2+P_2(x^2+y^2+z^2)+P_4(x^4+y^4+z^4)\right]U=EU, \tag{17}$$

where M is the mass of one atom and where

$$\epsilon=E+P_0/2. \tag{18}$$

The variables may be separated by letting $U(x,y,z)=u(x)v(y)w(z)$, and we obtain three equations of the form

$$\left[-\frac{\hbar^2}{2M}\frac{d^2}{dx^2}+P_2x^2+P_4x^4\right]u(x)=E'u(x). \tag{19}$$

To find the energy eigenvalues of Eq. (19) P_4x^4 may be treated as a perturbing potential so that the first-order eigenvalues become

$$\epsilon_{\chi mn}=P_0/2+\hbar\left(\frac{2P_2}{M}\right)^{\frac{1}{2}}(\chi+m+n+\tfrac{3}{2})+\frac{3}{4}\frac{\hbar^2}{M}\frac{P_4}{P_2}(\chi^2+m^2+n^2+\chi+m+n+\tfrac{3}{2}). \tag{20}$$

III. EQUATION OF STATE AND SPECIFIC HEATS c_p AND c_v

Letting $g=1$ for each separate eigenvalue, i.e., for each different value of χ, m, or n, we get for the partition function

$$Q=e^{-P_0/2kT}e^{-\frac{3}{2}W/kT}\left\{\sum_{n=0}^{\infty}\exp\left[-\frac{1}{kT}(nW+n^2Y)\right]\right\}^3, \tag{21}$$

where

$$W=\hbar(2P_2/M)^{\frac{1}{2}}+Y, \tag{22}$$

$$Y=3\hbar^2P_4/4MP_2. \tag{23}$$

[5] J. H. Henkel, Ph.D. thesis, Brown University (1954).

Y should be small compared to W if P_4x^4 is a perturbing potential so that we can expand $\exp(-n^2Y/kT)$ in a series. Keeping the first three terms we have that

$$\exp(-n^2Y/kT)=1-\frac{n^2Y}{kT}+\frac{1}{2}\left(\frac{n^2Y}{kT}\right)^2. \tag{24}$$

The question arises over what temperature range we may make this expansion safely. We can answer this best by examining the free energy, which becomes, after substituting Eq. (24) in (21) and keeping terms to the second degree in Y,

$$\begin{aligned} f&=-kT\ln Q \\ &=P_0/2+\tfrac{3}{2}W+3kT\ln(1-e^{-x}) \\ &\quad+3Y\frac{e^x+1}{(e^x-1)^2}-\frac{3}{2}\frac{Y^2}{W}\frac{x(e^{3x}+10e^{2x}+9e^x)}{(e^x-1)^4}, \end{aligned} \tag{25}$$

where

$$x=W/kT. \tag{26}$$

As T becomes very small the thermal part of the fourth and fifth terms approaches zero very rapidly. Therefore, we may make the expansion (24) for small T provided $Y\ll W$.

The equation of state using Eq. (2) becomes

$$\begin{aligned} -3\beta a^2P&=-\frac{1}{2}\frac{\partial P_0}{\partial a}+\frac{3}{2}\frac{\partial W}{\partial a}\left[\frac{e^x+1}{e^x-1}-2X\frac{x(e^{2x}+3e^x)}{(e^x-1)^3}\right. \\ &\quad\left.+X^2\frac{x^2(e^{4x}+23e^{3x}+47e^{2x}+9e^x)}{(e^x-1)^5}\right] \\ &\quad+3\frac{\partial Y}{\partial a}\left[\frac{e^x+1}{(e^x-1)^2}-X\frac{x(e^{3x}+10e^{2x}+9e^x)}{(e^x-1)^4}\right], \end{aligned} \tag{27}$$

where we have introduced the term

$$X=Y/W. \tag{27'}$$

The specific heat at constant volume per atom c_v becomes

$$\begin{aligned} c_v&=k\frac{\partial}{\partial T}\left[T^2\frac{\partial}{\partial T}\ln Q\right]_a \\ &=3k\left[\frac{x^2e^x}{(e^x-1)^2}-XK_1+X^2K_2\right], \end{aligned} \tag{28}$$

where

$$K_1=\frac{x^3(e^{3x}+8e^{2x}+3e^x)}{(e^x-1)^4}-\frac{2x^2(e^{2x}+3e^x)}{(e^x-1)^3} \tag{29}$$

and

$$\begin{aligned} K_2&=\frac{x^2(e^{3x}+10e^{2x}+9e^x)}{(e^x-1)^4}-\frac{2x^3(e^{4x}+23e^{3x}+47e^{2x}+9e^x)}{(e^x-1)^5} \\ &\quad+\frac{1}{2}\frac{x^4(e^{5x}+50e^{4x}+210e^{3x}+130e^{2x}+9e^x)}{(e^x-1)^6}. \end{aligned} \tag{30}$$

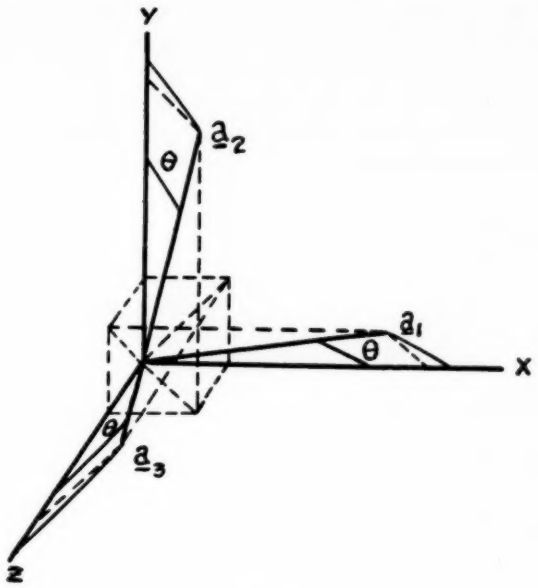

FIG. 2.

To obtain the specific heat at constant pressure c_p use is made of the standard form

$$c_p-c_v=-T\left(\frac{\partial V}{\partial T}\right)_P^2\left(\frac{\partial P}{\partial V}\right)_T, \tag{31}$$

where the partial derivatives in (31) are obtained from the equation of state (27).

IV. THE ELASTIC COEFFICIENT C_{44}

To obtain C_{44} consider the deformation as shown in Fig. 2 where the vectors (a_1,a_2,a_3) become

$$\begin{aligned} a_1&=a\cos\theta i+a\frac{\sin\theta}{\sqrt{2}}j+a\frac{\sin\theta}{\sqrt{2}}k, \\ a_2&=a\frac{\sin\theta}{\sqrt{2}}i+a\cos\theta j+a\frac{\sin\theta}{\sqrt{2}}k, \\ a_3&=a\frac{\sin\theta}{\sqrt{2}}i+a\frac{\sin\theta}{\sqrt{2}}j+a\cos\theta k, \end{aligned} \tag{32}$$

and where the strain components become

$$\begin{aligned} &e_1=e_2=e_3=0, \\ &e=e_4=e_5=e_6=\sqrt{2}\sin\theta\cos\theta+\frac{\sin^2\theta}{2}. \end{aligned} \tag{33}$$

Then the elastic coefficients C_{44} are given by (5) which may be written

$$3\beta a^2C_{44}=\frac{\partial^2 f}{\partial e^2}=\frac{1}{2}\frac{\partial^2 f}{\partial\theta^2}-\frac{1}{2\sqrt{2}}\frac{\partial f}{\partial\theta}, \tag{34}$$

where the derivatives are evaluated at $\theta=0$.

The potential energy P is given by (10), where now P_0, P_2, and P_4 are functions of θ. The elastic coefficients depend mainly on P_0 so that only the first two terms in the expansion, (24), or the first four terms of (25) will be kept. Denoting differentiation with respect to θ by primes and letting

$$T_L=\sum_{-\infty}^{+\infty}{}'\frac{i^2j^2+j^2k^2+k^2i^2}{[i^2+j^2+k^2]^L}$$
$$+3\sum_{-\infty}^{+\infty}\frac{i^2(j+\tfrac{1}{2})^2+(j+\tfrac{1}{2})^2(k+\tfrac{1}{2})^2+i^2(k+\tfrac{1}{2})^2}{[i^2+(j+\tfrac{1}{2})^2+(k+\tfrac{1}{2})^2]^L}, \quad (35)$$

we obtain for $\theta=0$

$$P_0'=0,$$
$$P_0''=\frac{2N(N+2)A}{a^N}T_{N/2+2},$$
$$P_2'=0,$$
$$P_2''=\frac{(N-1)N(N+2)(N+4)A}{3a^{N+2}}T_{N/2+3}, \quad (36)$$
$$P_4'=0,$$
$$P_4''=\frac{(N-1)N(N+1)(N+2)(N+4)(N+6)}{36a^{N+4}}T_{N/2+4}.$$

Also, for $\theta=0$, we obtain

$$Y'=0, \quad Y''=\frac{3\hbar^2}{4M}\left[\frac{P_4''}{P_2}-\frac{P_4P_2''}{P_2^2}\right],$$
$$W'=0, \quad W''=\frac{\hbar}{(2M)^{\frac{1}{2}}}\frac{P_2''}{(P_2)^{\frac{1}{2}}}+Y'', \quad (37)$$

whence Eq. (34) becomes

$$6\beta a^3C_{44}=P_0''/2+\tfrac{3}{2}W''\frac{(e^x+1)}{(e^x-1)}$$
$$+3Y''\frac{e^x+1}{(e^x-1)^2}-3XW''\frac{x(e^{2x}+3e^x)}{(e^x-1)^3}. \quad (38)$$

V. THE ELASTIC COEFFICIENT C_{11}

To obtain C_{11} consider the deformation given by a simple extension along the x axis as shown in Fig. 3. The vectors (a_1,a_2,a_3) become

$$a_1=\xi ai, \quad a_2=aj, \quad a_3=ak, \quad (39)$$

so that

$$e_2=e_3=e_4=e_5=e_6=0,$$

and

$$e_1=\tfrac{1}{2}(\xi^2-1). \quad (40)$$

Then

$$C_{11}=\frac{1}{\beta a^3}\frac{\partial^2 f}{\partial e_1^2}=\frac{4}{\beta a^3}\frac{\partial^2 f}{\partial(\xi^2)^2}. \quad (41)$$

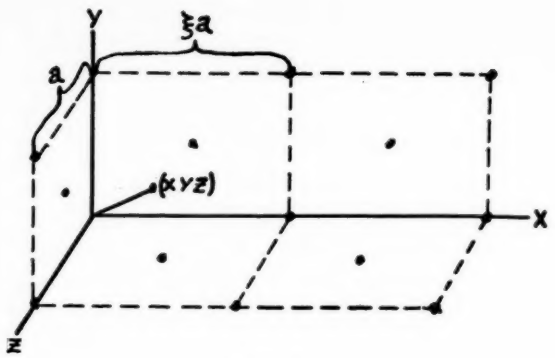

FIG. 3.

Making the assumption that each atom moves in a field due to all the other atoms at rest in their mean positions, the potential energy P is given by a form (8) where ia and $(i+\frac{1}{2})a$ have been replaced by $i\xi a$ and $(i+\frac{1}{2})\xi a$, respectively. The expansion (9) now takes the form

$$P=P_0/2+P_{x^2}x^2+P_{y^2}(y^2+z^2)+P_{x^4}x^4$$
$$+P_{y^4}(y^4+z^4)+P_{x^2y^2}(x^2y^2+x^2z^2)+P_{y^2z^2}y^2z^2, \quad (42)$$

where P_0, P_{x^2}, etc. are functions of a and ξ.

Letting

$$G_L=\sum_{-\infty}^{+\infty}{}'\frac{i^4+j^4+k^4}{[i^2+j^2+k^2]^L}$$
$$+3\sum_{-\infty}^{+\infty}\frac{i^4+(j+\tfrac{1}{2})^4+(k+\tfrac{1}{2})^4}{[i^2+(j+\tfrac{1}{2})^2+(k+\tfrac{1}{2})^2]^L}, \quad (43)$$

and denoting differentiation with respect to (ξ^2) by primes, the following are derived for $\xi=1$,

$$P_0''=\frac{N(N+2)A}{12a^N}G_{N/2+2},$$
$$P_{x^2y^2}=\frac{N(N+2)A}{12a^{N+4}}[(N+4)(N+6)T_{N/2+4}$$
$$-(2N+5)D_{N/2+2}],$$
$$P'_{x^2}=\frac{N(N+2)A}{12a^{N+2}}[3D_{N/2+1}-(N+4)G_{N/2+3}],$$
$$P'_{y^2}=\frac{N(N+2)A}{12a^{N+2}}[D_{N/2+1}-(N+4)T_{N/2+3}],$$
$$P_5=P''_{x^2}+2P''_{y^2}$$
$$=\frac{(N-1)N(N+2)(N+4)A}{24a^{N+2}}G_{N/2+3}, \quad (44)$$
$$P_6=P'_{x^4}+\tfrac{1}{3}P'_{x^2y^2}=\frac{(N-1)N(N+2)(N+4)A}{144a^{N+4}}$$
$$\times[3D_{N/2+2}-(N+6)G_{N/2+4}],$$

$$P_7=P'_{y^4}+\tfrac{1}{6}P'_{x^2y^2}+\tfrac{1}{6}P'_{y^2z^2}$$
$$=\frac{(N-1)N(N+2)(N+4)A}{144a^{N+4}}\times[D_{N/2+2}-(N+6)T_{N/2+4}],$$
$$P_8=(P''_{x^4}+\tfrac{1}{3}P''_{x^2y^2})+2(P''_{y^4}+\tfrac{1}{6}P''_{y^2z^2}+\tfrac{1}{6}P''_{x^2y^2})$$
$$=\frac{(N-1)N(N+1)(N+2)(N+4)(N+6)A}{288a^{N+4}}G_{N/2+4}.$$

The author has shown[5] in another place that the elastic coefficient is given by

$$\frac{\beta a^3}{4}C_{11}=\frac{P_0''}{2}+\frac{W_3}{2}\frac{e^x+1}{e^x-1}-\frac{[(W_1')^2+2(W_2')^2]}{W}\frac{xe^x}{(e^x-1)^2}+W_4\frac{e^x+1}{(e^x-1)^2}-\left[XW_3+2W_5\frac{W_1'}{W}+4\frac{W_6W_2'}{W}\right]x\frac{e^{2x}+3e^x}{(e^x-1)^3}+X\frac{[(W_1')^2+2(W_2')^2]}{W}\frac{x^2(e^{3x}+8e^{2x}+3e^x)}{(e^x-1)^4}-\frac{2W_7(W_1'-W_2')^2}{W^2}\frac{x^2e^{2x}}{(e^x-1)^4},\quad(45)$$

where x is given by (26), W by (22), X by (27′) and where

$$W_1'=\frac{\hbar}{(2M)^{\frac{1}{2}}}\frac{P'_{x^2}}{(P_2)^{\frac{1}{2}}}+W_5,$$
$$W_2'=\frac{\hbar}{(2M)^{\frac{1}{2}}}\frac{P'_{y^2}}{(P_2)^{\frac{1}{2}}}+W_6,$$
$$W_5=\frac{3\hbar^2}{4M}\frac{P_6}{P_2}-\frac{3}{4}\frac{\hbar^2}{M}\frac{P_4P'_{x^2}}{P_2^2}+\frac{\hbar^2}{8M}\frac{P_{x^2y^2}}{P_2^2}(P'_{x^2}-P'_{y^2})$$
$$W_6=\frac{3\hbar^2}{4M}\frac{P_7}{P_2}-\frac{3\hbar^2}{4M}\frac{P_4P'_{y^2}}{P_2^2}-\frac{P_{x^2y^2}}{16P_2^2}(P'_{x^2}-P'_{y^2}),$$
$$W_3=\frac{\hbar}{(2M)^{\frac{1}{2}}}\frac{P_5}{(P_2)^{\frac{1}{2}}}-\frac{\hbar}{2(2M)^{\frac{1}{2}}}\frac{[(P'_{x^2})^2+2(P'_{y^2})^2]}{P_2^{\frac{3}{2}}}+W_4,\quad(46)$$
$$W_4=\frac{3\hbar^2}{4M}\frac{P_8}{P_2}-\frac{3\hbar^2}{2M}\frac{P'_{x^2}P_6}{P_2^2}-\frac{3\hbar^2}{M}\frac{P'_{y^2}P_7}{P_2^2}-\frac{3\hbar^2}{4M}\frac{P_4P_5}{P_2^2}+\frac{3\hbar^2}{2M}\frac{P_4}{P_2^3}[(P'_{x^2})^2+2(P'_{y^2})^2]-\frac{\hbar^2}{8M}\frac{P_{x^2y^2}}{P_2^3}(P'_{x^2}-P'_{y^2})^2,$$
$$W_7=\frac{\hbar^2}{2M}\frac{P_{x^4y^2}}{P_2}.$$

Here P_2 and P_4 for $\xi=1$ are given by (14) and (15).

VI. CALCULATIONS

The values of D_L have been found by Lennard-Jones and Ingham.[6] They have been checked by the author for $L=3$, 4, 5, 6, and 7 by performing the summations up to $r^2=i^2+j^2+k^2=8^2$ and then integrating from $r=8$ to infinity. The values obtained are

$$D_3=\ 115.631$$
$$D_4=\ 204.831$$
$$D_5=\ 393.960$$
$$D_6=\ 776.440$$
$$D_7=1543.551.$$

The following values of G_L were found by a similar procedure:

$$G_5=\ 61.5261$$
$$G_6=105.6417$$
$$G_7=200.062$$
$$G_8=391.252$$
$$G_9=774.788.$$

Since $D_L=G_{L+2}+2T_{L+2}$, the following are obtained:

$$T_5=\ 27.0526$$
$$T_6=\ 49.5948$$
$$T_7=\ 96.9487$$
$$T_8=192.5943$$
$$T_9=384.382.$$

The constants A and B for argon were evaluated through use of the heat of sublimation U_0 and the lattice constant a_0 for crystalline argon at temperature $T=0°\text{K}$ and pressure $p=0$. The following values of A and B were used

$$A=2.194\times10^{-88}\text{ erg cm}^{10},$$
$$B=1.538\times10^{-58}\text{ erg cm}^{6}.\quad(47)$$

These lead to

$$U_0=1.412\times10^{-13}\text{ erg/atom}=2032\text{ cal/mole}$$
$$a_0=5.399\times10^{-8}\text{ cm}\quad(48)$$

which compare with the following values adopted by most authors[6–8]:

$$U_0=2030\text{ cal/mole},$$
$$a_0=\ 5.40A^0.\quad(49)$$

Buckingham[8] obtained the following values of A and B from the virial coefficients

$$A=2.05\times10^{-88}\text{ erg cm}^{10},$$
$$B=1.37\times10^{-58}\text{ erg cm}^{6}.\quad(50)$$

[6] J. E. Lennard-Jones and A. E. Ingham, Proc. Roy. Soc. (London) **A107**, 636 (1925).
[7] M. Kunimune, Progr. Theoret. Phys. (Japan) **5**, 412 (1950).
[8] R. A. Buckingham, Proc. Roy. Soc. (London) **A168**, 264 (1938).

TABLE I. a is expressed in Angstrom units, T is expressed in degrees Kelvin, and P is expressed in 10^7 dynes/cm².

T \ a	5.38	5.40	5.42	5.44	5.46	5.48
0	25.08	−1.73	−26.33			
5						
10	25.43	−1.35	−25.87	−48.39	−68.96	−87.77
15	27.73	1.15	−23.21	−45.48	−65.84	−84.42
20	32.79	6.46	−17.66	−39.72	−59.85	−78.22
25	40.09	13.93	−10.01	−31.89	−51.84	−70.04
30	48.85	22.83	−0.98	−22.74	−42.58	−60.67
35	58.61	32.68	8.96	−12.74	−32.51	−50.55
40	69.04	43.15	19.46	−2.20	−21.96	−39.99
45	79.91	54.02	30.34	8.68	−11.09	−29.12
50	91.06	65.17	41.46	19.78	00.00	−18.07
55	102.43	76.50	52.76	31.04	11.22	−6.89
60	113.93	87.96	64.18	42.41	22.54	4.37

The calculated equation of state is shown in Table I, and the calculated specific heats are shown in Table II along with the experimental ones obtained by Clusius.[9] In the calculations of the specific heats, thermal expansion was not neglected. The thermal expansion was obtained from Table I by assuming that the vapor pressure of solid argon is zero. Also shown in Table II are the calculated values of X given by (27′). As may be seen $Y \ll W$ so that the expansion (24) is permissible. The contribution to the specific heat by the term $3kX^2K_2$ is small, being less than 0.5 percent of the total calculated values for all temperatures shown.

Stewart,[10] at Harvard University, has obtained experimentally the pressure-volume curve for solid argon at 65°K. He has found that under a pressure of 1000 kg/cm², the volume decreased to $(0.9528 \pm 0.0014)V$, where V is the volume at zero pressure. From Table I the corresponding volume decreases to $0.9500V$ at 60°K.

The bulk modulus $K=\frac{1}{3}(C_{11}+2C_{12})$ was obtained from Table I by numerical differentiation. Its thermal dependence is shown in Table III along with the calculated values of C_{11}, C_{12}, C_{44}, and $C_{11}-C_{12}$. These elastic coefficients were calculated at zero pressure, thus allowing for thermal expansion. Also shown in Table III are the space-average values of $C_{11}(\bar{C}_{11})$

TABLE II. Specific heats in cal/mole.

T	c_v	c_p(calc)	c_p(exp) Clusius	X
10°	0.49	0.49	0.84	0.0187
15°	1.72	1.75	1.91	0.0188
20°	2.86	2.95	2.82	0.0189
25°	3.66	3.85	3.70	0.0191
30°	4.20	4.50	4.39	0.0194
35°	4.55	4.98	4.88	0.0197
40°	4.79	5.35	5.29	0.0200
45°	4.95	5.66	5.61	0.0204
50°	5.07	5.91	5.92	0.0208
55°	5.14	6.15	6.13	0.0213
60°	5.20	6.37	6.37	0.0218

[9] K. Clusius, Z. physik Chem. **B31**, 459 (1936).
[10] J. W. Stewart, personal interview.

given by

$$\bar{C}_{11}=C_{11}+\tfrac{4}{5}\left(C_{44}-\frac{C_{11}-C_{12}}{2}\right), \tag{51}$$

and the isothermal velocity $(\bar{C}_{11}/\rho)^{\frac{1}{2}}$, where ρ is the density of the solid argon.

Barker, Dobbs, and Jones[11] report a value of 1600 meters/sec for the velocity of sound in polycrystalline argon at 60°K. We may note from Table II that for 60°K $\gamma=c_p/c_v=1.225$ so that for 60°K

$$\left(\gamma\frac{\bar{C}_{11}}{\rho}\right)^{\frac{1}{2}}=1.61\times10^5 \text{ cm/sec.} \tag{52}$$

It is not quite correct to say that $(\gamma\bar{C}_{11}/\rho)^{\frac{1}{2}}$ is the adiabatic velocity of compressional waves but it is a fair approximation. The adiabatic coefficients C_{11}, C_{12}, and C_{44} may be obtained by replacing the Helmholtz free energy per particle f in Eqs. (3) to (5) by the internal energy per particle ϵ where

$$\epsilon=f+TS, \tag{53}$$

and S is the entropy per particle.

TABLE III. Elastic coefficient in 10^{10} dynes/cm².

T	K	C_{11}	C_{44}	C_{12}	$C_{11}-C_{12}$	$\bar{C}_{11}$	$\sqrt{\bar{C}_{11}/\rho}$
10	2.317	3.269	2.066	1.841	1.428	4.351	1.607×10^5
15	2.281	3.229	2.062	1.807	1.422	4.310	1.600
20	2.219	3.161	2.054	1.748	1.413	4.239	1.588
25	2.143	3.078	2.041	1.676	1.402	4.150	1.575
30	2.064	2.989	2.026	1.602	1.387	4.055	1.560
35	1.978	2.895	2.008	1.520	1.375	3.951	1.544
40	1.893	2.801	1.988	1.439	1.362	3.847	1.527
45	1.805	2.707	1.967	1.354	1.353	3.740	1.510
50	1.720	2.613	1.943	1.274	1.339	3.631	1.493
55	1.634	2.522	1.917	1.190	1.332	3.523	1.475
60	1.555	2.433	1.889	1.116	1.317	3.418	1.457

DISCUSSION OF RESULTS

We cannot expect the elementary form for the interaction potential to fit the true form very well. Kunimune[7] calculated theoretically the repulsive interaction energy between two argon atoms and fitted the potential curve with curves of the form A/r^N where A and N are constants and N being approximately 10 or 12. Here there were points in the smoothed curves that deviated from the theoretical ones by approximately 25 percent. Therefore, Eqs. (47) and (50) agree reasonably well.

Equation (28) represents a correction to the Einstein form for c_v, and we cannot therefore expect it to agree for very low temperatures, which is verified in Table II for $T=10$°K. However, above 15°K the agreement is very good, being 3 percent off in the range 15°K to 25°K and less than one percent for the range 45°K to 60°K.

Above 25°K the elastic coefficients appear to be

[11] Barker, Dobbs, and Jones, Phil. Mag. 44, 1182 (1953).

linear functions of temperature agreeing with the statement made by Zener[12] that "the normal variation of the elastic coefficients with temperature is linear over a wide temperature range." It does not appear that any of the elastic coefficients will vanish in the neighborhood of 84°K indicating melting as predicted by Born.[4] The agreement between the value 1.61×10^5 cm/sec given in Eq. (52) and the value 1.60×10^5cm/sec reported by Barker, Dobbs, and Jones is remarkable.

[12] C. Zener, *Elasticity and Anelasticity* (University of Chicago Press, Chicago, Illinois, 1948), p. 24.

It is well to note that the Cauchy relation "$C_{44}=C_{12}$" was not obtained even though central forces were assumed. This shows that the thermal motion makes a very significant contribution to the elastic coefficients. Only for very low temperatures where the thermal motion is small does the Cauchy relation tend to be valid.

The author wishes to thank Professor R. B. Lindsay under whose supervision this research was carried out, and the Office of Naval Research for its financial support.

THE JOURNAL OF CHEMICAL PHYSICS VOLUME 23, NUMBER 4 APRIL, 1955

On the Structure of a Detonation Front*

W. R. GILKERSON† AND NORMAN DAVIDSON
Gates and Crellin Laboratories of Chemistry, California Institute of Technology, Pasadena, California‡

(Received July 19, 1954)

An effort was made to observe the structure of the reaction zone for a detonation in a gas. Detonations in a 50 percent H_2:50 percent O_2 mixture at 0.035 atmos pressure containing 1 percent I_2 were initiated by shock waves in a shock tube. Because of ignition delays and the short length of tube available, the detonations did not settle down to a steady state and were of unexpectedly high velocity. The iodine served as a colorimetric indicator for the shock front. The light output of the detonation is a step function of time with a front coincident with the shock front within 2–3 μsec. The experiment indicates that the reaction zone is less than 10^4 collisions thick. A crude theoretical estimate of the reaction zone thickness of 1000–4000 collisions is made. Possible chain initiating steps are also considered.

THE von Neumann theory of detonation[1] assumes that the front consists of a shock wave which compresses and heats the unburned gas, thereby initiating combustion, and a reaction zone in which the temperature rises and the density falls as the combustion proceeds. The plane behind the reaction zone where the high temperature equilibrium essentially obtains is called the Chapman-Jouget (CJ) plane for an ordinary detonation.

The experiment described herein is an attempt to observe the thickness of the reaction zone for a detonation in a hydrogen-oxygen gas mixture in a glass tube. It has been successful only in establishing an upper limit for the thickness of this zone under certain special conditions. Kistiakowsky[2] has observed the density profile for a detonation in a mixture of oxygen, acetylene, and methyl bromide, presumably at 1 atmos initial pressure, by x-ray absorption, and reports that in this system the reaction zone is less than 1 mm thick.

The basic idea of the experiment is to observe a detonation in a H_2-O_2 mixture containing a small amount of I_2. Light absorption provides information about the concentration of iodine and therefore about the shock front. This can be compared with the position of the combustion zone as manifested by light emission by the reacting mixture.

The experiment was carried out in a shock tube, and some of its features may be described by reference to Fig. 1(a). When the membrane breaks, the expansion of the high pressure gas, hydrogen, into the low pressure reaction mixture results in a strong shock wave which initiates combustion. We call the resulting detonation a supported detonation because the "push" by the high pressure driving gas prevents the formation of a rarefaction wave behind the CJ plane, as is characteristic of an ordinary detonation. For the actual pressure ratios used, the detonation is somewhat stronger than is a free detonation. This subject is discussed in detail below.

EXPERIMENTAL

The shock tube and our general techniques have been described previously.[3] The driving section is a 180-cm length of 15-cm diameter steel pipe. The shock wave section is a 140-cm length of 15-cm alu-

* Research supported by the Office of Naval Research, Project NR 051-248.

† Present address: Department of Chemistry, University of South Carolina, Columbia, South Carolina.

‡ Contribution No. 1923.

[1] Referred to, for example, by Berets, Greene, and Kistiakowsky, J. Am. Chem. Soc. **72**, 1080 (1950).

[2] G. B. Kistiakowsky, J. Chem. Phys. **19**, 1611 (1951).

[3] Britton, Davidson, and Schott, Discussions Faraday Soc. **17**, 58 (1954).

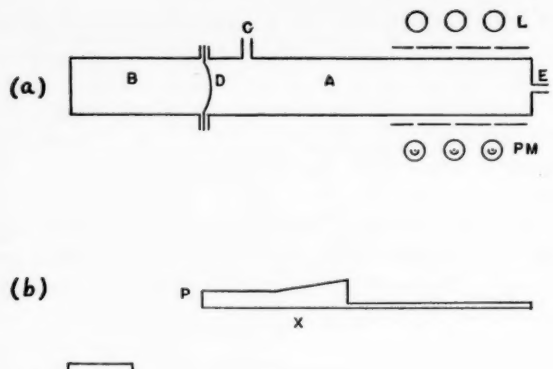

FIG. 1. (a) Schematic diagram of apparatus. *B*, driving gas (H_2); *D*, diaphragm; *A*, driven gas (H_2,O_2); *L*, lights; *PM*, photomultipliers; *C*, to vacuum line; *E*, gas inlet; Fig. (b)–(d) Pressure, *P*, as a function of distance, *x*, at sometime after the bursting of the diaphragm or the beginning of detonation for a free detonation, (b); a supported detonation, (c); an insufficiently supported detonation, (d). The dotted lines in (c) and (d) indicate the contact surface between expanded, cold driving gas and shocked, combusted, driven gas.

minum pipe and a 150 cm length of 15-cm Pyrex pipe. Cellulose acetate membranes are clamped between the steel and aluminum sections. The shock wave chamber could be evacuated to 0.5 μ pressure and degassed or leaked at a rate less than 0.1μ min^{-1}. Tank hydrogen and oxygen (Linde) are passed over Drierite and through flowmeters. They are mixed, and then passed through the pressure-reducing iodine-saturating system described previously.[3] After the tube was filled, a sample of the mixture was withdrawn into a one liter bulb and ignited by a hot platinum wire. The water produced was taken up by Drierite. From the pressure before and after combustion, the ratio of oxygen to hydrogen, *L* (Table I) was computed. This analysis was reproducible and accurate to ±0.6 percent.

TABLE I. Observed velocities of supported detonations.[a]

Experiment No.	*B*	S_{12} (cm/sec×10^{-5})	S_{23}	T_s °K	exp (−17 000/*RT*)	*L*
1	121	2.43	2.50	2060	1/62	0.982
2	120.5	2.55	2.69	2130	1/54	0.877
3	120	2.52	2.71	···	···	0.989
4	98.9	2.54	2.72	···	···	0.902
5	98.0	2.75	3.46	···	···	0.958
6	96.7	2.91	2.89	2680	1/24	0.993
7	96.2	2.95	3.06	2760	1/22	0.967
8	91.4	3.07	3.56	···	···	0.967
9	87.5	3.65	3.71	···	···	0.881

[a] *B*=bursting pressure ratio; S_{ij}=velocity between stations *i* and *j*; T_s=computed temperature behind shock for velocity S_{12}, assuming no combustion, and that $C_p=7/2R$; *L*=mole ratio of O_2 to H_2.

"SUPPORTED" DETONATION

The symbols to be used in this discussion are: P=pressure, W=mean molecular weight of unreacted gas, V=volume per W grams of gas, H=enthalpy per W grams, S=shock velocity, S_f=velocity of a free detonation calculated using the Chapman-Jouguet condition, v=material velocity of gas in laboratory system. Subscripts 1 and 2 refer to unshocked and shocked gas at chemical equilibrium respectively.

As is well known, the P, V behavior of a fluid subject to shock compression is defined by the Rankine-Hugoniot (RH) equation, $(P_2-P_1)(V_2+V_1)=2(H_2-H_1)$. This with the perfect gas law and the thermodynamic conditions for chemical equilibrium between the various components can be used to define the behavior of a detonating mixture, and the RH curve so calculated for 50 percent H_2:50 percent O_2 at an initial pressure of 0.035 atoms is illustrated in Fig. 2.

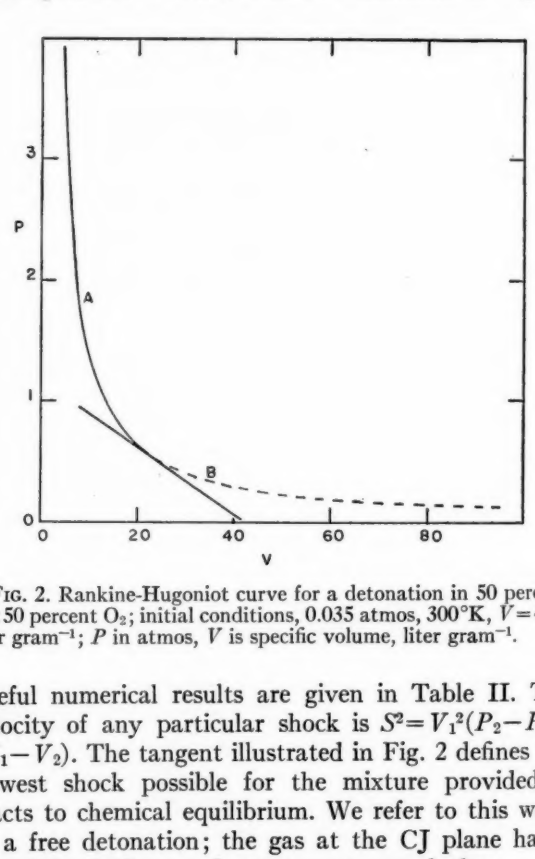

FIG. 2. Rankine-Hugoniot curve for a detonation in 50 percent H_2:50 percent O_2; initial conditions, 0.035 atmos, 300°K, V=41.4 liter gram^{-1}; P in atmos, V is specific volume, liter gram^{-1}.

Useful numerical results are given in Table II. The velocity of any particular shock is $S^2=V_1^2(P_2-P_1)/(V_1-V_2)$. The tangent illustrated in Fig. 2 defines the slowest shock possible for the mixture provided it reacts to chemical equilibrium. We refer to this wave as a free detonation; the gas at the CJ plane has a material velocity v and a temperature such that

$$S-v=V_2(P_2-P_1)^{\frac{1}{2}}(V_1-V_2)^{-\frac{1}{2}}$$

is the local sound velocity. For a shock proceeding to point *A* of Fig. 2, the velocity is greater than that for a free detonation, the temperature is higher, and $S-v$ is locally subsonic. For a shock proceeding to point *B*, the velocity S is greater than that for a free detonation, the temperature is lower, and $S-v$ is supersonic.

Figures 1(b)–(d) illustrate pressure profiles for

several possible experiments. Figure 1(b) is for a free detonation originating at the closed end of a tube. A rarefaction originates at the same end and follows the detonation. In a shock tube configuration with a sufficiently large bursting pressure ratio, the pressure profile will be that of Fig. 1(c). The push by the driving gas is sufficient to suppress the rarefaction and give a step function shape to the pressure wave. If the bursting pressure ratio is insufficient for the expanding gas from the driving chamber to reach the velocity v at the pressure P_2 which obtains at the CJ plane for a supported detonation, then the situation is as depicted in Fig. 1(d). There is a rarefaction behind the detonation front, and the velocity of the front is the same as that for a free detonation.

The equation relating the velocity v_4 and pressure P_4 of the gas from the driving chamber expanding from the pressure, P_3, if the initial velocity of sound be a_3 is

$$v_4=(2a_3/\gamma-1)[1-(P_3/P_4)^{(\gamma-1)/2\gamma}].$$

By matching v_4 and P_4 to v_2 and P_2, the shock velocity vs bursting pressure graph in Fig. 3 is obtained. The upper arm of the curve is the predicted steady state detonation velocity as a function of bursting pressure for an ideal shock tube. The lower dotted arm of the curve represents computed velocities for a transition to the dotted arm of the RH curve, Fig. 2. Gas on this arm of the RH curve is in an unstable condition in that the velocity $S-v$ is supersonic and a shock transition to the upper arm of the RH curve is possible. The transition to the dotted arm of the curve is impossible in the von Neumann description of a detonation in which combustion is preceded by a shock wave. It is conceivable if the combustion is initiated by the diffusion of free radicals ahead of the shock zone, and takes place in the few mean free paths that constitute the shock zone. Very high velocities for rather low bursting pressures are possible for this hypothetical case.

The computed free detonation velocity for 50 percent H_2:50 percent O_2 at 0.035 atmos is 2.20×10^5 cm/sec. The velocity at an initial pressure of 1 atmos is 2.33×10^5 cm/sec[1]; at the lower pressure, more enthalpy is absorbed in dissociation processes.

The experimental results are not suitable for quantitative comparison with Fig. 3. It should be remarked, however, that the effect of a small amount of iodine on the calculated curve would be quite small.

RESULTS AND DISCUSSION

Successful detonations occurred with bursting pressure ratios of 87 or greater, but did not occur with bursting pressure ratios, B, below 80. The theoretical B to just support a free detonation is 35, and shock tube experience indicates that a pressure *ca* 10 percent higher might actually be required. Presumably the failure to obtain detonations at low B is because the shock wave resulting when the membrane breaks is too weak to initiate combustion. The calculated temperature for $B=85$, for a pure shock tube experiment with no combustion is 1140°K. It may be recalled that Fay[4] observed the surprisingly low shock ignition temperature for stoichiometric H_2:O_2 of 400°K. It is not possible to say which of the many differences between the two experiments is responsible for the striking difference in results. One important possibility is that iodine added in our experiments inhibits ignition.

It is the general belief that it is difficult to maintain stable free detonations at low pressures. Mooradian and Gordon[5] report stable free detonations initiated by shock waves in a 1 in. pipe for an initial pressure of 0.125 atmos. They also report stable detonations in 1:10 knallgas:argon at 1 atmos pressure. The low pressure (0.035 atmos initial pressure) detonations achieved here are presumably due to the fact that the detonations were supported, and indeed overdriven,

TABLE II. Calculated properties in 50 percent H_2:50 percent O_2 detonations.[a]

P_2/P_1	V_1/V_2	T_2 °K	S cm/sec $\times10^{-5}$	OH	H	O	H_2	O_2	H_2O
				mole fractions					
112	8.90	3750	3.62	0.179	0.133	0.205	0.0760	0.209	0.199
75.3	6.94	3500	3.57	0.168	0.0915	0.153	0.0670	0.244	0.276
16.0	1.84	3000	2.20	0.124	0.0492	0.0811	0.0545	0.256	0.435
9.50	1.15	2900	3.09	0.114	0.0441	0.0736	0.0505	0.262	0.456
3.46	0.444	2750	···	0.104	0.0430	0.0702	0.0485	0.268	0.467

[a] (Initial conditions, 0.035 atmos, 300°K, thermodynamic data from "Selected values of chemical thermodynamic properties," National Bureau of Standards, Series III, 1950).

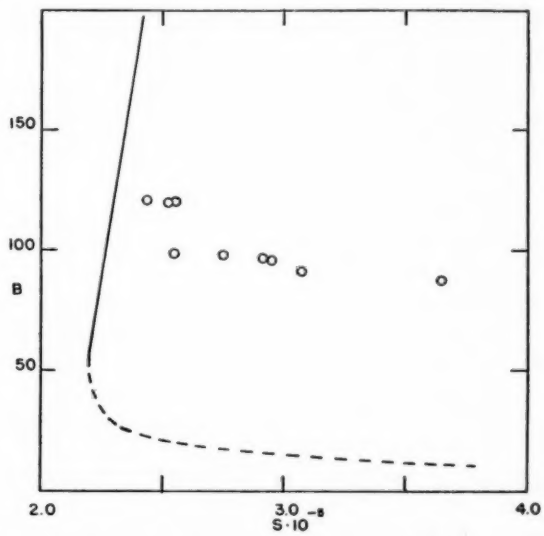

FIG. 3. The bursting pressure ratio, B, *vs* velocity, S, cm sec^{-1}; ——, calculated for the solid arm of the RH curve, Fig. 2; – – –, calculated for the dotted (unstable) arm of the RH curve, Fig. 2; O, experimental points, stations 1–3, Table I.

[4] J. Fay, *Fourth Symposium on Combustion* (Williams and Wilkins Company, Baltimore, Maryland, 1953), p. 501.

[5] A. J. Mooradian and W. E. Gordon, "Gaseous detonation III. Detonation limits in hydrogen-oxygen mixtures" Office of Naval Research report, Task Order I, with the University of Missouri (1950). See also Ph.D. thesis by A. J. M.

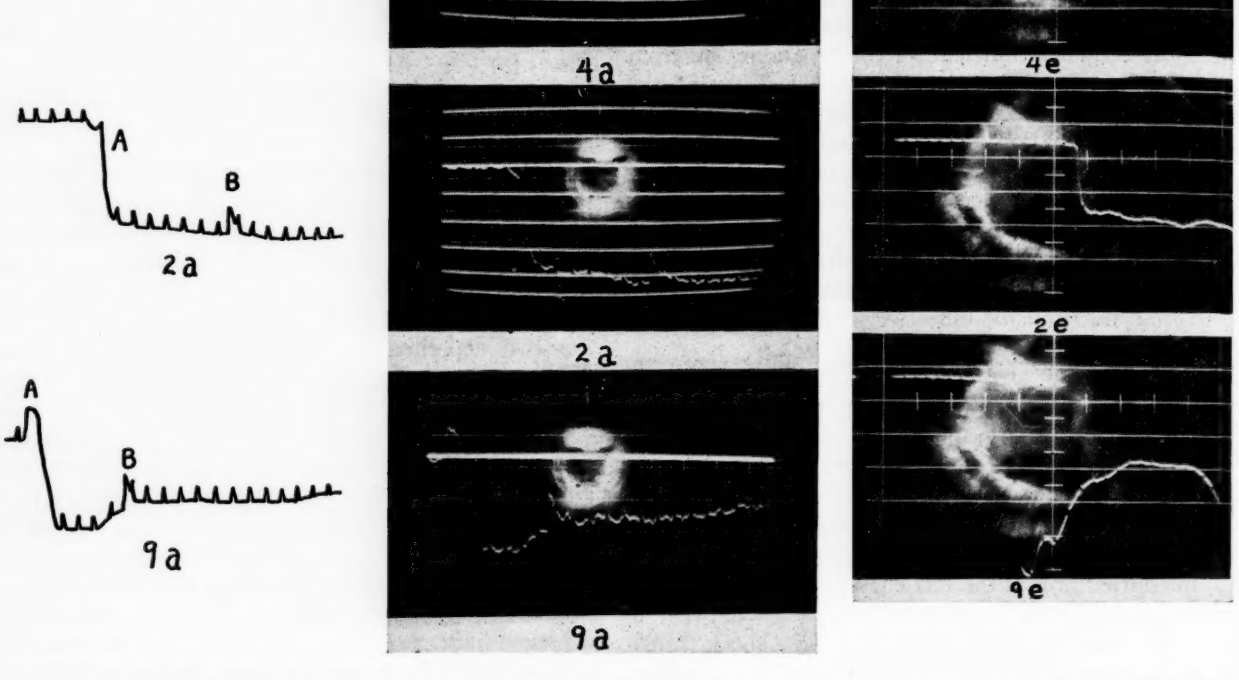

FIG. 4. Oscillograph records of photocurrent for some experiments. *4a*, *2a*, and *9a* are principally light absorption records at station 2 for experiments *4*, *2*, *9* of Table I. *A*, increase (or decrease *9a*) of light upon passage of the shock front. *B*, timing pulse from trigger circuit when shock passes station 3. The smudges are cathode glow on the *CRO* screen and are not significant. The small pips are 10 μsec timing markers. The smooth horizontal traces are either voltage calibrations or the cm rulings on the *CRO* screen. In *4a*, the light filter was the 487 mμ interference filter plus the 3385 Corning cut-off filter. The increase in light at the shock front is 1.7 times that expected for complete dissociation of the I_2, the additional amount being due to light emission. In *2a*, the cut-off filter was omitted, permitting more transmission of blue light. The increase in photocurrent is 3.7 times that expected for complete dissociation of the I_2. *4e*, *2e*, *9e* are light emission records at station 3 through a Corning 5562 blue filter (360–500 mμ). The slit geometry at the two stations was about the same, but the photoelectric sensitivity at station 3 was adjusted to be 1/120 that at station 2.

so that quenching by the rarefaction wave is absent, and due to the large tube diameter, which de-emphasizes attenuation by the walls.

Photoelectric measurements were obtained at three stations 240 cm (16 tube diameters), 260, and 280 cm from the membrane. Observations were made with light beams defined by 2.5-cm by 1-mm slits. The collimation was such that for perfect alignment of the slits and tube, a 3-mm length of the tube was observed by the photomultiplier for light absorption, and a 5-mm length for light emission. A signal due to absorption of blue green light at station 1 was used for triggering the oscilloscope sweeps. Light absorption measurements were made at station two with blue green light from a projection lamp passed through an interference filter with a maximum at 487 mμ and a half-width of 8 mμ, and a transmission of the order of $\frac{1}{2}$–1 percent through the rest of the spectrum. In some experiments a sharp cut Corning filter (No. 3385) opaque for wavelengths less than 480 mμ was used also. In others, this cut-off filter was omitted, and the light emission by the detonation, which is principally blue light, was superimposed on the light absorption changes. Light output of blue light (Corning filter No. 5562) was observed at station 3. Time intervals between the several stations were measured on the oscilloscope traces. In some runs, the time interval between the first and third stations was also measured with a Potter 1.6-Megacycle Counter Chronograph; these results agreed with the oscilloscope measurements.

Table I shows quantitative data for most of the experiments. The photoelectric signals of transmission of blue green light, Fig. 4, at station 2 show that (a) for typical experiments, there is no observed compression of the iodine, but that it disappears directly at the shock front; (b) the light output of the detonation is coincident with the shock front within the rise time of either signal (2–3 μsec). The calculated shock temperatures before combustion, T_s, Table I, are sufficiently high so that the thermal dissociation of iodine[3] is

sufficiently fast to account for (a), without invoking an increased rate of removal of iodine by the combustion process or by an increased rate of thermal dissociation due to combustion.

Observation (b) is, we believe, the most important result of this investigation. The reaction zone is less than 2–3 μsec or 4–6 mm thick.[6]

The light emission, as observed at station 3, consists principally of blue light and is a step function of time. There is no buildup of the luminosity nor is there a peak due to chemiluminescence of the reaction zone.

Figure 4(c) is an atypical record that was obtained only once. One sees compression of the iodine followed by a long delay with very little dissociation (temperature below 1200°K) followed by a detonation front which is luminous and where the iodine rapidly disappears. We believe that this is due to delayed ignition of the gas behind the shock, so that the pure shock (no combustion) has reached the second light station before the detonation catches up with and merges with the shock. (The recorded velocities for this experiment are not significant because of uncertainties as to the optical signal at station 1 which triggered the various timing circuits.)

In typical experiments Table I shows that the shocks are accelerating as they proceed downstream; although for pure shock waves, the velocities are quite steady.[3] Furthermore, the velocities are much higher than the theoretically expected value. Unusually high unsteady velocities at the inception of detonation are commonly observed.[7,8] Probably in all of our experiments, combustion did not begin immediately when the membrane broke, but was delayed until the shock propagated some distance downstream. When combustion starts, an unsteady very fast detonation moves up and merges with the shock. A longer tube than was available for the present investigation would be required in order for the steady state behavior of the system to be established.

Assuming that the average number of collisions per second per molecule at room temperature at 1 atmos pressure is 10^{10}, an average compression factor of 3.5 for the reaction zone to the CJ plane, and an average temperature of *ca* 2700°, the observation that the reaction zone is less than 5 mm thick means that the reaction is complete in less than 9×10^8 collisions. Without attempting a complete solution of the flame equations,[9] it is possible to make a rough estimate of the time for complete combustion as follows.

Assume the divergent chain reaction scheme,

	ΔE (kcal)
$H+O_2 \xrightarrow{k_1} OH+O$	17.0
$O+H_2 \rightarrow OH+H$	3.0
$OH+H_2 \rightarrow HOH+H$	−15.5

At the temperature of a detonation, the conventional low temperature chain breaking step, $H+O_2\rightarrow HO_2$, is not of great importance because of the instability of HO_2. Three body chain terminations like $H+H+M \rightarrow H_2+M$ have k's of the order[3] of 10^{-32} atom^{-2} cc^2 sec^{-1}; even if all of the gas were dissociated into atoms or radicals, their concentration would be *ca* 2×10^{18} cc^{-1}, and the half time for recombination of the order of $10^{32}/(4\times10^{36})=2.5\times10^{-5}$ sec or 2.5×10^4 collisions and this type of termination would not affect the reaction kinetics very much.

Reaction (1) is probably the slow step in the divergent chain. One can therefore treat OH and O as intermediates present at low concentration to which the steady state approximation applies, and consider the time rate of change of the hydrogen atom concentration. The resulting equation is $d(H)/dt=2k_1(O_2)$, and the solution for constant $k_1(O_2)$ is $(H)=(H)_0e^{2k_1(O_2)t}$. Each chain cycle creates two H atoms and two HOH molecules. In the final mixture, there are *ca* 10^{18} molecules/cc. If $(H)_0=1$ atom/cc, the time required for complete reaction is $18\times2.3/(2k_1\times O_2)=20$ chain cycles.

Baldwin and Walsh[10] have argued that at 520°C, $k_1=10^{-14}$ atom^{-1} cc sec^{-1}, although Lewis and von Elbe[11] recommend $k_1=10^{-17}$.

The value 10^{-14} equated to $PZ\exp(-17\,000/RT)$ gives P approximately unity. Referring to the initial temperature of the shocked gas, Table I, the Boltzmann factor for k_1, at 2060° is 1/62, at 2700° it is 1/22, and at the equilibrium temperature of *ca.* 3400° it is 1/10. At 1580°, the temperature of the shocked uncombusted

[6] Professor G. B. Kistiakowsky, while reviewing this manuscript, has very generously transmitted the following communication to us: "Using the x-ray absorption technique, we have now observed reaction zones (as zones of high initial density) in $2H_2-O_2$ mixtures at pressures from 85 to 20 mm (with some Xe added to increase x-ray absorption). The waves were not overdriven but steady and of normal velocity; the duration of the reaction zone varies from a couple μsec at the highest to 20 μsec at the lowest pressure, changing roughly as $1/P^2$. There seems to be no induction period . . . . I suspect that the overdrive and the presence of iodine must have somehow reduced the duration of the zone in the present experiments, or that the light emission starts as soon as reaction starts, not when it essentially ends, and then continues." These results predict that the time of passage of the reaction zone at the pressure used by us would be 11 μsec for a free detonation. The approximate calculations presented further on in the present paper predict a difference of a factor of about three between a free detonation and the overdriven detonations studied here, so that the time of passage of the reaction zone would be 3–4 μsec, which is only slightly larger than the upper limit estimated by us. The possible explanations proffered by GBK for any such differences are eminently reasonable.

[7] Berets, Greene, and Kistiakowsky, J. Am. Chem. Soc. **72**, 1086 (1950).

[8] A. J. Mooradian and W. E. Gordon, J. Chem. Phys. **19**, 1166 (1951).

[9] Hirschfelder, Curtiss, and Campbell, *Fourth Symposium on Combustion* (Williams and Wilkins Company, Baltimore, 1953), p. 190.

[10] R. R. Baldwin and A. D. Walsh, Discussions Faraday Soc. **17**, 96 (1954).

[11] B. Lewis and G. von Elbe, *Combustion, Flames and Explosions of Gases* (Academic Press, Inc., New York, 1951), p. 59.

gas in a free detonation, the Boltzmann factor is 1/200. The initial rate of the reaction will always be the slowest, and we may estimate therefore a thickness of the reaction zone of the order of $20\times200=4000$ collisions with O_2 molecules for a free detonation and $20\times60=1200$ collisions for some of the supported detonations of Table I. These estimates are consistent with the experimental observation that the reaction zone is less than 10^4 total collisions thick. If P, the steric factor for reaction (1) were 0.01 or less, the reaction zone would probably be thick enough to be observed in our experiment. Indeed, the arguments presented above indicate that if a decrease by a factor of ten in the number of collisions to be resolved could be achieved, the structure of the reaction zone could be observed, at least coarsely.

The activation energy of 17 kcal for the rate determining step (1) means that this reaction occurs at only a small fraction of the pertinent collisions even at *ca* 2000°K and excludes the possibility mentioned previously of the reaction occurring ahead of the shock wave leading to a transition to the lower arm of the RH curve.

It is of interest to make some equally crude calculations about the chain initiating step. Assume that it is $H_2+O_2=2OH$. Using the approximate rule for reactions of this type that the activation energy in the exothermic direction is 0.25 times the sum of the bond energies, $E_{ACT}=D_{H_2}+D_{O_2}-(\frac{1}{2})D_{OH}\cong70$ kcal. Assuming a steric factor of 0.1 and a rate constant $10^{-11}\exp(-70\,000/RT)$ $atom^{-1}$ cc sec^{-1} and $(H_2)=(O_2)=10^{18}$, the initial rate of production of OH radicals is 10^{18} cc^{-1} sec^{-1} at 2000° and 10^{16} cc^{-1} sec^{-1} at 1580; in each case, the rate is ample to initiate the divergent chain.

The relative importance of chain initiation by diffusion of radicals into unreacted gas may be estimated as follows. Let l be the thickness of the reaction zone and c_0 the concentration of H atoms (the most diffusible species) at equilibrium, and D their diffusion coefficient. In a system of coordinates sitting on the shock wave, the number of H atoms diffusing upstream across any plane into unreacted gas is Dc_0/l. The volume of gas flowing across the same plane is $S(V_2/V_1)$, (V_1/V_2 is the compression factor) so that the volume rate of production of H atoms by diffusion is $(Dc_0l/S)(V_1/V_2)$. For $D=5$ cm^2 sec^{-1}, which is reasonalbe for our experiment, $c_0=10^{17}$ atom/cc, and $l=10^{-1}$ cm; this is 10^{11} atom cc^{-1} sec^{-1}, $10^{-7}-10^{-5}$ less than the estimated rate of initiation by chemical reaction.

ACKNOWLEDGMENT

We are grateful to Dr. Arthur Bennett and Professor G. B. Kistiakowsky for stimulating advice and discussion.

Acid Catalysis in the Thermal Decomposition of Ammonium Nitrate*

BERNARD J. WOOD AND HENRY WISE
Jet Propulsion Laboratory, California Institute of Technology, Pasadena 3, California
(Received July 29, 1954)

Experimental measurements of the kinetics of thermal decomposition of ammonium nitrate have been made in the temperature range from 443 to 553°K. The results indicate that the degradation of ammonium nitrate is an autocatalytic liquid-phase reaction, the rate of which is proportional to the product of the mass of salt and the concentration of acid. The activation energy for this process is found to be 31.4 kcal. Adjustment of the concentration of acid present offers an effective means for the control of the rate of thermal degradation of ammonium nitrate.

THE isolation of nitric acid as an intermediate in the thermal decomposition of ammonium nitrate was reported by Veley.[1] Subsequent measurements[2,3] correlated the amount of acid formed during a given time interval of reaction to the initial mass of ammonium nitrate. Nevertheless the mechanism of the thermal degradation of the salt[4,5] and in particular the influence of the acid produced in the reaction are not known in any detail. In the present analysis a detailed determination has been carried out of the effect of acid on the kinetics of thermal decomposition of ammonium nitrate.

EXPERIMENTAL PROCEDURE

Weighed samples of ammonium nitrate† were placed into carefully dried Pyrex tubes which were subsequently evacuated and sealed. The sealed tubes were immersed for their entire length in an electrically heated constant-temperature oil bath for various time intervals. The hot samples were quickly cooled to room temperature and subsequently frozen in liquid nitrogen for at least 5 minutes. The frozen ampoules were then broken, their contents washed into clean beakers with CO_2-free water, and the resulting solutions titrated successively for acid with standard potassium hydroxide and for ammonium ion with formaldehyde solution.[6]

In order to provide a definite correlation between the rate of decomposition of ammonium nitrate and the amount of nitric acid present, experiments were also carried out in which known quantities of nitric acid were added to the salt in the sealed vessel before heating was commenced. Quantitative transfer of a small but definite quantity of acid was effected in the following manner. A glass reservoir of freshly distilled nitric acid and the ampoule to be charged with acid were connected through separate inlets to a storage bulb of known volume. The vapor pressure of the acid[7] was adjusted to the desired value by submerging the acid reservoir in a thermostated bath. By opening the intervening stopcock, nitric acid vapor was allowed to distill into the storage bulb until the equilibrium vapor pressure had been established. Then the established concentration of acid isolated in the storage bulb of known volume was allowed to distill into the evacuated ampoule which contained NH_4NO_3. To insure complete transfer of the vapor from the bulb to the ampoule, the NH_4NO_3 was immersed in liquid nitrogen and sealed off while still frozen. The quantity of nitric acid introduced was analyzed volumetrically, and good agreement was found between the experimental value and that calculated from the vapor-pressure data for nitric acid.[7] The reaction products were analyzed by a procedure identical to that employed in the rate measurements with pure ammonium nitrate.

EXPERIMENTAL RESULTS

The experimental measurements indicate that the initial rate of decomposition of ammonium nitrate is proportional to the mass of salt as shown in Fig. 1.

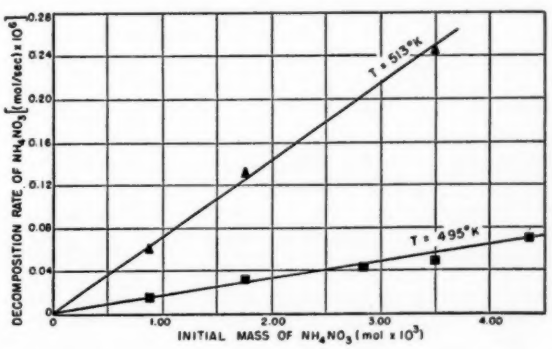

FIG. 1. Initial rate of thermal decomposition as a function of mass of ammonium nitrate.

* This paper presents the results of one phase of research carried out at the Jet Propulsion Laboratory, California Institute of Technology, under contract No. DA-04-495-ORD18 sponsored by the Department of the Army Ordnance Corps.

[1] V. H. Veley, J. Chem. Soc. **43**, 370 (1883).

[2] H. L. Saunders, J. Chem. Soc. **121**, 698 (1922).

[3] M. S. Shah and T. M. Oza, J. Chem. Soc. **1932**, 725.

[4] A. J. B. Robertson, J. Soc. Chem. Ind. **67**, 221 (1948).

[5] L. Friedman and J. Bigeleisen, J. Chem. Phys. **18**, 1325 (1950).

† The manufacturer's lot analysis ("Baker's Analyzed") lists the following impurities:

Insoluble matter	0.005%	heavy metals (as Pb)	0.0002%
Cl^-	0.0002%	Fe	0.0001%
PO_4^{---}	0.0001%	NO_2	0.0005%
SO_4^{--}	0.0005%	nonvolatile matter	0.0005%

Passes ACS neutrality test.

[6] K. Marcali and W. Rieman, Ind. Eng. Chem., Anal. Ed. **18**, 709 (1946).

[7] E. P. Egan, Ind. Eng. Chem., Anal. Ed. **37**, 303 (1945).

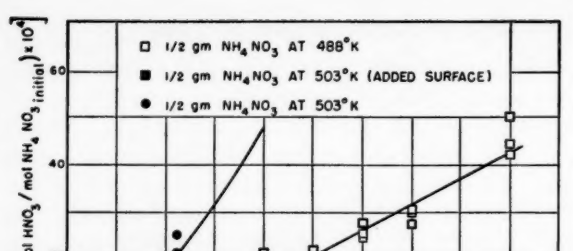

FIG. 2. Rate of formation of acid during thermal decomposition of ammonium nitrate.

However, quantitative analysis of the products further demonstrates an increasing rate in the production of nitric acid during the course of the reaction (Fig. 2). It is apparent therefore that the thermal degradation of ammonium nitrate takes place in the liquid phase and is autocatalyzed by acid.

In order to determine the effect of acid on the rate of reaction of ammonium nitrate a number of experiments were carried out in the presence of various amounts of nitric acid which were added to samples of salt before heating. The results of these measurements (Table I) combined with the effect of ullage on the amount of ammonium nitrate decomposed (Table III) indicate that the initial rate of chemical transformation is proportional to the concentration of acid in the sample. The experimental results may therefore be fitted to a rate law of the following form:

$$-\frac{1}{V}\frac{da}{dt}=k\frac{a}{V}\frac{b}{V} \tag{1}$$

where a and b represent the number of moles of ammonium nitrate and acid, respectively, and V, the volume of the liquid melt. Since V is proportional to the mass of ammonium nitrate (neglecting the relatively small volume of acid) the rate of disappearance of the salt (in moles/sec) is also given by

$$-\frac{da}{dt}=\frac{k}{V}ab=k'b. \tag{2}$$

TABLE I. Initial rate of decomposition of ammonium nitrate in the presence of nitric acid.

Temperature (°K)	Initial mass of reactants NH_4NO_3 (mole $\times 10^3$)	HNO_3 (mole $\times 10^5$)	Initial decomposition rate (mole sec^{-1}) $\times 10^6$
448	6.25	1.0	0.008
448	6.25	11.5	0.075
488	6.25	0.09	0.013
488	6.25	2.0	0.25
488	6.25	11.5	1.2

TABLE II. Effect of nitric acid on decomposition of ammonium nitrate at 448°K.

Initial mass of reactants mole $\times 10^3$ NH_4NO_3	HNO_3	Mass of NH_4NO_3 decomposed[a] mole $\times 10^3$
12.56	0.046	0.21
12.50	0.046	0.16
6.21	0.046	0.14
6.13	0.046	0.12
6.39	0.046	0.19
2.99	0.046	0.17
3.21	0.046	0.13
6.25	0.10	0.35

[a] Heating period: 2000 sec; volume of reaction vessel: 4 cc.

Consequently the mass rate of decomposition of the salt is a function only of the mass of acid present in the melt. This functional relationship is borne out by the data in Table II. In these experiments the initial mass of nitric acid in the sample was kept constant,‡ however its concentration was varied by the use of different amounts of ammonium nitrate.

Based on the rate law [Eq. (1)], the rate constant may be evaluated over the range of temperatures studied (Fig. 3) and the following rate equation results

$$\frac{k}{V}=10^{14.2}e^{-31400/RT}\ \text{mole}^{-1}\ \text{sec}^{-1}. \tag{3}$$

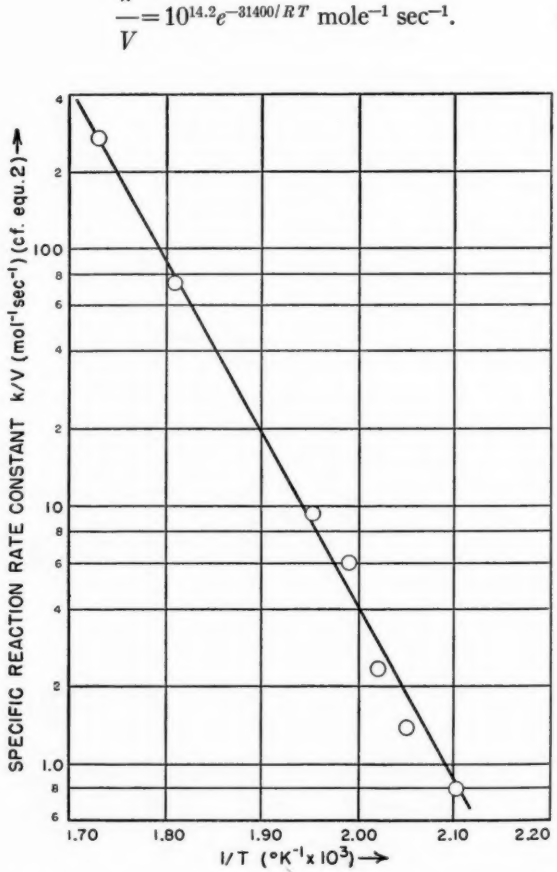

FIG. 3. Specific reaction rate constant as a function of temperature.

‡ Except for the last measurement in Table II.

Of special interest is the inhibition in decomposition rate observed during the course of the reaction (Fig. 4). This gradual decrease in the rate of decomposition is particularly pronounced in those samples of ammonium nitrate to which a relatively large amount of nitric acid originally was added.

Experimental measurements showed conclusively that the rate of decomposition of ammonium nitrate is not affected by such products of reaction as water vapor§ and nitrous oxide. However the addition of gaseous ammonia at an initial pressure of 100 mm Hg|| almost completely inhibited the reaction at 513°K. Additional experiments in which the pressure of ammonia was reduced to 10 mm Hg|| still showed inhibition although to a lesser degree. This effect is obviously due to the neutralization of the acid formed as an intermediate in the reaction. Since the solubility of ammonia in liquid ammonium nitrate is smaller than that of the acid, the inhibition does not occur until a sufficiently high concentration of ammonia has accumulated in the vapor phase. This effect is further demonstrated by increasing the volume of the sealed reaction vessel containing the ammonium nitrate (Table III).

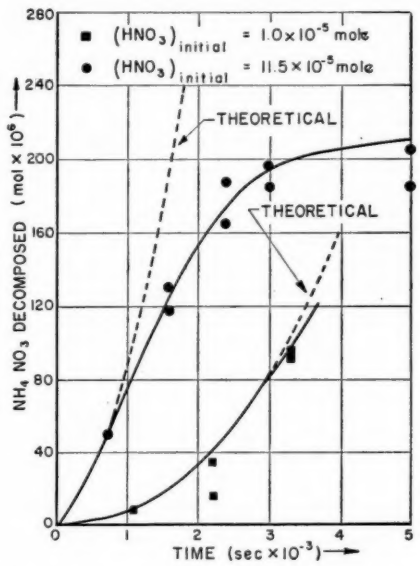

FIG. 4. Decomposition of ammonium nitrate in the presence of nitric acid as a function of time. (c=0.9, Eq. (4) and (6)).

Similarly a marked reduction in the rate of decomposition of ammonium nitrate results from the addition of surface (glass wool) to the sealed tube containing the reactants. Thus in the presence of added surface the concentration of nitric acid and the amount of ammonium nitrate decomposed was materially reduced (Table IV). At the same time the formation of nitrogen dioxide was apparent.¶ These observations are in agreement with the reported heterogeneous nature of the thermal decomposition of nitric acid.[8]

TABLE III. Effect of ullage on the thermal decomposition of ammonium nitrate heated 10 000 seconds at 488°K.

Initial mass of NH_4NO_3 (mole×10⁵)	Mass decomposed (mole×10⁵) in reactor of volume		
	2 cc	4 cc	50 cc
3.125	0.16	...	0.16
6.25	0.27	...	0.28
12.50	0.35	0.42	0.50

ANALYSIS OF RESULTS

The course of the thermal decomposition as measured by the rate of disappearance of ammonium nitrate exhibits the characteristics of a second-order, autocatalytic transformation. It is of interest that the experimental measurements have demonstrated a linear relationship between the rate of decomposition of ammonium nitrate and the rate of formation of nitric acid, i.e. $-c(da/dt)=(db/dt)$ where c represents an empirical constant whose value $0<c<1$. Consequently at any time t

$$b=c(a_0-a)+b_0 \tag{4}$$

where the subscript zero refers to the initial condition at $t=0$. Integration of Eq. (2) yields therefore

$$kt=\frac{V}{(b_0+ca_0)}\ln\frac{a_0b}{b_0a} \tag{5}$$

or,

$$k't=-\frac{1}{c}\ln\frac{b}{b_0}.$$

From Eq. (5) the initial mass of acid b_0 present in the reactant sample may be found by graphical analysis. Thus a plot of $\ln(b/a)$ *versus* time should produce a straight line whose intercept on the ordinate permits the calculation of b_0. Such an analysis of the experimental data is presented in Fig. 5.

TABLE IV. Decomposition of ammonium nitrate in the presence of nitric acid at 488°K.

Reaction time (sec)	Initial mass of reactants (mole×10⁵)		Mass of NH_4NO_3 decomposed (mole×10⁵)
	NH_4NO_3	HNO_3	
3000	12.50	...	0.17
3000	12.50	0.10	0.22[a]
3000	12.50	0.10	0.77

[a] With surface added.

§ Friedman and Bigeleisen (see reference 5) reported that small amounts of water vapor catalyzed the decomposition; however, such an effect could not be demonstrated in our experimental measurements.

|| Measured at 300°K

¶ Under these experimental conditions continuous removal of acid from the liquid phase occurs as long as the rate of thermal decomposition of acid is fast relative to the rate of vaporization.

[8] Johnston, Foering, Tao, and Messerly, J. Am. Chem. Soc. **73**, 2319 (1951).

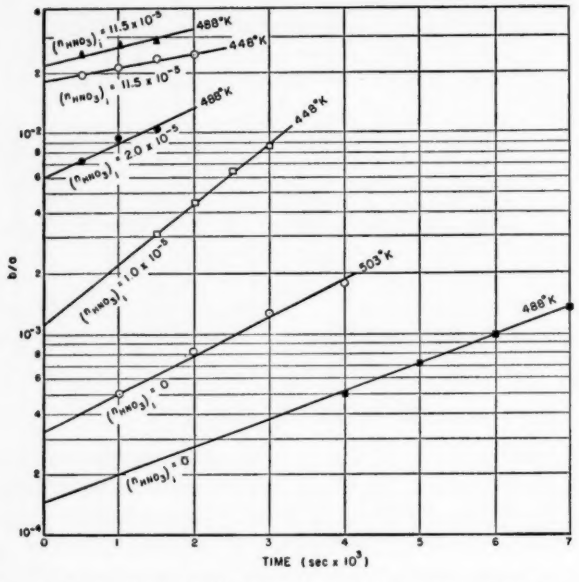

FIG. 5. Evaluation of initial mass of acid in liquid melt of ammonium nitrate (initial mass of $NH_4NO_3 = 6.25 \times 10^{-3}$ mole).

The lower two curves, which represent rate measurements in the absence of added nitric acid, yield from their intercepts on the ordinate 0.09×10^{-5} mole of acid at 488°K and 0.2×10^{-5} mole of acid at 503°K present at the beginning of the chemical transformation. The remaining curves in Fig. 5 represent experimental measurements in which nitric acid was initially added to the sample. The initial mass of nitric acid evaluated from these curves is in good agreement with the amount of acid actually introduced into the sealed reaction tubes (see Table V). The presence of acid at the onset of thermal decomposition of ammonium nitrate is in accordance with the qualitative observation that acid can be detected in a sample of the salt heated slightly above its melting point, a temperature at which the rate of decomposition of the material is extremely slow. During the initial stages of reaction the experimental results can be fitted to a theoretical curve based on Eq. (4) which has the form

$$a = (ca_0 + b_0)/[c + (b_0/a_0)e^{(kt/V)(a_0 + cb_0)}]. \quad (6)$$

After prolonged periods of heating, however, the experimental data** begin to diverge from the theoretical curve, especially in the cases in which relatively large amounts of acid were originally added to the sample (Fig. 4). These deviations are undoubtedly due to the loss of nitric acid from the liquid phase where it exerts its autocatalytic action. The accumulation of nitric acid in the vapor phase was observed indirectly at 488°K upon the addition of glass wool to the sealed tube containing the reacting material. As shown by the data in Fig. 2, a marked diminution in the final quantity of HNO_3 was observed in the presence of added surface. At the same time the formation of nitrogen dioxide in the gas phase became apparent.

It is also to be remembered that the thermal decomposition of ammonium nitrate involves the evolution of ammonia, the solubility of which in liquid ammonium nitrate is very much smaller than that of nitric acid. Thus, in a closed reaction vessel as employed in these experiments, sufficient ammonia may accumulate in the vapor phase to inhibit the reaction. This effect is readily demonstrated by varying the volume of the sealed reaction vessel containing the ammonium nitrate (Table III).

A mechanism for the thermal decomposition of ammonium nitrate which is consistent with the observed data and with those obtained by other investigations[5,9]

TABLE V. Initial mass of nitric acid added to NH_4NO_3.[a]

Temperature (°K)	Added	Mass of acid (mole×10⁵) Calculated from Fig. 5
448	1.0	0.7
448	11.5	11.3
488	0	0.09
488	2.0	3.7
488	11.5	13.7
503	0	0.2

[a] Initial mass of ammonium nitrate $= 6.25 \times 10^{-3}$ mole; reactor volume = 2 cc.

may be postulated:

$$NH_4NO_3 \rightarrow NH_3 + HNO_3 \quad (A)$$

$$H^+ + NH_4NO_3 \rightarrow [NH_2NO_2] + H_3O^+ \quad (B)$$

$$[NH_2NO_2] \rightarrow N_2O + H_2O. \quad (C)$$

This sequence of reactions exhibits the catalytic effect of the acid†† and the inhibitory influence of ammonia on the decomposition of ammonium nitrate. Equation (B) represents the slow step in the mechanism. Such a dehydration mechanism is based on the findings[5,9] that a N−N bond is formed during the thermal degradation of the salt. On the basis of our work no definite conclusion can be drawn concerning the identity of the intermediate. However, isotopic analysis[5] points to the formation of an unsymmetrical compound such as nitramide (NH_2NO_2) which yields the final products by further dehydration.

** Expressed in the form: $(a_0 - a)$ *vs* time.

[9] J. T. Kummer, J. Am. Chem. Soc. **69**, 2559 (1947).

†† Experimental data by H. A. Bent, [thesis, University of California (1952)] indicate that sulfuric acid has a similar catalytic effect.

Potential at Zero Charge for Reversible and Ideal Polarized Electrodes

PAUL RÜETSCHI* AND PAUL DELAHAY
Department of Chemistry, Louisiana State University, Baton Rouge, Louisiana
(Received August 19, 1954)

The potential at zero charge for an ideal polarized electrode, as measured with respect to some reference electrode, varies linearly with the work function of the metal, while this potential for a reversible electrode is independent of the nature of the electrode. This observation is verified experimentally for Ag, Cd, Cu, Ga, Hg, Ni, Pb, Pt, and Tl in the case of ideal polarized electrodes and for Ag, Au, Bi, Cu, Hg, and Pt for reversible electrodes. It is shown that the difference between the Volta potentials from electrode to solution for an ideal polarized electrode at zero charge is approximately −0.33 volt, and that the difference between the Galvani potentials is equal to the surface potential of the electrode. The difference of Volta potentials for a reversible electrode at zero charge varies linearly with the electronic work function of the metal.

INTRODUCTION

THE potential at which the charge at an interface electrode-solution is equal to zero can be determined experimentally for conditions under which electron transfer across the interface is either possible or virtually impossible. Determinations in which electron transfer is possible are carried out with a reversible electrode. Measurements for which electron transfer is virtually impossible are made with what Grahame[1,2] has called an "ideal polarized electrode." A mercury electrode in an electrolyte to which no mercurous ions or other reducible or oxidizable substance are added behaves almost as an ideal polarized electrode.[2] Potentials at zero charge, as measured against some reference electrode, may be very different (as much as one volt) according to whether one or the other method is applied. The reason for this difference was the object of a controversy between Billiter[3] and Palmaer,[4] but the argument was never settled. The fundamental difference between the two types of measurement is discussed quantitatively in this paper.

The relationship between potential at zero charge and work function of the metal has already been discussed by several authors. Veselovsky[5] pointed out that the difference between the zero charge potentials for silver and mercury electrodes is virtually equal to the difference between the work functions of these metals. According to Grahame,[2] Frumkin[6] expressed similar ideas more than twenty years ago. Vasenin[7] recently pointed out that a plot of potential at zero charge (measured with respect to some reference electrode) against work function for various metals has a slope smaller than unity. This result was accounted for by the action of multipoles of the solvent at the interface electrode solution. As far as we know no distinction between data obtained with ideal polarized and reversible electrodes is made by these Russian authors.

In the following discussion we shall use the Galvani, Volta, and surface potentials introduced by Lange.[8–10] The definition of these potentials will be briefly recalled. The Galvani or inner potential, φ, of a phase is defined as the electrical work involved in bringing a unit positive charge from infinity into the phase. The Volta or outer potential, ψ, of a phase is defined as the work required to bring a unit positive charge from infinity to a point just outside the phase where the influence of the image force is negligible, i.e., at about 10^{-4} cm from the surface of the phase in a state equivalent to the Schottky state.[11] The meaning of the expression "just outside the phase" is discussed by Adam.[12] The surface potential, χ, of a phase is defined by the electrical work involved in transferring a unit positive charge from a point just outside the phase into the phase. The difference between the Volta potentials of two phases is a well-defined and measurable quantity, while the corresponding difference of Galvani potentials cannot be measured and, according to Guggenheim,[13] cannot even be defined. Strehlow,[14] although he recognizes that differences of Galvani potentials cannot be measured, adopts the less extreme and more fruitful approach that such differences of potential could in principle be calculated.

The above potentials are related by the equation[8–10]

$$\varphi=\psi+\chi. \tag{1}$$

The emf across a complete electrochemical cell can be computed from Galvani or Volta potentials as indicated in Fig. 1, where V represents either φ or ψ.

* Postdoctoral fellow, 1953–1954.
[1] D. C. Grahame and R. B. Whitney, J. Am. Chem. Soc. **64**, 1548 (1942).
[2] D. C. Grahame, Chem. Revs. **41**, 441 (1947).
[3] J. Billiter, Z. Elektrochem. **8**, 638 (1902); Z. physik. Chem. **51**, 166 (1905).
[4] W. Palmaer, Z. Elektrochem. **9**, 754 (1903); Z. physik. Chem. **59**, 129 (1907).
[5] V. J. Veselovsky, Acta Physicochim. U.R.S.S. **11**, 815 (1939).
[6] A. N. Frumkin, Colloid Symposium Annual **7**, 89 (1930).
[7] R. M. Vasenin, Zhur. Fiz. Khim. **27**, 878 (1953).
[8] E. Lange, *Handbuch der Experimentalphysik* (Akademische Verlagsgesellschaft, Leipzig, 1933), Vol. 12, Pt. 2, p. 267 ff.
[9] O. Klein and E. Lange, Z. Elektrochem. **43**, 570 (1937).
[10] E. Lange, Z. Elektrochem. **55**, 76 (1951); **56**, 94 (1952).
[11] W. Schottky and Rothe, *Handbuch der Experimentalphysik* (Akademische Verlagsgesellschaft, Leipzig, 1928), Vol. 12, Pt. 2, p. 145 ff.
[12] N. K. Adam, *The Physics and Chemistry of Surfaces* (Oxford University Press, London, England, 1941), third edition, p. 303.
[13] E. A. Guggenheim, J. Phys. Chem. **33**, 842 (1929); **34**, 1758 (1930).
[14] H. Strehlow, Z. Elektrochem. **56**, 119 (1952).

METAL	SOLUTION	Hg_2^{++} in KCl	MERCURY	METAL
I	II	III	IV	I

$$E = (V_I - V_{II}) + (V_{II} - V_{III}) + (V_{III} - V_{IV}) + (V_{IV} - V_I)$$

FIG. 1. Schematic diagram of electrochemical cell.

IDEAL POLARIZED ELECTRODES

Consider the cell of Fig. 1 and assume that metal I—solution II is an ideal polarized electrode. The phases III and IV form a normal calomel electrode, which is connected to metal I. The emf of the cell is the sum of the differences of the Galvani or Volta potentials. The emf is positive when electrode I on the left is positive with respect to electrode I on the right. The difference of potential for the interface I–II depends on the adsorption of ions and on the orientation of multipoles of the solvent (water) in II. The charge at the interface can be changed by applying a voltage to the cell, and the emf corresponding to zero charge at the interface I–II can be determined by several methods described in Butler's review.[15] For example, the emf of the cell of Fig. 1, when metal I is mercury, is in the immediate vicinity of −0.50 volt in the absence of an electrocapillary active species in solution.[2]

If metal I is changed, it is observed that the emf of the cell corresponding to zero charge varies. A plot of experimental values of the emf of the cell against the work function[16] of metal I is shown in Fig. 1.[17] A few experimental potentials at zero charge are not plotted in Fig. 2 because of the uncertainty on the corresponding work functions. Thus, data[18] for zinc (−0.63 volt) and tellurium (+0.61 volt) are not shown. Data for platinum are uncertain, and the potential at zero charge, +0.28 volt, instead of the value +0.42 volt plotted in Fig. 2, is quoted by Butler.[19] The value of the work function of platinum is, at any rate, rather uncertain.[16] The points (solid circles) of Fig. 1 cluster along a line having a slope of one. If one accepts this value of the slope, the difference of Volta potentials for an ideal polarized electrode is constant. The argument is as follows.

The difference of Volta potentials $\psi_{IV}-\psi_I$ in the expression of the emf of the cell of Fig. 1 varies as the metal is changed. In view of the definition of the work function, one has[10,20]

$$\psi_{IV}-\psi_I=-(W_{IV}-W_I) \qquad (2)$$

where the W's are the work functions expressed in volts. The difference between the work functions accounts for the experimental variations of the emf at zero charge for different metals, and consequently the term $\psi_I-\psi_{II}$ in the expression of V (Fig. 1) is independent of the nature of metal I. In other words the difference of Volta potentials at zero charge for ideal polarized electrodes is constant regardless of the nature of the electrode. It should be noted that this conclusion was reached from experimental results, and was not deduced from *a priori* considerations. The difference of Volta potentials at zero charge can be evaluated as follows.

The difference of Volta potentials for the normal calomel electrode $\psi_{Hg}-\psi_{III}$, as measured by Klein and Lange,[9] is +0.17 volt. Since the emf for the cell of Fig. 1 is practically −0.50 when the metal I is mercury, the difference of Volta potentials, $(\psi_I-\psi_{II})_{z.c.}$, for the ideal polarized electrode at zero charge is −0.33 volt. This value is approximate since the datum and Klein and Lange is affected by the errors resulting from experimental difficulties.

The calculation of the difference of Galvani potentials would require the value of the difference between the surface potentials of phases I and II. The surface potential for aqueous solutions against an inert gas was evaluated as −0.36 volt by Strehlow.[14] It is essentially independent of the electrolyte[14,21] (no electrocapillary active substance present) at least for not too concentrated solutions, say, less than 0.1 M. The surface potential primarily results from the orientation of

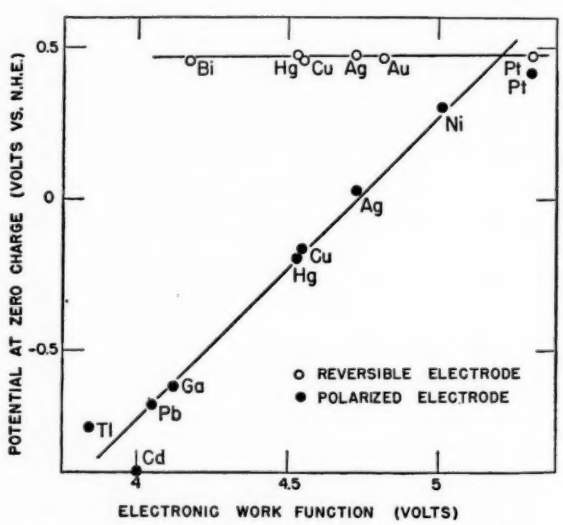

FIG. 2. Experimental potentials at zero charge against the work function of the electrode.

[15] J. A. V. Butler, in *Electrical Phenomena at Interfaces*, J. A. V. Butler, Editor (Methuen, London, England, 1951), pp. 30–74.

[16] Work function values from *Handbook of Chemistry and Physics*, C. D. Hodgman, Editor (Chemical Rubber Publishing Company, Cleveland, Ohio, 1951), pp. 2128–2131.

[17] Potentials at zero charge: T. Veslovsky, Acta Physicochim. U.R.S.S. **11**, 815 (1939) for Ag; J. Billiter, Z. Elektrochem. **14**, 624 (1908) for Cu; E. Murtazaev and J. Gorodetzkaja, Acta Physicochem. U.R.S.S. **4**, 75 (1936) for Ga; D. C. Grahame, Chem. Revs. **41**, 441 (1947) for Hg; R. Parsons, Z. Elektrochem. **55**, 113 (1951) for Ni; Borisova, Ershler, and Frumkin, J. Phys. Chem. U.S.S.R. **22**, 925 (1948) for Pb; J. Billiter, Z. Elektrochem. **8**, 638 (1902) for Pt; A. Frumkin, J. Colloid Sci. **1**, 277 (1946), and Borisova, Ershler, and Frumkin, Zhur. Fiz. Khim. **22**, 925 (1948) for Tl; A. Frunkin, Vestnik Moskov Univ. **7**, No. 9, 37 (1952) for Cd.

[18] See last reference in footnote 17.

[19] See reference 15, p. 41.

[20] P. Van Rysselberghe, J. Chem. Phys. **21**, 1550 (1953).

[21] A. Frumkin, J. Chem. Phys. **7**, 552 (1939).

water multipoles—mainly dipoles—with their positive poles toward the inert gas. On the basis of the value $\chi_{II} = -0.36$ volt one deduces from Eq. (1) the difference between Galvani potentials

$$\varphi_I - \varphi_{II} = (\psi_I - \psi_{II}) + (\chi_I - \chi_{II}), \quad (3)$$

or, in view of the value -0.33 volt for the difference between the ψ's (see the foregoing) at zero charge,

$$(\varphi_I - \varphi_{II})_{z.c.} = -0.33 + 0.36 + \chi_I. \quad (4)$$

This shows that the difference between Galvani potentials for an ideal polarized electrode at zero charge is virtually equal to the surface potential of the metal. Again, it should be emphasized that there is some uncertainty on the data used in this calculation.

The same conclusion can be deduced from the value of the difference of Galvani potentials of 0.495 volt calculated by Latimer, Pitzer, and Slansky[22] for the normal calomel electrode. As was pointed out by several authors,[14,20,21,23,24] the surface potential of mercury must be added to the calculated value of 0.495 volt. Thus,

$$(\varphi_{Hg} - \varphi_{III})_{N.C.E.} = +0.50 + \chi_{Hg}. \quad (5)$$

If metal I of Fig. 1 is mercury, the emf of the cell, which is the sum of the Galvani potentials, is -0.50 volt.[2] Thus

$$-0.50 = (\varphi_I - \varphi_{II})_{z.c.} + (\varphi_{III} - \varphi_{Hg})_{N.C.E.} \quad (6)$$

if one makes the justifiable assumption that the difference of Galvani potentials between the solutions II and III can be neglected in this approximate calculation.[10] By combining Eqs. (5) and (6) one obtains

$$(\varphi_I - \varphi_{II})_{z.c.} = \chi_{Hg}, \quad (7)$$

which is precisely Eq. (4) as written for the particular case of mercury.

[22] Latimer, Pitzer, and Slansky, J. Chem. Phys. **7**, 108 (1939).
[23] W. C. Burgers, Chem. Weekblad, **39**, No. 16–17, 1 (1942).
[24] R. Piontelli, *Int. Committee Electrochem. Therm. Kin. Proc. 2nd Meeting, Tamburini, Milan, 1951*, pp. 344–369.

REVERSIBLE ELECTRODES

Potentials at zero charge for reversible electrodes have been measured by varying the ratio of the activities of the species involved in the reversible electrode until zero charge is obtained. Experimental results[25] are given in Fig. 2, which shows conclusively that the potential at zero charge is independent of the work function of the metal. The result can be explained by considering the cell of Fig. 1. If metal I is changed the difference between the Volta potentials for phases IV and I varies because of variation of the work function of metal I. However, the difference between the Volta potentials between I and II is changed by the same amount as for IV and I, because electrons are now transferred across the interface I–II. This is the situation encountered in the measurement of reduction potentials with an inert electrode. The emf of the cell is then independent of the nature of the inert electrode. One deduces from the foregoing considerations that the difference of Volta potentials for reversible electrodes at zero charge varies linearly with the electronic work function of the metal.

CONCLUSION

Differences between experimental potentials at zero charge as obtained with reversible and ideal polarized electrodes can be accounted for on the basis of considerations based on Galvani, Volta, and surface potentials.

ACKNOWLEDGMENT

The authors gladly acknowledge the support of this investigation by the Office of Naval Research. Mr. Gleb Mamantov translated some of the Russian papers quoted in this study.

[25] Experimental data: K. Bennewitz and J. Schulz, Z. physik. Chem. **124**, 115 (1926) for Ag and Cu; K. Bennewitz and A. Delijannis, *ibid.* **154**, 113 (1931) for Hg; W. A. Patrick and C. L. Littler, J. Phys. Chem. **54**, 1016 (1950) for Ag, Au, and Pt; H. S. Oel and H. Strehlow, Z. physik. Chem. (Frankfurt, N. F) **1**, 241 (1954) for Bi. The latter authors also confirmed the previous results for Hg, Au, Pt, and Cu.

Substituted Methanes. XXI. Calculated and Observed Wave Numbers, and Calculated Thermodynamic Properties, for Bromodeuteromethane and Bromodideuteromethane

JEROME M. DOWLING
Spectroscopy Laboratory, Department of Physics, Illinois Institute of Technology, Chicago 16, Illinois*
(Received April 8, 1954)

Using potential energy constants obtained from CH_3Br and CD_3Br, wave numbers (fundamentals) for CH_2DBr and CHD_2Br were calculated by means of the Wilson FG matrix method with a potential energy function containing all possible second degree terms. The calculated values of the wave numbers were then used to assign existing infrared and Raman spectral data for these molecules. Then the heat content, free energy, entropy, and heat capacity for the ideal gaseous state at 1 atmos pressure were calculated for 12 temperatures from 100 to 1000°K with a rigid rotator, harmonic oscillator approximation.

INTRODUCTION

IN a previous investigation,[1] Raman and infrared spectral data, assignments, potential energy constants, and calculated thermodynamic properties were given for CH_3Br and CD_3Br. A similar treatment has been carried out for CH_2DBr and CHD_2Br, except that no spectral data were obtained.

The wave numbers corresponding to the fundamental vibrational frequencies of CH_2DBr and CHD_2Br were calculated with potential constants obtained from CH_3Br and CD_3Br.[1] In addition the heat content, free energy, entropy, and heat capacity were calculated for the ideal gaseous state.

TABLE I. Raman and infrared spectral data, assignments and calculated wave numbers for CH_2DBr.

Infrared Courtoy σ_g[a]	Raman Hemptinne $\Delta\sigma_1$[b]	σ_c	Theoretical assignment	Type
	583	596	σ_6	a'
755	765	760	σ_5	a'
920		929	$(\sigma_5+\sigma_9)-\sigma_5$	A''
935		929	σ_9	a''
1004		994	$\sigma_2-\sigma_8$	A''
1106		1101	$(\sigma_5+\sigma_9)-\sigma_6$	A''
1212	1216	1223	σ_4	a'
1241		1276	σ_8	a''
1460		1458	σ_3	a'
1684		1690	$\sigma_5+\sigma_9$	A''
	2235	2222	σ_2	a'
2994	2988	3008	σ_1	a'
2830[c]		2818	$\sigma_2+\sigma_6$	A'
2995		3008	σ_1	a'
		3081	σ_7	a''
3635		3636	$3\sigma_4$	A'
3670		3664	$\sigma_6+\sigma_7$	A''
3690		3695	$\sigma_2+\sigma_3$	A'
3755		3750	$\sigma_1+\sigma_5$	A'
3860		3836	$\sigma_7+\sigma_5$	A''
3955		3930	$\sigma_1+\sigma_9$	A''
4250		4236	$\sigma_1+\sigma_8$	A''
4450		4455	$\sigma_1+\sigma_3$	A'
4880		4882	$(\sigma_6+\sigma_7)+\sigma_4$	A''
5300		5316	$\sigma_2+\sigma_7$	A''
5930		5915	$2\sigma_3+\sigma_1$	A'
6500		6512	$(\sigma_2+\sigma_7)+\sigma_4$	A''

[a] σ_g = data obtained for gaseous state.
[b] σ_l = data obtained for liquid state.
[c] Data obtained with quartz prism.

* Publication No. 102.

[1] Weissman, Bernstein, Rosser, Meister, and Cleveland, J. Chem. Phys. **23**, 544 (1955).

SYMMETRY, SELECTION RULES, AND ASSIGNMENTS

The CH_2DBr and CHD_2Br molecules have the symmetry of the C_{1h} point group and thus have 9 normal vibrations, 6 of type a' and 3 of type a''. All fundamentals, overtones, and combinations are allowed in both the Raman and infrared spectra. The a' lines should be polarized while the a'' lines should be depolarized.

PREVIOUS DATA AND ASSIGNMENTS

The infrared spectrum of a mixture of CH_2DBr and CHD_2Br has been obtained by Courtoy and Hemptinne[2] while the Raman spectrum of a mixture of CH_2DBr and CHD_2Br in the liquid state has been investigated by Hemptinne.[3] The assignments are given in Tables I

TABLE II. Raman and infrared spectral data, assignments and calculated wave numbers for CHD_2Br.

Infrared Courtoy σ_g[a]	Raman Hemptinne $\Delta\sigma_1$[b]	σ_c	Theoretical assignment	Type
	573	576	σ_6	a'
625		626	$\sigma_8-\sigma_5$	A''
		690	σ_5	a'
709		727	σ_9	a''
829		837	$(\sigma_5+\sigma_9)-\sigma_6$	A''
979		984	$\sigma_7-\sigma_3$	A''
1049	1029	1057	σ_4	a'
1139		1146	$2\sigma_6$	A'
1295		1299	σ_3	a'
1316		1302	σ_8	a''
1410		1399	$\sigma_5+\sigma_9$	A''
1437		1418	$2\sigma_9$	A'
1736		1739	$\sigma_4+\sigma_5$	A'
2092		2098	$2\sigma_4$	A'
2188	2185	2168	σ_2	a'
		2279	σ_7	a''
2855[c]		2852	$\sigma_7+\sigma_6$	A''
2882		2878	$\sigma_2+\sigma_5$	A'
2955		2969	$\sigma_7+\sigma_5$	A''
3017	3019	3046	σ_1	a'
3235		3237	$\sigma_2+\sigma_4$	A'
3335		3328	$\sigma_7+\sigma_4$	A''
5030		5043	$(\sigma_7+\sigma_6)+\sigma_2$	A''

[a] σ_g = data obtained for gaseous state.
[b] σ_l = data obtained for liquid state.
[c] Data obtained with quartz prism.

[2] C. Courtoy and M. de Hemptinne, Ann. Soc. Sci. Bruxelles **60**, 122 (1946).

[3] M. de Hemptinne, Trans. Faraday Soc. **42**, 5 (1946).

TABLE III. Bond distances; products of inertia; symmetry numbers; and masses of the C, H, Br, and D atoms.

	CH_2DBr	CD_2HBr
C−D	1.093 A	1.093 A
C−H	1.093 A	1.093 A
C−Br	1.910 A	1.910 A
$I_{xx}I_{yy}I_{zz}$	1.3181×10^{4} (awu $A^2)^3$	1.9189×10^{4} (awu $A^2)^3$
Symmetry number	1	1

$m_C = 12.010$ awu
$m_H = 1.008$ awu
$m_D = 2.01418$ awu
$m_{Br} = 79.916$ awu

TABLE IV. Calculated and most probable values of the wave numbers (fundamentals) of CH_2DBr and CHD_2Br.[a]

Designation	Type	CH_2DBr Calc	CH_2DBr Obs	CHD_2Br Calc	CHD_2Br Obs
σ_1	a'	3008	2995	3046	3017
σ_2	a'	2222	2235[b]	2168	2188
σ_3	a'	1458	1460	1299	1295
σ_4	a'	1223	1212	1057	1049
σ_5	a'	760	755	690	
σ_6	a'	596	583[b]	576	573[b]
σ_7	a''	3081		2279	
σ_8	a''	1276	1241	1302	1316
σ_9	a''	929	935	727	709

[a] σ = wave number in K (kayser, cm^{-1}). All the fundamentals are nondegenerate (degeneracy = 1).
[b] Values for liquid (Raman). All others for the gaseous state.

and II. Infrared bands at 785, 803, 2564, 7120, and 8850 K as well as a Raman line at 811 K remain unassigned. These bands may have been due to impurities present in the mixture of CH_2DBr and CHD_2Br.

NORMAL COORDINATE TREATMENT

A normal coordinate treatment (Wilson FG matrix method),[4] using the most general quadratic potential energy function, was carried out for both molecules. The symmetry coordinates and the F and G matrix elements are not given because they are formally the same as those of Weber *et al.*[5] Values for the masses and bond lengths that were used to calculate G matrix elements are listed in Table III. The calculated and most probable values of the wave numbers (fundamentals) for CH_2DBr and CD_2HBr are given in Table IV.

The potential constants were transferred directly from CH_3Br and CD_3Br.[1]

THERMODYNAMIC PROPERTIES

The heat content, free energy, entropy, and heat capacity at constant pressure for CH_2DBr and CHD_2Br with a rigid rotator, harmonic oscillator approximation for the ideal gaseous state at 1 atmos pressure, were calculated for 12 temperatures in the 100 to 1000°K range.

[4] E. B. Wilson, Jr., J. Chem. Phys. **7**, 1047 (1939); **9**, 76 (1941).
[5] Weber, Meister, and Cleveland, J. Chem. Phys. **21**, 930 (1953).

TABLE V. Heat content, free energy, entropy, and heat capacity for CH_2DBr for the ideal gaseous state at 1 atmos pressure.[a]

T	$(H^0-E_0^0)/T$	$-(F^0-E_0^0)/T$	S^0	C_p^0
100	7.95	43.97	51.92	7.99
200	8.14	49.52	57.66	8.91
273.16	8.51	52.11	60.62	10.19
298.16	8.67	52.86	61.53	10.67
300	8.68	52.91	61.60	10.70
400	9.42	55.51	64.93	12.58
500	10.23	57.70	67.92	14.27
600	11.03	59.64	70.66	15.71
700	11.79	61.39	73.18	16.94
800	12.50	63.01	75.51	18.00
900	13.16	64.53	77.69	18.91
1000	13.78	65.94	79.73	19.70

[a] In this and the next table, T is in °K and the other quantities are in cal deg^{-1} $mole^{-1}$.

TABLE VI. Heat content, free energy, entropy, and heat capacity for CHD_2Br for the ideal gaseous state at 1 atmos pressure.

T	$(H^0-E_0^0)/T$	$-(F^0-E_0^0)/T$	S^0	C_p^0
100	7.95	44.38	52.33	8.00
200	8.22	49.94	58.17	9.27
273.16	8.71	52.57	61.28	10.79
298.16	8.90	53.34	62.25	11.33
300	8.92	53.40	62.32	11.36
400	9.78	56.08	65.86	13.35
500	10.68	58.36	69.04	15.05
600	11.63	60.38	71.91	16.49
700	12.32	62.22	74.54	17.72
800	13.07	63.91	76.98	18.76
900	13.75	65.49	79.24	19.65
1000	14.38	66.97	81.36	20.41

The values used for the bond distances, products of inertia, and symmetry numbers are given in Table III. The values used for the fundamentals were the observed values of the wave numbers (fundamentals) listed in Table IV. In the three instances where there are no observed values the calculated values were used. The thermodynamic functions so obtained are listed in Tables V and VI.

ACKNOWLEDGMENTS

This work was part of a research program which has been aided by a contract with the Office of Ordnance Research, U. S. Army; and by grants from the Research Corporation, the American Academy of Arts and Sciences, and the Socony-Vacuum Laboratories. The author and his associates is thankful for this assistance.

Substituted Methanes. XXV. Potential Constants and Calculated Thermodynamic Properties of Dibromofluoromethane*

HIROMU MURATA,† ANN PALM, AND ARNOLD G. MEISTER
Spectroscopy Laboratory,‡ Department of Physics, Illinois Institute of Technology, Chicago 16, Illinois
(Received July 30, 1954)

On the basis of previous Raman data, a reasonable set of potential constants was calculated for $CHFBr_2$ by the Wilson method, assuming a most general quadratic potential energy function. The thermodynamic properties—heat content, free energy, entropy, and heat capacity—for the ideal gaseous state at 1 atmos pressure were computed for 12 temperatures from 100 to 1000°K.

INTRODUCTION

RAMAN displacements and relative intensities have been reported by Glockler and Leader,[1] while Delwaulle and Francois[2] also determined quantitatively the polarization state of the Raman lines with the exception of the one associated with the C—H stretching vibration whose depolarization factor was estimated. Heat capacities for three temperatures have been calculated by a semi-empirical method,[3,4] and more recently Gelles and Pitzer[5] computed the heat capacity, heat content, free energy and entropy.

NORMAL COORDINATE TREATMENT

Since the $CHFBr_2$ molecule possesses a C_s symmetry, its nine fundamentals consisting of $6a'$ and $3a''$ type vibrations, are both infrared and Raman active. A normal coordinate treatment had not been carried out for the molecule, so that it seemed desirable to undertake such an investigation. On the basis of the observed fundamentals given in Table I, a set of potential constants were determined by the Wilson FG matrix method and the use of a potential energy function that contained all second degree terms. The symmetry coordinates and the notation for the potential constants have been described in detail in previous publications from this laboratory.[6,7] Initially, the potential constants were transferred from such molecules as $CHClBr_2$,[8] $CHBrF_2$,[9] and $CHBrCl_2$.[6] After several modifications, a set of potential constants (see Table II) was obtained that afforded a better than 2 percent agreement between the observed and calculated wave numbers as shown in Table I. It was difficult to attain a closer agreement, in particular for ν_4 and ν_5, since the diagonal F matrix elements associated with these fundamentals affected both wave numbers.

TABLE I. Observed and calculated wave numbers of the fundamentals of liquid $CHFBr_2$.

Raman: Delwaulle and Francois $\Delta\nu$	I	ρ	Raman: Glockler and Leader $\Delta\nu$	I	Probable value	ν_c	Assignment	Type
172	s	0.53	171.4	10	171	174	ν_6	a'
296	m	6/7	296.5	5	296	297	ν_9	a''
359	s	0.3	359.0	9	359	353	ν_5	a'
620	s	0.2	620.4	10	620	611	ν_4	a'
704	m	6/7	704.9	4	704	703	ν_8	a''
1063	w	0.6	1064.0	2	1064	1065	ν_3	a'
1171	w	0.8	1169.6	1	1170	1170	ν_7	a''
1295	m	0.4	1293.2	6	1294	1296	ν_2	a'
3015	s	p	3017.2	6	3016	3017	ν_1	a'

$\Delta\nu$ is the Raman displacement in cm^{-1} (K); I is the estimated relative intensity; s=strong, m=medium, w=weak; ν_c is the calculated wave number in cm^{-1} (K); ρ=depolarization factor; p=polarized.

TABLE II. Potential constants for $CHFBr_2$.[a]

Constant	Value	Constant	Value
f_b	2.9467[b]	$f_f{}^{bb}$	−0.24933
f_f	5.9558	$f_f{}^{bh}$	−0.17433
f_h	5.0428	$f_f{}^{fh}$	0.44000
f_{bf}	0.85000	$f_h{}^{bb}$	0.15001
f_{bh}	0.59044	$f_h{}^{bf}$	0.00000
f_{fh}	1.0200	$f_h{}^{bh}$	0.23250
f_{bb}	1.2726	$f_h{}^{fh}$	0.30001
$f_b{}^b$	0.47827	$f_{bb}{}^{bf}$	0.12500
$f_b{}^f$	0.65000	$f_{bf}{}^{b'f}$	−0.21710
$f_b{}^h$	0.05890	$f_{bf}{}^{bh}$	−0.01342
$f_f{}^h$	0.25305	$f_{bf}{}^{fh}$	−0.07539
$f_b{}^{bf}$	0.30998	$f_{bh}{}^{b'b}$	−0.03933
$f_b{}^{b'f}$	−0.11000	$f_{bh}{}^{b'h}$	−0.01853
$f_b{}^{bb}$	0.54639	$f_{bh}{}^{fh}$	0.11181
$f_b{}^{bh}$	0.23026	$f_{bh}{}^{b'f}$	−0.11342
$f_b{}^{fh}$	−0.19444	$f_{fh}{}^{bb}$	0.00371
$f_b{}^{b'h}$	−0.18144		
$f_f{}^{bf}$	0.24732		

[a] Bond stretching constants are in md/A; bond-angle interaction constants are in md/rad; and angle, and angle-angle interaction constants, are in md A/rad².
[b] The use of 5 significant figures is not justified but, they are retained in order to secure internal consistency in the calculations.

THERMODYNAMIC PROPERTIES

The heat content, free energy, entropy, and heat capacity at constant pressure were calculated for 12

* Presented in part at the Symposium on Molecular Structure and Spectroscopy, The Ohio State University, Columbus, Ohio, June 1954.
† Present address: Osaka Municipal Technical Research Institute, Osaka, Japan.
‡ Publication No. 108.
[1] G. Glockler and G. F. Leader, J. Chem. Phys. **8**, 699 (1940).
[2] M. L. Delwaulle and F. Francois, *Contribution to the Study of Molecular Structure* (Maison Desoer, Liège, Belgium, 1947–48), p. 119.
[3] G. Glockler and W. E. Edgell, J. Chem. Phys. **9**, 527 (1941).
[4] G. Glockler and W. E. Edgell, Ind. Eng. Chem. **34**, 532 (1942).
[5] E. Gelles and K. S. Pitzer, J. Am. Chem. Soc. **75**, 5259 (1953).
[6] Weber, Meister, and Cleveland, J. Chem. Phys. **21**, 930 (1953).
[7] Davis, Cleveland, and Meister, J. Chem. Phys. **20**, 454 (1952).
[8] Pontarelli, Meister, Cleveland, Voelz, Bernstein, and Sherman, J. Chem. Phys. **20**, 1949 (1952).
[9] Palm, Voelz, and Meister, J. Chem. Phys. **23**, 726 (1955).

temperatures from 100–1000°K using the probable values of the observed wave numbers listed in Table I. Except for the values at 400°K given by Gelles and Pitzer,[5] the present results were found to be in good agreement with theirs and will not be repeated. However, at 400°K the values of the heat content, free energy, entropy and heat capacity were found to be 12.83, 67.69, 80.51, and 17.57 cal deg^{-1} $mole^{-1}$, respectively. For the same temperature Pitzer and Gelles[5] give the values 12.96, 67.79, 80.75, and 17.87 cal deg^{-1} $mole^{-1}$, respectively. For the entropy and heat capacity the difference between the two sets of values is greater than it should be for two independent investigations, and when these two thermodynamic functions are plotted against the absolute temperature a smooth curve results in each case for the results of the present investigation, while the point at 400°K for the Gelles and Pitzer data departs considerably from the curve drawn with their data. Hence, it appears their results are in error at this temperature. A value of 1.723×10^{7} (awu A^2) was used for the product of the moments of inertia ($I_A I_B I_C$) in the present investigation.

ACKNOWLEDGMENTS

This work was part of a research program which has been aided by a contract with the Office of Ordnance Research, U. S. Army; and by grants from the Research Corporation, the American Academy of Arts and Sciences, and the Socony-Vacuum Laboratories. The authors are thankful for this assistance.

THE JOURNAL OF CHEMICAL PHYSICS VOLUME 23, NUMBER 4 APRIL, 1955

Cl^{35} Pure Quadrupole Resonances in Acid Chlorides and Chlorates*

P. J. Bray
Department of Physics, Rensselaer Polytechnic Institute, Troy, New York
(Received August 19, 1954)

The pure quadrupole resonances of Cl^{35} in acid chlorides of some aliphatic dicarboxylic acids have been observed. No resonances have been found in acid chlorides of aliphatic monocarboxylic acids which retain the unsubstituted CH_3 configuration at the chain end not occupied by the COCl group. This absence of resonances is attributed to possible randomness in the crystal structure or thermally activated low-frequency reorientations of groups within the molecule.

Resonances have also been measured in several chlorates, sulfuryl chloride, iodine monochloride, iodine trichloride, and selenium tetrachloride. Structural and bonding discussions are given for the latter two compounds.

PURE quadrupole resonances of Cl^{35} have been observed in a number of acid chlorides and metallic chlorates and several other interesting compounds. The resonances were detected with a self-quenching superregenerative oscillator, amplified by a Tektronix type 122 preamplifier and displayed on an oscilloscope. Table I contains the frequencies measured at liquid nitrogen temperature.

The acyl chlorine values of Table I are relisted in Table II together with other published values. Attempts to locate the Cl^{35} resonance in acetyl chloride have proved unsuccessful so far. The resonance is predicted between 27.5 and 28 Mc/sec on the basis of the known acetyl bromide resonance frequencies[1] and the ratio 6.5 of Br^{81} resonances to Cl^{35} resonances in such similar compounds as observed by Zeldes and Livingston.[2] The factor 6.5 is found to hold in the ratio of Br^{81} to Cl^{35} resonances in benzoyl bromide[1] and benzoyl chloride.[3]

The upper four resonances in dichloroacetyl chloride should be compared with the 37.979 and 38.807 Mc/sec values measured by Allen[4] for dichloroacetic acid. Similar comparison for chloroacetyl chloride can be made with the 36.131 and 36.429 Mc/sec values[4] in chloroacetic acid. It is apparent that there are two nonequivalent environments for dichloroacetyl chloride molecules in the crystal. This compound will not crystallize as the temperature is lowered but solidifies instead into a transparent glass-like material. On melting, nuclei of crystallization (which are translucent) appear suddenly as the last glassy material disappears. If the temperature is immediately lowered, crystal growth occurs from these seeds. A number of other compounds have exhibited this behavior. Many others, unfortunately, simply supercool to the amorphous glass and melt completely without the appearance of seed crystals.

In general, the search for acyl chlorine resonances has met with surprising lack of success. Table III contains compounds in which no resonance has been observed to date in the frequency regions indicated. Further, more careful searches over wider frequency ranges are in progress on some of the compounds.

* Research supported by grants from the National Science Foundation and the Rensselaer Polytechnic Institute Research Grants Committee.
[1] P. J. Bray, J. Chem. Phys. **22**, 1787 (1954).
[2] H. Zeldes and R. Livingston, J. Chem. Phys. **21**, 1418 (1953).
[3] D. W. McCall and H. S. Gutowsky, J. Chem. Phys. **21**, 1300 (1953).
[4] H. C. Allen, J. Am. Chem. Soc. **74**, 6074 (1952).

TABLE I. Cl^{35} pure quadrupole resonances at liquid nitrogen temperature.

Compound	Frequency (megacycles per second)	Approximate signal-to-noise ratio
dichloroacetyl chloride[a]	39.386±0.017	3
$CHCl_2COCl$	39.189±0.017	3
	38.521±0.017	2 or 3
	38.353±0.017	2 or 3
	32.962±0.017	2 or 3
	32.147±0.017	2 or 3
chloroacetyl chloride	37.517±0.004	2 to 3
$CH_2ClCOCl$	30.437±0.004	<2
oxalyl chloride	33.621±0.002	12 to 15
ClCOCOCl		
succinyl chloride	30.217±0.002	12 to 15
$ClCO(CH_2)_2COCl$		
adipyl chloride[b]	28.978±0.002	2 to 20
$ClCO(CH_2)_4COCl$		
sebacyl chloride[c]	29.118±0.002	2
$ClCO(CH_2)_8COCl$		
fumaryl chloride[c]	30.970±0.002	5 to 6
ClCOCH=CHCOCl	30.380±0.002	5 to 6
2-furoyl chloride	30.726±0.004	3 or 4
OCH=CHCH=CCOCl		
2,4-dichlorobenzoyl	37.145±0.004	3
chloride[c]	37.038±0.004	3
$Cl_2C_6H_3COCl$	35.923±0.004	2
	35.834−0.004	2
	31.086±0.004	1½
	31.039±0.004	1½
copper chlorate[c]	30.064±0.002	13 to 16
$Cu(ClO_3)_2\cdot 6H_2O$		
magnesium chlorate[c]	29.885±0.002	3
$Mg(ClO_3)_2\cdot 6H_2O$		
strontium chlorate[c]	29.869±0.002	6
$Sr(ClO_3)_2$		
β-iodine monochloride	37.202±0.002	3 or 4
ICl		
iodine trichloride[d]	35.680±0.004	2½
ICl_3 (I_2Cl_6)	33.916±0.004	1½
selenium tetrachloride	36.794±0.004	<2
$SeCl_4$	36.171±0.004	2
	35.696±0.004	2
	35.041±0.004	2 to 3
	34.685±0.004	<2
	34.534±0.004	3
sulfuryl chloride[a]	37.822±0.017	4 or 5
SO_2Cl_2	37.613±0.017	4 or 5
dichlorodiphenyl-	39.039±0.004	2 to 3
trichloroethane	38.814±0.004	2 to 3
	38.487±0.004	2 to 3
(DDT)	34.977±0.004	2
$CCl_3CH(C_6H_4Cl)_2$	34.868−0.004	2

[a] Resonance appears as a series of humps on the oscilloscope so that location of center pip is uncertain to half of the quench frequency.
[b] Resonance became progressively smaller as compound was exposed to air and became brown in color.
[c] Preliminary measurements made by D. Esteva.
[d] This measurement made in conjunction with Dr. G. D. Watkins.

During the investigations, care was taken to minimize the extent of reaction of the acid chlorides with water vapor. All compounds were placed in vials in liquid nitrogen shortly after opening their containers which were sealed glass ampoules in many cases. Investigations for quadrupole resonances were carried out within a short time after the freezing.

It is interesting to note that quadrupole resonances have been found only in those paraffins with COCl groups on both ends of the chain.[5] In compounds with the methyl group left at one end of the chain, the COCl group will be subject to perturbing fields from the end CH_3 groups on neighboring chains. If the crystal structure is insensitive to the orientation of the chains as far as the COCl and CH_3 ends are concerned, the COCl groups may see random numbers of COCl and CH_3 groups on the nearest chain ends. Such randomness in the environment may broaden the resonance beyond the sensitivity of normal detection methods.

The method suggested by Dean[6] might be used in this case. If a small percentage of the COCl substituted paraffin can be incorporated in the crystal form of the unsubstituted paraffin, all COCl groups should see CH_3 groups almost exclusively and the weak resonance can be detected by lock-in amplifier and recorder techniques.

An alternative explanation for the lack of observable acyl chlorine resonances in the substituted paraffins may involve rotation of the CH_3 groups at low frequencies about the end C−C axis in the chains. Such reorientations at rates of several kilocycles/sec have been found at liquid nitrogen temperature in *n*-pentane and *n*-hexane by Rushworth.[7] If a broadening mechanism involving low-frequency CH_3 group rotation is active, it may also explain the failure to detect quadrupole resonances in the chloro- and bromo-toluenes.

Investigation of these substituted paraffins should be made at liquid helium temperature. In at least some of them, the methyl group rotation (if present) should be frozen in at 4°K. In other cases, if the melting point is sufficiently high, investigation at a temperature high enough to assure rotation at a frequency which is large compared to the line width expected for the rigid lattice structure might yield a resonance.

The resonance frequencies for three chlorates appearing in Table I should be compared with the values[8,9] of 30.632 Mc/sec in $NaClO_3$, 28.953 Mc/sec in $KClO_3$, and 29.922 Mc/sec in $Ba(ClO_3)_2\cdot H_2O$. Extensive search has not as yet detected the Cl^{35} resonance in silver chlorate though the Br resonances in silver bromate are known.[10] The silver chlorate sample used may be impure.

The I resonances in the interhalogen compounds ICl and ICl_3 have been measured.[11,12] Although the location of ICl molecules in the unit cell of rhombic β-ICl is not known, one might anticipate two Cl^{35} resonances with a separation of 200 kc/sec or so on the basis of the two I^{127} lines with a separation of about 2.6 Mc/sec found

[5] In the case of the acetyl chlorides, resonances are found when one, two, or three chlorine atoms are substituted for hydrogens. No resonance appears in unsubstituted acetyl chloride.
[6] C. Dean, thesis, Harvard University, 1952.
[7] F. A. Rushworth, Proc. Roy. Soc. (London) **A222**, 526 (1954).
[8] Wang, Townes, Schawlow, and Holden, Phys. Rev. **86**, 809 (1952).
[9] P. J. Bray and P. J. Ring, J. Chem. Phys. **21**, 2226 (1953).
[10] Shimomura, Kushida, Inoue, and Imaeda, J. Chem. Phys. **22**, 350 (1954).
[11] H. G. Dehmelt, Z. Physik **130**, 356 (1951).
[12] G. D. Watkins (private communication).

in this compound by Dehmelt.[11] The Cl^{35} resonance observed does not have a very sharp line shape but appears to be only a single line. Since one of the I^{127} lines is very weak in comparison to the other, further search for a weak second Cl^{35} line is in progress. No resonance is observed in cubic α-ICl (MP=27.2°C) which is achieved by slow crystallization of ICl in a refrigerator. The β-ICl form (MP=13.9°C) is achieved by rapid crystallization over liquid nitrogen in a Dewar.

Recent x-ray analysis[13] shows that crystalline triclinic ICl_3 actually is constructed of planar I_2Cl_6 molecules. In each molecule, the six chlorine atoms are divided into two noticeably different groups positionwise with respect to the iodine atoms. There are four chlorine atoms in one group and two in the other. The method of superposition of layers in the crystal apparently distorts each molecule slightly so that each of these groups is further split in two though not by much. The two observed resonances are both weak and tend to appear as a series of humps rather than sharp lines possibly as a result of smearing arising from unresolvable splitting in the two major groups. The lower frequency line is definitely weaker.

TABLE II. Resonance frequencies of Cl^{35} in the COCl group.

Compound	Frequency	Structural formula
ethyl chloroformate[a]	33.858	$Cl-C(=O)-O-C_2H_5$
trichloroacetyl chloride[b]	33.721	$Cl-C(=O)-CCl_3$
oxalyl chloride	33.621	$Cl-C(=O)-C(=O)-Cl$
dichloroacetyl chloride	32.962 32.147	$Cl-C(=O)-CHCl_2$
diethylcarbamyl chloride[c]	31.877	$Cl-C(=O)-N(C_2H_5)-C_2H_5$
dimethylcarbamyl chloride[c]	31.8	$Cl-C(=O)-N(CH_3)-CH_3$
2,4-dichlorobenzoyl chloride	31.086 31.039	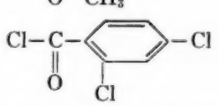
fumaryl chloride	30.970 30.380	$Cl-C(=O)-C(H)=C(H)-C(=O)-Cl$
2-furoyl chloride	30.726	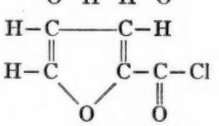
chloroacetyl chloride	30.437	$Cl-C(=O)-CH_2Cl$
succinyl chloride	30.217	$Cl-C(=O)-(CH_2)_2-C(=O)-Cl$
benzoyl chloride[c]	29.93	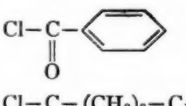
sebacyl chloride	29.118	$Cl-C(=O)-(CH_2)_8-C(=O)-Cl$
adipyl chloride	28.978	$Cl-C(=O)-(CH_2)_4-C(=O)-Cl$

[a] T. L. Weatherly and Q. Williams, J. Chem. Phys. **22**, 958 (1954).
[b] See reference 4 in text.
[c] See reference 3 in text.

[13] K. H. Boswijk and E. H. Wiebenga, Acta Cryst. **7**, 417 (1954).

TABLE III. Compounds in which investigation has failed to detect Cl^{35} quadrupole resonance.

Compound		Frequency range searched (Mc/sec)
propionyl chloride	CH_3CH_2COCl	27–41
n-caproyl chloride	$CH_3(CH_2)_4COCl$	24–36
caprylyl chloride	$CH_3(CH_2)_6COCl$	25–36
pelargonyl chloride	$CH_3(CH_2)_7COCl$	24–36
lauroyl chloride	$CH_3(CH_2)_{10}COCl$	24–40
myristoyl chloride	$CH_3(CH_2)_{12}COCl$	24–36
palmitoyl chloride	$CH_3(CH_2)_{14}COCl$	24–36
iso-valeryl chloride	$(CH_3)CHCH_2COCl$	24–36
iso-caproyl chloride	$(CH_3)_2CH(CH_2)_2COCl$	24–36
α-ethyl-*n*-butyryl chloride	$CH_3CH_2CH(C_2H_5)COCl$	25–35
phenylacetyl chloride	$C_6H_5CH_2COCl$	24–36
hydrocinnamoyl chloride	$C_6H_5CH_2CH_2COCl$	25–35
phenoxyacetyl chloride	$C_6H_5OCH_2COCl$	24–36
α-phenoxypropionyl chloride	$C_6H_5OCH(CH_3)COCl$	24–36
m-nitrobenzoyl chloride	$NO_2C_6H_4COCl$	27–40
p-nitrobenzoyl chloride	$NO_2C_6H_4COCl$	27–40
3,5-dinitrobenzoyl chloride	$(NO_2)_2C_6H_3COCl$	27–40
o-chlorobenzoyl chloride	ClC_6H_4COCl	27–40
3,4-dichlorobenzoyl chloride	$Cl_2C_6H_3COCl$	24–36
m-bromobenzoyl chloride	BrC_6H_4COCl	28–40
anisoyl chloride	$CH_3OC_6H_4COCl$	24–36
o-ethoxybenzoyl chloride	$C_2H_5OC_6H_4COCl$	24–40
p-ethoxybenzoyl chloride	$C_2H_5OC_6H_4COCl$	27–40
p-*n*-amoxybenzoyl chloride	$CH_3(CH_2)_4OC_6H_4COCl$	27–40
diphenylcarbamyl chloride	$(C_6H_5)_2NCOCl$	27–40
crotonyl chloride	$CH_3CH=CHCOCl$	24–36
1-naphthoyl chloride	$C_{10}H_7COCl$	24–36

The six resonances in $SeCl_4$ are not surprising in view of the four to sixteen resonances found in tetrachlorides of C, Ge, Si, Sn, and Ti.[14,15] Noting the very close spacing of lines observed by Livingston with a regenerative oscillator,[14] it is very possible that there are actually more than six lines in $SeCl_4$. Measurement of the weak resonances in this compound is very difficult, and at times the observer thought there were as many as eight resonances. Lines separated by less than the quench frequency (30 to 40 kc/sec) could probably not be resolved with the present super-regenerative apparatus. A regenerative oscillator is under construction for observation of such closely spaced resonances as those in selenium tetrachloride and 2,4-dichlorobenzoyl chloride.

Robinson, Dehmelt, and Gordy[16] have constructed a plot for Group IV tetrahalides of $1-|U_p|$ *versus* the

[14] R. Livingston, J. Phys. Chem. **57**, 496 (1953).
[15] H. G. Dehmelt, J. Chem. Phys. **21**, 380 (1953).
[16] Robinson, Dehmelt, and Gordy, J. Chem. Phys. **22**, 511 (1954).

electronegativity difference of the bonded atoms. U_p is the number of unbalanced p electrons on the halogen and is given by $|U_p| = |(eqQ)_{\text{molecule}}|/2|(eqQ)_{\text{atom}}|$. For chlorine quadrupole resonances, $|(eqQ)_{\text{molecule}}|$ is taken as twice the observed resonance frequency. If the value $1-|U_p| = 0.33$ to 0.37 for $SeCl_4$ is plotted against 0.7[17] or 0.6[18] as the Se—Cl electronegativity difference, the point falls on the line of points[16] of C, Ge, and Sn tetrahalides or deviates toward the silicon tetrahalide line of points which is different owing to the appreciable double-bond character in these compounds.[19]

Selenium, a third row element, would not be expected to show appreciable double-bond character in $SeCl_4$. One can obtain some idea of the double-bond character in the manner outlined by Mays and Dailey.[20] Using the published data[21] for the Se—Cl bond length in $SeCl_4$ and the single-bond and double-bond covalent radii[18] for Se and Cl, one finds for $SeCl_4$ approximately 21 percent ionic character, 73 percent single-bond character, and 6 percent double-bond character. This calculation assumes 15 percent s-p hybridization in the bonds.

In this comparison of $SeCl_4$ and Group IV tetrahalides, it must be remembered that selenium differs from the Group IV elements by lacking two p-shell electrons rather than by having two. Furthermore, published x-ray data[21] indicate that the tetrahedral structure model is probably only approximate in $SeCl_4$. It is possible then that the agreement of the $SeCl_4$ data with the trend in C, Ge, and Sn tetrahalides is fortuitous.

The resonances in sulfuryl chloride (distorted tetrahedral molecule)[22,23] can be compared with those in thionyl chloride[14] ($SOCl_2$, pyramidal configuration)[23] and in substituted benzenesulfonyl chlorides[3,24] ($C_6H_5SO_2Cl$).

The higher frequency group of lines in DDT presumably originates in the CCl_3 group since all reported resonances of Cl^{35} in the CCl_3 group in compounds containing this configuration fall in the 38 to 41 Mc/sec region at liquid nitrogen temperature. In particular, chloral hydrate $CCl_3CH(OH)_2$ also displays three resonances between 38 and 40 Mc/sec at this temperature.[4] Similarly, most singly substituted chlorobenzenes (with the exception of some *ortho* substituted compounds) give rise to Cl^{35} resonances between 34 and 36 Mc/sec at liquid nitrogen temperature. The two lower frequency resonances in DDT are then very probably due to the phenyl group chlorines.

The appearance of a single resonance in oxalyl chloride apparently confirms the presence of only one isomer in the crystalline state of the compound.[25] If both the *cis*-form and *trans*-form were present, two resonances should appear since the intra-molecular chlorine separations would differ in the two isomers. Nuclear magnetic resonance investigation of liquid oxalyl chloride might determine whether both isomers are present in the liquid state since the diamagnetic shielding of the chlorine nuclei in the two isomers may differ enough to produce an observable chemical splitting.

Most of the COCl substituted paraffins in Table III were investigated by Miss Dinorah Esteva. Further acknowledgment of her aid is noted in Table I.

I have benefited from discussions with Dr. S. C. Bunce of the Rensselaer Polytechnic Institute Chemistry Department and Dr. G. D. Watkins of the General Electric Research Laboratory; and equally helpful was correspondence with Dr. R. Bersohn, Department of Chemistry, Cornell University, and Dr. R. E. Kagarise, Naval Research Laboratory, Washington, D. C.

[17] M. Haissinsky, J. phys. radium **7**, 7 (1946).
[18] L. Pauling, *The Nature of the Chemical Bond* (Cornell University Press, Ithaca, 1944).
[19] A. L. Schawlow, J. Chem. Phys. **22**, 1211 (1954).
[20] J. Mays and B. P. Dailey, J. Chem. Phys. **20**, 1695 (1952).
[21] P. W. Allen and L. E. Sutton, Acta Cryst. **3**, 76 (1950).
[22] A. F. Wells, *Structural Inorganic Chemistry* (Oxford University Press, New York, 1950).
[23] D. E. Martz and R. T. Lagemann, J. Chem. Phys. **22**, 1193 (1954).
[24] P. J. Bray and D. Esteva, J. Chem. Phys. **22**, 570 (1954).
[25] R. E. Kagarise, J. Chem. Phys. **21**, 1615 (1953).

On the Helical Configuration of a Polymer Chain

TAKEHIKO SHIMANOUCHI AND SAN-ICHIRO MIZUSHIMA
Chemical Laboratory, Faculty of Science, Tokyo University, Hongo, Tokyo, Japan
(Received August 3, 1954)

A mathematical expression for the helical configuration of a polymer chain has been derived as a function of the bond lengths, bond angles, and internal rotation angles. The result of the calculation has been applied to the determination of stable configurations of several polymer chains.

I. INTRODUCTION

A GENERAL interest has been aroused in helical configurations of chain molecules in the field of high polymers, especially of proteins,[1] nucleic acids,[2] starches,[3] etc. It would, therefore, be interesting to derive a mathematical expression of chain configurations as a function of bond lengths, bond angles, and internal rotation angles, since in setting up a polymer model we can try with different values of these parameters lying in a range of values predicted from the study of simpler molecules as a structural unit of the corresponding polymer. The last parameter is concerned with the internal rotation about a single bond as axis, which has been considered to be free in many mathematical papers dealing with various problems of polymer chains. However, considerable evidence has been accumulated to indicate that the barrier to internal rotation has a height of few kilocalories per mole or more and the chain tends to have a configuration corresponding to the minima of the hindering potential.[4] Therefore, if the configuration does not correspond to these minima, the internal forces, such as internal hydrogen bonds, should be strong enough to compensate the excess of energy arising from the hindering potential to internal rotation.

We have already published a note[5] dealing with a special case of this problem. Since then an interesting paper by Low and Grenville-Wells[6] on the mathematical treatment of polypeptide configurations became available to us. However, this paper did not take the internal rotation angle as a parameter and, furthermore, it referred to a special case of polypeptides as our previous note,[5] we, therefore, would like to discuss a more general mathematical formulation in the present communication.

[1] See, for example, a discussion on the structure of proteins Proc. Roy. Soc. (London) **B141**, 1–103 (1953).
[2] J. D. Watson and F. H. C. Crick, Nature **171**, 737 (1953).
[3] R. E. Rundle and R. R. Baldwin, J. Am. Chem. Soc. **65**, 554 (1943); R. E. Rundle and D. French, *ibid.* 1707 (1943).
[4] As to the summary of this work, see, for example Mizushima, Morino, and Shimanouchi, J. Phys. Chem. **56**, 324 (1952); S. Mizushima, *Structure of Molecules and Internal Rotation* (Academic Press, Inc., New York, 1954).
[5] T. Shimanouchi and S. Mizushima, J. Chem. Soc. Japan **74**, 755 (1953).
[6] B. W. Low and H. J. Grenville-Wells, Proc. Natl. Acad. Sci. **39**, 785 (1953).

II. DERIVATION OF THE GENERAL EXPRESSION

Suppose that the skeleton of a polymer chain has a configuration as shown in Fig. 1 and let the bond length, bond angle, and internal rotation angle be denoted by r_{ij}, ϕ_{ijk}, and τ_{ijkl}, respectively, where i, j, k, and l are any four consecutive numbers specifying skeletal atoms. These atoms lie on a helix which can be described by three coordinates, ρ_i, θ_{ij}, and d_{ij}, where ρ_i is the distance of the ith atom from the axis of the helix and θ_{ij} and d_{ij} are, respectively, the angle of rotation about the axis and the translation along the axis on passing from the ith atom to the jth. (See Fig. 2.)

The mathematical treatment is simplest, if the skeleton contains only one kind of atom where the values of r, ϕ, τ, ρ, θ, and d are all independent of subscripts. It is, however, evident that even for two or more than two kinds of skeletal atoms, a similar treatment can be made, if we take account of a specific atom in the structural unit of the polymer chain. We shall first obtain the expression of ρ, θ, and d as a function of r, ϕ, and τ in the simplest case.

Let us choose sets of right-handed rectangular coordinate systems in the following way (see Fig. 3). The origin of the coordinate system i coincides with the position of the ith atom with its X_i axis on $r_{i,i+1}$ or the

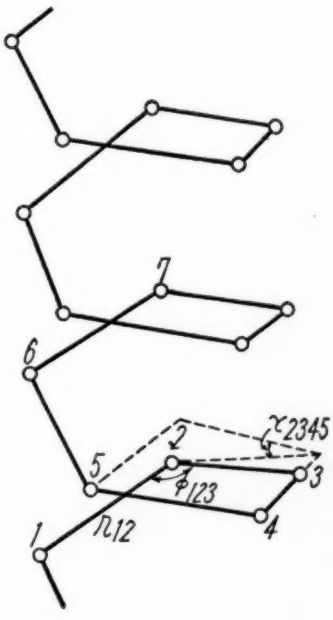

FIG. 1. Helix and internal coordinates.

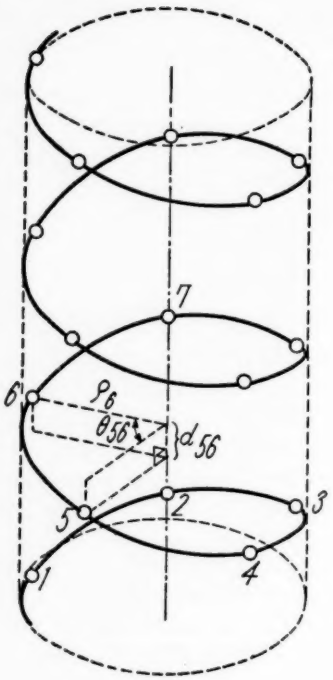

FIG. 2. Helix and cylindrical coordinates.

bond connecting the ith atom to the $i+1$th. The Y_i axis lies in the plane determined by the two bonds $r_{i,i+1}$ and $r_{i-1,i}$ in such a way that the angle between $r_{i-1,i}$ and the positive direction of Y_i is acute. The positive direction of Z_i axis is so taken as to make the coordinate system right-handed, as referred to in the foregoing. Then it can be shown (according to the calculation of Eyring[7]) that the transformation of the ith coordinates (X_i, Y_i, Z_i) into the $i-1$th $(X_{i-1}, Y_{i-1}, Z_{i-1})$ is expressed as

$$\mathbf{X}_{i-1}=\mathbf{A}\mathbf{X}_i+\mathbf{B}, \tag{1}$$

where $\mathbf{X}_i$ is a column vector with elements X_i, Y_i, and Z_i,

$$\mathbf{A}=\begin{pmatrix} -\cos\phi & -\sin\phi & 0 \\ \sin\phi\cos\tau & -\cos\phi\cos\tau & -\sin\tau \\ \sin\phi\sin\tau & -\cos\phi\sin\tau & \cos\tau \end{pmatrix} \tag{2}$$

and

$$\mathbf{B}=\begin{pmatrix} r \\ 0 \\ 0 \end{pmatrix}. \tag{3}$$

Let us choose other sets of right-handed rectangular coordinate systems (ξ_i, η_i, ζ_i) as follows (see Fig. 3). The origin of the ith coordinates coincides with the foot of the perpendicular to the axis of the helix drawn from the ith atom, the ξ_i axis being on this perpendicular with its positive direction pointing towards the ith atom. The ζ_i axis lies on the axis of the helix and the η_i axis is perpendicular to both ξ_i and ζ_i. Then the transformation of the ith coordinates (ξ_i, η_i, ζ_i) into the $i-1$th can be expressed as

$$\xi_{i-1}=\mathbf{N}\xi_i+\mathbf{L}, \tag{4}$$

where ξ_i is a column vector with elements ξ_i, η_i, and ζ_i,

$$\mathbf{N}=\begin{pmatrix} \cos\theta & -\sin\theta & 0 \\ \sin\theta & \cos\theta & 0 \\ 0 & 0 & 1 \end{pmatrix}, \tag{5}$$

and

$$\mathbf{L}=\begin{pmatrix} 0 \\ 0 \\ d \end{pmatrix}. \tag{6}$$

Let us now discuss the relation between the two kinds of coordinate systems referred in the foregoing. The transformation of ξ_i into $\mathbf{X}_i$ can be calculated as

$$\mathbf{X}_i=\mathbf{T}(\xi_i+\mathbf{S}), \tag{7}$$

where

$$\mathbf{T}=\begin{pmatrix} t_{11} & t_{12} & t_{13} \\ t_{21} & t_{22} & t_{23} \\ t_{31} & t_{32} & t_{33} \end{pmatrix} \tag{8}$$

and

$$\mathbf{S}=\begin{pmatrix} -\rho \\ 0 \\ 0 \end{pmatrix}. \tag{9}$$

Here $\mathbf{T}$ is an orthogonal matrix whose elements are determined so as to make the three relations (1), (4), and (7) consistent.

From (1) and (7), we have

$$\mathbf{T}(\xi_{i-1}+\mathbf{S})=\mathbf{A}\mathbf{T}(\xi_i+\mathbf{S})+\mathbf{B}, \tag{10}$$

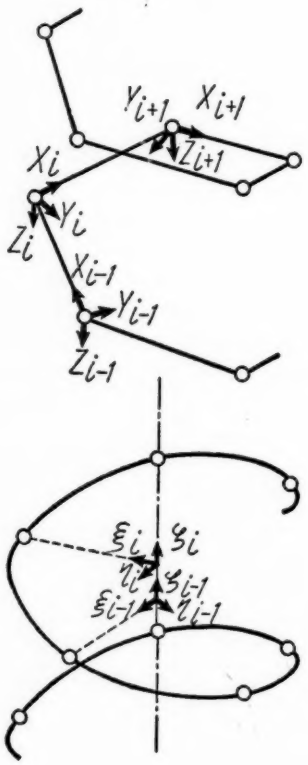

FIG. 3. The two sets of rectangular coordinate systems.

[7] H. Eyring, Phys. Rev. **39**, 746 (1932).

which can be rewritten as

$$\xi_{i-1}=\mathbf{T}^{-1}\mathbf{A}\mathbf{T}\xi_i+(\mathbf{T}^{-1}\mathbf{A}\mathbf{T}-\mathbf{E})\mathbf{S}+\mathbf{T}^{-1}\mathbf{B}, \quad (11)$$

where $\mathbf{E}$ is a unit matrix. This equation should be identical with Eq. (4) and, accordingly, we have

$$\mathbf{N}=\mathbf{T}^{-1}\mathbf{A}\mathbf{T} \quad (12)$$

$$\mathbf{L}=(\mathbf{T}^{-1}\mathbf{A}\mathbf{T}-\mathbf{E})\mathbf{S}+\mathbf{T}^{-1}\mathbf{B}. \quad (13)$$

We see from Eq. (12) that the orthogonal transformation applied to $\mathbf{A}$ gives $\mathbf{N}$ and, therefore, the sum of diagonal elements of these two matrices should be the same. Accordingly, we have from Eqs. (2) and (5)

$$1+2\cos\theta=-\cos\phi-\cos\phi\cos\tau+\cos\tau. \quad (14)$$

The final result is obtained by combining Eqs. (3), (6), (9), (13), and (14):

$$\cos\theta=\tfrac{1}{2}[-\cos\phi+\cos\tau-\cos\phi\cos\tau-1], \quad (15)$$

$$d^2=r^2(1-\cos\tau)(1-\cos\phi)/(3+\cos\phi-\cos\tau+\cos\phi\cos\tau), \quad (16)$$

$$\rho^2=2r^2(1+\cos\phi)/(3+\cos\phi-\cos\tau+\cos\phi\cos\tau)^2. \quad (17)$$

These three equations determine the configuration of the helix in terms of bond lengths r, bond angles ϕ, and internal rotation angles τ.

III. STABLE CONFIGURATIONS OF *n*-PARAFFINS AND POLYOXYMETHYLENE

Let us first apply the three expressions to the determination of stable configurations of long chain *n*-paraffins. The equilibrium τ values of *n*-paraffins have been shown to be 180° (*trans*) or about ±60° (*gauche*) by our spectroscopic measurement.[4]

For $\tau=180°$, Eq. (2) is reduced to

$$\mathbf{A}=\begin{bmatrix}-\cos\phi & -\sin\phi & 0\\ -\sin\phi & \cos\phi & 0\\ 0 & 0 & -1\end{bmatrix}$$

and from Eq. (15), we have

$$\theta=180°.$$

The corresponding configuration is the extended form in which all the molecules of solid *n*-paraffins have been shown to exist by our Raman measurement.[8]

For $\tau=60°$, we have

$$\mathbf{A}=\begin{bmatrix}-\cos\phi & -\sin\phi & 0\\ \frac{1}{2}\sin\phi & -\frac{1}{2}\cos\phi & -\frac{\sqrt{3}}{2}\\ \frac{\sqrt{3}}{2}\sin\phi & -\frac{\sqrt{3}}{2}\cos\phi & \frac{1}{2}\end{bmatrix}$$

[8] S. Mizushima and T. Shimanouchi, J. Am. Chem. Soc. **71**, 3411 (1949).

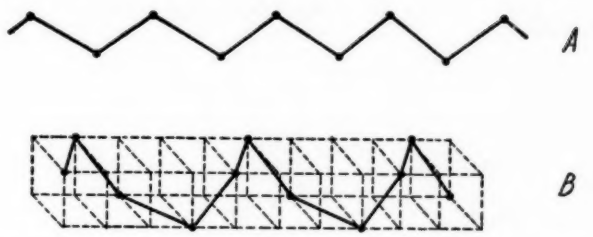

FIG. 4. The two configurations of *n*-paraffin and polyoxymethylene.

and Eqs. (15), (16), (17) become

$$\cos\theta=-(1+3\cos\phi)/4$$

$$d=\{(1-\cos\phi)/(5+3\cos\phi)\}^{\frac{1}{2}}r$$

$$\rho=2\sqrt{2}(1+\cos\phi)^{\frac{1}{2}}r/(5+3\cos\phi).$$

Assuming ϕ to be tetrahedral, we have

$$\theta=90°$$

$$d=\rho=r/\sqrt{3}.$$

The helix having these values of parameters is shown in Fig. 4B. Actually we have no corresponding example in the case of *n*-paraffins. However, polyoxymethylene has been shown to have a helical configuration with

$$\theta=80°$$

$$d=1.93\text{ A}.$$[9]

Assuming the C−O bond length to be 1.49 A, we have

$$r/\sqrt{3}=1.71\text{ A}.$$

Therefore, all the stable positions of internal rotation in polyoxymethylene can be concluded to be almost the *gauche*. This is in agreement with the experimental result obtained for $Cl-CH_2-O-CH_2-Cl$ which has a configuration similar to polyoxymethylene.[10]

IV. STABLE CONFIGURATIONS OF POLYPEPTIDE CHAIN

The polypeptide chain contains three kinds of internal rotation axes, −CO−NH−, −CHR−CO−, and −NH−CHR−, the corresponding azimuthal angle being designated by τ_1, τ_2, and τ_3, respectively. Further let us denote bond distances r_1, r_2, r_3 and bond angles ϕ_1, ϕ_2, ϕ_3 in the unit of the chain as shown in Fig. 5. Then the values of θ, d, and ρ of an α-carbon atom can be calculated similarly as above except for the expressions of A and B in Eqs. (2) and (3), which are changed to

$$\mathbf{A}=\mathbf{A}_3\mathbf{A}_1\mathbf{A}_2, \quad (18)$$

$$\mathbf{B}=\mathbf{A}_3\mathbf{A}_1\mathbf{B}_2+\mathbf{A}_3\mathbf{B}_1+\mathbf{B}_3, \quad (19)$$

[9] E. Sauter, Z. physik chem. **B21**, 186 (1933).

[10] M. Katayama and Y. Morino, Repts. Radiation Chem. Research Inst. **4**, 1 (1949).

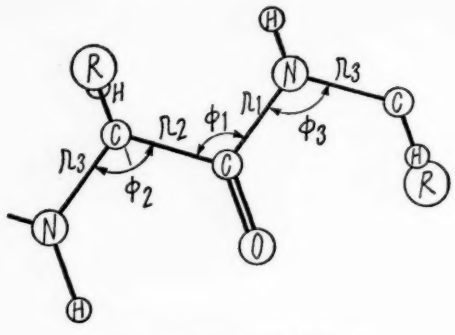

FIG. 5. The polypeptide chain.

where

$$\mathbf{A}_i=\begin{pmatrix} -\cos\phi_i & -\sin\phi_i & 0 \\ \sin\phi_i\cos\tau_i & -\cos\phi_i\cos\tau_i & -\sin\tau_i \\ \sin\phi_i\sin\tau_i & -\cos\phi_i\sin\tau_i & \cos\tau_i \end{pmatrix}, \quad (20)$$

$$\mathbf{B}_i=\begin{pmatrix} r_i \\ 0 \\ 0 \end{pmatrix}, \quad (21)$$

$i=1, 2, 3.$

With the relations (18) and (19) of **A** and **B** we have the expressions for **N** and **L** identical with Eqs. (12) and (13).

The equations for θ, d, and ρ referred to in our previous paper[5] can then be derived from Eqs. (15), (16), and (17) by denoting the elements of **A** and **B** as follows:

$$\mathbf{A}=\begin{pmatrix} a_{11} & a_{12} & a_{13} \\ a_{21} & a_{22} & a_{23} \\ a_{31} & a_{32} & a_{33} \end{pmatrix} \quad (22)$$

$$\mathbf{B}=\begin{pmatrix} b_1 \\ b_2 \\ b_3 \end{pmatrix}. \quad (23)$$

Then we have

$$\cos\theta=(a_{11}+a_{22}+a_{33}-1)/2, \quad (24)$$

$$d^2=[b_1(a_{13}+a_{31})+b_2(a_{23}+a_{32}) +b_3(a_{33}-a_{11}-a_{22}+1)]^2/(3-a_{11}-a_{22}-a_{33}) \times(a_{33}-a_{11}-a_{22}+1), \quad (25)$$

$$\rho^2=(b_1^2+b_2^2+b_3^2-d^2)/(3-a_{11}-a_{22}-a_{33}). \quad (26)$$

The helical configuration of a polypeptide chain is determined from Eqs. (24), (25), and (26), if we know the values of r, ϕ, and τ. The values of the former two parameters (or the bond lengths and bond angles) lie in a narrow range, but that of the last parameter can take two quite different values except for τ_1 or the azimuthal angle of internal rotation about $-CO-NH-$ axis which always take a value corresponding to the planar *trans* configuration of the peptide bond.[11] The equilibrium values of τ_2 and τ_3 correspond either to the *trans*-configuration or to the *gauche*-configuration, where the latter differs from the former by a τ value not much different from 120°. These different values of τ give rise to different stable configurations of a polypeptide chain.

Let us designate by $\angle t$ and $\angle g$ the values of τ corresponding to the *trans*- and the *gauche*-configurations. Then the equilibrium values of τ_1, τ_2, and τ_3 for some of the polypeptide models are expressed as follows:

(a) $\tau_1=\tau_2=\tau_3=\angle t$ for the extended configuration corresponding to the structure of β keratin proposed by Meyer and Mark.[12]

(b) $\tau_1=\angle t$, $\tau_2=-\angle g$, and $\tau_3=\angle g$ for the folded configuration corresponding to the structure of α protein proposed by Shimanouchi and Mizushima[13] and by Ambrose *et al.*[14]

(c) $\tau_1=\angle t$, $\tau_2=\angle g$, and $\tau_3=-\angle g$ for the folded configuration proposed by Huggins.[15]

(d) $\tau_1=\angle t$, $\tau_2=\angle g$, and $\tau_3=\angle g$ or $\tau_1=\angle t$, $\tau_2=-\angle g$, and $\tau_3=-\angle g$ for α helices of Pauling and Corey.[16]

The details of the discussion on the relative stability of these configurations and of others will be given elsewhere.[17]

V. STABLE CONFIGURATIONS OF CELLULOSE

The molecules of cellulose consist of pyranose rings. If we number the atoms of a cellulose molecule as shown in Fig. 6, the azimuthal angles of internal rotation

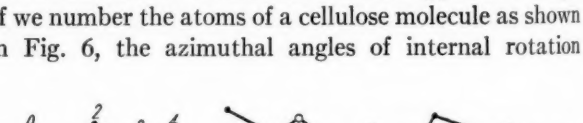

FIG. 6. The atomic arrangement in cellulose.

become:

$$\tau(0123)=180°,$$
$$\tau(1234)=60°,$$
$$\tau(2345)=180°,$$
$$\tau(3456)=-120°,$$
$$\tau(4567)=-120°.$$

[11] Mizushima, Shimanouchi, Nagakura, Kuratani, Tsuboi Baba, and Fujioka, J. Am. Chem. Soc. **72**, 3490 (1950).

[12] K. H. Meyer and H. Mark, Ber. deut. chem. Ges. **61**, 1932 (1928).

[13] T. Shimanouchi and S. Mizushima, Kagaku **17**, 24, 52 (1947); Bull. Chem. Soc. Japan **21**, 1 (1948).

[14] E. J. Ambrose and W. E. Hanby, Nature **163**, 483 (1949); Ambrose, Elliot, and Temple, Nature **163**, 859 (1949).

[15] M. L. Huggins, Chem. Revs. **32**, 195 (1943).

[16] Pauling, Corey, and Branson, Proc. Natl. Acad. Sci. **37**, 205 (1951).

[17] A part of this discussion has been given in reference 5. See also S. Mizushima, *Advances in Protein Chemistry* (Academic Press, Inc., New York, 1954), Vol. IX.

Furthermore, if we rewrite Eq. (1) as

$$\mathbf{X}_{i-1}=\mathbf{A}_{i-1,i}\mathbf{X}_i+\mathbf{B}_{i-1,i},$$

we have

$$\mathbf{A}=\mathbf{A}_{12}\mathbf{A}_{23}\mathbf{A}_{34}\mathbf{A}_{45}\mathbf{A}_{56},$$
$$\mathbf{B}=\mathbf{A}_{12}\mathbf{A}_{23}\mathbf{A}_{34}\mathbf{A}_{45}\mathbf{B}_{56}+\mathbf{A}_{12}\mathbf{A}_{23}\mathbf{A}_{34}\mathbf{B}_{45}+\mathbf{A}_{12}\mathbf{A}_{23}\mathbf{B}_{34}+\mathbf{A}_{12}\mathbf{B}_{23}+\mathbf{B}_{12}$$

in place of Eqs. (18) and (19) of the preceding section.

Using τ values just shown and assuming the bond angle ϕ to be tetrahedral angle and bond lengths of C−C and C−O to be 1.54 A, we can calculate the θ and d values of the cellulose helix as

$$\theta=180°,$$
$$d=(10.9/2)\text{A}.$$

The latter can be considered to be in good agreement with the value (10.3/2)A (or half the fiber period) obtained from the diffraction experiment on cellulose,[18] if we take into account the approximation made in this calculation.

[18] See, for example, K. H. Meyer and H. Mark, *Hochpolymere Chemie II* (Akademische Verlagsgesellschaft, Leipzig, Germany, 1940).

THE JOURNAL OF CHEMICAL PHYSICS VOLUME 23, NUMBER 4 APRIL, 1955

On the Electronic Structure and Electronic Spectra of Ethylene-Like Molecules*†

ROBERT G. PARR,‡ *Department of Chemistry, Carnegie Institute of Technology, Pittsburgh, Pennsylvania, and Department of Theoretical Chemistry, University of Cambridge, Cambridge, England*

AND

RUDOLPH PARISER, *Jackson Laboratory, E. I. duPont de Nemours and Company, Wilmington, Delaware*

(Received July 9, 1954)

A previously given theory of the electronic spectra and electronic structure of complex unsaturated molecules is applied to *ethylene-like molecules*, molecules such as ethylene itself, propylene or formaldehyde, which have two π electrons and two atomic π orbitals available for π-bond formation. Relations are derived among electronic excitation energies, intensities of electronic transitions, extra-ionic resonance energies and dipole moments of such molecules. Relative electronegativities are shown to play an important role in these relations, where the *effective electronegativity* of an atom is Mulliken's electronegativity (the mean of the appropriate atomic valence-state ionization potential and electron affinity) plus the total attraction of the valence electron of the atom for all other atoms in the molecule.

The analysis yields the result that the dipole moment due to a slight bond heteropolarity is proportional to the electronegativity difference of the bonded atoms, the extra-ionic resonance energy to its square. Proportionality factors are given absolutely by the theory. It is pointed out that the theory of a two-electron σ bond is formally the same, moreover, so that a derivation is provided for the familiar electronegativity relations of Pauling. Theoretical and empirical values for the proportionality factors are found to agree reasonably well for both π bonds and σ bonds.

The formulas given cover multiple perturbations of any type which may be considered not to add (or subtract) π electrons or π orbitals. They thus provide a scheme for quantitative evaluation of *inductive effects* in ethylene-like molecules. Systematic consideration of *mesomeric effects* is deferred, but an outline of the procedure which may be used for their study is given, using mono-substituted ethylene as an example.

To illustrate the use of the formulas, to bring out the relationships between the method and the work of other authors, and to see whether the method has promise for σ-electron systems, calculations are made of the electronic spectrum of ethylene, the twisting force constant of ethylene, the ionization potential and electron affinity of ethylene, the electronic spectrum and dipole moment of formaldehyde, and the electronic spectrum, ionization potential, and binding energy of the hydrogen molecule.

I. INTRODUCTION

RECENTLY there have been presented the elements of a theory designed for the quantitative correlation and prediction of those properties of complex unsaturated organic molecules, such as color, intensity of color, and resonance energy, which are qualitatively attributable to the unsaturation, or π electrons of these molecules.[1–3]

The theory differs from conventional ones in several important ways, some rather subtle, and it is a semi-empirical theory which may require modification as experience with its application accumulates. In order that the crucial points involved may be fully bared, Sec. II of the present paper is devoted to a summary of the main ideas and approximations in the theory.

Sections III–V give the application of the theory to two-π-electron, ethylene-like molecules (e.g., propylene or formaldehyde). Section III contains a derivation of

* Work assisted in part by the Office of Naval Research, U. S. Navy, through Contract Nonr-493(00) with the Carnegie Institute of Technology.

† Contribution No. 166 from Jackson Laboratory, E. I. duPont de Nemours and Company, Wilmington, Delaware.

‡ John Simon Guggenheim Memorial Foundation Fellow and Fulbright Research Scholar at the University of Cambridge, 1953–1954.

[1] R. Pariser and R. G. Parr, J. Chem. Phys. **21**, 466 (1953).

[2] R. Pariser and R. G. Parr, J. Chem. Phys. **21**, 767 (1953). The argument given on p. 769 of this paper in favor of using lower penetration integral values than calculated theoretically is not correct. The actual formal relation between the electron affinity A and self-penetration integral (1:11) is $A=(1:11)-T$, where T is the kinetic energy of a π electron in the negative ion (a relatively large quantity). The authors are indebted to Dr. F. O. Ellison for pointing out this error.

[3] F. G. Fumi and R. G. Parr, J. Chem. Phys. **21**, 1864 (1953). In Table I of this paper, for boldface $\mathbf{g}$ read $\bar{g}$.

the basic formulas that obtain when such molecules are treated as two-π-electron, two-π-orbital systems, and Sec. IV gives some illustrative calculations. The formulas given cover *inductive* effects of substituents in such molecules. The way in which *mesomeric* effects may be considered is discussed in Sec. V.

The theory may be applied formally to σ as well as to π bonds. Section VI contains some calculations on the hydrogen molecule exploring this possibility.

The relationship of the theory to recent work of others is discussed at appropriate places in the text and summarized in Sec. VII, where certain general conclusions are also stated.

II. SUMMARY OF THE METHOD

This theoretical method represents an attempted synthesis of some of the best elements of the simpler and more empirical approaches to the electronic structure of unsaturated molecules and some of the best elements of the more complex and more purely theoretical approaches. The method may be said to have seven characteristics. (1) Only π electrons are explicitly considered. (2) Corrections are made for the inadequacies of considering only π electrons. (3) Many-electron molecular wave functions are built from one-electron $2p\pi$ atomic orbitals. (4) Empirical elements are included. (5) Ionic and covalent states are properly located on the energy scale relative to one another and mixed in proportions determined by quantum-mechanical calculation. (6) Repulsions between π electrons are included. (7) The treatment of repulsions between π electrons is simplified. From a realistic point of view each of these characteristics seems desirable. Most past theories have had one or more of them, but few have had many.

There are five steps in the application of the theory to a given molecule. The first three steps span the formal procedure while the last two delineate the manner in which the calculations are carried out.[4]

Step 1. The Hamiltonian operator determining the π-electronic motions is written in the form

$$\mathbf{H}=\Sigma_i\mathbf{H}_{\text{core}}(i)+\tfrac{1}{2}\Sigma_{ij}(e^2/r_{ij}), \tag{1}$$

where the sums are over all π electrons i and j.

Step 2. Wave functions for the various π-electronic states of the molecule are formed from normalized Slater atomic $2p\pi$ orbitals χ_p by first forming orthonormal molecular orbitals

$$\phi_i=\Sigma_p C_{ip}\chi_p, \tag{2}$$

then forming appropriate orthonormal antisymmetrized products[5]

$$\Phi=(n!)^{-\frac{1}{2}}\begin{vmatrix}(\phi_1\alpha)^1 & (\phi_1\beta)^1 & \cdots\\ (\phi_1\alpha)^2 & (\phi_1\beta)^2 & \cdots\\ \cdot & \cdot & \cdot\\ \cdot & \cdot & \cdot\end{vmatrix}\equiv(1\bar{1}\cdots), \tag{3}$$

and finally forming linear combinations of the Φ

$$\Psi=A_1\Phi_1+A_2\Phi_2+\cdots. \tag{4}$$

Step 3. The values of the π-electron energy E are determined by solution of a secular equation

$$|(H_{mn}-\delta_{mn}E)|=0, \tag{5}$$

and the coefficients A_m are determined by solution of simultaneous equations.

$$\Sigma_m A_m(H_{mn}-\delta_{mn}E)=0, \tag{6}$$

where $H_{mn}=\int\Phi_m^*\mathbf{H}\Phi_n d\nu$ and $\delta_{mn}=1$ if $m=n$, $=0$ otherwise.

Step. 4. The integrals H_{mn} are expressed[6] in terms of core integrals.

$$I_{ij}=\int\phi_i^*(1)\mathbf{H}_{\text{core}}(1)\phi_j(1)d\nu(1), \tag{7}$$

and electronic repulsion integrals,

$$(ij|kl)=\int\phi_i^*(1)\phi_k^*(2)(e^2/r_{12})\phi_j(1)\phi_l(2)d\nu(1)d\nu(2), \tag{8}$$

over molecular orbitals. Using Eq. (2), these integrals are then expressed in terms of the coefficients C_{ip}, core integrals over atomic orbitals,

$$\alpha_p=\int\chi_p^*(1)\mathbf{H}_{\text{core}}(1)\chi_p(1)d\nu(1) \tag{9}$$

and

$$\beta_{pq}=\int\chi_p^*(1)\mathbf{H}_{\text{core}}(1)\chi_q(1)d\nu(1), \tag{10}$$

and electronic repulsion integrals over atomic orbitals,

$$(pq|rs)=\int\chi_p^*(1)\chi_r^*(2)(e^2/r_{12})\chi_q(1)\chi_s(2)d\nu(1)d\nu(2). \tag{11}$$

Step 5. The integrals over atomic orbitals are obtained as follows. (a) Integrals α_p are calculated from atomic valence-state ionization potentials I_p using formulas of the type

$$\alpha_p=-I_p-\Sigma'_{s\neq p}(s:pp)-\Sigma'_{q\neq p}(qq|pp), \tag{12}$$

where the sum over s is over all atoms in the molecule except the pth, the sum over q is over those atoms in the molecule other than the pth which contribute π electrons to the group being considered, and $(s:pp)$ is the potential energy of attraction of an electron in the orbital χ_p for the atom s *including its π electron* (if it bears any).

(b) Integrals β_{pq} are treated as empirical properties of bonds; β_{pq} is taken to be zero if atoms p and q are non-neighbors.

(c) In determining the coefficients C_{ip}, that is in evaluating the orthogonality integrals $\int\phi_i^*(1)\phi_j(1)d\nu(1)=\delta_{ij}$, and in computing the integrals $(ij|kl)$, the approximation of zero differential overlap is invoked, namely,

$$\chi_p^*(1)\chi_q(1)d\nu(1)=0, \tag{13}$$

when χ_p and χ_q are on different atoms. This has the effect of making

$$S_{pq}=\int\chi_p^*(1)\chi_q(1)d\nu(1)=\delta_{pq} \tag{14}$$

and causing only integrals of the type $(pp|qq)$ to appear in the final expressions for electronic repulsion integrals.

(d) Integrals $(pp|pp)$ are calculated from atomic valence-state ionization potentials I_p and atomic valence-state electron affinities A_p using formulas of the type

$$(pp|pp)=I_p-A_p. \tag{15}$$

(e) Integrals $(pp|qq)$, $p\neq q$, are calculated for large distances from theoretical formulas for appropriate atomic orbitals; for small distances they are obtained from empirical fitting of

[4] See references 1 and 2 for more details. Some minor modifications have been made in the procedures there described.

[5] Intermediate between the single-determinant type functions of Eq. (3) and the final linear combinations of Eq. (4) there will often be certain linear combinations of determinants determined from molecular symmetry or by resolution of spin degeneracies. Symbols Φ (with appropriate subscripts) will sometimes be used for such functions.

[6] Computation of matrix elements for a Hamiltonian operator like that of Eq. (1) between determinantal functions like those of Eq. (3) is a standard procedure, described in full for example in E. U. Condon and G. H. Shortley, *Theory of Atomic Spectra* (Cambridge University Press, Cambridge, 1935).

data or from smooth curves drawn to make the theoretical curves go into the zero-distance $(pp|pp)$ values given by Eq. (15). Integrals $(s:pp)$ are calculated from theoretical formulas where possible; otherwise estimated.

Step 1 is a mathematical expression of the π-electron approximation while steps 5(d) and 5(e) correct for the errors accompanying it.[2,7] Steps 2 and 3 described the manner in which total wave functions are built from atomic wave functions, assigning weights to different contributing structures by quantum-mechanical calculation.[1] Steps 5(a), 5(b), 5(d), and 5(e) show how empirical data, in the main atomic, are introduced, while Step 5(d) provides means for properly locating covalent and ionic states on the energy scale.[2,7] The inclusion of r_{nj} terms in the Hamiltonian operator in Step 1 brings the electronic repulsion problem out in the open to be faced squarely, and Step 5(c) provides a simple way to deal with this problem.[1,8]

III. ETHYLENE-LIKE MOLECULES: THEORY

Now consider a molecule having two $2p\pi$ atomic orbitals, χ_a and χ_b, on neighboring atoms a and b, and two π electrons, what may be called an *ethylene-like molecule*. The Hamiltonian operator will be

$$\mathbf{H}=\mathbf{H}_{\text{core}}(1)+\mathbf{H}_{\text{core}}(2)+(e^2/r_{12}). \tag{16}$$

The most convenient molecular obritals are those appropriate for the homonuclear case (e.g., ethylene itself), namely,

$$\phi_1=2^{-\frac{1}{2}}(\chi_a+\chi_b),\quad \phi_2=2^{-\frac{1}{2}}(\chi_a-\chi_b). \tag{17}$$

Assignment of the two electrons to these orbitals in all possible ways and antisymmetrization yield six determinants, which in turn give three singlet wave functions,

$$\Phi_1=(1\bar{1}),\quad \Phi_2=(2\bar{2}),\quad \Phi_V=2^{-\frac{1}{2}}[(1\bar{2})+(2\bar{1})], \tag{18}$$

and three degenerate triplet wave functions,

$$\Phi_T=(12)\quad\text{or}\quad(\bar{1}\bar{2})\quad\text{or}\quad 2^{-\frac{1}{2}}[(1\bar{2})-(2\bar{1})]. \tag{19}$$

The three singlet functions will in general mix to give three functions, Ψ_N, Ψ_V, Ψ_Z, approximating successive singlet-state wave functions of the molecule, each of the form

$$\Psi_\cdot=A_{\cdot 1}\Phi_1+A_{\cdot 2}\Phi_2+A_{\cdot V}\Phi_V; \tag{20}$$

whereas any one of the triplet functions is already the best such function obtainable from the given starting atomic orbitals:

$$\Psi_T=\Phi_T. \tag{21}$$

In the homonuclear case, Φ_V does not interact with Φ_1 and Φ_2, and the function Ψ_N is an admixture of Φ_1 and Φ_2 only, the mixing giving the π bond appropriate covalent and ionic character. The mixing of Φ_V with Φ_1 and Φ_2 in the heteronuclear case produces an additional stabilization energy which may be termed the *extra-ionic resonance energy*.[9]

Formulas for the nonzero matrix elements of H between the various Φ functions in terms of integrals over molecular orbitals are as follows:[6,10]

$$\begin{aligned}
H_{11}&=2I_{11}+(11|11),\\
H_{22}&=2I_{22}+(22|22),\\
H_{VV}&=I_{11}+I_{22}+(11|22)+(12|12),\\
H_{TT}&=I_{11}+I_{22}+(11|22)-(12|12),\\
H_{12}&=(12|12),\\
H_{1V}&=2^{\frac{1}{2}}[I_{12}+(11|12)],\\
H_{2V}&=2^{\frac{1}{2}}[I_{21}+(22|21)].
\end{aligned} \tag{22}$$

The integrals over molecular orbitals in turn are expressible in terms of integrals over atomic orbitals:

$$\begin{aligned}
I_{11}&=\tfrac{1}{2}(\alpha_a+\alpha_b)+\beta_{ab},\\
I_{22}&=\tfrac{1}{2}(\alpha_a+\alpha_b)-\beta_{ab},\\
I_{12}&=I_{21}=\tfrac{1}{2}(\alpha_a-\alpha_b),\\
(11|11)&=(22|22)=(11|22)=\tfrac{1}{4}[(aa|aa)\\
&\qquad+(bb|bb)+2(aa|bb)]\equiv J,\\
(12|12)&=\tfrac{1}{4}[(aa|aa)+(bb|bb)-2(aa|bb)]\equiv K,\\
(11|12)&=(22|21)=\tfrac{1}{4}[(aa|aa)-(bb|bb)]\equiv L.
\end{aligned} \tag{23}$$

One also has, from Eqs. (12) and (15),

$$\begin{aligned}
\alpha_a+\tfrac{1}{2}(aa|aa)&=-\tfrac{1}{2}(I_a+A_a)\\
&\qquad-\textstyle\sum'_{s\neq a}(s:aa)-(aa|bb),\\
\alpha_b+\tfrac{1}{2}(bb|bb)&=-\tfrac{1}{2}(I_b+A_b)\\
&\qquad-\textstyle\sum'_{s\neq b}(s:bb)-(aa|bb).
\end{aligned} \tag{24}$$

With

$$\begin{aligned}
y_a&\equiv\tfrac{1}{2}(I_a+A_a)+\textstyle\sum'_{s\neq a}(s:aa),\\
y_b&\equiv\tfrac{1}{2}(I_b+A_b)+\textstyle\sum'_{s\neq b}(s:bb),
\end{aligned} \tag{25}$$

and

$$Y\equiv y_a-y_b, \tag{26}$$

Eq. (22) thus becomes

$$\begin{aligned}
H_{11}&=\alpha_a+\alpha_b+2\beta_{ab}+J,\\
H_{22}&=H_{11}-4\beta_{ab},\\
H_{VV}&=H_{11}-2\beta_{ab}+K,\\
H_{TT}&=H_{11}-2\beta_{ab}-K,\\
H_{12}&=K,\\
H_{1V}&=H_{2V}=-2^{-\frac{1}{2}}Y.
\end{aligned} \tag{27}$$

The quantities $\frac{1}{2}(I+A)$ being the absolute electro-

[7] R. Pariser, J. Chem. Phys. **21**, 568 (1953). Compare W. Moffitt, Proc. Roy. Soc. (London) **A210**, 224 (1951), and see discussion in Secs. IV, VI, and VII.

[8] R. G. Parr, J. Chem. Phys. **20**, 1499 (1952).

[9] L. Pauling, *Nature of the Chemical Bond* (Cornell University Press, Ithaca, 1939), Chapter II.

[10] R. G. Parr and B. L. Crawford, Jr., J. Chem. Phys. **16**, 526 (1948). This paper contains detailed derivations of the formulas for the matrix elements for ethylene itself, both in its equilibrium and twisted configurations.

negativities of Mulliken,[11] the quantities y may reasonably be called *effective electronegativities* and Y is then an electronegativity difference.

If the energy relative to H_{11} is denoted by W, that is, if

$$W \equiv E - H_{11}, \tag{28}$$

the secular equation for the singlet states now reads

$$\begin{vmatrix} -W & K & -2^{-\frac{1}{2}}Y \\ K & -W-4\beta_{ab} & -2^{-\frac{1}{2}}Y \\ -2^{-\frac{1}{2}}Y & -2^{-\frac{1}{2}}Y & -W-2\beta_{ab}+K \end{vmatrix} = 0, \tag{29}$$

(1) (2) (V)

while the equation for the triplet state is simply

$$W = -2\beta_{ab} - K. \tag{30}$$

Successive roots of the singlet equation being called W_N, W_V, W_Z, the root of the triplet equation W_T, solution of these equations for a given molecule will give a set of approximate π-electron energy levels, $E_N \leqslant E_V \leqslant E_Z$ and E_T, and a set of approximate π-electron wave functions, Ψ_N, Ψ_V, Ψ_Z, and Ψ_T. Corresponding *total energies* will be π-electron energies plus core energies; a significant part of the latter will be the potential energy of repulsion between the π-electron bearing centers, in this case (for all levels) $+(aa|bb)$. (The $+$charges in C^+-C^+ should be interpreted as charges vacated by the π electrons, not nuclear charges, a point that apparently has been overlooked heretofore.)

The dipole moment for any state of the molecule and transition moments between any two states can be determined if the matrix elements

$$\mathbf{M}_{mn} = \int \Phi_m^* \mathbf{M} \Phi_n d\nu \tag{31}$$

are known, where

$$\mathbf{M} = \sum_t e_t \mathbf{r}_t, \tag{32}$$

$\mathbf{r}_t$ being the vectorial distance of the tth charged particle in the molecule from an arbitrary origin and e_t its charge. (The molecule as a whole is assumed neutral.) In general there will be contributions to $\mathbf{M}$ both from the underlying core structure and from the π electrons,

$$\mathbf{M} = \mathbf{M}_{\text{core}} + \mathbf{M}_\pi \tag{33}$$

and the latter contribution will be given by

$$\mathbf{M}_\pi = e\sum_i \mathbf{r}_i, \tag{34}$$

where e is the absolute value of the charge on an electron and the sum is over all π electrons.

The natural origin for the vectors $\mathbf{r}_i$ in this case is the midpoint between the two π-electron bearing centers, for then $\mathbf{M}_{\text{core}}$ will vanish when there is high symmetry. Further, if Cartesian coordinates are employed, with the positive z axis along the line of centers from a toward b, the x and y components of $\mathbf{M}_\pi$ also vanish, leaving

$$\mathbf{M} = -e[z(1)+z(2)]\mathbf{k}, \tag{35}$$

where $z(i)$ is the z coordinate of electron i and $\mathbf{k}$ is a unit vector along the z axis. Thus, one only needs matrix elements of $z(i)$ to obtain the π components of the $\mathbf{M}_{mn}$ of Eq. (31), $\mathbf{M}_{mn}{}^\pi$. Using[12]

$$\begin{aligned} \int \chi_a^*(i) z(i) \chi_a(i) d\nu(i) &= -\tfrac{1}{2}R, \\ \int \chi_b^*(i) z(i) \chi_b(i) d\nu(i) &= +\tfrac{1}{2}R, \\ \int \chi_a^*(i) z(i) \chi_b(i) d\nu(i) &= 0, \end{aligned} \tag{36}$$

where R is the internuclear distance, one obtains (by explicit expansion of the $\mathbf{M}_{mn}{}^\pi$ in terms of these basic integrals) the following results:

$$\begin{bmatrix} \mathbf{M}_{11}{}^\pi & \mathbf{M}_{12}{}^\pi & \mathbf{M}_{1V}{}^\pi \\ \mathbf{M}_{21}{}^\pi & \mathbf{M}_{22}{}^\pi & \mathbf{M}_{2V}{}^\pi \\ \mathbf{M}_{V1}{}^\pi & \mathbf{M}_{V2}{}^\pi & \mathbf{M}_{VV}{}^\pi \end{bmatrix} = \begin{bmatrix} 0 & 0 & 2^{-\frac{1}{2}}eR\mathbf{k} \\ 0 & 0 & 2^{-\frac{1}{2}}eR\mathbf{k} \\ 2^{-\frac{1}{2}}eR\mathbf{k} & 2^{-\frac{1}{2}}eR\mathbf{k} & 0 \end{bmatrix}, \tag{37}$$

$$(\mathbf{M}_{TT}{}^\pi) = (0);$$

matrix elements connecting singlet states with the triplet state are zero.

Equations (29) and (37) show that although the functions Φ_1, Φ_2, and Φ_V are associated with zero moment, a mixture of them has a moment if it contains both Φ_V and one of Φ_1 and Φ_2. Thus the dipole moment associated with the ground-state function,

$$\Psi_N = A_{N1}\Phi_1 + A_{N2}\Phi_2 + A_{NV}\Phi_V, \tag{38}$$

is

$$\begin{aligned} (\boldsymbol{\mu}_\pi/eR\mathbf{k}) &= 2^{\frac{1}{2}}(A_{N1}+A_{N2})A_{NV} \\ &\doteq (A_{N1}+A_{N2})^2 Y/(-W_N-2\beta+K). \end{aligned} \tag{39}$$

The transition moment between any two such Ψ functions is similarly expressible in terms of the corresponding A coefficients.

When Y is small, that is, when the π bond is only slightly heteropolar, Eq. (39) yields

$$\begin{aligned} (\boldsymbol{\mu}_\pi/eR\mathbf{k}) &\doteq (A_{N1}+A_{N2})^2 Y/(E_V-E_N) \\ &\doteq Y/(E_V-E_N), \end{aligned} \tag{40}$$

where $E_V - E_N$ is the excitation energy from the ground state to the first singlet excited state. Letting Δ denote the extra-ionic resonance energy, in this case one

[11] R. S. Mulliken, J. Chem. Phys. **2**, 782 (1934). For later numerical values, see H. A. Skinner and H. O. Pritchard, Trans. Faraday Soc. **49**, 1254 (1953).

[12] One could at this stage, if one wished, relax the condition of zero differential overlap, which would make the third integral in Eq. (36) in general not zero and give rise to a "homopolar" moment.

also has

$$2\Delta \doteq (A_{N1}+A_{N2})^2 Y^2/(E_V-E_N) \doteq Y^2/(E_V-E_N) \quad (41)$$

and

$$\Delta \doteq \tfrac{1}{2}(\boldsymbol{\mu}_x/eR\mathbf{k})^2/(E_V-E_N). \quad (42)$$

The quantity 2Δ is also the amount the excitation energy of the first singlet excited state V increases under a small inductive effect—the "blue shift" of the $N-V$ transition.

IV. ETHYLENE-LIKE MOLECULES: ILLUSTRATIVE CALCULATIONS

A number of calculations will now be carried out to exhibit the extent to which the formulas of the previous section are quantitatively applicable in simple cases. Each of the examples chosen will require a more detailed consideration of the theoretical quantities involved than the one before, and two or more calculations sometimes will be performed using numerical values obtained through considerations of different degrees of refinement. It is hoped that in this way both the limitations and the advantages of the method will be made plain.

A. The Electronic Spectrum of Ethylene

In a symmetrical case such as ethylene itself, the secular equations (29) and (30) reduce to the following simpler forms:

$$\begin{vmatrix} -W & K \\ K & -W-4\beta \end{vmatrix} = 0 \quad (\text{roots } W_N, W_Z),$$
$$W_V = -2\beta+K, \quad (43)$$
$$W_T = -2\beta-K.$$

Here

$$W \equiv E-H_{11}, \quad H_{11}=2\alpha+2\beta+J;$$
$$J \equiv \tfrac{1}{2}[(aa|aa)+(aa|bb)], \quad (44)$$
$$K \equiv \tfrac{1}{2}[(aa|aa)-(aa|bb)];$$

and

$$\alpha \equiv \alpha_a = \alpha_b, \quad \beta \equiv \beta_{ab}.$$

The quantity 2α enters all electronic energy levels additively and so cancels out in the computation of electronic excitation energies. For the computation of the electronic spectrum one thus needs values for β, $(aa|aa)$ and $(aa|bb)$. The theoretical values of $(aa|aa)$ and $(aa|bb)$ for Slater $2p\pi$ carbon atomic orbitals with effective charge 3.18 and 1.353 A $a-b$ distance are 16.93 and 9.26 ev.[13] In accordance with Eq. (15), however, an empirical value is to be preferred for $(aa|aa)$, namely, $11.54-0.46=11.08$ ev.[11] These values give $J=10.17$ and $K=0.91$ ev. There remains β, which is to be determined empirically from molecular data. Now it seems fairly sure (although it is not certain) that the 7.6 ev band of ethylene represents the $N-V$ transition.[14] Assuming this assignment to be correct, β may be given the value, -3.31 ev, which makes E_V-E_N come out to be 7.6 ev. The complete energy level scheme then obtained is as follows:

$$\left.\begin{aligned} E_N &= H_{11}-0.06 \text{ ev}, \\ E_V-E_N &= 7.60 \text{ ev}, \\ E_T-E_N &= 5.78 \text{ ev}, \\ E_Z-E_N &= 13.32 \text{ ev}. \end{aligned}\right\} \quad \left[\begin{aligned} \beta &= -3.31 \text{ ev}, \\ (aa|aa) &= 11.08 \text{ ev}, \\ (aa|bb) &= 9.26 \text{ ev}. \end{aligned}\right] \quad (45)$$

Since there is strong indirect evidence that the state T in ethylene lies at about 6.4 ev,[15] these results are in good agreement with experiment.

As a second calculation, the values of $(aa|aa)$ and $(aa|bb)$ may be corrected for the errors inherent in the zero differential overlap approximation. This may be done by adding to the first and subtracting from the second the quantity

$$\tfrac{1}{2}S^2[(aa|aa)-(aa|bb)] = \tfrac{1}{2}(0.28)^2(1.82) = 0.07 \text{ ev},$$

where S is the overlap integral between orbitals χ_a and χ_b.[13] The justification for this has been given elsewhere;[3] in brief the situation is that the integrals over atomic orbitals are best interpreted as integrals over the orthonormalized atomic orbitals of Löwdin[16] and that in the two-center case the corrections that must be applied to Slater integrals $(aa|aa)$ and $(aa|bb)$ to bring them approximately into the corresponding Löwdin integrals are plus and minus the above quantity. This correction produces no change in J but makes K now 0.98 ev. Again β is -3.31 ev, and the complete energy level scheme is as follows:

$$\left.\begin{aligned} E_N &= H_{11}-0.07 \text{ ev}, \\ E_V-E_N &= 7.60 \text{ ev}, \\ E_T-E_N &= 5.64 \text{ ev}, \\ E_Z-E_N &= 13.31 \text{ ev}. \end{aligned}\right\} \quad \left[\begin{aligned} \beta &= -3.31 \text{ ev}, \\ (aa|aa) &= 11.15 \text{ ev}, \\ (aa|bb) &= 9.19 \text{ ev}. \end{aligned}\right] \quad (46)$$

These results are not significantly different from the aforementioned.

Here β has been interpreted as a purely empirical property of a carbon-carbon bond. One might hope to compute β theoretically, and indeed, as Moffitt and Scanlan[17] and Moser[18] have shown in detail (and the present authors have confirmed), when this is done making reasonable assumptions reasonable results are obtained. But this may not always be the best approach. After all the model is crude; theoretical elucidation of β will help in estimating its changes under small perturbations, but for obtaining its absolute value in a given case it seems only sensible to try to use actual experimental data in that or a similar case.

[13] Reference 10 contains the integrals required for ethylene. A somewhat superior tabulation is that of H. J. Kopineck, Z. Naturforsch. **5a**, 420 (1950).

[14] P. G. Wilkinson and J. L. Johnston, J. Chem. Phys. **18**, 190 (1950).

[15] W. Potts, Ph.D. thesis, University of Chicago, 1953.

[16] P. O. Löwdin, J. Chem. Phys. **18**, 365 (1950).

[17] W. Moffitt and J. Scanlan, Proc. Roy. Soc. (London) **A218**, 464 (1953); **A220**, 530 (1953).

[18] C. M. Moser, J. Chem. Phys. **21**, 2098 (1953). RGP is indebted to Dr. Moser for a helpful discussion.

The quantity $(aa|bb)$ has here been calculated theoretically and the $T-V$ split has come out in good agreement with the observed 1.2 ev. In an earlier calculation,[2] when the triplet state was as yet unlocated, a lower value of $(aa|bb)$, 7.38 ev, was used, and the $T-V$ split came out to be 3.1 ev, appreciably smaller than the uncorrected molecular orbital value of 10.4 ev, but larger than the observed 1.2 ev. Actually, the previous downward adjustment of $(aa|bb)$ was made in order to fit the benzene spectrum. A corresponding adjustment was not found necessary in the diatomic molecule O_2,[3] and a simple rationalization can in fact be given for such a downward adjustment in polyatomic but not in diatomic cases. Terms $(aa|bb)$ in ethylene arise only when each atom holds a π electron, thus: $\dot{C}-\dot{C}$. In benzene, on the other hand, terms $(aa|bb)$ will sometimes arise involving electrons on negatively charged carbon atoms, as in structures

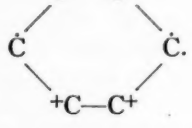

On the average a lower Z might thus be appropriate for benzene.

B. The Twisting Frequency of Ethylene[10]

Within the accuracy of the theory, Eqs. (43) and (44) hold for ethylene whether it is in its planar, equilibrium configuration, or in a twisted configuration. The only difference is that in the latter case when the CH_2 groups are twisted an angle φ with respect to one another the major axes of the orbitals χ_a and χ_b are inclined at that angle too. The basic quantities in the formulas which depend on φ are β and $(aa|bb)$; α depends on φ also but only through $(aa|bb)$:

$$\alpha=-I_a-\sum'_{s\neq a}(s:aa)-(aa|bb). \tag{47}$$

The dependences of β and $(aa|bb)$ on φ are given by the formulas[19]

$$\beta=\cos\varphi\beta_0 \tag{48}$$

and

$$(aa|bb)=\cos^2\varphi(aa|bb)_0+\sin^2\varphi(aa|bb)_{90}, \tag{49}$$

where the subscripts 0 and 90 indicate angles of inclination of orbital χ_b with respect to orbital χ_a.

The theoretical value of $(aa|bb)_{90}$ for Slater $2p\pi$ atomic orbitals with effective charge 3.18 and $a-b$ distance 1.353 A is 9.00 ev.[13] This is all that is necessary in addition to the values of $(aa|bb)_0$ and β_0 previously given in order to fix the variation with twisting of any of the energy levels. The variation in the total energy, E_N, of the state N with a small amount of twisting will in particular determine the twisting force constant, k, and hence the twisting frequency, ω, of the normal molecule:[10]

$$k=(\partial^2 E_N/\partial\varphi^2)_{\varphi=0}$$
$$\omega=560k^{\frac{1}{2}} \quad (\omega \text{ in cm}^{-1},\ k \text{ in ev}). \tag{50}$$

In the planar configuration the contribution of Φ_2 to Ψ_N (as determined above) is so small that the approximation $\Psi_N\doteq\Phi_1$ is very good in the neighborhood of equilibrium. The π-electron energy will then be $E_N \doteq H_{11}$, and the total energy will be this plus a core term which is a constant plus $(aa|bb)$ [see the discussion following Eq. (30)]:

$$\begin{aligned}E_N&=E_N+(aa|bb)+\text{constant}\doteq H_{11}+(aa|bb)+\text{constant}\\&=2\alpha+2\beta+J+(aa|bb)+\text{constant}\\&=\text{constant}+\cos\varphi[2\beta_0]-\cos^2\varphi[\tfrac{1}{2}(aa|bb)_0]\\&\qquad-\sin^2\varphi[\tfrac{1}{2}(aa|bb)_{90}].\end{aligned} \tag{51}$$

Thus

$$k\doteq-2\beta_0+[(aa|bb)_0-(aa|bb)_{90}]. \tag{52}$$

Or, introducing numerical values from Eq. (45),

$$k\doteq 6.62+0.26=6.88 \text{ ev},$$
$$\omega\doteq 1470 \text{ cm}^{-1}. \tag{53}$$

The corresponding experimental values are $k=3.36$ ev and $\omega=1027$ cm^{-1},[20] so that the computed force constant is too high by a factor of two.

The calculation can be corrected for the effect of overlap without great difficulty. It will be shown in Eq. (66) that a better formula for α than Eq. (47) includes a term $-S\beta$. Following through the effect of this correction, instead of the approximate result $k\doteq-2\beta_0$ of Eq. (52), one gets, using $S=S_0\cos\varphi$, the results $k\doteq-2[(1-S_0)/(1+S_0)]\beta_0=-1.2\beta_0=3.97$ ev, $\omega\doteq 1120$ cm^{-1}.

In view of the fact that in these calculations hyperconjugation, which favors twisted ethylene, has been neglected, either of these results may be regarded as quite satisfactory. Mulliken estimates the hyperconjugative correction to the twisting frequency to be about 120 cm^{-1},[21] which would make the value calculated here first too high, the value calculated second just right, but this last very good agreement should probably not be taken too seriously. The significant result is that the electronic repulsion plays but a small part in determining the twisting frequency. *The twisting force constant for a π bond is essentially proportional to the core beta for that bond.* This opens up the possibility of getting at the quantities beta through infrared spectroscopic data.

All of the states N, T, V, and Z could be plotted as functions of φ using the formulas given above. Curves so obtained may not have more than semi-quantitative

[19] Reference 10 contains detailed derivations. The present $(aa|bb)_0$ and $(aa|bb)_{90}$ are the $(aa|bb)$ and $(aa|b_xb_x)$ of reference 10.

[20] R. L. Arnett and B. L. Crawford, Jr., J. Chem. Phys. **18**, 118 (1950).

[21] R. S. Mulliken and C. C. J. Roothaan, Chem. Revs. **41**, 219 (1947).

validity, however. All things considered,[22] perhaps the best approximate view would be that π-electronic repulsion terms remain unchanged when the molecule is twisted, the π bond beta decreasing toward zero but hyperconjugative effects increasing in partial compensation.

C. The Ionization Potential and Electron Affinity of Ethylene

The formal determination of the ionization potential and electron affinity of ethylene by the present theory is very straightforward. For the $C_2H_4^+$ ion, there is one electron in the orbital ϕ_1; the π-electron energy therefore is

$$E(C_2H_4^+)=\alpha+\beta. \tag{54}$$

For the $C_2H_4^-$ ion, there are two electrons in ϕ_1, one in ϕ_2; the π-electron energy therefore is

$$E(C_2H_4^-)=3\alpha+\beta+3J-K. \tag{55}$$

Comparing these formulas with the corresponding formula for ethylene itself (neglecting the small effect of configuration interaction),

$$E(C_2H_4)=2\alpha+2\beta+J, \tag{56}$$

One obtains for the ionization potential the formula

$$I=-\alpha-\beta-J, \tag{57}$$

for the electron affinity the formula

$$A=-\alpha+\beta-2J+K, \tag{58}$$

and for their sum the formula

$$I+A=-2\alpha-3J+K. \tag{59}$$

There are a number of ways of looking at these formulas. The simplest is to interpret Eq. (57) as giving the core parameter α in terms of the observed ionization potential. Since I is 10.62 ev[23] for ethylene, one gets, in this way, using Eq. (45), values for the other quantities,

$$\begin{aligned}&\alpha=-10.62+3.31-10.17=-17.48 \text{ ev},\\ &A=17.48-3.31-2(10.17)+0.91=-5.26 \text{ ev},\\ &I+A=2(17.48)-3(10.17)+0.91=5.36 \text{ ev}.\end{aligned} \tag{60}$$

The electron affinity of ethylene is unknown. While it may well be negative, it is not likely as negative as -5 ev, as will be further discussed below.

It would be asking more of the theory to require it to predict both I and A. For a first try at this, one may merely substitute the theoretical expression for α, Eq. (47) into Eqs. (57)–(59), giving the following formulas:

$$\begin{aligned}I&=(I_a+P)-\tfrac{1}{2}(aa|aa)+\tfrac{1}{2}(aa|bb)-\beta\\ &=y_a+[\tfrac{1}{2}(aa|bb)-\beta],\end{aligned} \tag{61A}$$

$$\begin{aligned}A&=(A_a+P)+\tfrac{1}{2}(aa|aa)-\tfrac{1}{2}(aa|bb)+\beta\\ &=y_a-[\tfrac{1}{2}(aa|bb)-\beta],\end{aligned} \tag{62A}$$

$$I+A=I_a+A_a+2P=2y_a. \tag{63A}$$

Here P is the (always positive) penetration $\sum'_{s\neq a}(s:aa)$ and y_a is the effective electronegativity of atom a as defined in Eq. (25). These formulas are most interesting and suggestive, but they fail when put to quantitative test. For, using numerical values from Eq. (45), they give $y_a\geqq 6.00$ ev, $I\geqq 6.00+(4.63+3.31)=13.94$ ev, $A\geqq 6.00-(4.63+3.31)=-1.94$ ev, $I+A\geqq 12.00$ ev. That is, the ionization potential comes out much higher than the atomic ionization potential instead of lower.

Here now is something quite wrong. While molecular orbital theories in the past have not been spectacularly successful in predicting ionization potentials, they have not generally been off this much.[24] There must have been a gross error brought into the present theory through the zero differential overlap approximation, through the atoms-in-molecules correction of Eq. (15), or through superposition of the two.

To take the zero differential overlap approximation first, allowance for its effect does indeed relieve the situation somewhat. For, as has been shown elsewhere,[3] the empirical α and β which are so important in determining I and A are not to be identified with the corresponding theoretical quantities α_t and β_t, but instead (in the diorbital case) with

$$\alpha=(\alpha_t-S\beta_t)/(1-S^2) \tag{64}$$

and

$$\beta=(\beta_t-S\alpha_t)/(1-S^2), \tag{65}$$

where S is the overlap integral between χ_a and χ_b. Since Eq. (47) is really an expression for α_t, not α, the correct formula for α is not Eq. (47) but

$$\alpha=\alpha_t-S\beta=-I_a-\sum'_{s=a}(s:aa)-(aa|bb)-S\beta. \tag{66}$$

This gives the following formulas alternative to Eqs. (61A)–(63A):

$$\begin{aligned}I&=(I_a+P)-\tfrac{1}{2}(aa|aa)+\tfrac{1}{2}(aa|bb)-(1-S)\beta\\ &=y_a+[\tfrac{1}{2}(aa|bb)-\beta]+S\beta,\end{aligned} \tag{61B}$$

$$\begin{aligned}A&=(A_a+P)+\tfrac{1}{2}(aa|aa)-\tfrac{1}{2}(aa|bb)+(1+S)\beta\\ &=y_a-[\tfrac{1}{2}(aa|bb)-\beta]+S\beta,\end{aligned} \tag{62B}$$

$$\begin{aligned}I+A&=I_a+A_a+2P+2S\beta\\ &=2y_a+2S\beta.\end{aligned} \tag{63B}$$

With the same numerical values as before, these

[22] The zero differential overlap approximation may be expected to be too severe to allow correct predictions in all cases of the directions of changes of electronic repulsion energies under minor perturbations. Thus under the zero differential overlap approximation the quantity K is bigger by about 0.1 ev for perpendicular ethylene than for planar ethylene, but without this approximation the change is 0.2 ev in the opposite direction. See reference 10.

[23] R. E. Honig, J. Chem. Phys. **16**, 105 (1948).

[24] See, for example, R. G. Parr and R. S. Mulliken, J. Chem. Phys. **18**, 1338 (1950).

formulas give $y_a \geqq 6.00$ ev, $I \geqq 13.94-0.277(3.31)$ 13.02 ev, $A \geqq -2.86$ ev, $I+A \geqq 10.16$ ev. The ionization potential is still too high.

In order that the effect of the atoms-in-molecules correction both alone and superposed upon the zero differential overlap approximation may be examined, it is convenient to have displayed the precise way in which electronic repulsion integrals over molecular orbitals have been handled in the present problem. The integrals which enter are the integrals $(11|11)$, $(22|22)$, $(11|22)$, and $(12|12)$ of Eq. (22). In effect these have been computed by first writing out complete formulas for them, namely,[10]

$$\begin{aligned}(11|11)&=\tfrac{1}{2}(1+S)^{-2}[(aa|aa)+(aa|bb)\\&\qquad+2(ab|ab)+4(aa|ab)],\\(22|22)&=\tfrac{1}{2}(1-S)^{-2}[(aa|aa)+(aa|bb)\\&\qquad+2(ab|ab)-4(aa|ab)],\\(11|22)&=\tfrac{1}{2}(1-S^2)^{-1}[(aa|aa)+(aa|bb)-2(ab|ab)],\\(12|12)&=\tfrac{1}{2}(1-S^2)^{-1}[(aa|aa)-(aa|bb)];\end{aligned}\tag{67}$$

then replacing these formulas by simpler ones,

$$\begin{aligned}(11|11)&=(22|22)=(11|22)\\&=\tfrac{1}{2}[(aa|aa)+(aa|bb)]\equiv J,\\(12|12)&=\tfrac{1}{2}[(aa|aa)-(aa|bb)]\equiv K;\end{aligned}\tag{68}$$

and *then* applying the atoms-in-molecules correction,

$$(aa|aa)=I_a-A_a.\tag{69}$$

There are two possible attitudes to adopt. The first, which corresponds to the procedure of Moser,[18] is that the justification for passing from Eqs. (67) to equations like Eqs. (68) lies in Mulliken-type approximation formulas,[25]

$$\begin{aligned}(ab|ab)&\doteq\tfrac{1}{2}S^2[(aa|aa)_t+(aa|bb)],\\(aa|ab)&\doteq\tfrac{1}{2}S[(aa|aa)_t+(aa|bb)],\end{aligned}\tag{70}$$

relating the quantities $(ab|ab)$ and $(aa|ab)$ to the *theoretical* $(aa|aa)_t$ value (subscript t for theoretical). According to this view Eq. (69) should be applied *before* the approximations of Eq. (70) are made, not after, so that, up to terms in S^2, Eqs. (68) should be replaced by the formulas,

$$\begin{aligned}(11|11)&=J+S[(aa|aa)_t-(aa|aa)],\\(22|22)&=J-S[(aa|aa)_t-(aa|aa)],\\(11|22)&=J,\quad(12|12)=K,\end{aligned}\tag{71}$$

where $(aa|aa)_t$ denotes the theoretical as contrasted to the empirical value of $(aa|aa)$. Taking cognizance of just which integral enters each energy formula, one thus obtains a third set of formulas for I, A, and $I+A$, namely;

$$\begin{aligned}I&=(I_a+P)-\tfrac{1}{2}(aa|aa)+\tfrac{1}{2}(aa|bb)\\&\qquad-(1-S)\beta-S[(aa|aa)_t-(aa|aa)]\\&=y_a+[\tfrac{1}{2}(aa|bb)-\beta]-S[-\beta+(aa|aa)_t\\&\qquad-(aa|aa)],\end{aligned}\tag{61C}$$

$$\begin{aligned}A&=(A_a+P)+\tfrac{1}{2}(aa|aa)-\tfrac{1}{2}(aa|bb)+(1+S)\beta\\&=y_a-[\tfrac{1}{2}(aa|bb)-\beta]+S\beta,\end{aligned}\tag{62C}$$

$$\begin{aligned}I+A&=I_a+A_a+2P-S[-2\beta\\&\qquad+(aa|aa)_t-(aa|aa)]\\&=2y_a-S[-2\beta+(aa|aa)_t-(aa|aa)].\end{aligned}\tag{63C}$$

These formulas give $y_a \geqq 6.00$ ev, $I \geqq 13.02-0.277(16.93-11.08)=11.40$ ev, $A \geqq -2.86$ ev, $I+A \geqq 8.54$ ev. The ionization potential is better, but still too high by more than 0.8 ev.

The second possible attitude, which corresponds closely to Moffitt's procedure[17,26] and which allows the retention of the relative simplicity of Eqs. (61B)-(63B), is that Eqs. (70) hold approximately in the generalized sense required in order that Eq. (68), and hence Eqs. (61B)-(63B), hold with all integrals given values appropriately adjusted to make up for the inadequacies of the π-electron approximation, that is, to take account of polarization of σ electrons, variation of effective charge with degree of ionicity, and so on. This attitude, which the authors in fact prefer, may seem very blasé in the face of the $I \geqq 13.02$ ev computed from Eq. (61B) as compared with the $I \geqq 11.40$ ev computed from Eq. (61C). However, one's reaction must be tempered by the fact that if one uses purely theoretical values in Eq. (61B) throughout, that is, if one makes no atoms-in-molecules correction whatever, one obtains $I \geqq 11.54-\tfrac{1}{2}(16.93-9.26)+0.723\times(3.31)=10.10$ ev, which is a very satisfactory result indeed. (The corresponding result computed without invoking zero differential overlap and including an estimate of the penetration term P is $I=10.90$ ev.)[10] Actually, the authors do not feel that this calculation using a theoretical $(aa|aa)$ value is just right either, but it does illustrate how very sensitive the theoretical expression for I is to parameter values—all that is needed for I to come out slightly less than I_a is for $[(aa|aa)-(aa|bb)]$ to exceed $-2(1-S)\beta$ slightly, and this could come about in several ways.

These two attitudes in fact represent two distinct versions of the π-electron approximation. At infinite distance there is no difference between the two; they both satisfy Moffitt's demand that the theory be made to give correct relative energies for dissociation products.[27] But at a finite distance there is a difference.

A decision between the alternative interpretations cannot be made without a good deal more information. Experimentally, values of electron affinities would be very useful; theoretically, detailed studies of simple

[25] R. S. Mulliken, J. Chim. Phys. **46**, 497 (1949).

[26] Compare the discussion in Sec. VI.

[27] W. Moffitt, Proc. Roy. Soc. (London) **A210**, 246 (1951).

cases including explicit consideration of σ electrons are required.[28]

D. A Heteropolar Application of Formaldehyde

The analysis above having shown that the empirical α which enters the formulas of Sec. III is not strictly α_t but $\alpha_t - S\beta$, one may well question the applicability of those formulas in Sec. III which were derived on the assumption $\alpha = \alpha_t$, that is, the formulas involving the electronegativity difference Y. The saving feature is that the same correction applies to α_a as to α_b, so that corrections cancel out in the difference $\alpha_a - \alpha_b$. The definitions of effective electronegativities y and electronegativity differences Y may thus be left unchanged. One must merely bear in mind that corrections $-S\beta$ should be applied when ionization potentials, electron affinities or total π-electron energies are being computed, but they may be ignored when spectroscopic intervals are being considered.

Unfortunately there is not a wealth of examples for which the equations of Sec. III apply and sufficient data are available for checking the theory. Thus, in the case of propylene, hyperconjugation (mesomeric) effects are superposed on inductive effects; in the case of formaldehyde lone pair and sigma-bond moments obscure the dipole moment data and the first main absorption band has been attributed to excitation of one of the lone-pair electrons. This does not mean that the equations of Sec. III are useless but only that careful and detailed studies, both experimental and theoretical, are required before they can be applied with confidence. In particular, mesomeric and inductive effects, when both present, have to be considered simultaneously, then disentangled. How this can be done is indicated in Sec. V.

With the understanding then that the calculation is exploratory rather than definitive, the formaldehyde molecule, $H_2C=O$, will now be considered. The relevant data are: dipole moment 2.34 D,[29] carbon-oxygen distance 1.22 A,[30] $N-V$ π-electron transition 1560 A or 8.0 ev.[31] The questions here asked will be: (1) Are these data consistent with each other according to the present theory? (2) If these data are consistent, with what empirical electronegativity difference Y do they correspond? (3) If these data are consistent, how does the empirical Y compare with one estimated from atomic effective electronegativities y?

The $N-V$ transition of ethylene being 7.6 ev, there is a small blue shift in going from ethylene to formaldehyde, which is in accordance with the predictions of Sec. III. In fact, this blue shift is approximately 2Δ, twice the extra-ionic resonance energy, as given by Eqs. (41) and (42). Thus Eq. (42) gives $(\mathfrak{y}_\pi/eR\mathbf{k})^2 = (0.4/7.6) = 0.0526$, $(\mathfrak{y}_\pi/eR\mathbf{k}) = 0.23$, $|\mathfrak{y}_\pi| = (0.23)(4.8) \times (1.22) \times 10^{-18}$ esu $= 1.3$ D. The lone-pair moment might be of the same order as in the water molecule, 1.5 D or so,[32] which makes this computed π moment reasonable, the sigma-bond moment presumably being small.[33] The answer to question (1) is therefore: Yes.

Too many factors enter the dipole moment to allow an empirical π-electronegativity difference to be determined from the experimental moment. The spectroscopic shift may be used to determine it, however, Eq. (41) giving $Y^2 = (0.4)(7.6) = 3.04$, $Y = 1.7$ ev.

To compare this empirical Y with one obtained from atomic electronegativities, one needs the appropriate I and A for the oxygen atom. If sp^2 hybridization is assumed (the precise hybridization for oxygen in formaldehyde is not known), these are the p-electron values for 0 in the valence state sp^5, V_2, namely, $I = 17.91$ ev, $A = 4.85$ ev.[11] Thus $\frac{1}{2}(I+A) = 11.38$ ev for oxygen, which combined with the carbon value 6.00 ev obtained above gives $Y = y_O - y_C = 5.4 - (P_C - P_O)$ ev, where P_O is the attraction of an oxygen π-electron for a neutral $-CH_2$ group and P_C the attraction of a carbon π electron for the two H atoms and a neutral O atom. P_C presumably exceeds P_O, but just how much is hard to say without detailed calculations. The empirical and theoretical Y therefore would appear to be in at least rough agreement.

In this calculation it has been implicitly assumed that the quantity $H_{VV} - H_{11} = 2\beta_{ab} + K$ is the same for formaldehyde as for ethylene, which by no means need be the case. A change in this quantity could produce a "homopolar shift" either to the red or blue which would be superposed upon the blue shift previously computed.

V. ETHYLENE-LIKE MOLECULES: MESOMERIC *VERSUS* INDUCTIVE EFFECTS

The formulas of Sec. III cover the effects of substitutions or other perturbations in ethylene-like molecules only in so far as they do not entail changes in the number of π electrons or π orbitals that need to be considered. These are commonly known as *inductive* effects. If substitutions or other perturbations change the number of π electrons or π orbitals, *mesomeric* effects will also enter.[34]

To see how mesomeric and inductive effects may be treated simultaneously yet kept sensibly separate, consider the specific example of one more π orbital and two more π electrons, as in monofluoroethylene or propylene. Let the newly available orbital be χ_s on atom s, substituent atom on atom a; one then has the

[28] Strictly speaking, no one of the quantities α, β, J, and K is the same for $C_2H_4^+$ as for C_2H_4 or for $C_2H_4^-$.

[29] J. N. Shoolery and A. H. Sharbaugh, Phys. Rev. **82**, 95 (1951).

[30] G. Herzberg, *Infrared and Raman Spectra of Polyatomic Molecules* (D. Van Nostrand Company, Inc., New York, 1945), p. 440.

[31] W. C. Price, J. Chem. Phys. **3**, 256 (1935); A. D. Walsh, Proc. Roy. Soc. (London) **A185**, 176 (1946).

[32] J. A. Pople, J. Chem. Phys. **21**, 2234 (1953).

[33] The dipole moments of alcohols, ethers, and like molecules presumably are due in large part to lone-pair moments.

[34] Before mesomeric and inductive effects can be quantum-mechanically treated, they must be quantum-mechanically defined; this paragraph gives such a definition.

three $2p\pi$ atomic orbitals χ_s, χ_a, χ_b, and four π electrons. This problem could be treated from scratch afresh, but it is better merely to modify the analysis of the inductive effect already given. In place of the four starting functions of Eqs. (18) and (19), one now has nine, six singlet and three triplet:

$$\begin{aligned}
\Phi_1&=(1\bar{1}s\bar{s}),\quad \Phi_2=(2\bar{2}s\bar{s}),\\
\Phi_V&=2^{-\frac{1}{2}}[(1\bar{2}s\bar{s})+(2\bar{1}s\bar{s})],\\
\Phi_{V'}&=2^{-\frac{1}{2}}[(1\bar{1}s\bar{2})+(1\bar{1}2\bar{s})],\\
\Phi_{V''}&=2^{-\frac{1}{2}}[(2\bar{2}s\bar{1})+(2\bar{2}1\bar{s})],\\
\Phi_{V'''}&=(1\bar{1}2\bar{2}),\\
\Phi_T&=2^{-\frac{1}{2}}(1\bar{2}s\bar{s})-(2\bar{1}s\bar{s})],\\
\Phi_{T'}&=2^{-\frac{1}{2}}[(1\bar{1}s\bar{2})-(1\bar{1}2\bar{s})],\\
\Phi_{T''}&=2^{-\frac{1}{2}}[(2\bar{2}s\bar{1})-(2\bar{2}1\bar{s})].
\end{aligned}\tag{72}$$

Here only one component of each triplet function has been included, and s has been used to indicate χ_s.

At the stage corresponding to the previous Eqs. (22) and (23), the formulas for matrix elements between starting functions are as follows:

$$\begin{aligned}
H_{11}&=\alpha_a+\alpha_b+2\alpha_s+2\beta_{ab}+J+4J_s+J_{ss},\\
H_{22}&=H_{11}-4\beta_{ab},\\
H_{VV}&=H_{11}-2\beta_{ab}+K,\\
H_{TT}&=H_{11}-2\beta_{ab}-K,\\
H_{V'V'}&=H_{T'T'}=H_{11}-\beta_{ab}+[\tfrac{1}{2}(\alpha_a+\alpha_b)\\
&\qquad -\alpha_s+2J-K-J_s-J_{ss}],\\
H_{V''V''}&=H_{T''T''}=H_{11}-3\beta_{ab}+[\tfrac{1}{2}(\alpha_a+\alpha_b)\\
&\qquad -\alpha_s+2J-K-J_s-J_{ss}],\\
H_{V'''V'''}&=H_{11}-2\beta_{ab}+[(\alpha_a+\alpha_b)\\
&\qquad -2\alpha_s+5J-2K-4J_s-J_{ss}];
\end{aligned}\tag{73}$$

$$\begin{aligned}
H_{12}&=K,\\
H_{1V}&=H_{2V}=2^{-\frac{1}{2}}(\alpha_a-\alpha_b+2L+4L_s),\\
H_{1V'}&=H_{2V''}=H_{V'V'''}=H_{V''V'''}=\beta_{as},\\
H_{1V''}&=H_{1V'''}=H_{2V'}=H_{2V'''}=H_{VV'''}=0,\\
H_{VV'}&=H_{VV''}=-H_{TT'}=H_{TT''}=-2^{-\frac{1}{2}}\beta_{as},\\
H_{V'V''}&=H_{T'T''}=-\tfrac{1}{2}(\alpha_a-\alpha_b+4L+2L_s).
\end{aligned}\tag{74}$$

Here J, K, and L are the quantities defined in Eq. (23),

$$\begin{aligned}
J_{ss}&\equiv(ss|ss),\quad J_s\equiv(11|ss)=(22|ss)\\
&=\tfrac{1}{2}[(aa|ss)+(bb|ss)],
\end{aligned}\tag{75}$$

$$L_s\equiv(12|ss)=\tfrac{1}{2}[(aa|ss)-(bb|ss)].$$

The α's can be expressed in terms of effective electronegativities much as before. With y_a and y_b given by Eqs. (25),

$$y_s{}^+\equiv\tfrac{1}{2}(I_s+I_s{}^+)+\sum{}'_{t\neq s}(t:ss),\tag{76}$$

and

$$(ss|ss)=I_s{}^+-I_s,\tag{77}$$

Where I_s and $I_s{}^+$ are the first and second ionization potentials of atom s (the electron affinity and first ionization potential of ion s^+), one has in fact

$$\begin{aligned}
\alpha_a&=-y_a-\tfrac{1}{2}(aa|aa)-(aa|bb)-2(aa|ss),\\
\alpha_b&=-y_b-\tfrac{1}{2}(bb|bb)-(aa|bb)-2(bb|ss),\\
\alpha_s&=-y_s{}^+-\tfrac{1}{2}(ss|ss)-(aa|ss)-(bb|ss).
\end{aligned}\tag{78}$$

Accordingly, with

$$Y_s\equiv y_s{}^+-\tfrac{1}{2}(y_a+y_b)\tag{79}$$

and $Y\equiv y_a-y_b$ as before, Eqs. (43) and (44) become

$$\begin{aligned}
H_{11}&=\alpha_a+\alpha_b+2\beta_{ab}+J-2y_s{}^+,\\
H_{22}&=H_{11}-4\beta_{ab},\\
H_{VV}&=H_{11}-2\beta_{ab}+K,\\
H_{TT}&=H_{11}-2\beta_{ab}-K,\\
H_{V'V'}&=H_{T'T'}=H_{11}-\beta_{ab}\\
&\qquad +(Y_s+\tfrac{1}{2}J-\tfrac{1}{2}K-J_s-\tfrac{1}{2}J_{ss}),\\
H_{V''V''}&=H_{T''T''}=H_{11}-3\beta_{ab}\\
&\qquad +(Y_s+\tfrac{1}{2}J-\tfrac{1}{2}K-J_s-\tfrac{1}{2}J_{ss}),\\
H_{V'''V'''}&=H_{11}-2\beta_{ab}+(2Y_s+2J-K-4J_s);
\end{aligned}\tag{80}$$

and

$$\begin{aligned}
H_{12}&=K,\\
H_{1V}&=H_{2V}=-2^{-\frac{1}{2}}Y,\\
H_{1V'}&=H_{2V''}=H_{V'V'''}=H_{V''V'''}=\beta_{as},\\
H_{1V''}&=H_{1V'''}=H_{2V'}=H_{2V'''}=H_{VV'''}=0,\\
H_{VV'}&=H_{VV''}=-H_{TT'}=H_{TT''}=-2^{-\frac{1}{2}}\beta_{as},\\
H_{V'V''}&=H_{T'T''}=\tfrac{1}{2}(Y-2L+2L_s).
\end{aligned}\tag{81}$$

Introducing the abbreviations

$$\begin{aligned}
W&\equiv E-H_{11},\quad W_2\equiv H_{22}-H_{11}=-4\beta_{ab},\\
W_V&\equiv H_{VV}-H_{11}=-2\beta_{ab}+K,\\
W_T&\equiv H_{TT}-H_{11}=-2\beta_{ab}-K,\\
W_{V'}&\equiv H_{V'V'}-H_{11}=-\beta_{ab}\\
&\qquad +(Y_s+\tfrac{1}{2}J-\tfrac{1}{2}K-J_s-\tfrac{1}{2}J_{ss})\\
&\qquad =H_{T'T'}-H_{11}\equiv W_{T'},\\
W_{V''}&=H_{V''V''}-H_{11}=-3\beta_{ab}\\
&\qquad +(Y_s+\tfrac{1}{2}J-\tfrac{1}{2}K-J_s-\tfrac{1}{2}J_{ss})\\
&\qquad =H_{T''T''}-H_{11}\equiv W_{T''},\\
W_{V'''}&=H_{V'''V'''}-H_{11}=-2\beta_{ab}+(2Y_s+2J-K-4J_s),
\end{aligned}\tag{82}$$

the secular equation for the singlet states will now read

$$\begin{vmatrix} (1) & (2) & (V) & (V') & (V'') & (V''') \\ -W & K & -2^{-\frac{1}{2}}Y & \beta_{as} & 0 & 0 \\ K & W_2-W & -2^{-\frac{1}{2}}Y & 0 & \beta_{as} & 0 \\ -2^{-\frac{1}{2}}Y & -2^{-\frac{1}{2}}Y & W_V-W & -2^{-\frac{1}{2}}\beta_{as} & -2^{-\frac{1}{2}}\beta_{as} & 0 \\ \beta_{as} & 0 & -2^{-\frac{1}{2}}\beta_{as} & W_{V'}-W & \frac{1}{2}Y-L+L_s & \beta_{as} \\ 0 & \beta_{as} & -2^{-\frac{1}{2}}\beta_{as} & \frac{1}{2}Y-L+L_s & W_{V''}-W & \beta_{as} \\ 0 & 0 & 0 & \beta_{as} & \beta_{as} & W_{V'''}-W \end{vmatrix} = 0, \quad (83)$$

while that for the triplet states will read

$$\begin{vmatrix} (T) & (T') & (T'') \\ W_T-W & 2^{-\frac{1}{2}}\beta_{as} & -2^{-\frac{1}{2}}\beta_{as} \\ 2^{-\frac{1}{2}}\beta_{as} & W_{T'}-W & \frac{1}{2}Y-L+L_s \\ -2^{-\frac{1}{2}}\beta_{as} & \frac{1}{2}Y-L+L_s & W_T''-W \end{vmatrix} = 0. \quad (84)$$

These two equations are generalizations of Eqs. (29) and (30).

Equation (83) submits to the following physical interpretation. The 1×1 secular equation obtained by ignoring all elements except the one in the upper left-hand corner corresponds to the simplest molecular orbital wave function for a homopolar bond. The 2×2 equation similarly obtained keeping only the upper left 2×2 block corresponds to an improved wave function for a homopolar system: molecular orbital + configuration interaction ≡ Heitler-London + ionic terms. The 3×3 equation from the upper left corner corresponds to a wave function corrected for bond heteropolarity (inductive effect). The full 6×6 equation corresponds to a wave function further improved by resonance interactions with the substituent s (inductive effect+mesomeric effect). And the 5×5 equation obtained by ignoring the third row and third column corresponds to a wave function for a homopolar bond in resonance interaction with a substituent (mesomeric effect only). Equation (84) can be interpreted similarly.

Quantitative calculations with these equations will not be undertaken here, but a few general points may be noted. The extent of inductive effects on the ground state is roughly measured by (Y/W_V), the extent of mesomeric effects by $(\beta_{as}/W_{V'})$. When both effects are small they will be additive (solve Eq. (84) by perturbation theory), but they will in general mix in a complicated way.

Mesomeric effects on dipole moments and transition moments can be brought in by straightforward extension of Eqs. (35)–(39). Other properties could be similarly treated.

Much work will have to be done to assess the inductive and mesomeric effects of various substituents on the basis of this theory, even in ethylene-like molecules. On the one hand data must be sought which will aid in the assignment of values to the parameters β and y; on the other hand theoretical studies of quantities such as these will be useful.

VI. ON THE POSSIBLE APPLICATION OF THE THEORY TO SIGMA BONDS

If a theory as simple as the present one could be applied to sigma bonds explicitly, it would provide a very useful tool for correlation and prediction of spectroscopic and other properties of molecules of all kinds, not just the π-electron systems so far considered. In this section the possibility will be examined of applying the formulas of Sec. III to molecules containing one two-electron sigma bond—*hydrogen-like molecules*.

Without question the theory is at least formally, and hence qualitatively applicable. The treatment given can be carried over in its entirety to the H_2 molecule, for example, and there corresponds to the usual molecular orbital treatment including configuration interaction (or, equivalently, to the usual Heitler-London treatment including ionic terms). Furthermore, for the heteropolar case the dipole moment—extra-ionic resonance energy—electronegativity difference formulas are of just the form prescribed by Pauling.[9] So the formulation of Sec. III at least has heuristic value when applied to sigma bonds.

Whether the formulation transcends heuristic value may be tested at two levels. One may inquire whether the theoretical and empirical (Pauling) proportionality factors in the dipole moment—extra-ionic resonance energy—electronegativity difference relations are in agreement. Or, one may test the scheme by explicit application to determine electronic energy levels and other properties for simple examples such as the H_2 molecule, making quantitative comparisons with corresponding nonempirical treatments as one goes along. In the following paragraphs, these viewpoints will be taken in turn.

A. Electronegativity Relations for a Hydrogen-Like Molecule

For the hydrogen molecule itself, H_2, $E_V-E_N=12.47$ ev and $R=0.7417$ A.[35,36] Inserting these figures in Eq. (40) one thus has for a hydrogen-like molecule

$$\mu(\text{Debye}) \doteq (Y_M/12.47)(4.80)(0.74) = 0.285Y_M = 0.90Y_P, \quad (85)$$

[35] G. Herzberg, *Spectra of Diatomic Molecules* (D. Van Nostrand Company, Inc., New York, 1950).

[36] For a list of the vertical excitation energies and ionization potential of H_2 which are required here, see Table III of reference 25.

where Y_M is the electronegativity difference in electron volts, Mulliken's scale, and Y_P is the electronegativity difference on Pauling's scale, related to Y_M through[11]

$$Y_M = 3.15 Y_P. \tag{86}$$

Similarly, Eq. (41) yields

$$\Delta(\text{kcal/mole}) \doteq \tfrac{1}{2}(Y_M^2/12.47)(23.06) = 0.925 Y_M^2 = 9.18 Y_P^2. \tag{87}$$

The corresponding empirical formulas of Pauling are[9]

$$\mu(\text{Debye}) = 1.00 Y_P(\text{empirical}) \tag{88}$$

and

$$\Delta(\text{kcal/mole}) = 23.06 Y_P^3(\text{empirical}). \tag{89}$$

Equations (85) and (87) are in reasonable accord with these, which lends confidence that the equations of Sec. III are semiquantitatively applicable to sigma bonds. However, one should note that Pauling's formulas were not really designed for molecules very similar to H_2 in their electronic structure but rather for molecules such as the hydrogen halides, the alkali halides, the mixed halogens, and so on. In such molecules: (a) the electronegativity differences are of the same order of magnitude as the $N-V$ transition energy, not much smaller as Eqs. (40)–(42) require; (b) lone pairs almost always contribute to the dipole moment (this will in general be the case whenever the bond is formed between hydribized orbitals, as opposed to pure s or pure p orbitals); and (c) one of the two bonded atoms is usually much smaller than the other, which presumably makes penetration contributions to electronegativity differences substantial. And one must also point out that $E_V - E_N$ in such molecules is less than in hydrogen, R more, so that the proportionality factor between μ(Debye) and Y_P becomes greater than unity.

It should be in quite a different context that Eqs. (40)–(42) as applied to sigma bonds would be most useful. Thus one could predict from Eq. (42) that the fractional blue shift of the first $^1\Sigma_g^+ - {}^1\Sigma_u^+$ transition in ethane brought on by a small *inductive* perturbation would be approximately equal to the square of the corresponding dipole moment increment in units of eR. Such a decrease in color accompanying an increase in the extra-ionic character of the bond is in agreement with the qualitative considerations of Pitzer and Hildebrand on "color and bond character."[37]

B. Some Calculations on the Hydrogen Molecule

In practice one does not use theories of electronic structure to predict internuclear distances in complex molecules but one proceeds from known internuclear distances to the prediction of other properties. Accordingly, the calculations here reported for the hydrogen molecule all take the internuclear distance to be the observed 0.74 A.[35]

[37] K. S. Pitzer and J. H. Hildebrand, J. Am. Chem. Soc. **63**, 2472 (1941).

The properties to be considered, and their experimental magnitudes,[38] are as follows:

$$\begin{aligned} &\text{First Singlet Excitation Energy} \equiv E_V - E_N = 12.5 \text{ ev}, \\ &\text{First Triplet Excitation Energy} \equiv E_T - E_N = 10.3 \text{ ev}, \\ &\text{First Ionization Potential} \equiv I = 16.5 \text{ ev}, \\ &\text{Binding Energy} \equiv 2E_H - E_N = 4.8 \text{ ev}. \end{aligned} \quad \text{(Experimental)} \tag{90}$$

The problem is to account for these properties as well as possible with a theory in which the electronic wave function for the molecule is constructed from $1s$ atomic orbitals on the two atoms with effective charge $Z \doteq 1$ (the Slater effective charge in this case!).

It will be convenient to display first the results of the relevant purely theoretical calculations, which can be carried out in this case without difficulty because all required integrals may be found in the literature.[39] The most general wave function that can be constructed from the given atomic orbitals is the molecular orbital wave function including configuration interaction (or, equivalently, the Heitler-London wave function including ionic terms), which has been considered by many authors, most recently by Scherr.[40] This wave function has just the form of Eq. (20) (with $A_{.V} = 0$ by symmetry and the normalizing factors for the molecular orbitals containing the overlap integral); the energy formulas have just the form of Eqs. (22). Results for four different values of the effective charge Z are as follows:

$$\begin{aligned} &Z = 0.72,\ 1.07,\ 1.43,\ 1.79; \\ &E_V - E_N = 13.7,\ 23.1,\ 30.9,\ 38.8 \text{ ev}; \\ &E_T - E_N = 8.5,\ 14.9,\ 19.1,\ 23.0 \text{ ev}; \\ &I = 16.3,\ 16.2,\ 14.7,\ 9.1 \text{ ev}; \\ &2E_H - E_N = -2.9,\ 1.6,\ 2.6, \\ &\qquad -5.3 \text{ ev}. \end{aligned} \quad \text{(Purely Theoretical)} \tag{91}$$

There is little encouraging about these results. The mean value of the singlet and triplet excitation comes out about right for $Z = 0.7$, but the singlet-triplet split is more than twice its observed value for this Z, much greater still for larger Z. The binding energy does not even come out positive for this Z; it is positive and somewhat more than one-half its observed value for $Z = 1.4$. (The best result obtained if both Z and R are adjusted to give minimum energy is $2E_H - E_N = 4.03$ ev for $R = 0.7400$ A and $Z = 1.193$.)[41] The ionization potential is better, but one should note here that what one is really computing is the ionization potential

[38] See reference 36. The "experimental" values are in part determined from accurate theoretical calculations.

[39] J. O. Hirschfelder and J. W. Linnett, J. Chem. Phys. **18**, 130 (1950).

[40] C. W. Scherr, J. Chem. Phys. **22**, 149 (1954).

[41] S. Weinbaum, J. Chem. Phys. **1**, 593 (1933).

increment in going from the hydrogen atom ($I=13.6$ ev) to the hydrogen molecule.

An interesting point may be made in passing. The variational principle applies strictly to these calculations for the states T and V (as well as for N): the best triplet wave function is the one which makes E_T an absolute minimum, and similarly with the singlet. The figures in Eq. (91) show that the best Z for the states T and V is on the order of 0.7, far from the best for the ground state. And further, the excitation energies themselves come out better for this Z. The implication is: *In variational calculations of spectroscopic intervals, lower Z values for atomic orbitals may be appropriate than are given by Slater's rules.*

Before turning to simplified methods of calculation, theoretical values for the electronic repulsion integrals which enter the calculations may be quoted. These are (formally) the integrals of Eq. (67):

$$\begin{aligned} &Z=0.72,\ 1.07,\ 1.43,\ 1.79;\\ &S=0.858,\ 0.725,\\ &\qquad 0.586,\ 0.458;\\ &(11|11)=11.50,\ 16.34,\\ &\qquad 20.51,\ 24.13 \text{ ev};\\ &(22|22)=11.96,\ 16.92,\\ &\qquad 21.30,\ 25.23 \text{ ev};\\ &(11|22)=11.33,\ 16.06,\\ &\qquad 20.26,\ 24.03 \text{ ev};\\ &(12|12)=2.61,\ 4.15,\ 5.91,\ 7.91 \text{ ev}. \end{aligned} \quad \begin{matrix}\\ \\ \\ \\ \\ \\ \\ \\ \\ \\ \\ \\ \text{(Purely}\\ \text{Theoretical)}\end{matrix} \quad (92)$$

The constancy of the first three integrals even with S as high as 0.86 is striking and suggests that a simplified treatment of these integrals should be possible. The zero differential overlap approximation, that is, Eq. (68), yields the following results:

$$\begin{aligned} &Z=0.72,\ 1.07,\ 1.43,\ 1.79;\\ &(11|11)=(22|22)=(11|22)\equiv J\\ &\quad =11.48,\ 16.28,\\ &\qquad 20.46,\ 24.17 \text{ ev};\\ &(12|12)\equiv K\\ &\quad =0.69,\ 1.97,\ 3.87,\ 6.24 \text{ ev}. \end{aligned} \quad \begin{matrix}\\ \\ \\ \\ \\ \\ \\ \\ \text{(Zero}\\ \text{Differential}\\ \text{Overlap}\\ \text{Approximation)}\end{matrix} \quad (93)$$

These values are satisfactory for all but K, which comes out too small. Since K determines the singlet-triplet split and molecular orbital calculations of this quantity tend to come out too high (which may be called the singlet-triplet split catastrophe of molecular orbital theory), one might use the numerical values of Eq. (93) as an artificial means of improving the calculated spectrum without changing much else. The atoms-in-molecules correction affords another, non-artificial means for removing the singlet-triplet catastrophe, however, so that here the difference in the K values in Eqs. (92) and (93) will be regarded as undesirable. The difference can be removed by correcting for overlap. A method for doing this approximately was used in Sec. IV in going from Eq. (45) to Eq. (46). More exactly, one may merely retain the $1-S^2$ in the denominator in the expression for K:

$$J=\tfrac{1}{2}[(aa|aa)+(aa|bb)],$$
$$K=\tfrac{1}{2}(1-S^2)^{-1}[(aa|aa)-(aa|bb)]. \quad (94)$$

This amounts to assuming the Mulliken formulas of Eq. (70) exact without subsequently neglecting terms proportional to S^2. The following integral values are thus obtained:

$$\begin{aligned} &Z=0.72,\ 1.07,\ 1.43,\ 1.79;\\ &(11|11)=(22|22)=(11|22)\equiv J\\ &\quad =11.48,\ 16.28,\\ &\qquad 20.46,\ 24.17 \text{ ev};\\ &(12|12)\equiv K\\ &\quad =2.61,\ 4.15,\\ &\qquad 5.91,\ 7.91 \text{ ev}. \end{aligned} \quad \begin{matrix}\\ \\ \\ \\ \\ \\ \\ \\ \text{(Mulliken}\\ \text{Approximation)}\end{matrix} \quad (95)$$

The agreement between the values of Eq. (95) and the exact values of Eq. (92) is both startling and encouraging; *to obtain simplified schemes for treating sigma electrons one may apply Mulliken-type approximation formulas throughout, almost with abandon.*

Combined with theoretically calculated core integrals, the electronic repulsion integrals of Eq. (95) lead to essentially the same molecular properties as did the integrals of Eq. (92), that is, to essentially the (unsatisfactory) results of Eq. (91). There remains to see first whether the results can be improved by applying atoms-in-molecules corrections and then whether core integrals could be evaluated better empirically than theoretically. (Empirical evaluation of core integrals without first application of atoms-in-molecules corrections cannot be of much help because the singlet-triplet catastrophe would remain.)

If S^2 were negligible, the way to apply atoms-in-molecules corrections would be merely to replace the theoretical $(aa|aa)_t$ in J and K with the empirical value

$$(aa|aa)=I_H-A_H=13.60-0.75=12.85 \text{ ev}.^{11}$$

That is, one would subtract a quantity

$$\delta\equiv\tfrac{1}{2}[(aa|aa)_t-12.85)] \quad (96)$$

from both J and K. Actually S^2 is not negligible in this case, so that replacement of $(aa|aa)_t$ with 12.85 is not quite equivalent to correcting J and K as indicated, and one must be careful what one does (compare the discussion in Sec. IV.D). Moffitt's own procedure would be to subtract δ from J and K except in the matrix element $H_{12}=K$, for which the correction according to him would be $-(1+S^2)\delta/(1-S^2)$.[17] This procedure will be employed here, although results

not much different would be obtained if the same correction, simply $-\delta$, were applied to K everywhere. (H_{12} is of secondary importance in determining the energy level scheme.) Corrected values for the electronic repulsion integrals then are as follows:

$$\begin{aligned} &Z=0.72,\ 1.07,\ 1.43,\ 1.79;\\ &J=11.82,\ 13.58,\ 14.72,\ 15.39\text{ ev};\\ &K=2.95,\ 1.45,\ 0.17,\ -0.77\text{ ev};\\ &H_{12}=4.67,\ -3.54,\ -5.85,\ -5.44\text{ ev}. \end{aligned} \quad \begin{matrix}\text{(Mulliken Approximation and Moffitt Correction)}\\ \\ \\ \\ \end{matrix} \quad (97)$$

The independent core integrals may be taken as the molecular integrals I_{11} and I_{22}, related to α and β through the identities

$$I_{11}=(\alpha+\beta)/(1+S),\quad I_{22}=(\alpha-\beta)/(1-S). \quad (98)$$

Purely theoretically, one finds:

$$\begin{aligned} &Z=0.72,\ 1.07,\ 1.43,\ 1.79;\\ &I_{11}-E_H=-13.89,\ -18.46,\ -20.94,\ -18.65\text{ ev};\\ &I_{22}-E_H=-2.91,\ -0.37,\ 3.59,\ 11.31\text{ ev}. \end{aligned} \quad \begin{matrix}\\ \text{(Purely Theoretical)}\\ \\ \\ \end{matrix} \quad (99)$$

These values then give:[42]

$$\begin{aligned} &Z=0.72,\ 1.07,\ 1.43,\ 1.79;\\ &E_V-E_N=15.0,\ 20.6,\ 25.4,\ 29.7\text{ ev};\\ &E_T-E_N=9.2,\ 17.7,\ 25.1,\ 31.2\text{ ev};\\ &I=16.7,\ 18.8,\ 20.5,\ 17.4\text{ ev};\\ &2E_H-E_N=-2.5,\ 4.2,\ 8.4,\ -2.9\text{ ev}. \end{aligned} \quad \begin{matrix}\\ \text{(Mulliken Approximation, Moffitt Correction and Theoretical Treatment of the Core)}\\ \\ \\ \\ \end{matrix} \quad (100)$$

Comparison of these results with the purely theoretical results of Eq. (91) and the experimental results of Eq. (90) shows that application of the Moffitt correction has improved the singlet-triplet split a great deal and the binding energy somewhat,[43] but it has left the mean of the singlet and triplet excitation energies still too high for $Z\doteq 1$.

Finally, empirical adjustment of core integrals may be carried out. Taking I_{11} and I_{22} to fit the observed singlet excitation energy and the binding energy, for example, one obtains:

$$\begin{aligned} &Z=0.72,\ 1.07,\ 1.43,\ 1.79;\\ &E_V-E_N=12.5,\ 12.5,\ 12.5,\ 12.5\text{ ev};\\ &E_T-E_N=6.6,\ 9.6,\ 12.2,\ 14.0\text{ ev};\\ &I=15.8,\ 13.0,\ 13.2,\ 12.1\text{ ev};\\ &2E_H-E_N=4{,}8.\ 4.8,\ 4.8,\ 4.8\text{ ev}. \end{aligned} \quad \begin{matrix}\\ \text{Mulliken Approximation, Moffitt Correction and Empirical Treatment of the Core)}\\ \\ \\ \\ \end{matrix} \quad (101)$$

The values of the core integrals which give these results are as follows:

$$\begin{aligned} &Z=0.72,\ 1.07,\ 1.43,\ 1.79;\\ &I_{11}-E_H=-12.8,\ -12.4,\ -12.9,\ -12.7\text{ ev};\\ &I_{22}-E_H=-4.4,\ -2.0,\ -2.0,\ -0.6\text{ ev}. \end{aligned} \quad \begin{matrix}\\ \text{(Empirical)}\\ \\ \\ \end{matrix} \quad (102)$$

One could alternatively fit the observed ionization potential, but then the binding energy comes out poorly. Again (compare Sec. IV.C) the atoms-in-molecules correction is seen to improve the situation as regards the electronic spectrum but to be of no help in the matter of the ionization potential. Thus, such corrections are promising but must be applied with care. The binding energy of 8 volts obtained in Eq. (100) is an example of the sort of false result one may get—the shelter of the variational principle has been lost, so to speak; it has been replaced by the firm but open base of atomic energy levels.

VII. DISCUSSION

Commentary on particulars having been included in previous sections, the discussion in the present section will be of a general nature.

First, a few remarks will be made about the proposed formula for the effective electronegativity of an atom a in a diatomic molecule, Eq. (25):

$$y_a\equiv\tfrac{1}{2}(I_a+A_a)+P_a. \quad (103)$$

Here I_a and A_a are the valence-state ionization potential and electron affinity of atom a, respectively, I_a also a function of the valence state of the positive ion, A_a also a function of the valence state of the negative ion; and P_a is the total attraction of the valence electron on atom a for all other atoms in the molecule in their (perhaps hypothetical) neutral condition. If in a diatomic molecule there is a net positive charge Q transferred from atom b to atom a as the result of a greater electronegativity of atom b than of atom a, in the final actual state of the molecule the separate atoms will not be neutral—the original electronegativity difference will have been compensated in part. In fact,

[42] In the calculation of $2E_H-E_N$, the binding energy, the nuclear repulsion term $e^2/R=19.47$ ev must be included in E_N.

[43] Scherr (reference 40) has also noted that the Moffitt correction improves the binding energy of hydrogen computed in this manner for $Z\doteq 1$.

theoretical work of Mulliken[44] has shown that the effective electronegativity after such a charge transfer would be

$$z_a \equiv \tfrac{1}{2}(I_a+A_a)+\tfrac{1}{2}Q(I_a-A_a)+P_a. \qquad (104)$$

This equation should give the residual electronegativity of atom a in the final molecule, but Eq. (103) seems a better measure of the tendency for charge to be transferred between neutral atoms as they are forming a bond. Mulliken's formula for effective electronegativity is not actually Eq. (104) but what one obtains from it upon inserting the atoms-in-molecules formula $A_a=I_a-(aa|aa)$. Put the other way around, the atoms-in-molecules correction reduces Mulliken's formula to Eq. (104), which in turn reduces to Eq. (103) when Q is set equal to zero. Equation (103) is a slight modification of Mulliken's own original electronegativity definition.[11] Whether the penetration terms P can be effectively computed is problematical, but their physical implications should be born in mind in any case.

The present method may be said to be both an approximation to the method of Moffitt and a modification of it. If core integrals are computed theoretically and all integrals of the type $(aa|bb)$ strictly interpreted as integrals over Slater orbitals of fixed predetermined Z values, then the two methods should give much the same results, the extent of their divergence being determined by errors (if any) in Mulliken-type approximation formulas and the size of certain terms of order S^2 neglected in the present method. If on the other hand core integrals or integrals $(aa|bb)$ are adjusted empirically, there is a difference. Moffitt appears undecided as to the desirability of evaluating core integrals empirically;[45] to the present authors it seems best to so treat them, and integrals $(aa|bb)$ as well.

Several general suggestions regarding quantum-chemical techniques are implicit in the work of the previous sections. It may be well to make them explicit:

(1) For heteronuclear molecules which have natural homonuclear analogs, in the sense that propylene is "like" ethylene or pyridine is "like" benzene, variational calculations of wave functions may conveniently be carried out starting from functions which are correct (or approximately correct) wave functions for various states of the analogs. Electronegativity differences then enter final formulas in a perspicuous way.

(2) Quantum-mechanical definition (and treatment) of inductive and mesomeric effects of molecular perturbations may be achieved as follows. Suppose one has a molecule (or portion of a molecule) adequately described using a given number of atomic orbitals and considering explicitly a given number of electrons (that such a description must exist is axiomatic in chemical discussions of this topic). Inductive effects of a perturbation will be those that can be accounted for without increasing the number of electrons or the number of orbitals in the description; mesomeric effects will be those that cannot be so accounted for; i.e. the difference between total effects and inductive effects.

(3) Since a great saving of labor results when Mulliken-type approximation formulas [see Eq. (70)] are used to simplify molecular calculations, widespread application of such formulas profitably may be made in contexts in which high accuracy is not required.[46]

The purpose of this paper has been not to obtain specific numerical results for specific cases, but to obtain insight regarding the validity of the methods being employed. Tables of "final results" for ethylene, formaldehyde, and hydrogen intentionally have therefore been omitted. The conclusions of the work are rather of a qualitative type:

(1) The natural way in which electronegativities enter the formulas shows that the formulation is itself natural.

(2) The theory is quantitatively successful enough for ethylene, formaldehyde, and hydrogen to encourage further extensive applications to π-electron systems and intensive studies of σ-electron systems.

(3) The inclusion of spectra, ionization potentials, and binding energies in a single semiempirical scheme will not be easy, even for a class of related molecules (e.g. alternant hydrocarbons). Very careful studies of parameter values are required to achieve this.

Much experience thus remains to be gained, but one may proceed to acquire it with confidence.

In conclusion, attention may be called to recent vigorous work of Dr. J. A. Pople developing and applying a method very similar to the one that has been here advocated.[47] RGP is indebted to Dr. Pople for a number of helpful discussions.

[44] See reference 25, especially Sec. 17. The authors are grateful to Professor Mulliken for helpful correspondence concerning this material.

[45] See, however, W. Moffitt, Proc. Roy. Soc. (London) **A210**, 224 (1951) and, more recently, W. Moffitt, J. Chem. Phys. **22**, 320 (1954). In both papers core integrals are treated empirically to great advantage.

[46] Compare Barker, Eyring, Thorne, and Baker, J. Chem. Phys. **22**, 699 (1954).

[47] J. A. Pople, Trans. Faraday Soc. **49**, 1375 (1953); A. Brickstock and J. A. Pople, Trans. Faraday Soc. **50**, 901 (1954).

Substituted Methanes. XXII.* Infrared Spectra of $CHBrF_2$, and Potential Constants and Calculated Thermodynamic Properties of $CHBrF_2$ and $CDBrF_2$

ANN PALM, FRED L. VOELZ, AND ARNOLD G. MEISTER
Spectroscopy Laboratory,† Department of Physics, Illinois Institute of Technology, Chicago 16, Illinois
(Received May 2, 1954)

The near infrared spectrum of gaseous bromodifluoromethane was obtained using a Perkin-Elmer Model 21 Spectrometer equipped with a NaCl prism. A set of potential constants was determined for $CHBrF_2$ by means of the Wilson FG matrix method, using a potential energy function with all possible second degree terms. The same potential constants were used to calculate the fundamentals of $CDBrF_2$. Finally the heat content, free energy, entropy, and heat capacity were calculated for 12 temperatures from 100 to 1000°K, for the ideal gaseous state at 1 atmos pressure, using the observed fundamentals for $CHBrF_2$ and the calculated ones for $CDBrF_2$.

INTRODUCTION

PRIOR to this investigation, the infrared spectrum of $CHBrF_2$ had been obtained by Plyler and Acquista.[1] No data could be found in the literature for the Raman spectrum but an attempt was made to predict, by a graphical method, the wave numbers for the fundamental vibrations.[2] Stepanov,[3] using a simple valence force potential function, calculated the wave numbers of all the fundamentals. For the higher wave numbers his predicted values agreed very well with those observed in the infrared, but for the lower wave numbers the agreement is not as good. So, it was felt that a normal coordinate treatment, using the most general quadratic potential function, should be carried out and this was done in the present investigation. Values for the thermodynamic functions of $CHBrF_2$ have been calculated by Gelles and Pitzer[4] but no observed values were found. No previous vibrational spectral data or thermodynamic functions could be found for $CDBrF_2$.

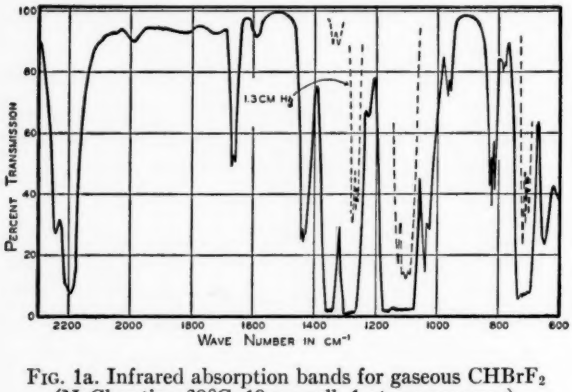

FIG. 1a. Infrared absorption bands for gaseous $CHBrF_2$ (NaCl optics, 30°C, 10-cm cell, 1 atmos pressure).

EXPERIMENTAL RESULTS

The sample of $CHBrF_2$ was obtained through the courtesy of Dr. R. C. McHarness of the Jackson Laboratory of E. I. duPont de Nemours and Company. Since the substance is a gas at room temperature, the infrared spectrum of the gas was obtained with a Perkin-Elmer Model 21 spectrometer equipped with a NaCl prism. A 10 cm gas cell was used with pressures of 1 atmos or less, depending on the intensity of the band being investigated. The data obtained are in satisfactory agreement with the previously reported values of Plyler and Acquista[1] and both sets of data along with the probable assignments are given in Table I. Since the $CHBrF_2$ molecule has the symmetry of the C_s point group, six of its fundamentals belong to the a' type while the remaining three are of the a'' type. All fundamentals, overtones, and combinations are allowed in both the infrared and the Raman spectrum. The observed infrared spectrum is shown in Fig. 1.

NORMAL COORDINATE TREATMENT

A Wilson[5] FG matrix calculation of the wave numbers of the fundamentals was undertaken to verify the assignments and to test the transferability of potential constants from structurally related molecules. The descriptive notation introduced by Davis *et al.*[6] was

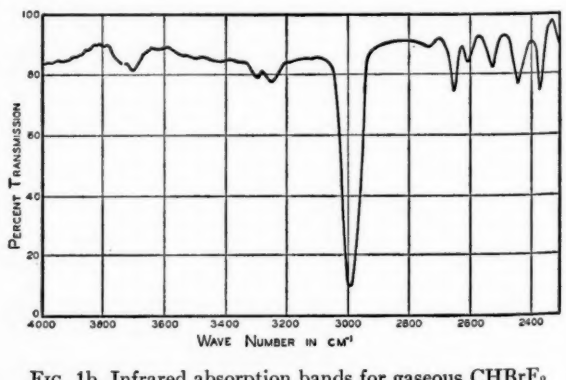

FIG. 1b. Infrared absorption bands for gaseous $CHBrF_2$ (NaCl optics, 30°C, 10-cm cell, 1 atmos pressure).

* For previous papers of this series, see J. Chem. Phys. **18**, 346, 1073, 1076, 1081 (1950); **19**, 119, 784, 1561 (1951); **20**, 454, 1949, 1979 (1952); **21**, 158, 189, 242, 930, 1778, 1781, 1903 (1953); J. Opt. Soc. Am. **43**, 1061 (1953); J. Chem. Phys. **22**, 193, 1042 (1954); **23**, 700 (1955).

† Publication No. 103.

[1] E. K. Plyler and N. Acquista, J. Research Natl. Bur. Standards **48**, 92 (1952).

[2] G. Glockler and G. R. Leader, J. Chem. Phys. **8**, 699 (1940).

[3] B. I. Stepanov, Compt. rend. acad. sci. U.R.S.S. **45**, 56 (1944).

[4] E. Gelles and K. S. Pitzer, J. Am. Chem. Soc. **75**, 5259 (1953).

[5] E. B. Wilson, Jr., J. Chem. Phys. **7**, 1047 (1939); **9**, 76 (1941).

[6] Davis, Cleveland, and Meister, J. Chem. Phys. **20**, 454 (1952).

TABLE I. Infrared spectral data and assignments for bromodifluoromethane.[a]

	Plyler and Acquista			Present results				
	ν	I		ν	I	ν_C	Assignment	Type
	240[b]	···				244	ν_6	a'
	323	vw				323	ν_9	a''
P	572	···						
Q	577	s				579	ν_5	a'
R	584	···						
	644	m		646	m	646	$2\nu_9$	A'
P	708	···	P	709	···			
Q	718	s	Q	717	vs	708	ν_4	a'
R	724	···	R	724	···			
	···			781		785	$\nu_8-\nu_9$[c]	A'
P	810	···	P	811	···			
Q	818	w	Q	818	m	817	$\nu_5+\nu_6$	A'
R	824	···	R	825	···			
	875	vw	P	884	···			
			Q	892	s	900	$\nu_5+\nu_9$[c]	A''
	893	vw	R	896	···			
				959	w	958	$\nu_4+\nu_6$	A'
	964	vw		965	w	957	$\nu_2-\nu_9$	A''
	···			1021	m	1021	$\nu_7-\nu_9$	A'
	1033	m		1033	s	1040	$\nu_2-\nu_6$,	A'
							$\nu_4+\nu_9$	A''
P	1099	···	P	1101	···			
Q	1108	s	Q	1110	vs	1107	ν_8	a''
R	1123	···	R	1123	···			
	1135	s		1136	vs	1130	ν_3	a'
	1185	w		···		1198	$\nu_4+2\nu_6$	A'
	···			1221	m	1223	$\nu_5+2\nu_9$[c]	A'
P	1274	···	P	1274	···			
Q	1280	s	Q	1280	vs	1276	ν_2	a'
R	1289	···	R	1289	···			
P	1337	···	P	1339	···			
Q	1344	s	Q	···	vs	1344	ν_7	a''
R	1351	···	R	1351	···			
			P	1429	···			
	1434	w	Q	1433	m	1436	$2\nu_4$	A'
			R	1441	···			
	1600	vw		1600	w	1603	$\nu_2+\nu_9$	A''
				1667	m	1667	$\nu_7+\nu_9$	A'
	1675	vw		1679	m	1685	$\nu_5+\nu_8$	A''
				1726	vw	1723	$\nu_1-\nu_2$	A'
	1926	w		···		1921	$\nu_5+\nu_7$	A''
	1988	vw		1995	w	1998	$\nu_2+\nu_4$	A'
	2197	m		2203	s	2216	$2\nu_8$	A'
	2252	w		2250	m	2243	$\nu_3+\nu_8$	A''
	2352	vw		2369	w	2388	$\nu_8+\nu_2$	A''
	2438	vw		2443	w	2452	$\nu_8+\nu_7$	A'
	2525	vw		2539	w	2539	$2\nu_8+\nu_9$,	A''
							$2\nu_4+\nu_8$	A''
	2610	vw		2623	w	2624	$\nu_2+\nu_7$	A''
	2659	vw		2669	w	2688	$2\nu_7$	A'
				2753	w	2763	$\nu_1-\nu_6$	A'
	3003	s		3013	vs	3003	ν_1	a'
	3267	vw		3267	w	3243	$\nu_1+\nu_6$	A'
				3316	w	3326	$\nu_1+\nu_9$	A''
	3716	vw		3713	w	3721	$\nu_1+\nu_4$	A'
				3749	w	3759	$\nu_2+\nu_3+\nu_7$	A''
	4080	w		···		4111	$\nu_1+\nu_8$	A''
	4237	w		···		4283	$\nu_1+\nu_2$	A'

[a] ν = wave number in cm^{-1} (K); I = estimated relative intensity (vs = very strong, s = strong, m = medium, w = weak, vw = very weak); ν_c = calc value.
[b] Predicted wave number from combination bands.
[c] Tentative assignments.

used for the potential constants and the internal coordinates. The symmetry coordinates used, and, therefore, the elements of the F and G matrices are formally the same as those given in paper XIV of this series.[7]

In the first attempt to calculate the fundamentals,

[7] Weber, Meister, and Cleveland, J. Chem. Phys. **21**, 930 (1953).

TABLE II. Potential constants for $CHBrF_2$, CBr_2F_2, CHF_3, and CH_2F_2.[a]

Type	$CHBrF_2$	CBr_2F_2	CHF_3	CH_2F_2
f_b	3.30000[b]	2.9132	···	···
f_f	6.27990	6.1400	6.2460	6.2279
f_h	4.97680	···	5.0323	4.9645
$f_b{}^f$	0.66281	0.66281	···	···
$f_b{}^h$	0.05890	···	···	···
$f_f{}^f$	0.93260	0.80996	0.87900	0.86095
$f_f{}^h$	0.25305	···	0.25305	0.25305
$f_b{}^{bf}$	0.15000	0.28016	···	···
$f_b{}^{bh}$	0.37500	···	···	···
$f_b{}^{ff}$	−0.24000	−0.24816	···	···
$f_b{}^{fh}$	−0.17000	···	···	···
$f_h{}^{bh}$	0.23249	···	···	···
$f_h{}^{bf}$	0.15000	···	···	···
$f_h{}^{ff}$	0.25000	···	···	0.40000
$f_h{}^{fh}$	0.32000	···	···	0.30547
$f_f{}^{bf}$	0.29605	0.29605	···	···
$f_f{}^{bf'}$	−0.27382	−0.27382	···	···
$f_f{}^{bh}$	−0.18000	···	···	···
$f_f{}^{ff}$	0.40000	0.37704	0.41959	0.41770
$f_f{}^{fh}$	0.43933	···	0.43933	0.45725
$f_f{}^{f'h}$	−0.21967	···	−0.21967	−0.23759
f_{bf}	1.07858	1.1750	···	···
f_{bh}	0.63789	···	···	···
f_{ff}	2.13953	1.5409	2.1523	2.1112
f_{fh}	0.89222	···	0.94629	0.94629
$f_{bf}{}^{bf'}$	−0.01122	0.11594	···	···
$f_{bf}{}^{bh}$	0.32194	···	···	···
$f_{bf}{}^{ff}$	0.04750	0.045877	···	···
$f_{bf}{}^{fh}$	−0.07500	···	···	···
$f_{bf}{}^{f'h}$	0.02500	···	···	···
$f_{bh}{}^{ff}$	0.05000	···	···	···
$f_{bh}{}^{fh}$	0.10000	···	···	···
$f_{ff}{}^{fh}$	0.25910	···	0.31007	0.32874
$f_{fh}{}^{f'h}$	0.08898	···	0.17900	0.13964

[a] Bond stretching and bond interaction constants are expressed in md/A; angle-bond interaction constants are in md/rad; and angle, and angle-angle interaction constants are in md A/rad^2.
[b] This number of significant figures is not justified except that they are necessary to give the best reproduction of the observed wave numbers and to secure internal consistency in the calculations.

potential constants were transferred mainly from CF_3H,[8] CBr_2F_2,[9] CF_3Br,[10] and $CHBrCl_2$.[11] The final set of potential constants is given in Table II along with similar potential constants for CBr_2F_2, CF_3H, and CH_2F_2 for comparison. In cases where values for potential constants had not been obtained from previous investigations in this laboratory on halogen substituted methanes, simplifying assumptions, such as $f_{bf}{}^{bh}=f_{ff}{}^{h}$ or $f_b{}^{fh}=f_b{}^{ch}$, were made. The modified potential constants given in Table II furnish a set of wave numbers for the fundamentals that are within two percent or less of the observed values. Closer reproduction of the observed values could be attained only at the expense of distorting some of the potential constants from the pattern already obtained from previously investigated halogenated methanes. This was found to be especially true for the C−Br stretching constant (f_b), since the value given in Table II is somewhat larger than for

[8] Decker, Meister, and Cleveland, J. Chem. Phys. **19**, 784 (1951).
[9] Decker, Meister, Cleveland, and Bernstein, J. Chem. Phys. **21**, 1781 (1953).
[10] McGee, Cleveland, Meister, Decker, and Miller, J. Chem. Phys. **21**, 242 (1953).
[11] Unpublished investigation of S. R. Polo and A. G. Meister.

TABLE III. Calculated and observed values of the fundamentals of gaseous $CHBrF_2$ and $CDBrF_2$.

Type	Frequency	Wave number in cm^{-1} (K) $CHBrF_2$ Calculated	$CHBrF_2$ Observed	$CDBrF_2$ Calculated
a'	ν_1	3003	3003	2208
a'	ν_2	1276	1280	1134
a'	ν_3	1130	1135	1019
a'	ν_4	708	718	623
a'	ν_5	579	577	578
a'	ν_6	244	240[a]	240
a''	ν_7	1344	1344	1109
a''	ν_8	1107	1108	977
a''	ν_9	323	323	323

[a] Predicted wave number from combination bands.

TABLE IV. Heat content, free energy, entropy, and heat capacity of $CHBrF_2$ for the ideal gaseous state at 1 atmos pressure (cal $mole^{-1}$ deg^{-1}).

T(°K)	$(H^0-H_0^0)/T$	$-(F^0-H_0^0)/T$	S^0	C_p^0
100	8.26	49.93	58.19	9.21
200	9.39	55.99	65.38	11.77
273.16	10.26	59.05	69.31	13.48
298.16	10.56	59.96	70.51	14.04
300	10.57	60.02	70.59	14.08
400	11.72	63.22	74.95	16.17
500	12.79	65.95	78.74	17.87
600	13.75	68.37	82.12	19.20
700	14.61	70.56	85.17	20.24
800	15.36	72.56	87.92	21.06
900	16.03	74.41	90.44	21.72
1000	16.63	76.15	92.78	22.26

other brominated methanes. This change is believed due to differences in anharmonicity corrections in going from one halogenated methane to another when potential constants are transferred. The largest difference between the present calculated values and those of Stepanov[3] exists for the ν_6 fundamental since the values found in each case were 244 and 380 cm^{-1}, respectively.

The set of potential constants determined for $CHBrF_2$ were then used to calculate the wave numbers of the fundamentals of $CDBrF_2$. These values are given in Table III and as a check the Teller-Redlich product rule[12,13] was used. Using the calculated fundamentals of $CDBrF_2$ and the observed fundamentals of $CHBrF_2$ the ratios for the a' and a'' wave numbers was found to be 0.50906 and 0.72701, respectively, while the product rule gives 0.51477 and 0.71908. The close agreement between the calculated and expected ratios indicates that the values given for the wave numbers of the fundamentals of $CDBrF_2$ in Table III should be reasonable.

[12] G. Herzberg, *Infrared and Raman Spectra of Polyatomic Molecules* (D. Van Nostrand Company, Inc., New York, 1947), p. 232.

[13] K. S. Pitzer, *Quantum Chemistry* (Prentice-Hall, Inc., New York, 1953), p. 452.

TABLE V. Heat content, free energy, entropy, and heat capacity of $CDBrF_2$ for the ideal gaseous state at 1 atmos pressure (cal $mole^{-1}$ deg^{-1}).

T(°K)	$(H^0-H_0^0)/T$	$-(F^0-H_0^0)/T$	S^0	C_p^0
100	8.27	50.01	58.28	9.22
200	9.46	56.09	65.55	12.05
273.16	10.42	59.18	69.60	14.06
298.16	10.75	60.11	70.86	14.71
300	10.77	60.17	70.94	14.75
400	12.07	63.46	75.53	17.05
500	13.25	66.28	79.53	18.83
600	14.30	68.79	83.09	20.17
700	15.21	71.06	86.28	21.19
800	16.01	73.15	89.16	21.98
900	16.71	75.07	91.78	22.59
1000	17.32	76.98	94.21	23.08

TABLE VI. Bond distances, masses, and principal moments of inertia for $CHBrF_2$ and $CDBrF_2$.

	$CHBrF_2$	$CDBrF_2$
C—H	1.093[a]	...
C—F	1.36	1.36
C—Br	1.91	1.91
C—D	...	1.093
I_{xx}	172.7	176.1
I_{yy}	214.8	216.0
I_{zz}	51.63	53.81
m_C = 12.01139		m_{Br} = 79.9105
m_H = 1.00785		m_F = 19.0000
m_D = 2.01418		

[a] Bond distances, moments of inertia, and masses are in A, awu A^2, and awu, respectively.

THERMODYNAMIC PROPERTIES

The heat content, free energy, entropy, and heat capacity at constant pressure for $CHBrF_2$ and $CDBrF_2$ were calculated for 12 temperatures in the 100°K to 1000°K range, using a rigid rotator, harmonic oscillator approximation for the ideal gaseous state at 1 atmos pressure. These values appear in Tables IV and V, while the values used for the bond distances, masses, and principal moments of inertia are given in Table VI. The observed fundamentals listed in Table III were used for $CHBrF_2$ and the calculated fundamentals for $CDBrF_2$. All fundamentals are nondegenerate and the symmetry number is 1. Tetrahedral angles were assumed for both molecules.

Gelles and Pitzer[4] have calculated thermodynamic functions for $CHBrF_2$ and their results are in reasonable agreement with the present investigation.

ACKNOWLEDGMENTS

This investigation was part of a research program which has been aided by a contract with the Office of Ordnance Research, U. S. Army; and by grants from the American Academy of Arts and Sciences, the Research Corporation, and the Socony-Vacuum Laboratories. The authors are thankful for this assistance.

Dissociation by Impacts of the Second Kind

W. E. GROTH, *Gibbs Chemical Laboratory*

AND

O. OLDENBERG, *Lyman Laboratory of Physics, Harvard University,* Cambridge, Massachusetts*

(Received May 28, 1954)

The process by which an excited Kr atom in an impact of the second kind dissociates an N_2 molecule is investigated by comparison with related processes. (1) The production of free N atoms is not due to an atom transfer reaction. (2) It is not due to the "resonance" transfer of electronic energy of Kr′ directly into vibrational energy of N_2 leading to dissociation. (3) It is due to the transfer of electronic energy of Kr′ into electronic energy of N_2. The simplest interpretation is the production of a repulsive level of N_2 which immediately dissociates.

IN the present paper we try to analyze an important photochemical process, the dissociation of a molecule by an impact of the second kind, more specifically, the photochemical dissociation of the nitrogen molecule by excited krypton. This process was recently experimentally investigated by one of us.[1] The mixture of Kr and N_2 was intensely illuminated with the light from a krypton lamp. This light (several lines near 1200 A) produced only the lowest excited levels of the Kr atoms, near 10 ev. (The higher energy lines are less intensely emitted from the lamp, less strongly absorbed by the Kr gas, and, moreover, hardly transmitted by the LiF window.) Hence we are concerned with the effect of Kr′ (10 ev) on nitrogen molecules. We shall compare this collision process with the most thoroughly explored process of this type, that is, the dissociation of H_2 by excited Hg atoms described by Cario and Franck[2] in their first exploration of impacts of the second kind.

We shall discuss three possible effects of the impact, (1) the *atom transfer reaction* forming, for example, HgH, (2) the straight chemical dissociation which is due to excitation of *vibrational energy*, and (3) the dissociation which is due to excitation of electronic energy of the molecule.

(1) ATOM TRANSFER REACTION

The experiment of Cario and Franck proved only that excited mercury atoms when colliding with hydrogen molecules generate free hydrogen atoms. It remained uncertain whether the collision $Hg'+H_2$ dissociates the hydrogen molecule into free atoms or instead binds one of the atoms to the Hg, thus producing HgH+H. This latter result may be assumed, at least as an alternative, since in the same experiment the HgH spectrum was observed.[3] There is no such alternative in the collision of an excited Kr atom with a nitrogen molecule since the Kr atom in its normal state, being a rare gas atom, is unable to form a stable molecule, KrN. It is true that the excited atom, Kr′, may be able to form a molecule. However, we must assume that the excited atom Kr′ consumes its energy of excitation (10 ev) in dissociating an N_2 molecule (energy of dissociation 9.76 ev) so that for the eventual formation of a molecule by the same process only non-excited Kr is available. Hence one must conclude that Kr′ dissociates the N_2 into free atoms, which is different from the case just considered in which the formation of HgH is an alternative.

(2) TRANSFER OF ELECTRONIC ENERGY INTO VIBRATION

Conventionally, the transfer of energy in an impact of the second kind is supposed to show a preferred probability in the case of resonance. In our case resonance implies that the impact of the second kind transfers electronic energy directly into *vibration* of such an amount that dissociation occurs, excluding the excitation of any other degree of freedom. However, the application of the idea of resonance to this particular impact of the second kind has been questioned.[4]

We may as well investigate the reverse process, i.e., the recombination of a pair of atoms which, in a triple collision, transfer their total energy to a third body and so excite its electronic system. The experimental evidence regarding the reverse process is as follows. Atomic hydrogen excites only the *D* lines of the spectrum of sodium atoms although the recombination energy available (4.48 ev) would be sufficient to excite two more lines of the principal series.[5] Their absence proves that the total energy of recombination is not transferred to the electronic system of the colliding Na atom. Vice versa, it is not to be expected that an atom with just sufficient energy of excitation will dissociate a hydrogen molecule, although the condition of "resonance" is fulfilled.

The evidence based on excitation of the atomic spectrum of mercury by active nitrogen, i.e., atomic nitrogen, is similar but less conclusive. We shall accept

* This work is connected with a research program supported by the Air Force Cambridge Research Center and the Office of Naval Research.

[1] W. Groth, Z. physik. Chem. **1**, 300 (1954).
[2] G. Cario and J. Franck, Z. Physik **11**, 161 (1922).
[3] J. Kaplan, Nature **123**, 162 (1929).
[4] O. Oldenberg, Phys. Rev. **87**, 786 (1952).
[5] F. L. Mohler, Phys. Rev. **29**, 419 (1927).

the value 9.76 ev for the energy of dissociation.[6] Active nitrogen excites mercury atoms up to an energy of 9.51 ev. However, the next higher level, at 9.65 ev, fails to appear even after a forty times longer exposure. Furthermore, the high levels up to 9.51 ev show spectral lines with intensities *decreasing toward the limit*, indicating the increasingly rare occurrence of the higher levels.[7] This observation demonstrates that there is no probability for the *total* energy of recombination of N+N to be transferred to the excitation of Hg. Vice versa, there is no probability for the excitation energy of Hg (if exceeding 9.76 ev) to be *totally* transferred into the dissociation of a N_2 molecule. In other words, there is no reason for the conventional assumption that resonance gives a preference to the total transfer of electronic energy of an atom into vibrational energy, in particular dissociation, of a molecule. Hence we should not assume that excited Kr (10 ev) transfers its energy directly into vibration or dissociation of the N_2 molecule ($D=9.76$ ev).

(3) TRANSFER OF ELECTRONIC INTO ELECTRONIC ENERGY

Laidler[8] investigated several cases of impacts of the second kind in which the excitation energy of atoms dissociates molecules. Among his cases is the dissociation of H_2 by the impact of Hg′. Laidler explored all possible potential *curves* of the diatomic molecules HgH and H_2. By interpolation he found the potential *surfaces* of the three-atomic complex HgH_2. Intersections between two such surfaces indicate radiationless transitions. The principal limitation for such transitions is Wigner's rule which postulates that the sum of the electron spins is not changed by the transition. According to this theory the transition from the initial Hg+H_2 to the final Hg+H+H leads over as many as four intermediate potential surfaces, each individual transition obeying Wigner's rule. An alternative, simpler scheme is given by the transition $Hg(^3P_1)+H_2(^1\Sigma)\rightarrow Hg(^1S_0)+H_2(^3\Sigma)\rightarrow Hg(^1S)+H+H$, that is, the transfer of electronic energy from Hg′ into the repulsive level $^3\Sigma_u^+$ of the H_2 molecule which immediately dissociates.[9] However, Dr. Laidler kindly called my attention to the fact that presumably this simple reaction requires a considerable activation energy since the repulsive level of H_2 shows a steep rise of potential energy for decreasing distance of the atoms. At the normal nuclear distance of H_2 this potential energy is even twice as large as the energy of dissociation. It is true that the approach of Hg′ distorts this curve. This effect is visualized by the potential surfaces of Hg′+H+H which were plotted by Laidler.[8] The distortion, however, is presumably not strong enough to lower the potential barrier sufficiently. (Although the potential surfaces are known only for collinear approach of the three atoms involved, one may guess that for any other approach, too, such a barrier would exist.) The activation energy is neither supplied by the temperature nor by the energy of the $Hg(^3P_1)$. This consideration leaves little chance for the simple and otherwise plausible process mentioned.

A remarkable feature of the transfer, irrespective of its interpretation, is its great probability as is evident from the following estimate: Stuart[10] found that as little as 0.2 mm of hydrogen reduced the intensity of the resonance radiation of mercury to one-half of its original value. Beutler and Rabinowitsch[11] computed the corresponding effective distance of approach between Hg′ and H_2 to be 5.2 A.[12] Hence we must assume that the transfer of energy from Hg′ to H_2, whatever the detail of the process is, takes place over a distance of the order of magnitude 5.2 A, that is, seven times the internuclear distance of the H_2 molecule.

For the transfer of the energy of 10.0 ev of Kr′ to the N_2 molecule the complete system of possible potential surfaces has not been explored. However, the simple transfer of electronic energy into a repulsive level of the N_2 molecule may occur. It is true that the collision considered does not readily generate the repulsive level $^5\Sigma$ because of Wigner's rule. However, the level $^3\Sigma$ may be produced[13] at an energy in the continuous range above the limit of dissociation and so generate the pair of N atoms.

Our argument throws light on a related problem: the dissociation of the N_2 molecule by *electron impact*. Since all excited states of the N_2 molecule have potential minima not much shifted from that of the normal state, electron impact fails to endow the excited electronic state of N_2 with strong vibration. This theory explains the observed fact that the upper electronic levels of the N_2 molecule when excited by electron impact show little vibration. How is this fact reconciled with the other fact that active nitrogen manifests an ample percentage of dissociation? Presumably, electron impact excites repulsive levels which immediately dissociate. In addition, "dissociative recombination" as suggested by Mitra[14] is expected to contribute to the

[6] A. G. Gaydon, *Dissociation Energies* (John Wiley and Sons, Inc., New York, 1947), p. 159; G. Cario and L. H. Reinecke, Abhandl. der braunschweig. wiss. Ges. **1**, 8 (1949); Kistiakowsky, Knight, and Malin, J. Am. Chem. Soc. **73**, 2972 (1951); A. E. Douglas, Can. J. Phys. **30**, 302 (1952); Y. Tanaka (private communication); J. M. Hendrie, J. Chem. Phys. **22**, 1503 (1954).

[7] J. Okubo and H. Hamada, Phil. Mag. **5**, 375 (1928).

[8] K. J. Laidler, J. Chem. Phys. **10**, 46 (1942).

[9] A. S. Coolidge, Phys. Rev. **65**, 236 (1944).

[10] H. A. Stuart, Z. Physik **32**, 262 (1925).

[11] H. Beutler and E. Rabinowitsch, Z. physik. Chem. **8**, 403 (1930).

[12] The large value of this distance may suggest that a small part of the energy of Hg′, that is, the energy $^3P_1-^3P_0=0.219$ ev, is transferred into vibration of the H_2 molecule provided that this transfer is preferred by resonance. This, however, cannot happen since the lowest vibrational quantum of H_2 has an energy as high as 0.544 ev. Furthermore, a resonance transfer into several rotational quanta of H_2 is not to be expected since it would violate the conservation of angular momentum.

[13] G. Herzberg, *Spectra of Diatomic Molecules* (D. Van Nostrand Company, Inc., New York, 1950), second edition, p. 355.

[14] S. K. Mitra, Phys. Rev. **90**, 516 (1953).

production of free N atoms. This process which may be written

$$N_2^+ + e \rightarrow N' + N'$$

was suggested by Bates[15] as mainly responsible for the recombination of electrons and ions in the gas phase. Thus we understand that in an electric discharge through nitrogen dissociation occurs although no strongly vibrating molecules are produced.

We conclude that the dissociation of N_2 by excited Kr atoms may be interpreted by the intermediate excitation of a repulsive level of the molecule which immediately, i.e., within the time of one vibration, decomposes. The direct transfer of vibrational energy leading to dissociation seems less plausible.

[15] D. R. Bates, Phys. Rev. **78**, 492 (1950).

THE JOURNAL OF CHEMICAL PHYSICS VOLUME 23, NUMBER 4 APRIL, 1955

Measurement of Bond Moments in C_2H_2 and C_2D_2 from Infrared Intensities

EDWARD C. WINGFIELD AND JOSEPH W. STRALEY
Department of Physics, University of North Carolina, Chapel Hill, North Carolina
(Received August 16, 1954)

The absolute infrared absorption intensities in the active bending vibration ν_5 in C_2H_2 and C_2D_2 have been measured using the extrapolation method of Wilson and Wells. The intensities observed are $A_5(C_2H_2) = 2170 \times 10^{10}$ cycles/sec cm at NTP and $A_5(C_2D_2) = 1040 \times 10^{10}$ cycles/sec cm at NTP. These values indicate the bond moment associated with the CH and the CD bonds are $\mu_{CH} = 0.999 \pm 0.035$ debye and $\mu_{CD} = 0.941 \pm 0.033$ debye, respectively.

INTRODUCTION

THE work of Wells and Wilson[1] has made the measuring of the intensity of an infrared absorption band a well-established though remaining a somewhat difficult procedure. This paper will describe the measurement of the intensity of the bands associated with the infrared active bending mode in C_2H_2 and C_2D_2 and will indicate the conclusions that have been reached from this information.

By way of background it should be noted that the intensity of the asymmetric stretching vibration ν_3 in C_2H_2 located at 3287 cm^{-1} has been reported by Callomon, McKean, and Thompson.[2] They have found that the intensity of this band equals 835×10^{10} cycles/sec cm at NTP. From this measurement they have deduced the dependence of bond moment on internuclear distance $\partial\mu/\partial r_{CH}$ equals ± 1.6 debyes/A.

The infrared-active fundamental ν_5 is located at 729 cm^{-1} (13.7μ) and 539 cm^{-1} (18.6μ) in C_2H_2 and C_2D_2, respectively. Measurement of the intensities of these bands determine the magnitude of the bond moments associated with the CH and the CD bonds.

The technique of determining the absolute intensity of an absorption band in the gaseous state has been adequately discussed in the literature.[3-5] A Perkin-Elmer Model 112 double pass spectrometer equipped with NaCl and KBr prisms was used in this experiment. The gas under study was contained in a high pressure cell 5 centimeters long at partial pressures in the range from zero to a maximum of 4 cm Hg. Broadening of the rotational structure was attained through the use of nitrogen from a commercial cylinder at a pressure of 200 psi. To minimize error due to "envelope" effect the instrument was operated at minimum slit-maximum gain consistent with securing an intelligible record. The 13.7μ band in C_2H_2 was observed using a NaCl prism and with an equivalent slit width of 3.16 cm^{-1}; the 18.6μ band in C_2D_2 was observed using a KBr prism and an equivalent slit width of 2.13 cm^{-1}.

[1] E. Bright Wilson and A. J. Wells, J. Chem. Phys. **14**, 578 (1946).
[2] Callomon, McKean, and Thompson, Proc. Roy. Soc. (London) A208, 341 (1951).
[3] Welsh, Pashlen, and Dunn, J. Chem. Phys. **19**, 340 (1951).
[4] David Z. Robinson, J. Chem. Phys. **19**, 881 (1951).
[5] G. E. Hyde and D. F. Hornig, J. Chem. Phys. **20**, 647 (1952).

ACETYLENE

The acetylene used in this investigation was obtained from a lecture bottle furnished by Matheson Chemical Company. Its purity was rated at 99.5 percent. In order to remove the acetone which is always present in acetylene that is stored under pressure, the gas was filtered through sulfuric acid contained in three wash bottles equipped with siltered glass tips. This filtering process may introduce SO_2 and acid spray. These impurities, if present, were removed by filtering the gas through a dilute NaOH solution followed by a drying agent.

To determine the intensity of an infrared absorption band it is necessary to determine values of the quantity $\int \ln T_0/T d\nu$, where T_0 and T represent the radiant energy of the incident and transmitted beam in the frequency range $d\nu$. The values of this integral were determined by numerical integration and were plotted as a function of "equivalent path" L_e as in Fig. 1. The quantity L_e may be given the physical interpretation

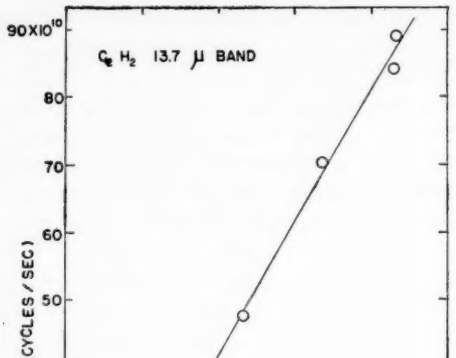

FIG. 1. Integrated apparent absorption coefficient as a function of equivalent path length at NTP for the 729 cm^{-1} band of C_2H_2 at a total pressure of 200 psi.

that it represents the length of cell which at atmospheric pressure would contain the same number of effective gas molecules as the actual cell. The slope of this curve at $L_e=0$ yields the intensity of the absorption band.

To verify our determination of the limiting value of the slope of this curve, values of the apparent intensity based on the experimentally determined points were plotted as a function of L_e. These data showed a trend that was best represented as a straight line of negative slope whose intercept at $L_e=0$ equals the intensity of the band.

The probable error in this quantity is estimated at 7 percent. This error was reached by making a least squares analysis of the deviations of the apparent intensities from the line referred to above. To this was added an estimate of the maximum error inherent in the technique. These included errors due to stray light, impurities in the sample, interaction of the sample with the broadening gas, and the envelope effect.

The intensity of the band in this way was determined to equal 2170±150 cycles/sec cm at NTP.

DEUTEROACETYLENE

The sample of deuteroacetylene used in this experiment was prepared by a method outlined by Leith and Morse.[6] The gas was obtained by adding heavy water to calcium carbide which reacts according to the equation,

$$CaC_2+2D_2O\rightarrow Ca(OD)_2+C_2D_2.$$

The gas was purified by being passed successively through a cold trap utilizing dry ice and acetone, three wash bottles containing sulfuric acid, and a final drying tower containing P_2O_5.

The experimental values of the integrated apparent absorption coefficient for the ν_5 fundamental in C_2D_2 are plotted as a function of L_e in Fig. 2. The intensity of the band is thereby found to be equal to 1040±70 $\times10^{10}$ cycles/sec cm at NTP where the value quoted and the probable error was determined as in the previous case.

CALCULATION OF BOND MOMENTS

It has been amply demonstrated through the analysis of the structure of vibration-rotation bands and through evidence secured by the Raman effect that both C_2H_2 and C_2D_2 are linear and symmetrical. These molecules, therefore, belong to the point group $D_{\infty h}$. Each possesses five fundamental vibrational modes only two of which are active in the infrared. The mode ν_5 of symmetry class π_u is the only mode of that particular class. The symmetry coordinate R_5 is therefore a linear function of the normal coordinate Q_5.

Wu,[7] utilizing the earlier work of Colby,[8] has shown that a suitable symmetry coordinate can be defined by

$$R_5=\frac{y_1+y_4}{2}-\frac{y_2+y_3}{2},$$

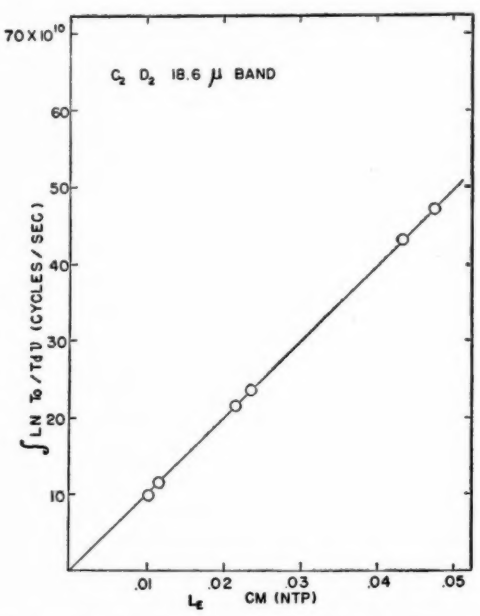

FIG. 2. Integrated apparent absorption coefficient as a function of equivalent path length at NTP for the 539 cm^{-1} band of C_2D_2 at a total pressure of 200 psi.

[6] L. C. Leith and A. T. Morse, Can. J. Chem. **30**, 924 (1952).

[7] T. Y. Wu, *Vibrational Spectra and Structure of Polyatomic Molecules* (National University of Peiking, Kun-Ming, China, 1939), p. 179.

[8] W. F. Colby, Phys. Rev. **47**, 388 (1935).

where y_1, y_2, y_3, and y_4 represent the off-axis displacements of the H, C, C, and H atoms, respectively. The normal coordinate associated with this mode can then be shown to be given by

$$Q_5=(\mu')^{\frac{1}{2}}R_5,$$

where the reduced mass μ' is given by

$$\mu'=2mM/(M+m),$$

where m and M represent the mass of the hydrogen and the carbon atoms, respectively.

We will let μ_T represent the total dipole moment of the molecule and μ_{CH} represent the dipole moment associated with the CH bond. We will assume that the total dipole moment is equal to the vector sum of the bond moments associated with the CH (or CD) bonds. By virtue of the symmetry of the molecule we will assume that there is no bond moment associated with the CC bond. We will further assume that the CH bond moments remain constant in magnitude and continue to lie along the bonds during the bending of the molecule. As a convention regarding the direction of the bond dipoles we will think of a positive bond moment as one that is directed out from the carbon atom, i.e., a positive value of μ_{CH} is associated with the condition that the hydrogen atoms constitute regions of net positive charge.

In the bending mode ν_5 the change in the total dipole moment is related to the vector change in the bond dipole by

$$\Delta\mu_T=2\Delta\mu_{CH}.$$

Assuming the bond dipole to remain parallel to the bond during the vibration,

$$\frac{\Delta\mu_{CH}}{\mu_{CH}}=\frac{\Delta R_5}{a},$$

where a represents the CH bond length. For small oscillations

$$\frac{\Delta\mu_{CH}}{\Delta R_5}=\frac{\partial\mu_{CH}}{\partial R_5}=\frac{\mu_{CH}}{a}.$$

Since

$$\frac{\partial\mu_T}{\partial R_5}=\frac{\partial\mu_T}{\partial Q_5}\frac{\partial Q_5}{\partial R_5},$$

it follows that

$$\frac{2\mu_{CH}}{a}=(\mu')^{\frac{1}{2}}\frac{\partial\mu_T}{\partial Q_5}.$$

The intensity of an infrared absorption band is related to the quantity $\partial\mu_r/\partial Q_5$ through the equation

$$A_5=\frac{2N\pi}{3c}\left(\frac{\partial\mu_T}{\partial Q_5}\right)^2,$$

where N represents the number of molecules per cm³ at NTP and the factor of 2 on the right has been introduced because we are here dealing with a doubly degenerate mode.

Combining the above equations,

$$\mu_{CH}=\pm\frac{a}{2}(\mu')^{\frac{1}{2}}\left(\frac{3A_5c}{2N\pi}\right)^{\frac{1}{2}}.$$

Substituting the measured values of A_5, the known value of the CH bond length a ($1.057\pm0.003\times10^{-8}$ cm),[9] and other physical constants into this equation it is found that $\mu_{CH}=\pm(0.999\pm0.035)$ debye and that $\mu_{CD}=\pm(0.941\pm0.033)$ debye.

It is to be observed that these measurements are in essential agreement with the value quoted by Kelly, Rollefson, and Schurin[10] who found through measurements of the index of refraction of acetylene that the bond moment associated with the CH bond equals $\pm(1.05\pm0.01)$ debye.

This experiment sheds no further light on the question of the sign of the bond moment. There can be no doubt that the magnitude of the CH bond moment varies markedly from one compound to another depending in some manner upon the environment in which the H atom finds itself. The argument of Coulson[11] that the bond moment associated with the CH bond is negative appears to be valid for methane. That it cannot be immediately inferred that this moment is also negative in acetylene can be seen from the fact that in certain other compounds positive values have been reported.[12] In a comparison of magnitudes and trends in a series of compounds Gent[13] has expressed the view that the polarity of the CH bond in acetylene is definitely positive. Further experiments will be required to establish the sign of many of these bond moments conclusively.

ACKNOWLEDGMENT

This work was financed in part by a grant from the National Science Foundation. We must also express our admiration of the skill with which Mr. Nestore DiCostanzo constructed the high pressure cell used in this work among other items vital to our progress.

[9] Herzberg, Patat, and Verleger, Z. Physik **102**, 1 (1936).
[10] Kelly, Rollefson, and Schurin, J. Chem. Phys. **19**, 1595 (1951).
[11] C. A. Coulson, Trans. Faraday Soc. **38**, 433 (1942).
[12] A. R. H. Cole and H. W. Thompson, Trans. Faraday Soc. **46**, 203 (1950).
[13] W. L. G. Gent, Quart. Rev. (London) **2**, 383 (1948).

Interaction of Methylene Deformation Frequencies in Paraffin Crystals II. A Theoretical Treatment of the Interaction of Vibrations

RICHARD S. STEIN
Department of Chemistry, University of Massachusetts, Amherst, Massachusetts
(Received August 20, 1954)

The splitting of the methylene deformation frequencies in crystals of *n*-paraffins is described in terms of interaction between nearest-neighbor molecules. On the basis of a simplified model, the order of magnitude of the splitting may be accounted for. Polarization behavior and changes occurring upon heating, cooling, and deuteration are described in terms of this model.

IN a previous paper[1] it was concluded that the splitting of the CH_2 rocking and bending deformation frequencies in the normal form of the crystals of paraffin hydrocarbons arises from a perturbation of the vibrations of a free paraffin molecule by the field of the crystal. The crystal structures of some *n*-paraffins ($C_{29}H_{60}$ and $C_{30}H_{62}$) have been determined by Müller[2] while that of polythene has been determined by Bunn[3] (Fig. 1). It is noted that in each unit cell there are two pairs of nearest neighbor hydrogen atoms (H_2 and H_3, and H_4 and H_7 in the figure) which are separated by 2.5 A while the next nearest neighbor hydrogen atoms (e.g., H_1 and H_5) are about 2.8 A apart. Calculation indicates that the interaction between these would only be 1/10 of that between the nearest neighbor pair. For this discussion, only the interaction between nearest neighbors will be considered. It will be assumed (for simplicity) that the C_A-C_B bonds and the C_C-C_D bonds are perpendicular.

Let us consider two of the interacting CH_2 groups (Fig. 2). Let θ_0 be the normal H−C−H bond angle and V_0 be the potential energy associated with this angle in the isolated molecule. The frequency of one of the modes of CH_2 deformation will be $\nu_0=(1/2\pi)(k_0/\mu)^{\frac{1}{2}}$, where μ is an effective mass and k_0 a force constant defined by

$$k_0=\partial^2V_0/\partial\alpha^2.$$

($\alpha=\theta/2$.) In the crystal, the potential energy becomes

$$V=V_0+V',$$

where V' is the potential energy of interaction between the nearest-neighbor hydrogen atoms. The frequency will change to $\nu=(1/2\pi)(k/\mu)^{\frac{1}{2}}$ where

$$k=\frac{\partial^2V}{\partial\alpha^2}=\frac{\partial^2V_0}{\partial\alpha^2}+\frac{\partial^2V'}{\partial\alpha^2}.$$

Therefore, if μ remains unchanged,

$$\nu=\nu_0\left[1+\frac{1}{k_0}\left(\frac{\partial^2V'}{\partial\alpha^2}\right)\right]^{\frac{1}{2}}.$$

($\partial^2V'/\partial\alpha^2$) will depend upon the phase relationships between the deformations of the CH_2 groups. Born and von Karman[4] have shown that in a crystal such interaction leads to a distribution of modes of vibration which has maxima corresponding to adjacent CH_2 groups vibrating in-phase and 180° out-of-phase. For large crystals, these maxima are very sharp, and modes corresponding to phase relationships very close to the above are the only important ones.

Let us consider the in-phase rocking mode (where the hydrogen atoms are moving in the manner indicated by the arrows in Fig. 2). It is apparent that

$$\frac{\partial^2V'}{\partial\alpha^2}=\left(\frac{\partial^2V'}{\partial r^2}\right)\left(\frac{\partial r}{\partial\alpha}\right)^2+\left(\frac{\partial V'}{\partial r}\right)\left(\frac{\partial^2 r}{\partial\alpha^2}\right).$$

The second term is small compared to the first. ($\partial^2V'/\partial r^2$) is a function of r alone. The equation

$$V'=-\frac{4.31\times10^{-60}}{r^6}+7.7\times10^{-10}\exp(-4.58\times10^8 r)$$

has been proposed by Müller.[5] ($\partial^2V'/\partial r^2$), designated by

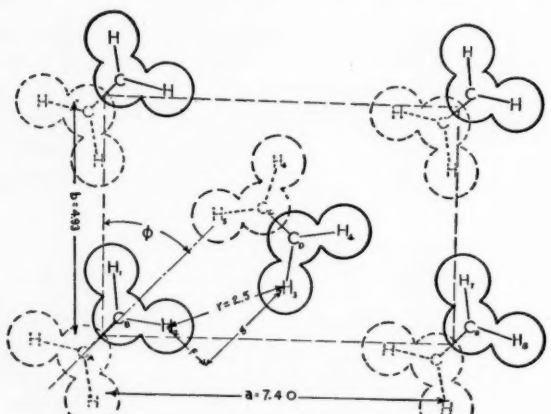
H
C
H
H
C
H
H
H

β, obtained from this equation is plotted in Fig. 3.

Since r is a function of f and g,

$$\left(\frac{\partial r}{\partial \alpha}\right)=\frac{f}{r}\left(\frac{\partial f}{\partial \alpha}\right)+\frac{g}{r}\left(\frac{\partial g}{\partial \alpha}\right),$$

where for this mode

$$\left(\frac{\partial f}{\partial \alpha}\right)=l(\sin\alpha-\cos\alpha)$$

and

$$\left(\frac{\partial g}{\partial \alpha}\right)=l(\sin\alpha+\cos\alpha).$$

l is the C−H bond length. Thus

$$\left(\frac{\partial r}{\partial \alpha}\right)^2=l^2\left[1+\left(\frac{g^2-f^2}{r^2}\right)\sin\theta-\left(\frac{2fg}{r^2}\right)\cos\theta\right]=1.92l^2$$

and

$$\nu=\nu_0\left(1+\frac{1.92l^2\beta}{k_0}\right)^{\frac{1}{2}}.$$

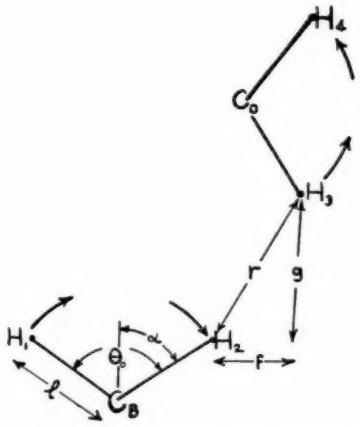

FIG. 2. The interaction between two nearest-neighbor CH_2 groups. $f=0.9$ A, $g=2.3$ A, $r=2.5$ A, $\theta_0=110°$. The curved arrows indicate the relative motions of the hydrogen atoms in the "in-phase rocking mode" of deformation.

The out-of-phase mode will be similar except that

$$\left(\frac{\partial f}{\partial \alpha}\right)=-l(\sin\alpha+\cos\alpha)$$

$$\left(\frac{\partial g}{\partial \alpha}\right)=l(\sin\alpha-\cos\alpha)$$

$$\left(\frac{\partial r}{\partial \alpha}\right)^2=l^2\left[1-\left(\frac{g^2-f^2}{r^2}\right)\sin\theta+\left(\frac{2fg}{r^2}\right)\cos\theta\right]=0.08l^2$$

and

$$\nu=\nu_0\left(1+\frac{0.08l^2\beta}{k_0}\right)^{\frac{1}{2}}.$$

Thus, it is predicted that as a result of interaction between molecules in the crystal, the CH_2 rocking frequency ν_0 (721 cm^{-1}) in the isolated molecule should be split into two components, the out-of-phase component being at a frequency very slightly higher than ν_0, and the in-phase component at a considerably higher frequency. The two components are observed at 721 cm^{-1} and 731 cm^{-1}.

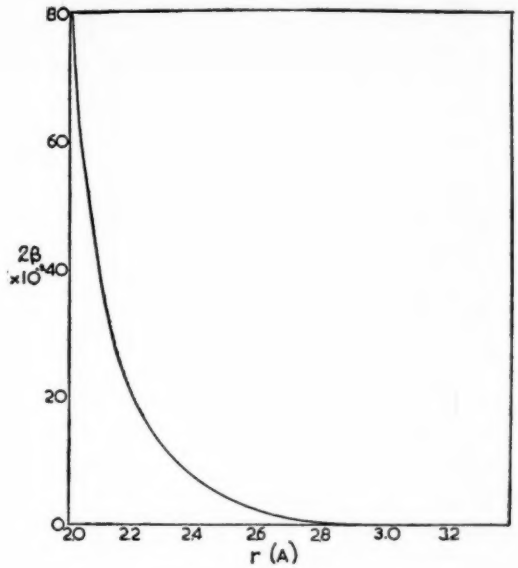

FIG. 3. The variation of β with r.

The following predictions may also be made:

(1) Both components should only be observed for radiation polarized perpendicular to the c-axis of the n-paraffin or polythene crystal. The out-of-phase rocking mode (lower frequency) should be polarized along the b crystal axis [Fig. 4(a)] while the in-phase rocking mode (higher frequency) should be polarized along the a-axis [Fig. 4(b)]. This is in agreement with the observations of Krimm.[6]

(2) The extension of the above treatment to the symmetrical CH_2 deformation frequency (1460 cm^{-1}) leads to the prediction that in the normal form of the crystal, the in-phase mode should be the lower frequency and should be polarized along the a-axis while the out-of-phase mode should be the higher frequency and should be polarized along the b-axis. Krimm has found[6] the opposite polarization behavior for the monoclinic form of crystals of n-$C_{36}H_{74}$. He believes that in this form, the chains are tilted and that his observations for this form are in agreement with the above theory.[7]

(3) The separation of the components of the doublet depends upon the ratio β/k_0. Less separation would be expected for the 1460 cm^{-1} doublet than for the 721 cm^{-1} doublet since k_0 is larger for the former. For the former one finds about 6 cm^{-1} separation at 1460 cm^{-1} as compared with 10 cm^{-1} at 721 cm^{-1}.

(4) The separation is proportional to ν_0. Thus if ν_0 is changed by changing the effective mass μ by deutera-

[6] S. Krimm, J. Chem. Phys. **22**, 567 (1954).
[7] S. Krimm (personal communication).

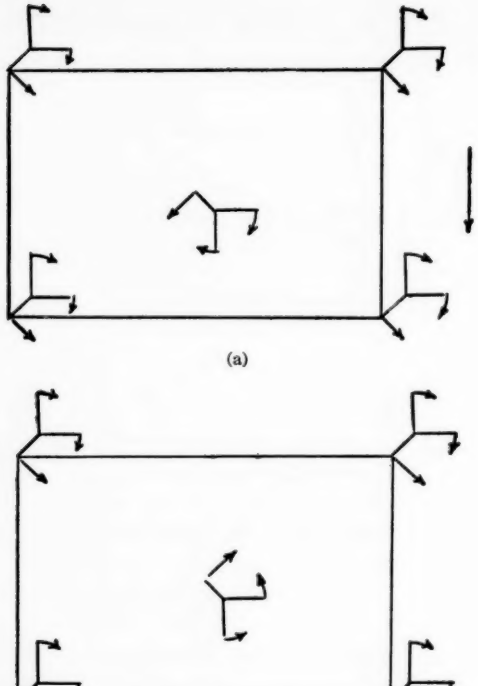

FIG. 4. The direction of the electric vector for absorption of polarized infrared radiation for (a) the out-of-phase rocking mode (lower frequency) and (b) the in-phase rocking mode (higher frequency).

tion, the doublet separation decreases in the same ratio as does ν_0. This has been reported.[1]

(5) The interaction force constant β depends upon r and will change if r is changed (e.g., by changing the temperature). The change in the frequency of the lower frequency component of the 721 cm^{-1} doublet with temperature will be

$$\left(\frac{\partial \nu}{\partial T}\right)=\frac{0.04l^2}{k_0}\left(\frac{\partial \beta}{\partial r}\right)\left(\frac{\partial r}{\partial T}\right),$$

while for the high frequency component

$$\left(\frac{\partial \nu}{\partial T}\right)=\frac{0.98l^2}{k_0}\left(\frac{\partial \beta}{\partial r}\right)\left(\frac{\partial r}{\partial T}\right)$$

(neglecting the temperature dependence of l and k_0). Thus, the position of the high frequency component would be considerably more temperature dependent than that of the low in agreement with experiment.[1,8] If $(\partial r/\partial T)$ is estimated from the coefficient of expansion, one calculates that the frequency of the 731 cm^{-1} component should shift toward higher frequencies by about 2 cm^{-1} on cooling from room temperature to liquid nitrogen temperature. The observed shift is 3 cm^{-1}.[1] The 721 cm^{-1} should shift less than 0.01 cm^{-1}. The observed shift is about 0.5 cm^{-1}. It is reasonable that the high frequency component should become sharper at lower temperatures.[8] Thermal motion within the crystal will result in β being a function of time and position. As the crystal is cooled, the distribution of values for β becomes narrower.

(6) On heating n-paraffin crystals through the λ-point, there is a 5–10 percent increase in one of the dimensions of the unit cell[9,10] in addition to the onset of free rotation[11] or randomness of orientation about the long axis of the paraffin chains. As a result, there would be an appreciable decrease in the average value of β and the splitting should become negligible above the λ point, in agreement with experiment.[1]

The author is indebted to G. B. B. M. Sutherland, Elliott Montroll, J. E. Lennard-Jones, Norman Sheppard, and Samuel Krimm for many helpful discussions and suggestions, as well as to the U. S. National Research Council for a fellowship which made this work possible.

[8] King, Hainer, and McMahon, J. Appl. Phys. **20**, 559 (1949).
[9] Sayer, Patterson, and Keays, J. Am. Chem. Soc. **66**, 179 (1944).
[10] A. Müller, Proc. Roy. Soc. (London) **A138**, 514 (1934).
[11] L. Pauling, Phys. Rev. **36**, 430 (1930).

Mean Amplitudes of Thermal Vibrations in Polyatomic Molecules. III. The Generalized Mean Amplitudes

YONEZO MORINO AND EIZI HIROTA
Department of Chemistry, Faculty of Science, Tokyo University, Bunkyo-ku, Tokyo, Japan
(Received April 14, 1954)

James' theory of the effect of molecular vibrations upon the diffraction pattern is revised and extended, including the parallel as well as perpendicular vibrations of atom pairs. Corresponding to these vibrations the mean square amplitudes, parallel and perpendicular, and the mean cross products are defined, and a method of calculating them by means of normal modes of vibration is derived. At the same time the effect of molecular symmetry upon mean amplitudes is discussed with the result that some of them are essentially reduced to zero because of the symmetry.

I. AN EXTENSION OF JAMES' THEORY OF THE THERMAL VIBRATIONS OF POLYATOMIC MOLECULES

ABOUT twenty years ago James[1] discussed first the influence of thermal vibrations of molecules upon the x-ray diffraction patterns. As the mathematical treatment of electron diffraction by gaseous molecules is entirely identical with that of x-ray diffraction by the molecules, his final formula has frequently been applied to electron diffraction. It is, however, to be noted that his treatment was aimed mainly at the scattering of x-ray but not of electron beam. The wavelength of the former, usually 1.54 A, is about twenty times larger than that of the electron beam ($\lambda\sim 0.06$ A). It follows from this that the derivation used and the conclusion obtained by James ought to be re-examined when applied to the scattering of electron beam. Debye[2] treated the effect of the thermal vibration on the electron diffraction patterns, but his theory was confined to the case of diatomic molecules. Karle and Karle[3] discussed extensively the scattering of electron beams by gaseous molecules from the theoretical as well as the experimental standpoint, and confirmed James' result that when the thermal motion of atoms in a molecule is taken into consideration, the theoretical intensity curve for the rigid molecule,

$$I=k\sum_{i\neq j}\sum f_if_j\frac{\sin sl_{ij}}{sl_{ij}}, \tag{1}$$

must be replaced in the first approximation by

$$I=k\sum_{i\neq j}\sum e^{-A_{ij}}f_if_j\frac{\sin sl_{ij}}{sl_{ij}}; \tag{2}$$

where $A_{ij}=s^2\langle\Delta l_{ij}^2\rangle/2$, $\langle\Delta l_{ij}^2\rangle^{\frac{1}{2}}$, denoting the root-mean-square amplitude along the equilibrium direction of the atom pair i and j. They calculated the effect of the higher terms but their result seems to contain some mistakes. Under these circumstances it is desirable to revise James' theory to take correctly into account the effect of the vibration perpendicular to the equilibrium direction of the atom pair. At the same time, it would be worth while to derive a straightforward method of calculation of the generalized mean amplitudes, just as those for the parallel vibration presented in the preceding paper.[4]

A. Intensity Function

Now consider a particular atom pair (i,j) in a molecule. Following the method of James [reference 1, Eq. (32)], we define the six quantities;

$$\begin{aligned} &A=\tfrac{1}{2}s^2\langle\Delta z^2\rangle, \quad B=\tfrac{1}{2}s^2\langle\Delta x^2\rangle, \quad C=\tfrac{1}{2}s^2\langle\Delta y^2\rangle,\\ &D=\tfrac{1}{2}s^2\langle\Delta z\Delta x\rangle, \quad E=\tfrac{1}{2}s^2\langle\Delta x\Delta y\rangle, \quad F=\tfrac{1}{2}s^2\langle\Delta y\Delta z\rangle, \end{aligned} \tag{3}$$

where the z axis represents the equilibrium direction of the atom pair, the x and y axes the directions perpendicular to it, and Δz, Δx, and Δy the differences of the displacements of the two atoms in the directions of the three axes: $\Delta z=\Delta z_i-\Delta z_j$, etc. We may call $\langle\Delta z^2\rangle$ the *mean square "parallel" amplitude*, $\langle\Delta x^2\rangle$ and $\langle\Delta y^2\rangle$ the *mean square "perpendicular" amplitudes*, and $\langle\Delta z\Delta x\rangle$, $\langle\Delta x\Delta y\rangle$, and $\langle\Delta y\Delta z\rangle$ the *mean cross products*.

The intensity of the coherent molecular term of the electron diffraction due to the atom pair i and j is given by [reference 1, Eq. (33)],

$$\bar{M}_{ij}=f_if_j\int\cos(\lambda a)\exp[-(A\lambda^2+B\mu^2+C\nu^2+2D\lambda\mu+2E\mu\nu+2F\nu\lambda)]\Omega d\omega, \tag{4}$$

where

$$f_i=\frac{8\pi^2me^2}{h^2}\cdot\frac{Z_i-F_i}{s^2}, \tag{5}$$

and

$$\lambda=\cos\varphi, \quad \mu=\sin\varphi\cos\epsilon, \quad \nu=\sin\varphi\sin\epsilon, \tag{6}$$

$$\Omega d\omega=\frac{1}{4\pi}\sin\varphi d\varphi d\epsilon, \tag{7}$$

and

$$a=sl_{ij}. \tag{8}$$

[1] R. W. James, Physik. Z. **33**, 737 (1932).
[2] P. Debye, J. Chem. Phys. **9**, 55 (1941).
[3] J. Karle and I. L. Karle, J. Chem. Phys. **17**, 1052 (1949); **18**, 957, 963 (1950).
[4] Morino, Kuchitsu, Takahashi, and Maeda, J. Chem. Phys. **21**, 1927 (1953).

Putting the exponential function in the integrand equal to $1-(A\lambda^2+B\mu^2+C\nu^2+2D\lambda\mu+2E\mu\nu+2F\nu\lambda)$, integrating and then inserting $\exp(-A)$ tentatively in place of $(1-A)$, James obtained the following equation:

$$\bar{M}_{ij}=f_if_j\left[\frac{\sin a}{a}e^{-A}+\left(A-\frac{B+C}{2}\right)(2\pi)^{\frac{1}{2}}a^{-\frac{1}{2}}J_{\frac{1}{2}}(a)\right]. \quad (9)$$

This treatment depends upon the assumption that the six quantities defined by Eqs. (3) are essentially small at all the s values. But this is not always legitimate in the case of electron diffraction, because it frequently occurs that A is larger than 1, so that the convergency of the expansion of the exponential function with regards to A is not fulfilled unless the higher terms are taken into account. In fact, if Eq. (9) is used as it is, a peculiar result will often be found; the second term is definitely larger than the first.

Our procedure is as follows: taking out the factor $\exp(-A)$ from the integrand of Eq. (4) and transforming the variable φ to $\lambda=\cos\varphi$, we have

$$I=\bar{M}_{ij}/f_if_j=\frac{e^{-A}}{4\pi}\int_0^{2\pi}d\epsilon\int_{-1}^{+1}\cos(a\lambda)\times\exp[P(1-\lambda^2)]\exp[Q\lambda(1-\lambda^2)^{\frac{1}{2}}]d\lambda, \quad (10)$$

where

$$P=A-B\cos^2\epsilon-C\sin^2\epsilon-2E\sin\epsilon\cos\epsilon, \quad (11)$$

and

$$Q=-2D\cos\epsilon-2F\sin\epsilon. \quad (12)$$

The two exponential functions being expanded, Eq. (10) is expressed as a product of the two infinite series:

$$I=\frac{e^{-A}}{4\pi}\int_0^{2\pi}d\epsilon\int_{-1}^{+1}\cos(a\lambda)\sum_{n=0}^{\infty}\sum_{m=0}^{\infty}\frac{P^n}{n!}\frac{Q^m}{m!}\times(1-\lambda^2)^n\lambda^m(1-\lambda^2)^{m/2}d\lambda. \quad (13)$$

Each term of the integrand is an even or odd function of λ according to whether m is even or odd. The odd terms disappear on integrating from -1 to $+1$, so that it is only the even terms $m=2k$ that are to be considered. Expressing the integral by Bessel functions,[5] we obtain

$$I=\frac{e^{-A}}{4\pi}\sum_{n=0}^{\infty}\sum_{k=0}^{\infty}(-1)^k\pi^{\frac{1}{2}}\frac{(n+k)!}{n!(2k)!}\left(\frac{d}{da}\right)^{2k}\times\left[\left(\frac{2}{a}\right)^{n+k+\frac{1}{2}}J_{n+k+\frac{1}{2}}(a)\right]\int_0^{2\pi}P^nQ^{2k}d\epsilon. \quad (14)$$

As shown in Appendix I, each term in Eq. (14) has the form of

$$\left(\frac{P}{a}\right)^n\left(\frac{Q^2}{a}\right)^k\left(\frac{c_1}{a}+\frac{c_2}{a^2}+\cdots\right), \quad (15)$$

where $c_1, c_2, \cdots$ are quantities composed of $\sin a$ or $\cos a$ multiplied by some numerical coefficients. P/a is approximately $s\langle\Delta l^2\rangle/l$, and Q^2/a is $s^3\langle\Delta l^2\rangle^2/l$, both increasing with s. It has been found that in the usual case mean amplitudes $\langle\Delta l^2\rangle^{\frac{1}{2}}$ have a magnitude of $0.04l$. Thus P/a is smaller than 0.1 in the usual regions of $s(s<30)$ and $l(l<5$ A). Therefore, in the summation of Eq. (14) it is sufficient to take into account only the first two terms, $n=0$ and 1, and in the expansion of Eq. (15) the higher terms, except the first two are safely neglected to keep the same order of magnitude. On the other hand Q^2/a is not always smaller than 1. At the limit mentioned above, indeed, it becomes larger than 10, so that the summation over k must be carried out to infinite terms. By a simple manipulation as shown in Appendix I, we finally obtain

$$I=e^{-A}\frac{\sin\gamma}{a}+10e^{-A}\frac{\sin\gamma}{a^3}G^2-10e^{-A}\frac{\cos\gamma}{a^4}G^4-2e^{-A}\frac{\cos\gamma}{a^2}\left(A-\frac{B+C}{2}\right)-4e^{-A}\frac{\sin\gamma}{a^3}\times[(A-B)D^2+(A-C)F^2-2DEF], \quad (16)$$

where

$$\gamma=a-2G^2/a, \quad (17)$$

and

$$G^2=D^2+F^2. \quad (18)$$

It should be pointed out that this formula has two outstanding features: the first is that every term contains the exponential factor $\exp(-A)$. This exponential factor is important to make the correction term small even at large values of s. The other remarkable point is that every term contains sine or cosine functions of $\gamma=a-2G^2/a$, instead of $\sin a$ or $\cos a$. This affords to each term of the intensity function a phase shift defined by

$$\Delta s=2G^2/al, \quad (19)$$

which increases rapidly with s^3. In the case mentioned previously, $2G^2/al\cong s^3\langle\Delta l^2\rangle^2/l^2=(0.04)^4l^2s^3$, and, for instance, at $l=2$ A and $s=30$, the phase shift becomes 0.27.

If we put $G=0$, that is, $D=F=0$, Eq. (16) is reduced to be

$$I=e^{-A}\frac{\sin a}{a}-2e^{-A}\frac{\cos a}{a^2}\left(A-\frac{B+C}{2}\right)+\cdots, \quad (20)$$

which coincides with James' final formula, except one factor, $\exp(-A)$, in the second term.

Karle and Karle[6] gave the intensity function involving the correction factor in this order of approximation, but unfortunately their expression contains several mistakes (exponential factor in Eqs. (16), (24), (25), and (26) in reference 6). If they are corrected, it takes

[5] E. T. Whittaker and G. N. Watson, *Modern Analysis* (Cambridge University Press, New York, 1927), p. 366.

[6] J. Karle and I. L. Karle, J. Chem. Phys. **18**, 957 (1950).

the form of

$$I=e^{-A}\frac{\sin a}{a}-2e^{-A}\frac{\cos a}{a^2}\left(A-\frac{B+C}{2}\right)$$
$$-2e^{-A}\frac{\cos a}{a^2}(D^2+F^2)+\cdots, \quad (21)$$

which corresponds to the expansion of Eq. (16) in the case when $G^2/a\ll 1$. Needless to say, this condition is often but not always satisfied as shown in the foregoing.

It should be noted that the discussion stated above depends upon the first Born approximation that no phase shifts take place by the scattering processes at the atoms. As was recently pointed out by Schomaker and Glauber,[7] these phase shifts cannot be neglected, especially when the atomic numbers of the two scattering atoms are quite different. This effect affords the intensity $\bar{M}_{ij}\cos\delta s$ in place of that given by the fundamental Eq. (4), where δs denotes the difference of the phase shift caused by the scattering at the atoms i and j. Bartell and Brockway,[8] estimated that $\delta\cong 2\times 10^{-3}\Delta Z$ for 40-kv electrons and for argon or even lighter atoms, ΔZ being the difference of the atomic numbers of the two atoms. This provides the final Eq. (16) with a correction term of

$$-\tfrac{1}{2}\delta^2 s^2 I=-\tfrac{1}{2}\delta^2 s^2 e^{-A}\frac{\sin\gamma}{a}+\cdots. \quad (22)$$

For a pair of carbon and chlorine atoms ($\Delta Z=11$) it amounts to 0.20 at $s=30$.

B. Radial Distribution Function

The corresponding extension of the radial distribution function is now treated, which is obtained from two different sides, one based upon the Fourier transform of the intensity function and the other on the direct consideration of the probability distribution of the distance between the given atoms. The latter method which is more straightforward than the former will mainly be discussed in the following.

At a particular instant the distance l of the atom pair i and j deviates from the equilibrium one, l_{ij}, the deviation having not only the z component ($\Delta z=\Delta z_i-\Delta z_j$) but also the x and y components ($\Delta x=\Delta x_i-\Delta x_j$ and $\Delta y=\Delta y_i-\Delta y_j$, respectively). Thus, expanded in terms of these quantities, l is given by

$$l=[(l_{ij}+\Delta z)^2+(\Delta x)^2+(\Delta y)^2]^{\frac{1}{2}}$$
$$=l_{ij}+\Delta z+[(\Delta x)^2+(\Delta y)^2]/2l_{ij}+\cdots. \quad (23)$$

The small displacements, Δz, Δx, and Δy, may be expressed in terms of normal coordinates Q_n's: i.e.,

$$\Delta z=\sum_n A_nQ_n,\ \Delta x=\sum_n B_nQ_n,\ \text{and}\ \Delta y=\sum_n C_nQ_n. \quad (24)$$

The probability distribution function $P(l)dl$, expressing the probability that l will be found in the interval $(l, l+dl)$, or $(l-dl/2, l+dl/2)$, can be obtained by the integral

$$P(l)dl=\int_{-\infty}^{+\infty}\cdots\int\Delta\prod_n W_n dQ_n, \quad (25)$$

where

$$W_n=\left(\frac{H_n}{\pi}\right)^{\frac{1}{2}}\exp[-H_nQ_n^2], \quad (26)$$

with

$$H_n=\frac{4\pi^2\nu_n}{h}\operatorname{tgh}\frac{h\nu_n}{2kT}. \quad (27)$$

$\langle\Delta Q_n^2\rangle=1/2H_n$ is the mean square amplitude of the normal vibration Q_n. The function Δ introduced in the integrand of Eq. (25), is only a formal device so as to restrict the integration in Eq. (25) to the range of $(l-dl/2, l+dl/2)$. This function is the well-known discontinuous integral of Dirichlet,[9]

$$\Delta=\frac{1}{\pi}\int_{-\infty}^{+\infty}\frac{\sin\alpha\rho}{\rho}\exp(i\rho\gamma)d\rho, \quad (28)$$

which is equal to 1 whenever $-\alpha\leqq\gamma\leqq\alpha$ and is zero otherwise. Taking

$$\alpha=dl/2, \quad (29)$$

and

$$\gamma=l_{ij}-l+\sum_{n=1}^{N}A_nQ_n+\frac{1}{2l_{ij}}\sum_{m=1}^{N}\sum_{l=1}^{N}$$
$$\times(B_mB_l+C_mC_l)Q_mQ_l, \quad (30)$$

Eq. (25) is the complete expression for the probability function:

$$P(l)dl=\frac{dl}{2\pi}\int_{-\infty}^{+\infty}\cdots\int\exp[i\rho(l_{ij}-l)]$$
$$\times\exp\left[i\rho\sum_{n=1}^{N}A_nQ_n+\frac{i\rho}{2l_{ij}}\sum_{m=1}^{N}\sum_{l=1}^{N}(B_mB_l\right.$$
$$\left.+C_mC_l)Q_mQ_l\right]\left(\frac{H_1}{\pi}\right)^{\frac{1}{2}}\cdots\left(\frac{H_N}{\pi}\right)^{\frac{1}{2}}$$
$$\times\exp[-\sum_{n=1}^{N}H_nQ_n^2]dQ_1\cdots dQ_N. \quad (25')$$

The second exponential factor in Eq. (25′) is approximated by

$$\exp\left[i\rho\sum_n A_nQ_n+\frac{i\rho}{2l_{ij}}\sum_m\sum_l(B_mB_l+C_mC_l)Q_mQ_l\right]$$
$$\cong\exp[i\rho\sum_n A_nQ_n]+\exp[i\rho\sum_n A_nQ_n]$$
$$\times\frac{i\rho}{2l_{ij}}\sum_m\sum_l(B_mB_l+C_mC_l)Q_mQ_l. \quad (31)$$

[7] V. Schomaker and R. Glauber, Nature **170**, 290 (1952); R. Glauber and V. Schomaker, Phys. Rev. **89**, 667 (1953). See also J. A. Hoerni and J. A. Ibers, Phys. Rev. **91**, 1182 (1953).

[8] L. S. Bartell and L. O. Brockway, Nature, **171**, 978 (1953).

[9] S. Chandrasekhar, Revs. Modern Phys. **15**, 1 (1943): especially pp. 8–10 and 80–81.

Corresponding to this, $P(l)dl$ is divided into two parts, the one is

$$P_1(l)dl=\frac{dl}{2\pi}\int_{-\infty}^{+\infty}d\rho\,\exp[i\rho(l_{ij}-l)]\prod_{n=1}^{N}\left(\frac{H_n}{\pi}\right)^{\frac{1}{2}}$$
$$\times\int_{-\infty}^{+\infty}\exp\left[-H_n\left(Q_n-\frac{i\rho A_n}{2H_n}\right)^2-\frac{A_n^2}{4H_n}\rho^2\right]dQ_n, \quad (32a)$$

and the other is

$$P_2(l)dl=\frac{dl}{2\pi}\int_{-\infty}^{+\infty}d\rho\,\exp[i\rho(l_{ij}-l)]\frac{i\rho}{2l_{ij}}\left(\frac{H_1}{\pi}\right)^{\frac{1}{2}}\cdots\left(\frac{H_n}{\pi}\right)^{\frac{1}{2}}$$
$$\times\int_{-\infty}^{+\infty}\cdots\int\exp\left[-\sum_{n=1}^{N}H_n\left(Q_n-\frac{i\rho A_n}{2H_n}\right)^2-\sum_{n=1}^{N}\frac{A_n^2}{4H_n}\rho^2\right]$$
$$\times\sum_{m=1}^{N}\sum_{l=1}^{N}(B_mB_l+C_mC_l)Q_mQ_l dQ_1\cdots dQ_N. \quad (32b)$$

The approximation used in Eq. (31) is valid only when

$$\frac{\rho}{2l_{ij}}\sum_{m=1}^{N}\sum_{l=1}^{N}(B_mB_l+C_mC_l)Q_mQ_l\ll 1, \quad (33)$$

where ρ is extended from $-\infty$ to $+\infty$ but contributes effectively to the integral only in the range $|\rho|<2/\langle\Delta l^2\rangle^{\frac{1}{2}}$. The double sum $\sum_m\sum_l(B_mB_l+C_mC_l)Q_mQ_l$, on the other hand, is of the order of $\langle\Delta l^2\rangle$, so that the factor (33) is roughly equal to $\langle\Delta l^2\rangle^{\frac{1}{2}}/l_{ij}\cong 0.04$, hence the validity of Eq. (33) may be secured in almost all the cases.

Now the integration of Eqs. (32) is carried out by several steps of rather lengthy calculations, with the results that

$$P_1(l)=\frac{1}{(2\pi\langle\Delta z^2\rangle)^{\frac{1}{2}}}\exp\left[-\frac{(l-l_{ij})^2}{2\langle\Delta z^2\rangle}\right], \quad (34a)$$

and

$$P_2(l)=\frac{1}{(2\pi\langle\Delta z^2\rangle)^{\frac{1}{2}}}\cdot\frac{l-l_{ij}}{l_{ij}}\left[\frac{\langle\Delta x^2\rangle+\langle\Delta y^2\rangle}{2\langle\Delta z^2\rangle}\right.$$
$$\left.-\frac{\langle\Delta z\Delta x\rangle^2+\langle\Delta z\Delta y\rangle^2}{2\langle\Delta z^2\rangle^2}\left\{3-\frac{(l-l_{ij})^2}{\langle\Delta z^2\rangle}\right\}\right]$$
$$\times\exp\left[-\frac{(l-l_{ij})^2}{2\langle\Delta z^2\rangle}\right], \quad (34b)$$

where it is to be noted that

$$\sum_{n=1}^{N}\frac{A_n^2}{2H_n}=\langle\Delta z^2\rangle=\frac{2A}{s^2},\quad \sum_{n=1}^{N}\frac{B_n^2}{2H_n}=\langle\Delta x^2\rangle=\frac{2B}{s^2},$$
$$\sum_{n=1}^{N}\frac{C_n^2}{2H_n}=\langle\Delta y^2\rangle=\frac{2C}{s^2},$$

and

$$\sum_{n=1}^{N}\frac{A_nB_n}{2H_n}=\langle\Delta z\Delta x\rangle,\quad \sum_{n=1}^{N}\frac{A_nC_n}{2H_n}=\langle\Delta z\Delta y\rangle. \quad (35)$$

The modified radial distribution function used by Karle and Karle is obtained from $P(l)$ by the following transformation,*

$$f(l)=\frac{1}{4}\left(\frac{\pi}{b}\right)^{\frac{1}{2}}\int_{-\infty}^{+\infty}\frac{P(R)}{R}\exp\left[-\frac{(R-l)^2}{4b}\right]dR. \quad (36)$$

It is easily evaluated by introducing Eqs. (34). The result is

$$f(l)=\left(\frac{\pi}{2(\langle\Delta z^2\rangle+2b)}\right)^{\frac{1}{2}}\frac{1}{2l_{ij}}\left\{1-\sigma\frac{l-l_{ij}}{l_{ij}}\right\}$$
$$\times\exp\left[-\frac{(l-l_{ij})^2}{2(\langle\Delta z^2\rangle+2b)}\right], \quad (37)$$

where

$$\sigma=\frac{1}{(\langle\Delta z^2\rangle+2b)}\left[\langle\Delta z^2\rangle-\frac{\langle\Delta x^2\rangle+\langle\Delta y^2\rangle}{2}\right.$$
$$\left.+\frac{\langle\Delta z\Delta x\rangle^2+\langle\Delta z\Delta y\rangle^2}{2(\langle\Delta z^2\rangle+2b)}\left(3-\frac{(l-l_{ij})^2}{\langle\Delta z^2\rangle+2b}\right)\right]. \quad (38)$$

The effects of the perpendicular amplitudes and the cross products are entirely involved in the term σ, which is usually positive near the equilibrium distance, and makes the deviation of $f(l)$ from the Gaussian type larger towards the shorter distance and smaller towards the longer.

Fourier transform of the intensity function:

$$f(l)=\int_0^{\infty}sI(s)\exp(-bs^2)\sin(sl)ds, \quad (39)$$

gives the completely coincident result with Eq. (37), when the intensity function is approximated by Eq. (21). The artificial reducing factor $\exp(-bs^2)$ in Eq. (39), which was usually used in the analysis of electron diffraction patterns, makes the contribution of $sI(s)$ to $f(l)$ somewhat trivial when s is large, so that it is permitted to replace the rigorous Eq. (16) by Eq. (21), because the difference between them lies almost in the region of large s values.

Such being the case, it seems doubtful whether the radial distribution function modified by use of the factor $\exp(-bs^2)$ is the best one for the discussion of the perpendicular components of the mean amplitudes. Since the effect of the perpendicular motion appears appreciably only in the part of the intensity function of large s values, it may be promising to devise a trans-

* Karle's reducing factor $\exp(-as^2)$ is written here $\exp(-bs^2)$ instead.

formation factor[10] which lays greater stress on this part of the function.

As described in the preceding section, the consideration of the second Born approximation introduced a correction term $\frac{1}{2}\delta^2 s^2 I$ to the intensity function [see Eq. (22)]. This provides, instead of Eq. (39),

$$f(l)=\int_0^\infty sI(s)(1-\tfrac{1}{2}\delta^2 s^2)\exp(-bs^2)\sin sld s, \quad (40)$$

which may be approximated by

$$f(l)=\int_0^\infty sI(s)\exp[1-(b+\tfrac{1}{2}\delta^2)s^2]\sin sld s. \quad (41)$$

Thus in the final formulas for the modified radial distribution function, (37) and (38), the factor $2b$ should be replaced by $2b+\delta^2$.

II. CALCULATION OF THE GENERALIZED MEAN AMPLITUDES

The generalized mean amplitudes consist of six quantities introduced by Eqs. (3): the first is the *mean square parallel amplitude* $\langle\Delta z^2\rangle$, other two are the *mean square perpendicular amplitudes*, $\langle\Delta x^2\rangle$ and $\langle\Delta y^2\rangle$, and the last three are the *mean cross products*, $\langle\Delta z\Delta x\rangle$, $\langle\Delta x\Delta y\rangle$, and $\langle\Delta y\Delta z\rangle$. In the previous article[11] the term *mean amplitude* was used as an abbreviation of *root mean square amplitude*. For the treatment of the generalized mean amplitudes, however, it may be more natural to define the six components of the mean amplitudes in terms with the dimension of cm^2 as stated above, because the cross products are sometimes negative. Of course their signs are trivial, depending upon the direction of the coordinate axes assumed. However, the product term *DEF* which appears in Eq. (16), has a definite sign decided by those of the cross terms, irrespective of the directions of the coordinate axes. Therefore the sign of each term of mean amplitudes is reserved for the time being, referring to an assumed set of axes.

A. Normal Coordinate Treatment

Every motion of atoms in a molecule is given by the superposition of the normal modes of vibration, as was shown in the preceding paper[4] for the parallel mean amplitudes. In order to obtain the precise expression for all the components of the generalized mean amplitudes, it is necessary to correlate the Cartesian coordinates x's directly to the normal coordinates Q's. According to Wilson,[12] the Cartesian coordinate matrix $\mathbf{X}$ is connected with the internal coordinate matrix $\mathbf{R}$ through the transformation matrix $\mathbf{A}$ of the dimension of $(3N, 3N-6)$, which are complemented by adding the zero submatrix of the dimension of $(3N,6)$ representing six conditions of no translation and of no rotation of the molecule as a whole:†

$$\mathbf{X}=\mathbf{AR}, \quad (42)$$

or conversely,

$$\mathbf{R}=\mathbf{BX}, \quad (43)$$

so that

$$\mathbf{AB}=\mathbf{B'A'}=\mathbf{E}, \quad (44)$$

where $\mathbf{E}$ is a unit matrix, and $\mathbf{A'}$ denotes the transposed matrix of $\mathbf{A}$. The symmetry coordinate matrix $\mathbf{S}$ is also introduced, correlating with $\mathbf{R}$ and $\mathbf{Q}$ by the relations:

$$\mathbf{S}=\mathbf{UR}, \quad (45)$$

and

$$\mathbf{S}=\mathfrak{L}\mathbf{Q}. \quad (46)$$

Now the kinetic energy in Cartesian coordinates,

$$2\mathbf{T}=(d\mathbf{X}/dt)'M(d\mathbf{X}/dt), \quad (47)$$

can be transformed by Eq. (42) into an expression in the internal coordinates:

$$2\mathbf{T}=(d\mathbf{R}/dt)'\mathbf{A'MA}(d\mathbf{R}/dt), \quad (48)$$

where $\mathbf{M}$ is a diagonal matrix of $3N$ dimension, consisting of the masses m_i's of all the atoms. According to Wilson, Eq. (48) is to be equal to

$$2\mathbf{T}=(d\mathbf{R}/dt)'\mathbf{G}^{-1}(d\mathbf{R}/dt), \quad (49)$$

so that

$$\mathbf{G}^{-1}=\mathbf{A'MA}, \quad (50)$$

or

$$\mathbf{A}=\mathbf{M}^{-1}\mathbf{B'G}^{-1}. \quad (51)$$

In order to use amply the symmetry, the Cartesian coordinates are expressed by the normal coordinates through the matrix $\mathbf{U}$ which includes the symmetry properties of the molecule. Combining Eq. (42) with Eqs. (45), (46), and (51), and introducing the relations of

$$\mathfrak{G}=\mathbf{UGU'}, \quad (52)$$

and

$$\mathfrak{L}\mathfrak{L}'=\mathfrak{G}, \quad (53)$$

we obtain‡

$$\mathbf{X}=\mathbf{M}^{-1}\mathbf{B'U'}(\mathfrak{L}^{-1})'\mathbf{Q}. \quad (54)$$

This relation requires the knowledge of $\mathbf{B}$ and $(\mathfrak{L}^{-1})'$, the former being rather easily obtained from the s-vector diagram,[13] while the latter making necessary the manipulation of $\mathfrak{L}$ and then the inversing calculation of $\mathfrak{L}$ into $\mathfrak{L}^{-1}$.

Now the small displacement of the x coordinate of

[10] J. Waser and V. Schomaker, Revs. Modern Phys. **25**, 671 (1953).

[11] Morino, Kuchitsu, and Shimanouchi, J. Chem. Phys. **20**, 726 (1952).

[12] E. B. Wilson, Jr., J. Chem. Phys. **7**, 1047; **9**, 76 (1941).

† The matrix $\mathbf{A}$ and $\mathbf{B}$ should not be confused with A and B defined by Eqs. (3).

‡ This relation has been obtained by Crawford and Fletcher. See B. L. Crawford, Jr., and W. H. Fletcher, J. Chem. Phys. **19**, 141 (1951).

[13] E. B. Wilson, Jr., J. Chem. Phys. **9**, 76 (1941).

the ith atom is given by

$$x_i=\sum_{l,m,k} M^{-1}{}_i B'_{il} U'_{lm} (\mathfrak{L}^{-1})'_{mk} Q_k, \tag{55}$$

then

$$x_i-x_j=\sum_{l,m,n} (M^{-1}{}_i B'_{il}-M^{-1}{}_j B'_{jl}) U'_{lm} (\mathfrak{L}^{-1})'_{mk} Q_k. \tag{56}$$

We may conveniently introduce an operator $\mathbf{D}_{ij}{}^x$, which, when operated on the matrix $\mathbf{M}^{-1}\mathbf{B}'$, gives a column matrix $(M^{-1}{}_i B'_{il}-M^{-1}{}_j B'_{jl})$, the suffix x of $\mathbf{D}_{ij}{}^x$ denoting the operation with regard to the x coordinate. Thus Eq. (56) can be expressed in such a way that

$$x_i-x_j=[\mathbf{D}_{ij}{}^x(\mathbf{M}^{-1}\mathbf{B}')]'\mathbf{U}'(\mathfrak{L}^{-1})'\mathbf{Q}. \tag{57}$$

And the mean square of (x_i-x_j) is given by

$$\langle(x_i-x_j)^2\rangle=[\mathbf{D}_{ij}{}^x(\mathbf{M}^{-1}\mathbf{B}')]'\mathbf{U}'(\mathfrak{L}^{-1})' \times\langle\mathbf{Q}^2\rangle\mathfrak{L}^{-1}\mathbf{U}[\mathbf{D}_{ij}{}^x(\mathbf{M}^{-1}\mathbf{B}')]. \tag{58}$$

The mean amplitudes in the direction of y and z axes are given in similar forms. Further, the cross products are expressed analogously as

$$\langle(x_i-x_j)(y_i-y_j)\rangle=[\mathbf{D}_{ij}{}^x(\mathbf{M}^{-1}\mathbf{B}')]'\mathbf{U}'(\mathfrak{L}^{-1})' \times\langle\mathbf{Q}^2\rangle\mathfrak{L}^{-1}\mathbf{U}[\mathbf{D}_{ij}{}^y(\mathbf{M}^{-1}\mathbf{B}')]. \tag{59}$$

B. Approximate Method of Calculation

The approximate method presented in the preceding article[4] was based upon an asymptotic expansion of the hyperbolic cotangent function for the mean amplitudes of the normal coordinates:

$$\langle\mathbf{Q}^2\rangle=kT\mathbf{\Lambda}^{-1}+\frac{h^2}{64\pi^2kT}\mathbf{E}. \tag{60}$$

Inserting Eq. (60) in Eq. (58), and then applying the relations

$$\mathfrak{L}\mathbf{\Lambda}^{-1}\mathfrak{L}'=\mathfrak{F}^{-1}, \tag{61}$$

and

$$(\mathfrak{L}^{-1})'\mathfrak{L}^{-1}=\mathfrak{G}^{-1}, \tag{62}$$

we have

$$\langle(x_i-x_j)^2\rangle=kT[\mathbf{D}_{ij}{}^x(\mathbf{M}^{-1}\mathbf{B}')]'\mathbf{U}'\mathfrak{G}^{-1}\mathfrak{F}^{-1}\mathfrak{G}^{-1}\mathbf{U} \times[\mathbf{D}_{ij}{}^x(\mathbf{M}^{-1}\mathbf{B}')]+\frac{h^2}{64\pi^2kT}[\mathbf{D}_{ij}{}^x(\mathbf{M}^{-1}\mathbf{B}')]' \times\mathbf{U}'\mathfrak{G}^{-1}\mathbf{U}[\mathbf{D}_{ij}{}^x(\mathbf{M}^{-1}\mathbf{B}')]. \tag{63}$$

Since

$$\mathbf{G}^{-1}=\mathbf{U}'\mathfrak{G}^{-1}\mathbf{U}, \tag{64}$$

and

$$\mathbf{F}^{-1}=\mathbf{U}'\mathfrak{F}^{-1}\mathbf{U}, \tag{65}$$

Eq. (63) is expressed in terms of the internal coordinates as follows:

$$\langle(x_i-x_j)^2\rangle=kT[\mathbf{D}_{ij}{}^x(\mathbf{M}^{-1}\mathbf{B}')]'\mathbf{G}^{-1}\mathbf{F}^{-1}\mathbf{G}^{-1} \times[\mathbf{D}_{ij}{}^x(\mathbf{M}^{-1}\mathbf{B}')]+\frac{h^2}{64\pi^2kT}[\mathbf{D}_{ij}{}^x(\mathbf{M}^{-1}\mathbf{B}')]' \times\mathbf{G}^{-1}[\mathbf{D}_{ij}{}^x(\mathbf{M}^{-1}\mathbf{B}')]. \tag{66}$$

From Eq. (51)

$$\mathbf{G}^{-1}=(\mathbf{B}^{-1})'\mathbf{M}\mathbf{B}^{-1}, \tag{67}$$

therefore, the kth term of the column matrix $[\mathbf{D}_{ij}{}^x(\mathbf{M}^{-1}\mathbf{B}')]\mathbf{G}^{-1}$, becomes

$$\begin{aligned}([\mathbf{D}_{ij}{}^x(\mathbf{M}^{-1}\mathbf{B}')]'\mathbf{G}^{-1})_k &=\sum_{l,m}(M^{-1}{}_i B'_{il}-M^{-1}{}_j B'_{jl})(B^{-1})'_{lm} M_m (B^{-1})_{mk}\\ &=A_{ik}-A_{jk}=[D_{ij}{}^x(A)]_k,\end{aligned} \tag{68}$$

since

$$\sum_l B'_{il}(B^{-1})'_{lm}=1 \text{ for } m=i, \text{ and } 0 \text{ otherwise.} \tag{69}$$

Further the second term of Eq. (66) can be simplified as

$$\begin{aligned}[\mathbf{D}_{ij}{}^x(\mathbf{M}^{-1}\mathbf{B}')]'\mathbf{G}^{-1}[\mathbf{D}_{ij}{}^x(\mathbf{M}^{-1}\mathbf{B}')] &=\sum_k (A_{ik}-A_{jk})(B_{ki}M^{-1}{}_i-B_{kj}M^{-1}{}_j)\\ &=\frac{1}{M_i}+\frac{1}{M_j}.\end{aligned} \tag{70}$$

Therefore the mean amplitude for a perpendicular vibration is given by

$$\langle(x_i-x_j)^2\rangle=kT[\mathbf{D}_{ij}{}^x(\mathbf{A})]'\mathbf{F}^{-1}[\mathbf{D}_{ij}{}^x(\mathbf{A})] +\frac{h^2}{64\pi^2kT}\left(\frac{1}{M_i}+\frac{1}{M_j}\right). \tag{71}$$

For the parallel mean amplitude, similar argument leads that

$$\langle(z_i-z_j)^2\rangle=kT[\mathbf{D}_{ij}{}^z(\mathbf{A})]'\mathbf{F}^{-1}[\mathbf{D}_{ij}{}^z(\mathbf{A})] +\frac{h^2}{64\pi^2kT}\left(\frac{1}{M_i}+\frac{1}{M_j}\right), \tag{72}$$

and for the mean cross products

$$\langle(z_i-z_j)(x_i-x_j)\rangle=kT[\mathbf{D}_{ij}{}^z(\mathbf{A})]'\mathbf{F}^{-1}[\mathbf{D}_{ij}{}^x(\mathbf{A})]. \tag{73}$$

It should be pointed out that in Eq. (73) the second term is dropped out, because it is easily shown that

$$[\mathbf{D}_{ij}{}^z(\mathbf{M}^{-1}\mathbf{A})]'\mathbf{G}^{-1}[\mathbf{D}_{ij}{}^x(\mathbf{M}^{-1}\mathbf{A})]=0, \tag{74}$$

since, according to Eq. (69)§

$$\sum_k A_{ik}{}^z B_{ki}{}^x=0, \quad \text{and} \quad \sum_k A_{jk}{}^z B_{ki}{}^x=0. \tag{75}$$

As shown in Appendix II, if the parallel displacement of the distance between the ith and jth atoms be taken as one of the internal coordinates, the element of the column matrix $\mathbf{D}_{ij}{}^z(\mathbf{A})$ is 1 for this coordinate and zero

§ $A_{ik}{}^z$ denotes the element which gives the z component of the displacement of the ith atom. Therefore $\Sigma_k A_{ik}{}^z B_{ki}{}^x$ is a nondiagonal element of the unit matrix and vanishes.

for all the others, and Eq. (72) is simplified to be

$$\langle(z_i-z_j)^2\rangle=kT(F^{-1})_{R_{ij}}+\frac{h^2}{64\pi^2kT}\left(\frac{1}{M_i}+\frac{1}{M_j}\right), \quad (76)$$

where $(F^{-1})_{R_{ij}}$ denotes‖ the diagonal element of the inverted matrix $\mathbf{F}^{-1}$ corresponding to the parallel displacement of the atomic distance. For the cross products containing the parallel displacement as one of its component the following relations are derived:

$$\langle(z_i-z_j)(x_i-x_j)\rangle=kT(F^{-1})_{R_{ij}}[D_{ij}{}^x(A)]_{R_{ij}}, \quad (77a)$$

and

$$\langle(z_i-z_j)(y_i-y_j)\rangle=kT(F^{-1})_{R_{ij}}[D_{ij}{}^y(A)]_{R_{ij}}, \quad (77b)$$

where $[D_{ij}{}^y(A)]_{R_{ij}}$ is the element of the column matrix with regard to the same internal coordinate. It is very interesting to note that both the cross products, (77a) and (77b), are given by the same force constants as those for the parallel square amplitude.

The conclusions stated before hold not only for the bond distance but also for any nonbonded atom pairs. As evident from the argument described in Appendix II, they result from the fact that the parallel displacement of the atomic distance can be taken as one of the internal coordinates of the molecule. In the preceding paper[4] the same formula was derived for bond distances, whereas those of the nonbonded distances were obtained by expanding them in terms of the usual internal coordinates composed of the small displacements of bond distances and bond angles. Needless to say, the small displacement of the distance of any pair of atoms can be taken as one of the internal coordinates, so that the above conclusions can be used for any atom pair.

At a first glance the method described here seems to be more available than those in the preceding paper. In the new treatment, however, we must transform the **F** matrix into a new set of coordinates including the displacement of the said distance, and then carry out the inversion of the matrix **F**. Therefore, it seems doubtful whether this method is easier to deal with than the former one.

For the perpendicular amplitudes and the cross product between them such a simplification cannot be obtained, and Eqs. (71) and (73) have to be used, in which the most laborious task is to compute **A** from **B**. In actual cases the matrix **A** can be obtained easily by Eq. (51) by calculating the inverse matrix $\mathbf{G}^{-1}$ and then multiplying it with **B′**. It is also preferable to calculate the matrix elements by use of symmetry coordinates rather than by internal coordinates, because the factorization of the matrices by the symmetry properties of the molecule simplifies the calculation.

‖ Rigorously speaking, the diagonal element of the $\mathbf{F}^{-1}$ matrix should be expressed as $(F^{-1})_{R_{ij},R_{ij}}$, which is, however, written simply $(F^{-1})_{R_{ij}}$.

III. SYMMETRY CONSIDERATION OF THE MEAN AMPLITUDES

It can be easily shown that symmetry consideration not only simplifies the calculation of the mean amplitudes but also gives useful information whether they are essentially zero or not. The symmetry of the molecule is introduced into the calculation through the transformation matrix **U**, and the normal vibrations are factored into subgroups which are discriminated by being symmetric, antisymmetric, or degenerate with respect to the symmetry elements. But it often happens that a subgroup has no genuine modes of normal vibrations, because the normal modes belonging to this group are either the translation or the rotation of the molecule as a whole. At the same time, if the coordinate axes are suitably selected, the three components of the displacements of a distance can be allowed to belong to any one of the symmetry groups. Sometimes it may happen that one of them falls into the subgroup which has no genuine modes of vibration stated previously. This means that the displacement component is not realized in the motion of the molecule, that is, it has zero magnitude of amplitude. Thus the mean square amplitudes of this displacement as well as the mean cross products composed of it should eventually disappear.

For instance, a nonlinear triatomic molecule has three normal vibrations which are located on the molecular plane, so that the perpendicular displacements of any atomic distances are zero, and the terms, $\langle\Delta y^2\rangle$, $\langle\Delta y\Delta z\rangle$, $\langle\Delta y\Delta x\rangle$, which contain the displacement Δy, perpendicular to the molecular plane, disappear. Another example is a linear triatomic molecule ABA $(\mathbf{D}_{\infty h})$[14]: it has four normal vibrations; two are on the axis, one belonging to the type $\sum_g{}^+$ and the other to the type $\sum_u{}^-$. The other two vibrations are perpendicular to the axis, degenerate and antisymmetric to the center of symmetry i and belong to the type Π_u. Whereas, the perpendicular components of the displacement between the end atoms belong to the type Π_g which contains no normal modes of vibrations. Thus the two perpendicular terms $\langle\Delta x^2\rangle$ and $\langle\Delta y^2\rangle$ and, accordingly, the three cross products are all eliminated.

A more outstanding example is the Cl···Cl pairs in carbon tetrachloride. These pairs lie on a plane of symmetry; Δz and one of perpendicular displacements Δx are located on the plane, while the other one Δy is perpendicular to the plane. As is well known, the normal vibrations of this molecule consist of four vibrations belonging to A_1, E, and F_2 subgroups of $\mathbf{T}_d$ point group, and they are all symmetric with respect to this plane. Therefore, $\langle\Delta y^2\rangle$ substantially disappears, while $\langle\Delta z^2\rangle$ and $\langle\Delta x^2\rangle$ do not.

Another rule which is more applicable than the argument described above is that the cross products between the two displacement components which belong

[14] G. Herzberg, *Molecular Spectra and Molecular Structure* (D. Van Nostrand Company, Inc., New York, 1945), Vol. II, pp. 119 and 272.

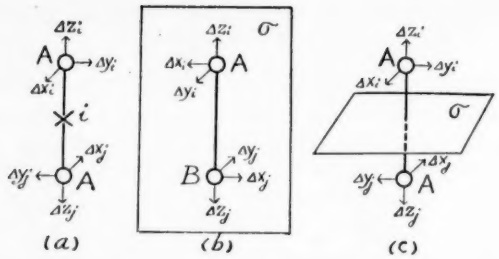

FIG. 1. The displacements of an atom pair and the symmetry.

to different subgroups have no finite values. It will be clarified by the following examples. Let the equilibrium position of the atomic distance AB be on the z axis, and let the molecule have a symmetry or symmetries which are covering operations of AB, that is, by which the atoms AB interchange their positions, or remain at their original positions. In the first example [see Fig. 1(a)], the pair of atoms AA has a center of symmetry i at the middle point of the distance, and the three components, Δz, Δx, and Δy, are symmetrically transformed by the symmetry operation; while in the second case [Fig. 1(b)], where the atomic distance AB is located on the plane of symmetry σ the two components in the plane, Δz and Δx are symmetrically transformed but Δy the component perpendicular to the plane is antisymmetrically transformed by the reflection to this plane. In the former case any cross products have the property of being composed of the normal vibrations symmetric to i, while in the latter case the normal modes of vibrations belonging to the symmetric group have displacements in the directions of the z and x axes but no finite components in the y axis. At the same time the antisymmetric vibrations have displacements in the y axis, but no components in the x and z axes. Therefore, the cross terms $\langle\Delta x\Delta y\rangle$ and $\langle\Delta y\Delta z\rangle$ vanish in this molecule, although $\langle\Delta z\Delta x\rangle$ as well as the square terms, $\langle\Delta x^2\rangle$, $\langle\Delta y^2\rangle$, and $\langle\Delta z^2\rangle$ have finite magnitudes. In the last example shown in Fig. 1(c), where the symmetry plane bisects the atomic distance AA, the reflection to the plane σ, transforms Δz symmetrically but Δx and Δy antisymmetrically, so that the cross terms $\langle\Delta z\Delta x\rangle$ and $\langle\Delta z\Delta y\rangle$ vanish in this case in spite of the finite magnitude of $\langle\Delta x\Delta y\rangle$. In Table I some of the important cases of various symmetry elements are tabulated. In the third, fourth, and fifth columns the symbols $+$, $-$, and e denote, respectively, that the corresponding components of the displacements are symmetric, antisymmetric, and degenerate with respect to the operation.

TABLE I. The mean cross products with respect to the covering operation of the atomic distance.

Symmetry	Relative position of the atomic distance with respect to the symmetry elements	Δz	Δx	Δy	$D(zx)$	$E(xy)$	$F(yz)$
(1) i	i is located at the center of the AB.	+	+	+	$\neq 0$	$\neq 0$	$\neq 0$
(2) $\parallel\sigma$	AB lies on the plane y axis being taken perpendicularly to the plane.	+	+	−	$\neq 0$	0	0
(3) $\perp\sigma$	$AB(A=B)$ is bisected by the plane perpendicularly.	+	−	−	0	$\neq 0$	0
(4) $\parallel C_2$	AB lies on the axis.	+	−	−	0	$\neq 0$	0
(5) $\perp C_2$	$AB(A=B)$ is perpendicular and Δx is parallel to the axis.	+	−	+	0	0	$\neq 0$
(6) $\parallel C_n(n\geqq 3)$	AB lies on the axis.	+	e	e	0	$\neq 0$	0

This rule will prove of wider application, when the atom pair has two or more covering operations. For instance, when AB lies on the crossing line of the two planes of symmetry perpendicular to each other (see Table II), the molecule has at least the symmetry C_{2v} by these two symmetry elements, and the normal modes are grouped into four types: A_1, A_2, B_1, and B_2. The three components of the displacements belong to

TABLE II. The crossed mean amplitudes when the atomic distance is on the crossing line of the two planes of symmetry.

Displacement	$\sigma(zx)$	$\sigma'(zy)$	Symmetry type
Δz	+	+	A_1
Δx	+	−	B_1
Δy	−	+	B_2
$D(zx)=E(xy)=F(yz)=0$			

different symmetry types, Δz to A_1 type symmetric to both planes, Δx to B_1 type symmetric to σ, and antisymmetric to σ', and the component Δy belongs to the class B_2 antisymmetric to σ, and symmetric to σ'. Therefore, the cross products $\langle\Delta z\Delta x\rangle$, $\langle\Delta z\Delta y\rangle$, and $\langle\Delta x\Delta y\rangle$ completely disappear in this case. Some examples of the combinations of the covering operations are listed in the following:

(I) The Cases when All the Mean Cross Products Vanish: $D=E=F=0$

(1) $\parallel\sigma+\parallel\sigma'(C_{2v})$: AB lies on the crossing line of the two planes of symmetry σ and σ'.

(2) $\parallel\sigma+\perp\sigma'(C_{2v})$: $AB(A=B)$ lies on one plane σ, and is bisected by the second plane σ' perpendicular to the former σ.

(3) $\parallel\sigma+\perp C_2(C_{2v})$: $AB(A=B)$ lies on the plane σ and is bisected perpendicularly by the axis C_2 locating on the plane σ.

(4) $\parallel\sigma+\parallel C_n(n\geqq 2)(C_{nv})$: AB lies on the axis C_n and on the plane σ.

(5) $\perp\sigma+\perp C_2(C_{2h})$: $AB(A=B)$ is bisected perpendicularly by the plane σ and by the axis C_2 locating on the plane σ.

(6) $\perp C_2+\parallel C_n(n\geqq 2)(D_n)$: $AB(A=B)$ lies on the axis C_n, and is bisected by the axis C_2 perpendicular to the C_n axis.

(II) The Cases when the Mean Cross Products Are Zero Except One Term

(7) $\parallel\sigma+\perp C_2(C_{2h})$: $AB(A=B)$ lies on the plane σ, but it is bisected by the axis C_2 perpendicular to the plane σ, the y axis being taken parallel to the C_2 axis. The result is: $E(xy)=F(yz)=0$, but $D(zx)\neq 0$.

TABLE III. Some examples of the mean cross products in simple molecules.

Molecule	Atom pair	$D(zx)$	$E(xy)$	$F(yz)$	Symmetrics
H_2O (triangular)	H···H	0	0	0	$\parallel\sigma+\perp\sigma'$
	H−O	$\neq 0$	0	0	$\parallel\sigma$
H_2CO (planar)	C=O	0	0	0	$\parallel\sigma+\parallel C_2$
	H···H	0	0	0	$\parallel\sigma+\perp C_2$
	H···O	$\neq 0$	0	0	$\parallel\sigma$
	C···H	$\neq 0$	0	0	$\parallel\sigma$
BCl_3 (planar regular triangular)	B−Cl	0	0	0	$\parallel\sigma+\parallel\sigma'$
	Cl···Cl	0	0	0	$\parallel\sigma+\perp\sigma'$
		(All cross terms vanish.)			
CH_3Cl (symmetrical top-like)	C−Cl	0	0	0	$\parallel\sigma+\parallel C_3$
	C−H	$\neq 0$	0	0	$\parallel\sigma$
	H−H	0	$\neq 0$	0	$\perp\sigma$
	Cl···H	0	$\neq 0$	0	$\perp\sigma$
CH_2Cl_2 (deformed tetrahedral)	C−Cl	$\neq 0$	0	0	$\parallel\sigma$
	C−H	$\neq 0$	0	0	$\parallel\sigma$
	Cl···Cl	0	0	0	$\parallel\sigma+\perp\sigma'$
	H···H	0	0	0	$\parallel\sigma+\perp\sigma'$
	H···Cl	$\neq 0$	0	0	$\parallel\sigma$
CCl_4 (regular tetrahedral)	C−Cl	0	0	0	$\parallel\sigma+\parallel C_3$
	Cl···Cl	0	0	0	$\parallel\sigma+\perp\sigma'$
		(All cross terms vanish.)			
cis-$C_2H_2Cl_2$ (planar)	C=C	0	0	0	$\parallel\sigma+\parallel C_2$
	H···H	0	0	0	$\parallel\sigma+\perp C_2$
	Cl···Cl	0	0	0	$\parallel\sigma+\perp C_2$
	all other pairs	$\neq 0$	0	0	$\parallel\sigma$
trans-$C_2H_2Cl_2$ (planar)	C=C	$\neq 0$	0	0	$\parallel\sigma+\perp C_2$
	Cl···Cl (*trans*)	$\neq 0$	0	0	$\parallel\sigma+\perp C_2$
	H···H (*trans*)	$\neq 0$	0	0	$\parallel\sigma+\perp C_2$
	all other pairs	$\neq 0$	0	0	$\parallel\sigma$
C_2H_4 (planar)	C=C	0	0	0	$\parallel\sigma+\parallel\sigma'$
	H···H(CH_2)	0	0	0	$\parallel\sigma+\perp\sigma'$
	H···H (*cis*)	0	0	0	$\parallel\sigma+\perp\sigma'$
	H···H (*trans*)	$\neq 0$	0	0	$\parallel\sigma+\perp C_2$
	all other pairs	$\neq 0$	0	0	$\parallel\sigma$
SF_6 (regular octahedral)	S−F	0	0	0	$\parallel\sigma+\parallel\sigma'$
	F···F	0	0	0	$\parallel\sigma+\perp\sigma'$
		(All cross terms vanish.)			
C_6H_6 (regular hexagonal)	C−C	0	0	0	$\parallel\sigma+\perp\sigma'$
	C···C	0	0	0	$\parallel\sigma+\perp\sigma'$
	C−H	0	0	0	$\parallel\sigma+\parallel\sigma'$
	H···H	0	0	0	$\parallel\sigma+\perp\sigma'$
	C···H	$\neq 0$	0	0	$\parallel\sigma$

(8) $\perp\sigma+\parallel C_n(n\geqq 2)(C_{nh})$: $AB(A=B)$ lies on the axis C_n, but it is bisected by the plane σ, which is perpendicular to the C_n axis. The z axis is taken parallel to C_n, and x and y axes to the plane σ. The result is: $D(zx)=F(yz)=0$, but $E(xy)\neq 0$.

It should be noted that the existence of the center of symmetry is of no use, since as indicated in Table I, it does not separate the three components of the displacements.

As the molecules which we are interested in, usually contain many atom pairs of this sort, the consideration described above will enable us to simplify further treatment. Some examples are shown in Table III. It will be seen that the atom pairs having two covering operations except the center of symmetry have no cross terms in almost all the cases. The pairs of C−C, *trans* Cl···Cl, and *trans* H···H in *trans*-dichloroethylene molecule, as well as the H···H pairs at the *trans*-position in ethylene molecule, etc., provide the exceptions due to the argument described in (II-7).

In actual cases the process of treatment is to be reversed. The symmetry properties should be considered first, then the nonvanishing components of the mean amplitudes are calculated by the method described in Sec. II, and finally the intensity curve and the modified radial distribution curve are computed by the formulas presented in Sec. I to compare with those obtained by the experiment.

In conclusion, the authors are grateful for aid from the Scientific Research Encouragement Grant given by the Department of Education of Japan in support of this research.

APPENDIX I

The integration of Eq. (14):

$$I=\frac{e^{-A}}{4\pi}\sum_{n=0}^{\infty}\sum_{k=0}^{\infty}(-1)^k(\pi)^{\frac{1}{2}}\frac{(n+k)!}{n!(2k)!}\left(\frac{d}{da}\right)^{2k}\times\left[\left(\frac{2}{a}\right)^{n+k+\frac{1}{2}}J_{n+k+\frac{1}{2}}(a)\right]\int_0^{2\pi}P^nQ^{2k}d\epsilon, \quad \text{(A1)}$$

is carried out as follows: Since

$$J_{p+\frac{1}{2}}(a)=(-1)^pa^{p+\frac{1}{2}}\left(\frac{2}{\pi}\right)^{\frac{1}{2}}\left(\frac{1}{a}\frac{d}{da}\right)^p\left\{\frac{\sin a}{a}\right\}, \quad \text{(A2)}$$

we have

$$\left(\frac{d}{da}\right)^{2k}\left[\left(\frac{2}{a}\right)^{n+k+\frac{1}{2}}J_{n+k+\frac{1}{2}}(a)\right]=I_p\left\{(-1)^{n+k}\frac{2^{n+k+1}}{(\pi)^{\frac{1}{2}}}\times\left(\frac{i^{n+3k}e^{ia}}{a^{n+k+1}}-\frac{(n+5k)(n+k+1)}{2}\times\frac{i^{n+3k-1}e^{ia}}{a^{n+k+2}}+\cdots\right)\right\}, \quad \text{(A3)}$$

where I_p denotes the imaginary part.

As described in Sec. I, the summation of the series over n suffices to take the first two terms $n=0$, and 1, while that over k should be taken to the infinite terms. The integral to be calculated is divided into two parts;

$$I=I_0+I_1, \quad \text{(A4)}$$

with

$$I_0=\frac{e^{-A}}{4\pi}\sum_{k=0}^{\infty}(-1)^k(\pi)^{\frac{1}{2}}\frac{k!}{(2k)!}\left(\frac{d}{da}\right)^{2k}\times\left[\left(\frac{2}{a}\right)^{k+\frac{1}{2}}J_{k+\frac{1}{2}}(a)\right]\int_0^{2\pi}Q^{2k}d\epsilon, \quad \text{(A5)}$$

and

$$I_1=\frac{e^{-A}}{4\pi}\sum_{k=0}^{\infty}(-1)^k(\pi)^{\frac{1}{2}}\frac{(k+1)!}{(2k)!}\left(\frac{d}{da}\right)^{2k}\times\left[\left(\frac{2}{a}\right)^{k+\frac{3}{2}}J_{k+\frac{1}{2}}(a)\right]\int_0^{2\pi}PQ^{2k}d\epsilon. \quad \text{(A6)}$$

If we put

$$D=G\cos\epsilon_0, \quad F=G\sin\epsilon_0, \quad \text{(A7)}$$

then

$$Q=-2G\cos(\epsilon-\epsilon_0), \quad \text{(A8)}$$

and we have

$$\int_0^{2\pi}Q^{2k}d\epsilon=(4G^2)^k\int_0^{2\pi}\cos^{2k}(\epsilon-\epsilon_0)d\epsilon=2\pi G^{2k}\frac{(2k)!}{(k!)^2}. \quad \text{(A9)}$$

By similar procedure we obtain

$$\int_0^{2\pi}PQ^{2k}d\epsilon=2\pi G^{2k}\left[\frac{(2k)!}{(k!)^2}A+\frac{(2k)!}{(k-1)!(k+1)!}\times(B\sin^2\epsilon_0+C\cos^2\epsilon_0-2E\sin\epsilon_0\cos\epsilon_0)-\frac{1}{4}\frac{(2k+2)!}{[(k+1)!]^2}(B+C)\right]. \quad \text{(A10)}$$

Inserting Eq. (A9) into (A5) and neglecting the higher ones than the first two terms in the expansion of Eq. (A3), we have

$$I_0=I_p\left\{e^{-A}\frac{e^{ia}}{a}\sum_{k=0}^{\infty}\frac{1}{k!}\left(-\frac{2iG^2}{a}\right)^k\left(1-\frac{5k(k+1)}{2}\frac{1}{ia}\right)\right\}$$
$$=\frac{e^{-A}}{a}I_p\left\{e^{ia}\sum_{k=0}^{\infty}\frac{1}{k!}\left(-\frac{2iG^2}{a}\right)^k+10\frac{G^2}{a^2}\sum_{k=0}^{\infty}\frac{1}{(k-1)!}\times\left(-\frac{2iG^2}{a}\right)^{k-1}-10i\frac{G^4}{a^3}\sum_{k=0}^{\infty}\frac{1}{(k-1)!}\times\left(-\frac{2iG^2}{a}\right)^{k-2}\right\}; \quad \text{(A11)}$$

and by summing up the infinite series into exponential forms it may be written as

$$I_0=\frac{e^{-A}}{a}I_p\left\{e^{i\gamma}+10\frac{G^2}{a^2}e^{i\gamma}-10i\frac{G^4}{a^3}e^{i\gamma}\right\}=e^{-A}\frac{\sin\gamma}{a}+10e^{-A}G^2\frac{\sin\gamma}{a^3}-10e^{-A}G^4\frac{\cos\gamma}{a^4}, \quad \text{(A12)}$$

where

$$\gamma=a-2G^2/a. \quad \text{(A13)}$$

For the calculation of the second integral it suffices to take the first term in the expansion of (A3),

$$I_1=e^{-A}I_p\left\{-\frac{2ie^{ia}}{a^2}\sum_{k=0}^{\infty}\frac{1}{k!}\left(-\frac{2iG^2}{a}\right)^k \times[(k+1)A-(2k+1)(B+C)/2+k(B\sin^2\epsilon_0 +C\cos^2\epsilon_0-2E\sin\epsilon_0\cos\epsilon_0)]\right\}, \quad \text{(A14)}$$

and by similar procedure we obtain

$$I_1=-2\frac{e^{-A}}{a^2}I_p\left\{ie^{i\gamma}\left(A-\frac{B+C}{2}\right)+e^{i\gamma}\frac{2G^2}{a} \times(A-B\cos^2\epsilon_0-C\sin^2\epsilon_0-2E\sin\epsilon_0\cos\epsilon_0)\right\}$$
$$=-2e^{-A}\frac{\cos\gamma}{a^2}\left(A-\frac{B+C}{2}\right)-4e^{-A}\frac{\sin\gamma}{a^3} \times[AG^2-BD^2-CF^2-2DEF]. \quad \text{(A15)}$$

Hence, Eqs. (A12) and (A15) being combined, the final expression becomes

$$I=e^{-A}\frac{\sin\gamma}{a}+10e^{-A}G^2\frac{\sin\gamma}{a^2}-10e^{-A}G^4\frac{\cos\gamma}{a^4} -2e^{-A}\frac{\cos\gamma}{a^2}\left(A-\frac{B+C}{2}\right)-4e^{-A}\frac{\sin\gamma}{a^3} \times[(A-B)D^2-(A-C)F^2-2DEF]. \quad \text{(A16)}$$

APPENDIX II

It is easily proved as follows that $[\mathbf{D}_{ij}{}^z(\mathbf{A})]$ has the form of $(1,0,0,0,\cdots)$, where z indicates the parallel displacement of a given atomic distance. Let the equilibrium position of the pair of atoms (i,j) be on the z axis, and the parallel displacement of this distance, $R_{ij}=\Delta z_i-\Delta z_j$, be taken as one of the internal coordinates. If we put R_{ij} at the first element of the column matrix of the internal coordinates, $\mathbf{R}$, and z_i, z_j at the first and second elements of $\mathbf{X}$, the $\mathbf{B}$ matrix has the form of

$$R_{ij}=\begin{matrix}&\Delta z_i&\Delta z_j&&&\\ R_1&1,&-1,&0,&0,&\cdots\\ R_2&B_{21},&B_{22},&B_{23},&B_{24},&\cdots\\ R_3&B_{31},&B_{32},&B_{33},&B_{34},&\cdots\end{matrix}. \quad \text{(A17)}$$

Then the elements of the inverted matrix of $\mathbf{B}$ are give by

$$A_{11}=|B|_{11}/det|B|, \quad A_{21}=|B|_{12}/det|B|, \quad \cdots$$
$$A_{12}=|B|_{21}/det|B|, \quad A_{22}=|B|_{22}/det|B|, \quad \cdots \quad \text{(A18)}$$

where $|B|_{ij}$ denotes the cofactor of the term B_{ji}. Expanding $det|B|$ with respect to the first row, we find

$$det|B|=|B|_{11}-|B|_{12}. \quad \text{(A19)}$$

Therefore,

$$A_{11}-A_{21}=1. \quad \text{(A20)}$$

It can be easily shown by Eq. (A18) that

$$A_{1l}-A_{2l}=0, \quad \text{(A21)}$$

in case when $l\neq 1$. Therefore, the column matrix $\mathbf{D}(\mathbf{A})$ with regard to the parallel component of the displacement of the atomic distance R_{ij}, is reduced to

$$[\mathbf{D}_{ij}{}^z(A)]=(1,0,0,0,\cdots). \quad \text{(A22)}$$

Thus the matrix of the first term in Eq. (72) is simplified to be

$$[\mathbf{D}_{ij}{}^z(\mathbf{A})]'\mathbf{F}^{-1}[\mathbf{D}_{ij}{}^z(\mathbf{A})]=(F^{-1})_{Rij}, \quad \text{(A23)}$$

for the parallel vibration of the distance. Moreover, since $[\mathbf{D}_{ij}{}^z(\mathbf{A})]'\mathbf{F}^{-1}$ has only one element of finite magnitude $(F^{-1})_{Rij}$, the multiplication of matrices, $[\mathbf{D}_{ij}{}^z(\mathbf{A})]'\mathbf{F}^{-1}[\mathbf{D}_{ij}{}^x(\mathbf{A})]$ appeared in Eq. (73) is reduced to a simple multiplication of one term of $(F^{-1})_{Rij}$ with the corresponding one $[D_{ij}{}^x(A)]_{Rij}$.

Letters to the Editor

THIS section will accept reports of new work, provided these are terse and contain few figures, and especially few half-tone cuts. The Editorial Board will not hold itself responsible for opinions expressed by the correspondents. Contributions to this section should not exceed 600 words in length and must reach the office of the Editor not later than the 15th of the second month preceding that of the issue in which the Letter is to appear. No proof will be sent to the authors. A publication charge of $10.00 per Letter is made which, when honored, will entitle the Institution to 100 free reprints.

Concentration Dependence of Chemical Exchange and NMR Multiplet Structure in Water-Ethanol Mixtures

IRVING WEINBERG AND JOHN R. ZIMMERMAN
Magnolia Petroleum Company, Field Research Laboratories, Dallas, Texas
(Received February 11, 1955)

GUTOWSKY[1,2] and his co-workers have made extensive studies of chemical shifts of magnetic resonance single-line spectra arising from fast chemical phenomena. Abnormal proton line width broadening of certain paramagentic aqueous systems has also been attributed to fast proton exchange.[3,4] In ethanol, Arnold and Packard[5] found the position of the proton resonance of the OH group to be temperature and concentration dependent. Under all of these conditions, the position of the single resonance line is a number average of the chemical shifts of the nuclei in the absence of any exchange. In cases of molecular association or complexing it would be advantageous to be able to study the individual molecular species. However, fast proton exchange usually interferes with such an observation. Since in ethyl alcohol small concentrations of water do not wash out the spin-spin structure in the OH resonance, it was felt that the association of ethyl alcohol and water might possibly be subject to study by nuclear resonance methods. Thenceforth, a preliminary investigation of this possibility has been made. All observations were carried out at room temperature by means of the Varian, V-4300 high resolution spectrometer at a dc magnetic field of approximately 9500 gauss. Chemical shifts were referenced with respect to the central spectrum of the CH_3 resonance in ethyl alcohol.

It was found that the presence of water in solution has a marked effect on chemical shifts of both the ethanol OH and associated H_2O lines. As shown in Fig. 1, no measurable changes in chemical shift occur until in the vicinity of 20 percent water concentration. Fast exchange begins in this region and the two lines rapidly coalesce. Under conditions of fast exchange, the molecular ratio of water and alcohol molecules calculated from the experimental chemical shifts in Fig. 1 is almost 1/1—actually 0.95/1. This corresponds to 27 percent by weight of water in solution. The average lifetime of a proton in the OH state at the critical concentration is approximately 0.05 second. Additional exchange processes are suggested by the fact that at high water concentrations the chemical shift of the coalesced line does not change appreciably.

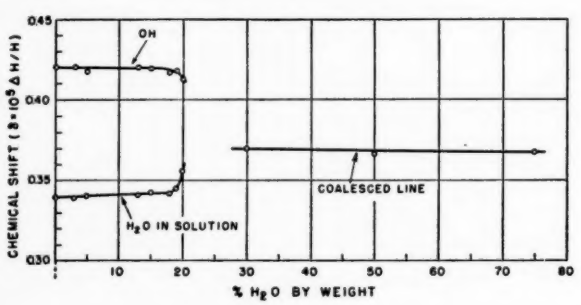

FIG. 1.

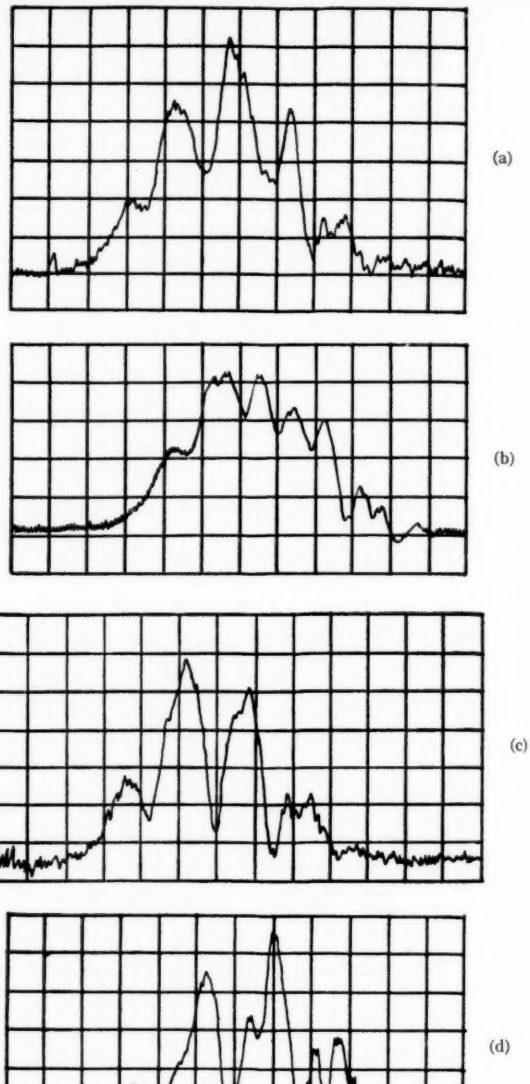

FIG. 2. CH_2 resonance of ethyl alcohol-water mixture. (a) Less than 0.1 percent H_2O. (b) 13 percent H_2O. (c) 20 percent H_2O. (d) 50 percent H_2O.

In the region, shown in Fig. 1, where fast exchange does not appear to be present, changes in spin-spin structure of both the OH and CH_2 multiplets are observed. For example, variations of the CH_2 multiplet structure are shown in Fig. 2. Whereas in water-free ethanol some of the splittings are essentially coincident from the combined effect of OH and CH_3 interactions with the CH_2 group, the concentrations just prior to the region of fast exchange exhibit an expected effect of association by an apparent alteration of the coupling between the CH_2 and OH groups. Of course, when fast exchange sets in, the spin-spin interactions between the OH and CH_2 groups are washed out.

Since ethyl alcohol has been found to be so extremely sensitive to small impurities, some of our arguments based on these observations may be premature. With this thought in mind, we are investigating various techniques for producing "pure" alcohol and water. We hope to learn more about the state of association and exchange processes of the alcohol-water mixture with further refined measurements, including higher spectral resolution, of these observed effects. The influence of temperature on the exchange system and critical concentration should be a convenient and worthwhile parameter to study.

[1] H. S. Gutowsky and A. Saika, J. Chem. Phys. **21**, 1688 (1953).
[2] H. S. Gutowsky and S. J. Fujiwara, J. Chem. Phys. **22**, 1782 (1954).
[3] J. R. Zimmerman, J. Chem. Phys. **21**, 1605 (1953).
[4] J. R. Zimmerman, J. Chem. Phys. **22**, 950 (1954).
[5] J. T. Arnold and M. E. Packard, J. Chem. Phys. **19**, 1608 (1951).

Simultaneous Vibrational Transitions in Liquids

J. A. A. KETELAAR AND F. N. HOOGE
Laboratory for General and Inorganic Chemistry of the University of Amsterdam, Amsterdam, The Netherlands
(Received February 10, 1955)

As a sequel to the recent discovery of simultaneous vibrational transitions in compressed gas mixtures,[1] e.g., CO_2+N_2 CO_2+O_2, and CO_2+H_2, we have also investigated liquid mixtures.

The infrared absorption spectrum of a mixture of equal parts by volume of bromine and carbon disulfide (0.54 mole fraction of bromine) in a cell with a light path of 5 mm did indeed show on both sides of the very heavy band of CS_2 at 1510 cm^{-1} a band which was not present in the spectra of either of the components in 5 mm thickness (Fig. 1). The carbon disulfide used was purified by prolonged shaking with bromine, elimination of the bromine with copper turnings and destillation.[2] The pure bromine used was specially made in an all glass apparatus without the use of any grease or other organic compounds.[3] Its infrared spectrum did show the complete absence of any absorbing impurities, which are always present in commercial preparations.

With a saturated solution of iodine in carbon disulfide (14.5g I_2 in 100g solution) in a layer of 1 cm also two new bands were observed, again on both sides of the CS_2 band at 1510 cm^{-1}.

Observed: $Br+CS_2$: 1807, 1204 cm^{-1}; I_2+CS_2: 1710, 1307 cm^{-1}.
Calculated:[4] $1510\pm306.1=1816$, 1204 cm^{-1}; $1510\pm203.1=1713$, 1307 cm^{-1}.

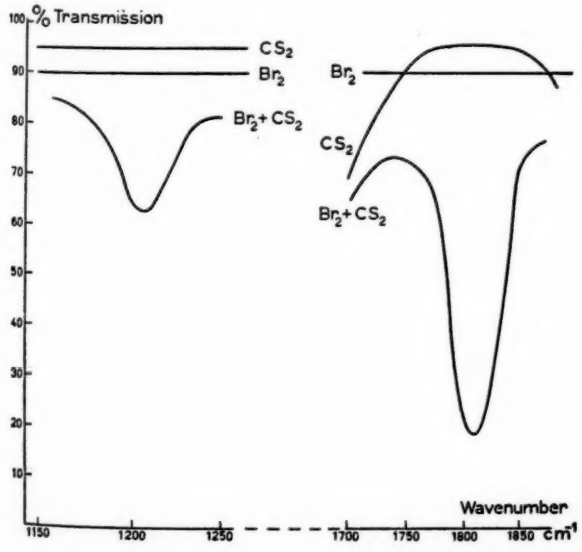

FIG. 1. Transmission curves for CS_2, Br_2, and a mixture with X $Br_2=0.54$; Cell thickness 5 mm.

The value of 1510 cm^{-1} taken for ν_3 (asymmetric vibration) of carbon disulfide is the value found by us in dilute solutions of CS_2 in bromine; for pure CS_2 this frequency is given as 1515 cm^{-1}.

We conclude that in these liquid mixtures, just as in gases, simultaneous vibrational transitions exist. In these cases we have not only observed the sum frequencies but also the difference frequencies as was predicted by one of us. (On the basis of a theory analogous to the polarizability theory of the Raman-effect.[5])

The intensity ratio of difference band to sum band in first approximation is given by: $I_0/I_S=\exp(-h\nu/kT)$ with ν the vibrational frequency of the bromine (iodine) molecule. The ratio observed for optical densities at the top of the absorption band CS_2+Br_2:0.19, CS_2+I_2:0.36 is very close to the calculated value: 0.22 and 0.35, respectively.

The dependence of the intensities on concentration and temperature will be studied next. Other mixtures, e.g., with CCl_4, will be also investigated. However with components with more complicated molecules the lack of transparency in rather thick layers will prevent the detection of simultaneous vibrational transitions in most cases.

This work is part of the research program of the "Stichting voor Fundamenteel Onderzoek der Materie" (Foundation for Fundamental Research of Matter, F.O.M.) and was made possible by financial support from the Nederlandse Organisatie voor Zuiver Wetenschappelijk "Onderzoek" (Netherland Organisation for Pure Research, Z.W.O.).

[1] J. Fahrenfort and J. A. A. Ketelaar, J. Chem. Phys. **22**, 1631 (1954).
[2] A. Chenevier, Z. anal. Chem. **31**, 68 (1892).
[3] A. Scott, J. Chem. Soc. **103**, 847 (1913).
[4] Liquid bromine $\nu=306.1$ cm^{-1}, H. Stammreich and R. Forneris, J. Chem. Phys. **22**, 1624 (1954). Bromine vapor 316.8 cm^{-1} iodine (vapor) $\nu=213.3$ cm^{-1}, quoted by G. Herzberg, *Spectra of Diatomic Molecules*, second edition, p. 541.
[5] J. A. A. Ketelaar, "Estimated value for liquid state: 203 cm^{-1}," Convegno intern. di Fisica dell'infrarosso, Parma, September 3–7, 1954 (to be published).

Virial Coefficients of Benzene-Cyclohexane Mixtures, and Theories of Liquid Solutions

F. G. WAELBROECK
Laboratoire de Chimie-Physique II. Université Libre de Bruxelles, Brussels, Belgium
(Received January 20, 1955)

THE cell model of the liquid state has been used by Prigogine and co-workers[1] to evaluate the "second-order terms" in the expansion of the free energy and, hence, the excess thermodynamic properties of liquid solutions. These authors assumed that, for homopolar, quasi-spherical molecules[2]

$$\epsilon_{12}=(\epsilon_{11}\epsilon_{22})^{\frac{1}{2}}, \quad (1)$$

$$r_{12}=(r_{11}+r_{22})/2. \quad (2)$$

ϵ_{ij} and r_{ij} are the coordinates of the minimum in the intermolecular potential energy curve of molecules i and j.

On the other hand, Longuet-Higgins[3] has shown that the first-order deviation from the laws of perfect solutions is independent of the structure of the solution, and may be expressed in terms of

$$d_{12}=(2\epsilon_{11}-\epsilon_{11}-\epsilon_{22})/\epsilon_{11}. \quad (3)$$

d_{12} measures, for most solutions, the deviations from (1). Longuet-Higgins tests his theory by comparing the d_{12} values deduced from various excess properties of the same mixture.

The properties of some solutions, however, [CH_4/CO;[4] $CCl_4/C(CH_3)_4$][5] cannot be represented, even qualitatively, by this theory of conformal solutions, and must undoubtedly be attributed to the above mentioned higher-order (and structure-dependent) terms. It may thus be wondered whether the agreement obtained

TABLE I. Virial coefficients of $C_6H_6(B_{11})$, $C_6H_{12}(B_{22})$ and their mixture (B_{12}) as functions of the temperature T(°C). For each gas: in brackets, number of experiments carried out, then, value of the virial coefficient and average deviation from the mean (cc mole^{-1}). B_{12} was calculated from: $B_m = x_1^2B_{11} + 2x_1x_2B_{12} + x_2^2B_{22}$; x_1, x_2 are the molar fractions; B_m the apparent virial coefficient of the mixture.

T (°C)	$-B_{11}(C_6H_6)$			$-B_{22}(C_6H_{12})$			$-B_{12}$ (Mixture)		
42°				(1)	1518				
47°				(2)	1435	±9			
50°				(2)	1382	±13			
55°				(2)	1355	±16	(3)	1227	±30
58°	(2)	1125	±7	(2)	1301	±3			
60°	(7)	1117	±11	(6)	1268	±13	(9)	1203	±23
62°	(1)	1103							
65°	(5)	1088	±2	(6)	1236	±11	(16)	1158	±12
68°	(2)	1054	±11						
70°	(7)	1035	±11	(8)	1180	±10	(9)	1109	±20
75°	(5)	1011	±9	(4)	1171	±3	(5)	1075	±9

by Longuet-Higgins for a certain number of solutions is not due to his treatment of d_{12} as a parameter which can be arbitrarily adjusted.

Accurate measurements of the second virial coefficients of benzene, cyclohexane and of their mixture, have been carried out[6] in an apparatus analogous to that of Eucken and Mayer.[7] The experimental results (Table I) are compared (Fig. 1) with previous determinations.[8]

These measurements allow a determination of d_{12} if, as is assumed in practically all the theories of liquid solutions: a) The intermolecular potential-energy curves of identical, or different, molecules lead to a corresponding state law, and b) r_{12} is given by (2). It follows from a) that the plots of the reduced virial coefficients $B_{ij}^* = B_{ij}/V_{ij}^{cr}$ *versus* the reduced temperatures $T_{ij}^* = T/T_{ij}^{cr}$ should coincide, and that

$$T_{ij}^{cr} = k\epsilon_{ij} \quad V_{ij}^{cr} = k'(r_{ij})^3. \tag{4}$$

k and k' are constants, independant of the nature of i and j; T_{11}^{cr}, T_{22}^{cr}, V_{11}^{cr}, V_{22}^{cr} the critical constants of the pure substances; T_{12}^{cr}, V_{12}^{cr} those of an hypothetical substance with interactions identical to the 1–2 intermolecular potential. From assumption b) and Eq. (4): $V_{12}^{cr} = [(V_{11}^{cr})^{\frac{1}{3}} + (V_{22}^{cr})^{\frac{1}{3}}]^3/8$.

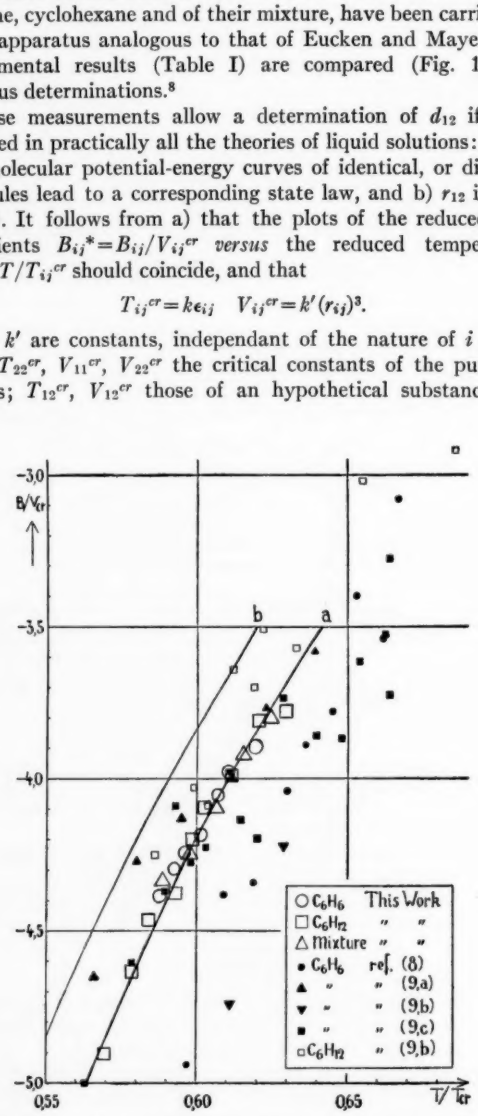

FIG. 1. Plot of the reduced virial coefficients as functions of the reduced temperatures. The critical constants V_{cr} and T_{cr} were taken from K. A. Kobe and R. E. Lynn, Jr., Chem. Revs. **52**, 117 (1953).

Figure 1 shows that, in the temperature range studied, and within the limits of experimental uncertainties, the pure substances appear to obey a corresponding state law. The plot $B_{12}^* = f[T/(T_{11}^{cr} \cdot T_{22}^{cr})^{\frac{1}{2}}]$ also coincides with curve (a) obtained for the pure substances. The theory of conformal solutions predicted, from the experimental excess properties, that, if the first-order derivatives of the free energy are predominant, $d_{12} \sim -0.065$ for this mixture[3]; if such had been the case, the B_{12} values, plotted as indicated above, would have fallen on curve (b).

The maximum possible error on a single B_{12} measurement corresponds to an uncertainty of slightly less than ±0.04 on d_{12}. Each B_{12} value plotted being the average of from 3 to 16 experiments, we may conclude that, if assumptions a) and b) are valid, $d_{12} = 0.00 \pm 0.02$ for the C_6H_6/C_6H_{12} mixture, and that the excess properties of this liquid solution must probably be attributed to structure-dependent (second- and higher-order) terms in the expansion of the free energy.

The author wishes to thank the Institut pour l'Encouragement de la Recherche Scientifique dans l'Industrie et l'Agronomie (IRSIA) for a grant which has made this research possible.

[1] I. Prigogine and G. Garikian, Physica **16**, 239 (1950). I. Prigogine and V. Mathot, J. Chem. Phys. **20**, 49 (1952). I. Prigogine and A. Bellemans, Disc. Faraday Soc. **15**, 80 (1953). I. Prigogine and S. Lafleur, Acad. Roy. Belg. Bull. classe Sci. **40**, 484 (1954).
[2] Other cases can be readily considered, but require the use of one or more adjustable parameters.
[3] H. C. Longuet-Higgins, Proc. Roy. Soc. (London) **A205**, 247 (1951).
[4] V. Mathot and A. Desmyter, J. Chem. Phys. **21**, 782 (1953).
[5] V. Mathot (to be published).
[6] A detailed description of these experiments will be published in the Bull. soc. chim. Belg.
[7] A. Eucken and L. Mayer, Z. physik chem. **B5**, 452 (1929).
[8] (a) Bax-tendale and Enüstün. Phil. Trans. Roy. Soc. (London) **A243**, 176 (1951). (b) Lambert, Roberts, Rowlinson, Wilkinson, Proc. Roy. Soc. (London) **A196**, 113 (1949). (c) Francis, McGlashan, Hamann, and McManamey, J. Chem. Phys. **20**, 1341 (1952).

Intrinsic Viscosity of Polymethylmethacrylate

ANTON PETERLIN
Institute "Jozef Stefan," Ljubljana, Yugoslavia
(Received February 7, 1955)

SCHULZ and collaborators[1] have measured the intrinsic viscosity of polymethylmethacrylate in different solvents in a very wide range of molecular weights, from $M = 400$ to 10^7. At large M the log $[\eta]$ *vs* log M plot (Fig. 1) yields a straight line, the intrinsic viscosity being very well represented by the Houwink-Mark relation $[\eta] = K.M^a$. In benzene as solvent $K = 0.38 \cdot 10^{-2}$ cm^3/g, $a = 0.79$. At lower M, however, the viscosity curve shows a markedly lower slope quite contrary to the theoretical prediction for linear chains.

Since side chains lower the intrinsic viscosity[2] we have considered a more elaborated model of PMMA. The monomer unit has two side groups: $-CH_3$ and $-COOCH_3$. The latter one is a chain with three links: $-CO-O-CH_3$. In the case of pure head-to-tail polymerization the macromolecule has the structure

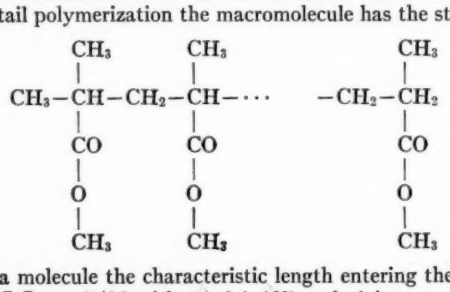

In such a molecule the characteristic length entering the Flory's relation $[\eta] = \Phi \cdot d^3/M$ with $\Phi = 2.1 \cdot 10^{23}$ mole^{-1} is not more the end-to-end distance but the gyration radius ρ introduced by Stockmayer and Zimm[3] in the light scattering investigation of

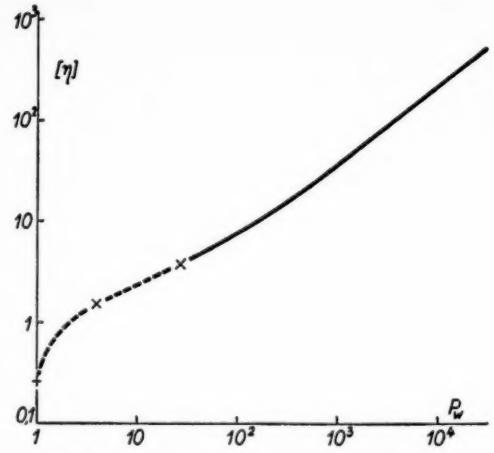

FIG. 1. Intrinsic viscosity of PMMA in benzene (Meyerhoff, see reference 1). The monomer (methylisobutyrate) was measured in acetone (Peterlin).

branched chains and by Brini and Benoit[4] in the treatment of the viscosity of singly branched tertiary alcohols. In order to conform with the case of unbranched molecules, we have to put $d^2=6\rho^2$. Attributing to every group the same statistical weight, the gyration radius is given by

$$\rho^2=\frac{1}{2N^2}\sum_j\sum_k\langle r^2_{jk}\rangle_{Av} \qquad (1)$$

where $N=6P$ is the number of groups in the P-mer and r_{jk} the distance between the ϑ-th and the k-th group. Neglecting any volume and interaction effect and taking

$$\langle r_n^2\rangle_{Av}=b^2[n(1-\cos^2\alpha)-2\cos\alpha+2\cos^{n+1}\alpha]/(1-\cos\alpha)^2 \qquad (2)$$

as the square average of the distance of two groups with n links between them, we get with $b=1.54$A and $\cos\alpha=\frac{1}{3}$ the curve d^3/M of Fig. 2. It has the same characteristics as the experimental intrinsic viscosity curve although there is, of course, no perfect fit due to the many over-simplifications in the model. So, for instance, owing to the undisturbed random walk formula (Eq. (2)) the limiting viscosity function has the slope 0.5 instead of the experimental value 0.79.

The most important feature is the low slope at small DP where the many side chains give the PMMA molecule a rather sphere-like appearance. A very similar structure has the polystyrene molecule with the large benzene ring as the side chain of the monomer unit. Indeed the viscosity behavior[1,5] coincides very closely with that of PMMA. The same applies to polyisobutylene.[6]

Further the steep increase in viscosity from the monomer to the dimer has to be noted. Experimentally the increase is still larger than can be understood by the molecular structure of the solvent. At equal size, shape, and force field of the molecules of the solvent and the solute intrinsic viscosity vanishes. Since the difference between the molecule of MMA monomer and of benzene is not very large, a constant amount has to be subtracted from the calculated $[\eta]$ of PMMA in order to get the true intrinsic viscosity and especially the transition to the pure solvent. Then the theoretical curve fits better the experimental one.

The nearly constant value of $[\eta]$ between $P=2$ and 5 in the calculated curve is very likely due to the neglect of the volume effect. The oligomer[7] is surely more extended than our model thus yielding a larger slope of the viscosity curve.

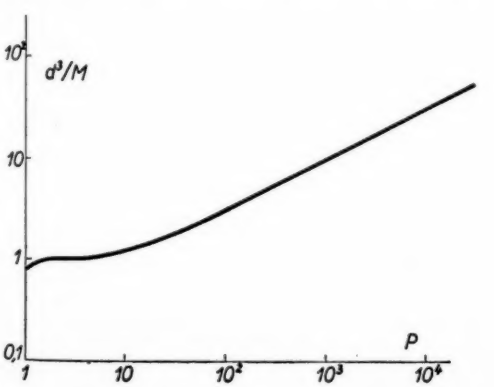

FIG. 2. The calculated value $(\rho\sqrt{6})^3/M$ for the simplified PMMA model.

[1] K. G. Schön and G. V. Schulz, Z. physik Chem. **2**, 197 (1954); G. Meyerhoff, paper read before the Int. Congr. Macromol. Chem., Torino, October 1954.
[2] Staudinger, Bier, and Lorentz, Makromol. Chem. **3**, 251 (1949).
[3] W. H. Stockmayer and B. M. Zimm, J. Chem. Phys. **17**, 1301 (1949).
[4] M. Brini and H. Benoit, paper read before the Int. Congr. Macromol. Chem., Torino, October, 1954.
[5] H. Marzolph and G. V. Schulz, Makromol. Chem. **13**, 120 (1954).
[6] T. G. Fox and P. J. Flory, J. Phys. Colloid Chem. **53**, 197 (1947); W. R. Krieghaum and P. J. Flory, J. Am. Chem. Soc. **75**, 1775 (1953).
[7] A. Peterlin, Int. Coll. *Macromolecules in Solution* (Paris, 1948), p. 70.

On the $^4\Pi$ State of the O_2^+ Molecule

A. BUDÓ AND I. KOVÁCS
Central Research Institute for Physics, Department of Spectroscopy, Budapest, Hungary
(Received December 28, 1954)

IN the case of the $^4\Pi$ electron state of the O_2^+ molecule the splitting of the multiplet term, taken as a function of the rotational quantum number $\mathfrak{F}$—according to Nevin's rotational analysis[1] of the $^4\Sigma_g^--{}^4\Pi_u$ bands—does not agree well with the formulas derived by Brandt[3] on the basis of van Vleck's theory.[2] The above $^4\Pi$ state is the only fine-structure $^4\Pi$ term known up to now. Theoretical considerations indicate that the deviations in the relative positions of the components of the $^4\Pi$ term, as compared with those expected theoretically, may be due to an interaction of these components with one or more $^2\Pi$ term. Such an interaction between terms of different multiplicities is being transmitted by the operator $\Sigma a_i(l_iS_i)$ of the orbit-spin interaction.[4] In the term scheme of the O_2^+ molecule $^2\Pi$ terms can indeed be found relatively near to the $^4\Pi$ term considered here.

For short we denote these Π terms successively by $^2\Pi^a$, $^4\Pi$, $^2\Pi^b$, $^2\Pi^c$, $^2\Pi^d$.

In the wave equation $[H-V(r)]\phi=0$ of the stationary molecule H_0 is the part of H not containing spin-terms, so that approximately $H=H_0+\Sigma a_i(l_iS_i)=H_0+H_p$. The eigenfunctions ϕ_0 of the wave equation $[H_0-V(r)]\phi_0=0$ belonging to the five states mentioned were constructed as linear combinations of such zero-order eigenfunctions of the five-electron system which appear in the form of determinants. We used in the approximation of the coefficients on the one hand Mulliken's derivation[5] of the five states from the states of O_2, on the other hand, the values of the multiplet constants A of the known first three terms/$A=195$, -48 and 8.2 cm^{-1}/.

Turning from the stationary molecule to that with oscillating and rotating nuclei, we worked out the matrix elements of the operator H_1+H_p with the help of the eigenfunctions of $\psi_0=\phi_0Ru$. Here H_1 represents the terms neglected in the separation of the complete wave equation, R is the eigenfunction of the wave equation of the oscillator, and u that of the symmetric top. We find in the approximation used here an interaction between the term components $^4\Pi$, $^2\Pi^b$, and $^2\Pi^c$. Correspondingly we obtain the term values of the components of $^4\Pi$ from the four suitable eigenvalues of an 8-row matrix H'. Transforming H' with the help of a matrix S, so that the $^4\Pi$ part of $S^{-1}H'S$ is diagonal, four diagonal elements of this part represent Brandt's energy expression W_k. However, as the result of the interaction of the $^4\Pi$ term with the $^2\Pi$ terms, the other parts of the matrix give further

terms $(W_k'-W_k)$; in particular, we obtain from the perturbation calculation of nondegenerate systems in second approximation

$$W_k'-W_k=\alpha(S_{2k}^2+S_{3k}^2), \quad (k=1,2,3,4), \tag{1}$$

where

$$\alpha=\frac{\rho^2}{\nu(^4\Pi,^2\Pi^b)}+\frac{\sigma^2}{\nu(^4\Pi,^2\Pi^c)}. \tag{2}$$

Here ρ and σ are the following matrix elements of the operator H_p: $\rho=H_p(^4\Pi_{\frac{1}{2}},^2\Pi_{\frac{1}{2}}^b)=-81.3$ cm^{-1}, $\sigma=H_p(^4\Pi_{\frac{1}{2}},^2\Pi_{\frac{1}{2}}^c)=152.8$ cm^{-1}. The meaning of S is given by formula (9) of an earlier paper[6] by the authors.

Thus, from the above considerations follows that the interaction with the $^2\Pi$ terms results in the following deviations in the distances between the components of the $^4\Pi$ term as compared with the values expected from Brandt's formulas:

$$\Delta W_{ki}'-\Delta W_{ki}=(W_k'-W_i')-(W_k-W_i)$$
$$=\alpha(S_{2k}^2+S_{3k}^2-S_{2i}^2-S_{3i}^2). \tag{3}$$

In Fig. 1 the deviations observed, S. Nevin, Table XX, are indicated by circles, those calculated theoretically according to

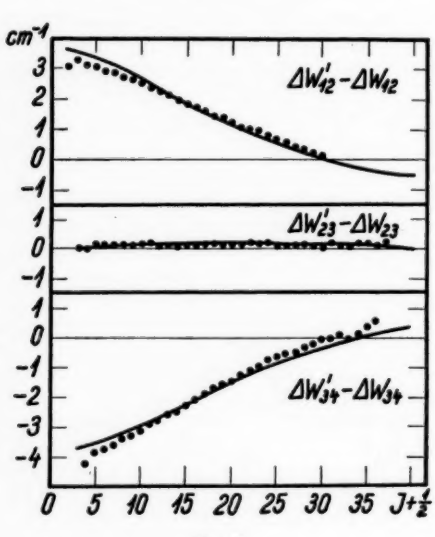

FIG. 1.

(3) with $\alpha=-3.712$ cm^{-1} by full lines. The agreement can be regarded as satisfactory.

A more detailed report will be published in *Acta Physica Hungarica*.

[1] T. E. Nevin, Trans. Roy. Soc. (London) **237**, 471 (1938).
[2] J. H. van Vleck, Phys. Rev. **33**, 467 (1929).
[3] W. H. Brandt, Phys. Rev. **50**, 778 (1936).
[4] J. H. van Vleck, Phys. Rev. **40**, 544 (1932); A. Budó and I.Kovács, Z. Physik **109**, 393 (1938); 111, 633 (1939).
[5] R. S. Mulliken, Revs. Modern Phys. **4**, 51 (1932).
[6] A. Budó and I. Kovács, Physik Z. **45**, 122 (1944).

Small Grating Spectrometer for the Far Infrared Region

EARLE K. PLYLER AND NICOLO ACQUISTA
National Bureau of Standards, Washington 25, D. C.
(Received January 26, 1955)

IT is now possible to measure spectra with a CsI prism to 50 microns.[1] Other materials have been considered to make it possible to extend the range to longer wavelengths. In fact, a prism of crystal quartz with a 7.5° refracting angle has been

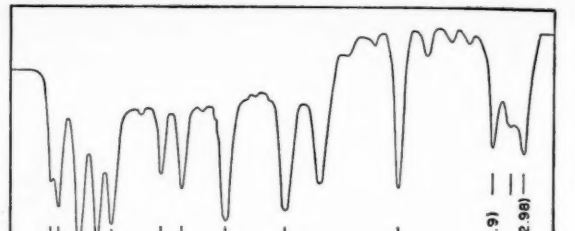

FIG. 1. The water vapor spectrum recorded with a 320 lines/in. grating. The upper curve is the second-order spectrum and the lower curve is the third-order spectrum. Overlapping of the two orders occurs at 305 cm^{-1}.

used in a spectrometer, and energy was recorded in the 150 micron region, but the resolution was low. Also no appreciable energy was detected between 50 and 80 microns. This would be a disadvantage in the use of a quartz prism as many molecules would have absorption bands in this region. The problem of measurements beyond 50 microns was then approached by placing a small grating in a spectrometer in place of the Littrow mirror and with the prism removed. Two gratings were available. They had a ruled surface of about $2\frac{1}{4}\times3$ inches and were ruled with 320 lines/in. and 180 lines/in. A thermocouple with a CsI window was suitable to 56 microns. Another thermocouple with a crystal quartz window was used in the region from 50 to 125 microns.

Special attention is necessary to the problem of stray radiation in the long wavelength region. The stray radiation was greatly reduced by the use of reflection gratings and reststrahlen plates. The two small plane mirrors immediately in front of and behind the exit slit of the spectrometer were replaced by two plane gratings, and the plane mirror in the source box of the spectrometer was replaced by a reststrahlen plate of NaCl, KBr, or CsBr.

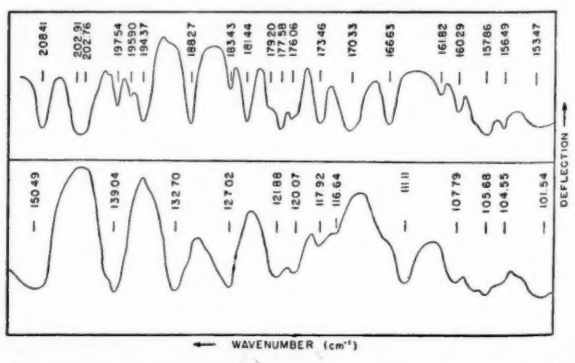

FIG. 2. The upper curve is the first-order spectrum of water vapor from 150 to 200 cm^{-1} as observed with the 320 lines/in. grating. The lower curve is the water vapor spectrum from 100 to 150 cm^{-1} as observed with a 180 lines/in. grating.

A system which was equally as effective as the gratings and the reststrahlen plates in the removal of stray radiation consisted in the use of blackened silver mirrors which were first roughened with fine emery cloth. These reflection filters have been described previously.[1] Since the quartz window on the thermocouple absorbed the radiation from 6 to 45 microns the second order from the grating did not overlap the first order except in the region from 90 to 125μ when the silver reflectors were used.

With these changes in the optical system just mentioned it was found that energy could be observed from the globar source with the same amplifier which was used for the near infrared region.

Figure 1 shows the water vapor absorption lines from 23.5 to 33.5μ as observed with the 320 lines/in. grating. The top curve is the second-order and the bottom curve is the third-order spectrum. The five lines in the region of 395 cm^{-1} are well resolved by the instrument. The strong absorption line at 340 cm^{-1} was not reported in the earlier experimental work for this region.

Figure 2 shows the region from 50 to 65μ as observed with the 320 lines/in. grating in the upper curve, and the lower curve is for the region from 65 to 100μ which was measured with the 180 lines/in. grating. Also the region from 100 to 125μ was measured by the use of a CsBr reflector. Slits of 1.8 mm were necessary for these measurements.

Other gratings and reststrahlen plates can be used to obtain the best resolution for a particular region. For measurements at wavelengths greater than 125 microns CsI plates would be necessary and a grating of 120 to 150 lines/in. would aid in increasing the energy. One grating with about 240 lines/in. would make it possible to cover the region from 50 to 100 microns with good resolution.

[1] N. Acquista and Earle K. Plyler, J. Opt. Soc. Am. **43**, 977 (1953).

Relation between the Surface Potential and the Interaction Energy in the Case of Some Hydrogen Films

J. C. P. MIGNOLET
Institut W. Spring, Université de Liège, Liège, Belgium
(Received December 20, 1954)

SOME time ago, Boudart[1] presented stimulating ideas regarding the interaction between adatoms and proposed a relation between the differential interaction energy (Δq) and the change in work function ($\Delta\varphi$) of the surface caused by the film. Adopting Boudart's approach, the writer has compared the surface potential (defined by $\mathcal{U}=-\Delta\varphi$), the differential energy of interaction, and the integral energy of interaction (ΔQ) in the case of some hydrogen films for which data were available *viz.*, WH, NiH, and FeH. It is thus found that, for nearly complete films,

$$\Delta q/\mathcal{U}=1.10\pm0.16 \text{ electrons per atom,}$$

$$\Delta Q/\mathcal{U}=0.47\pm0.11 \text{ electron per atom, and}$$

$$\Delta q/\Delta Q=2.46\pm0.36 \text{ electrons per atom.}$$

Within the mean deviations, the ratios agree with the relations:

$$\Delta q=e\mathcal{U} \tag{1}$$

$$\Delta Q=e\mathcal{U}/2 \tag{2}$$

$$\Delta q=2\Delta Q \tag{3}$$

where e denotes the charge of the electron.

The first relation differs from Boudart's by a factor 2. Boudart was led to a wrong value of $\Delta q/\mathcal{U}$ because, for the WH film, he used Bosworth's value which the author[2] has shown to be erroneous[3] and for the NiH film, he incorrectly chose the Δq value from Beeck's data[4]. Boudart's derivation of his relation is not correct either since the double layer is built by putting the charges at half the distance between their centers of gravity.

The interpretation of the first relation raises an interesting problem. The following explanation is proposed. The adsorption of hydrogen on the metals considered is essentially covalent.[1,5] The hydrogen supplies an electron and an orbital to the bond. The contribution of the metal is the important point. It is suggested that (1) the site supplies a vacant orbital and (2) the electron comes from the highest occupied level of the conductibility band. This means that the adsorption of an atom requires the excitation of an electron from the conductibility band into a vacant orbital. The adsorption causes a displacement of electrons outward and a lowering of the highest occupied level and consequently an increase in φ. This accounts for the negative sign of the hydrogen films.[6]

As the surface is being covered, the highest occupied level falls down and the excitation energy for the transfer increases. The contribution of this step to the differential energy of interaction is simply $e\Delta\varphi$. We thus get Eq. (1) directly if there is no other significant contribution, and furthermore the relation appears to be valid for all values of θ.

Relation (2) can be deduced from the definition of ΔQ and Δq by the relation

$$\Delta Q\equiv\frac{1}{\theta}\int_0^\theta \Delta q d\theta=\frac{e}{\theta}\int_0^\theta \Delta\varphi d\theta \tag{4}$$

if $\Delta\varphi$ varies proportionally with θ.

A detailed article including a discussion of relation (3) will be published soon.

I am much indebted to Professor L. D'Or for a discussion of the problem and to the Fonds National de la Recherche Scientifique for a "mandat d'associé" and the Union Minière du Haut-Katanga for its financial aid to our laboratory.

[1] M. Boudart, J. Am. Chem. Soc. **74**, 3556 (1952).
[2] J. C. P. Mignolet, Rec. trav. chim. (to be published).
[3] It is -0.48 v *in vacuo* instead of -1.04 v.
[4] It is difficult to understand why Boudart chose 10 kcal/mole. From O. Beeck's Fig. 14 [*Advances in Catalysis* (Academic Press, Inc., New York, 1950), II, p. 174], we find 16 kcal/mole.
[5] D. D. Eley, Disc. Faraday Soc. **8**, 34 (1950).
[6] Until convincing evidence is produced, it is considered that the positive surface potential found by C. W. Oatley [Proc. Phys. Soc. (London) **551**, 318 (1939)] is not correct.

Heats of Adsorption on Metal Surfaces

M. BOUDART
Chemical Engineering Laboratory, Princeton University, Princeton, New Jersey
(Received January 12, 1955)

DECREASES of heats of chemisorption on solids are commonly attributed to either *a priori* heterogeneity of the surface (planes, edges, corners, etc.) or repulsive interactions between adsorbed species. In a paper[1] quoted by Mignolet in the preceding letter, I have discussed data relative to clean metal adsorbents and a few adsorbates. From observations relative to the simultaneous adsorption of hydrogen and nitrogen on iron films,[2] I concluded, with Beeck, that the first explanation was unsatisfactory. From calculations of repulsive interactions, I concluded, with Rideal and Trapnell,[3] that this second alternative fell short of explaining the heat decrease by an order of magnitude. I attempted therefore to explain the adsorption-heat data by means of a classical double layer through which bonding electrons must penetrate upon adsorption. While this idea was not essentially new, I succeeded in showing that this effect, which I termed "induction," could explain *the order of magnitude* of the observed heat effects. To do this, I used contact potential data then available and made the rough but not unreasonable assumption, that the centroid of the charge distribution in the

double layer was approximately situated midway between its positive and negative ends.

The assumption of a smeared out classical double layer offers serious difficulties at low coverage. Gomer[4] attempted to remedy this situation by calculating the field of a plane array of dipoles. So doing, he had to leave out entirely the characteristics of the metal. As a result, he obtained fields which on the metal side at least would extend into the metal interior much more deeply than our normal intuition of metal behavior would permit.

The assumption of midway centroid of charge is undoubtedly susceptible of considerable refinement. On the basis of new data, Mignolet proposes a modified correlation between changes in adsorption heats and contact potentials differing by a factor of two from what I suggested originally. While this correction factor is the maximum that my interpretation will take, it is not in contradiction with it.

In order to explain the negative sign of the vacuum side of the double layer of hydrogen on tungsten, I pictured the proton imbedded below the outermost lattice planes. One of the advantages of this idea is that it explains the reversal of the sign of the adsorbed hydrogen layer observed by Mignolet[5] when hydrogen is adsorbed in excess of the "complete film."

The final answer to the problems discussed here will only be provided by quantum-mechanical calculations more elaborate than practically feasible so far, or, as appears more likely, by painstaking experimental work on clean single-crystal planes.

[1] M. Boudart, J. Am. Chem. Soc. **74**, 3556 (1952).
[2] O. Beeck, *Advances in Catalysis* (Academic Press, Inc., New York, 1950), Vol. II.
[3] E. K. Rideal and B. M. W. Trapnell, J. chim. phys. **47**, 126 (1950).
[4] R. Gomer, J. Chem. Phys. **21**, 1869 (1953).
[5] J. C. P. Mignolet, J. Chem. Phys. **20**, 341 (1952).

Experimental Evidence for the Existence of Abnormal OH Rotational "Temperatures" in Low-Pressure Flames*

HERBERT P. BROIDA AND HENRY J. KOSTKOWSKI
National Bureau of Standards, Washington, D. C.
(Received January 12, 1955)

RELATIVE intensities of the $^2\Sigma \rightarrow {}^2\pi$ transition of OH in many hydrocarbon flames at low pressures were shown by Gaydon and Wolfhard[1] to be characterized by rotational 'temperatures" many times larger than the calculated adiabatic temperatures. Their conclusion that these rotational distributions have a nonthermal origin has been questioned by Penner[2,3] on the basis that similar effects would be observed in thermally populated systems with large self-absorption. It appeared worthwhile, therefore, to measure the *OH absorption* in a low-pressure flame for which abnormal "temperatures" have been observed. This note reports some preliminary measurements.

Flames possessing the aforementioned abnormality were obtained by burning premixed acetylene and oxygen on a 5-cm diameter burner at pressures from 1.5 to 6 mm Hg. Spectroscopic measurements on these flames were made with a scanning, grating monochromator[4] using photomultiplier detection.[5] The rotational "temperatures" of OH in the $^2\Sigma$ state, obtained from conventional logarithmic plots, depended considerably on the position in and pressure of the flame. For example, at a pressure of 1.6 mm Hg the measured "temperature" at the base was 12 000°K and at 70 mm above the base 7400°K. At a pressure of 4 mm Hg the corresponding temperatures were 8000°K and 5000°K. Both flames contained 2 volumes of acetylene to 5 volumes of oxygen. The reproducibility and precision of the measured values is within 10 percent.

Having obtained flames with abnormal "temperatures," we carried out absorption measurements on the OH in these flames. In order to insure that the measured absorption was not influenced by the resolving power of the monochromator a line rather than a continuum source was used. The source was a discharge through water vapor at a pressure of 0.5 mm Hg.[6] The OH lines in this discharge, due to its low pressure and temperature, should be narrower than those in the flame. As a result, any absorption that occurs will be essentially at the peak of the lines. Furthermore an ac electronic amplifier was used which amplified the radiation from the discharge alone since only it was modulated by a metal chopper placed between the discharge and the flame. The OH line absorption, measured in this manner, was found to be very small. At 1.9 mm Hg in an acetylene-oxygen (in the ratio of 2 to 5) flame which was 7.5 cm thick, the greatest absorption of the strong $Q_1 5$ (0−0) line was only 15 percent. The absorption of the first line of the R_2 and second line of the P_1 branches was less than 3 percent and 5 percent, respectively.

The observed small absorption was confirmed by a two-path method suggested by Penner.[7] At the same position of the same flame on which the direct absorption measurements were made, the emission "temperatures" (as determined from the P_1 and R_2 branches) were 6600°K for the single path and 6900°K for the double path. This difference is well within the experimental error. The ratio of the double- to the single-path intensities also showed negligible absorption.

This consistent set of experimental results, which will be described in more detail in a forthcoming paper, shows that measured nonthermal rotational distributions of OH emission intensities in low-pressure acetylene flames are not caused by self-absorption.

* Supported in part by the Air Research and Development Command, Baltimore, Maryland.
[1] A. G. Gaydon and H. G. Wolfhard, Proc. Roy. Soc. (London) **A194**, 169 (1948).
[2] S. S. Penner, J. Chem. Phys. **20**, 507, 522 (1952).
[3] S. S. Penner, J. Chem. Phys. **20**, 1335 (1952).
[4] W. G. Fastie, J. Opt. Soc. Am. **42**, 641 (1952).
[5] This instrument was constructed by the research department of Leeds and Northrup Company and loaned to the Heat and Power Division of the National Bureau of Standards on a field trial arrangement.
[6] H. P. Broida and W. R. Kane, Phys. Rev. **89**, 1053 (1953).
[7] S. S. Penner, J. Chem. Phys. **20**, 1341 (1952).

Lowest Singlet Excited Levels of Naphthalene. II

ROLAND LEFEBVRE, *Centre de Chimie Théorique, 155 Rue de Sèvres, Paris 15°, France*
AND
CARL M. MOSER, *Pavillon Pasteur, Institut du Radium, 11 rue P. Curie, Paris 5°, France*
(Received February 11, 1955)

IN the course of calculations on the lowest excited states of naphthalene, the results of which have been previously summarized,[1] interesting relationships between various approximations concerning the calculation of the singlet excited states of naphthalene have been found.

Let us consider, in the manner of Dewar and Longuet-Higgins,[2] the four singlet excitations from the two highest bonding orbitals ϕ_m and ϕ_n to the two lowest antibonding orbitals $\phi_{n'}$ and $\phi_{m'}$. The energy involved in an excitation of an electron from ϕ_a to ϕ_b can be approximated as[3]:

$$E_1^{a,b} = E_0 \text{ (ground state)} + \epsilon_b - \epsilon_a - J_{ab} + 2K_{ab}.$$

To obtain the exact degeneracy between $m \rightarrow n'$ and $n \rightarrow m'$, which is fundamental to the theory of Dewar and Longuet-Higgins, it is sufficient to make the following assumptions: (a) The LCAO coefficients form a unitary matrix, and the antibonding orbitals can be deduced from the bonding orbitals by changing the sign of one of the sets of coefficients corresponding to the starred or unstarred atoms. (b) The molecular integrals can be approximated by retaining only the Coulomb atomic integrals. (c) The quantity $\int \chi_K H \chi_K dt$ which appears in the ϵ_i's is independent of K, and $\int \chi_K H^{\text{core}} \chi_e dt$ is retained only for $K=1$ and for

neighboring atoms (see Pople[4]). (a) and (b) ensure the equalities $J_{mn'}=J_{nm'}$ and $K_{mn'}=K_{nm'}$. If we add (c) then $\epsilon_{m'}-\epsilon_n=\epsilon_{n'}-\epsilon_m$.

We have applied these restrictions using the Hückel orbitals. The mixing of the B_{2u} functions appears to be more significant than that assumed by Dewar and Longuet-Higgins. However, with further restrictive conditions on the values of $\int\chi_K H\chi_\epsilon dt$ it is possible to find a small mixing in the B_{2u} case.

If, in the manner of Moffitt,[5] W.F.'s for the excited states are built from cyclic complex orbitals and derived by applying a perturbation to the cyclic molecule, this must necessarily be identical, in an explicit procedure, to the above if applied with the same assumptions to the real cyclic orbitals. (a) is satisfied; if we assume (b) the quantity responsible for the mixing of the functions built in analogy with the cyclic molecule can be expressed in the B_{1u} case in terms of off-diagonal elements of the H^{SCF} operator which plays formally the same role here as the mono-electronic operator $\mathbf{P}$ of Moffitt. In the B_{2u} case there are additional repulsion terms. If then we make for the $\int\chi_K H\chi_\epsilon dt$ the restrictions which are in common use in the simple LCAO theory, these off-diagonal elements reduce to that which comes from the cross bond.

These considerations can be easily extended to the other polyacenes.

The relation between these developments and the calculations previously reported[1] will be discussed in a forthcoming paper.

One of us (C.M.) wishes to acknowledge the grant of a U. S. Public Health Service Fellowship.

[1] C. M. Moser and R. Lefebvre, J. Chem. Phys. **23**, 598 (1955).
[2] M. S. J. Dewar and H. C. Longuet-Higgins, Proc. Phys. Soc. (London) **A67**, 795 (1954).
[3] C. C. J. Roothaan, Revs. Modern Phys. **23**, 69 (1951).
[4] J. A. Pople, Trans. Faraday. Soc. **49**, 1375 (1954).
[5] W. Moffitt, J. Chem. Phys. **22**, 320 (1954).

Effect of a Repulsive Force on the Scattering of Ions by Molecules

VERNON W. MYERS
Department of Physics, The Pennsylvania State University, State College, Pennsylvania
(Received February 7, 1955)

SIMONS and his co-workers have measured the cross section for the scattering of ions by molecules and have interpreted their results in terms of an attractive force. It may be of interest to consider the addition of a repulsive force. Let

$$V(r)=-\frac{K}{r^n}+\frac{L}{r^{2n}}. \tag{1}$$

A $2n$ repulsive potential is assumed for convenience in calculations. If the scattering is treated classically, and the small angle approximation is used, there results[1]

$$\frac{A}{r^n}-\frac{B}{r^{2n}}=\pm W\tan\phi. \tag{2}$$

$$A=\frac{\pi^{\frac{1}{2}}\Gamma(\frac{1}{2}n+\frac{1}{2})}{\Gamma(\frac{1}{2}n)},\quad B=\frac{\pi^{\frac{1}{2}}\Gamma(n+\frac{1}{2})}{\Gamma(n)}.$$

W in Eq. (2) is the kinetic energy of the ion at long distances from the molecule. The positive sign is chosen if $A/r^n>B/r^{2n}$, and the minus sign is chosen if $A/r^n<B/r^{2n}$, ϕ is the minimum scattering angle that results in an ion being scattered from the original beam. For Simon's apparatus,

$$\tan\phi=\frac{a}{l-x}. \tag{3}$$

$a=0.301$ cm, $l=4.18$ cm, and x is a variable lying between $0\leqslant x\leqslant l$. The combination of Eqs. (2) and (3) leads to the three roots:

$$r_\alpha{}^n=\frac{2B}{A-\left(A^2-\dfrac{4aBW}{l-x}\right)^{\frac{1}{2}}},$$
$$r_\beta{}^n=\frac{2B}{A+\left(A^2-\dfrac{2aBW}{l-x}\right)^{\frac{1}{2}}}, \tag{4}$$
$$r_\lambda{}^n=\frac{2B}{A+\left(A^2+\dfrac{4aBW}{l-x}\right)^{\frac{1}{2}}}.$$

$r_\alpha{}^n$ and $r_\beta{}^n$ are real when $A^2\geqslant 4aBW/(l-x)$. If $A^2<4aBW/(l-x)$, $r_\alpha{}^n$ and $r_\beta{}^n$ are complex and have no physical meaning. The probability of scattering in a ring of radius r and thickness dr is proportional to rdr. If $r>r_\alpha$ or $r_\gamma<r<r_\beta$, the scattering angle is less than the minimum angle required by Eq. (3). If $r_\beta<r<r_\alpha$ or if $r<r_\gamma$, the scattering angle is greater than the minimum. The scattering cross section for a particular x is

$$\sigma(x)=2\pi\int_0^{r_\gamma} rdr+2\pi\int_{r_\beta}^{r_\alpha} rdr=\pi(r_\alpha{}^2-r_\beta{}^2+r_\lambda{}^2). \tag{5}$$

When $r_\alpha{}^n$ and $r_\beta{}^n$ are complex, the scattering cross section is $\pi r_\gamma{}^2$. The effective scattering cross section is

$$\sigma_{\text{theo}}=\frac{\pi}{l}\int_0^l (r_\alpha{}^2-r_\beta{}^2+r_\gamma{}^2)dx. \tag{6}$$

Consider the application of this method to the scattering of $H_2{}^+$ by He[2]. Let

$$V(r)=-\frac{2.0}{r^4}+\frac{0.3}{r^6}, \tag{7}$$
$$V \text{ in ev},\quad r \text{ in } A,\quad A=4.7,\quad B=1.0.$$

Table I gives the comparison between theory and experiment. The agreement is only qualitative but seems satisfactory in view of the approximate model used. It should be noted that a more exact treatment of the scattering[2] reduces the coeff 2.0 of Eq. (7) to 1.5, and the coeff 0.3 would be reduced by a factor of two or greater.

TABLE I. A comparison of the experimental and theoretical scattering cross sections of $H_2{}^+-He$.

Kinetic energy of ion in ev	Experimental cross section in (A)^2	Theoretical cross section in (A)^2	Percent difference
4.0	8.8	8.1	8
48	2.4	1.7	30
118	1.4	1.1	20

[1] Simons, Fontana, Muschlitz, and Jackson, J. Chem. Phys. **11**, 307 (1943).
[2] Simons, Muschlitz, and Unger, J. Chem. Phys. **11**, 322 (1943).

Equivalent Circuit for a Coil Cell Used in rf Titrimetry

J. R. HASKINS, GEORGE HELLER, AND EUGENE MILLER
Research Division, Ordnance Missile Laboratories, Redstone Arsenal, Huntsville, Alabama
(Received February 7, 1955)

RECENTLY Hamme, Grove, and Kassner[1] reported on the application of measurements of conductance and susceptance of coil-type containers to high-frequency titrimetry. Specifically, they found that the characteristic variation of cell conductance with frequency depended on the properties of the liquid in the cell. An attempt to explain and predict this variation is reported in this present note.

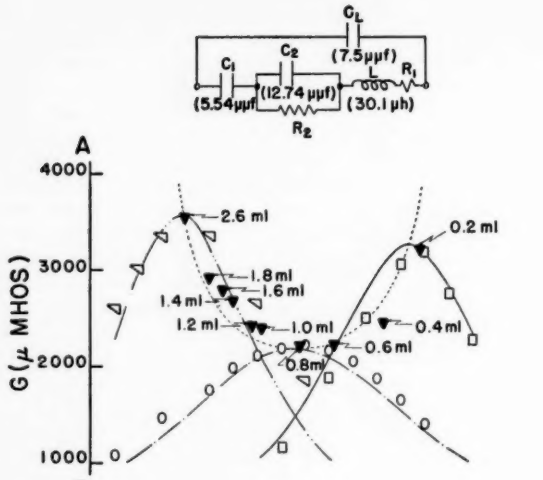

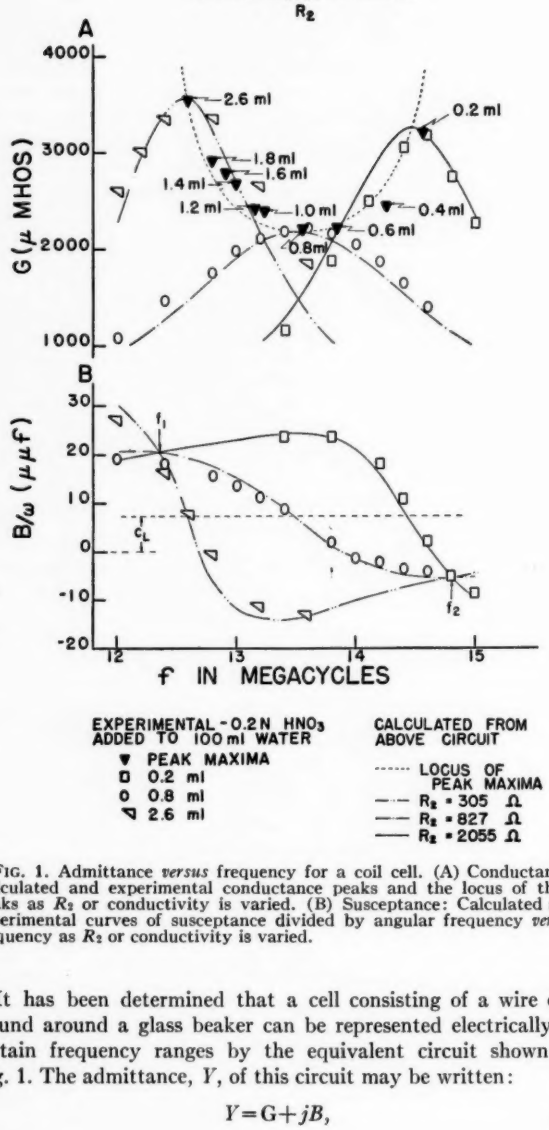

FIG. 1. Admittance *versus* frequency for a coil cell. (A) Conductance: Calculated and experimental conductance peaks and the locus of these peaks as R_2 or conductivity is varied. (B) Susceptance: Calculated and experimental curves of susceptance divided by angular frequency *versus* frequency as R_2 or conductivity is varied.

It has been determined that a cell consisting of a wire coil wound around a glass beaker can be represented electrically in certain frequency ranges by the equivalent circuit shown in Fig. 1. The admittance, Y, of this circuit may be written:

$$Y=G+jB, \tag{1}$$

where

$$G=\frac{\left[R_1+\dfrac{R_2}{1+\omega^2C_2^2R_2^2}\right]}{\left[R_1+\dfrac{R_2}{1+\omega^2C_2^2R_2^2}\right]^2+\left[\dfrac{1}{\omega C_1}-\omega L+\dfrac{\omega C_2R_2^2}{1+\omega^2C_2^2R_2^2}\right]^2} \tag{1.1}$$

$$B=\frac{\left[\dfrac{1}{\omega C_1}-\omega L+\dfrac{\omega C_2R_2^2}{1+\omega^2C_2^2R_2^2}\right]}{\left[R_1+\dfrac{R_2}{1+\omega^2C_2^2R_2^2}\right]^2+\left[\dfrac{1}{\omega C_1}-\omega L+\dfrac{\omega C_2R_2^2}{1+\omega^2C_2^2R_2^2}\right]^2}+\omega C_L. \tag{1.2}$$

L represents the inductance of the coil; R_1 the resistance of the coil; C_1 a capacitance depending on the beaker glass, insulation of the wire, air space between turns, etc.; C_2 and R_2 a capacitance and resistance depending on the liquid in the beaker; C_L the lead wire capacitance; and ω the angular frequency.

It may be shown from Eqs. (1) that the maximum value of the conductance, G, will occur, in the first approximation, at a frequency where the first term in the expression for the susceptance, B, [Eq. (1.2)] is zero (when $B=\omega C_L$). From Eq. (1.2) it may be shown that, if R_2 is the only element of the equivalent circuit which is variable, the lowest frequency at which a conductance peak maximum may occur is given by:

$$f_1=\omega_1/2\pi=1/[2\pi(LC_1)^{\frac{1}{2}}] \quad \text{when} \quad R_2\to 0, \tag{2}$$

and the highest frequency at which it may occur is given by:

$$f_2=\omega_2/2\pi=(1/2\pi)[1/L(1/C_1+1/C_2)]^{\frac{1}{2}} \quad \text{when} \quad R_2\to\infty. \tag{3}$$

When $R_1\ll R_2/(1+\omega^2C_2^2R_2^2)$, the variation of the conductance peak maximum, $G_{\max}$, with frequency, ω, may be shown to be related to R_2 and these limiting frequencies (ω_1) and (ω_2) by:

$$G_{\max}=(1+\omega^2C_2^2R_2^2)/R_2,$$
$$\text{where} \quad R_2^2=(1/\omega^2C_2^2)[(\omega^2-\omega_1^2)/(\omega_2^2-\omega^2)]. \tag{4}$$

A General Radio Twin-T impedance bridge was used to measure conductance and susceptance of a cell consisting of 60 turns of No. 18 shellacked copper wire wrapped around a 180 ml Berzelius beaker containing 100 ml of distilled water. The conductivity of the water contained in the cell was varied by adding small quantities of 0.2N nitric acid. The measurements were taken at room temperature. The resultant data are plotted in Fig. 1, together with variations predicted by Eqs. (1) and (4).

The correspondence between the calculated curves and the experimental data appears to justify using the proposed equivalent circuit as a basis for better understanding high-frequency titrimetry in a coil cell.

[1] Hamme, Grove, and Kassner, J. Chem. Phys. **22**, 944 (1954).

Some Comments on the Frontier Orbital Theory of the Reactions of Conjugated Molecules

H. H. GREENWOOD
Sir John Cass College, Aldgate, London E.C. 3, England
(Received December 13, 1954)

THE molecular-orbital theory of the reactions of conjugated molecules introduced by Wheland and Pauling[1] associates the ease of ionic attack with the charge density and polarizability at a given atom of attack. Coulson and Longuet-Higgins[2] deduced the formula

$$\delta\mathcal{E}=q_r\delta\alpha_r+\tfrac{1}{2}\pi_{r,r}\delta\alpha_r^2+\cdots \tag{1}$$

where the change $\delta\alpha_r$ in Coulomb integral is assumed to be due to the presence of the charged reagent in the neighborhood of the rth atom under attack, and suggested that $\delta\mathcal{E}$ represent the change in π-electron energy in the early stages of reaction. Fukui *et al.*[3] have recently shown that the density distribution in the unperturbed ground state of the frontier electrons which occupy the least bound occupied level of the π-electron system may be used to predict the positions of electrophilic attack. The method has been extended to account for nucleophilic and free radical attack.[4] It was concluded that the frontier electrons are to be distinguished as primarily concerned in bond formation at the position of attack.

The frontier orbital interpretation appears, from a comparison of the numerical results obtained, to be consistent with Eq. (1). Analysis of the change in π-electron configuration associated with the change $\delta\mathcal{E}$ of (1) for electrophilic attack ($\delta\alpha_r$ negative) reveals the following properties:

(1) The amplitude of the MO describing the lowest π-electron energy level increases at the position of attack, and decreases elsewhere.

(2) The amplitudes of all other MO's including the frontier orbitals decrease at the position of attack.

These results mean that the polarization of the π-electron system

by a positively charged reagent according to (1) brings towards the position of attack the π-electron pair occupying the most tightly bound energy level. Simultaneously all other pairs are progressively removed from this region. The physical implications of (1) are therefore inconsistent with bond formation by the frontier electrons.

In the same way nucleophilic attack, represented by $\delta\alpha_r$ positive in (1) produces a reduced amplitude of the frontier electrons at the region of attack, a result incompatible with the frontier-orbital hypothesis.

Of the two theories which correlate equally well with experimental data, the frontier-orbital concept is more readily acceptable by comparison with conventional bonding by the least-bound electrons of the reacting systems. Nevertheless polarization of the π-electron system by the ionic reagent itself precludes this hypothesis by reason of the physical- and quantum-mechanical principles controlling the charge shifts.[5]

The frontier orbitals appear to be significant in the case of free-radical attack. The charge-distribution method associates the ease of radical attack with the free valence F_r at an atom[6] which may be related to the change in π-electron energy due to a change in resonance integral of the bonds adjacent to the position of attack. The corresponding change in π-electron configuration results in a reduction in amplitude at the position of attack of all MO's except the frontier orbitals. These are not, however, distorted towards the region of attack, but remain distributed throughout the conjugated system, and tend to form a degenerate pair of zero-binding energy. A suitable linear combination of this pair produces an orbital localized at the position of attack, and a second confined to the conjugated system exclusive of this position. Hund's rule[7] requires the two available electrons to be placed one in each orbital, thus accounting for the provision of a free electron at the position of radical attack.

[1] G. W. Wheland and L. Pauling, J. Am. Chem. Soc. **57**, 2086 (1935).
[2] C. A. Coulson and H. C. Longuet-Higgins, Proc. Roy. Soc. (London) **192A**, 16 (1947).
[3] Fukui, Yonezawa, and Shingu, J. Chem. Phys. **20**, 722 (1952).
[4] Fukui, Yonezawa, Nagata, and Shingu, J. Chem. Phys. **22**, 1433 (1954).
[5] H. H. Greenwood, J. Am. Chem. Soc. (to be published).
[6] C. A. Coulson, Disc. Faraday Soc. No. **2**, 9 (1947).
[7] C. A. Coulson, *Valence* (Clarendon Press, Oxford, England, 1952), pp. 36, 98.

Methyl and Phenyl Affinities of Aromatic Compounds

D. H. HEY AND G. H. WILLIAMS
King's College, Strand, London, W.C.2., England
(Received January 28, 1955)

MEASUREMENTS have recently been reported by M. Levy and M. Szwarc[1] of "relative methyl affinities" of a number of aromatic compounds. These quantities are, in fact, relative reactivities towards attack by methyl radicals arising from the decomposition of acetyl peroxide. It is of interest to note that the numerical values of the relative methyl affinities are very close to those of the relative rates of attack by phenyl radicals, arising from the decomposition of benzoyl peroxide and from other sources, on the same aromatic compounds. The measurement of these quantities, which in Levy and Szwarc's terminology could be called "relative phenyl affinities," has been reported by the present authors and their co-workers.[2-9] The results of these investigations are summarized and, where the quantities are available, compared with the corresponding relative methyl affinities, in Table I.

The agreement between the values of the two quantities for naphthalene and for diphenyl is striking, and the values reported for pyridine are at least of the same order of magnitude.

As well as the relative rates of attack tabulated in Table I we have measured the ratios of the various isomers formed in the phenylation of the aromatic compounds, and from the two sets of measurements calculated partial rate factors representing the reactivities of the various individual positions in the aromatic nuclei in terms of the reactivity of any one position in benzene. The partial rate factors were compared with those computed from the results of molecular-orbital calculations by a number of workers,[10-17] and the substantial agreement between theory and experiment noted In addition, the increase in methyl (or phenyl) affinity with increasing conjugation in the aromatic system, which was pointed out by Levy and Szwarc, was also noted by the present authors.[2]

TABLE I.

Compound	Relative phenyl affinity	Relative methyl affinity
Benzene	1	1
Toluene	1.9	
*tert*Butylbenzene	0.87	
p-di-*tert*Butylbenzene	0.63	
Naphthalene	23.9	22
Diphenyl	4.0	5
Pyridine	1.04	3
Nitrobenzene	4.0	
Fluorobenzene	1.3	
Chlorobenzene	1.4	
Brombenzene	1.7	
Iodobenzene	1.8	
p-Dichlorobenzene	2.7	
sym-Trichlorobenzene	5.0	

Extensions of this work to include other aromatic systems, and other aryl radicals, will be published later.

[1] M. Levy and M. Szwarc, J. Chem. Phys. **22**. 1621 (1954).
[2] D. H. Hey and G. H. Williams, Discussions Faraday Soc. **14**, 216 (1953).
[3] Augood, Hey, and Williams, J. Chem. Soc. 2094 (1952).
[4] Augood, Hey, and Williams, J. Chem. Soc. 44 (1953).
[5] Augood, Cadogan, Hey, and Williams, J. Chem. Soc. 3412 (1953).
[6] Cadogan, Hey, and Williams, J. Chem. Soc. 794 (1954).
[7] Hey, Stirling, and Williams, J. Chem. Soc. 2747 (1954).
[8] Cadogan, Hey, and Williams, J. Chem. Soc. 3352 (1954).
[9] Hey, Pengilly, and Williams (to be published).
[10] G. W. Wheland, J. Am. Chem. Soc. **69**, 900 (1942).
[11] C. Sandorfy, Bull. Soc. Chim. **16**, 615 (1949).
[12] C. A. Coulson and H. C. Longuet-Higgins, Proc. Roy. Soc. (London) **A193**, 447 (1948).
[13] W. A. Brown, Quart. Rev. **6**, 63 (1952).
[14] P. Yvan, Compt. rend. **229**, 622 (1949).
[15] F. Seel, Z. Elektrochem. **52**, 191 (1948).
[16] F. Seel, Z. Naturforsch. **3a**, 35 (1948).
[17] Burkitt, Coulson, and Longuet-Higgins, Trans. Faraday Soc. **47**, 553 (1951).

Invariance of Integrated Transmittance and Total Fractional Transmission with Experimental Slit Function*

C. R. DEPRIMA AND S. S. PENNER
California Institute of Technology, Pasadena, California
(Received January 27, 1955)

IT is well known to spectroscopists that the integrated transmittance and total fractional transmission are, in principle, independent of experimental slit width under the conditions usually satisfied in experimental work. A recent discussion of this problem for a triangular slit function has been given, for example, by Nielsen, Thornton, and Dale.[1] It is the purpose of the present note to re-examine this question in more general terms and to specify the requirements under which the experimental results are, in principle, independent of the experimental slit function.

Consider the spectral region between the wave numbers ω_1 and $\omega_2(\omega_1<\omega_2)$ which are selected in such a way that for $\omega \leqslant \omega_1 + \Delta\omega^*$ and for $\omega \geqslant \omega_2 - \Delta\omega^*$ the spectral absorption coefficient $P(\omega)$ vanishes. The functional form of $P(\omega)$ in the range $\omega_1+\Delta\omega^* < \omega < \omega_2-\Delta\omega^*$ is arbitrary. The spectral region from ω_1 to ω_2 is scanned with an instrument which can be described by a slit function $g(|\omega'-\omega|,b,c)$ such that the instrument responds to the wave number ω' when it is set at ω. The slit function is assumed to vanish for $|\omega'-\omega| \geqslant \Delta\omega^*$. The parameters b and c are dependent

on the nature of the instrument selected for study. Representative slit functions are triangular, trapezoidal, or Gaussian.[1]

Let $I^0(\omega)$ represent the incident intensity, $I(\omega)$ is the transmitted intensity, $P(\omega)$ equals the spectral absorption coefficient, and X is the optical density. The integrated transmittance is then

$$\int_{\omega_1}^{\omega_2} T(\omega)d\omega=\int_{\omega_1}^{\omega_2} \times\left(\frac{\int_{\omega-\Delta\omega^*}^{\omega+\Delta\omega^*} I^0(\omega')\{\exp[-P(\omega')X]\}g(|\omega'-\omega|,b,c)d\omega'}{\int_{\omega-\Delta\omega^*}^{\omega+\Delta\omega^*} I^0(\omega')g(|\omega'-\omega|,b,c)d\omega'}\right)d\omega. \quad (1)$$

For spectrographs with reasonable resolution the intensity $I^0(\omega')$ may be taken as constant in the wave number range $\omega-\Delta\omega^* \leqslant\omega' \leqslant\omega+\Delta\omega^*$, i.e., $I^0(\tau+\omega)=I^0(\omega)$ for $|\tau| \leqslant\Delta\omega^*$. Hence, introducing an appropriate change of variables and changing the order of integration, we find

$$\int_{\omega_1}^{\omega_2} T(\omega)d\omega=\left[\int_{-\Delta\omega^*}^{\Delta\omega^*} g(|\tau|,b,c)d\tau\right]^{-1}\int_{\omega_1}^{\omega_2}\left(\int_{-\Delta\omega^*}^{\Delta\omega^*} \{\exp[-P(\tau+\omega)X]\}g(|\tau|,b,c)d\tau\right)d\omega=\left[\int_{-\Delta\omega^*}^{\Delta\omega^*} g(|\tau|,b,c)d\tau\right]^{-1} \times\int_{-\Delta\omega^*}^{\Delta\omega^*} g(|\tau|,b,c)\left(\int_{\omega_1+\tau}^{\omega_2+\tau} \{\exp[-P(\omega)X]\}d\omega\right)d\tau. \quad (2)$$

However, since $|\tau| \leqslant\Delta\omega^*$ the stated requirements for $P(\omega)$ imply that

$$\int_{\omega_1+\tau}^{\omega_2+\tau} \{\exp[-P(\omega)X]\}d\omega=\int_{\omega_1}^{\omega_2} \{\exp[-P(\omega)X]\}d\omega. \quad (3)$$

Consequently Eq. (2) reduces to

$$\int_{\omega_1}^{\omega_2} T(\omega)d\omega=\int_{\omega_1}^{\omega_2} \{\exp[-P(\omega)X]\}d\omega. \quad (4)$$

The experimental conditions which must be met in order to justify the use of Eq. (4) are seen to be the following: (a) if the slit function vanishes for $|\omega'-\omega| \geqslant\Delta\omega^*$ and $P(\omega)$ vanishes for $\omega \leqslant\omega_1{}^0$ and $\omega \geqslant\omega_2{}^0$, we must scan at least over the spectral range from $\omega_1=\omega_1{}^0-\Delta\omega^*$ to $\omega_2=\omega_2{}^0+\Delta\omega^*$[2]; (b) the incident intensity $I^0(\omega)$ must be a slowly varying function of ω such that $I^0(\omega+\tau) \simeq I^0(\omega)$ for $|\tau| \leqslant\Delta\omega^*$.

The total fractional transmission of a spectral region T_R is defined by the relation

$$T_R=\frac{\int_{\omega_1}^{\omega_2}\left(\int_{\omega-\Delta\omega^*}^{\omega+\Delta\omega^*} I^0(\omega')\{\exp[-P(\omega')X]\}g(|\omega'-\omega|,b,c)d\omega'\right)d\omega}{\int_{\omega_1}^{\omega_2}\left(\int_{\omega-\Delta\omega^*}^{\omega+\Delta\omega^*} I^0(\omega')g(|\omega'-\omega|,b,c)d\omega'\right)d\omega}. \quad (5)$$

Proceeding as before, it is readily seen that Eq. (5) becomes

$$T_R=\frac{\int_{-\Delta\omega^*}^{\Delta\omega^*} g(|\tau|,b,c)d\tau\int_{\omega_1+\tau}^{\omega_2+\tau} I^0(\omega)\{\exp[-P(\omega)X]\}d\omega}{\int_{-\Delta\omega^*}^{\Delta\omega^*} g(|\tau|,b,c)d\tau\int_{\omega_1+\tau}^{\omega_2+\tau} I^0(\omega)d\omega}.$$

Hence, if $I^0(\omega)$ has the same values at corresponding points in the spectral ranges, $\omega_1-\Delta\omega^* \leqslant\omega \leqslant\omega_1+\Delta\omega^*$ and $\omega_2-\Delta\omega^* \leqslant\omega \leqslant\omega_2+\Delta\omega^*$, respectively, then

$$T_R=\frac{\int_{\omega_1}^{\omega_2} I^0(\omega)\{\exp[-P(\omega)X]\}d\omega}{\int_{\omega_1}^{\omega_2} I^0(\omega)d\omega}, \quad (6)$$

provided the previously stated conditions are met for the slit function and absorption coefficient. The conclusion that $I^0(\omega)$ is arbitrary, except in the neighborhood of the ends of the integration interval, is interesting and physically plausible.

* Supported by the Office of Naval Research under Contract Nonr-220(03), NR 015 401.

[1] Nielsen, Thornton, and Dale, Revs. Modern Phys. **16**, 307 (1944).

[2] We must choose the integration interval larger by at least $\Delta\omega^*$ on either end than the range for which $P(\omega)$ is nonzero because, in principle, the spectrometer will show absorption when it is set within a range $\Delta\omega^*$ of the nearest absorbing region.

Microwave Spectrum and Planarity of the Ring of Trimethylene Oxide

JOSE FERNANDEZ, ROLLIE J. MYERS, AND WILLIAM D. GWINN
Department of Chemistry and Chemical Engineering, University of California, Berkeley, California

(Received February 11, 1955)

OUR interest in trimethylene oxide $CH_2-CH_2-CH_2$ (O bridging the two end carbons) stems from the recent work in infrared and Raman spectroscopy which indicates that cyclobutane[1] probably has a puckered ring. In the four-membered rings, the classical ring strain would tend to make the ring planar, while the preferred staggered configuration of the hydrogens in internal rotation would tend to make the ring puckered. Trimethylene oxide, having fewer hydrogens, would have less tendency to have a puckered ring, and the microwave work was undertaken to attempt to determine whether or not the ring is planar and to determine the structure of the molecule.

The microwave spectrum has been investigated in the region from 16 to 42 kmc/sec. The spectrum is very rich, due to the occurence of a large number of Q branch lines for the ground and excited ring bending vibrational states of the molecule. Several lines have been assigned to the ground and first excited states, and a few to the second and third. A list of transitions, rotational constants, and moments of inertia is given in Table I.

Planar trimethylene oxide would have approximately equally spaced vibrational levels with statistical weights of 7 and 9. The intensities of rotational transitions for the ground and excited vibrational states would be in the ratio of $7:9\exp(-E_1/kT):7\exp(-E_2/kT)$—for $A\leftrightarrow B_a$ transitions and $9:7\exp(-E_1/kT):9\times\exp(-E_2/kT)$—for $B_b\leftrightarrow B_c$ transitions, where E_1 and E_2 are the energy levels of the first two vibrational states. If the molecule were bent and the two positions were separated by a high potential barrier at the planar position, the vibrational levels would coalesce in pairs and the statistical weights of each pair would be the same. If the two minima were separated by a low barrier, the statistical weights would be the same as for a planar molecule but the separation of the ground and first excited vibrational levels would be much less than that for the first and second excited vibrational levels. In trimethylene oxide the intensities of four rotational transitions were measured for several vibrational states and the accuracy was sufficient to determine that the statistical weights were necessary (i.e., the vibrational levels are single levels), and that E_1 was approximately 60 cm^{-1} and that

TABLE I.

Ground vibrational state			First excited vibrational state		
A	12 045.2	Mc/sec	A	12 058.0	Mc/sec
B	11 734.0	Mc/sec	B	11 726.0	Mc/sec
C	6730.7	Mc/sec	C	6772.6	Mc/sec
I_A	41.96509	amuA^2	I_A	41.92082	amuA^2
I_B	43.07823	amuA^2	I_B	43.10776	amuA^2
I_C	75.10116	amuA^2	I_C	74.63631	amuA^2

	Assigned transitions in Mc/sec			
	Ground vibrational state		First excited vibrational state	
Transition	Experimental	Calculated	Experimental	Calculated
$1_{10}-2_{11}$	41 932.7	(41 932.7)	41 950.5	(41 950.5)
$1_{11}-2_{12}$	31 926.0	(31 926.0)	32 043.4	(32 043.4)
$1_{01}-2_{02}$	32 223.3	32 223.3	32 358.6	32 361.9
$0_{00}-1_{01}$	18 465.0	18 464.7	18 498	18 498.6
$3_{12}-3_{21}$	16 490.2	(16 490.2)	16 443.8	(16 443.8)
$4_{22}-4_{41}$	17 268.2	17 268.3	17 283.2	17 284.1
$5_{32}-5_{51}$	18 346.5	(18 346.5)	18 452.1	(18 452.1)
$6_{33}-6_{52}$	26 081	26 080.6	25 928	25 925.9
$7_{43}-7_{62}$	26 333	26 333.0	26 215	26 216.7
$7_{53}-7_{52}$	24 592	24 593.2	24 240	24 240.6
$8_{63}-8_{62}$	23 890	23 890.2	23 460	23 458.3
$8_{53}-8_{72}$	26 725	26 724.7	26 665	26 668.1
$9_{73}-9_{72}$	22 976	22 979.9		

E_2 was less than 200 cm^{-1}. Therefore, we conclude that trimethylene oxide has a planar ring.

From the measurement of the Stark effect, the dipole moment was observed to be 1.93 ± 0.01 D and there was no evidence of any contribution from a component of the dipole perpendicular to the ring. From this we can come to the independent conclusion that trimethylene oxide has a planar ring. If the barrier were very high, the Stark effect would be very sensitive to a perpendicular component of the dipole, and an upper limit of 0.01 D could be set. This would correspond to the impossible situation of a high barrier separating two minima only 0°40′ apart. If the barrier were lower, the Stark effect calculations would be influenced by the broken degeneracy of the double minima vibrational levels. Detailed calculations have been made and if the separation of the first two levels is less than 2 cm^{-1} the possibility of a double minima vibration can be eliminated. If the splitting were greater than 2 cm^{-1} we should notice the splitting of the rotational line of some of the excited ring bending vibrational levels. We do not observe any splitting. Therefore trimethylene oxide is planar.

The out-of-plane contribution to the moments of inertia is $\frac{1}{2}(I_A+I_B-I_C)$. Since trimethylene oxide has a planar ring, the H−C−H angle may be calculated to be 112° if the C−H length is assumed to be 1.08 A.

Work with deuterated trimethylene oxide is in progress, and it is hoped that it will be possible to determine the complete structure of the molecule.

[1] Rathjens, Freeman, Gwinn, and Pitzer, J. Am. Chem. Soc. **75**, 5634 (1953).

Erratum: Polymorphism in Solution of *cis*- and *trans*-β-Methoxy-*p*-Nitrochalcone

[J. Chem. Phys. **22**, 1943–1944 (1954)]

Yoshiyuki Urushibara, Fujiro Iimura, and Kenro Ikeda
Department of Chemistry, The University of Tokyo, Bunkyo-ku, Tokyo

TABLE I should be printed as follows:

TABLE I. Polymorphism and ultraviolet absorption spectra of β-methoxy-*p*-nitrochalcone.

	M.p. °C[a]	λ max (mμ) in *n*-heptane	Stability in heptane	λ max (mμ) in alcohol	λ max (mμ) in $CHCl_3$	Stability in $CHCl_3$
cis-form	57–60 88	245 (1.45)[c]	rather stable	249 (1.60)	252 (1.60)	
	55–58 67–69	251 (1.45)		260 (1.70)		equilib. p.t. 263 (1.60)
	76–79[b] 78–81 89.5–90.5[b] 97[b]	255 (1.65)	most stable (*ca* equilib. p.t.)	265 (1.60)	260 (1.70)	
	117–120	260 (1.80)				
	132–135	264 (1.80)			266.5 (1.60)	rather stable
trans-form	78–81 125–128	difficulty soluble		252 (1.70) 325 (1.00)		
	65.5–67	255 (1.40) 308 (1.30)		262 (1.40) 313 (1.30)		
	107–110	262 (1.70) 311 (1.30)		267 (1.40) 316 (1.20)		
	70–72	difficultly soluble		320 (1.30)		

[a] Unsharp M.p. of some species may be ascribed to the increased velocity of transition at elevated temperatures.
[b] Confirmed to be a pure polymorph, and not a mixture by x-ray analyses.
[c] In brackets: molecular extinction coefficient $\times10^{-4}$.

Radiation Induced Equilibrium of Hydrogen-Deuterium Mixtures*

S. O. Thompson and O. A. Schaeffer
Department of Chemistry, Brookhaven National Laboratory, Upton, Long Island, New York

(Received December 13, 1954)

IT has been reported[1] that hydrogen-tritium equilibrium mixtures show a 12 percent discrepancy between the experimental and the theoretical value of the equilibrium constant. To account for the discrepancy one alternative explanation suggested possible evidence for a change in the calculated thermodynamic constant because of the radiation field. As such an effect would be rather novel, the radiation induced exchange equilibrium between hydrogen and deuterium was investigated.

In order to minimize as much as possible systematic instrumental errors, radiation equilibrated mixtures were compared directly to catalytically equilibrated mixtures. The hydrogen and deuterium were purified by diffusion through palladium thimbles. Roughly equimolar mixtures of hydrogen and deuterium were prepared manometrically for the equilibrations. Polonium-210 alpha particles and 2-Mev Van de Graaff electrons were used as sources of radiation. The comparison samples were equilibrated over nickel at 20°C.

All analyses were performed with a Consolidated Nier Isotope Ratio Mass Spectrometer employing electrostatic scanning. The filament emission and other instrumental parameters were kept as uniform as possible. In order to obtain consistent and reproducible results, the following procedure was used. The irradiated sample was allowed to flow through the spectrometer for ten minutes and then three successive determinations were made at intervals of five minutes. The spectrometer was then pumped out for ten minutes and a catalytically equilibrated sample was treated in the same manner. This procedure gave about ±2 percent reproducibility. The test used for establishing that the equilibrium value had in fact been reached for the catalytically equilibrated samples was to equilibrate for 4 hours and for 45 hours. When analyzed in the mass spectrometer, the values of the equilibrium constants were 3.17 and 3.20 for the 4- and 45-hour samples, respectively.

In Table I the catalytic and radiation induced equilibrium constants are compared directly for three determinations using polonium-210 alpha rays and one determination using 2-Mev Van de Graaff electrons. In every case the radiation value and the catalytic value analyzed at the same time agree within the experimental precision of about one percent. The 45-hour catalytically equilibrated sample was used for all the comparison analyses. The equilibrium constant varies from determination to determination by considerably more than this, which is probably due to different relative sensitivities of the instrument for H_2, HD, and

TABLE I. Radiation and catalytic induced equilibration of hydrogen and deuterium.

Method of equilibration	Time of irradiation, (min)	Pressure mm of Hg	Mole percent D_2	Mole percent HD	Mole percent H_2	$K_s=\frac{(HD)^2}{(H_2)(D_2)}$
2-Mev electrons	108	215	12.33	42.96	44.71	3.35
Nickel catalyst			41.86	44.22	13.92	3.36
Po-210 alphas	5100	220	32.02	46.79	21.20	3.23
Nickel catalyst			41.40	44.00	14.60	3.20
Po-210 alphas	1080	110	32.12	46.36	21.52	3.11
Nickel catalyst			40.56	44.12	15.32	3.13
Po-210 alphas	3960	240	29.85	47.05	23.09	3.21
Nickel catalyst			39.19	44.85	15.97	3.21
Average value						3.23 ± 0.07
Theoretical value[a]						3.25

[a] H. C. Urey, J. Chem. Soc. **1947**, 562.

D_2 on different days. The over-all average of the equilibrium constant agrees well with the calculated value as shown in Table I.

The half-times for the reaction were determined from plots of percent HD formed *vs* the time of irradiation. These were 3.7 and 38 minutes for electrons and alpha particles, respectively. As shown in Table I all the irradiated samples were exposed for at least 25 half-times and as a result should be at equilibrium.

The radiation intensity was of the order of 10^{12} to 10^{14} ion pairs produced per second. The G values were 9×10^3 and 4×10^4 molecules formed per 100 ev for electrons and alpha particles, respectively, and these values were estimated from range-energy curves and the radiation intensity. For the 2-Mev electrons the intensity was measured with a collector behind the cell; the entire beam passed through the cell. The alpha source strength was calculated from the known source strength and an estimated geometry factor. In these experiments the radiation intensities were of the same order as those used in the hydrogen-tritium work and the ionization density of the radiating particles used bracketed those of the 5-kev tritium beta particles.

It seems quite clear that there is no appreciable discrepancy between the position of the radiation induced hydrogen-deuterium exchange equilibrium and the thermodynamically calculated value. In view of this it is unlikely that the radiation induced H_2-T_2 exchange equilibrium is especially different from the thermodynamically calculated value.

* Research carried out under the auspices of the U. S. Atomic Energy Commission.

[1] Mattraw, Pachucki, and Dorfman, J. Chem. Phys. **20**, 926 (1952).

Molecular Orbital Approximation to Electron-Spin Coupled Nuclear Spin-Spin Interactions in Molecules

HARDEN MCCONNELL
Shell Development Company, Emeryville, California
(Received January 7, 1955)

THE indirect magnetic interaction between magnetic nuclei in molecules that gives rise to fine-structure multiplets in the high-resolution nuclear magnetic resonance spectra of liquid or gaseous samples has been interpreted by Ramsey and Purcell[1,2] in terms of a second-order coupling between the magnetic moments associated with electron-spin and nuclear-spin angular momenta. These authors, and Gutowsky, McCall, and Slichter,[3] have used James-Coolidge and Heitler-London wave functions to approximate this coupling for nuclei directly bonded to one another. In order to obtain further information as to what factors determine the relation between molecular electronic structure and indirect nuclear spin coupling constants, we have applied the second-order (electron-spin)-(nuclear-spin) Hamiltonian given by Ramsey[2] to an antisymmetrized single product-type molecular spin-orbital function

$$\Psi_0=\frac{1}{\sqrt{N!}}\sum_P(-1)^P P\psi_1(1)\alpha(1)\psi_1(2)\beta(2)\psi_2(3)\alpha(3)\cdots \times\psi_M(N-1)\alpha(N-1)\psi_M(N)\beta(N), \quad (1)$$

where

$$\psi_i=\sum_j a_{ji}\phi_j^{(i)} \quad (2)$$

and where $\phi_j^{(i)}$ is an atomic (or hybrid) orbital centered on nucleus j. When the energy of interaction between nuclei N and N' is expressed by the equation,

$$\epsilon_{NN'}=\gamma_N\gamma_{N'}I_N\cdot I_{N'}J_{NN'}, \quad (3)$$

then the spin-spin coupling constant $J_{NN'}$ which is obtained using (1) and (2), is, to a good approximation,

$$J_{NN'}=\frac{1}{2\Delta E}\sum_{i,j}^{M,M}a_{Ni}a_{Nj}a_{N'i}a_{N'j}Q_{ij}^{NN'}$$

$$Q_{ij}^{NN'}=(\phi_N^{(i)}(k)\phi_N^{(i)}(k)\,|\,R(k,l)\,|\,\phi_{N'}^{(i)}(l)\phi_{N'}^{(i)}(l))$$

$$R(k,l)=4\beta^2\hbar^2\left[(3\cos^2\vartheta_{kl}-1)+\left(\frac{8\pi}{3}\right)\delta(r_{kN})\delta(r_{lN'})\right]\left[\frac{1}{r_{kN}^3}\frac{1}{r_{lN'}^3}\right] \quad (4)$$

$\cos\vartheta_{kl}=(r_{kN}\cdot r_{lN'})/(r_{kN}r_{lN'})$.

In (4) ΔE is an effective electronic excitation energy, of the order of electron-volts.

Important limitations on the result in (4) are: Uncertainties in appropriate ΔE values limit the quantitative application of (4) to comparisons of $J_{NN'}$'s within the same molecule; also, both configuration interaction and magnetic orbital terms[2] are neglected. Nevertheless, some properties shown by (4) should be helpful for semiempirical correlations of coupling constants. These are: (1) Valence electrons in the higher energy molecular orbitals, and not "inner shell" electrons, are primarily responsible for nuclear spin coupling. (2) For some molecular systems (e.g., aromatic hydrocarbons) there can exist a class of molecular orbitals such that $Q_{ij}^{NN'}=Q^{NN'}=$constant for all i and j within that class. These orbitals contribute $(\frac{1}{2}\Delta E)Q^{NN'}(\sum_i a_{Ni}a_{N'i})^2$ to the coupling between N and N'; $\sum_i a_{Ni}a_{N'i}$ is closely related to the "bond-order" as defined by Coulson and Longuet-Higgins when N and N' are directly bonded to one another.[4] The quantity $(\sum_i a_{Ni}a_{N'i})^2$, and hence some $J_{NN'}$'s, may not vary monotonically with internuclear distance. (3) If $Q_{ij}^{NN'}$ involves pure p orbits on N and N', $Q_{ij}^{NN'}$ will contain the factor $(3\cos^2\theta-1)$ where, for a rigid molecular framework, θ is the angle between the axes of the p orbitals. Thus, bond-angles can play a role in determining coupling constants. (4) From (4) it is seen that it is likely that both positive and negative $J_{NN'}$'s will be found experimentally.

A detailed discussion of the derivation and applications of (4) will be given in a subsequent communication

[1] N. F. Ramsey and E. M. Purcell, Phys. Rev. **85**, 143 (1952).
[2] N. F. Ramsey, Phys. Rev. **91**, 303 (1953).
[3] Gutowsky, McCall, and Slichter, J. Chem. Phys. **21**, 279 (1953).
[4] C. A. Coulson and H. C. Longuet-Higgins, Proc. Roy. Soc. (London) **A191**, 39 (1947); **A193**, 447 (1948).

Depolarization of Light Scattered by Polymolybdates in Acid and Basic Solutions

P. K. KATTI AND V. N. WANCHOO
Department of Applied Science, Delhi Polytechnic, Delhi, India
(Received January 10, 1955)

RECENTLY Kestigian and Stein[1] have used the light-scattering technique of Zimm[2] for determining the molecular weights M of sodium molybdate in two broad ranges of pH 6.5−7.5 and 2.5−4.0. They have shown that in the former range M is 480 ± 10 whereas in the acid range M is 2500 ± 1000, a result which they regard is in confirmity with the earlier observations of Jander[3] on the aggregation of molybdates in acid solutions. The present note deals with depolarization measurements of light (we have used sunlight with a green filter) transversely scattered by sodium molybdate solutions of different pH. The experimental arrangement is described in an earlier paper by one of us.[4] It is similar to that of R. S. Krishnan,[5] and Doty and Kaufmann.[6] Colorless dust-free solutions of sodium molybdate of different pH were prepared by the method of Lochet,[7] Kestigian and Stein.

Table I gives the value of depolarization at different pH for a solution of 1 percent concentration.

TABLE I. Variation of depolarization values with pH.

pH	1.4	1.8	4.0	6.0	8.3
%	0.9	4.5	9.5	6.9	4.9
%	36	70	85	95	100
M (approx) (From Jander's curve)	~2200	~2000	~900	~500	~200

It is well known that the depolarization, ρ_h (ratio I_v/I_h of the vertically polarized component, I_v, to that of the horizontally polarized component, I_h, when the incident beam is horizontally polarized) is of interest in studying the changes in the size of the molecular aggregates in the neighborhood of 100$\mu\mu$. If the size of the scattering centers is not much larger than 100$\mu\mu$ then I_h can be treated as due to the superposition of two independent components I_{ha} and I_{hs} due to the anisotropy and the size respectively of the molecular aggregates. I_{ha} is always equal to I_v. The magnitude of I_{hs} for scattering centers of various sizes has been investigated by Mie.[8] When the size is small ($r \ll 100\mu\mu$) the Mie component is zero and $\rho_h = 1$ or 100 percent. As the particle size increases the contribution of the Mie component to I_h slowly increases. The consequent continuous decrease of ρ_h in this region therefore offers a sensitive test of the increase in the size of the aggregates.

The values of ρ_h (Table I) show that ρ_h is equal to 100 percent for basic solutions and decreases with the increase in pH until its value reaches 36 percent at pH 1.4. The above variations of ρ_h clearly indicate that the size of the molecules in sodium molybdates solutions varies over a wide range with the decrease in the pH from molecular dimensions in basic solutions to large aggregates of the order of 100$\mu\mu$ at 1.4 pH. It is interesting to note that the increase in the size of the molecules as suggested by the decrease in ρ_h is in close agreement with the scheme suggested by Jander.

Values of ρ_v-depolarization with incident vertically polarized light, indicate that the molybdate molecules are anisotropic both in acid and basic solutions except in the neighborhood of pH 1.4 where the large aggregates are more or less spherical.

Investigations on the depolarization values and the molecular weights of sodium molybdate in solutions of different concentrations at very small intervals of pH are in progress and will be discussed elsewhere.

Our thanks are due to Professor D. S. Kothari for his interest in this investigation.

[1] Kestigian, Colodny, and Stein, J. Chem. Phys. **21**, 952 (1953).
[2] B. H. Zimm, J. Chem. Phys. **16**, 1099 (1948).
[3] Jander, Z. anorg. Chem. **229**, 129 (1936) and earlier papers.
[4] P. K. Katti, Proc. Indian Acad. Sci. **28**, 216 (1948).
[5] R. S. Krishnan, Proc. Indian Acad. Sci. **1(A)**, 782 (1935).
[6] Doty and Kaufmann, J. Phys. Chem. **49**, 583 (1945).
[7] Lochet, Compt. rend. **230**, 2137 (1950).
[8] Mie, Ann. Physik **25**, 377 (1908).

Thermodynamic Functions for Silane

AUBREY P. ALTSHULLER
2715 E. 116th Street, Cleveland 20, Ohio
(Received February 14, 1955)

ALTHOUGH the vibrational frequencies for silane were determined and assigned some years ago,[1-3] only recently has the Si—H interatomic distance been determined accurately.[4-6] Thus the data necessary to calculate the thermodynamic functions C_p^0, $(H^0-H_0^0)T$, $-(F^0-H_0^0)/T$, and S^0 are available. The thermodynamic functions for SiH_4 do not appear to have been calculated previously over a range of temperatures.

Recent infrared and microwave measurements indicate that the Si—H interatomic distance of 1.44_5A[3] or 1.45_6[7] obtained from an analysis of the rotational fine structure of SiH_4[3] are too small.

TABLE I. Thermodynamic functions for silane in the ideal gas state in cal/deg/mole.

T °K	C_p^0	$(H^0-H_0^0)/T$	$-(F^0-H_0^0)/T$	S^0
200	8.48	8.06	37.13	45.19
250	9.28	8.23	38.94	47.17
298.16	10.22	8.47	40.41	48.88
350	11.29	8.82	41.78	50.60
400	12.29	9.19	42.99	52.18
500	14.12	10.00	45.12	55.12
600	15.73	10.84	47.00	57.84
700	17.13	11.64	48.73	60.37
800	18.32	12.41	50.33	62.74
900	19.33	13.13	51.83	64.96
1000	20.19	13.80	53.25	67.05
1100	20.90	14.41	54.59	69.00
1200	21.51	14.98	55.86	70.84
1300	22.02	15.51	57.08	72.59
1400	22.44	15.99	58.24	74.23
1500	22.81	16.43	59.36	75.79

Recent infrared measurements under high resolution of SiH_3D,[4] and microwave measurements on SiH_3Cl,[5,4] SiD_3Cl,[6,4] SiD_3F[6] give a r_{SiH} distance of 1.48±0.01A. Therefore, the moment of inertia of silane has the value $(9.78\pm0.14)\times10^{-40}$ g-cm^2. The vibrational frequencies of silane[3] are $\nu_1(1)=2187.0$ cm^{-1}; $\nu_2(2)=975.6$ cm^{-1}; $\nu_3(3)=2190.6$ cm^{-1}; and $\nu_4(3)=914.2$ cm^{-1}.

Using these data, the values of the thermodynamic functions C_p^0, $(H^0-H_0^0)/T$, $-(F^0-H_0^0)/T$ and S^0 for silane have been calculated in the temperature range from 200° to 1500°K. The rigid rotator-harmonic oscillator approximation was used for the ideal gas at a pressure of one atmosphere. The values of the thermodynamic functions are listed in Table I.

The uncertainties in $(F^0-H_0^0)/T$ and S^0 resulting from the uncertainty in the moment of inertia amount to ±0.04 cal/deg/mole. Small uncertainties in the vibrational frequencies and the uncertainty resulting from the use of the rigid rotator-harmonic oscillator approximation, may bring the total uncertainties in the thermodynamic functions to about ±0.1 cal/deg/mole. At temperatures near 1000°K and above, neglect of anharmonicity and other effects may increase the uncertainties further.

The specific heat and heats of transition and fusion have been determined calorimetrically[8] between 11° and 161.5°K. The calorimetric value of the entropy at 161.5°K (b.p. of silane) is 43.2±0.2 eu. The spectroscopic value of the entropy at 161.5°K of 43.4±0.1 eu is in good agreement with the calorimetric value.

[1] W. B. Steward and H. H. Nielsen, Phys. Rev. **47**, 828 (1935).
[2] F. B. Stitt and D. M. Yost, J. Chem. Phys. **4**, 82 (1936).
[3] Tindal, Straley, and Nielsen, Phys. Rev. **62**, 151 (1942).
[4] S. R. Polo and M. K. Wilson, J. Chem. Phys. **22**, 1559 (1954).
[5] Dailey, Mays, and Townes, Phys. Rev. **76**, 136 (1949).
[6] Bak, Bruhn, and Rastrup-Anderson, J. Chem. Phys. **21**, 752, 753 (1953).
[7] G. Herzberg, *Infrared and Raman Spectra of Polyatomic Molecules* (D. Van Nostrand Company, Inc., New York, 1945).
[8] K. Clusius, Z. physik. Chem. **B23**, 213 (1933).

Study of Chelation through Raman Effect

P. G. PURANIK
Physical Laboratories, Osmania University, Hyderabad, India
(Received August 31, 1954)

USING a Fuess glass spectrograph having a dispersion of 19 cm^{-1} per mm in the λ4358A region and a Hilger Raman source, an intense Raman spectrum of salicylaldehyde has been recorded in twenty minutes. The Raman frequencies are 151(5b), 268(6), 299(2), 413(4), 453(8), 565(7), 669(2), 773(0), 890(1), 1033(8), 1120(3), 1154(7), 1230(9), 1282(4), 1324(10), 1378(2), 1462(10), 1581(8), 1623(6), 1648(6), 1669(9), 3057±23(lb). Shifts in the C=O frequency of this aldehyde caused by mixing phenol and methyl alcohol with it are measured and given in Table I.

The results given above show that the behavior of the C=O frequency in this case is reverse of what it is in the nonchelate ketones, aldehydes, and esters, when they are mixed with acceptor

TABLE I. C=O frequency in mixtures of salicylaldehyde with phenol and methyl alcohol.

Pure aldehyde	Mixture with phenol by vol.		Mixture with methyl alcohol by vol.		
...	1:0.5	1:1	1:1	1:4	1:9
1669	1669	1674	1675	1672	1670

solvents. In the case of nonchelate aldehydes, the carbonyl frequency is diminished, while in salicylaldehyde the C=O frequency is seen to increase.

When a chelate compound like salicylaldehyde, in which the chelation has already caused a diminution in the frequency of the C=O bond to 1669, is placed in an environment of molecules, like phenol or methyl alcohol, furnishing the acceptor hydrogen, the donor oxygen of the C=O group of the aldehyde is confronted with two acceptor hydrogens, one of the OH group of the aldehyde itself, and the other of the OH group of phenol or methyl alcohol. Under such circumstances, the increase in the C=O frequency, due to the presence of the molecules furnishing acceptor hydrogen, suggests that the force due to chelation is being opposed by the force due to intermolecular hydrogen bonding with the phenol or methyl alcohol molecules. Thus the acceptor hydrogen of phenol or methyl alcohol, by opposing the force of chelation, is trying to restore the strength of carbonyl bond to the normal magnitude in a nonchelate structure. Therefore the C=O frequency, instead of decreasing which would have been the case if it had already not diminished due to chelation, is now increasing.

The results obtained with phenol do not go beyond demonstrating the restoration of the strength of the link, because of the experimental limitation in getting a mixture of high concentration of phenol, in a clear liquid form. Methyl alcohol proves more helpful. At 50 percent concentration of the alcohol, the increase in the frequency of the C=O bond reaches the maximum value. Thereafter, on increasing the alcohol content further, the C=O frequency begins to decrease, suggesting that the chelation has completely broken down and the intermolecular hydrogen bonding has set in. At 90 percent concentration of the alcohol, the value of the C=O frequency reaches 1670 cm^{-1}.

Thus, salicylaldehyde provides an example where the transition from inter-molecular hydrogen bonding to inter-molecular hydrogen bonding can be studied by Raman effect.

The author expresses his thanks to Professor S. Bhagavantam for his guidance and suggestions.

Radio-Frequency Vibrational Absorption in Piezoelectric Crystals

JULES DUCHESNE AND ANDRÉ MONFILS*
Institut d'Astrophysique, Université de Liège, Cointe-Sclessin, Belgium
(Received February 14, 1955)

THE method used is similar to that employed in nuclear quadrupole spectroscopy,[1] but with the sample placed in a condenser instead of in the coil of the oscillating circuit. In these conditions, it could be expected that piezoelectric crystals would give rise to discrete acoustic absorption. This effect has now indeed been observed at about 30 Mc in the case of some antibiotics (levo- and racemic chloramphenicol, and oxytetracyclin[2]).

The present report refers mainly to the study of levo-chloramphenicol, though the behavior of the other two compounds is similar. The spectrum consists of a great number of lines whose widths vary from about 2 to 20 kc, for temperatures between 77 and 300°K. Up to the present we have investigated the spectral interval from 15 to 50 Mc. Our spectrum covers this entire region; further work outside these limits would, of course, reveal a greater extension. The main characteristics may be summarized as follows:

(1) A saturation effect of the lines occurs from which a relaxation time τ has been determined. The value obtained is about one second at 263°K for every line considered.
(2) A definite and reversible shift of the lines with temperature has been observed, and this may be expressed by the formula

$$\frac{\Delta\nu}{\Delta T}=-\mathbf{\Delta}(T)\nu, \tag{1}$$

where $\mathbf{\Delta}(T)$, which is itself a function of temperature, represents the displacement per degree. This factor has been found to be very sensitive to small structural changes of the substances. In this respect, it may be pointed out that $\mathbf{\Delta}(T)$ is increased by a factor of two on going from levo- to recemic chloramphenicol at 220°K. Thermodynamic research by Grüneisen has led him to formulate the following law[3] connecting lattice frequencies and specific volume:

$$\frac{d(\ln\nu)}{d(\ln V)}=-\gamma, \tag{2}$$

where γ is Grüneisen's constant. On comparing formulas (1) and (2) it is easy to deduce

$$\gamma=\mathbf{\Delta}\frac{(T)}{\alpha},$$

where α, which also depends on temperature, is the thermal expansion coefficient (in volume) of the substance. Taking into account that, according to our measurements, $\mathbf{\Delta}$ equals 10^{-4}/degree at 300°K for levo-chloramphenicol, and assuming for α the reasonable value of 10^{-4}/degree, it is deduced that $\gamma=1$. This compares satisfactorily with the values between 1 and 3 obtained for several compounds from thermodynamic measurements.[3]

The lattice vibrational origin of the spectra is thus confirmed. Obviously we now have a very direct method for the investigation of the fundamental properties of solid matter. Furthermore, it appears to be of wide application and may be invaluable in the study of the most complex compounds and in the distinguishing of substances of almost identical structure. Further research is being carried out in our laboratory, particularly in the field of biology.

A detailed account of this work will be published elsewhere in the near future.

* Chargé de Recherches du Fonds National Belge de la Recherche Scientifique.
[1] R. Livingston, Ann. N. Y. Acad. Sci. **55**, No. 5, 800 (1952); J. Duchesne and A. Monfils, Rev. Univ. Mines, Liège, 9e série, **T.X**, No. 9, 599 (1954).
[2] For a description of the compounds see: J. D. Dunitz, J. Am. Chem. Soc. **74**, 995 (1952); M. Welsch, Chapter "Antibiotiques" in *Pharmacodynamie Biochimique* (Sciences et Lettres, Liège, 1954), pp. 478 and 487.
[3] J. C. Slater, *Introduction to Chemical Physics* (McGraw-Hill Book Company, Inc., New York, 1939), pp. 217 and 451.

Erratum: $J=0\rightarrow1$ Rotational Transition of Trifluoroiodomethane

[J. Chem. Phys. **22**, 2094 (1954)]

FRED STERZER
Department of Physics, College of Engineering, New York University, University Heights, New York, New York

INSTEAD of "dipole moment of $1.018^{-18}\pm0.1$ esu cm" it should read: "dipole moment of $(1.0\pm0.1)\times10^{-18}$ esu cm."

Errata: Time Lag in the Self-Nucleation

[J. Chem. Phys. 22, 1614 (1954)]

HIROMU WAKESHIMA
The Kobe University of Mercantile Marine, Kobe, Japan

Page	line			
1615	12	$N(g)$	should read	$1/N(g)$
1615	21 and 27	$kT/4\chi^*$	should read	$kT/2\chi^*$
1615	35	$kT/4\pi D^*\chi^*$	should read	$kT/2D^*\chi^*$
1615	38	$4D^*\chi^*/kT$	should read	$2D^*\chi^*/kT$
1615	53	$kT/4D^*\chi^*$	should read	$kT/2D^*\chi^*$
1615	54	0.4×10^{-6} sec	should read	0.8×10^{-6} sec

Exp: Six Potential and Properties of Gases

M. P. MADAN
Department of Physics, University of Lucknow, India

(Received September 28, 1954)

MASON[1] has recently reported the transport property collision integrals for the gases whose molecules obey an exp:six potential energy of the form

$$E(r)=\frac{\epsilon}{1-6/\alpha}\left\{\frac{6}{\alpha}\exp[\alpha(1-r/r_m)]-(r_m/r)^6\right\}.$$

It is well known that the coefficient of thermal diffusion[1] is far more sensitive to the type of molecular interaction than the elementary gas coefficients and thus a determination of the laws of molecular interaction from thermal diffusion based on an exponential potential form, which is more realistic than the widely used Lennard-Jones 12:6 potential, will be much more accurate and useful.

The formulas for various gas coefficients have been given by Mason.[1] To decide upon the parameter α of Eq. (1), the thermal separation ratio R_T was calculated to its first and second approximations for values of $\alpha=12$ to $\alpha=17$. A comparison of these values with extensive experimental data of Stier[2] for argon and rather less extensive data of Davenport and Winter[3] for O_2, N_2, and methane suggested $\alpha=14$ for argon and methane and $\alpha>16$ for O_2 and N_2, through the values for latter gases are not conclusive enough due to their restricted data, nevertheless these values are in agreement with those found by Mason and Rice.[4]

TABLE I. Values of the force constants from thermal diffusion.

	Argon					Methane		
	$[R_T]_1$			$[R_T]_2$				
Temp. (°K)	ϵ/k (°K)	r_m (A)		ϵ/k (°K)	r_m (A)	Temp. (°K)	ϵ/k (°K)	r_m (A)
130	116.1	3.900		117.1	3.891	284	153.5	4.241
140	117.7	3.905		117.7	3.905	443	147.7	4.204
150	120.0	3.886		120.0	3.886			
180	120.0	3.889		120.0	3.889			
250	127.6	3.835		128.2	3.827			
300	136.3	3.794		136.3	3.794			
350	142.9	3.777		143.4	3.773			
400	147.1	3.766		150.4	3.753			
480	147.7	3.770		152.4	3.755			
530	148.9	3.776		153.2	3.768			

It was interesting to note that for values of $\alpha>14$ the thermal separation ratio R_T does not show an inversion of sign at low temperatures while there is sufficient theoretical and experimental evidence[5-7] that R_T does change sign at low temperatures, so the validity of exp:six potential for the values of the parameter $\alpha>14$ is open to question. This might be one of the important reasons that Mason and Rice[4] find the exp:six potential unsuccessful in dealing with nonspherical molecules which have a tendency for $\alpha>14$. Therefore the present investigations were restricted to argon and methane.

The values of the parameters ϵ and r_m have been evaluated using both $[R_T]_1$ and $[R_T]_2$ for the case of argon and for the case of methane by a procedure described in detail by Srivastava and Madan[7] (see Table I). Mason's[1] report also enabled to study the effect of second approximation to R_T on intermolecular force constants. The difference between $[R_T]_1$ and $[R_T]_2$ values which is about 7 percent produces a difference of about 1 percent in the values of ϵ up to 400°K, while for slightly higher temperatures the difference is within 5 percent taking also into account the most probable graphical and computational errors and this clearly indicates that the error involved in taking $R_T=[R_T]$, is considerably less and lies well within the experimental errors in the measurement of R_T. Similar results have also been obtained by Saxena and Srivastava[8] for the case of 12:6 potential.

TABLE III. Coefficient of self-diffusion using force constants from thermal diffusion; D_{11} in $cm^2\ sec^{-1}$.

	Temp. (°K)	Exp:six (present work)	12:6 (present work)	12:6 (reference 11)	Exptl. (reference 12)
Argon	353.2	0.247	0.245	0.245	0.249
	295.2	0.178	0.177	...	0.178
	273.2	0.155	0.154	0.154	0.156
	194.7	0.0824	0.0815	...	0.0830
	90.2	0.0181	0.0178	...	0.0180
	77.7	0.0134	0.0132	0.0133	0.0134
Methane	353.2	0.308	0.309	0.293	0.318
	298.2	0.226	0.227	...	0.240
	273.2	0.192	0.192	0.183	0.206
	194.7	0.100	0.100	...	0.0992
	90.2	0.0216	0.0214	0.0187	0.0266

For the sake of comparison, the force constants ϵ and r_m have also been evaluated by a method[9] using the temperature dependence of viscosity. These results have been extensively compared in Table II with the previous determination by Mason and Rice[4] and by others. The agreement between the force constants obtained by using different methods is remarkably good. To test the correctness of the parameters obtained the coefficient of self-diffusion was used to compare the experimental results with theory. The force constants used were those derived from thermal diffusion for the low temperature range 100–300°K (see Table II), as the experimental data on thermal diffusion usually refer to low temperatures. The results are also compared for the case of 12:6 potential using the force constants from thermal diffusion[7,10] and viscosity.[11] The agreement is very good for argon and good for methane (see Table III).

TABLE II. Comparison of values of force constants by different methods.

	Exp:six potential						12:6 potential			
	From thermal DiH (Present work)			From viscosity, virial and crystal properties (Reference 4)			From viscosity (Present work)		From thermal DiH (References 7, 10)		From viscosity (Reference 11)	
	α	ϵ/k	r_m	α	ϵ/k	r_m	ϵ/k	r_m	ϵ/k	r_m	ϵ/k	r_m
Argon	14	122.9	3.868	14	123.2	3.866	122.46	3.868	124.9	3.842	124	3.837
Methane	14	150.6	4.222	14	152.8	4.206	152.20	4.203	156.7	4.150	136.5	4.290

It is a pleasure to thank Professor B. N. Srivastava, Professor J. O. Hirschfelder, and Professor P. N. Sharma for useful advice and encouragement.

[1] E. A. Mason, J. Chem. Phys. **22**, 169 (1954).
[2] Stier, Phys. Rev. **62**, 548 (1942).
[3] Davenport and Winter, Trans. Faraday Soc. **47**, 1160 (1951).
[4] E. A. Mason and W. E. Rice, J. Chem. Phys. **22**, 843 (1954).
[5] Waldman, Z. Naturforsch. **A2**, 358 (1947).
[6] Troyer, van Itterbeek, and Rietveld, Physica **17**, 938 (1951).
[7] B. N. Srivastava and M. P. Madan, J. Chem Phys. **21**, 807 (1953).
[8] S. C. Saxena and B. N. Srivastava (to be published).
[9] B. N. Srivastava and M. P. Madan, Proc. Nat. Acad. Sci. India **21**, 254 (1952); Phil. Mag. **43**, 968 (1952).
[10] B. N. Srivastava and M. P. Madan, Proc. Phys. Soc. (London) **A66**, 277 (1953).
[11] Hirschfelder, Curtiss, and Bird. *The Molecular Theory of Gases and Liquids* (John Wiley and Sons, Inc. New York, 1954).
[12] E. B. Winn, Phys. Rev. **80**, 1024 (1950).

Proposed Structure of Certain Spinels at High Temperature*

WILLIAM T. HOLSER
Department of Geology, Cornell University, Ithaca, New York†
(Received December 23, 1954)

IN certain spinels (such as $Fe_2^{3+}Cu^{2+}O_4$) only a fraction λ of Fe^{3+} are in A (4-coordination) sites, and λ varies with temperature.[1,2] This departure from Verwey's[3] energy calculation for a purely inverse 2–4 or purely normal 2–3 structure, might occur by either (1) gradual disordering of cations among all A and B (6-coordination) sites, to completion at a critical temperature with cations in the same proportions (2:1) in both types of sites (λ changes from 0 or $\frac{1}{2}$ to $\frac{1}{3}$)[1]; or (2) gradual increase in the proportion of the inverse structure, if normal is calculated at 0°K, or vice versa, again to completion at a critical temperature (λ changes from 0 to $\frac{1}{2}$ or $\frac{1}{2}$ to 0).

The first possibility may be tested by an order parameter[4] $0=(P-P_d)/(P_0-P_d)$, where P is the probability that a particular type of site has the same kind of atom as in the completely ordered state at 0°/K, P_d is the probability that said site is so occupied in complete disorder, and P_0 is the probability for complete order. If, as in Fe_2CuO_4, the low-temperature ordered form is inverse; then $O_i=6\lambda-2$, and if normal, $O_n=1-3\lambda$. Bertaut's data[5] are replotted (Fig.1) in terms of O_i. For Fe_2CuO_4 O_i reaches 0 (complete disorder) at about 1150°C, but does not approach it in the sharply accelerated fashion usual in disorder.[6] Apparently $A-B$ disordering is not the principal cause of λ change in these spinels.

The second possibility is analogous to the polymorphism in one dimension exhibited by structures like SiC. These structures may be described[7,8] in terms of a distribution function $D_i=n_i/(n_n+n_i)=2\lambda$, where n_n and n_i are the numbers of (undefined) structural units or domains with the normal and inverse states, respectively. The change in λ with increasing temperature now represents an increase in proportion of higher energy, but still internally ordered, units. Bertaut's data are again replotted (Fig. 1) in terms of λ.

Mixing of structures at high temperatures gives[9] $(1-D_i)/D_i=\exp -V/kT$, where V is the energy difference between inverse and normal structures. Constant V would make $D(T)$ decrease slowly. The calculated (Coulomb) energy difference between inverse and normal states[3] is small and in the wrong direction, and therefore cannot predict a D_i-T curve. Furthermore, several factors may increase V and steepen $D(T)$ at high temperature:

1. Interaction.—Cooperation of the form $V=V_0D$, as in one-dimension polymorphs,[9] rapidly increases the high-temperature form at a critical temperature. If such a critical temperature occurs for these spinels, Fig. 1 indicates that it must be far above 1200°K. The interaction might also result in ordering among normal and inverse units, and further result in simple fractional values of λ,[9] but these lesser variations have not been detected.

2. Disordering of B atoms.—This decreases V,[3] and consequent rapid onset of B disordering in Fe_2CuO_4 at 1030°K[1] should result in a downward kink in the D_i-T curve, which the present data would not detect.

3. Decrease in covalency.—As vibrational energy increases with temperature, the probability decreases that A and O atoms are close to the ideal tetrahedral positions necessary for most effective covalent bonding.[10] Therefore V should decrease toward the calculated[3] Coulomb potential difference. In confirmation, the only compositions in which λ has been observed to depart from 0 or $\frac{1}{2}$ also reverse Verwey's rule at low temperature, due to 4-fold covalent bonding: Fe_2CuO_4, Fe_2MgO_4, Fe_2ZnO_4, Ga_2MgO_4.

The generally flat D_i-T curves indicate that the high-temperature structure of these spinels is probably some mixture of normal and inverse structures, with little real disordering of cations among A and B positions. The data are not of sufficient accuracy or temperature range to decide which of several possible factors effect this mixing. C. J. Schneer of the University of New Hampshire and A. E. Austin of Battelle Memorial Institute contributed significantly to this note.

* This work was supported in part by the Office of Naval Research and in part by the Geological Society of America.
† Present address: Battelle Memorial Institute, 505 King Avenue, Columbus 1, Ohio.
[1] E. F. Bertaut, J. phys. radium **12**, 252 (1951).
[2] Louis Neel, Ann. phys. **3**, 137 (1948).
[3] E. J. W. Verwey and E. L. Heilmann, J. Chem. Phys. **15**, 174 (1947); E. J. W. Verwey and others, Z. physik. Chem. **198**, 6 (1951).
[4] W. L. Bragg and E. J. Williams, Proc. Roy. Soc. (London) **145A**, 700 (1935).
[5] The values of λ listed by Weil, Bertaut, and Bochirol, J. phys. radium **11**, 208 (1950), are slightly lower than those graphed by Bertaut (footnote 1), so both are plotted here.
[6] J. M. Cowley, Phys. Rev. **77**, 669 (1950); D. Chipman and B. E. Warren, J. Appl. Phys. **21**, 696 (1950); J. M. Cowley, J. Appl. Phys. **21**, 24 (1950).
[7] C. J. Schneer, Bull. Geol. Soc. Am. **64**, 1471 (1953).
[8] C. J. Schneer, thesis, Cornell University, p. 29 (1954).
[9] See reference 8, pp. 42–47.
[10] H. D. Megaw, Acta Cryst. **7**, 188 (1954), has explained variations in the perovskite-type structures by a similar decrease of covalent bonding.

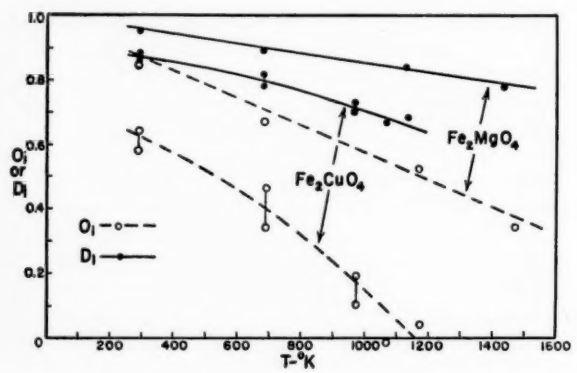

FIG. 1.

Reactor and Gamma-Ray Induced Coloring in Crystalline Quartz and Corning Fused Silica

PAUL W. LEVY
*Brookhaven National Laboratory, Upton, New York**
(Received January 26, 1955)

THE coloring induced in crystalline and amorphour silica by x-ray and nuclear radiations has been the subject of much recent work.[1,2] Attempts have been made to attribute the observed color centers to some property of the material, e.g., interstitial atoms, impurities, etc.[3,4] In this letter we will emphasize the coloring, or actually the lack of it, induced in Corning "purified" fused silica. Data on natural Brazilian crystalline quartz samples, cut from a single crystal, are included for comparison.

Samples of both materials 2 mm thick were irradiated in the Brookhaven reactor and with Co^{60} gamma rays. The Co^{60} gammas

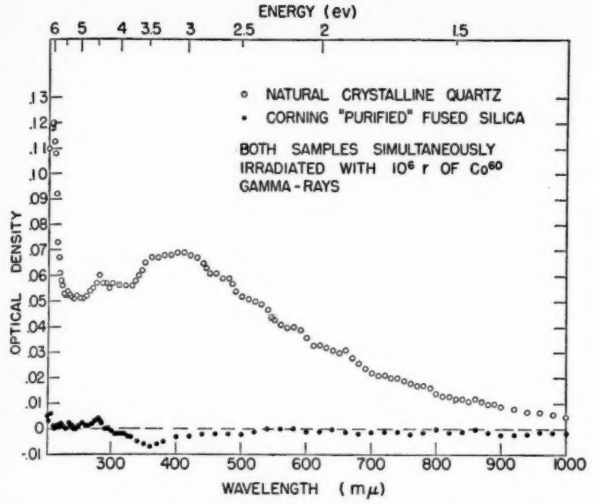
ENERGY (ev)
6 5 4 3.5 3 2.5 2 1.5
NATURAL CRYSTALLINE QUARTZ
CORNING "PURIFIED" FUSED SILICA
BOTH SAMPLES SIMULTANEOUSLY IRRADIATED WITH 10^6 r OF Co^{60} GAMMA-RAYS
OPTICAL DENSITY
WAVELENGTH (mμ)

FIG. 1. The change in optical density produced in natural Brazilian crystalline quartz and in Corning "purified" fused silica upon receiving 10^6 r of Co^{60} gamma rays at 30°C. All of the changes shown for the Corning sample may be instrumental.

are 1.1 and 1.3 Mev so that irradiated crystals were also subjected to a large number of recoil electrons and a broad spectrum of ionizing radiation extending down to visible light. The temperature of the Co^{60} facility is ≈30°C. From Fig. 1 one sees that 10^6r of gamma rays produced practically no coloring in the Corning material while in the crystalline material coloring occurs in broad bands, except for the band at ≈200 mμ which is quite narrow. All of the change observed in the Corning sample upon γ irradiation may be instrumental. The shape of the absorption spectra induced in all other types of fused silica that we have measured, subject to the same gamma-ray dose, is roughly the same as shown for this crystalline sample.

Samples were exposed to reactor irradiations in the "pneumatic tube" at 70°C. Here they are subject to fast and slow neutrons in addition to the radiation present in the cobalt sources. The reactor radiations colored a natural crystal throughout the visible and ultraviolet as shown by Fig. 2. Excepting the Corning silica, this coloring is similar to that we have found in all other fused and crystalline samples that were exposed in the reactor. With a few exceptions the curves we obtained are similar to the

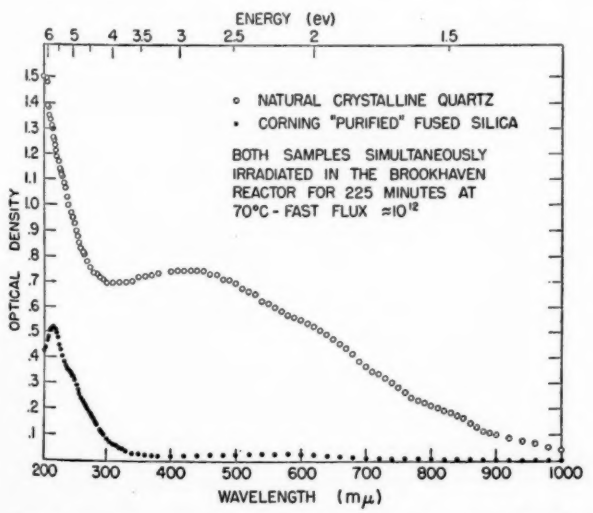
ENERGY (ev)
6 5 4 3.5 3 2.5 2 1.5
NATURAL CRYSTALLINE QUARTZ
CORNING "PURIFIED" FUSED SILICA
BOTH SAMPLES SIMULTANEOUSLY IRRADIATED IN THE BROOKHAVEN REACTOR FOR 225 MINUTES AT 70°C - FAST FLUX ≈10^{12}
OPTICAL DENSITY
WAVELENGTH (mμ)

FIG. 2. The change in optical density produced in natural Brazilian crystalline quartz and Corning "purified" fused silica by a 225-minute reactor irradiation at 70°C.

published ones. In contrast however, the Corning sample is very slightly colored in the reactor except for the strong band at 218 mμ, and a weak band near 242 mμ. This lack of coloring must be a property of the Corning silica since it was irradiated simultaneously with the other samples. In short reactor irradiations, during which the Corning material was subject to $<10^6$r, the 218-mμ band appears—indicating that this band, and also the 242-mμ band, are produced by reactor radiations and not gamma rays. Preliminary data for samples irradiated in the reactor at higher temperatures indicate that the maximum height of the bands in both fused and crystalline material is a function of temperature for a fixed neutron flux. The properties of Corning silica described here are similar to those we have reported for synthetic crystalline Al_2O_3.[5]

Two of the many ways of explaining the difference between the Corning and other silicas deserve mention. First, it may contain something which prevents it from being colored. For example, some glasses which normally are readily colored can be prevented from coloring if sufficient cerium is incorporated in them.[6] It is known that the Corning material contains water[7] (probably as OH ion) and other impurities given by Cohen.[4] Second, the Corning silica may be free of the impurities that could be responsible for the additional coloring in the other silica samples. Thus the bands at 218 mμ and near 242 mμ may be due to impurities or to some property of the lattice itself such as, e.g., interstitial Si or an electron trapped on an O vacancy. If this second alternative proves to be the case one must seriously consider the possibility that the band at 218 mμ in fused silica is due to the same electronic configuration as the band near 200 mμ in the crystal. These results and speculations are consistent with Cohen's[4] results if one assumes that the 218-mμ band is associated with interstitial silicon.

The author sincerely appreciates the cooperation of Dr. J. W. Michener of the Owens Corning Fiberglas Company, Newark, Ohio, who provided most of the Corning fused silica and of Dr. G. J. Dienes of Brookhaven National Laboratory for helpful discussions.

* Under the auspices of the U. S. Atomic Energy Commission.
[1] G. Mayer and J. Gueron, J. chim. phys. **49**, 204 (1952).
[2] F. S. Dainton and J. Rowbottom, Trans. Faraday Soc. **50**, 480 (1944). This article gives most of the pertinent references.
[3] R. Yokoto, J. Phys. Soc. Japan **7**, 316 (1952); Phys. Rev. **91**, 1013 (1953).
[4] A. J. Cohen, J. Chem. Phys. **23**, 765 (1955), this issue.
[5] P. W. Levy and G. J. Dienes, Phys. Rev. **94**, 1409 (1954); Proc. Phys. Soc. (London) (to be published).
[6] See for example the review article: K. Sun and N. J. Kreidel, Glass Ind. **33**, 511 (1952).
[7] H. Ritland, private communication.

Impurity Induced Color Centers in Fused Silica

ALVIN J. COHEN
Multiple Fellowship on Glass Science, Mellon Institute, Pittsburgh, Pennsylvania
(Received January 28, 1955)

SEVERAL workers [1-3] have associated color centers in fused silica having absorption maxima near 220, 300, and 540 mμ with the SiO_2 network alone and not with impurities present. The well-known absorption peak at 242 mμ found in many specimens of fused silica has been attributed to "interstitial" silicon atoms by Yokota[1] and to metallic impurity by Garino-Canina.[4]

In this laboratory experiments have been made on Heraeus Homogenized Ultrasil and Amersil grades of fused silica* and on Corning purified fused silica,† all of which initially lacked a 242 mμ peak.

By heating 1.5 mm thick wafers of Amersil silica to 1000–1400°C for 2.5 hours under reducing conditions using powdered sugar carbon, 325 mesh silicon or 180 mesh silicon carbide, we have produced the 242 mμ peak. Its optical density increases linearly with temperature of specimen treatment. Rapid cooling appeared

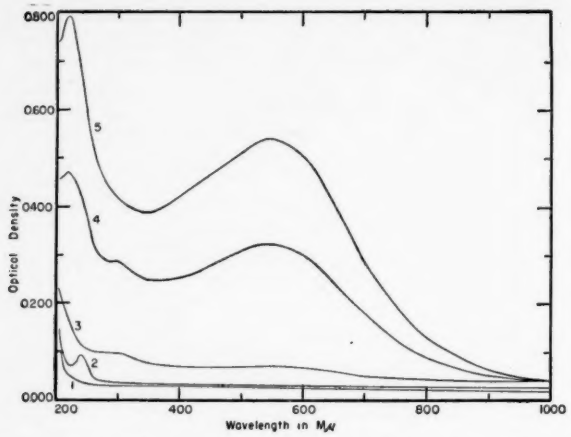

FIG. 1. Absorption spectra of x-rayed Amersil fused silica. (1) Original 1.5-mm thick polished wafer. (2) Heat treatment in silicon powder at 1400°C for 2.5 hours followed by quenching in air. (3) Original wafer without heat treatment x-rayed (50 kv, 20 ma) for 60 hours, 6.5 cm from Be window. (4) Heat treatment as in (2) followed by 5 hours of x-ray, same conditions as (3). (5) X-ray of (4) for total of 60 hours; 300 mμ peak has been saturated and smothered by the 220 mμ peak.

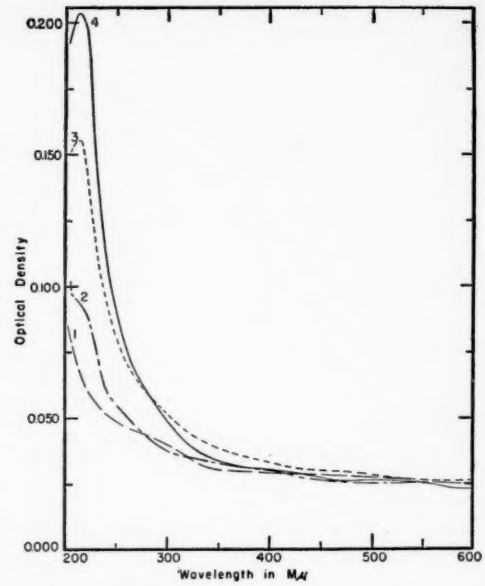

FIG. 2. Color center production in Corning purified silica. (1) Original 8-mm thick polished wafer. (2) After 144 hours x-ray treatment (50 kv, 20 ma). (3) After 298.5 hours at x-ray treatment. (4) After 313.5 hours x-ray treatment.

not to affect production of the peak; cooling to room temperature, however, was in the order of 1–5 minutes. Heating Amersil or Ultrasil under identical conditions in air but in absence of reducing agent failed to produce this peak. Heating Corning silica in air or with silicon or silicon carbide at 1400°C for 2.5 hours failed to produce the 242 mμ peak. We can conclude that the 242 mμ peak arises from reduction of some chemical impurity common to most commercial fused silica but absent in Corning material. Production of the 242 mμ peak is always accompanied by great enhancement of the 214, 300, and 540 mμ color centers, as shown in Fig. 1.

X-irradiation of Corning silica with 50 PKV, 20 ma tungsten radiation, 6 cm from the Be window of a Machlett AEG 50 tube, produces a color center at 214 mμ only after prolonged treatment, as shown in Fig. 2. No color centers are produced at 300 and 540 mμ in the Corning silica, in contrast to other commercial fused silicas; this indicates that production of these peaks requires chemical impurities. Even after heating a 1.5-mm thick wafer of Corning silica at 1400°C in silicon carbide for 2.5 hours and x-raying, no 300 and 540 mμ peaks appear. There is, however, slight enhancement of the 214 mμ peak as developed by long x-raying. Under identical conditions the 300 and 540 mμ peaks in Amersil are enhanced. Impurities responsible for these two peaks are therefore present in Amersil and absent in Corning silica. Residue remaining after dissolving these materials in hydrofluoric acid is less than 0.001 percent by weight in both cases. Emission analysis of residues shows that aluminum is present in greater amount, and titanium in equal or greater amount in Amersil; beryllium and germanium are present in Amersil and absent in Corning silica. Emission analysis of untreated pulverized samples indicates that aluminum, calcium, chromium, iron, and magnesium are present in the same orders of magnitude in both materials; copper and nickel are present in greater quantity in Amersil than in Corning. Boron if present in Amersil is less than 20 ppm. Water is present in both as indicated by presence of the first overtone at 1.4μ of the 2.8-μ band due to O−H bond stretching.

Earlier[5] the author suggested that color centers in α quartz were due to impurities, and that the impurity associated with the 540-mμ peak in fused silica is probably responsible for the peak in amethyst at the same wavelength. It is possible that the 214-mμ color center found in Corning purified silica and other silica after high-energy irradiation is associated with the silica network alone and does not require impurity atoms. Levy[6] has shown that reactor irradiation results in very strong enhancement of the 214-mμ band. It remains to be proven that this band is independent of impurities.

[1] R. Yokota, J. Phys. Soc. Japan **7**, 316 (1952).
[2] G. Mayer and J. Gueron, J. chim. phys. **49**, 204 (1952); (English translation) Glass Ind. **34**, 127 (1953).
[3] F. S. Dainton and J. Rowbottom, Trans. Faraday Soc. **50**, 480 (1954).
[4] V. Garino-Canina, Compt. rend. **238**, 1577 (1954).
* Obtained through the Amersil Company, Inc., Hillside, New Jersey.
† Courtesy of Corning Glass Works, Corning, New York.
[5] A. J. Cohen, J. Chem. Phys. (to be published).
[6] P. W. Levy, J. Chem. Phys. **23**, 764 (1955), preceding letter.